Universidade Federal de Pernambuco
Centro de Ciências da Saúde
Programa de Pós-Graduação em Ciências Farmacêuticas

PAULO ANDRÉ TEIXEIRA DE MORAES GOMES

Planejamento estrutural, síntese e avaliação das propriedades farmacológicas de inéditas tiazolil-hidrazonas derivadas da ftalimida e da isatina

Recife
2016

Paulo André Teixeira de Moraes Gomes

Planejamento estrutural, síntese e avaliação das propriedades farmacológicas de inéditas tiazolil-hidrazonas derivadas da ftalimida e da isatina

Tese submetida ao Programa de Pós-Graduação em Ciências Farmacêuticas do Centro de Ciências da Saúde da UFPE, como requisito parcial para o recebimento do Título de Doutor em Ciências Farmacêuticas.

Orientadora: Prof.ª Dr.ª Ana Cristina Lima Leite

Coorientador: Dr. Marcos Veríssimo de Oliveira Cardoso

Recife

2016

Catalogação na fonte
Bibliotecária: Mônica Uchôa, CRB4-1010

G633p Gomes, Paulo André Teixeira de Moraes.
Planejamento estrutural, síntese e avaliação das propriedades farmacológicas de inéditas tiazolil-hidrazonas derivadas da ftalimida e da isatina / Paulo André Teixeira de Moraes Gomes. – 2016.
225 f.: il.; tab.; 30 cm.

Orientadora: Ana Cristina Lima Leite.
Tese (Doutorado) – Universidade Federal de Pernambuco, CCS. Programa de Pós-Graduação em Ciências Farmacêuticas. Recife, 2016.
Inclui referências e apêndices.

1. Ftalimidas. 2. Isatina. 3.Tiazol. 4. Chagas. 5. Câncer. I. Leite, Ana Cristina Lima (Orientadora). II. Título.

615.3 CDD (23.ed.) UFPE (CCS2016-244)

PROPESQ
PRÓ-REITORIA PARA ASSUNTOS DE PESQUISA E PÓS-GRADUAÇÃO

UFPE

ATA DA OCTOGÉSIMA DEFESA DE TESE DE DOUTORADO DO PROGRAMA DE PÓS-GRADUAÇÃO EM CIÊNCIAS FARMACÊUTICAS DO CENTRO DE CIÊNCIAS DA SAÚDE DA UNIVERSIDADE FEDERAL DE PERNAMBUCO

Aos vinte e sete dias do mês de julho de dois mil e dezesseis, às quatorze horas, no Departamento de Ciências Farmacêuticas da Universidade Federal de Pernambuco, em sessão pública, teve início a defesa da Tese "**PLANEJAMENTO ESTRUTURAL, SÍNTESE E AVALIAÇÃO DAS PROPRIEDADES FARMACOLÓGICAS DE INÉDITAS TIAZOLIL-HIDRAZONAS DERIVADAS DA FTALIMIDA E DA ISATINA**" do aluno **Paulo André Teixeira de Moraes Gomes**, na área de concentração Fármacos e Medicamentos, sob a orientação da Prof.ª Dr.ª Ana Cristina Lima Leite. O doutorando **Paulo André Teixeira de Moraes Gomes** cumpriu todos os demais requisitos regimentais para a obtenção do grau de DOUTOR em Ciências Farmacêuticas. A Banca Examinadora indicada pelo colegiado do programa na Reunião ordinária do dia quatro de julho de dois mil e dezesseis, homologada pela Diretoria de Pós-Graduação, através do processo Nº 23076.031726/2016-81 em 11/07/2016, foi composta pelos Professores Doutores: Ana Cristina Lima Leite, do Departamento de Ciências Farmacêuticas da UFPE; Sebastião José de Melo, do Departamento de Antibióticos da UFPE; Mônica Camelo Pessoa de Azevedo de Albuquerque do Departamento de Medicina Tropical da UFPE; Moacyr Jesus Barreto de Melo Rêgo do Departamento de Bioquímica da UFPE e Gardênia Carmen Gadelha Militão do Departamento de Fisiologia e Farmacologia da UFPE. Após cumpridadas as formalidades, o candidato foi convidado a discorrer sobre o conteúdo da Tese. Concluída a explanação, o candidato foi arguido pela Banca Examinadora que, em seguida, reuniu-se para deliberar e conceder ao mesmo a menção APROVADO da referida Tese. A Senhora Presidente informou que ao aluno "Aprovado" terá o prazo de quarenta e cinco dias para a entrega dos exemplares definitivos do trabalho à Coordenação conforme regimento interno do Programa (Art. 35). E, para constar, lavrei a presente Ata que vai por mim assinada, Secretária de Pós-Graduação, e pelos membros da Banca Examinadora.

Recife, 27 de julho de 2016.

_____
Nerilin Trajano da Silva Neto

BANCA EXAMINADORA

Prof.ª Ana Cristina Lima Leite _____
Prof. Sebastião José de Melo _____
Prof.ª Mônica Camelo Pessoa de Azevêdo Albuquerque _____
Prof. Moacyr Jesus Barreto de Melo Rêgo _____
Prof.ª Gardênia Carmen Gadelha Militão _____
Paulo André Teixeira de Moraes Gomes _____

À minha mãe, Cristina Teixeira de Morais, pelo apoio, conselhos e orações que me ajudam a seguir atingindo meus objetivos.

À minha esposa, Ana Daura Travassos de Oliveira Moraes, por todo o amor e companheirismo que têm me transformado, a cada dia, em uma pessoa melhor.

Ao meu avô, Pedro Simões de Morais (*in memoriam*), ao meu irmão, Hugo Leonardo Simões Gomes (*in memoriam*).

AGRADECIMENTOS

Agradeço à minha orientadora, Prof.ª Dr.ª Ana Cristina, por ter me acolhido para sua equipe desde 2008. Por todas as oportunidades que tem me dado de crescer no meio acadêmico. Pela confiança que deposita em todos os alunos do LpQM. Pela liberdade que nos dá para desenvolvermos nossas habilidades no âmbito científico. Por ter acompanhado meu processo de amadurecimento profissional ao longo dos anos, desde a minha iniciação científica até o doutorado.

Ao meu coorientador, Dr. Marcos Cardoso, por ter me ajudado principalmente durante o processo de organização e elaboração de artigos. Ao meu "segundo coorientador", Dr. Diogo Rodrigo, que também me ajudou muito desde a iniciação científica até o doutorado.

A todos os meus amigos do LpQM, por todos esses anos de convivência, brincadeiras, conselhos e apoio. Em especial, às minhas ex-ICs, Miria e Lucianna, que hoje são doutorandas de sucesso. Ao doutorando Arsênio e à Dr.ª Edna, que trabalharam comigo durante o doutorado, contribuindo bastante para a produção do meu primeiro artigo. Ao doutorando Gevanio, que faz parte do grupo desde o tempo em que éramos ICs. À Thays, que fez parte do grupo durante a sua iniciação científica e me auxiliou muito na concretização desse trabalho.

À FACEPE, pela concessão da bolsa de doutorado. Ao Programa de Pós-Graduação em Ciências Farmacêuticas. A todos os colaboradores que tornaram esse trabalho possível: Prof.ª Dr.ª Valéria Pereira (Fiocruz-PE), Prof.ª Dr.ª Milena Botelho (Fiocruz-BA), Prof. Dr. Fábio Brayner (LIKA-UFPE) e Dr. Moacyr Rêgo (NUPIT-UFPE).

Aos meus familiares, que me dão muito orgulho, por serem pessoas de bem, esforçadas e que fizeram e fazem parte da formação do meu caráter. Principalmente à minha mãe (Cristina), por sempre ter sido uma guerreira e por, além de tantas outras coisas que ela fez e faz por mim, ter acreditado nos meus sonhos. Também à minha sogra (Valéria) e ao meu sogro (Inaldo), por serem minha família aqui em Recife.

À minha esposa (Daura), por ser minha companheira de todas as horas e uma amiga verdadeira. Pelo amor e por toda a felicidade que nos permitimos viver, e que, geralmente só é vivida na infância. Por todos os momentos de aprendizado e diversão e por tudo de bom que ainda virá. Por sermos crianças juntos.

E principalmente, a Deus. Essa energia que perpassa e constitui todo o Universo. Que está presente em tudo que é vivo e não vivo. Por me guiar pelo melhor caminho ao longo de toda minha jornada.

"*O senhor... Mire veja: o mais importante e bonito, do mundo, é isto: que as pessoas não estão sempre iguais, ainda não foram terminadas – mas que elas vão sempre mudando. Afinam ou desafinam. Verdade maior. É o que a vida me ensinou. Isso que me alegra, montão.*"

(João Guimarães Rosa, Grande Sertão: Veredas, 1956)

RESUMO

A identificação e utilização de estruturas privilegiadas como base para a obtenção de novas moléculas, tem se destacado como estratégia para a descoberta de novos fármacos. Como exemplos de estruturas privilegiadas podem ser citados os heterociclos ftalimida e isatina. Ambos são importantes grupos farmacofóricos conhecidos pelo amplo espectro de atividades biológicas que apresentam. Outro importante grupo farmacofórico que vem sendo bastante explorado e que está presente em moléculas quimicamente diversas e ativas para uma grande variedade de doenças é o heterociclo tiazol. Fazendo uso da estratégia de hibridização molecular foram obtidos inéditos compostos tiazóis derivados da ftalimida e da isatina. O presente trabalho está dividido em dois capítulos e explora duas das muitas atividades farmacológicas apresentadas pelos grupos farmacofóricos, a atividade antichagásica e a anticâncer. O primeiro capítulo apresenta o planejamento, a síntese, a caracterização estrutural, a avaliação quanto às propriedades antichagásicas de tiazóis derivados da ftalimida. Alguns dos compostos obtidos nessa primeira parte apresentaram potente inibição sobre a forma tripomastigota do parasito com baixa toxicidade em células esplênicas, e as relações estrutura-atividade resultantes são discutidas. Também são apresentadas alterações ultraestruturais que ftalil-1,3-tiazóis induzem sobre a morfologia do parasito, como o encurtamento do flagelo, condensação da cromatina, inchaço das mitocôndrias, alteração de reservosomos e dilatação do retículo endoplasmático. Juntos, estes dados revelam, pela primeira vez, uma nova série de compostos contendo ftalimido-tiazóis como base estrutural com potentes efeitos contra o *T. cruzi* e características de líder-similar ("lead-like") contra a doença de Chagas. Os resultados apresentados no primeiro capítulo foram publicados na *European Journal of Medicinal Chemistry*. O segundo capítulo apresenta o planejamento, a síntese empregada, a caracterização estrutural para a obtenção das séries de tiazóis inéditos derivados da isatina, assim como alguns resultados prévios de suas propriedades antitumorais. Nessa segunda parte da tese são apresentadas 29 moléculas, sendo 9 tiossemicarbazonas e 20 tiazóis. Nenhum dos compostos apresentou citotoxicidade na dose de 100 μM para células normais humanas. Embora não sejam conclusivos, resultados prévios indicam que alguns compostos intermediários apresentam importante atividade antitumoral, o que pode indicar que a síntese de derivados de tais compostos pode ser promissora para a obtenção de novos agentes antitumorais. De modo geral, pode-se concluir que a estratégia de utilização de estruturas privilegiadas como bases estruturais para a obtenção de novos compostos biologicamente ativos permitiu identificar potentes agentes antichagásicos, bem como encontrar um prévio direcionamento para síntese de novos protótipos a fármacos antitumorais.

Palavras-chave: Ftalimidas. Isatina. Tiazol. Chagas. Câncer.

ABSTRACT

The identification and use of privileged structures as a basis for obtaining new molecules, has excelled as a strategy for drug discovery. Examples of privileged structures can be cited the phthalimide and isatin heterocycles. Both are important pharmacophore groups known by the broad spectrum of biological activities that present. Another important pharmacophore which has been extensively explored and is present in various chemically active molecules and for a wide variety of diseases is the thiazole heterocycle. Making use of molecular hybridization strategy were obtained unpublished thiazoles compounds derived from phthalimide and isatin. This work is divided into two chapters and explores two of the many pharmacological activities presented by pharmacophore groups, the antichagasic and anti-cancer activity. The first chapter presents the planning, synthesis, structural characterization, antichagasic properties evaluation of phthalimido-thiazoles derivatives. Some of the compounds obtained in this first part showed potent inhibition on parasite trypomastigotes with low toxicity in spleen cells and the resulting structure-activity relationships are discussed. Also ultrastructural changes appear that phthalyl-1,3-thiazoles induce on the morphology of the parasite, such as the shortening of the flagellum, chromatin condensation, swelling of mitochondria, reservosomes change and dilatation of the endoplasmic reticulum. Together, these data revealed, for the first time, a novel series of phthalimido-thiazoles-structure-based compounds with potential effects against *T. cruzi* and lead-like characteristics against Chagas disease. The results showed in the first chapter were published in the European Journal of Medicinal Chemistry. The second chapter presents the planning, the synthesis used, the structural characterization to obtain the derivatives unpublished thiazoles series of isatin, as well as some preliminary results of its anti-tumor properties. In this second part of the thesis are displayed 29 molecules, 9 thiosemicarbazone and 20 thiazoles. Neither compound showed cytotoxicity in a dose of 100 uM to normal human cells. Although not conclusive, preliminary results indicate that some intermediates have significant antitumor activity, which may indicate that the synthesis of derivatives of such compounds can be promising for obtaining novel anticancer agents. In general, it can be concluded that the strategy of use of privileged structures as structural basis for obtaining new biologically active compounds identified potent antichagasic agents and find a previous guidance for synthesis of new prototypes to antitumor drugs.

Keywords: Phthalimide, isatin, thiazole, Chagas disease, cancer.

LISTA DE ESQUEMAS

LISTA DE FIGURAS

LISTA DE TABELAS

LISTA DE ABREVIATURAS

^{13}C-RMN: Ressonância Magnética Nuclear de Carbono;

^{1}H-RMN: Ressonância Magnética Nuclear de Prótons;

CCD: Cromatografia de camada delgada;

FDA: Food and Drug Administration;

IV: Infravermelho;

IV: Infravermelho;

OMS: Organização Mundial de Saúde;

PF: Ponto de fusão;

Rf: Fator de retenção;

REA: Relação estrutura-atividade.

PBMCs: Células mononucleares do sangue periférico (em inglês "peripheral blood mononuclear cell".

SUMÁRIO

1 INTRODUÇÃO

Estruturas privilegiadas são esqueletos moleculares com propriedades versáteis de ligação, de tal modo que um único grupamento é capaz de proporcionar ligantes potentes e seletivos para uma gama de diferentes alvos biológicos através da modificação de grupos funcionais. O resultado é a produção de ligantes de alta qualidade que fornecem uma base sólida para o desenvolvimento de novos fármacos (DESIMONE *et al.*, 2004). Dentre as estratégias que podem conduzir à descoberta de novos fármacos, a identificação e utilização dessas estruturas privilegiadas ganhou atenção especial quando comparada a outras estratégias (COSTANTINO & BARLOCCO, 2006).

Um exemplo de estrutura privilegiada é o heterociclo ftalimida (1,3-isoindolinadiona). Trata-se de uma imida aromática na qual dois grupos carbonila estão ligados a um grupo funcional amina, sendo um grupo de partida muito importante e muito utilizado na química orgânica (SHARMA *et al.*, 2010).

Derivados da ftalimida formam um interessante grupo de compostos que possui amplo espectro de propriedades farmacológicas (SUVARNA *et al.*, 2012), dentre as quais pode-se citar a atividade analgésica (ANTUNES *et al*. 2003), anticonvulsivante (BAILLEUX et al., 1994), antituberculose (JEAN *et al.*, 2009; BABU *et al.*, 2005), ansiolítica (HASSANZADEH *et al.*, 2007), anti-inflamatória (COLLIN *et al.*, 2001), antimicrobiana (PATEL *et al.*, 2004), antipsicótica (AL-RASHOOD *et al.*, 1988) e antiparasitária (TIMOTHY *et al.* 2012; MIGUEL *et al.*, 2014; SANTIAGO *et al.*, 2013), sendo também conhecida pelas atividades imunomoduladora, anti-angiogênica e anti-proliferativa (TEO, 2005).

Nosso grupo de pesquisa (Laboratório de Planejamento em Química Medicinal – LpQM – UFPE) tem explorado as propriedades farmacológicas de derivados ftalimídicos. Como resultado, foram identificados importantes protótipos a farmacos com potentes atividades antinflamatória (LEITE *et al.*, 2014), antiproliferativa (CARDOSO *et al.*, 2015), imunomoduradora (CARDOSO *et al.*, 2015; LEITE *et al.*, 2014; COÊLHO *et al.*, 2014; PESSOA *et al.*, 2010), antitumoral (PESSOA *et al.*, 2010) e antiparasitátira (SANTIAGO *et al.*, 2014) (**Figura 1**). A **Figura 2** apresenta dois exemplos de derivados ftalimídicos obtidos por nosso grupo.

Figura 1. Trabalhos publicados pelo LpQM envolvendo o núcle ftalimida.

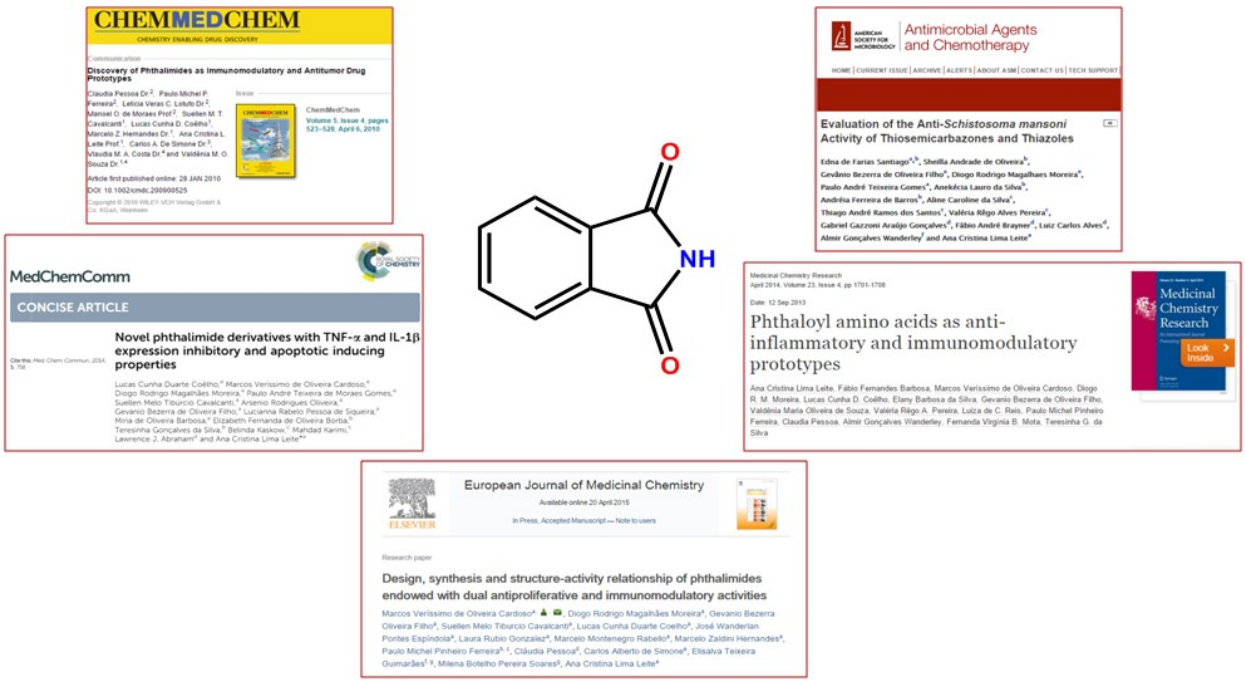

Fonte: Elaborado pelo autor.

Figura 2. Exemplos de derivados ftalimídicos: O composto **9c** com potente atividade imunomoduladora (COÊLHO et al., 2014) e o composto LpQM-45 como potente agente esquistossomicida (SANTIAGO et al., 2014).

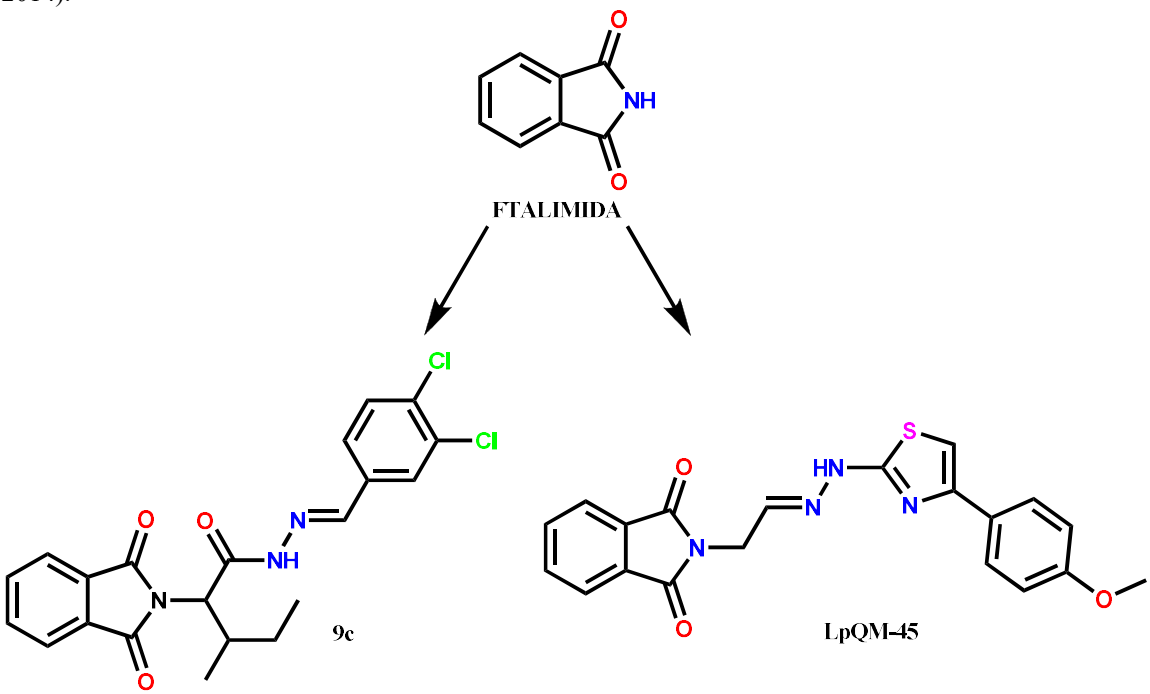

Fonte: Elaborado pelo autor.

Mais recentemente, nosso grupo decidiu explorar as propriedades farmacológicas dos derivados da isatina (1H-indol-2,3-diona). Trata-se de outro exemplo de estrutura privilegiada, sendo um importante composto heterocíclico do tipo indol (VINE *et al.*, 2009). O indol é um importante sistema heterocíclico por estar inserido em proteínas, por ser a base de vários fármacos, como a indometacina, e por fazer parte do esqueleto de alcaloides indóis – compostos biologicamente ativos de plantas, incluindo estricnina e LSD. A incorporação de um núcleo indol em compostos medicinais têm dado a esse heterociclo versátil um amplo espectro de atividades biológicas (**Figura 3**) (SHARMA *et al.*, 2010).

Figura 3. Núcleo Indol e suas principais atividades biológicas.

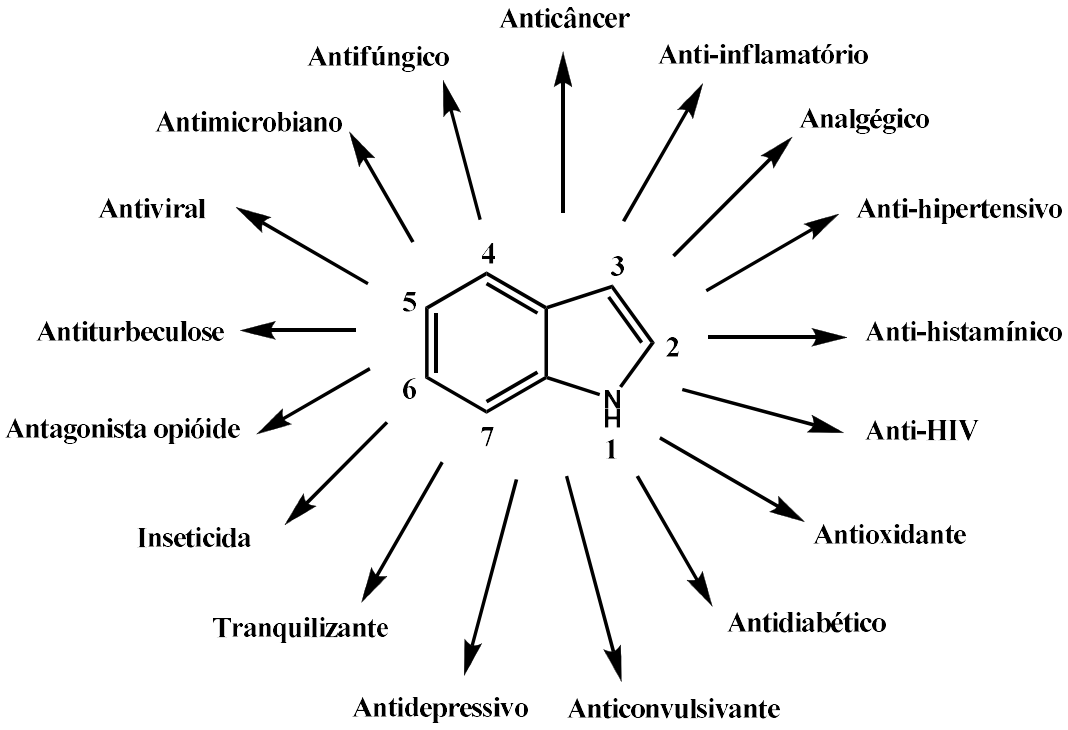

Fonte: Elaborado pelo autor.

Assim como o indol, tanto a isatina quanto seus derivados demonstram uma gama de atividades biológicas e farmacológicas, incluindo propriedades anticonvulsivante, antibacteriana, antifúngica, antiviral e anticâncer. Esse amplo espectro de atividade biológica tem sido facilitado pela versatilidade sintética da isatina, que permitiu a geração de um grande número de derivados estruturalmente diversos, incluindo análogos com substituição do anel aril e/ou derivação do nitrogênio da isatina e dos carbonos C2 e C3 (VINE *et al.*, 2009) (**Figura 4**).

Figura 4. Estrutura da isatina.

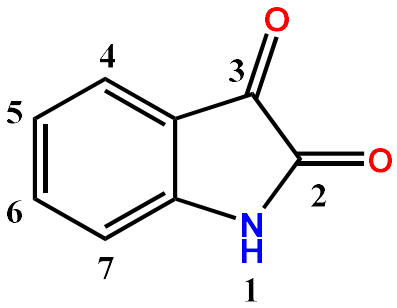

Fonte: Elaborado pelo autor.

Outro importante núcleo que também vêm sendo esplorados por nosso grupo são os tiazóis ou 1,3-tiazóis. Trata-se de um composto orgânico heterocíclico formado por um anel de cinco membros contendo três átomos de carbono, um de enxofre e um de nitrogênio (**Figura 5**). Os tiazóis são membros dos heterociclos azóis que incluem imidazóis e oxazóis. O anel tiazol é planar, e sua aromaticidade é caracterizada pela deslocalização de um par de elétrons do átomo de enxofre para completar os 6 elétrons π necessários para satisfazer a regra de Huckel (KASHYAP *et al.*, 2012).

Figura 5. Estrutura do anel heterocíclico Tiazol.

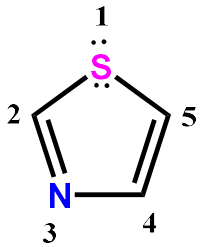

Fonte: Elaborado pelo autor.

Os derivados tiazólicos são conhecidamente uma classe de compostos com um amplo espectro de atividades biológicas, dentre as quais podem ser citadas a atividade antibacteriana, anti-inflamatória, imunomoduladora, anti-hipertensiva, anticonvulsivante, antidepressiva e anticâncer (MESHRAM *et al*., 2012). Alguns exemplos de compostos biologicamente ativos contendo o núcleo tiazol são o sulfatiazol (droga antimicrobiana), ritonavir (droga antirretroviral), abafungin (droga antifúngica), bleomicina e tiazofurin (fármacos antitumorais) (KASHYAP *et al.*, 2012) (**Figura 6**).

Figura 6. Compostos biologicamente ativos que apresentam tiazol em sua estrutura.

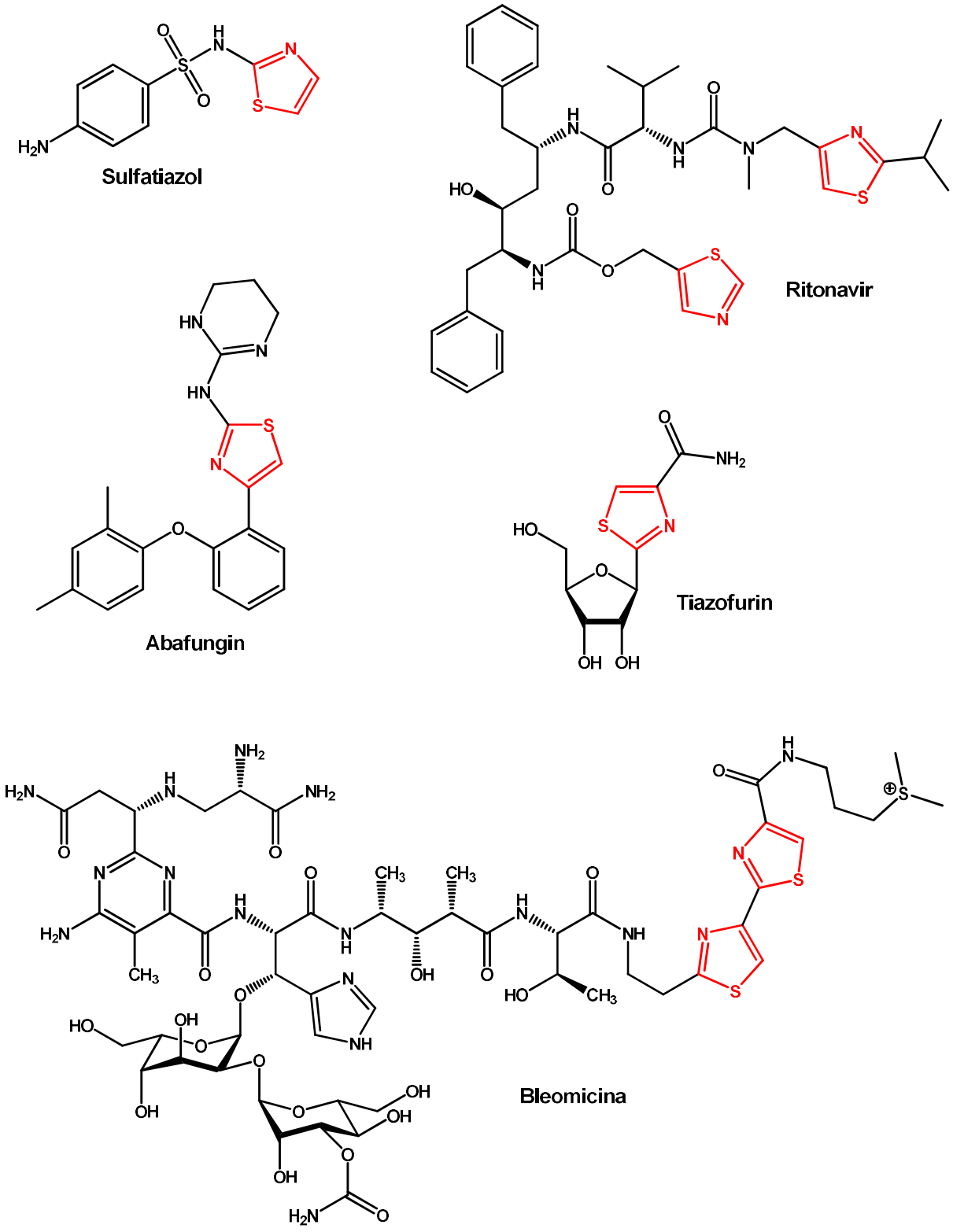

Fonte: Elaborado pelo autor.

O presente trabalho está dividido em dois capítulos e apresenta novos tiazóis derivados da ftalimida e da isatina, obtidos por meio da estratégia de hibridização estrutural, e explora

duas das muitas atividades farmacológicas apresentadas por esses grupos farmacofóricos, a atividade antichagásica e a anticâncer (**Figura 7**).

Figura 7. Amplo espectro de atividades dos núcleos ftalimida e isatina.

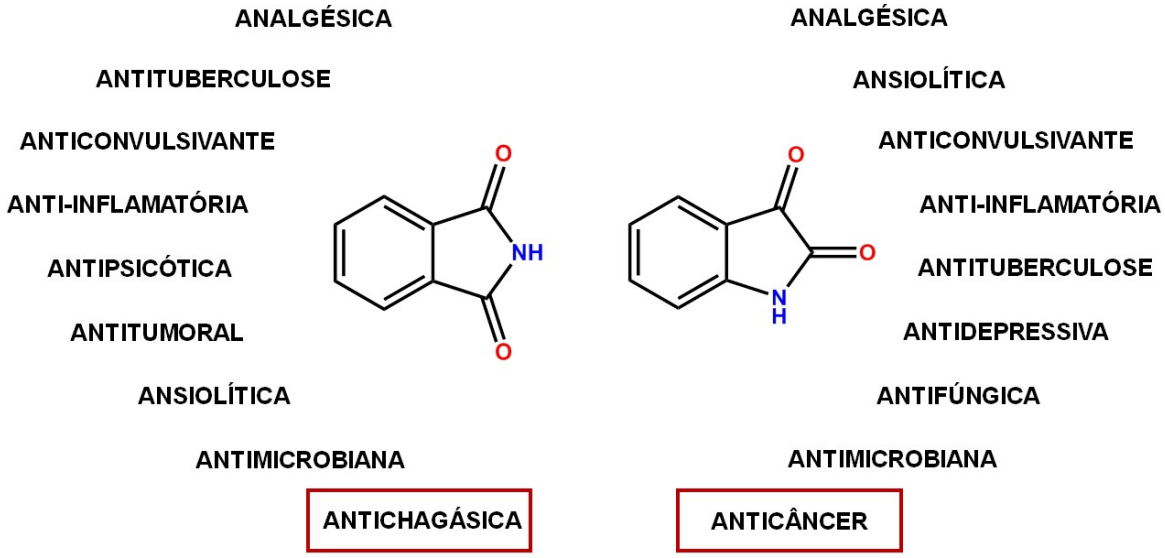

Em destaque, as atividades avaliadas neste trabalho. Fonte: Elaborado pelo autor.

O primeiro capítulo é intitulado "Ftalimido-tiazóis como blocos de construção e os seus efeitos sobre o crescimento e morfologia do *Trypanosoma cruzi*" e nele é apresentado o planejamento, a síntese, a caracterização estrutural, a avaliação quanto às propriedades antichagásicas de tiazóis derivados da ftalimida.

O segundo capítulo é intitulado "Planejamento estrutural, síntese e avaliação das propriedades antitumorais de inéditas tiazolil-hidrazonas derivadas da isatina" e nele é apresentado o planejamento, a síntese empregada, a caracterização estrutural para a obtenção das séries de tiazóis inéditos derivados da isatina, assim como alguns resultados prévios de suas propriedades antitumorais.

Desse modo, aqui é apresentada a investigação da eficácia da estratégia de hibridização estrutural, envolvendo as estruturas privilegiadas tiazol, ftalimida e isatina, com relação à potencialização das propriedades farmacológicas de tais compostos.

2 OBJETIVOS

2.1 Objetivo Geral

Este trabalho tem por objetivo identificar novos tiazóis biológicamente ativos, utilizando-se a estratégia de hibridização molecular. Desse modo, são investigadas as propriedades antichagásicas de tiazóis derivados da ftalimida e as propriedades antitumorais de tiazóis derivados da isatina.

2.2 Objetivos específicos

- Sintetizar uma série de tiazóis inéditos derivados da ftalimida;
- Sintetizar uma série de tiazóis inéditos derivados da isatina;
- Caracterizar e elucidar todos os compostos através de técnicas de Ressonância Magnética Nuclear de Prótons (^{1}H-RMN) e Carbono (^{13}C-RMN), Infravermelho (IV) e Análise Elementar;
- Analisar citotoxicidade celular frente a células esplênicas de camundongos BALB/c para os derivados da ftalimida;
- Avaliar a atividade antichagásica dos derivados da ftalimida frente às formas epimastigota e tripomastigota do *T. cruzi*;
- Avaliar as alterações ultraestruturais promovidas pelos derivados da ftalimida na forma tripomastigota do *T. cruzi*;
- Identificar o possível mecanismo de morte celular promovido pelos derivados da ftalimida na forma tripomastivota do *T. cruzi*;
- Avaliar a citotoxicidade dos derivados da isatina em células humanas mononucleares do sangue periférico;
- Avaliar as propriedades antitumorais dos derivados da isatina frente a diferentes linhagens de sélulas tumorais.

3 CAPÍTULO 1

Ftalimido-tiazóis como blocos de construção e os seus efeitos sobre o crescimento e morfologia do *Trypanosoma cruzi*

Artigo publicado na *Eur. J. Med. Chem.*

3.1 Revisão da Literatura

3.1.1 Doença de Chagas

Doença de Chagas, também conhecida como tripanossomíase americana, é uma doença potencialmente fatal causada pelo parasita protozoário *Trypanosoma cruzi* (*T. cruzi*). Estima-se que aproximadamente 6-7 milhões de pessoas seriam infectados em todo o mundo, principalmente na América Latina, onde a doença de Chagas é endêmica (WHO, 2015).

O ciclo de vida de *T. cruzi* é complexo, com vários estágios de desenvolvimento em insetos vetores e hospedeiros mamíferos. Tripomastigotas não replicativos, na corrente sanguínea, e amastigotas intracelulares replicativos, são as formas típicas do organismo, que são identificadas em hospedeiros mamíferos, enquanto epimastigotas replicativos estão presentes no vetor triatomíneo (**Figura 8**) (RASSI *et al.*, 2009).

Figura 8. Formas evolutivas do *Trypanosoma cruzi*.

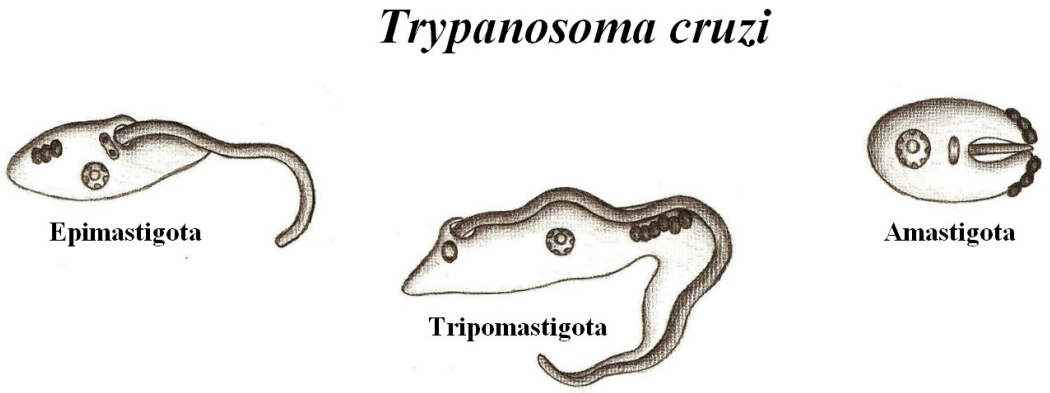

Fonte: Elaborado pelo autor.

Apesar dos esforços de muitos investigadores para pesquisar novos fármacos anti-Chagas, apenas um medicamento é usado atualmente em terapia, benznidazol (BDZ) (URBINA, 2002; PÉREZ-MOLINA *et al.*, 2013). A quimioterapia corrente para a doença de Chagas não é satisfatória devido à eficácia limitada do BDZ, particularmente durante a fase crônica, com efeitos secundários frequentes que podem levar à interrupção do tratamento (CARDOSO *et al.*, 2014).

Uma maneira pragmática para melhorar a qualidade dos candidatos a fármacos é melhorando a qualidade dos blocos de construção (reagentes) que são usados para sintetizá-las. Nossa estratégia está focada em subestruturas e suas propriedades, que tenham suas

atividades biológicas e boas propriedades fármaco-similar ("drug-like") preveamente conhecidas. Entre os grupos químicos explorados quanto à atividade anti-*T. cruzi*, tiazolil-hidrazonas são notáveis por terem uma ampla atividade biológica, especialmente antiparasitária (GAWANDE *et al.*, 2013; MASOUD *et al.*, 2012; MOREIRA *et al.*, 2012; PIZZO *et al.*, 2011). Caputo *et al.* têm demonstrado atividade tripanocida para uma série de 4-aril-tiazolil-hidrazonas (CAPUTTO *et al.*, 2012), que têm grandes e potentes atividades para todas as formas do parasito.

Nossa busca por novos fármacos antichagásicos desde 2006 têm nos levado a desenvolver uma variedade de tiossemicarbazonas e 1,3-tiazolil-hidrazonas como agentes tripanossomicidas (CARDOSO *et al.*, 2014; MOREIRA *et al.*, 2012; HERNANDES *et al.*, 2010; LEITE *et al.*, 2006; LEITE *et al.*, 2007; ESPÍNDOLA *et al.*, 2015; OLIVEIRA FILHO *et al.*, 2015). Em continuação de nossa busca por moléculas bioativas, nós evidenciamos que a derivatização do grupo tiossemicarbazona em um grupamento tiazol pode gerar novos modelos propensos a apresentar atividade anti-*T. cruzi* (CARDOSO *et al.*, 2014).

3.1.2 Derivados da ftalimida

Muito esforço tem sido investido para identificar as principais diferenças chaves entre fármacos e outros compostos orgânicos. É Esperado que bibliotecas de alta qualidade exibam similaridades com fármacos (drug-likeness) para produzir compostos com perfis farmacocinéticos e de segurança desejáveis. O grupo funcional ftalimida tem sido utilizado como uma ferramenta importante na síntese orgânica por proteger contra reações indesejadas. Muitas equipes de pesquisa têm usado esse núcleo como um bloco de construção para melhorar a qualidade do composto. De fato, derivados de ftalimida têm demonstrado um amplo espectro de propriedades farmacológicas, tais como analgésica (ALANAZI *et al.*, 2015), anticonvulsivante (KAMINSKI *et al.*, 2011), antituberculose (AKGÜN et al., 2012; ABDEL-AZIZ *et al.*, 2011), hipolipidémica (ABDEL-AZIZ *et al.*, 2011), ansiolítica (ALANAZI *et al.*, 2015), anti-inflamatória (ALANAZI *et al.*, 2015), antimicrobiana (AKGÜN *et al.*, 2012; SINGH *et al.*, 2015; ELUMALAI *et al.*, 2013) e antipsicótica (WILLIAMS *et al.*, 2011).

Por esse motivo, o nosso grupo de pesquisa tem explorado as propriedades farmacológicas dos derivados da ftalimida. Como resultado, foram identificados protótipos bioativos com potentes propriedades anti-inflamatórias (LEITE *et al.*, 2013), anti-

proliferativas (CARDOSO *et al.*, 2015), imunomoduladoras (LEITE *et al.*, 2013; COÊLHO et al., 2014; PESSOA *et al.*, 2010), anti-tumorais (CARDOSO *et al.*, 2015a), antiangiogénicas (COSTA *et al.*, 2015) e esquistossomicidas (SANTIAGO *et al.*, 2014). Como exemplo de atividade antiparasitária das ftalimidas pode-se citar o trabalho de Santiago *et al.*, que identificaram derivados ftalimido-tiazóis com potentes atividades esquistossomicidas. A ftalimida LpQM-45 causou alterações ultra-estruturais significativas, incluindo a destruição do tegumento em ambos vermes, machos e fêmeas (SANTIAGO *et al.*, 2014), no entanto, as suas propriedades antichagásicas não foram exploradas (**Figura 9**).

Figura 9. Exemplo de derivado da ftalimida com atividade antiparasitária.

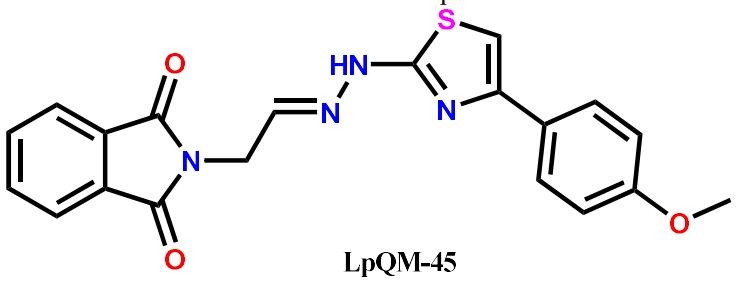

LpQM-45

Fonte: Elaborado pelo autor.

3.1.3 Planejamento das séries

Considerando os resultados promissores obtidos por compostos que contêm um anel tiazol e núcleos ftalimidas, eles foram escolhidos como grupos farmacofóricos de base para a obtenção de novos fármacos. Deste modo, foi sintetizado um conjunto de moléculas com os núcleos ftalimida e tiazol. Com o objetivo de formar uma biblioteca de compostos com essa estrutura de base, foram explorados substituintes em torno do anel fenil ligado em C4 no anel tiazol (compostos **2b-n**). Além disso, um grupo espaçador entre a ftalimida e o anel de tiazol foi inserido e um grupo fenil em N3 do anel tiazol, também foi introduzido (**6b-l**). Para investigar a influência da porção ftalimida na atividade anti-*T. cruzi*, 26 novos compostos foram testados *in vitro* contra as formas epimastigota e tripomastigota do parasito *T. cruzi*. Estudos ultraestruturais e análise de citometria de fluxo também foram investigados **(Figura 10)**.

Figura 10. Planejamento estrutural dos compostos propostos

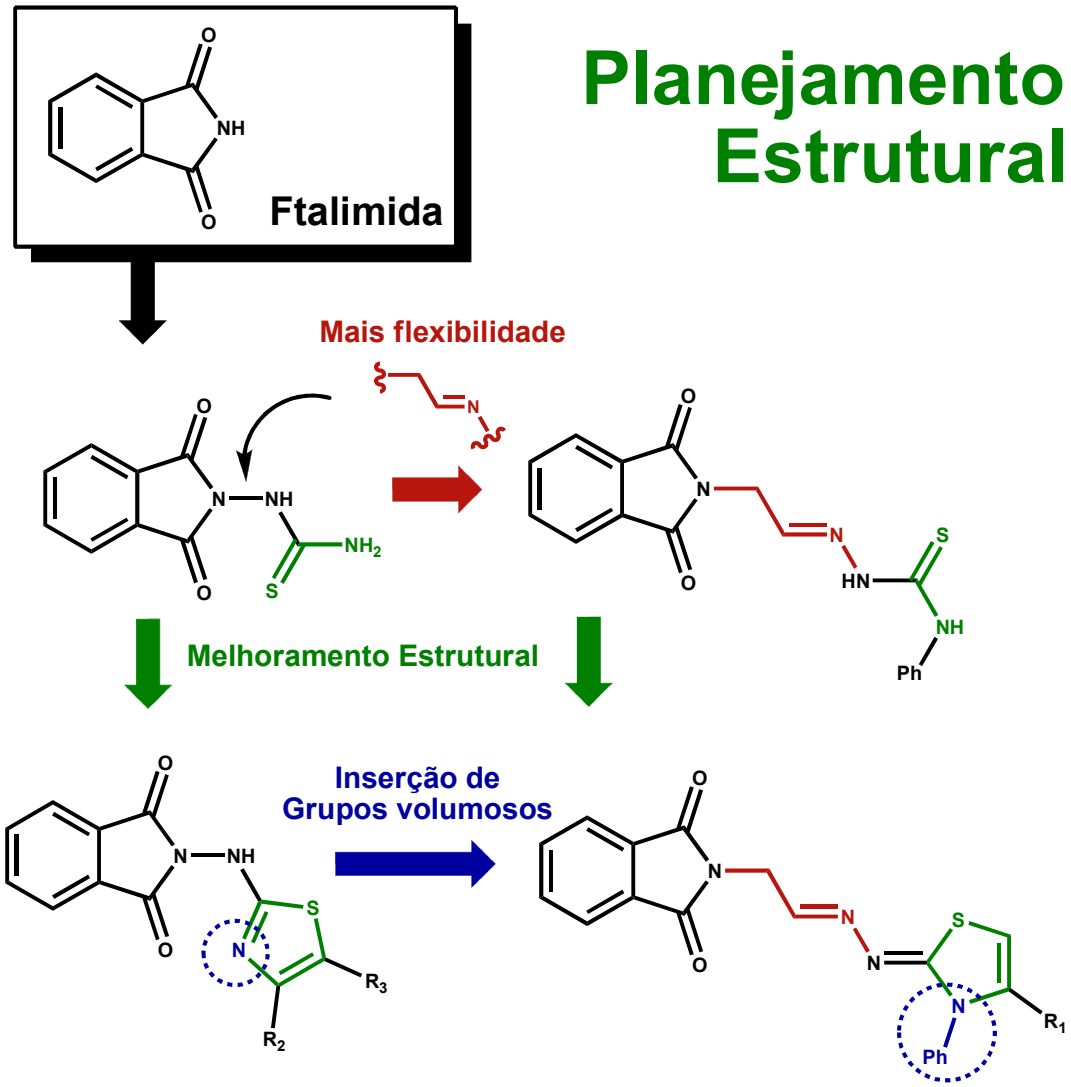

Fonte: Elaborado pelo autor.

3.2 Resultados e discussão

3.2.1 Parte química

Inicialmente, 14 ftalimido-tiazóis (**2a-n**) foram sintetizados em uma reação de duas etapas, seguindo os procedimentos relatados por Pessoa *et al.* (PESSOA *et al.*, 2010). Inicialmente, uma reação do anidrido ftálico com tiossemicarbazida, em DMF sob refluxo, durante 4 h, com uma quantidade catalítica de DMAP, levou-nos para o composto **1**. A síntese da série **2a-n** foi realizada através da ciclização de Hantsch entre o composto **1** e a adequada α-cetona halogenada (1,3-dicloroacetona para o composto **2a**), sob irradiação de ultrassom, a temperatura ambiente (ta) durante 1 h. Esta condição de reação conduziu a rendimentos médios de 36-65%. Para sintetizar a série **6a-l**, foi seguido o protocolo de reação relatado por Cardoso *et al.* (CARDOSO *et al.*, 2015a). Os compostos **6a-l** desejados foram obtidos pela reação do intermediário **5b** (ou **5a**, para o composto **6a**) com a adequada α-cetona-halogenada (1,3-dicloroacetona para o composto **6a**), através da ciclização de Hantsch, levando a bons rendimentos (46-82%) (**Esquema 1**). Todos os compostos sintetizados foram bem caracterizados por espectroscopia de infravermelho (IR), de ressonância magnética nuclear (RMN ^{1}H, ^{13}C), espectroscopia de massa (ESI-TOF) e, no caso de compostos **2e**, **2f** e **2g**, por análise de difração de raios-X de único cristal **(Figura 11)**.

Esquema 1: Síntese global dos compostos **2a-n** e **6a-l**.

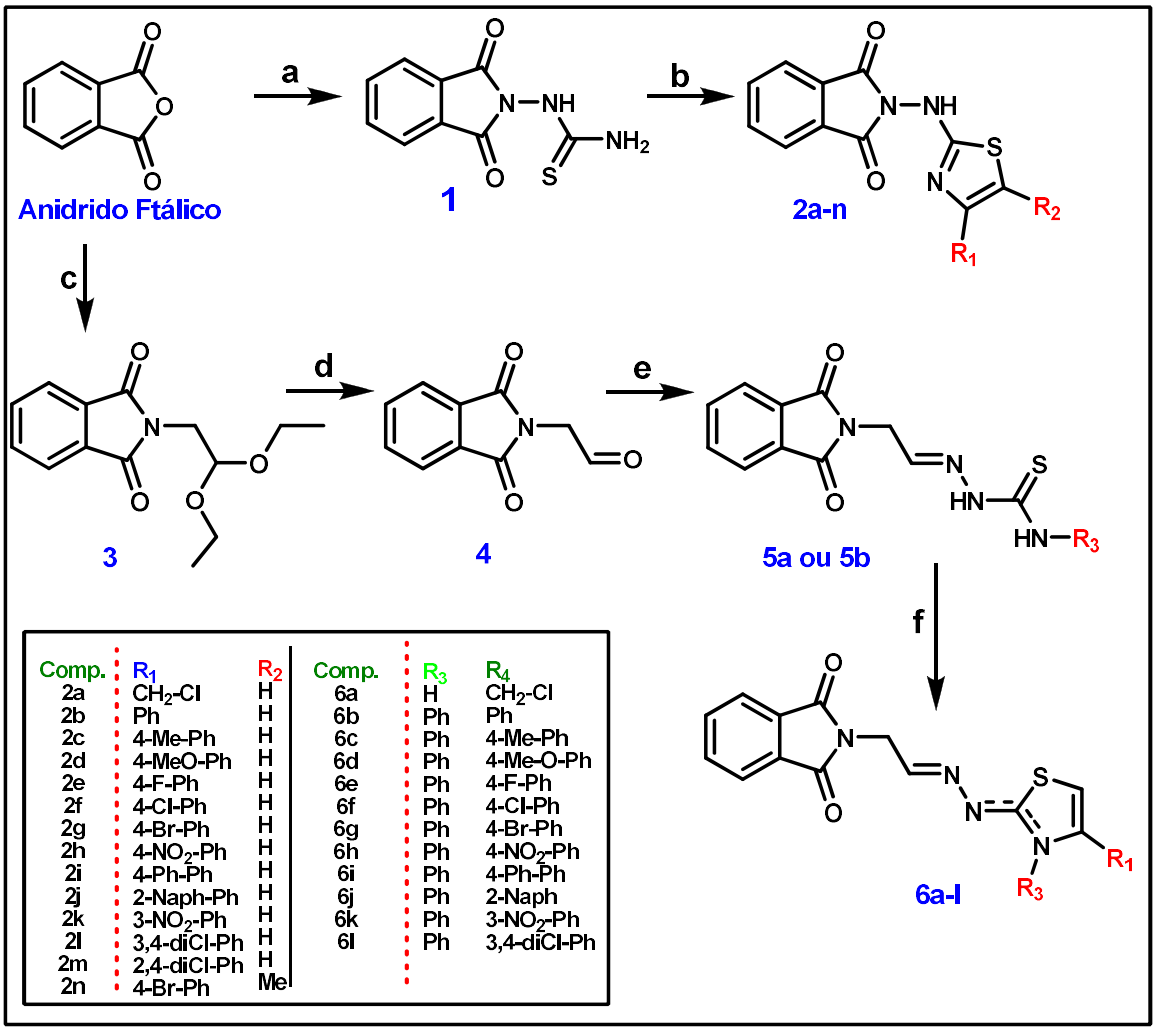

Comp.	R_1	R_2
2a	CH_2-Cl	H
2b	Ph	H
2c	4-Me-Ph	H
2d	4-MeO-Ph	H
2e	4-F-Ph	H
2f	4-Cl-Ph	H
2g	4-Br-Ph	H
2h	4-NO_2-Ph	H
2i	4-Ph-Ph	H
2j	2-Naph-Ph	H
2k	3-NO_2-Ph	H
2l	3,4-diCl-Ph	H
2m	2,4-diCl-Ph	H
2n	4-Br-Ph	Me

Comp.	R_3	R_4
6a	H	CH_2-Cl
6b	Ph	Ph
6c	Ph	4-Me-Ph
6d	Ph	4-Me-O-Ph
6e	Ph	4-F-Ph
6f	Ph	4-Cl-Ph
6g	Ph	4-Br-Ph
6h	Ph	4-NO_2-Ph
6i	Ph	4-Ph-Ph
6j	Ph	2-Naph
6k	Ph	3-NO_2-Ph
6l	Ph	3,4-diCl-Ph

Reagentes e condições: (a) tiossemicarbazida, DMF, DMAP, refluxo, 4 h; (b) correspondente α-cetona-halogenada (1,3-dicloroacetona para o composto **2a**), 2-propanol, ultrassom, ta, 1 h; (c) 1-aminoacetaldeído-dietil-acetal, tolueno, refluxo, DMAP, 2 h; (d) H_2SO_4 (70%), refluxo, 2 h; (e) tiossemicarbazida (**5a**) ou 4-fenil-3-tiossemicarbazida (**5b**), EtOH, HCl, refluxo, 4 h; (f) para **6a**, 1,3-dicloroacetona, DMF, ta, 1 h; para **6b-l**, corresponde α-cetona-halogenada, 2-propanol, ta, 1 h.

Figura 11. A estrutura molecular dos compostos entitulados mostrando o esquema de marcação atômica e de deslocamentos elipsóides no nível de probabilidade de 50%.

Composto 2f

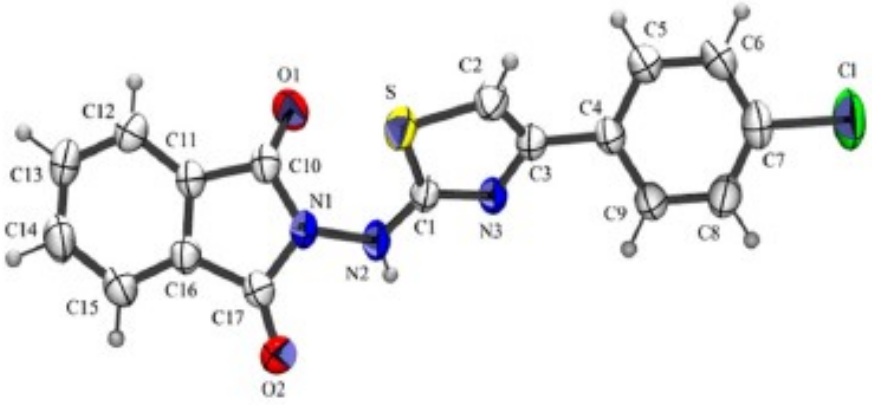

Composto 2g

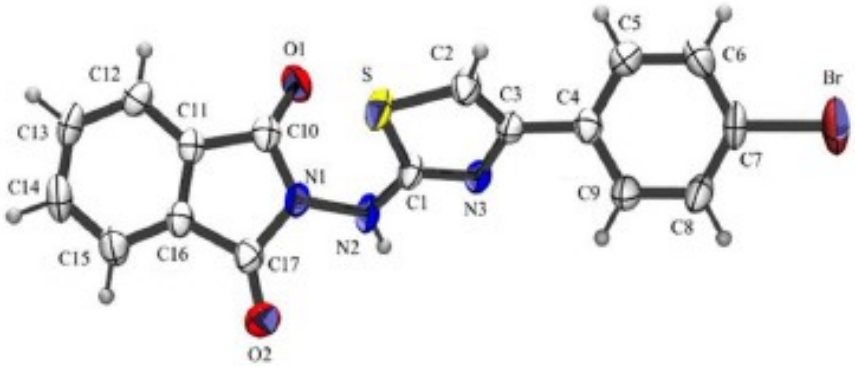

Composto 2e

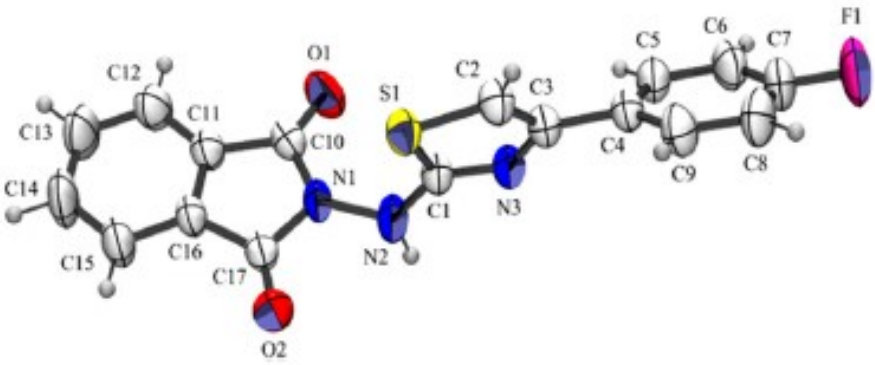

O espectro de RMN 1H de alguns compostos mostrou que a série de ftalimido-tiazóis 6a-l é constituída por diastereómeros. Em seguida, tentou-se definir a configuração do isômero maioritário por meio de análise cristalográfica. No entanto, não foi possível cristalizar os ftalimido-tiazóis 6a-l adequadamente para a análise de raios-X. Com base em compostos cristalizados anteriormente por nosso grupo, sugere-se que o isômero principal formado apresenta a configuração E-Z (**Figura 12**). De fato, para a ligação dupla C2=N2 da hidrazina é comumente atribuída a configuração E (CARDOSO *et al.*, 2014; CARDOSO *et al.*, 2015a; CARDOSO *et al.*, 2015b). No que diz respeito à ligação dupla N3=C3 exocíclica, sugere-se que a configuração predominante seja Z (MOREIRA *et al.*, 2012; MOREIRA *et al.*, 2014).

Figura 12. Representação dos isômeros do composto **6i**.

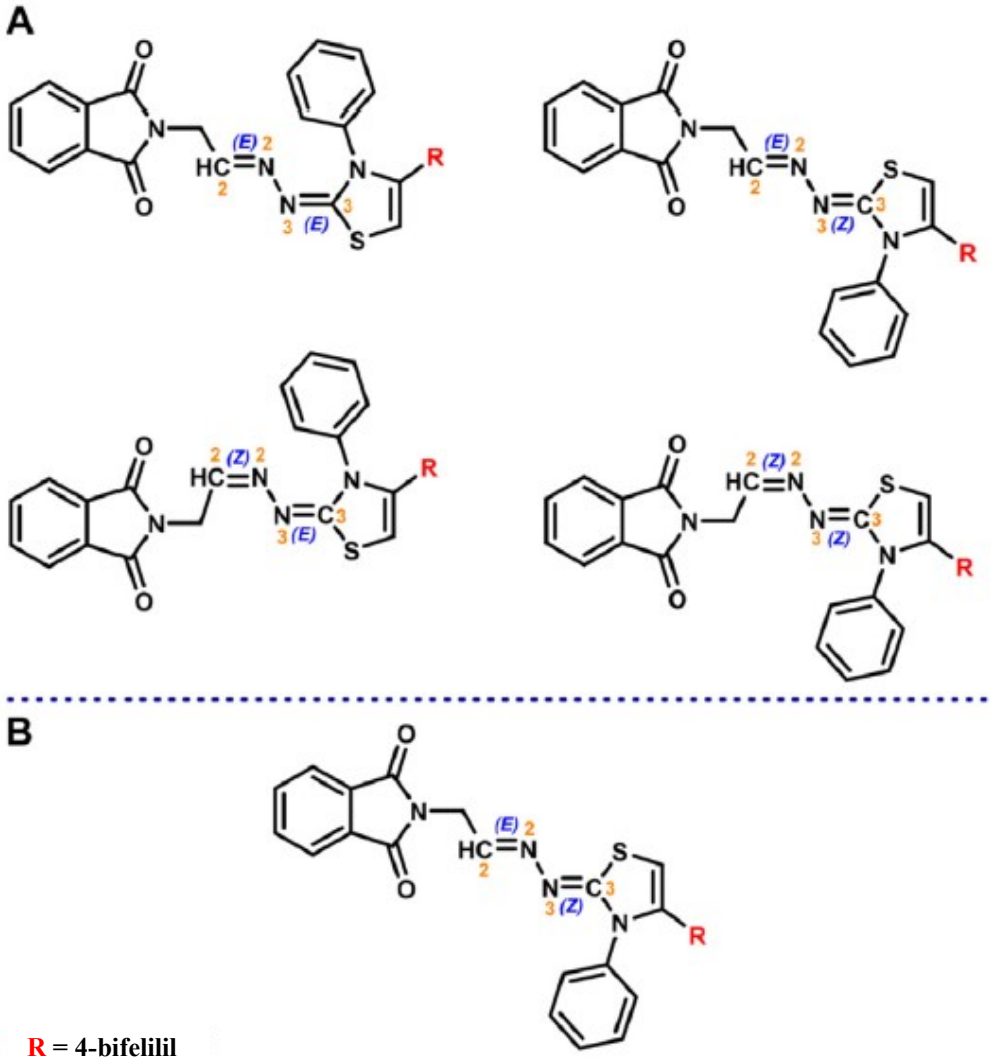

A- Possíveis isômeros do composto **6i**. B- Isômero majoritário sugerido para o composto **6i**.

3.2.2 Avaliação da atividade anti-*T. cruzi*

Tabela 1. Citotoxicidade e atividade tripanocida contra formas epimastigotas e tripomastigotas.

CÓDIGO	R1	R2	R3	Citotoxicidade µM [a]	IC_{50} Epimastigotas (*T. cruzi*) µM[b]	IC_{50} Tripomastigotas (*T. cruzi*) µM[c]
1	-	-	-	4,5	56,8	52,0
	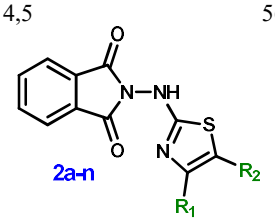					
	2a-n					
2a	Cl-Me	H	-	17,0	225,7	54,4
2b	Ph	H	-	3,1	70,2	107,5
2c	4-Me-Ph	H	-	14,9	70,4	107,0
2d	4-Me-O-Ph	H	-	14,2	6,4	50,3
2e	4-F-Ph	H	-	2,9	26,5	52,1
2f	4-Cl-Ph	H	-	2,8	30,6	86,2
2g	4-Br-Ph	H	-	2,5	14,8	89,8
2h	4-NO_2-Ph	H	-	2,7	13,3	84,9
2i	4-Ph-Ph	H	-	251,6	4,0	27,5
2j	2-Naph	H	-	269,2	8,0	4,7
2k	3-NO_2-Ph	H	-	2,7	43,2	91,1
2l	3,4-diCl-Ph	H	-	2,6	69,3	88,8
2m	2,4-diCl-Ph	H	-	12,8	10,1	22,7
2n	4-Br-Ph	Me	-	2,4	13,9	38,2
5b	-	-	-	50	36,9	ND
	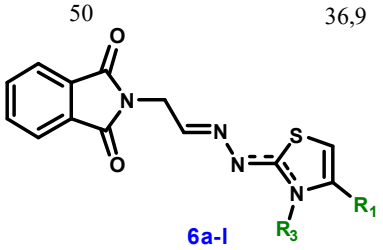					
	6a-l					
6A	Cl-Me	H	-	73,7	85,7	**2.2**
6B	Ph	H	Ph	228,1	ND	8,8
6C	4-Me-Ph	H	Ph	221,2	57,8	33,3
6D	4-Me-O-Ph	H	Ph	213,4	ND	10,0
6E	4-F-Ph	H	Ph	219,1	ND	73,8
6F	4-Cl-Ph	H	Ph	211,4	10,6	18,4
6G	4-Br-Ph	H	Ph	96,6	ND	9,7
6H	4-NO_2-Ph	H	Ph	206,8	12,2	**3,2**
6I	4-Ph-Ph	H	Ph	194,3	44.2	98,0
6J	2-Naph	H	Ph	204,9	11,9	**0,5**
6K	3-NO_2-Ph	H	Ph	103,4	6,0	**0,9**
6L	3,4-diCl-Ph	H	Ph	197,1	ND	ND
BZD	-	-	-	96,6	48,8	6,26

[a] Maior concentração não tóxica (> 90% de incorporação de timidina tritiada) em células esplênicas de ratos BALB/c.

[b] Determinada 11 dias após a incubação de epimastigotas com os compostos.[a,b] Apenas valores com um desvio padrão <10% foram incluídos. IC_{50} foi calculado a partir de pelo menos cinco concentrações, em triplicata (SD <10%). Bdz = benzonidazol; ND = Não determinado.

[c] Determinada 24 h após a incubação de tripomastigotas cepa Y com os compostos.

Inicialmente, os compostos **2a-n** foram planejados para melhorar a atividade tripanocida e a tolerância citotóxica com a ciclização da ftalimido-tiossemicarbazona ao anel ftalimido-tiazol. A partir dos resultados, observou-se que na maioria dos casos os novos ftalimido-tiazóis apresentaram alta atividade citotóxica em células esplênicas. Em oposição, só os compostos **2i** e **2j** apresentaram baixa citotoxicidade.

Quanto à atividade tripanocida em epimastigotas, observou-se que 16 compostos (de 28) apresentam melhor potência do que o benznidazol (**Tabela 1**). Entre os compostos da série **2a-n**, o **2i** foi o mais ativo, tanto entre os compostos da série quanto de todo o trabalho. O composto mais ativo na série **6** é o **6k**, um derivado contendo 3-NO_2, apresentando um IC_{50} de 6,0 mM. Observando-se compostos com substituintes retiradores (**2e-h**, **2k-n**), o composto com o substituinte 2,4-dicloro (**2m**) foi o mais ativo. Seu análogo di-substituído 3,4-dicloro (**2l**) apresenta a menor atividade tripanocida e elevada toxicidade nas células esplênicas de ratos BALB/c, denotando que a orientação dos substituintes é importante para a atividade. Observando os compostos substituíntes volumosos (fenil, 2-naftil e 4-bifenilil), na série **2a-n**, uma relação de LogP e atividade tripanocida (**Figura 13**) é observada, sendo o composto **2i** o mais ativo desta sub-série.

A tendência de substituintes volumosos observada para a série **2a-n** não é observada para a série **6a-l**, sendo o composto **6k** (3-NO_2) o mais ativo da série **6a-l**.

Figura 13. Evolução da atividade tripanocida para a forma epimastigota.

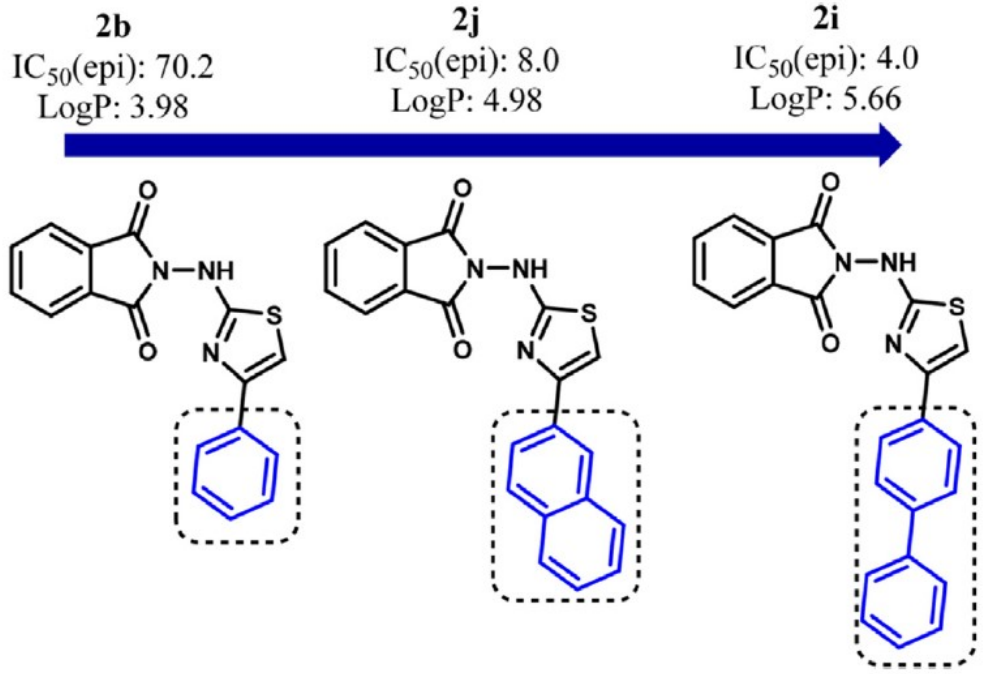

Quando se compara a atividade tripanocida da série **2a-n** dos derivados ftalimido-tiazóis contra a forma tripomastigota, o composto **2j** mostro ser o mais potente desta sub-série, apresentando níveis citotóxicos inferiores (269,2 μM) e atividade tripanocida equipotente em comparação com Bdz (4,7 *vs* 6,3 mM) (**Tabela 1**).

Não foi observada nenhuma correlação clara entre os tiazóis com substituintes em C4 e a atividade biológica. Por exemplo, 2-naftil é um substituinte volumoso presente em **2j**; No entanto, o composto **2i**, que também apresenta um substituinte volumoso bifenilil, não apresenta uma boa atividade. A influência do fenil ligado em C4 no anel tiazol também foi investigada, mas não foi observada nenhuma melhoria notável na atividade. Comparando-se o composto **2a** com o composto **2b**, que contém o fenil não substituído, foi observada uma diminuição da atividade tripanocida e maior citotoxicidade, enquanto os compostos com o fenil substituído mantiveram ou aumentaram ambas as atividades.

Uma otimização estrutural envolvendo a adição de um grupo espaçador (-CH2-CH=) entre a ftalimida e o núcleo tiazol foi realizada a fim de aumentar a flexibilidade das moléculas e investigar sua influência sobre as atividades biológicas (**Figura 14**). A substituição de H por um grupo fenil em N3 também foi realizada, para investigar a influência dos substituintes volumosos com base nos resultados dos compostos **2i** e **2j**, substituídos com 4-bifenilil e 2-naftil em C4, respectivamente, que exibiram menor citotoxicidade.

Figura 14. Otimização estrutural de compostos propostos.

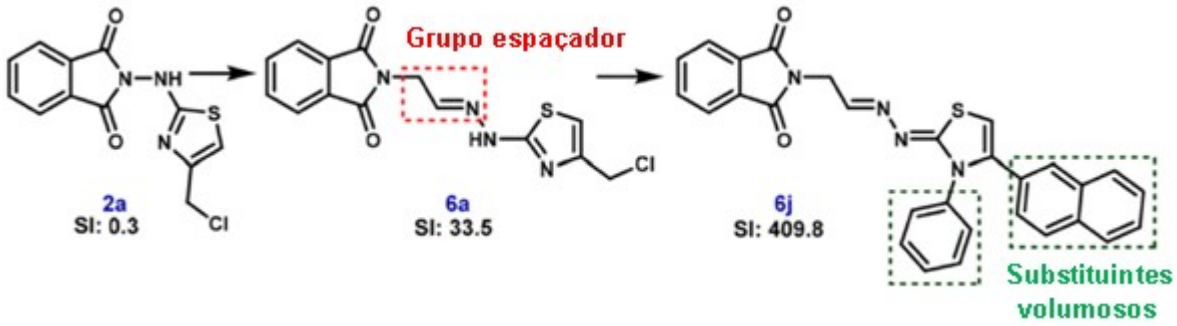

Índice de seletividade (SI) = concentração mais elevada não-tóxico em células esplênicas de ratos BALB/c/IC50 em tripomastigotas.

Compostos contendo um grupo espaçador (**6a-l**) e fenil em N3 (**6b-l**), em geral, apresentaram perfis de baixa citotoxicidade e melhoraram a atividade tripanocida para a forma tripomastigota, destacando-se os compostos **6a** (2,2 μM), **6h** (3,2 μM), **6j** (0,5 μM) e **6k** (0,9 μM). De fato, o composto **6j** apresentou um índice seletivo (IS, para a forma tripomastigota) de 409.8, sendo cerca de 27 vezes mais seletivo do que o Bdz (SI: 15.25), a droga padrão em uso clínico. Tal como observado na série **2a-n**, o composto substituído em C4 com clorometil (**6a**, 2,2 μM) foi mais ativo do que os compostos substituídos com fenil (**6b**, 8,8 mM); Entretanto, os compostos com fenil substituído **6j** (0,5 μM) e **6k** (0,9 μM) foram mais ativos que o **6a**. Comparando o composto **6a** com o **2a**, ambos substituídos com clorometil em C4 com a única diferença da presença do grupo espaçador em **6a**, uma melhora de 24 vezes na atividade tripanocida (2,2 *vs* 54,4 μM) e um aumento de 4 vezes na citotoxicidade (73,7 *vs* 17,0 μM) foram observados para **6a**. Os compostos **6k** e **6h**, ambos os compostos substituídos com nitro nas posições *meta* e *para*, respectivamente, apresentaram elevada atividade tripanocida com índices de seletividades de 114,9 e 64,6, respectivamente (**Tabela 1**). O composto **6e** (com o substituinte retirador de elétrons, flúor) e **6i** (com o substituinte 4-bifenilil) não apresentaram boa atividade tripanocida. O composto **6j**, que foi substituído com o substituinte volumoso 2-naftil, apresentou a maior atividade tripanocida.

Os estudos de SAR revelaram que uma série de ftalimido-tiazóis são interessantes compostos anti-*T. cruzi*, dos quais cinco novos compostos apresentaram baixa citotoxicidade em células esplênicas de ratos BALB/c e atividade anti-tripanocida contra a forma tripomastigota do parasito.

Congreve *et al.* propuseram uma regra-de-três (RO3) (CONGREVE *et al.*, 2003) representando um conjunto de diretrizes para a construção de uma biblioteca de grupamentos (peso molecular, < 300; cLogP, $\leq$ 3; número de doadores de ligações de hidrogénio, $\leq$ 3; e número de aceitadores de ligações de hidrogênio, $\leq$ 3). Recentemente, RO3 foi credenciada pela maioria dos químicos medicinais e poderia ser útil para a seleção de grupamento eficaz (CHEN *et al.*, 2015). Como pode ser visto na **Tabela 2**, os grupamentos ftalimida e tiazol estão de acordo com RO3.

Tabela 2. Cálculos da Regra-dos-três (RO3) dos grupamentos ftalimida e tiazol.

Regra	Ftalimida	Tiazol	Critério atendido
Peso molecular (<300)	147,13	85,12	Sim
cLogP (<3)	1,148	0,486	Sim
Número de doadores de ligação de hidrogênio (<3)	1	0	Sim
Número de aceptores de ligação de hidrogênio (<3)	2	1	Sim

O perfil tripanocida destes ftalimido-tiazóis revelou um grupo de compostos com base estrutural privilegiada que podem ser utilizados como blocos de construção para a obtenção de novos compostos de referência. Eles possuem algumas características estruturais, tais como pesos moleculares mais baixos, diminuição da complexidade e diminuição da hidrofobicidade, que são consistentes com as características de líder-similar ("lead-like"). Estes compostos podem ser utilizados para produzir ligações estruturalmente simples com atividade modesta, permitindo a posterior derivação, numa fase posterior para melhorar a afinidade e seletividade enquanto mantém características fármaco-similar ("drug-like").

3.2.3 Estudos ultraestruturais

Visando investigar os efeitos dos ftalimido-tiazóis na morfologia do parasito, o composto **6k**, um dos compostos mais ativos deste trabalho, foi seleccionado. Os efeitos ultraestruturais do **6k** em tripomastigotas após 24 horas foram analisados por Microscopia Eletrônica de Transmissão (TEM) e Microscopia Eletrônica de Varredura (SEM), na concentração de IC_{50} e duas vezes o valor de IC_{50} (**Tabela 1**), e a análise ultraestrutural apresentou várias alterações morfológicas (**Figura 15**).

A análise SEM mostrou que o tratamento com 0,9 μM (1 x IC50) e 1,8 μM (2 x IC50) do composto **6k** causou bolhas no flagelo e encurtamento do flagelo com uma diminuição drástica no número de parasitas, respectivamente (**Figura 15B-C**), enquanto o grupo controle manteve a sua morfologia típica (**Figura 15A**).

A análise TEM revelou que os parasitos não tratados apresentaram morfologias ultraestruturais normais de organelas, tais como cinetoplasto, núcleo, nucléolos, flagelo, os ribossomos e membranas de microtúbulos (**Figura 15D**), ao passo que os parasitas tratados com 0,9 μM de **6k** mostraram alterações nos reservosomos, e um grande número de células mostrou intensa vacuolização citoplasmática. Além disso, alterações da morfologia do parasito, grandes aglomerados de cromatina nuclear que se assemelhavam aos núcleos de células apoptóticas, inchaço das mitocôndrias e perda de material citoplasmático foram

observados (**Figura 15E-F**). Os parasitas tratados com 1,8 μM de **6k** apresentaram alterações da morfologia do parasito, condensação da cromatina anormal, retículo endoplasmático dilatado, vacuolização intensa no citoplasma, inchaço do cinetoplasto e alterações nos reservosomos-like (**Figura 15G**).

A análise ultraestrutural foi aplicada para explorar os danos induzidos pelos compostos em parasitos tripomastigotas do T. cruzi e claramente mostrou alterações morfológicas graves, das quais intensa vacuolização citoplasmática, condensação da cromatina, alterações nos reservosomos-like e inchaço das mitocôndrias foram as mais freqüentes. Estas alterações ultraestruturais são semelhantes aos descritos na literatura (GONZALES-PERDOMO *et al.*, 1990; SOUZA *et al.*, 2004; GARZONI *et al.*, 2004; BRAGA *et al.*, 2004; DANTAS *et al.*, 2006). A avaliação ultraestrutural indica uma ação dependente da dose porque uma diminuição drástica no número de parasitos foi observada com doses crescentes do composto.

Figura 15. Alterações ultraestruturais nas formas tripomastigotas do *T. cruzi* tratadas com **6k** observadas por SEM e TEM.

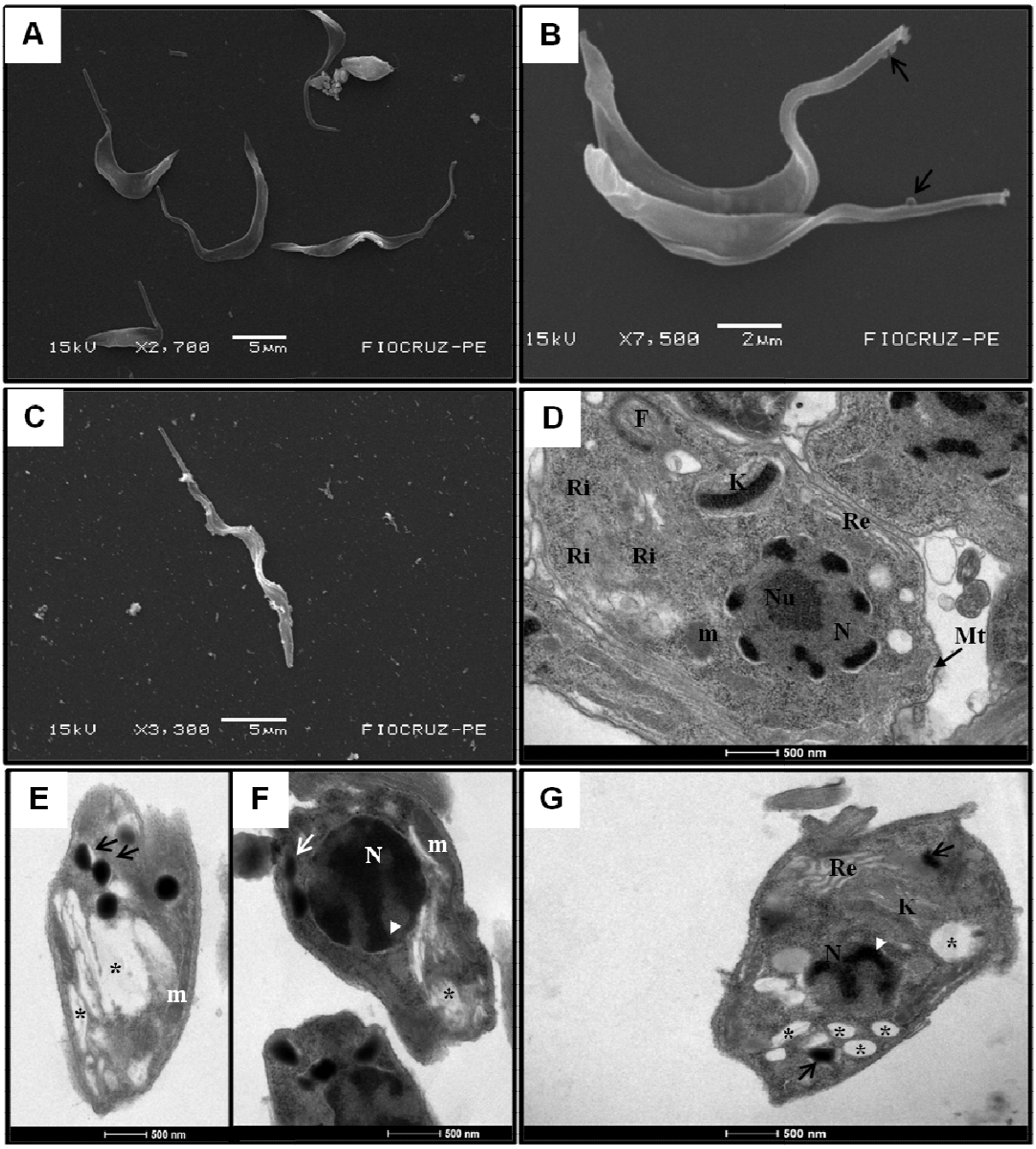

A- SEM das tripomastigotas não tratadas do controle mostrando o típico corpo alongado. B- SEM de parasitos tratados com 0,9 µM de **6k** mostrando bolhas no flagelo. C- SEM de parasitos tratados com 1,8 µM de **6k** mostrando redução drástica do número de parasitos e encurtamento do flagelo. D- TEM de tripomastigotas não tratadas mostrando a morfologia normal com cinetoplasto (K), núcleo (N), nucléolo (Nu), flagelo (F), ribossomos (Ri), mitocôndrias (m) e microtúbulos Mt). E e F TEM de parasitos tratados com 0,9 µM de **6k** que mostram alterações da morfologia do parasito, condensação da cromatina anormal (seta) no núcleo (N), inchaço da mitocôndria (m), alterações nos reservosomos (setas) e perda do material citoplasmático (asteriscos). G- TEM de parasitos tratados com 1,8 µM de **6k** que apresentam alterações da morfologia do parasito, condensação anormal de cromatina (seta), retículo endoplasmático dilatado (Re), intensa vacuolização no citoplasma (asterisco), inchaço do cinetoplasto (K) e alterações nos reservosomos-like (setas).

3.2.4 Análise de citometria de fluxo

Depois de confirmar que **6k** é um composto antiparasitário que afetou organização celular ultraestrutural, procurou-se determinar se **6k** causou a morte celular do parasito. Para este fim, cepas Y de tripomastigotas foram tratadas com diferentes concentrações de **6k**. Após 24 h de incubação, as células do parasito foram coradas com iodeto de propídio (PI) e anexina-V e analisadas por citometria de fluxo. Os resultados são mostrados na **Figura 16**.

Figura 16. % da análise de células PI-positivo em tratamento com **6k**.

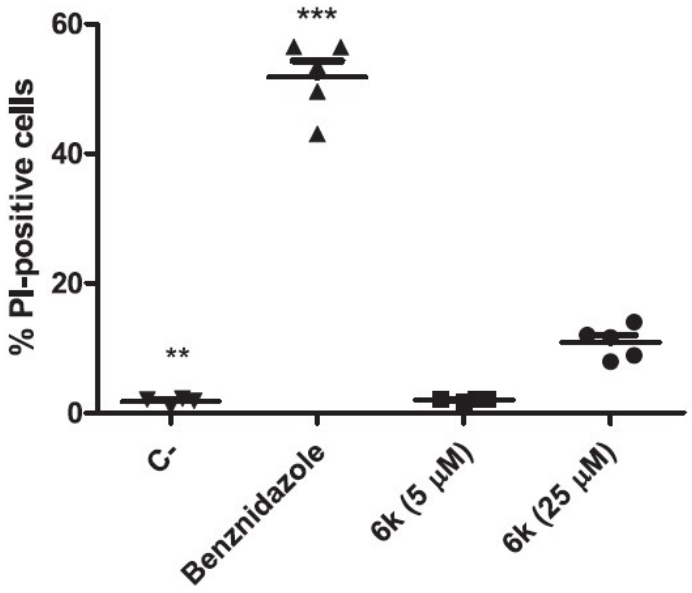

Tripomastigotas foram tratadas com o composto durante 24 horas e examinadas por citometria de fluxo com coloração de PI. (C-) sem tratamento; Concentração de droga é dada em parêntesis. Dois experimentos independentes, cada concentração em duplicado. *** P <0,0001 em comparação com (C-).

Em comparação com células não tratadas, o benznidazol resultou na coloração de PI em uma maneira dependente da concentração, enquanto que nenhuma coloração significativa de anexina-V foi observada (dados não mostrados). A 25 µM, benznidazol induziu 56 ± 6% da coloração PI em células do parasita. Na mesma concentração, o tratamento com o composto **6k** induziu coloração de PI em 11 ± 3% de células do parasito. Nenhuma coloração PI ou anexina-V foi observada durante o tratamento com **6k** (dados não mostrados). Portanto, estes ftalimido-tiazóis não destroem as células do parasito por processos clássicos de morte celular. Com base nas observações de microscopia electrônica, é possível que ftalimido-tiazóis diminuam a viabilidade do parasito, alterando a organização do citosol, causando principalmente intensa vacuolização citoplasmática.

3.3 Conclusão

Vinte e seis ftalimido-tiazóis foram obtidos com rendimentos razoáveis utilizando uma metodologia simples. Compostos com importante atividade tripanocida, especialmente os compostos **2j**, **6a**, **6h**, **6j** e **6k**, foram identificados. Citometria de fluxo e estudos ultraestruturais mostraram que o composto **6k** não mata o parasita através de necrose ou apoptose; no entanto, ele promoveu diversas alterações morfológicas no parasito. O composto **6j**, o agente tripanocida mais potente identificado neste trabalho, apresentou um índice de seletividade de 409, sendo cerca de 26 vezes mais seletivo que o BDZ, a droga padrão em uso clínico. Os nossos resultados indicaram que ftalimido-tiazóis podem ser utilizados como blocos de construção para criar candidatos promissores para o tratamento da doença de Chagas.

3.4 Seção experimental

3.4.1 Parte química

3.4.1.1 Equipamentos e reagentes

Todos os reagentes foram adquiridos a partir de fontes comerciais (Sigma-Aldrich, Acros Organics, Vetec or Fluka). O progresso das reações foi acompanhado por análise de cromatografia de camada delgada (CCD) (Merck, silica gel 60 F_{254} em folha de alumínio). As purezas dos compostos obtidos foram confirmadas por análise de combustão (para C, H, N e S) realizada utilizando um instrumento Carlo-Erba (modelo AE 1110). Os pontos de fusão foram determinados num aparelho de ponto de fusão electrotérmico capilar Fisatom 430D e não foram corrigidos. Os espectros de RMN foram medidos ambos em um Varian UnityPlus 400 MHz (400 MHz para 1H e 100 MHz para 13C) ou em um Bruker AMX-300 MHz (300 MHz para ^{1}H e 75,5 MHz para ^{13}C). DMSO-d_6 e D_2O foram adquiridas da CIL ou Sigma-Aldrich. Os deslocamentos químicos foram registrados em ppm, e as multiplicidades foram dadas como s (singuleto), d (dupleto), t (tripleto), m (multipleto), dd (dupleto duplo), e as constantes de acoplamento (*J*) em hertz. A espectrometria de massa foi realizada em um LC-TI-TOF (Shimadzu). A menos que especificado de outro modo, ESI foi conduzido no modo de íon positivo. As condições típicas foram as seguintes: tensão capilar de 3 kV, voltagem do cone de 30 V, e verificação de pico entre 50 e 1000 m/z. Os espectros de IV foram registados com um espectrofotómetro modelo Bruker IFS66 FT-IR utilizando pastilhas de KBr.

3.4.1.2 Procedimento geral para a síntese de 2a-n

O composto **1** foi preparado por meio da reação entre tiossemicarbazida e anidrido ftálico disponíveis comercialmente (razão molar 1:1) utilizando DMF sob refluxo na presença de uma quantidade catalítica de DMAP, durante 4 h. Esta condição de reação conduziu a um rendimento satisfatório (58%). Os ftalimido-tiazóiss (**2a-n**) foram preparados por meio de ciclização entre **1** e a respectiva cetona α-halogenada (1,3-dicloroacetona para o composto 2a), por meio de irradiação com ultrassom durante 1 hora, como anteriormente relacionados (CARDOSO *et al.*, 2014). Estas reações foram bem procedidas sob condições de ultrassons, à temperatura ambiente, utilizando 2-propanol como solvente, resultando em rendimentos satisfatórios (36-65%) e tempos de reação mais curtos (60 min, na maioria dos casos).

3.4.1.3 Procedimento para a síntese dos compostos intermediárioa 5a-b

O composto **3** foi preparado pela condensação de aminoacetaldeído dietil acetal com o anidrido ftálico comercialmente disponíveis (proporção 1:1 mol), utilizando tolueno em refluxo, na presença de uma quantidade catalítica de DMAP (rendimento de 52%) durante 2 horas. No passo seguinte, 2- (2,2-dietoxietil) isoindolina-1,3-diona (**3**) foi submetido à hidrólise ácida (ácido sulfúrico a 70%) em refluxo durante 2 h. Depois de a reação estar completa, deixou-se à temperatura ambiente e, em seguida, foi resfriada para induzir a precipitação. O precipitado formado foi filtrado através de um funil sinterizado com água destilada, obtendo-se 55% do produto puro. Para a síntese de **5a** e **5b**, 2- (1,3-dioxoisoindol-2-il) acetaldeído (**4**) reagiu com tiossemicarbazida (na razão de 1: 1) (para **5a**) ou 4-fenil-3-tiossemicarbazida (para **5b**), em etanol, sob refluxo, com uma quantidade catalítica de HCl (4 gotas) durante 4 h. As reações foram seguidas por análise de placa de cromatografia em camada delgada. O precipitado formado foi filtrado através de um funil sinterizado com etanol para se obter o produto puro (rendimento de 76% para **5a** e 70% para **5b**).

3.4.1.4 Procedimento para a síntese do 6a

Em um balão de fundo redondo foi adicionado 2-(2-(1,3-dioxoisoindolin-2-il) etilideno)hidrazinacarbotioamida (**5a**), 1,3-dicloroacetona e DMF. A mistura reacinal foi mantida à temperatura do ambiente em torno de 1 hora. A reaçãp foi acompanhada por placa cromatográfica de camada delgada. Após a adição de água, o produto precipita de forma pura.

3.4.1.5 Procedimento geral para a síntese do 6b-l

Em balão de fundo redondo foi adicionada 2-(2-(1,3-dioxoisoindolina-2-il)etilideno)-N-fenil-hidrazina-carbotioamida (**5b**), a respectiva cetona α-halogenada e 2-propanol. A mistura reacional foi mantida sob agitação magnética, à temperatura ambiente, durante 1 h. As reações foram seguidas por placa cromatográfica de camada delgada. O precipitado formado foi filtrado num funil sinterizado com água destilada, obtendo-se o produto puro.

3.4.1.6 Dados físico-químicos e elucidação estrutural

2a: 2-[4-(clorometil)tiazol-2-ilamino]isoindolina-1,3-diona

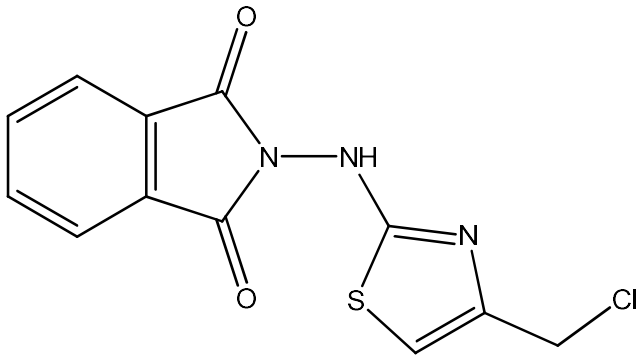

- Cristais brancos;
- Rendimento: 50%;
- PF (°C) 207-208;
- Rf: 0.53 (hexano / acetato de etila 1:1).
- IV (KBr, cm^{-1}): 3119,15 (NH), 1743,24 (C=O).
- RMN ^{1}H (300 MHz, DMSO-d_6), δ_{ppm}: 4,54 (s, 2H, CH_2), 7,03 (s, 1H, tiazol), 7,93-7,99 (m, 4H, Ar), 10,54 (s, 1H, NH).
- RMN ^{13}C (75,5 MHz, DMSO-d_6), δ_{ppm}: 41,1 (CH_2), 109,8 (CH, tiazol), 123,9 (CH, Ar), 129,4 (C, Ar), 135,4 (CH, Ar), 147,1 (C, tiazol), 165,6 (C=O), 168,3 (S-C=N, tiazol).
- Anal. Calcd para $C_{12}H_8ClN_3O_2S$: C, 49,07; H, 2,75; N, 14,31; S, 10,92. Encontrado: C, 48,50; H, 2,81; N, 14,34; S 10,43.
- HRMS: 294,0097 $[M+H]^+$.

2b: 2-(4-feniltiazol-2-ilamino)isoindolina-1,3-diona

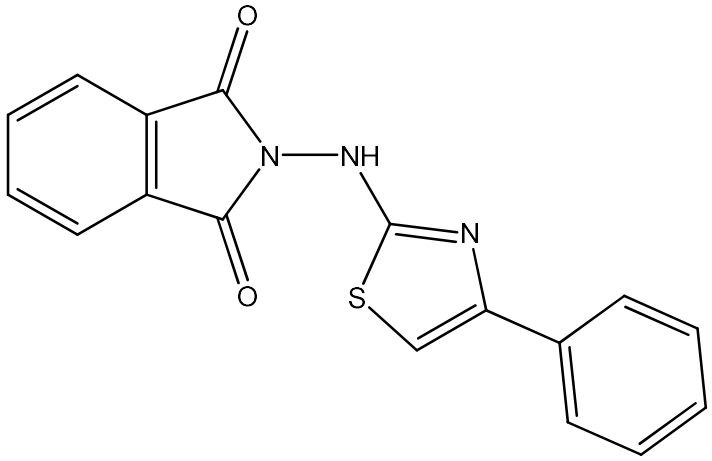

- Cristais amarelo-claros;
- Rendimento: 65%;
- PF (°C): 194-196;
- Rf: 0.60 (hexano / acetato de etila 1:1).
- IV (KBr, cm^{-1}): 3123,66 (NH), 1742,23 (C=O).
- RMN ^{1}H (400 MHz, DMSO-d_6), δ_{ppm}: 7,25 (t, J = 7,4 Hz, 1H, Ar), 7,33 (t, J = 7,4 Hz, 2H, Ar), 7,38 (s, 1H, tiazol), 7,70 (d, J = 7,6 Hz, 2H, Ar), 7,95-8,02 (m, 4H, Ar), 10,65 (s, 1H, NH).
- RMN ^{13}C (100 MHz, DMSO-d_6), δ_{ppm}: 104,8 (CH, tiazol), 123,8 (CH, Ar), 125,5 (CH, Ar), 127,7 (CH, Ar), 128,6 (CH, Ar) 129,3 (C, Ar), 133,9 (C, Ar), 135,4 (CH, Ar), 149,9 (C, tiazol), 165,5 (C=O), 167,6 (S-C=N, tiazol).
- Anal. Calcd para $C_{17}H_{11}N_3O_2S$: C, 62,08; H, 3,41; N, 12,98; S, 9,71. Encontrado: C, 63,54; H, 3,45; N, 12,53; S, 9,98.
- HRMS: 322,0619 $[M+H]^{+}$.

2c: 2-(4-p-toluiltiazol-2-ilamino)isoindolina-1,3-diona

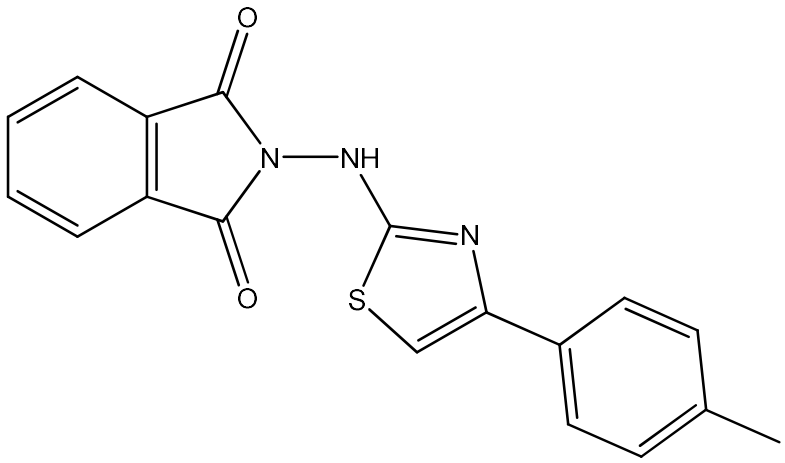

- Cristais amarelo-claros;
- Rendimento: 37%;
- PF (°C): 214-216;
- Rf: 0.65 (hexano / acetato de etila 1:1).
- IV (KBr, cm^{-1}): 3117,64 (NH), 1738,51 (C=O).
- RMN ^{1}H (400 MHz, DMSO-d_6), δ_{ppm}: 2,26 (s, 3H, CH_3), 7,14 (d, J = 6.8 Hz, 2H, Ar), 7,30 (s, 1H, tiazol), 7,59 (d, J = 6.8 Hz, 2H , Ar), 7,99 (m, 4H, Ar), 10,41 (s, 1H, NH).
- RMN ^{13}C (100 MHz, DMSO-d_6), δ_{ppm}: 20,8 (CH_3), 103,9 (CH, tiazol), 123,9 (CH, Ar), 125,5 (CH, Ar), 129,17 (CH, Ar), 129,3 (C, Ar), 131,4 (C, Ar), 135,4 (C, Ar), 137,1 (C, Ar), 150,2 (C, tiazol), 165,6 (C=O), 167,5 (S-C=N, tiazol).
- Anal. Calcd para $C_{18}H_{13}N_3O_2S$: C, 63,17; H, 3,81; N, 18,12; S, 9,17. Encontrado: C, 64.46; H, 3.91; N, 18.53; S, 9.56.
- HRMS: 336.0812 $[M+H]^+$.

2d: 2-[4-(4-metoxifenil) tiazol-2-ilamino]isoindolina-1,3-diona

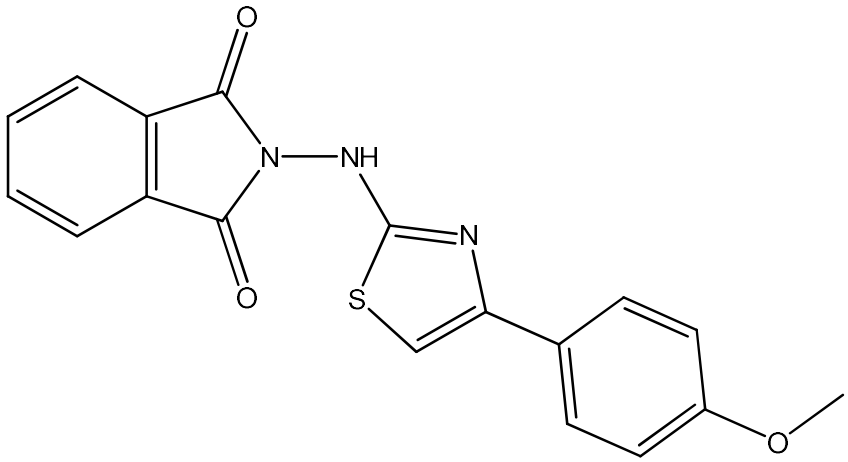

- Cristais amarelo-claros;
- Rendimento: 72%;
- PF (°C): 215-218;
- Rf: 0.53 (hexano / acetato de etila 3:2).
- IV (KBr, cm^{-1}): 3232,68 (NH), 1748,64 (C=O).
- RMN ^{1}H (300 MHz, DMSO-d_6), δ_{ppm}: 1,025 (s, 3H, CH_3), 6,90 (d, J = 11.6 Hz, 2H, Ar), 7,20 (s, 1H, tiazol), 7,62 (d, J = 11.6 Hz, 2H , Ar), 7,98 (m, 4H, Ar), 10,72 (s, 1H, NH).
- RMN ^{13}C (75,5 MHz, DMSO-d_6), δ_{ppm}: 25,5 (CH_3), 102,7 (CH, tiazol), 114,0 (CH, Ar), 123,9 (CH, Ar), 126,7 (C, Ar), 127,0 (CH, Ar), 129,4 (C, Ar), 135,4 (CH, Ar), 149,5 (C, tiazol), 158,6 (CO, Ar), 165,6 (C=O), 167,6 (S-C=N, tiazol).
- Anal. Calcd para $C_{18}H_{13}N_3O_3S$: C, 58,88; H, 3,87; N, 11,38; S, 8,77. Encontrado: C, 61,53; H, 3,73; N, 11,96; S, 9,13.
- HRMS: 352,0825 $[M+H]^+$.

2e: 2-[4-(4-fluorofenil)tiazol-2-ilamino]isoindolina-1,3-diona

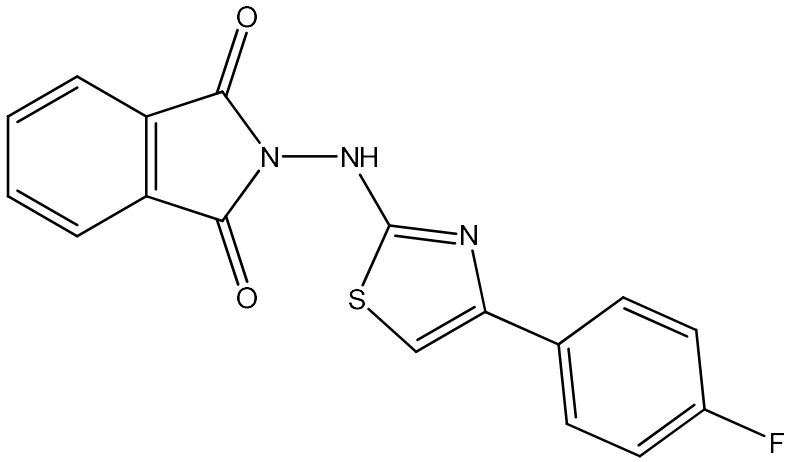

- Cristais amarelos;
- Rendimento: 51%;
- PF (°C): 208-210;
- Rf: 0,53 (hexano / acetato de etila 3:2).
- IV (KBr, cm^{-1}): 3130,14 (NH), 1743,63 (C=O).
- RMN ^{1}H (400 MHz, DMSO-d_6), δ_{ppm}: 7,17 (d, J = 17,6 Hz, 2H, Ar), 7,37 (s, 1H, tiazol), 7,73 (d, J = 14.0 Hz, 2H, Ar), 7,99 (m, 4H, Ar), 10,42 (s, 1H, NH).
- RMN ^{13}C (100 MHz, DMSO-d_6), δ_{ppm}: 104,6 (CH, tiazol), 115,4 (CH, Ar), 115,6 (CH, Ar), 123,9 (CH, Ar), 127,5 (CH, Ar), 129,3 (C, Ar), 135,4 (CH, Ar), 160,4 (C, tiazol), 162,9 (CF, Ar), 165,5 (C=O), 167,6 (S-C=N, tiazol).
- Anal. Calcd para $C_{17}H_{10}FN_3O_2S$: C, 60,32; H, 3,02; N, 12,32; S, 9,58. Encontrado: C, 60,17; H, 2,97; N, 12,38; S, 9,45.
- HRMS: 340,0566 $[M+H]^{+}$.

2f: 2-[4-(4-clorofenil)tiazol-2-ilamino]isoindolina-1,3-diona

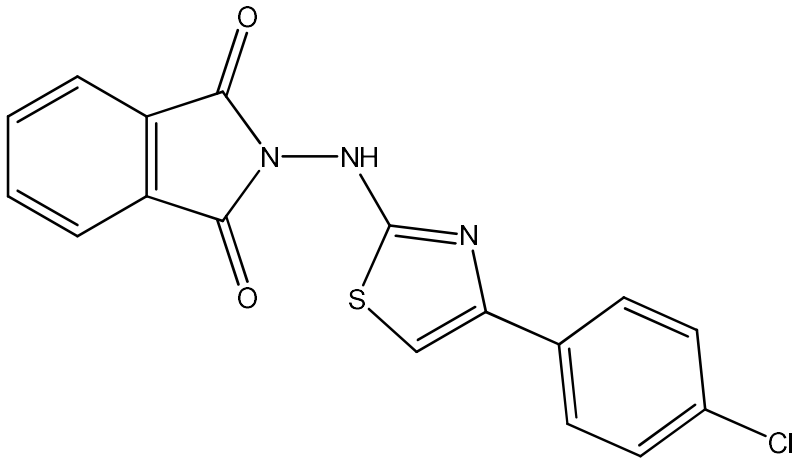

- Cristais amarelo-claros;
- Rendimento: 62%;
- PF (°C): 217-218;
- Rf: 0,53 (hexano / acetato de etila 1:1).
- IV (KBr, cm^{-1}): 3119,79 (NH), 1739,00 (C=O).
- RMN ^{1}H (400 MHz, DMSO-d_6), δ_{ppm}: 7,39 (d, J = 8,0 Hz, 2H, Ar), 7,46 (s, 1H, tiazol), 7,72 (d, J = 8 Hz, 2H, Ar). 7,99 (m, 4H, Ar), 10,46 (s, 1H, NH).
- RMN ^{13}C (100 MHz, DMSO-d_6), δ_{ppm}: 105,7 (CH, tiazol), 123,9 (CH, Ar), 127,3 (CH, Ar), 128,7 (CH, Ar), 129,3 (C, Ar) 132,2 (C, Ar), 132,9 (C, Ar), 135,4 (CCl, Ar), 148,9 (C, tiazol), 165,5 (C=O), 167,7 (S-C=N, tiazol).
- Anal. Calcd para $C_{17}H_{10}ClN_3O_2S$: C, 57,55; H, 2,96; N, 11,62; S, 9,03. Encontrado: C, 57,39; H, 2,83; N, 11,81; S, 9,01.
- HRMS: 356,0260 $[M+H]^{+}$.

2g: 2-[4-(4-bromofenil)tiazol-2-ilamino]isoindolina-1,3-diona

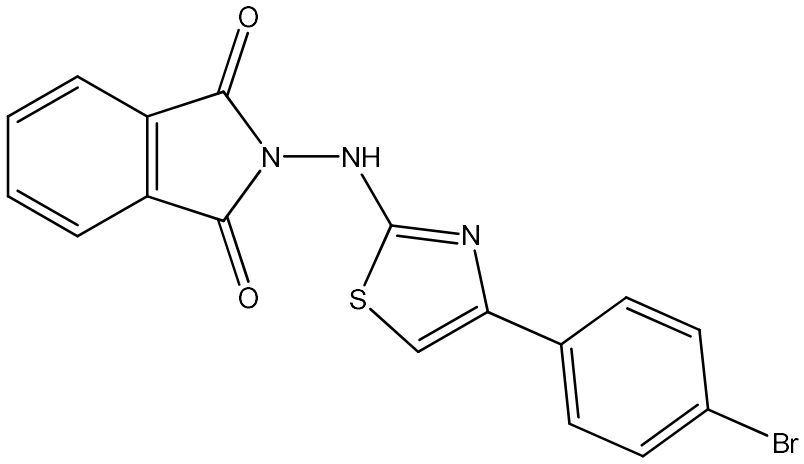

- Cristais amarelo-claros;
- Rendimento: 55%;
- PF (°C): 220-221;
- Rf: 0,68 (hexano / acetato de etila 1:1).
- IR (KBr, cm^{-1}): 3117,68 (NH), 1739,19 (C=O).
- RMN ^{1}H (400 MHz, DMSO-d_6), δ_{ppm}: 7,47 (s, 1H, tiazol), 7,53 (d, J = 8,4 Hz, 2H, Ar), 7,65 (d, J = 8,0 Hz, 2H, Ar), 7,96 (m, 4H, Ar), 10,46 (s, 1H, NH).
- RMN ^{13}C (100 MHz, DMSO-d_6), δ_{ppm}: 105,8 (CH, tiazol), 120,8 (CH, Ar), 123,9 (CH, Ar), 127,6 (CH, Ar), 129,3 (C, Ar) 131,6 (C, Ar), 135,4 (CBr, Ar), 148,9 (C, tiazol), 165,5 (C=O), 167,7 (S-C=N, tiazol).
- Anal. Calcd para $C_{17}H_{10}BrN_3O_2S$: C, 51,15; H, 2,58; N, 11,62; S, 9,03. Encontrado: C, 51,01; H, 2,52; N, 11,50; S, 8,91.
- HRMS: 401,9764 $[M+H]^{+}$.

2h: 2-[4-(4-nitrofenil)tiazol-2-ilamino]isoindolina-1,3-diona

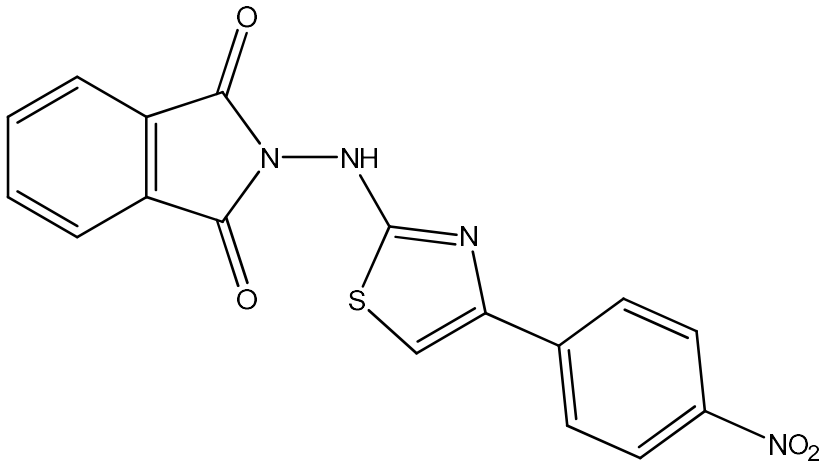

- Cristais amarelos;
- Rendimento: 41%;
- PF (°C): 239-240;
- Rf: 0,45 (hexano / acetato de etila 3:2).
- IV (KBr, cm^{-1}): 3309,85 (NH), 1724,82 (C=O).
- RMN ^{1}H (400 MHz, DMSO-d_6), δ_{ppm}: 7,77 (s, 1H, tiazol), 7,97 (m, 4H, Ar), 8,02 (d, J = 8,8 Hz, 2H, Ar), 8,21 (d, J = 8,8 Hz, 2H, Ar), 10,54 (s, 1H, NH).
- RMN ^{13}C (100 MHz, DMSO-d_6), δ_{ppm}: 109,6 (CH, tiazol), 123,9 (CH, Ar), 124,1 (CH, Ar), 126,4 (CH, Ar), 129,3 (CN Ar), 135,4 (CH, Ar), 139,9 (C, Ar), 146,3 (C, Ar), 147,9 (C, tiazol), 165,382 (C=O), 168,0 (S-C=N, tiazol).
- Anal. Calcd para $C_{17}H_{10}N_4O_4S$: C, 54,40; H, 2,87; N, 15,23; S, 9,11. Encontrado: C, 55,73; H, 2,75; N, 15,29; S, 8,75.
- HRMS: 367,0517 $[M+H]^{+}$.

2i: 2-[4-(bifenil-4-il)tiazol-2-ilamino]isoindolina-1,3-diona

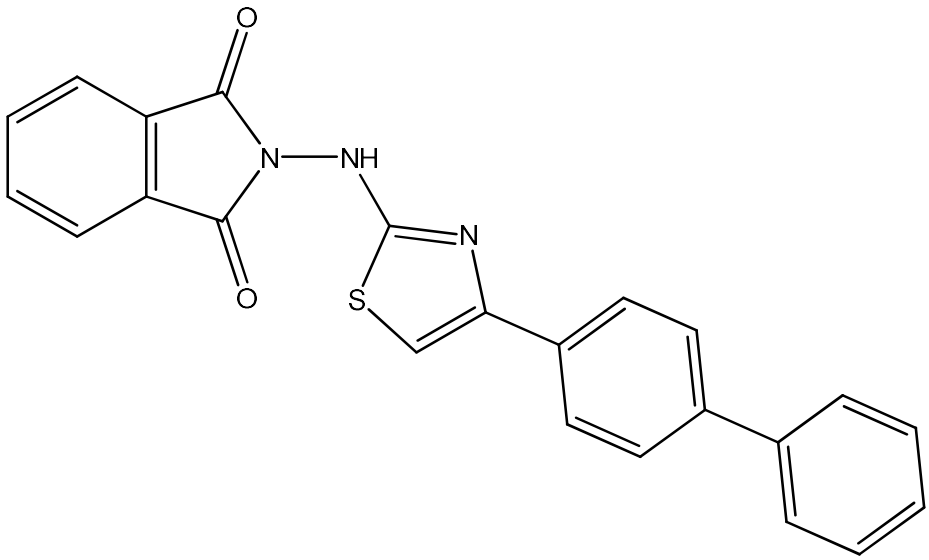

- Cristais amarelo-claros;
- Rendimento: 46%;
- PF (°C): 240-241;
- Rf: 0.65 (hexano / acetato de etila 3:2).
- IV (KBr, cm^{-1}): 3324,67 (NH), 1660,10 (C=O).
- RMN ^{1}H (300 MHz, DMSO-d_6), δ_{ppm}: 7,35 (s, 1H, tiazol), 7,48 (t, J = 10,0 Hz, 1H, Ar), 7,63 (m, 4H, Ar), 7,72 (d, J = 11,6 Hz, 2H, Ar), 7,82 (m, 4H, Ar) 7,96 (d, J = 11,6 Hz, 2H, Ar), 10,65 (s, 1H, NH).
- RMN ^{13}C (75,5 MHz, DMSO-d_6), δ_{ppm}: 103,4 (CH, tiazol), 126,5 (CH, Ar), 126,9 (CH, Ar), 127,5 (CH, Ar), 128,0 (CH, Ar) 129,0 (CH, Ar), 130,1 (CH, Ar), 131,5 (CH, Ar), 133,9 (C, Ar), 136,1 (CH, Ar), 139,0 (C, Ar), 139,7 (C Ar), 150,2 (C, tiazol), 167,6 (C=O), 168,3 (S-C=N, tiazol).
- Anal. Calcd para $C_{23}H_{15}N_3O_2S$: C, 66,81; H, 3,98; N, 10,48; S, 7,95. Encontrado: C, 66,50; H, 3,80; N, 10,57; S, 8,07.
- HRMS: 398,0958 $[M+H]^{+}$.

2j: 2-[4-(naftalen-2-il)tiazol-2-ilamino]isoindolina-1,3-diona

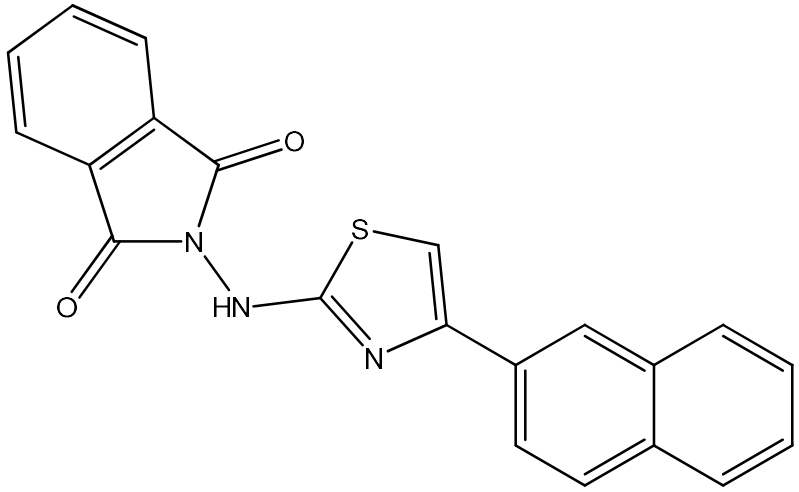

- Cristais amarelo-claros;
- Rendimento: 47%;
- PF (°C): 225-227;
- Rf: 0,50 (hexano / acetato de etila 3:2).
- IV (KBr, cm^{-1}): 3169,87 (NH), 1743,89 (C=O).
- RMN ^{1}H (400 MHz, DMSO-d_6), δ_{ppm}: 7,47 (t, 2H, Ar), 7,53 (s, 1H, tiazol), 7,87 (d, *J* = 11,6 Hz, 4H, Ar), 8,03 (m, 4H , Ar), 8,23 (s, 1H, Ar), 10,48 (s, 1H, NH).
- RMN ^{13}C (100 MHz, DMSO-d_6) δ_{ppm}: 105,5 (CH, tiazol), 123,9 (CH, Ar), 124,2 (CH, Ar), 126,1 (CH, Ar), 126,4 (CH, Ar) 127,1 (CH, Ar), 127,6 (CH, Ar), 128,1 (CH, Ar), 128,2 (CH, Ar), 129,3 (C, Ar), 131,5 (C, Ar), 132,4 (C, Ar), 133,0 (C, Ar), 135,4 (CH, Ar), 150,1 (C, tiazol), 165,6 (C=O), 168,0 (S-C=N, tiazol).
- Anal. Calcd para $C_{21}H_{13}N_3O_2S$: C, 64,89; H, 3,48; N, 11,45; S, 8,26. Encontrado: C, 67,91; H, 3,53; N, 11,11; S, 8,63.
- HRMS: 367,0517 $[M+H]^{+}$.

2k: 2-[4-(3-nitrofenil)tiazol-2-ilamino]isoindolina-1,3-diona

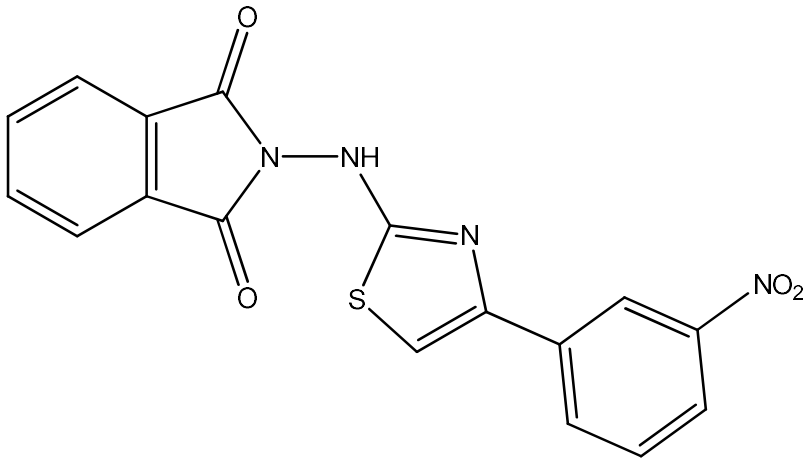

- Cristais amarelo-claros;
- Rendimento: 44%;
- PF (°C): 206-207;
- Rf: 0,55 (hexano / acetato de etila 3:2).
- IV (KBr, cm^{-1}): 3287,35 (NH), 1732,47 (C=O).
- RMN ^{1}H (300 MHz, DMSO-d_6) δ_{ppm}: 7,65 (t, J = 7,2 Hz, 1H, Ar), 7,73 (s, 1H, tiazol), 8,00 (m, 4H, Ar), 8,13 (m, 2H, Ar), 8,48 (s, 1H, Ar) 10,36 (s, 1H, NH).
- RMN ^{13}C (75,5 MHz, DMSO-d_6), δ_{ppm}: 107,7 (CH, tiazol), 119,9 (CH, Ar), 122,3 (CH, Ar), 123,9 (CH, Ar), 129,3 (CN, Ar) 130,3 (CH, Ar), 131,7 (CH, Ar), 135,5 (CH, Ar), 147,7 (C, Ar), 148,2 (C, tiazol), 165,5 (C=O), 168,2 (S-C=N, tiazol).
- Anal. Calcd para $C_{17}H_{10}N_4O_4S$: C, 53,04; H, 2,88; N, 15,49; S, 8,90. Encontrado: C, 54,73; H, 2,75; N, 15,29; S, 8,75.
- HRMS: 367,0517 $[M+H]^{+}$.

2l: 2-[4-(3,4-diclorofenil)tiazol-2-ilamino]isoindolina-1,3-diona

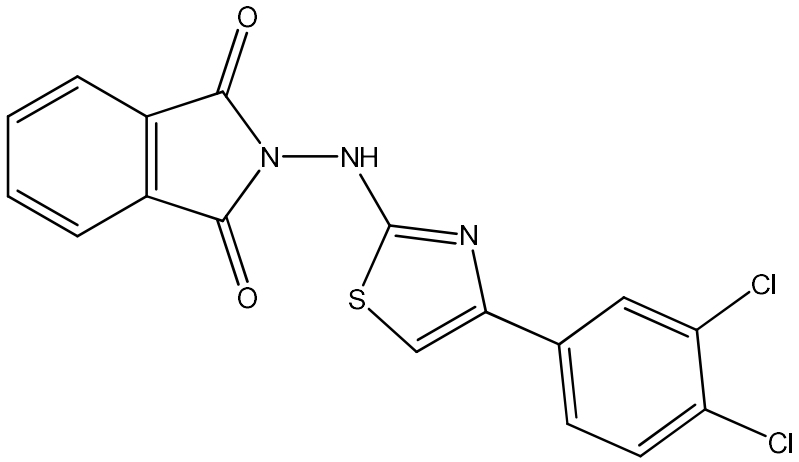

- Cristais amarelo-claros;
- Rendimento: 57%;
- PF (°C) 217-218;
- Rf: 0,53 (hexano / acatato de etila 3:2).
- IV (KBr, cm^{-1}): 3337,03 (NH), 1742,53 (C=O).
- RMN ^{1}H (300 MHz, DMSO-d_6), δ_{ppm}: 7,52 (s, 1H, tiazol), 7,62 (s, 1H, Ar), 7,68 (d, J = 2,1 Hz, 1H, Ar), 7,94 (d, J = 1,8 Hz, 1H , Ar), 8,00 (m, 4H, Ar), 10,51 (s, 1H, NH).
- RMN ^{13}C (75,5 MHz, DMSO-d_6), δ_{ppm}: 107,1 (CH, tiazol), 123,9 (CH, Ar), 127,1 (CH, Ar), 129,3 (CCl, Ar), 129,5 (CH, Ar), 130,9 (CCl, Ar), 131,4 (C, Ar), 134,5 (CH, Ar), 135,4 (C, Ar), 136,0 (CH, Ar), 147,9 (C, tiazol), 165,4 (C=O), 167,9 (S-C=N, tiazol).
- Anal. Calcd para $C_{17}H_9Cl_2N_3O_2S$: C, 51,19; H, 2,43; N, 11,04; S, 8,58. Encontrado: C, 52,32; H, 2,32; N, 10,77; S, 8,22.
- HRMS: 356,0260 $[M+H]^+$.

2m: 2-[4-(2,4-diclorofenil)tiazol-2-ilamino]isoindolina-1,3-diona

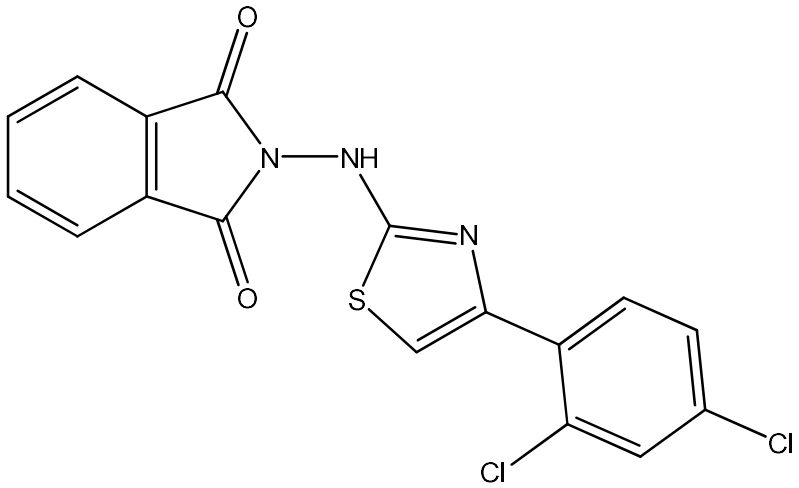

- Cristais incolores;
- Rendimento: 46%;
- PF (°C) 217-218;
- Rf: 0,55 (hexano / acetato de etila 3:2).
- IV (KBr, cm^{-1}): 3130,90 (NH), 1741,75 (C=O).
- RMN ^{1}H (400 MHz, DMSO-d_6), δ_{ppm}: 7,41 (d, *J* = 7,2 Hz, 1H, Ar), 7,45 (s, 1H, tiazol), 7,63 (s, 1H, Ar), 7,65 (d, *J* = 8,4 Hz, 1H, Ar). 7,97 (m, 4H, Ar), 10,46 (s, 1H, NH).
- RMN ^{13}C (100 MHz, DMSO-d_6), δ_{ppm}: 110,45 (CH, tiazol), 123,8 (CH, Ar), 127,5 (CH, Ar), 129,3 (CCl, Ar), 129,7 (CH, Ar), 131,5 (CCl, Ar), 131,5 (C, Ar), 132,1 (CH, Ar), 132,7 (C, Ar), 135,4 (CH, Ar), 145,4 (C, tiazol), 165,4 (C=O), 166,7 (S-C=N, tiazol).
- Anal. Calcd para $C_{17}H_9Cl_2N_3O_2S$: C, 52,25; H, 2,26; N, 10,50; S, 7,91. Encontrado: C, 52,32; H, 2,32; N, 10,77; S, 8,22.
- HRMS: 356.0260 $[M+H]^{+}$.

2n: 2-[4-(4-bromofenil)-5-metiltiazol-2-ilamino]isoindolina-1,3-diona

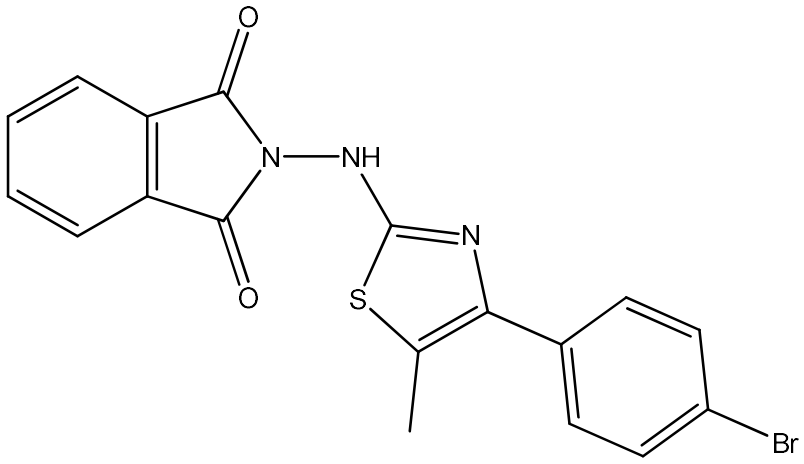

- Cristais amarelos;
- Rendimento: 36%;
- PF (°C) 235-236;
- Rf: 0,60 (hexano / acetato de etila 3:2).
- IV (KBr, cm^{-1}): 3188,90 (NH), 1745,97 (C=O).
- RMN ^{1}H (400 MHz, DMSO-d_6), δ_{ppm}: 2,36 (s, 3H, CH_3), 7,41 (d, J = 8,4 Hz, 2H, Ar), 7,55 (d, J = 8,4 Hz, 2H, Ar), 7,96 (m, 4H, Ar), 10,23 (s, 1H, NH);
- RMN ^{13}C (100 MHz, DMSO-d_6), δ_{ppm}: 12,1 (CH_3), 119,3 (CH, tiazol), 120,4 (C, Ar), 123,8 (CH, Ar), 129,3 (C, Ar), 129,8 (CH, Ar), 131,2 (CH, Ar), 133,7 (CBr, Ar), 135,3 (CH, Ar), 144,0 (C, tiazol), 163,5 (C=O), 165,5 (S-C=N, tiazol).
- Anal. Calcd para $C_{17}H_{12}BrN_3O_2S$: C, 51,75; H, 3,00; N, 9,93; S, 7,58. Encontrado: C, 52,19; H, 2,92; N, 10,10; S, 7,74.
- HRMS: 401,9764 $[M+H]^+$.

5a: (E)-2-[2-(1,3-dioxoisoindolin-2-il)etilideno]hidrazinacarbotioamida

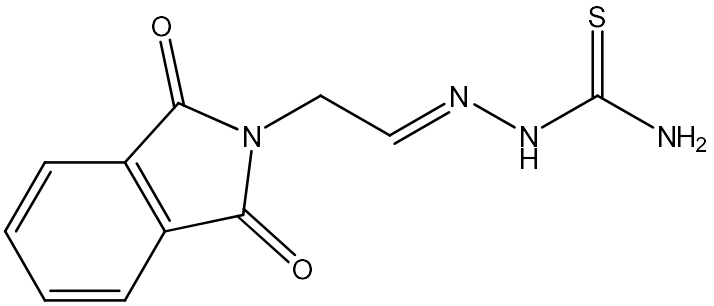

- Cristais brancos;
- Rendimento: 76%;
- PF (°C): 223-224;
- Rf 0,45 (hexano / acetato de etila 3:2);
- IV (KBr, cm^{-1}): 3423 e 3308 (N-H), 1769 e 1713 (C=O), 1602 (C=N);
- RMN ^{1}H (300 MHz, DMSO-d_6), δ_{ppm}: 4,36 (d, J = 3,6 Hz, 2H, CH_2), 7,36 (s, 1H, NH), 7,42 (t, J = 3,6 Hz, 1H, CH=N), 7,83-7,90 (m, 4H, Ar), 8,03 e 11,27 (s, 1H, NH_2);
- RMN ^{13}C (75,5 MHz, DMSO-d_6), δ_{ppm}: 40,1 (CH_2), 123,1 (Ar), 131,7 (Ar), 134,4 (Ar), 140,4 (C=N), 167,5 (C=O), 177,9 ($(NH)_2C=S$).

5b: (E)-2-[2-(1,3-dioxoisoindolin-2-il)etilidene]-N-fenil-hidrazinacarbotioamida

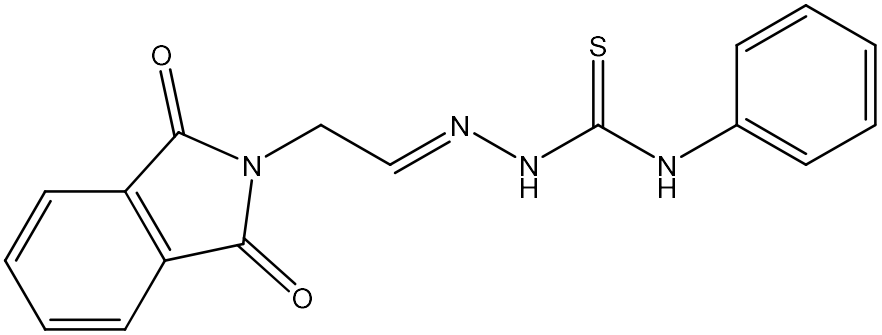

- Cristal branco;
- Rendimento: 70%;
- PF (°C): 174-176;
- Rf 0,52 (hexano / acetato de etila 3:2);
- RMN ^{1}H (300 MHz, DMSO-d_6), δ_{ppm}: 4,46 (d, J = 4,2 Hz, 2H, CH_3), 7,14 (t, J = 7,8 Hz, 1H, Ar), 7,29 (t, J = 7,8 Hz, 2H, Ar), 7,42 (d, J = 7,8 Hz, 2H), 7,52 (t, J = 4,2 Hz, 1H, Ar), 7,85-7,99 (m, 4H, Ar), 9,66 (s, 1H, NH), 11,72 (s, 1H, NH);
- RMN ^{13}C (75,5 MHz, DMSO-d_6), δ_{ppm}: 40 (CH_2), 123,2 (Ar), 124,7 (Ar), 125,1 (Ar), 128,1 (Ar), 131,7 (Ar), 134,5 (Ar), 138,7 (Ar), 140,9 (C=N), 167,6 (C=O), 175,8 ($(NH)_2C$=S).
- Anal. Calcd para $C_{17}H_{14}N_4O_2S$: C, 60,34; H, 4,17; N, 16,56; S, 9,48. Encontrado: C, 60,03; H, 4,45; N, 16,35; S, 11,30.

6a: (E)-2-(2-{2-[4-(clorometil)tiazol-2-il]hidrazona}etil)isoindolina-1,3-diona

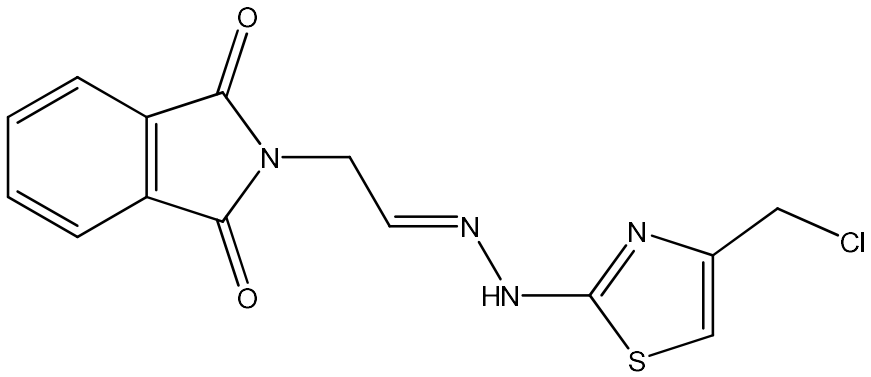

- Cristais brancos;
- Rendimentos: 82%;
- PF (°C): 191-193;
- Rf 0,23 (hexano / acetato de etila 3:2);
- IV (KBr, cm^{-1}): 3159.36 e 3113.44 (N-H), 1771.01 e 1717.67 (C=O), 1565.77 (C=N).
- RMN ^{1}H (400 MHz, DMSO-d_6), δ_{ppm}: 4.41 (d, J = 3.2 Hz, 2H, CH_2), 4.53 (s, 2H, CH_2), 6.76 (s, 1H, CH, tiazol), 7.32 (s, 1H, CH), 7.86-7.89 (m, 4H, CH Ar), 11.75 (s, 1H, NH);
- RMN ^{13}C (75.5 MHz, DMSO-d_6), δ_{ppm}: 38 (CH_2), 41.7 (CH_2), 107.9 (tiazol), 123.1 (Ar), 131.7 (Ar), 134.5 (Ar), 138.4 (tiazol), 147.8 (C=N), 167.5 (C=O), 168.6 (tiazol).
- Anal. Calcd para $C_{14}H_{11}ClN_4O_2S$: C, 50.23; H, 3.31; N, 16.74; S, 9.58. Encontrado: C, 49.91; H, 3.30; N, 16.82; S,10.03.
- HRMS: 335.0259 $[M+H]^+$.

6b: 2-((E)-2-{(Z)-[3,4-difeniltiazol-2(3H)-ilideno]hidrazona}etil)isoindolina-1,3-diona

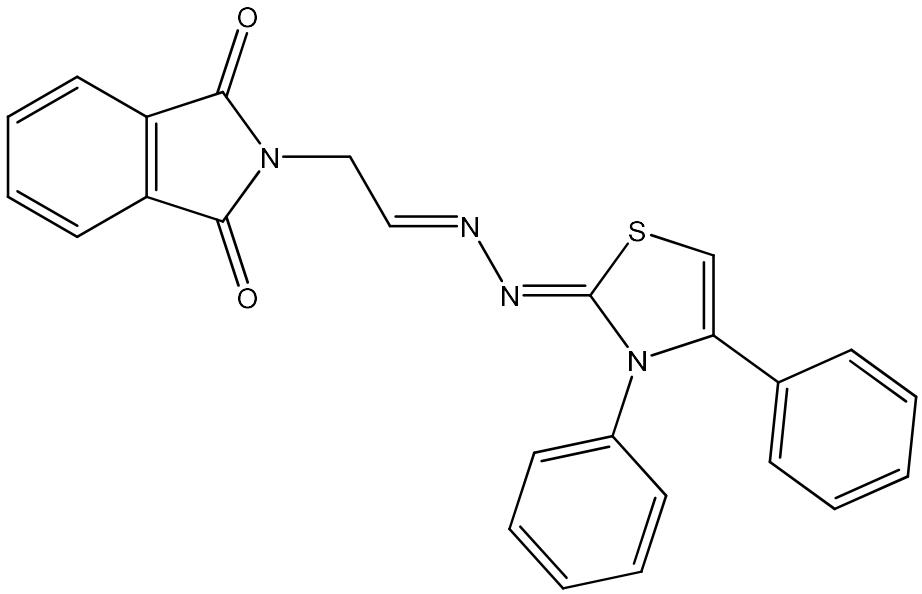

- Cristais laranjas;
- Rendimento: 56%;
- PF (°C): 196-198;
- Rf 0,46 (hexane / ethyl acetate 3:2);
- IV (KBr, cm^{-1}): 1712.40 (C=O).
- RMN ^{1}H (300 MHz, DMSO-d_6), δ_{ppm}: 4,42 (d, J = 3 Hz 2H, CH_2), 6,45 (s, 1H, CH, tiazol), 7,09-7,32 (m, 10H, CH Ar), 7,44 (t, J = 3 Hz, 1H, HC=N), 7,91-7,88 (m, 4H, CH Ar, ftalimida);
- RMN ^{13}C (75,5 MHz, DMSO-d_6), δ_{ppm}: 40,3 (CH_2), 104,2 (tiazol), 123,0 (Ar), 125,2 (Ar), 128,0 (Ar), 128,1 (Ar), 128,3 (Ar), 128,6 (Ar), 128,8 (Ar), 130,6 (Ar), 131,8 (Ar), 134,4 (Ar), 137,3 (Ar), 139,3 (tiazol), 148,2 (C=N), 167,5 (C=O), 169.9 (tiazol).
- Anal. Calcd for $C_{25}H_{18}N_4O_2S$: C, 68,48; H, 4,14; N, 12,78; S, 7,31. Encontrado: C, 66.88; H, 4.30; N, 12.48; S, 7.12.
- HRMS: 439.1028 $[M+H]^+$.

6c: 2-((E)-2-{((Z)-[(3-fenil-4-p-toluiltiazol-2(3H)-ilideno)]hidrazona)}etil)isoindolina-1,3-diona

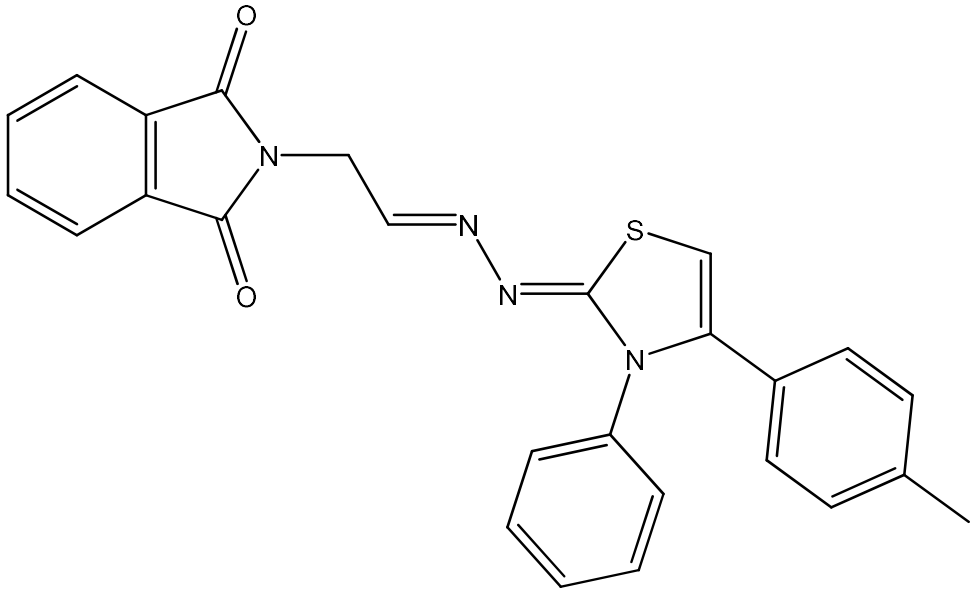

- Cristais amarelos;
- Rendimento: 52%;
- PF (°C) 156-158;
- Rf: 0,7 (hexano / acetato de etila 3:2).
- IV (KBr, cm^{-1}): 1712.39 (C=O).
- RMN ^{1}H (300 MHz, DMSO-d_6), δ_{ppm}: 2,19 (s, 3H,CH_3), 4,42 (d, J = 3 Hz, 2H, CH_2), 6,41 (s, 1H, CH tiazol), 6,95-6,99 (m, 4H, CH Ar), 7,17-7,45 (m, 6H, CH Ar), 7,88-7,95 (m, 4H, CH Ar ftalimida);
- RMN ^{13}C (75.5 MHz, DMSO-d_6), δ_{ppm}: 20,7 (CH_3), 38,9 (CH_2), 100,7 (CH, tiazol), 123,1 (Ar), 127,7 (Ar), 128,1 (Ar), 128,7 (Ar), 128,8 (Ar), 128,9 (Ar), 129,8 (Ar), 131,8 (Ar), 134,5 (Ar), 137,4 (Ar), 137,9 (Ar), 139,5 (tiazol), 148,2 (C=N), 167,6 (C=O), 170,1 (tiazol).
- Anal. Calcd para $C_{26}H_{20}N_4O_2S$: C, 69,01; H, 4,45; N, 12,38; S, 7,09. Encontrado: C, 68,66; H, 4,36; N, 12,12; S, 6,96.
- HRMS: 453.1138 $[M+H]^+$.

6d: 2-((E)-2-{(Z)-[4-(4-metoxifenil)-3-feniltiazol-2(3H)-ilideno]hidrazona}etil) isoindolina-1,3-diona

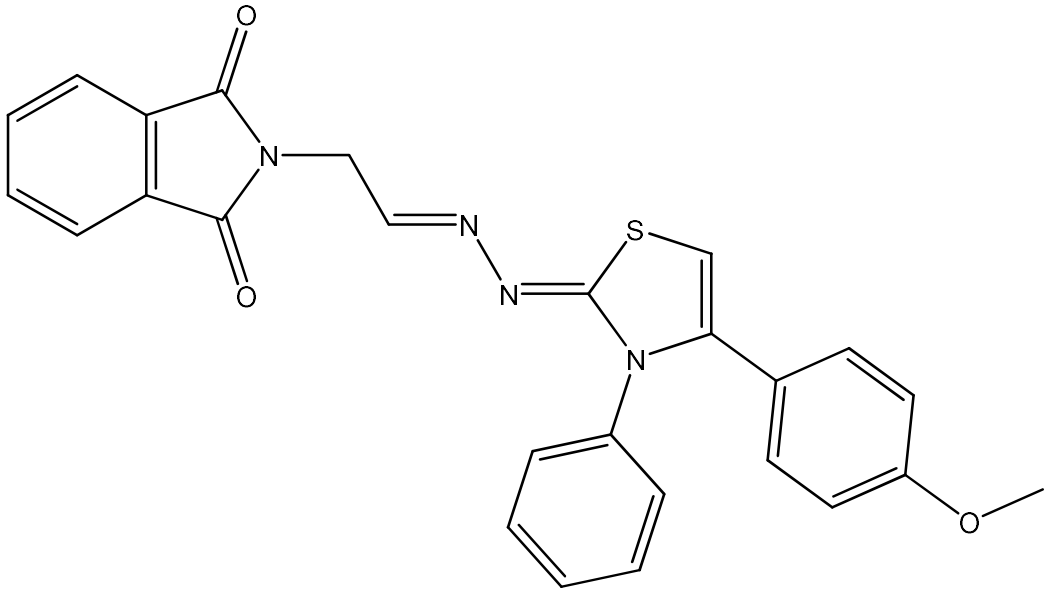

- Cristais amarelos;
- Rendimento: 54%;
- PF (°C): 173-175;
- Rf 0,49 (hexano / acetato de etila 3:2);
- IV (KBr, cm^{-1}): 1713.83 (C=O).
- RMN ^{1}H (300 MHz, DMSO-d_6), δ_{ppm}: 4,18 (s, 3H, CH_3), 4,44 (d, J = 3 Hz, 2H, CH_2), 6,83-8,10 (m, 14H, Ar);
- RMN ^{13}C (75.5 MHz, DMSO-d_6), δ_{ppm}: 40,1 (CH_2), 56,4 (CH_3), 104,3 (tiazol), 123,1 (Ar), 123,3 (Ar), 127,9 (Ar), 128,4 (Ar), 128,8 (Ar), 129,2 (Ar), 131,7 (Ar), 134,5 (Ar), 136,6 (Ar), 136,7 (Ar), 137,6 (Ar), 139,0 (tiazol), 146,8 (C=N), 167,5 (C=O), 169,6 (tiazol).
- Anal. Calcd para $C_{26}H_{20}N_4O_3S$: C, 66,65; H, 4,30; N, 11,96; S, 6,84. Encontrado: C, 65,60; H, 4,08; N, 11,85; S, 6,68.
- HRMS: 469.1276 $[M+H]^+$.

6e: 2-((E)-2-{(Z)-[4-(4-fluorofenil)-3-feniltiazol-2(3H)-ilideno]hidrazona}etil)isoindolina-1,3-diona

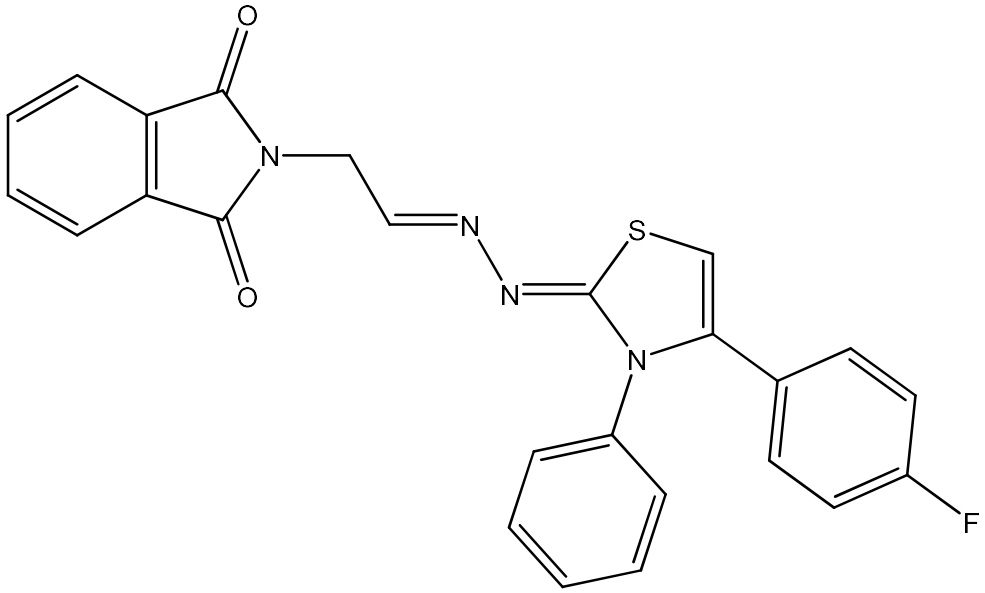

- Cristais amarelos;
- Rendimento: 50%;
- PF (ºC): 176-179;
- Rf: 0,63 (hexano / acetato de etila 3:2);
- IV (KBr, cm^{-1}): 1714.47 (C=O);
- RMN ^{1}H (300 MHz, DMSO-d_6), δ_{ppm}: 4,43 (d, J = 3 Hz, 2H, CH_2), 6,47 (s, 1H, CH tiazol), 7,02-7,36 (m, 9H, CH Ar), 7,45 (t, J = 3 Hz, 1H, CH), 7,86-7,95 (m, 4H, CH Ar ftalimida);
- RMN ^{13}C (75,5 MHz, DMSO-d_6), δ_{ppm}: 38,9 (CH_2), 101,3 (CH tiazol), 115,1 (Ar), 115,3 (Ar), 123,1 (Ar), 127.1 (Ar), 128,0 (Ar), 128,7 (Ar), 128,9 (Ar), 130,6 (Ar), 131,8 (Ar), 134,5 (Ar), 137,2 (Ar), 138,3 (tiazol), 148,3 (C=N), 160,2 e 163,4 (C-F), 167.6 (C=O), 169,9 (tiazol).
- Anal. Calcd para $C_{25}H_{17}FN_4O_2S$: C, 65,78; H, 3,75; N, 12,27; S, 7,02. Encontrado: C, 63,91; H, 3,79; N, 12,01; S, 6,94.
- HRMS: 457.1083 $[M+H]^{+}$.

6f: 2-(2-{(Z)-[4-(4-clorofenil)-3-feniltiazol-2(3H)-ilideno]hidrazona}etil)isoindolina-1,3-diona

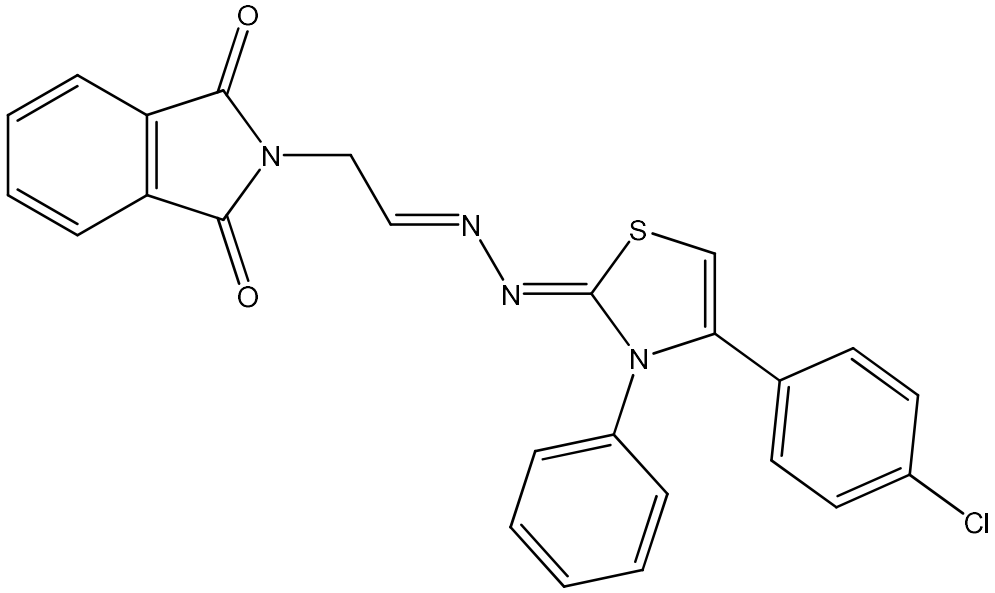

- Cristais amarelos;
- Rendimento: 58%;
- PF (°C): 176-179;
- Rf: 0,844 (hexano / acetato de etila 3:2);
- IV (KBr, cm^{-1}): 1717,30 (C=O).
- RMN ^{1}H (300 MHz, DMSO-d_6), δ_{ppm}: 4,41 (d, J = 3 Hz, 2H, CH_2), 6,50 (s, 1H, tiazol), 7,07-7,37 (m, 9H, Ar), 7,44 (t, J = 3 Hz, 1H) 7,85-7,94 (m, 5H, Ar);
- RMN ^{13}C (75.5 MHz, DMSO-d_6), δ_{ppm}: 56,0 (CH_2), 101,8 (tiazol), 123,1 (Ar), 127,9 (Ar), 128,1 (Ar), 128,6 (Ar), 128,9 (Ar), 129,5 (Ar), 129,9 (Ar), 131,8 (Ar), 133,1 (Ar), 134,5 (Ar), 137,2 (Ar), 138,7 (tiazol), 148,3 (C=N), 167,6 (C=O), 169,9 (tiazol).
- Anal. Calcd para $C_{25}H_{17}ClN_4O_2S$: C, 63,49; H, 3,62; N, 11,85; S, 6,78. Encontrado: C, 61,17; H, 3,43; N, 11,47; S, 6,79.
- HRMS: 473.0793 $[M+H]^+$.

6g: 2-((E)-2-{(Z)-[4-(4-bromophenyl)-3-phenylthiazol-2(3H)-ylidene]hydrazono}ethyl)isoindoline-1,3-dione

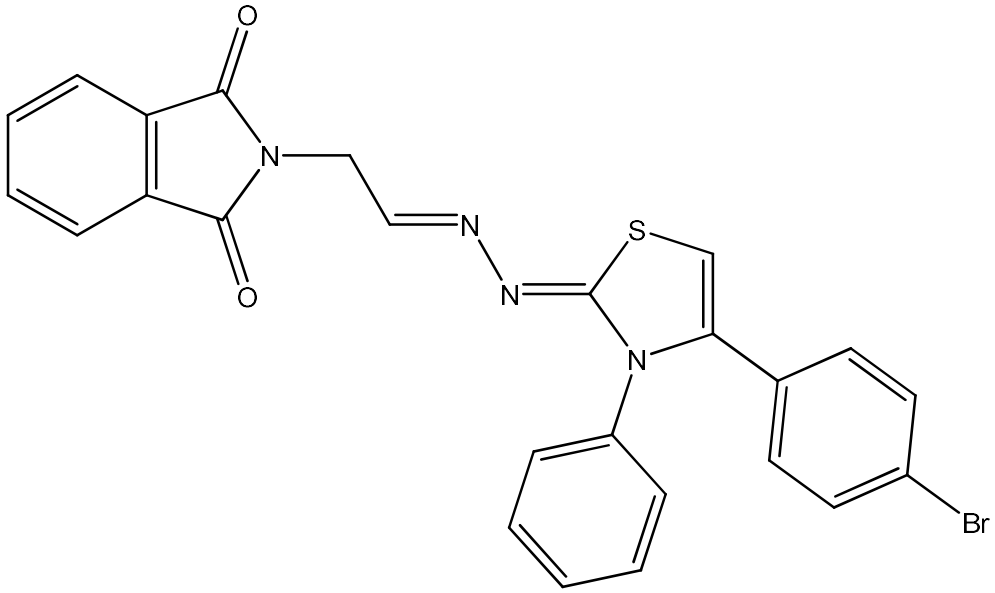

- Cristais brancos;
- Rendimento: 55%;
- PF (°C): 189-193;
- Rf: 0,73 (hexano / acetato de etila 3:2);
- IV (KBr, cm^{-1}): 1717.05 (C=O).
- RMN ^{1}H (300 MHz, DMSO-d_6), δ_{ppm}: 4,42 (d, J = 3 Hz, 2H, CH_2), 6,51 (s, 1H, tiazol), 7,01-7,94 (m, 14H, Ar);
- RMN ^{13}C (75,5 MHz, DMSO-d_6), δ_{ppm}: 39,3 (CH_2), 101,87 (tiazol), 121,7 (Ar), 123,1 (Ar), 127,9 (Ar), 128,6 (Ar), 128,9 (Ar), 129,8 (Ar), 130,1 (Ar), 131,2 (Ar), 131,8 (Ar), 134,5 (Ar), 137,2 (Ar), 138,1 (tiazol), 148,5 (C=N), 167,6 (C=O), 169,9 (tiazol).
- Anal. Calcd para $C_{25}H_{17}BrN_4O_2S$: C, 58,03; H, 3,31; N, 10,83; S, 6,20. Encontrado: C, 57,27; H, 3,28; N, 10,68; S, 6,06.
- HRMS: 517.0005 $[M+H]^{+}$.

6h: 2-((E)-2-{(Z)-[4-(4-nitrofenil)-3-feniltiazol-2(3H)-ilideno]hidrazona}etil)isoindolina-1,3-diona

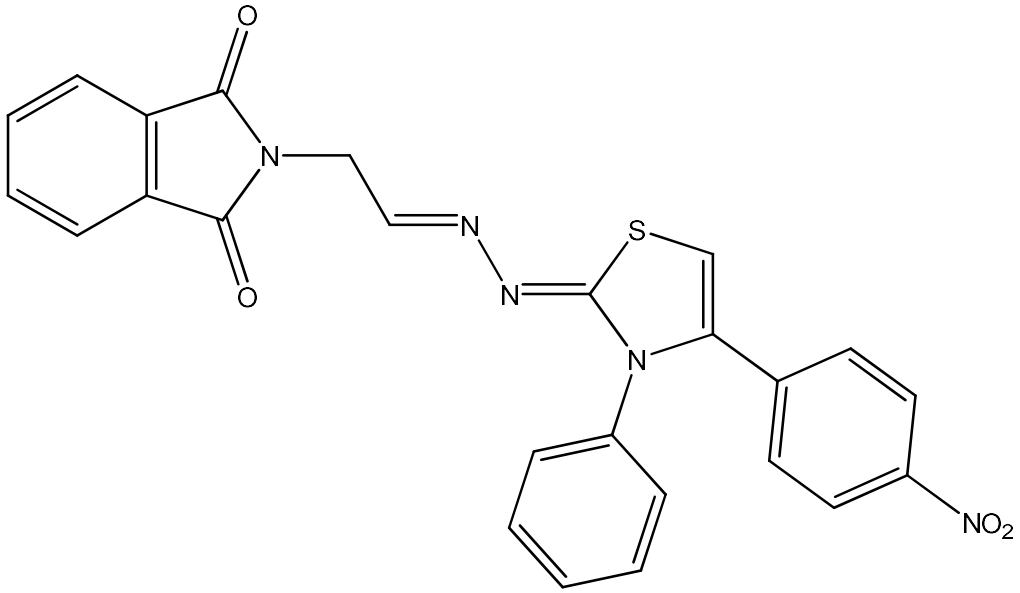

- Cristais laranjas;
- Rendimento: 46%;
- PF (°C): 186-189;
- Rf: 0,75 (hexano / acetato de etila 3:2).
- IV (KBr, cm^{-1}): 1713,38 (C=O).
- RMN ^{1}H (300 MHz, DMSO-d_6), δ_{ppm}: 4,45 (d, J = 3 Hz, 2H, CH_2), 6,78-8,10 (m, 15H, Ar);
- RMN ^{13}C (75.5 MHz, DMSO-d_6), δ_{ppm}: 40,1 (CH_2), 102,0 (tiazol), 123,2 (Ar), 123,3 (Ar), 124,5 (Ar), 128,0 (Ar), 128,4 (Ar), 129,0 (Ar), 131,7 (Ar), 131,7 (Ar), 134,5 (Ar), 136,7 (Ar), 137,4 (Ar), 138,7 (tiazol), 146,7 (C=N), 167,5 (C=O), 169,6 (tiazol).
- Anal. Calcd para $C_{25}H_{17}N_5O_4S$: C, 62,10; H, 3,54; N, 14,48; S, 6,63. Encontrado: C, 59,19; H, 3,65; N, 13,76; S, 6,93.
- HRMS: 484.0975 $[M+H]^{+}$.

6i: 2-((E)-2-{(Z)-[4-(bifenil-4-il)-3-feniltiazol-2(3H)-ilideno]hidrazona}etil)isoindolina-1,3-diona

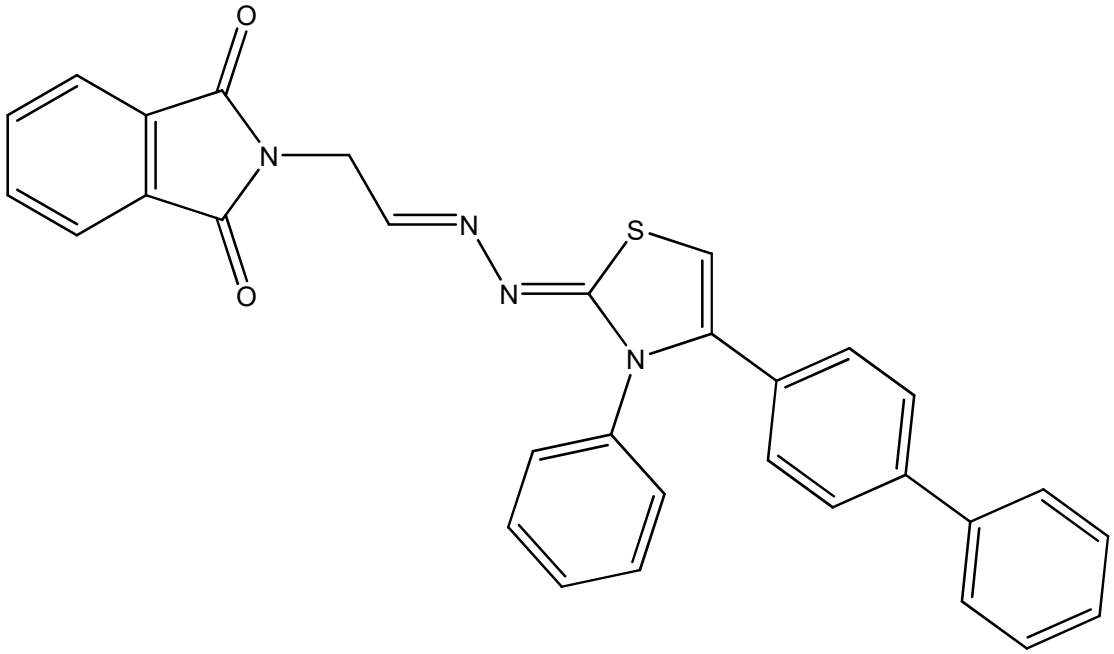

- Cristais amarelos;
- Rendimento: 73%;
- PF (°C) 157-159;
- Rf 0,43 (hexano / acetato de etila 3:2);
- IV (KBr, cm^{-1}): 1716,38 (C=O).
- RMN ^{1}H (400 MHz, DMSO-d_6), δ_{ppm}: 4,48 (d, J = 3,6 Hz, 2H, CH_2), 6,05 (s, 1H, tiazol), 7,00-7,82 (m, 19H, Ar);
- RMN ^{13}C (75.5 MHz, DMSO-d_6), δ_{ppm}: 39,2 (CH_2), 101,2 (tiazol), 123,3 (Ar), 126,8 (Ar), 126,9 (Ar), 127,7 (Ar), 128,3 (Ar), 128,4 (Ar), 128,5 (Ar), 128,6 (Ar), 128,7 (Ar), 128,8 (Ar), 129,2 (Ar), 129,6 (Ar), 132,3 (Ar), 133,9 (Ar), 133,9 (Ar), 139,9 (tiazol), 141,2 (C=N), 167,8 (C=O), 169,0 (tiazol).
- Anal. Calcd para $C_{31}H_{22}N_4O_2S$: C, 72,35; H, 4,31; N, 10,89; S, 6,23. Encontrado: C, 70,19; H, 4,32; N, 10,35; S, 6,53.
- HRMS: 515.1416 $[M+H]^{+}$.

6j: 2-((E)-2-{(Z)-[4-(naftalen-2-il)-3-feniltiazol-2(3H)-ilideno]hidrazona}etil)isoindolina-1,3-diona

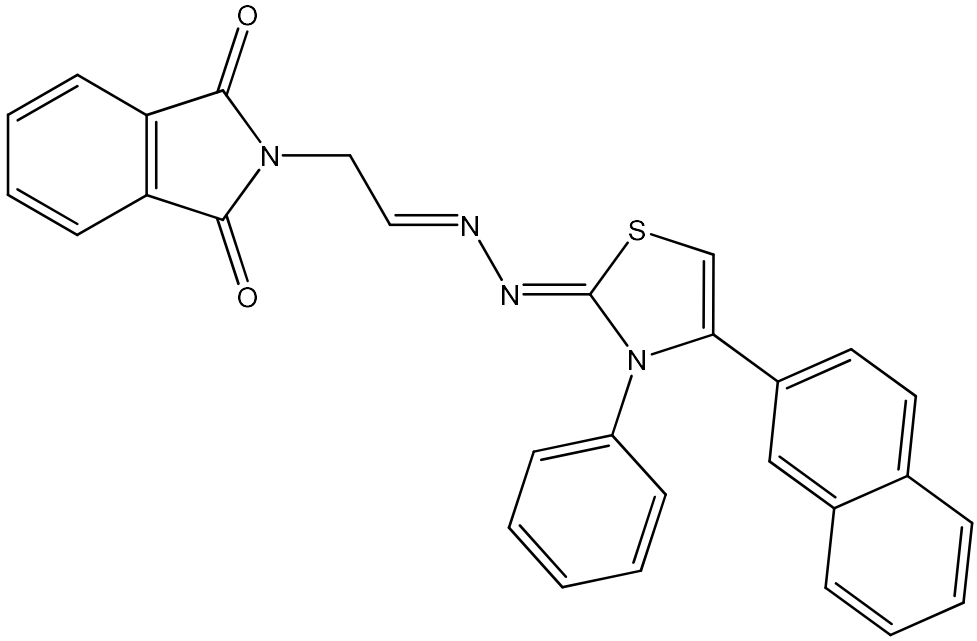

- Cristais amarelos;
- Rendimentos: 68%;
- PF (°C): 159-161;
- Rf 0,43 (hexano / acetato de etila 3:2);
- IV (KBr, cm^{-1}): 1713,93 (C=O).
- RMN ^{1}H (400 MHz, DMSO-d_6), δ_{ppm}: 4,56 (d, J = 4 Hz, 2H, CH_2), 6,18 (s, 1H, tiazol), 6,99-7,91 (m, 17H, Ar);
- RMN ^{13}C (75.5 MHz, DMSO-d_6), δ_{ppm}: 39,2 (CH_2), 101,6 (tiazol), 123,3 (Ar), 125,4 (Ar), 126,5 (Ar), 126,7 (Ar), 127,6 (Ar), 127,7 (Ar) 127,8 (Ar), 128,0 (Ar), 128,1 (Ar), 128,3 (Ar), 128,4 (Ar), 128,7 (Ar), 129,2 (Ar), 132,3 (Ar), 132,8 (Ar), 133,9 (Ar), 137,5 (Ar), 140,3 (tiazol), 149,5 (C=N), 167,8 (C=O), 171,0 (tiazol).
- Anal. Calcd para $C_{29}H_{20}N_4O_2S$: C, 71,29; H, 4,13; N, 11,47; S, 6,56. Encontrado: C, 70,09; H, 4,21; N, 11,41; S, 6,70.
- HRMS: 489.1296 $[M+H]^+$.

6k: 2-((E)-2-{(Z)-[4-(3-nitrofenil)-3-feniltiazol-2(3H)-ilideno]hidrazona}etil)isoindolina-1,3-diona

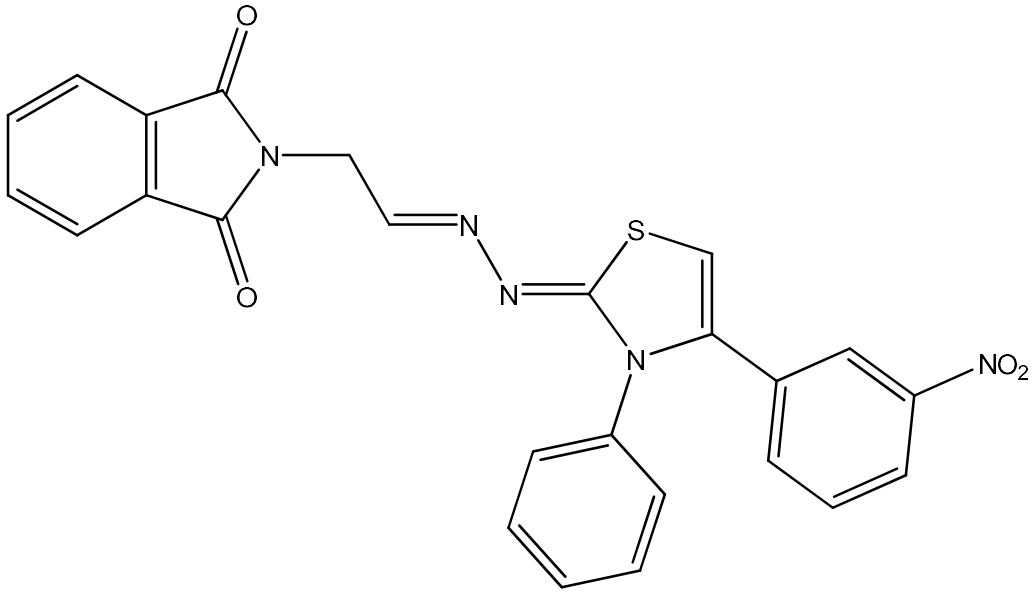

- Cristais amarelos;
- Rendimento: 63%;
- PF (°C): 154-154;
- Rf 0,34 (hexano / acetato de etila 3:2);
- IV (KBr, cm^{-1}): 1712,80 (C=O).
- RMN ^{1}H (300 MHz, DMSO-d_6), δ_{ppm}: 4,43 (d, J = 2,7 Hz, 2H, CH_2), 6,76 (s, 1H, CH tiazol), 7,25-7,38 (m, 5H, CH Ar), 7,48-7,51 (m, 3H, CH Ar), 7,86-7,95 (m, 6H, CH Ar), 8,07 (t, J = 2.4 Hz, 1H, HC=N);
- RMN ^{13}C (75,5 MHz, DMSO-d_6), δ_{ppm}: 39,3 (CH_2), 104,3 (tiazol), 123,2 (Ar), 123,4 (Ar), 123,6 (Ar), 128,8 (Ar), 128,9 (Ar), 129,1 (Ar), 129,3 (Ar), 129,5 (Ar), 129,6 (Ar), 130,0 (Ar), 130,3 (Ar), 135,0 (Ar), 135,6 (Ar), 138,8 (tiazol), 149,3 (C=N), 167,5 (C=O), 169,6 (tiazol).
- Anal. Calcd para $C_{25}H_{17}N_5O_4S$: C, 62,10; H, 3,54; N, 14,48; S, 6,63. Encontrado: C, 60,45; H, 3,70; N, 14,10; S, 6,48.
- HRMS: 484.0976 $[M+H]^+$.

6l: 2-((E)-2-{(Z)-[4-(3,4-diclorofenil)-3-feniltiazol-2(3H)-ilideno]hidrazona}etil) isoindolina-1,3-diona

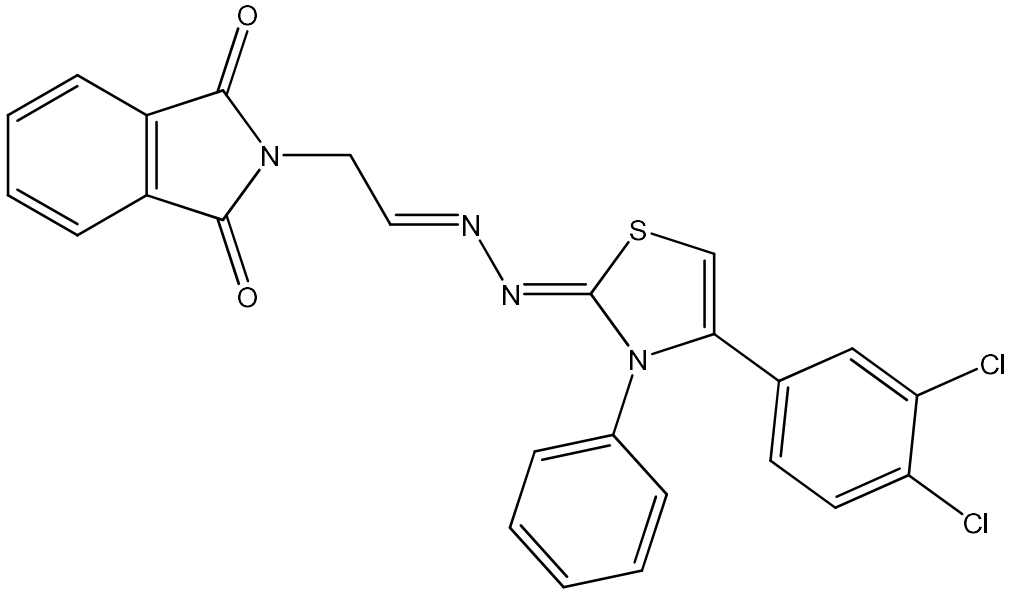

- Cristais amarelos;
- Rendimento: 48%;
- PF (ºC) 155-157;
- Rf: 0,89 (hexano / acetato de etila 3:2);
- IV (KBr, cm^{-1}): 1714,45 (C=O).
- RMN ^{1}H (300 MHz, DMSO-d_6), δ_{ppm}: 4,45 (d, J = 3 Hz, 2H, CH_2), 6,81-7,92 (m, 14H, Ar);
- RMN ^{13}C (75.5 MHz, DMSO-d_6), δ_{ppm}: 40,1 (CH_2), 104,6 (tiazol), 123,1 (Ar), 128,3 (Ar), 128,6 (Ar), 128,9 (Ar), 129,3 (Ar), 130,3 (Ar), 130,5 (Ar), 130,9 (Ar), 131,4 (Ar), 131,7 (Ar), 134,3 (Ar), 134,6 (Ar), 136,1 (Ar), 137,3 (tiazol), 149,2 (C=N), 167,5 (C=O), 169,6 (tiazol);
- Anal. Calcd para $C_{25}H_{16}Cl_2N_4O_2S$: C, 59,18; H, 3,18; N, 11,04; S, 6,32. Encontrado: C, 56,85; H, 3,30; N, 10,58; S, 6,02.
- HRMS: 507.0432 $[M+H]^+$

3.4.1.7 Análise de raio-X

As coletas de dados de difração de raios-X foram realizadas num difratômetro Kappa CCD-Enraf-Nonius (câmara CCD 95 milímetros em κ-goniostat) usando radiação de grafite monocromada MoKα (0,71073 Å) à temperatura ambiente. Os dados foram coletados usando o software COLLECT (COLLECT *et al.*, 1997) até 50 ° (2θ). Os parâmetros da célula unitária finais foram baseados em reflexões 15666, 9327 e 12333 para **2e**, **2f** e **2g**, respectivamente. Integração e dimensionamento das reflexões, bem como as correções para efeitos de Lorentz e de polarização foram realizadas com o sistema de programas HKL DENZO-SCALEPACK (OTWINOWSKI *et al.*, 1997). As estruturas dos compostos foram resolvidas através de métodos diretos com SHELXS-97 (SHELDRICK, 1997). O modelo foi refinado por matriz completa com mínimos quadrados em F2 usando SHELXL-97 (SHELDRICK, 1997). O programa ORTEP-3 (FARRUGIA, 1997) foi usado para representações gráficas, e o programa WinGX (FARRUGIA, 1999) foi usada para preparar o material para publicação. Todos os átomos de H foram localizados por considerações geométricas (C-H = 0.93 Å; N-H = 0,86 Å) e refinados usando um modelo de equitação com Uiso (H) = 1.5Ueq (C-metil) ou 1.2Ueq (outra). Um diagrama ORTEP-3 das moléculas é mostrado na Figura 11. Dados cristalográficos (excluindo fatores estrutura) para as estruturas relatados neste trabalho foram depositados junto do Centro de dados cristalográficos de Cambridge como material complementar (nº CCDC 1.411.254, 1.411.262 e 1.411.263).

3.4.2 Parte biológica

3.4.2.1 Análise biológica da toxicidade para esplenócitos

Os esplenócitos de camundongos BALB/c foram divididos em placas de 96 poços a uma densidade de 5 x 10^6 células por cavidade em meio RPMI-1640 contendo 10% de Soro Bovino Fetal inativado (FBS). Cada inibidor químico foi dissolvido em DMSO a uma concentração de 10 mg/ml, e, em seguida, a amostra foi diluída em série em meio RPMI-1640 suplementado com FBS a 10% a concentrações de 1,0, 5,0, 10, 25, 50 e 100 μg/mL , em triplicata. Como um controle positivo, saponina foi utilizada a uma concentração de 0,1 μg/mL, enquanto que o meio RPMI-1640 suplementado com 10% de FBS e DMSO foi usado como um controle negativo. Um total de 1,0 μCi de 3H-timidina foi adicionado a cada poço e a placa foi incubada durante 24 h a 37 ºC e 5% de CO2.

A placa foi então lida no leitor contador de irradiação beta (Multilabel Reader, Finlândia), e determinou-se a porcentagem de incorporação de timidina tritiada. As células que não foram tratadas com compostos (controles negativos) foram calculadas como 100% da incorporação de timidina tritiada (100% de células viáveis). Para as células tratadas com saponina, a viabilidade celular foi de 5%. Quando a percentagem de incorporação foi superior a 90%, a concentração da droga foi considerada como não tóxica para os esplenócitos.

3.4.2.2 Atividade antiproliferativa para a forma epimastigota

Epimastigotas de cepa Dm28c foram distribuídas em uma placa de 96 poços a uma densidade final de 10^6 células por poço. Cada inibidor químico foi dissolvido nos respectivos poços, em triplicata. Benznidazol foi usado como controles positivos neste ensaio. A placa foi então cultivada durante 4 dias a 27 °C. Após este tempo, aliquotas de cada poço foram recolhidas, e o número de parasitos foi calculado numa câmara de Neubauer. Epimastigotas não tratadas com os inibidores químicos (controle negativo) foram assumidas como 100% no número de parasitos. Determinaram-se as curvas de dose-resposta, e os valores de IC_{50} foram calculados usando pelo menos cinco concentrações (pontos de dados) e uma equação não linear (Prism, versão 4.0).

3.4.2.3 Toxicidade para tripomastigotas

Tripomastigotas da Cepa Y foram recolhidas a partir de sobrenadantes de células Vero e distribuídas numa placa de 96 poços a uma densidade final de 4×10^5 células por poço. Cada inibidor químico foi adicionado às cavidades, em triplicata. Benznidazol foi usado como controle positivo neste ensaio. A placa foi então cultivada durante 24 horas a 37 °C e 5% de CO_2. Após este tempo, aliquotas de cada poço foram recolhidas, e o número de parasitos viáveis (isto é, com a motilidade aparente) foi contado numa câmara de Neubauer. Os poços que não receberam os inibidores químicos foram assumidos como 100% no número de parasitos viáveis. Determinaram-se as curvas de dose-resposta, e os valores de IC50 foram calculados por regressão não linear (Prism, versão 4.0), utilizando pelo menos sete concentrações (pontos de dados).

3.4.2.4 Estudos ultraestruturais

Os parasitos foram cultivados durante 24 h em meio RPMI 1640 (Sigma-Aldrich, St. Louis, MO, EUA) tamponado em pH 7,5 e suplementado com HEPES (20 μM), 10% de soro fetal bovino, penicilina (100 U/ml) , e estreptomicina (100 μg/mL) contendo o composto **6k** na concentração IC_{50} e duas vezes o valor de IC_{50}. Os parasitos foram recolhidos, lavados em PBS e fixados com 2,5% de glutaraldeído, formaldeído a 4%, e tampão de cacodilato 0,1 M em pH 6,8. Eles foram, em seguida, pós-fixados em 2% de tetróxido de ósmio (OsO_4) num tampão de cacodilato 0,1 M em pH 6,8 e processados para microscopia eletrônica de transmissão (TEM) e microscopia electrônica de varredura (MEV).

Para a análise de MEV, os parasitos foram desidratados em etanol graduado e secados pelo método do ponto crítico com CO_2. As amostras foram montadas em bases de alumínio, revestidas com ouro e examinadas sob um microscópio JEOL-5600LV.

Para a análise de TEM, os parasitos foram desidratados numa série graduada de acetona e, finalmente, embebidos em EPON. As seções foram coradas com acetato de uranilo e citrato de chumbo e observadas com microscópio Tecnai spirit G2 Biotwin.

3.4.2.5 Iodeto de propídio e coloração anexina V

Tripomastigotas (1×10^7) foram incubadas durante 24 h a 37 °C na ausência ou presença do composto **6k**. Após a incubação, os parasitos foram marcados com iodeto de propídio (PI) e anexina V usando o kit de detecção de apoptose V-FITC anexina (Sigma-Aldrich), de acordo com as instruções do fabricante. Aquisição e as análises foram realizadas utilizando um citômetro de fluxo FACS Calibur (Becton Dickinson, CA, EUA) com o software FlowJo (Tree Star, CA, EUA). Um total de 30.000 eventos foi adquirido na região previamente estabelecida como formas tripomastigotas de *T. cruzi*. Foram realizados dois experimentos independentes.

4 CAPÍTULO 2

Planejamento estrutural, síntese e avaliação das propriedades antitumorais de inéditas tiazolil-hidrazonas derivadas da isatina

4.1 Revisão da Literatura

4.1.1 Câncer

Câncer (do grego *karkinos* – caranguejo) é um termo genérico para um grande grupo de doenças que podem afetar qualquer parte do corpo. Outros termos utilizados são tumores malignos e neoplasias (WHO, 2015). Uma característica comum aos tipos de câncer é a proliferação desordenada e a incapacidade de diferenciação celular normal. As células adquirem características de malignidade por meio do processo de progressão tumoral, que consiste no crescimento progressivo, na invasão e na formação de metástases (COSTA, 2011).

Hanahan e Weinberg descreveram em sua revisão de 2010, revisada em 2011, o conceito de "hallmarks" do câncer, que seriam as capacidades características que constituem o alicerce lógico para o entendimento dessa patologia. Os Hallmarks do câncer incluem: 1) manutenção de sinalização proliferativa, 2) evasão de supressores de crescimento, 3) ativação de invasão e metástase, 4) possibilidade de imortalidade replicativa, 5) indução de angiogenese e 6) resistência à morte celular (**Figura 17**). Adicionalmente, duas características cruciais que permitem a aquisição dos seis Hallmarks iniciais foram descritas. São essas: Instabilidade genômica e mutação, e inflamação promotora de tumor (HANAHAN & WEINBERG, 2010;HANAHAN & WEINBERG, 2011).

Figura 17. "Hallmarks" do câncer.

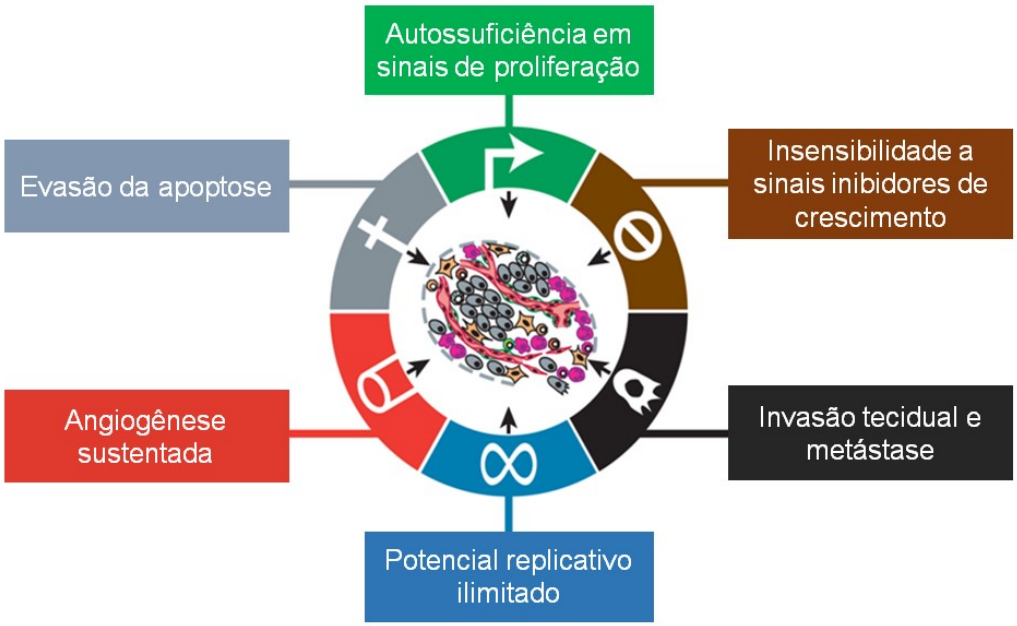

Adaptado de Hanahan; Weinberg, 2011.

As pesquisas em câncer tiveram, por muito tempo, um foco reducionista, baseado apenas nas células cancerosas e nos seus genes. Atualmente, os tumores são vistos como tecidos complexos, onde as células tumorais recrutam e subvertem tipos celulares normais, que servem como colaboradores na pauta neoplásica. As características fenotípicas do câncer não dependem unicamente das células tumorais (**Figura 18**) (HANAHAN, COUSSENS, 2012).

Figura 18. Tumores como tecidos complexos.

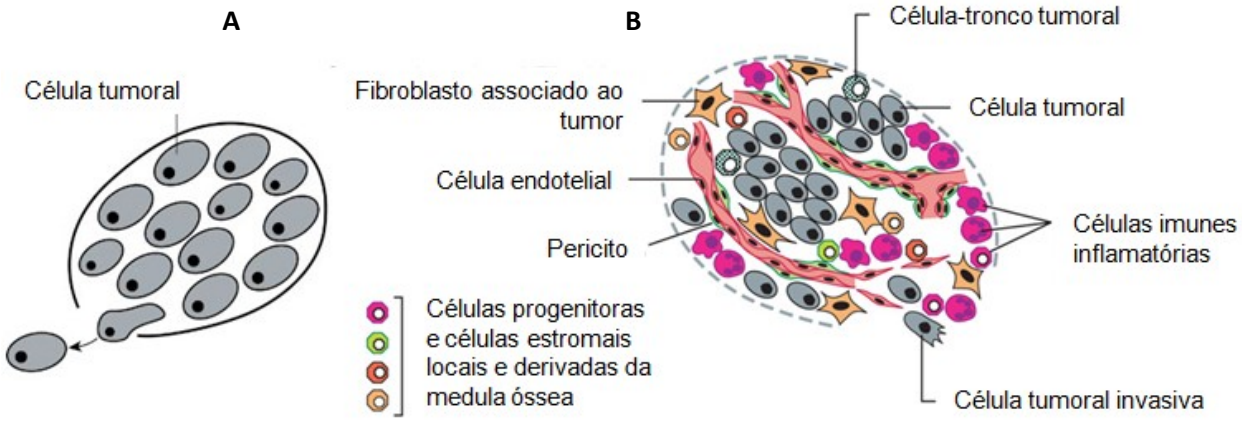

A – Visão reducionista. B – Concepção atual, considerando tanto as células tumorais como seu microambiente.
Fonte: Adaptado de Hanahan; Weinberg, 2000, 2011.

4.1.2 Epidemiologia do Câncer

Segundo a Organização Mundial de Saúde, o câncer continua sendo uma das principais causas de morte em todo o mundo. Estimou-se para 2012, cerca de 14 milhões de novos casos de câncer e 8,2 milhões de mortes relacionadas à esta doença. Ainda segundo dados da OMS, o número de novos casos de câncer deverá aumentar em cerca de 70% ao longo das próximas duas décadas (WHO, 2015).

Na ultima estimativa realizada pelo INCA (Instituto Nacional de Câncer) foi esperado para o ano de 2014, o surgimento de aproximadamente 576 mil casos novos de câncer no Brasil. Além disso, estima-se que a carga do câncer continuará aumentando nos países em desenvolvimento e crescerá ainda mais em países desenvolvidos se medidas preventivas não forem amplamente aplicadas. Em 2030, a carga global será de 21,4 milhões de casos novos de câncer e 13,2 milhões de mortes por câncer, em consequência do crescimento e do

envelhecimento da população, bem como da redução na mortalidade infantil e nas mortes por doenças infecciosas em países em desenvolvimento (INCA, 2014).

4.1.3 Quimioterapia do Câncer

A quimioterapia empregada para tratamento de pacientes com câncer é feita por meio do uso de agentes químicos isolados ou em combinação. Esta estratégia terapêutica é uma das principais atualmente utilizadas, podendo também ser empregada juntamente com outros métodos de forma adjuvante, quando usada após tratamento cirúrgico ou radioterápico curativo; ou previamente a uma remoção cirúrgica, geralmente para reduzir a massa tumoral minimizando a quantidade de lesões durante a cirurgia (COSTA-LOTUFO, 2010).

No entanto, o arsenal quimioterápico disponível para o tratamento do câncer apresenta vários problemas quanto à especificidade, agindo também em células normais, e potencialidade, apresentando valores ainda considerados pequenos de cura total. Além desses fatores, o desenvolvimento de resistência a múltiplas drogas é um elemento agravante e já com certa frequência de casos na terapêutica do câncer (SHUKLA *et al.*, 2012). Dessa forma, a pesquisa e desenvolvimento de novos fármacos para a quimioterapia do câncer se fazem necessários.

4.1.4 Derivados da isatina

Um conhecido grupo farmacofórico que apresenta uma notável e conhecida atividade antiproliferativa contra várias linhagens de células cancerosas é o heterociclo isatina (ABOUL-FADL *et al.*, 2012). A recente aprovação pela FDA do oxindol, malato de sunitinibe (**Figura 19**), como um inibidor de quinase para o tratamento do carcinoma renal avançado e tumores estromais gastrointestinais, destacou, ainda mais, o crescente interesse em isatinas como uma nova classe de agentes antineoplásicos. (MOTZER *et al.*, 2006).

Derivados da SU-5416 (semaxanib) e da SU-11248 (sunitinib) (**Figura 19**) são relatados como potentes inibidores das quinases dependentes de ciclina (CDKs), o que pode induzir apoptose em células de carcinoma de cólon. Shi *et al.* (1996) obtiveram derivados fenil-hidrazonas de isatinas (**Figura 19, I**) que também apresentam potente inibição de CDKs (SOLOMON *et al.*, 2009).

Além da potente inibição de quinase, o mecanismo de ação de outros derivados da isatina inclui a inibição e/ou modulação de proteases, inibição da tradução, da neovascularização e da polimerização da tubulina (VINE *et al.*, 2009). Abadi *et al.* (2006) identificaram as propriedades antitumorais e antiangiogênicas de imino 2-indolonas (**Figura 19, II**). Vine *et al*. (2009) sintetizaram diversos análogos da isatina substituída (**Figura 19, III**), e testaram em cinco linhas de células cancerígenas humanas, concluindo que isatinas substituídas podem ser efetivos fármacos anticâncer (SOLOMON *et al.*, 2009).

Figura 19. Exemplos de derivados da isatina que apresentam atividade antitumoral.

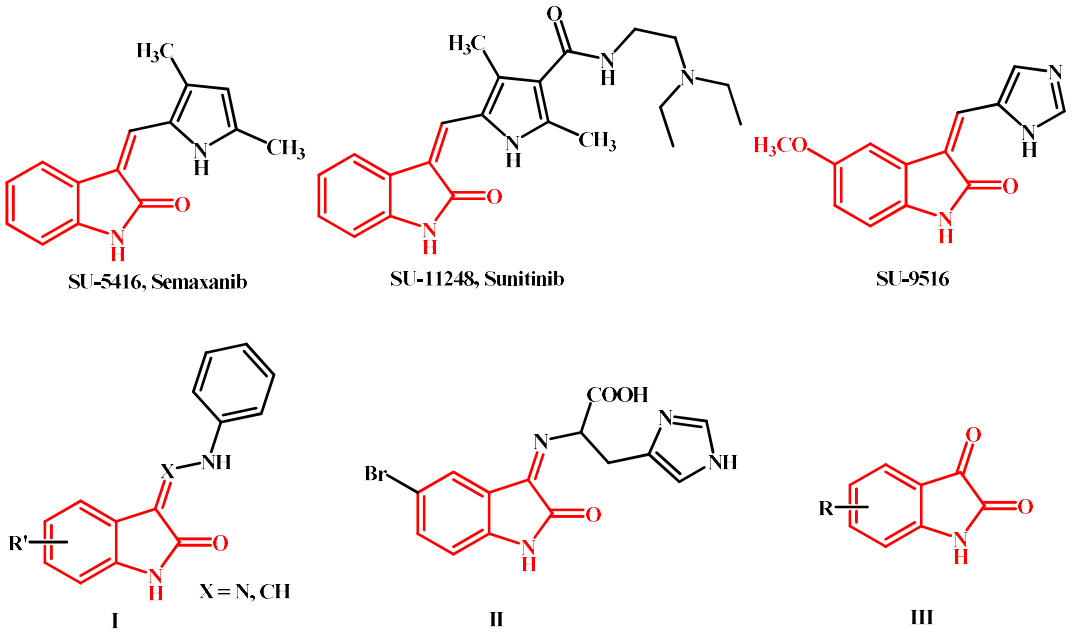

Fonte: Elaborado pelo autor.

4.1.5 Derivados do tiazol

Outra classe de compostos heterocíclicos que também se destacam pelo amplo espectro de atividades biológicas são os tiazóis. Dentre as atividades relatadas para esse núcleo farmacofórico, destaca-se a potente ação citotóxica frente a diferentes tipos de tumores tais como carcinoma de pulmão, adenocarcinoma de cólon, glioblastoma, melanoma, câncer de próstata e leucemia (LEFRANC et al., 2013; HASSAN et al., 2012; FALLAH-TAFTI et al., 2011; ALIABADI et al., 2010; SOUZA et al., 2005). Como exemplo de agentes antitumorais que apresentam tiazol em sua estrutura, podem ser citados a bleomicina e a tiazofurin (KASHYAP *et al.*, 2012) (**Figura 20**).

Figura 20. Exemplos de agentes antitumorais contendo o núcleo tiazol.

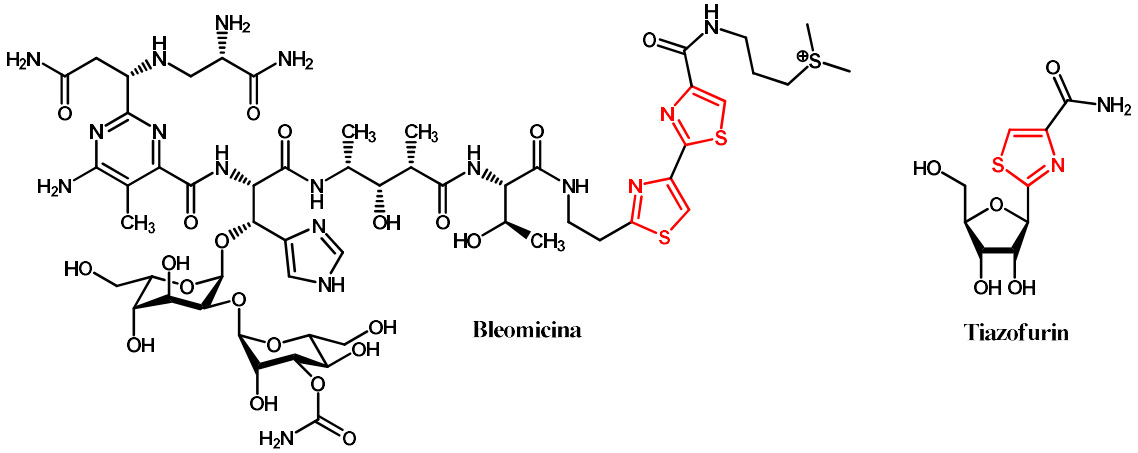

Fonte: Elaborado pelo autor.

4.1.6 Planejamento das séries

Frente ao exposto, os grupos isatina e tiazol foram escolhidos como grupos farmacofóricos de base, no intuito de obter novos agentes antitumorais. Desse modo, foi utilizada a estratégia química de hibridização molecular, onde as duas estruturas bioativas distintas foram unidas em uma nova estrutura. Com a utilização dessa estratégia pode-se obter um novo composto, conhecido como dual, misto ou duplo em propriedades farmacológicas, o que pode representar uma alternativa terapêutica muito interessante para determinadas fisiopatologias multifatoriais, como é o caso do câncer.

Vine e colaboradores (VINE *et al.*, 2007; VINE *et al.*, 2009) mostraram que algumas isatinas substituídas apresentam ação anticancerígena sobre células humanas de linfoma histiocítica (U937), principalmente as isatinas halogenadas e nitradas na posição C5. Por esse motivo, foram obtidas isatinas com um grupo nitro (NO_2) na posição C5 e isatinas com um halogênio nesta mesma posição. Escolheu-se o substituinte Cl para explorar os efeitos da presença de halogênios nessa posição. Também foram explorados substituintes em torno do anel fenil ligado ao anel tiazol em C4, além de serem feitas substituições na posição N3 também do anel tiazol.

A utilização dos substituintes halogenados possibilita, dentre outras coisas, a melhoria da absorção oral, da permeabilidade, da estabilidade metabólica e química, a formação de ligação halogênio no alvo farmacológico contribuindo para a estabilidade da ligação fármaco-receptor, além das contribuições estéricas dessa classe na interação com alvos farmacológicos (HERNANDES *et al.*, 2010).

Estas técnicas empregadas permitem uma análise da relação estrutura-atividade (SAR). As variações estruturais realizadas nas moléculas são confrontadas com as variações no potencial de atividade biológicas dessas moléculas. Dessa forma, pode-se apurar a especificidade de cada uma delas e observar quais variações foram benéficas ou prejudiciais para a atividade (**Figura 21**).

Figura 21. Planejamento estrutural dos compostos propostos

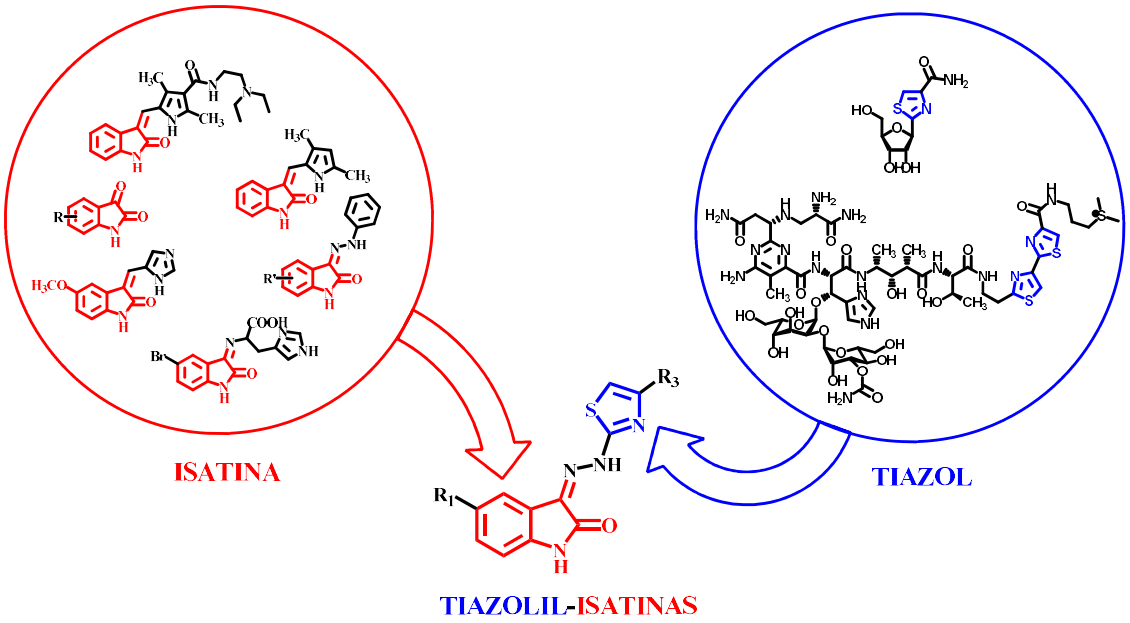

Fonte: Elaborado pelo autor.

4.2 Resultados e discussão

4.2.1 Parte Química

4.2.1.1 Obtenção da Série Química

Todos os compostos da série **PA01A-PA03L** foram obtidos por meio de uma metodologia simples, em duas etapas. Inicialmente foram obtidos nove compostos intermediários (tiossemicarbazonas). Dois dos intermediários que apresentam hidrogênio no radical $\mathbf{R_2}$ foram condensados com dez diferentes α-halo-cetonas, obtendo-se, desse modo, vinte tiazóis (**Esquema 2**).

Esquema 2. Esquema geral de síntese da série **PA1A-PA3L**.

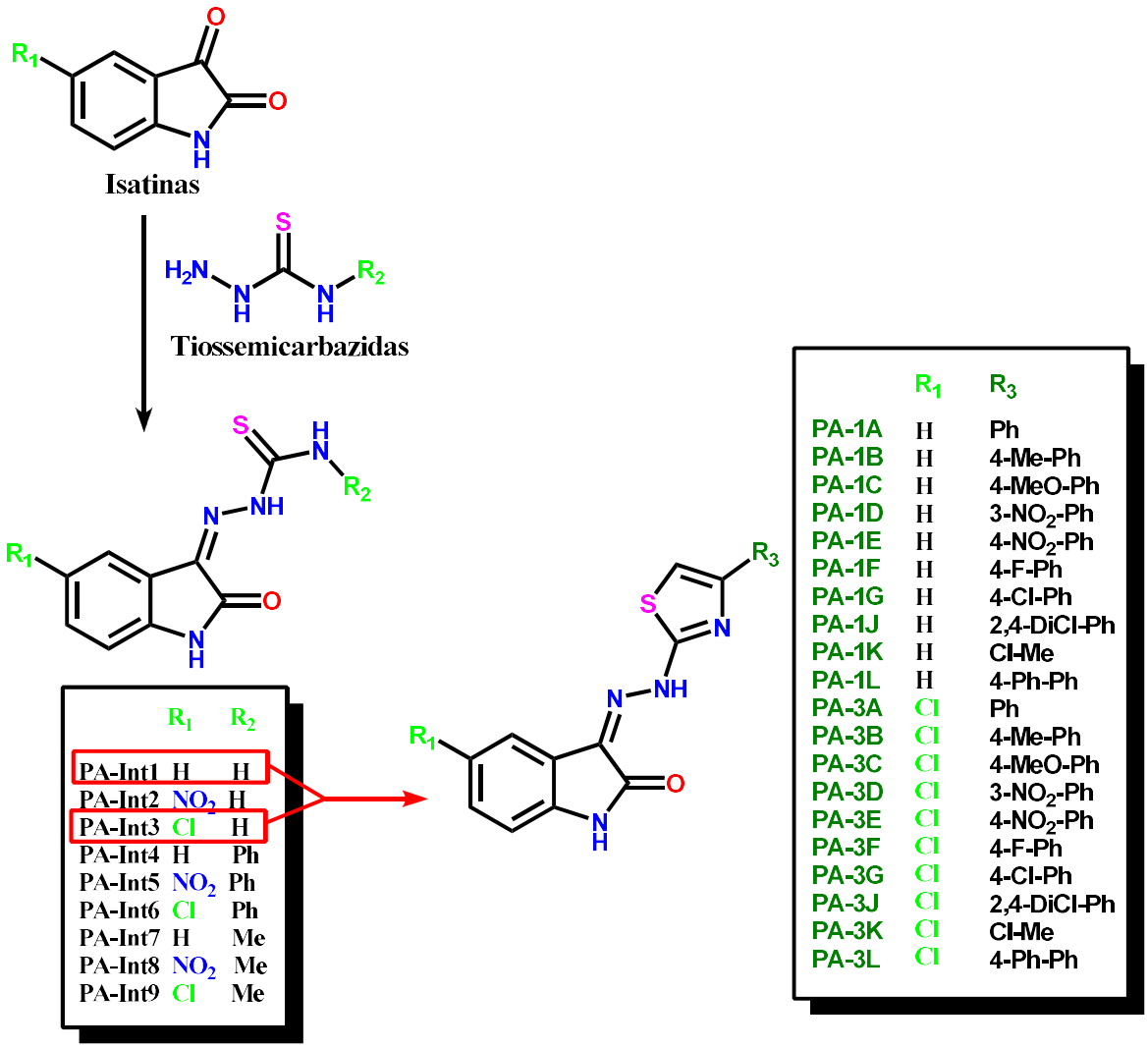

Fonte: Elaborado pelo autor.

4.2.1.1.1 Obtenção dos compostos intermediários (PAInt-1 a PA-Int9)

Para a obtenção dos compostos intermediários foi utilizada uma metodologia semelhante à de Karah, que trabalhou com derivados da isatina em 2002. Neste trabalho, Karah reagiu derivados da isatina com a tiossemicarbazida e obteve tiossemicarbazonas com altos rendimentos. A síntese é realizada em solução etanólica, sob refluxo, na presença de catalizador ácido (KARAH, 2002).

Tendo como base esta metodologia, foram obtidos os nove intermediários (**PA-Int1 à PA-Int9**) reagindo-se três diferentes isatinas (isatina, 5-nitroisatina e 5-cloroisatina), obtidas comercialmente, com três diferentes tiossemicarbazidas (tiossemicarbazida, fenil-tiossemicarbazida e metil-tiossemicarbazida), também obtidas comercialmente. As reações duraram em torno de três horas e os rendimentos foram de 60 à 85% (**Esquema 3**).

Esquema 3. Síntese dos compostos intermediários **PA-Int1 à PA-Int9**.

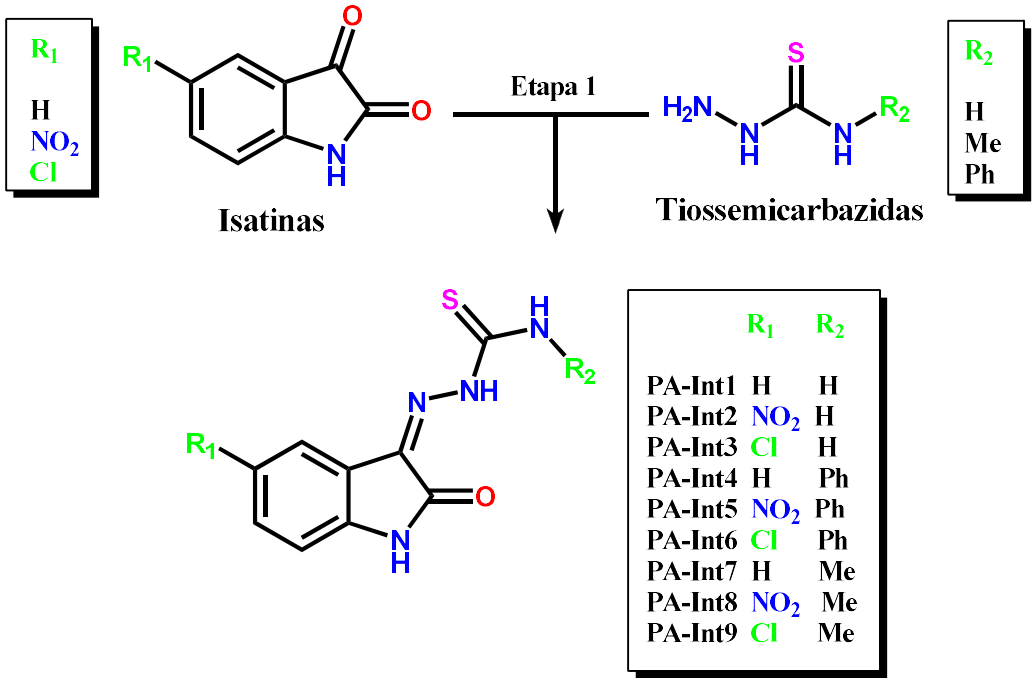

Reagentes e condições: Etanol, HCl, refluxo, 3h. Fonte: Elaborado pelo autor.

O mecanismo dessa síntese inicia-se com a protonação do oxigênio da carbonila para formar o intermediário íon oxônio. Em seguida ocorre um ataque nucleofílico do nitrogênio N-1 da tiossemicarbazida levando à formação do intermediário hemiaminal protonado, que,

por sua vez, perde uma molécula de água e, após neutralização, ocorre a formação da tiossemicarbazona (**Esquema 4**) (TENÓRIO & GÓES, 2005).

Esquema 4. Esquema da síntese das tiossemicarbazonas **PA-Int1 à PA-Int9**.

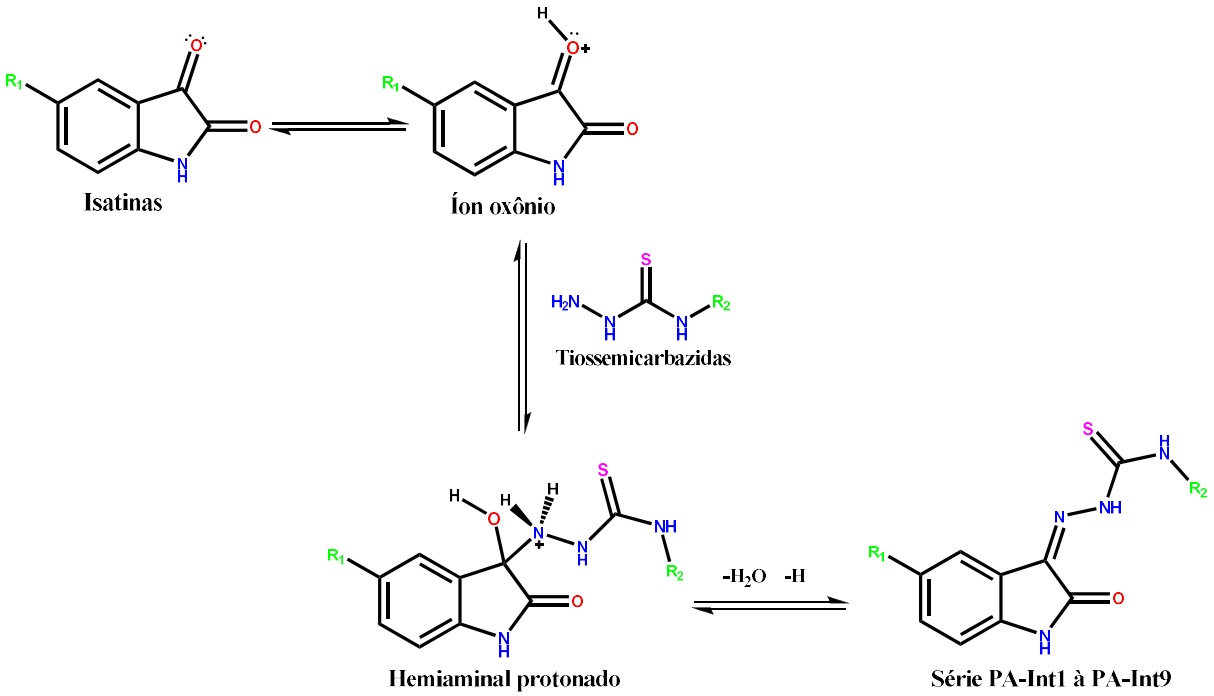

Fonte: Elaborado pelo autor.

4.2.1.1.2 Obtenção da série PA01A-PA03L

A segunda etapa da síntese aqui proposta consistiu na obtenção de trinta tiazóis inéditos que compõem a série **PA01A-PA03L**. Para tanto, foram escolhidas duas das tiossemicarbazonas sem substituintes na posição N3, sendo elas o **PA-Int1** e **PA-Int3**. Cada um desses intermediários foi condensado com dez diferentes α-halo-cetonas, seguindo-se a metodologia desenvolvida por Hantzsch em 1887 (SOUZA *et al*., 2005). Nesta metodologia as reações são desenvolvidas em agitação magnética sob refluxo (**Esquema 5**).

As tiossemicarbazonas, na presença de α-halogeno-cetonas, funcionam muito bem na síntese de tiazóis. Isto acontece porque as α-halogeno-cetonas são muito reativas frente ao grupo tioamida nucleofílico presente nas tiossemicarbazonas e, consequentemente, levam à ciclocondensação para formar o heterociclo (TENÓRIO & GÓES, 2005).

Esquema 5. Etapa 2: Síntese da série **PA01A-PA03L**.

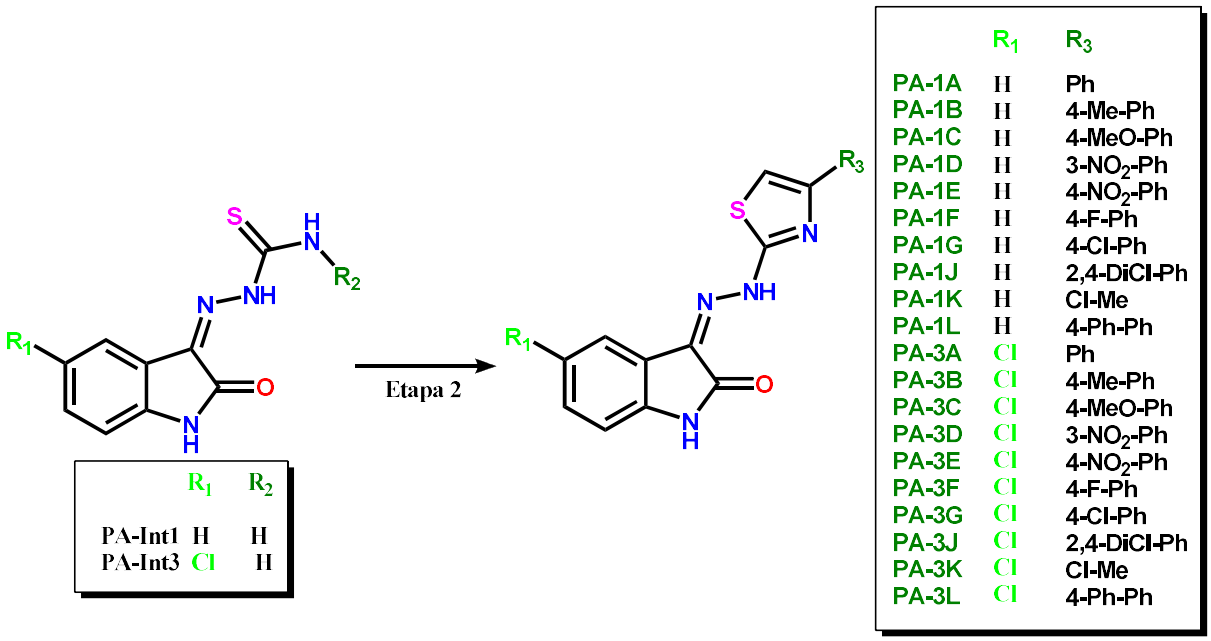

Reagentes e condições: respectivas α-halo-cetonas, isopropanol, refluxo, 2h. Fonte: Elaborado pelo autor.

O mecanismo da síntese de Hantzsch ocorre em três etapas. Inicialmente, o halogênio da α-halogeno-cetona sofre uma substituição nucleofílica, resultando em um sal S-alquiliminium, que sofre uma transferência de prótons. A ciclização produz um sal de 4-hidroxi-5-hidrotiazol, o qual é convertido em tiazol com eliminação de uma molécula de água (**Esquema 6**) (SILVA, 2009).

Esquema 6. Mecanismo de síntese da série de tiazóis **PA01A-PA03L**.

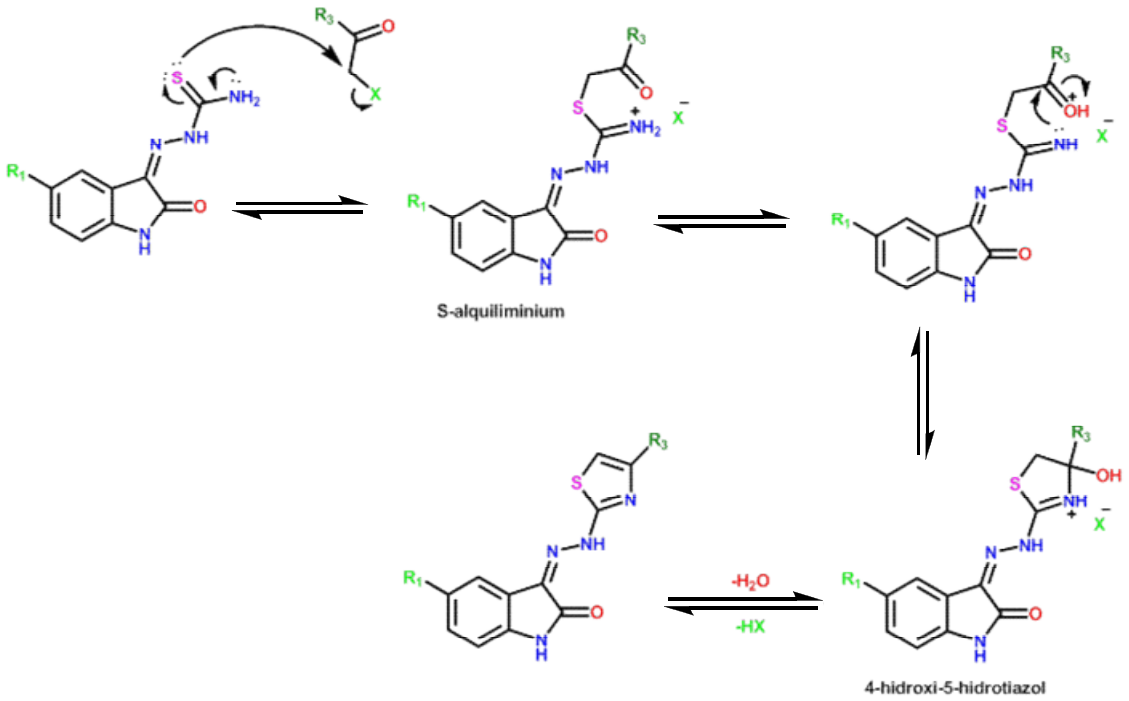

Fonte: Elaborado pelo autor.

4.2.1.2 Caracterização estrutural

Todos os 39 compostos (nove tiossemicarbazonas e trinta tiazóis) obtidos foram estruturalmente caracterizados utilizando-se as técnicas de Ressonância Magnética Nuclear de Prótons (RMN^{1}H), Ressonância Magnética Nuclear de Carbono (RMN^{13}C) e Infravermelho (IV). A seguir, será detalhado o processo de caracterização dos intermediários **PA-Int1** à **PA-Int9** e da série final de tiazóis **PA01A-PA03L**.

4.2.1.2.1 Caracterização dos intermediários PA-Int1 à PA-Int9

Para representar a caracterização dos compostos intermediários **PA-Int1** à **PA-Int9**, o composto **PA-Int1** foi escolhido como representante estrutural. Por meio da análise espectroscópica na região do infravermelho, pôde-se constatar a presença das principais bandas de absorção (**Figura 22**). A banda que aparece em 3235cm^{-1} sugere a deformação axial da ligação N-H. Em 1682 e 3145cm^{-1} pode-se observar bandas sugestivas da presença do grupo HN-C=O. Nas frequências de 1498 e 1137cm^{-1} pode-se identificar o estiramento C=S.

Figura 22. Espectro de infravermelho da molécula PA-Int1

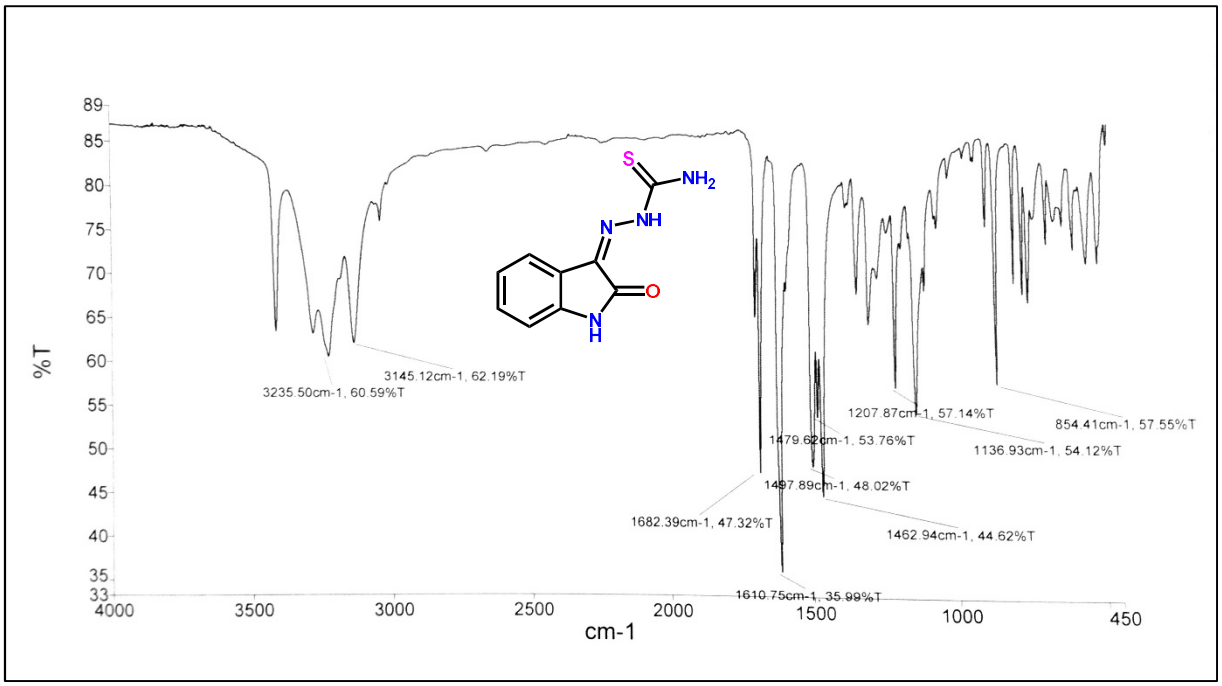

Fonte: Elaborado pelo autor.

A **Figura 23** apresenta os valores do espectro de RMN^{1}H do composto **PA-Int1**, onde foi constatada a presença de um dupleto em torno de 6.92 ppm, integrando para um hidrogênio, referente a um hidrogênio aromático. Em 7.08 ppm é observado um tripleto integrando para um hidrogênio, que também corresponde a um hidrogênio aromático. Assim como em 7.35 ppm também é observado um tripleto integrando para um hidrogênio de anel aromático. Outro dupleto de um hidrogênio de anel aromático é identificado em 7.65 ppm. Em 8.68 e 9.04 ppm encontram-se dois singletos referentes aos dois hidrogênios da amina primária (NH_2). Dois singletos, um em 11.2 ppm e outro em 12.47 ppm, correspondem aos dois hidrogênios das duas aminas secundárias (NH).

Figura 23. Espectro do RMN^{1}H para a molécula PA-Int1.

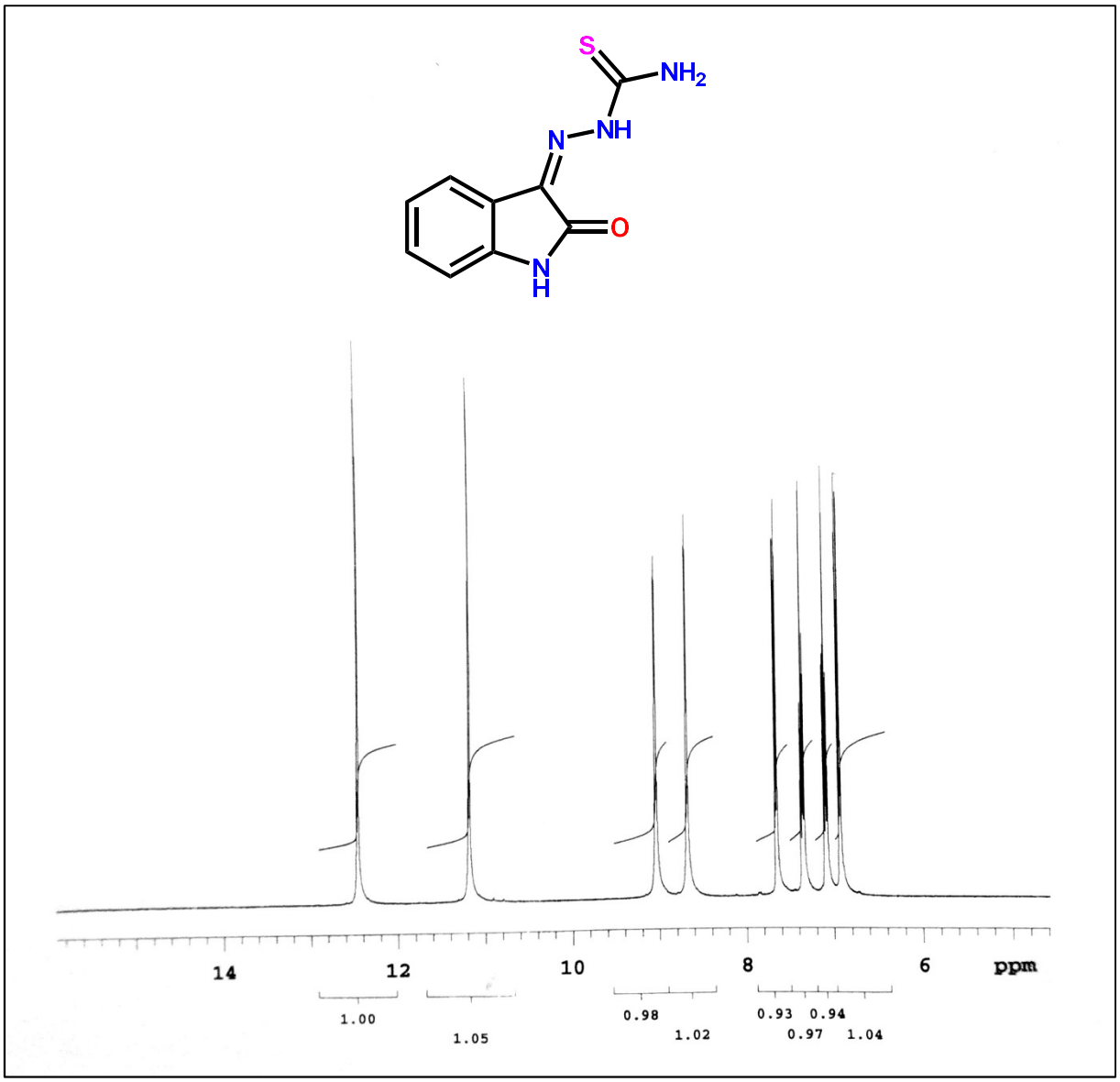

Fonte: Elaborado pelo autor.

Para confirmação dos carbonos presentes na molécula **PA-Int1**, foi utilizada a técnica de ressonância magnética nuclear de carbono 13 (**Figura 24**). Os picos que aparecem em 111.0, 119.9, 120.9, 122.4 e 131.2 ppm, correspondem aos carbonos aromáticos da molécula. O pico em 132.0 ppm corresponde ao C=N. O pico em 142.3 ppm corresponde ao carbono aromático que está ligado ao NH. Em 162.6 ppm encontra-se o pico correspondente ao carbono da carbonila. Já em 178.7 ppm está o pico característico do C=S

Figura 24. Espectro do RMN'C^{13} para a molécula PA-Int1.

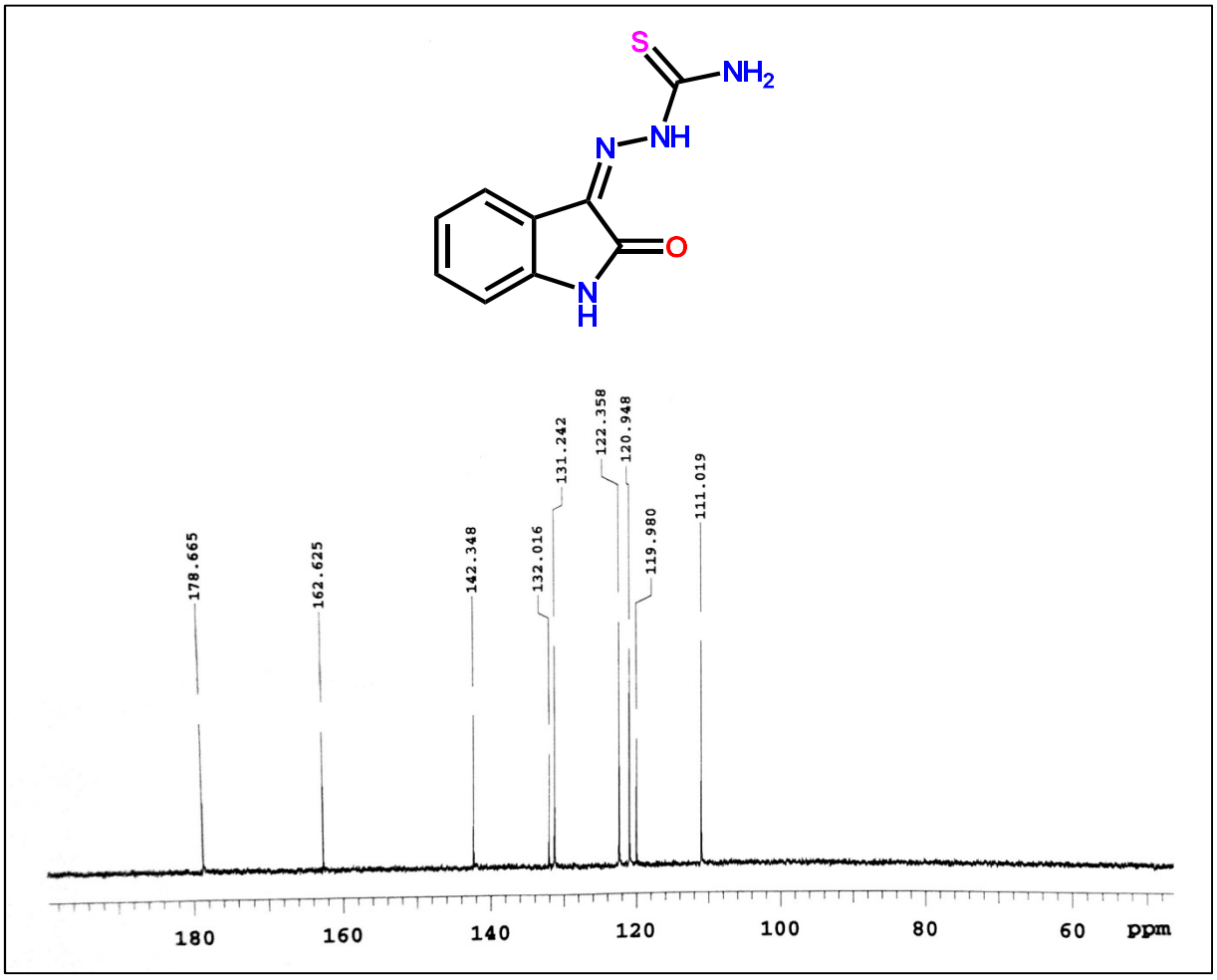

Fonte: Elaborado pelo autor.

4.2.1.2.2 Caracterização dos tiazóis PA01A-PA03L

Para representar a caracterização dos compostos intermediários **PA01A-PA03L**, foi escolhido o composto **PA01G**. Através da análise espectroscópica na região do infravermelho foi possível constatar as principais bandas de absorção (**Figura 25**). A banda em 3260 cm^{-1} sugere a deformação axial N-H. A banda em 1693 cm^{-1} corresponde ao HN-C=O.

Figura 25. Espectro de infravermelho da molécula **PA01G**

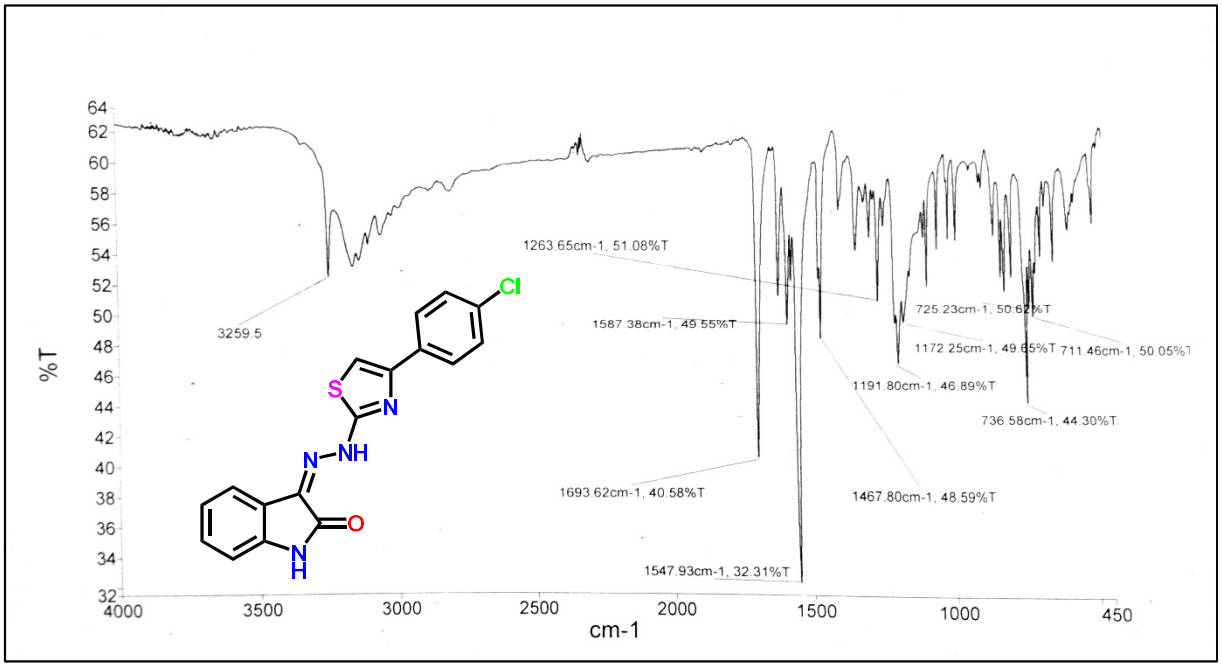

Fonte: Elaborado pelo autor.

A **Figura 26** apresenta os valores do espectro de RMN^{1}H do composto **PA01G**, onde foi constatada a presença de um dupleto integrando para um hidrogênio em 6.95 ppm, correspondente a um hidrogênio do anel aromático. Dois tripletos referentes a dois hidrogênios aromáticos foram identificados em 7.08 e 7.33 ppm. Dois dupletos integrando para um hidrogênio cada um, foram identificados em 7.46 e 7.52 ppm. Em 7.67 ppm encontra-se um singleto integrando para um hidrogênio aromático, sinal característico para indicar formação do anel tiazol. Em 7.90 ppm observa-se um dupleto referente a dois hidrogênios aromáticos. Em 11.23 e em 13.33 ppm aparecem dois singletos referentes aos dois hidrogênios das duas aminas secundárias (NH).

Figura 26. Espectro do RMN'H para a molécula **PA01G**.

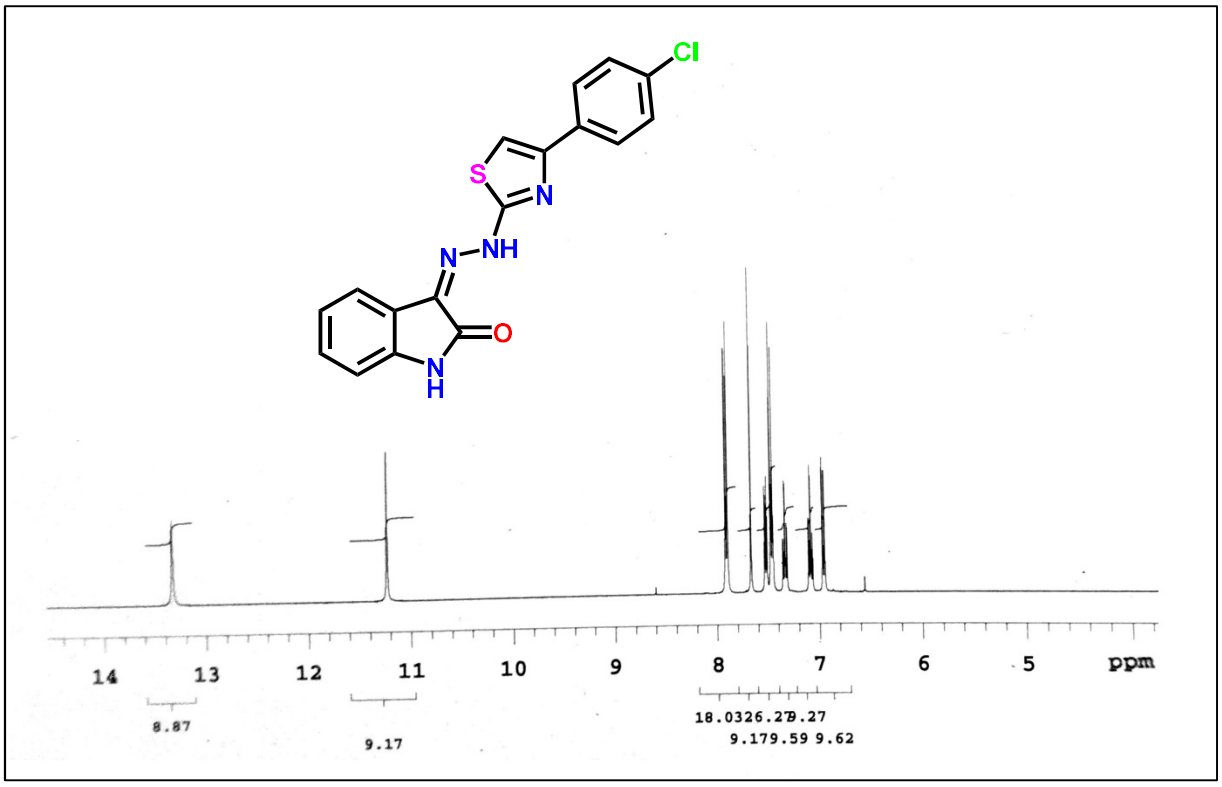

Fonte: Elaborado pelo autor.

Para confirmação dos carbonos presentes na molécula **PA01G**, foi utilizada a ressonância magnética nuclear de carbono 13 (**Figura 27**). Os picos em 107.5, 111.0, 119.8, 122.4 e 130.5 ppm correspondem a carbonos aromáticos. O pico em 119.7 ppm corresponde a um carbono aromático quaternário. Em 127.4 ppm observa-se um pico referente a dois carbonos aromáticos. O mesmo ocorre em 128.7 ppm. O pico em 132.2 ppm corresponde a um carbono quaternário ligado ao grupo fenil. O pico em 132.4 ppm corresponde ao C=N. Em 132.8 ppm observa-se o carbono quaternário aromático ligado ao cloro. Em 141.3 ppm encontra-se o carbono aromático ligado ao NH. Em 149.8 ppm está o C-N Aromático. Em 163.2 ppm está o carbono da carbonila (C=O). Por fim, o pico em 166.2 ppm corresponde ao carbono ligado ao nitrogênio e ao enxofre (N=C-S).

Figura 27. Espectro do RMN^{13}C para a molécula **PA01G**.

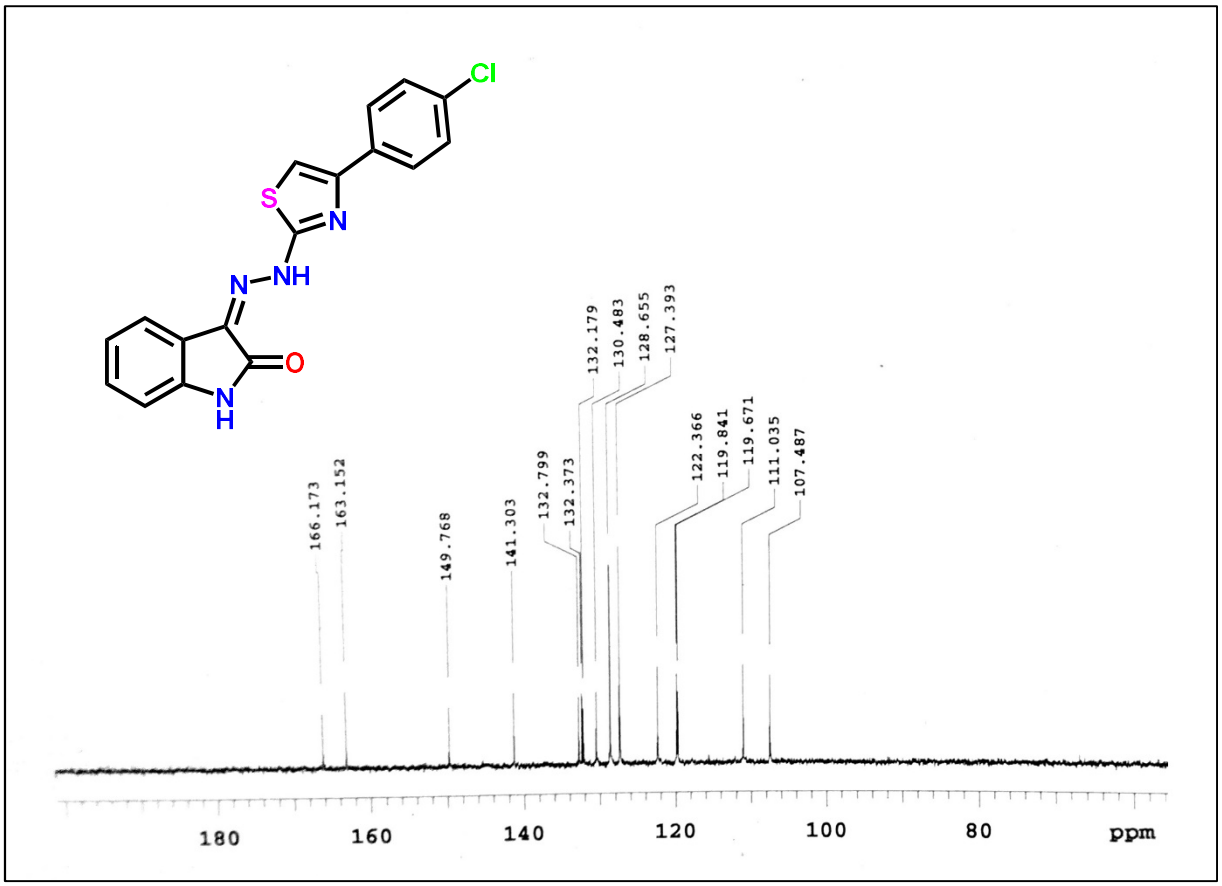

Além das análises descritas anteriormente, também foi possível realizar uma análise cristalográfica, utilizando um cristal obtido do composto **PA01G**. Com essa técnica foi possível confirmar a estrutura dos compostos obtidos. Também foi possível confirmar a planaridade da molécula (**Figura 28**).

Figura 28. Cristalografia da molécula **PA01G**.

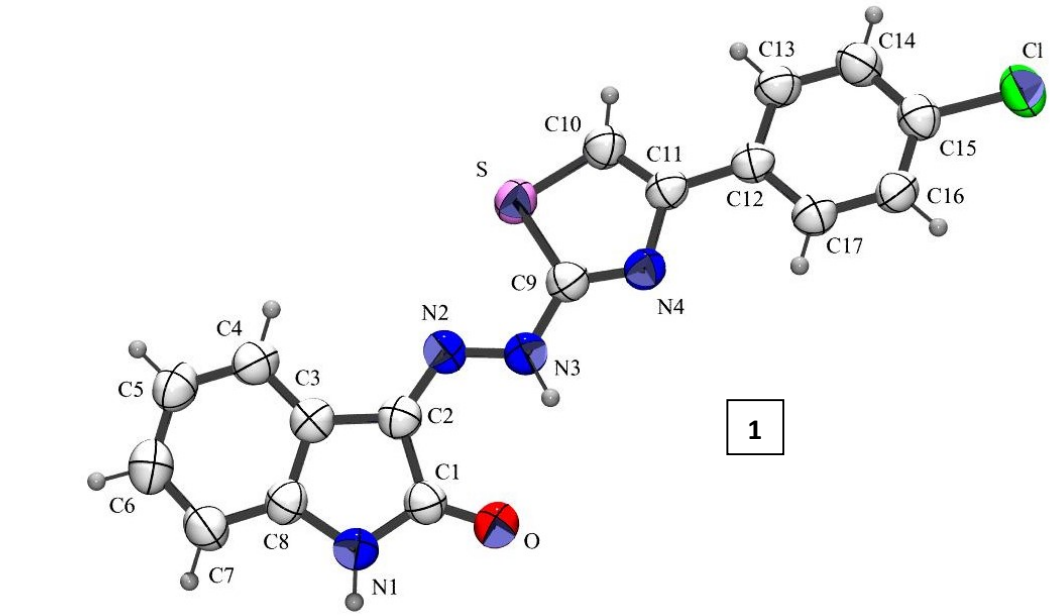

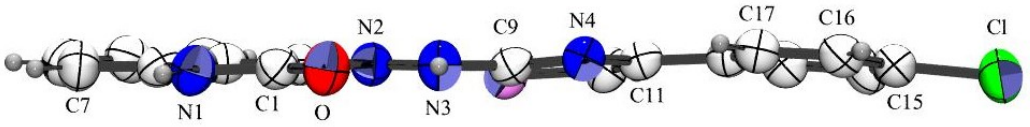

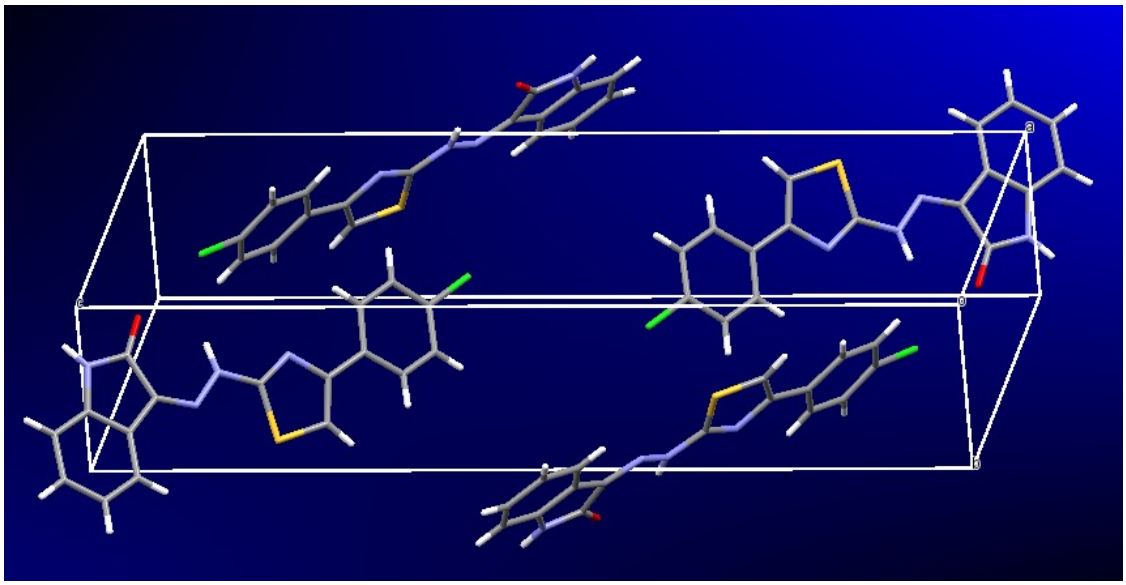

(1) Resolução estrutural da molécula **PA01G** por Difração de Raios X; (2) Projeção paralela aos anéis para visualização de planaridade da molécula; (3) Disposição das 4 moléculas na cela unitária geradas pela simetria do grupo espacial P21/c.

4.2.2 Parte Biológica

4.2.2.1 Avaliação da atividade antitumoral

Tabela 3. Toxicidade das séries PA1A-L, PA3A-L e PA-Int1-Int9.

Compostos	R_1	R_2	R_3	Citotoxicidade em PBMCs (µM)	Viabilidade celular (%) K-562	T-47D	HL-60/mx1	HeLa
			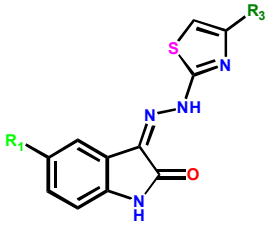					
PA1A	H	-	Ph	>100	104,0	101,0	77,2	68,5
PA1B	H	-	4-Me-Ph	>100	95,3	113,6	77,8	67,8
PA1C	H	-	4-MeO-Ph	>100	100,4	101,1	100,6	66,5
PA1D	H	-	3-NO2-Ph	>100	88,9	101,4	89,0	70,7
PA1E	H	-	4-NO2-Ph	>100	80,1	101,0	96,6	91,0
PA1F	H	-	4-F-Ph	>100	94,4	109,0	84,1	67,1
PA1G	H	-	4-Cl-Ph	>100	102,3	104,6	96,6	70,4
PA1J	H	-	2,4-DiCl-Ph	>100	93,3	90,2	89,6	75,5
PA1K	H	-	Cl-Me	61,43±0,035	128,2	108,5	71,6	79,6
PA1L	H	-	4-Ph-Ph	>100	101,5	92,9	77,5	80,2
PA3A	Cl	-	Ph	>100	123,4	96,2	93,3	74,2
PA3B	Cl	-	4-Me-Ph	>100	96,0	101,8	85,3	70,2
PA3C	Cl	-	4-MeO-Ph	>100	102,4	102,2	97,7	81,5
PA3D	Cl	-	3-NO2-Ph	>100	97,6	104,5	98,7	74,1
PA3E	Cl	-	4-NO2-Ph	>100	92,2	102,1	93,2	**56,0**
PA3F	Cl	-	4-F-Ph	>100	92,8	91,4	88,4	80,7
PA3G	Cl	-	4-Cl-Ph	>100	91,7	95,1	96,8	88,2
PA3J	Cl	-	2,4-DiCl-Ph	>100	110,7	92,3	88,6	72,7
PA3K	Cl	-	Cl-Me	>100	89,7	100,4	101,3	91,1
PA3L	Cl	-	4-Ph-Ph	>100	93,0	91,6	90,6	81,1
			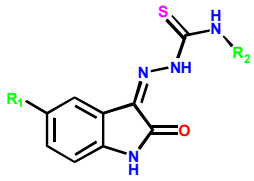					
PA-Int 1	H	H	-	>100	109,0	110,6	89,8	61,3
PA-Int 2	NO_2	H	-	>100	123,7	99,6	100,9	78,5
PA-Int 3	Cl	H	-	>100	124,0	104,2	76,2	80,4
PA-Int 4	H	Ph	-	>100	68,7	**47,7**	**6,3**	**39,2**
PA-Int 5	NO_2	Ph	-	>100	91,3	**52,5**	**10,4**	**28,0**
PA-Int 6	Cl	Ph	-	>100	**46,4**	**42,9**	**7,9**	**47,0**
PA-Int 7	H	Me	-	>100	112,7	89,2	109,6	95,6
PA-Int 8	NO_2	Me	-	>100	131,0	107,0	117,6	79,0
PA-Int 9	Cl	Me	-	>100	100,1	91,9	94,2	95,8

*****Os valores correspondem à média de três experimentos independentes. Os valores de desvio padrão foram menores que 15% em todos os casos.

Os compostos das séries **PA1A-L**, **PA3A-L** e os compostos intermediários **(PA-Int1-9)** foram avaliados quanto à toxicideda frente a células humanas mononucleares do sangue periférico (PBMCs). Como pode ser observado na **Tabela 3**, com excessão do **PA1K**, todos os compostos não apresentaram toxicidade mesmo na dose máxima testada (100 μM). O composto **PA1K** não apresenta um fenil ligado ao tiazol, diferente dos demais compostos da série **1A-L**, o que pode indicar que a presença do grupo fenil é importante na redução da citotoxicidade desses compostos.

Todos os compostos estão sendo testados quanto às suas propriedades antineoplásicas. Os compostos foram testados em quatro linhagens de células tumorais, duas linhagens de células aderentes, T-47D (Carcinoma ductal de mama) e HeLa (Adenocarcinoma cervical), e duas linhagens em suspensão, HL-60/mx1 (Leucemia aguda resistente a Etoposideo, Teniposideo e Bisantreno) e K-562 (Leucemia mielóide crônica), em única dose de 10 μM.

Os resultados, embora não sejam conclusivos, apresentam um prévio padrão de relação entre a estrutura dos compostos e a atividade apresentada até o momento. Os compostos intermediários **PA-Int4**, **PA-Int5** e **PA-Int6** apresentaram uma considerável redução da viabilidade celular das linhagens tumorais testadas, inclusive na linhagem que apresenta resistência a multiplas drogas (HL-60/mx1) (**Tabela 3**). Os três compostos apresentam em comum um fenil em N3. Tais resultados podem indicar que a presença desse substituinte é importante para a atividade antitumoral.

O composto **PA-Int6**, que apresenta, além do grupo fenil no nitrogênio, um cloro em C5 no grupo isatina, reduziu a viabilidade celular das quatro linhagens de cânceres testados. Esse resultado pode reforçar a importância da presença de halogênios nessa posição em isatinas, como já relatado na literatura (VINE *et al.*, 2007; VINE *et al.*, 2009). Com relação aos tiazóis, os dados ainda não são conclusivos.

4.3 Conclusão

Foram obtidos vinte e nove derivados do núcleo isatina, nove tiossemicarbazonas e vinte inéditas tiazolil-hidrazonas, utilizando-se uma metodologia simples e com bons rendimentos. Todos os compostos tiveram suas estruturas elucidadas pelas técnicas de RMN de H^1 e C^{13}, IV e espectroscopia de massas.

A maioria dos compostos não apresentou toxicidade frente a células normais humanas, na dose máxima testada (100 μM). Com relação às propriedades antineoplásicas, resultados preliminares indicam que a presença de um fenil em N3 nas tiossemicarbazonas **PA-Int4**, **PA-Int5** e **PA-Int6** é importante para a atividade antitumoral.

Os dados obtidos até o momento não são conclusivos. Mais testes devem ser realizados em outras linhagens de células tumorais para um melhor estudo da relação estrutura-atividade.

4.4 Perspectivas

Mais testes serão realizados para a obtenção de dados conclusivos com relação às propriedades antitumorais dos compostos apresentados, para um melhor estudo de relação estrutura-atividade.

Uma série de tiazóis derivados do **PA-Int2** (que apresenta o grupo nitro na posição C5 da isatina) será obtida, para uma melhor correlação entre os compostos, podendo-se analisar a importância de cada substituinte para a atividade antitumoral.

Com base nos dados obtidos até o momento, será realizada a síntese de três séries de tiazóis derivados dos três intermediários (**PA-Int4**, **PA-Int5** e **PA-Int6**) que apresentaram inibição das linhagens de células tumorais testadas.

De posse dos resultados biológicos, uma completa Relação Estrutura-Atividade (SAR) poderá ser realizada, para identificar quais substituintes que aumentam o potencial antitumoral dessas moléculas. Também será possível identificar quais moléculas apresentam um maior potencial para tornarem-se novos fármacos para a quimioterapia do câncer.

4.5 Seção experimental

4.5.1 Parte química

Os reagentes foram adquiridos da Acros Organics, Fluka, Vetec ou Sigma-Aldrich, enquanto que os solventes foram provenientes da Vetec ou Dinâmica. Os solventes deuterados (DMSO-d_6, $CDCl_3$, D_2O) são da marca Sigma.

As reações foram acompanhadas em cromatografia de camada delgada (CCD) utilizando sílica-gel 60 contendo indicador fluorescente F_{254} da marca Sigma. As placas cromatográficas foram visualizadas em uma lâmpada ultravioleta (365 ou 254nm).

Os pontos de fusão foram medidos em capilares usando um aparelho de Thomas Hoover e os valores não foram posteriormente corrigidos.

Para todos os compostos, foram feitas as análises de RMN de ^{1}H e ^{13}C e quando necessário, análises bidimensionais (DEPT), bem como a adição de D_2O para a localização dos sinais de NH. Todos os compostos foram solubilizados em DMSO-d_6. Os espectros de RMN ^{1}H e ^{13}C foram adquiridos nos instrumentos Varian modelo Unity Plus (400 MHz para ^{1}H; 100 MHz para ^{13}C) ou Bruker AMX (300 MHz para ^{1}H e 75.5 MHz para o ^{13}C), usando o tetrametilsilano como padrão interno. A multiplicidade dos sinais nos espectros de RMN ^{1}H foram designadas da seguinte forma: s / singleto; d / dubleto; t / tripleto; dd / duplo dupleto; q / quarteto; m / multipleto. Para os espectros de infravermelho, utilizou-se o instrumento Bruker (Modelo IFS 66) usando pastilhas de KBr.

4.5.1.1 Metodologia de Síntese

4.5.1.1.1 Síntese dos compostos intermediários PA-Int1 à PA-Int9: Em balão de fundo redondo, adicionou-se a respectiva isatina (indolina-2,3-diona; 5-nitroindolina-2,3-diona ou 5-cloroindolina-2,3-diona), a respectiva tiossemicabazida (hidrazinacarbotioamida; N-metil-hidrazinacarbotioamida ou N-fenil-hidrazinacarbotioamida) (na proporção 1:1), etanol (20ml) e HCl (7 gotas, cat.). A mistura reacional foi mantida em agitação magnética e refluxo por 3 horas. As reações foram acompanhadas por placa cromatográfica de camada delgada (CCD). O precipitado formado foi filtrado em funil sinterizado, obtendo-se o produto puro.

- **PA-Int1 =** 5,486 mmols indolina-2,3-diona, 5,486 mmols hidrazinacarbotioamida;
- **PA-Int2** = 5,486 mmols 5-nitroindolina-2,3-diona, 5,486 mmols hidrazinacarbotioamida;
- **PA-Int3** = 5,486 mmols 5-cloroindolina-2,3-diona, 5,486 mmols hidrazinacarbotioamida;
- **PA-Int4 =** 5,486 mmols indolina-2,3-diona, 5,486 mmols N-fenil-hidrazinacarbotioamida;
- **PA-Int5** = 5,486 mmols 5-nitroindolina-2,3-diona, 5,486 mmols N-fenil-hidrazinacarbotioamida;
- **PA-Int6** = 5,486 mmols 5-cloroindolina-2,3-diona, 5,486 mmols N-fenil-hidrazinacarbotioamida;
- **PA-Int7** = 5,486 mmols indolina-2,3-diona, 5,486 mmols N-metil-hidrazinacarbotioamida;
- **PA-Int8** = 5,486 mmols 5-nitroindolina-2,3-diona, 5,486 mmols N-metil-hidrazinacarbotioamida;
- **PA-Int9** = 5,486 mmols 5-cloroindolina-2,3-diona, 5,486 mmols N-metil-hidrazinacarbotioamida;

4.5.1.1.2. Síntese da série isatina-hidrazona-tiazóis (PA1A-PA3L): Em balão de fundo redondo, adicionou-se um dos dois intermediários sem substituintes na posição N (PA-Int1: 2-(2-oxoindolin-3-ilideno)hidrazinacarbotioamida ou PA-Int3: 2-(5-cloro-2-oxoindolin-3-ilideno)hidrazinacarbo-tioamida**)**, uma das dez α-halo-cetonas e isopropanol (20ml). A mistura reacional foi mantida sob refluxo por 2 horas. As reações foram acompanhadas por placa cromatográfica de camada delgada (CCD). O precipitado formado foi filtrado em funil sinterizado e recristalizado em THF, obtendo-se o produto puro.

- **PA01A =** 1,398 mmol de **PA-Int1,** 1,398 mmol de 2-bromo-acetofenona;
- **PA01B =** 1,398 mmol de **PA-Int1,** 1,398 mmol de 2-bromo-4'-metil-acetofenona;
- **PA01C =** 1,398 mmol de **PA-Int1,** 1,398 mmol de 2-bromo-4'-metoxi-acetofenona;
- **PA01D =** 1,398 mmol de **PA-Int1,** 1,398 mmol de 2-bromo-3'-nitro-acetofenona;
- **PA01E =** 1,398 mmol de **PA-Int1,** 1,398 mmol de 2-bromo-4'-nitro-acetofenona;
- **PA01F =** 1,398 mmol de **PA-Int1,** 1,398 mmol de 2-bromo-4'-fluor-acetofenona;
- **PA01G =** 1,398 mmol de **PA-Int1,** 1,398 mmol de 2-bromo-4'-cloro-acetofenona;

- **PA01J** = 1,398 mmol de **PA-Int1,** 1,398 mmol de 2, 2',4'-tricloro-acetofenona;
- **PA01K** = 1,398 mmol de **PA-Int1,** 1,398 mmol de 1,3-dicloroacetona;
- **PA01L** = 1,398 mmol de **PA-Int1,** 1,398 mmol de 2-bromo-4'-fenil-acetofenona.
- **PA03A** = 1,398 mmol de **PA-Int3,** 1,398 mmol de 2-bromo-acetofenona;
- **PA03B** = 1,398 mmol de **PA-Int3,** 1,398 mmol de 2-bromo-4'-metil-acetofenona;
- **PA03C** = 1,398 mmol de **PA-Int3,** 1,398 mmol de 2-bromo-4'-metoxi-acetofenona;
- **PA03D** = 1,398 mmol de **PA-Int3,** 1,398 mmol de 2-bromo-3'-nitro-acetofenona;
- **PA03E** = 1,398 mmol de **PA-Int3,** 1,398 mmol de 2-bromo-4'-nitro-acetofenona;
- **PA03F** = 1,398 mmol de **PA-Int3,** 1,398 mmol de 2-bromo-4'-fluor-acetofenona;
- **PA03G** = 1,398 mmol de **PA-Int3,** 1,398 mmol de 2-bromo-4'-cloro-acetofenona;
- **PA03J** = 1,398 mmol de **PA-Int3,** 1,398 mmol de 2, 2',4'-tricloro-acetofenona;
- **PA03K** = 1,398 mmol de **PA-Int3,** 1,398 mmol de 1,3-dicloroacetona;
- **PA03L** = 1,398 mmol de **PA-Int3,** 1,398 mmol de 2-bromo-4'-fenil-acetofenona.

4.5.1.2 Dados físico-químicos e elucidação estrutural

PA-Int1: (Z)-2-(2-oxoindolin-3-ilideno)hidrazinacarbotioamida

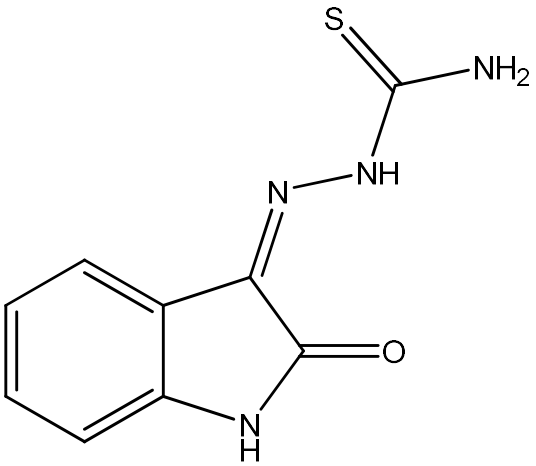

- Rendimento: 62%.
- Ponto de Fusão: 254 ^{o}C.
- Fator de Retenção (R_f): 0,53 (Sistema - 6:4 Tolueno/AcOEt).
- Infravermelho (KBr): 3235 (NH), 1682 e 3145 (HN-C=O), 1498 e 1137 (C=S) cm-1.
- RMN^{1}H (400 MHz, DMSO-d_6): δ 6.92 (d, 1H, *J* 7.6 Hz, ArH), 7.08 (t, 1H, *J* 7.6 Hz, ArH), 7.35 (t, 1H, *J* 7.6 Hz, ArH), 7.65 (d, 1H, *J* 7.6 Hz, ArH), 8.68 (s, 1H, NH_2), 9.04 (s, 1H, NH_2), 11.2 (s, 1H, NH), 12.47 (s, 1H, NH).
- RMN^{13}C (100 MHz, DMSO-d_6): δ 111.0 (CH, Ar), 119.9 (CH, Ar), 120.9 (C-Ar), 122.4 (CH, Ar), 131.2 (CH, Ar), 132.0 (C=N), 142.3 (C-NH, Ar), 162.6 (C=O), 178.7 (C=S).
- Fórmula Molecular: $C_9H_8N_4OS$.
- HRMS: 220,04 $[M+H]^+$.

PA-Int2: (Z)-2-(5-nitro-2-oxoindolin-3-ilideno)hidrazinacarbotioamida

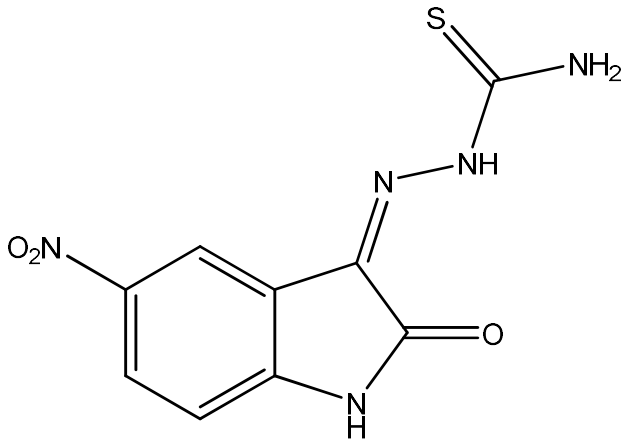

- Rendimento: 60%.
- Ponto de Fusão: 280 ^{o}C.
- Fator de Retenção (R_f): 0,50 (Sistema - 6:4 Tolueno/AcOEt).
- Infravermelho (KBr): 3276 (NH), 1697 e 3195 (HN-C=O), 1481 e 1139 (C=S) cm-1.
- RMN^{1}H (400 MHz, DMSO-d_6): δ 7.1 (d, 1H, *J* 8.4 Hz, ArH), 8.25 (d, 1H, *J* 8.4 Hz, ArH), 8.59 (s, 1H, ArH), 9.02 (s, 1H, NH_2), 9.18 (s, 1H, NH_2), 11.78 (s, 1H, NH), 12.21 (s, 1H, NH).
- RMN^{13}C (100 MHz, DMSO-d_6): δ 111.1 (CH, Ar), 116.4 (CH, Ar), 120.9 (C-Ar), 126.9 (CH, Ar), 129.9 (C=N), 142.7 (C-NO_2, Ar), 147.4 (C-NH, Ar), 162.9 (C=O), 178.8 (C=S).
- Fórmula Molecular: $C_9H_7N_5O_3S$.
- HRMS: 265,03 $[M+H]^{+}$.

PA-Int3: (Z)-2-(5-cloro-2-oxoindolin-3-ilideno)hidrazinacarbotioamida

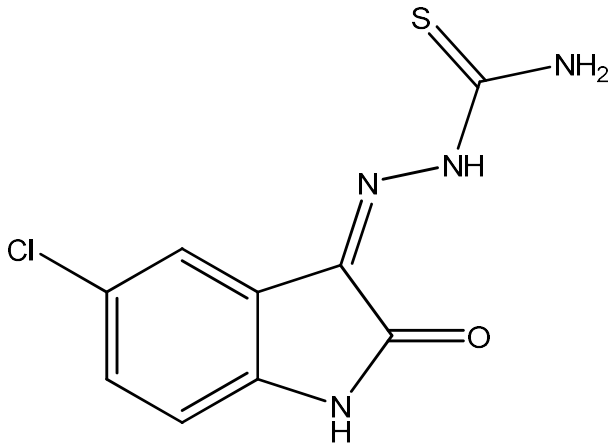

- Rendimento: 90%.
- Ponto de Fusão: 270 ^{o}C.
- Fator de Retenção (R_f): 0,66 (Sistema - 6:4 Tolueno/AcOEt).
- Infravermelho (KBr): 3219 (NH), 1697 e 3164 (HN-C=O), 1496 e 1143 (C=S) cm-1.
- RMN^{1}H (300 MHz, DMSO-d_6): δ 7.05 (d, 1H, *J* 8.4 Hz, ArH), 7.38 (d, 1H, *J* 8.4 Hz, ArH), 7.72 (s, 1H, ArH), 8.2 (s, 1H, NH_2), 8.57 (s, 1H, NH_2), 10.2 (s, 1H, NH), 12.62 (s, 1H, NH).
- RMN^{13}C (75.5 MHz, DMSO-d_6): δ 113.3 (2CH, Ar), 121.5 (C-Ar), 123.1 (CH, Ar), 128.4 (C-Cl, Ar), 131.4 (C=N), 141.8 (C-NH, Ar), 163.3 (C=O), 181.2 (C=S).
- Fórmula Molecular: $C_9H_7ClN_4OS$.
- HRMS: 254,00 $[M+H]^+$.

PA-Int4: (Z)-2-(2-oxoindolin-3-ilideno)-N-fenil-hidrazinacarbotioamida

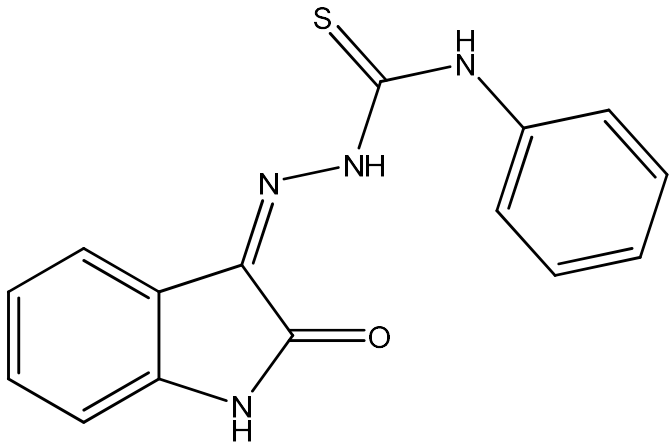

- Rendimento: 65%.
- Ponto de Fusão: 246 ^{o}C.
- Fator de Retenção (R_f): 0,77 (Sistema - 6:4 Tolueno/AcOEt).
- Infravermelho (KBr): 3298 (NH), 1694 (HN-C=O), 1496 e 1148 (C=S) cm-1.
- RMN^{1}H (300 MHz, DMSO-d_6): δ 7.04 (d, 1H, *J* 8.1 Hz, ArH), 7.11 (t, 1H, *J* 7.2 Hz, ArH), 7.25 (t, 2H, *J* 7.2 Hz, ArH), 7.4 (m, 3H, ArH), 7.75 (m, 3H, ArH), 10.14 (s, 1H, NH), 10.37 (s, 1H, NH), 12.95 (s, 1H, NH).
- RMN^{13}C (75.5 MHz, DMSO-d_6): δ 111.9 (CH, Ar), 121.2 (C-Ar), 121.9 (CH, Ar), 123.5 (CH, Ar), 125.3 (CH, Ar), 125.4 (CH, Ar), 126.7 (CH, Ar), 129.2 (2CH, Ar), 132.3 (CH, Ar), 132.5 (Ph-C-NH), 139.5 (C=N), 143.4 (C-NH, Ar), 163.6 (C=O), 177.4 (C=S).
- Fórmula Molecular: $C_{15}H_{12}N_4OS$.
- HRMS: 296,07 $[M+H]^{+}$.

PA-Int5: (Z)-2-(5-nitro-2-oxoindolin-3-ilideno)-N-fenil-hidrazinacarbotioamida

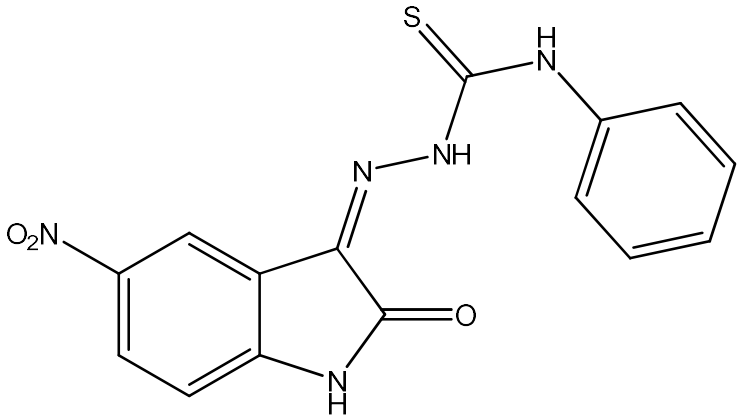

- Rendimento: 75%.
- Ponto de Fusão: 249 ^{o}C.
- Fator de Retenção (R_f): 0,60 (Sistema - 6:4 Tolueno/AcOEt).
- Infravermelho (KBr): 3303 (NH), 1695 e 3175 (HN-C=O), 1484 e 1148 (C=S) cm-1.
- RMN^{1}H (300 MHz, DMSO-d_6): δ 7.1 (d, 1H, *J* 9 Hz, ArH), 7.3 (t, 1H, *J* 6 Hz, ArH), 7.45 (t, 2H, *J* 6 Hz, ArH), 7.6 (d, 2H, *J* 6 Hz, ArH), 8.25 (d, 1H, *J* 9 Hz, ArH), 8.66 (s, 1H, ArH), 11.06 (s, 1H, NH), 11.83 (s, 1H, NH), 12.53 (s, 1H, NH).
- RMN^{13}C (75.5 MHz, DMSO-d_6): δ 111.2 (CH, Ar), 116.7 (CH, Ar), 120.9 (C-Ar), 126.0 (CH, Ar), 126.4 (CH, Ar), 127.0 (2CH, Ar), 128.5 (2CH, Ar), 130.2 (Ph-C-NH), 138.3 (C=N), 142.7 (C-NO_2, Ar), 147.4 (C-NH, Ar), 162.9 (C=O), 176.4 (C=S).
- Fórmula Molecular: $C_{15}H_{11}N_5O_3S$.
- HRMS: 341,06 $[M+H]^{+}$.

PA-Int6: (Z)-2-(5-cloro-2-oxoindolin-3-ilideno)-N-fenil-hidrazinacarbotioamida

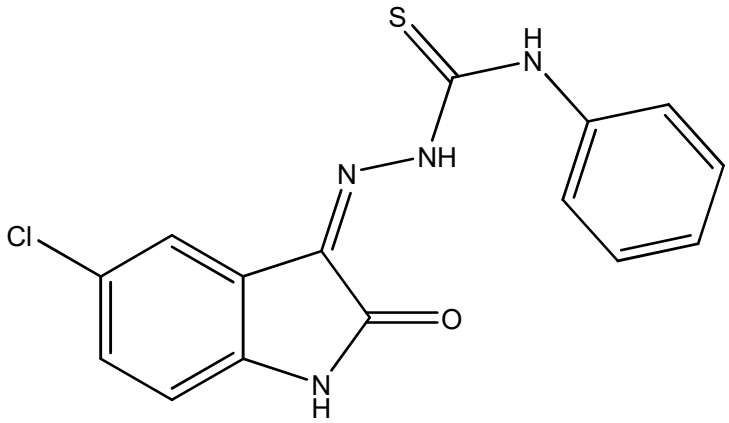

- Rendimento: 79%.
- Ponto de Fusão: 255 ^{o}C.
- Fator de Retenção (R_f): 0,68 (Sistema - 6:4 Tolueno/AcOEt).
- Infravermelho (KBr): 3317 (NH), 1691 e 3172 (HN-C=O), 1487 e 1158 (C=S) cm-1.
- RMN^{1}H (300 MHz, DMSO-d_6): δ 7.29 (t, 1H, *J* 7.5 Hz, ArH), 7.37 (d, 1H, *J* 2.1 Hz, ArH), 7.39 (d, 1H, *J* 2.1 Hz, ArH), 7.44 (t, 2H, *J* 7.5 Hz, ArH), 7.61 (d, 2H, *J* 7.5 Hz, ArH), 7.88 (s, 1H, ArH), 10.88 (s, 1H, NH), 11.33 (s, 1H, NH), 12.61 (s, 1H, NH).
- RMN^{13}C (75.5 MHz, DMSO-d_6): δ 112.5 (CH, Ar), 120.9 (CH, Ar), 121.8 (C-Ar), 125.7 (2CH, Ar), 126.6 (CH, Ar), 128.4 (2CH, Ar), 126.2 (C-Cl, Ar), 130.6 (CH, Ar), 131.0 (C=N), 138.27 (Ph-C-NH), 141.1 (C-NH, Ar), 162.4 (C=O), 176.3 (C=S).
- Fórmula Molecular: $C_{15}H_{11}ClN_4OS$.
- HRMS: 330,03 $[M+H]^{+}$.

PA-Int7: (Z)-N-metil-2-(2-oxoindolin-3-ilideno)hidrazinacarbotioamida

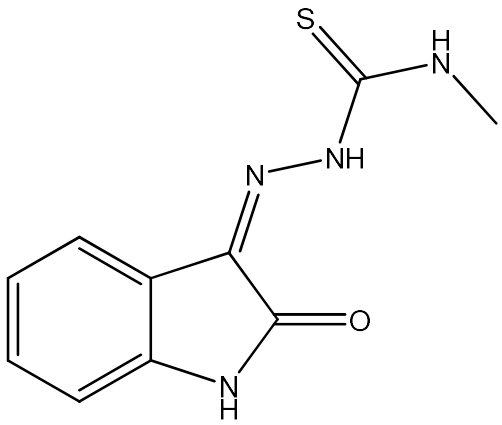

- Rendimento: 73%.
- Ponto de Fusão: 252 ^{o}C.
- Fator de Retenção (R_f): 0,64 (Sistema - 6:4 Tolueno/AcOEt).
- Infravermelho (KBr): 3230 (NH), 1708 e 3169 (HN-C=O), 1546 e 1149 (C=S) cm-1.
- RMN^{1}H (300 MHz, DMSO-d_6): δ 3.08 (d, 3H, *J* 4.8 Hz, CH_3), 6.91 (t, 1H, *J* 7.2 Hz, ArH), 7.09 (t, 1H, *J* 7.2 Hz, ArH), 7.33 (d, 1H, *J* 7.2 Hz, ArH), 7.63 (d, 1H, *J* 7.2 Hz, ArH), 9.23 (q, 1H, *J* 4.8 Hz, NH), 11.19 (s, 1H, NH), 12.59 (s, 1H, NH).
- RMN^{13}C (75.5 MHz, DMSO-d_6): δ 31.3 (CH_3), 111.0 (CH, Ar), 120.6 (CH, Ar), 119.9 (CH, Ar), 121.7 (C-Ar), 122.3 (CH, Ar), 132.4 (C=N), 142.2 (C-NH, Ar), 162.6 (C=O), 177.6 (C=S).
- Fórmula Molecular: $C_{10}H_{10}N_4OS$.
- HRMS: 234,06 $[M+H]^{+}$.

PA-Int8: (Z)-N-metil-2-(5-nitro-2-oxoindolin-3-ilideno)hidrazinacarbotioamida

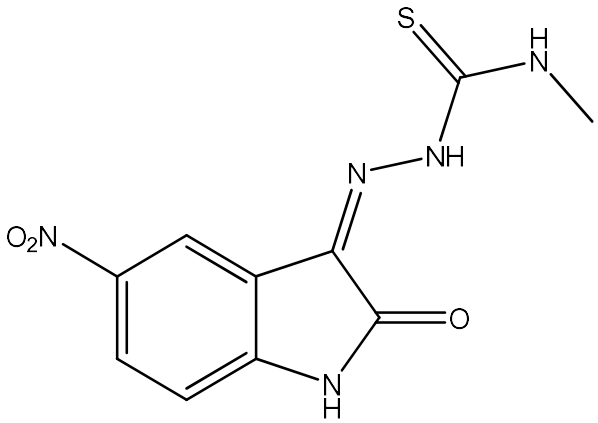

- Rendimento: 77%.
- Ponto de Fusão: 280 °C.
- Fator de Retenção (R_f): 0,62 (Sistema - 6:4 Tolueno/AcOEt).
- Infravermelho (KBr): 3343 (NH), 1622 e 3204 (HN-C=O), 1493 e 1132 (C=S) cm-1.
- RMN^{1}H (300 MHz, DMSO-d_6): δ 3.1 (d, 3H, *J* 4.5 Hz, CH_3), 7.1 (d, 1H, *J* 9 Hz, ArH), 8.24 (d, 1H, *J* 9 Hz, ArH), 8.51 (s, 1H, ArH), 9.49 (q, 1H, *J* 4.5 Hz, NH), 11.75 (s, 1H, NH), 12.34 (s, 1H, NH).
- RMN^{13}C (75.5 MHz, DMSO-d_6): δ 31.3 (CH_3), 111.1 (CH, Ar), 115.9 (CH, Ar), 120.9 (C-Ar), 126.6 (CH, Ar), 129.4 (C=N), 142.7 (C-NO_2, Ar), 147.1 (C-NH, Ar), 162.8 (C=O), 177.5 (C=S).
- Fórmula Molecular: $C_{10}H_9N_5O_3S$.
- HRMS: 279,04 $[M+H]^+$.

PA-Int9: (Z)-2-(5-cloro-2-oxoindolin-3-ilideno)-N-metil-hidrazinacarbotioamida

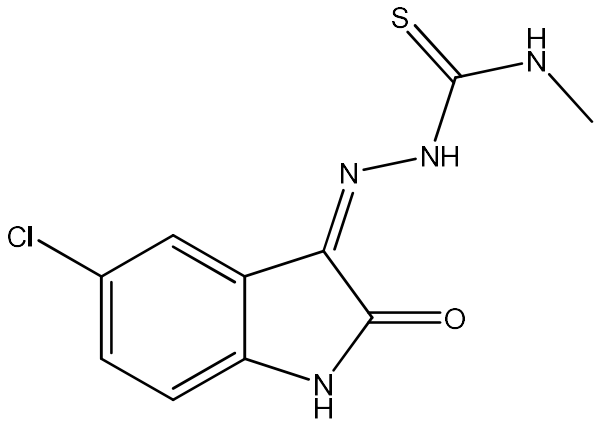

- Rendimento: 78%.
- Ponto de Fusão: 271 ^{o}C.
- Fator de Retenção (R_f): 0,68 (Sistema - 6:4 Tolueno/AcOEt).
- Infravermelho (KBr): 3247 (NH), 1698 (HN-C=O), 1548 e 1199 (C=S) cm-1.
- RMN^{1}H (300 MHz, DMSO-d_6): δ 3.08 (d, 3H, *J* 4.5 Hz, CH_3), 6.91 (d, 1H, *J* 8.1 Hz, ArH), 7.35 (d, 1H, *J* 8.1 Hz, ArH), 7.67 (s, 1H, ArH), 9.33 (q, 1H, *J* 4.5 Hz, NH), 11.27 (s, 1H, NH), 12.39 (s, 1H, NH).
- RMN^{13}C (75.5 MHz, DMSO-d_6): δ 31.3 (CH_3), 112.5 (CH, Ar), 120.2 (CH, Ar), 121.9 (C-Ar), 126.4 (C-Cl, Ar), 130.2 (CH, Ar), 130.2 (C=N), 140.8 (C-NH, Ar), 162.3 (C=O), 177.6 (C=S).
- Fórmula Molecular: $C_{10}H_9ClN_4OS$.
- HRMS: 268,02 $[M+H]^{+}$.

PA-1A: (Z)-3-[2-(4-feniltiazol-2-il)-hidrazona]indolin-2-ona

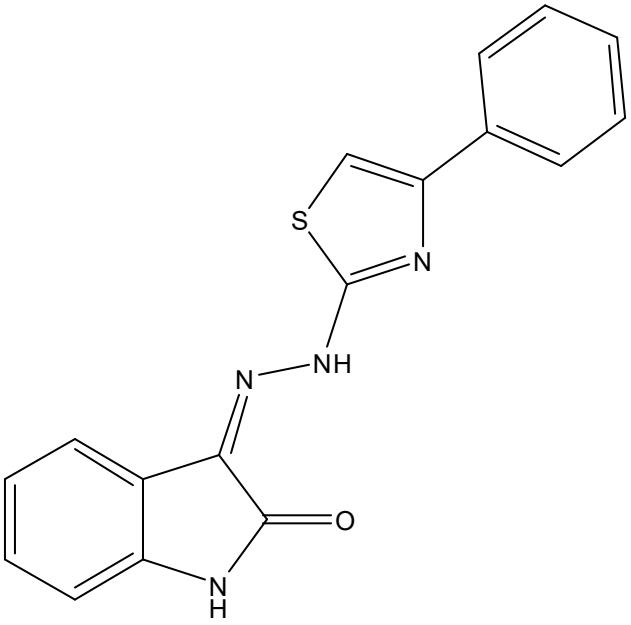

- Ponto de Fusão: 259-260 °C.
- Infravermelho (KBr): 3140 (NH), 1708 (HN-C=O).
- RMN^{1}H (300 MHz, DMSO-d_6): δ 7.02 (d, 2H, ArH), 7.46 (m, 6H, ArH), 7.88 (s, 1H, ArH), 8.41 (d, 1H, ArH), 11.22 (s, 1H, NH), 13.25 (s, 1H, NH).
- RMN^{13}C (75.5 MHz, DMSO-d_6): δ 106.7 (CH, Ar), 110.9 (CH, Ar), 119.7 (CH, Ar), 119.7 (C-Ar), 122.3 (CH, Ar), 125.6 (2CH, Ar), 127.9 (CH, Ar), 128.6 (2CH, Ar), 130.4 (CH, Ar), 132.1 (C-Ph), 133.8 (C=N), 141.2 (C-NH, Ar), 150.8 (C-N, Ar), 163.1 (C=O), 166.0 (N=C-S).
- Fórmula Molecular: $C_{17}H_{12}N_4OS$.
- HRMS: 320,07 $[M+H]^+$.

PA-1B: (Z)-3-[2-(4-toluiltiazol-2-il)-hidrazona]indolin-2-ona

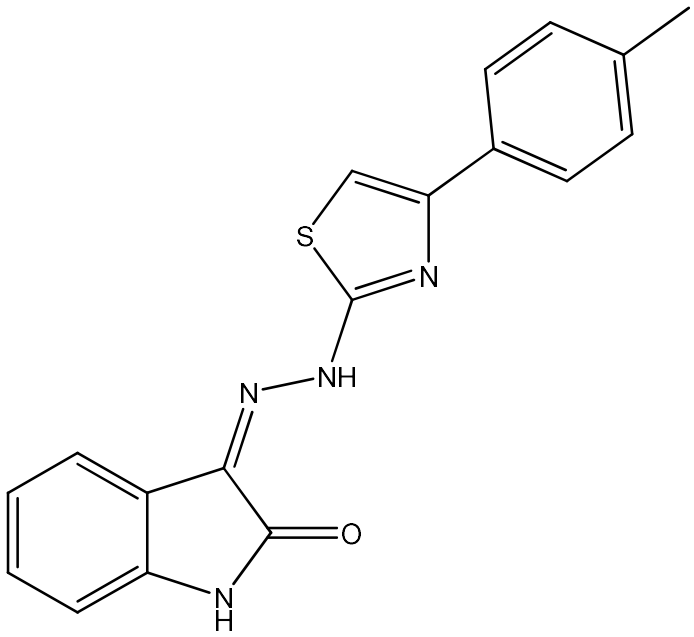

- Ponto de Fusão: 261-263 °C.
- Infravermelho (KBr): 3330 (NH), 1711 (HN-C=O).
- RMN^{1}H (300 MHz, DMSO-d_6): δ 2.32 (s, 3H, CH_3), 6.95 (m, 8H, ArH), 7.77 (s, 1H, ArH), 11.21 (s, 1H, NH), 13.26 (s, 1H, NH).
- RMN^{13}C (75.5 MHz, DMSO-d_6): δ 20.7 (CH_3), 105.8 (CH, Ar), 110.9 (CH, Ar), 119.7 (CH, Ar), 119.7 (C-Ar), 122.3 (CH, Ar), 125.6 (2CH, Ar), 129.1 (2CH, Ar), 130.4 (CH, Ar), 131.1 (CH, Ar), 132.0 (C-Ph), 137.2 (C=N), 141.2 (C-NH, Ar), 150.8 (C-N, Ar), 163.1 (C=O), 165.9 (N=C-S).
- Fórmula Molecular: $C_{18}H_{14}N_4OS$.
- HRMS: 334,09 $[M+H]^+$.

PA-1C: (Z)-3-{2-[4-(4-metoxifenil)tiazol-2-il]-hidrazona}indolin-2-ona

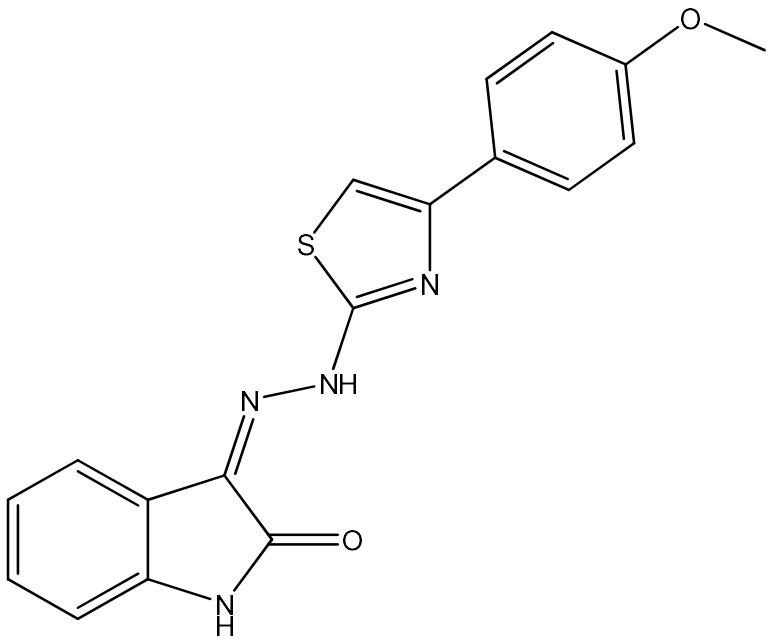

- Ponto de Fusão: 268 °C.
- Infravermelho (KBr): 3171 (NH), 1689 (HN-C=O).
- RMN^{1}H (300 MHz, DMSO-d_6): δ 3.8 (s, 3H, CH_3), 6.97 (d, 1H, *J* 7.5 Hz, ArH), 6.98 (d, 2H, *J* 8.7 Hz, ArH), 7.09 (t, 1H, *J* 7.5 Hz, ArH), 7.34 (t, 1H, *J* 7.5 Hz, ArH), 7.43 (s, 1H, ArH), 7.54 (d, 1H, *J* 7.5 Hz, ArH), 7.83 (d, 2H, *J* 8.7 Hz, ArH), 11.2 (s, 1H, NH), 13.32 (s, 1H, NH).
- RMN^{13}C (75.5 MHz, DMSO-d_6): δ 55.07 (CH_3), 104.5 (CH, Ar), 110.9 (CH, Ar), 113.9 (2CH, Ar), 119.7 (CH, Ar), 119.7 (C-Ar), 122.3 (CH, Ar), 126.8 (C-Ph), 127.0 (2CH, Ar), 130.3 (CH, Ar), 131.8 (C=N), 141.2 (C-NH, Ar), 150.9 (C-N, Ar), 159.0 (C-O, Ar), 163.1 (C=O), 165.8 (N=C-S).
- Fórmula Molecular: $C_{18}H_{14}N_4O_2S$.
- HRMS: 350,08 $[M+H]^+$.

PA-1D: (Z)-3-{2-[4-(3-nitrofenil)tiazol-2-il]-hidrazona}indolin-2-ona

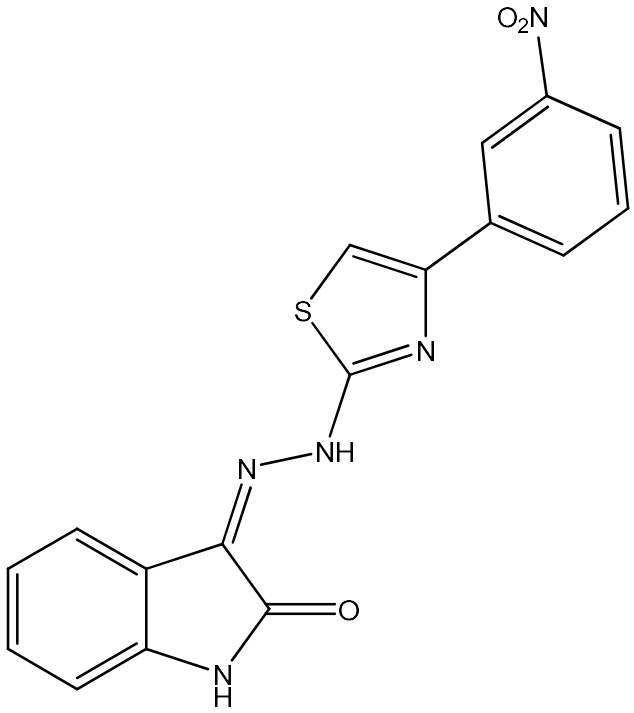

- Ponto de Fusão: 278-279 °C.
- Infravermelho (KBr): 3381 (NH), 1698 e 3181 (HN-C=O).
- RMN^{1}H (300 MHz, DMSO-d_6): δ 6.97 (d, 1H, *J* 7.5 Hz, ArH), 7.1 (t, 1H, *J* 7.5 Hz, ArH), 7.36 (t, 1H, *J* 7.5 Hz, ArH), 7.55 (d, 1H, *J* 7.5 Hz, ArH), 7.73 (t, 1H, *J* 7.8 Hz, ArH), 7.94 (s, 1H, ArH), 8.18 (d, 1H, *J* 7.8 Hz, ArH), 8.35 (d, 1H, *J* 7.8 Hz, ArH), 8.68 (s, 1H, ArH), 11.22 (s, 1H, NH), 13.37 (s, 1H, NH).
- RMN^{13}C (75.5 MHz, DMSO-d_6): δ 105.0 (CH, Tiazol), 119.2 (CH, Ar), 120.7 (CH-Ar), 123.0 (CH, Ar), 124.2 (CH, Ar), 125.6 (CH, Ar), 126.3 (CH, Ar), 128.9 (CH, Ar), 133.1 (CH, Ar), 134.2 (C=N), 139.0 (C, Ar), 141.3 (C-NH, Ar), 150.0 (C-N, Tiazol), 148.2 (C-NO_2, Ar), 169.1 (C=O), 170.5 (N=C-S, Tiazol).
- Fórmula Molecular: $C_{17}H_{11}N_5O_3S$.
- HRMS: 365,06 $[M+H]^+$.

PA-1E: (Z)-3-{2-[4-(4-nitrofenil)tiazol-2-il]-hidrazona}indolin-2-ona

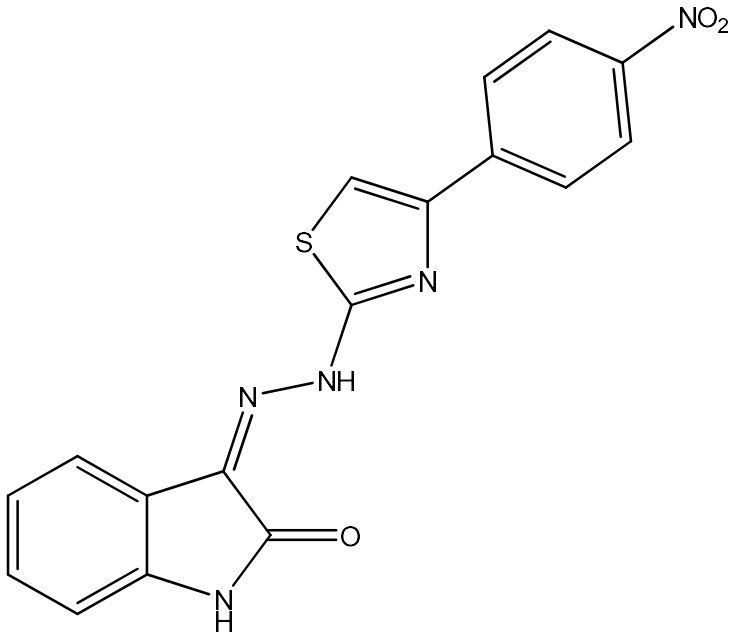

- Ponto de Fusão: 273 °C.
- Infravermelho (KBr): 3169 (NH), 1692 (HN-C=O).
- RMN^{1}H (300 MHz, DMSO-d_6): δ 6.96 (d, 1H, *J* 7.5 Hz, ArH), 7.09 (t, 1H, *J* 7.5 Hz, ArH), 7.34 (t, 1H, *J* 7.5 Hz, ArH), 7.53 (d, 1H, *J* 7.5 Hz, ArH), 7.96 (s, 1H, ArH), 8.15 (d, 2H, *J* 9 Hz, ArH), 8.26 (d, 2H, *J* 9 Hz, ArH), 11.21 (s, 1H, NH), 13.36 (s, 1H, NH).
- RMN^{13}C (75.5 MHz, DMSO-d_6): δ 110.9 (CH, Ar), 111.2 (CH, Ar), 115.6 (CH, Ar), 119.8 (C-Ar), 122.3 (CH, Ar), 123.9 (2CH, Ar), 126.5 (2CH, Ar), 130.6 (CH, Ar), 136.4 (C=N), 139.8 (C-Ph), 141.3 (C-NH, Ar), 146.5 (C-NO_2, Ar) 148.8 (C-N, Ar), 163.0 (C=O), 166.5 (N=C-S).
- Fórmula Molecular: $C_{17}H_{11}N_5O_3S$.
- HRMS: 365,06 $[M+H]^+$.

PA-1F: (Z)-3-{2-[4-(4-fluorofenil)tiazol-2-il]-hidrazona}indolin-2-ona

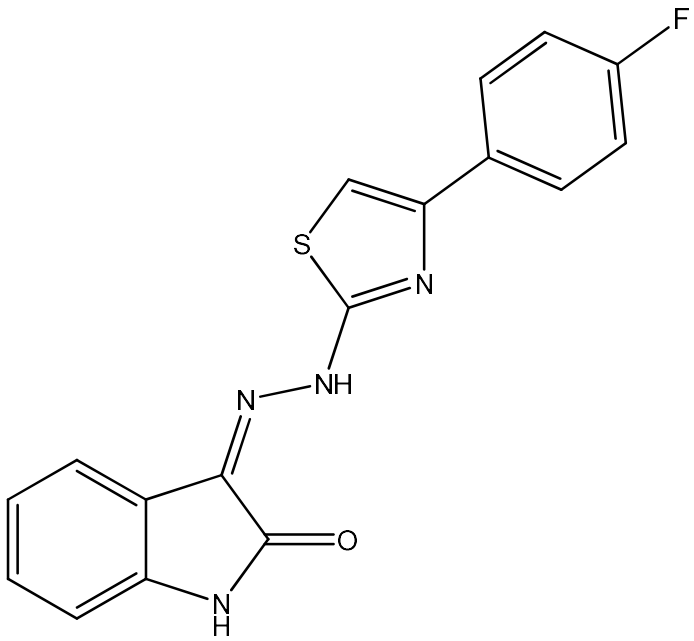

- Ponto de Fusão: 265-267 ^{o}C.
- Infravermelho (KBr): 3243 (NH), 1675 (HN-C=O).
- RMN^{1}H (400 MHz, DMSO-d_6): δ 6.95 (d, 1H, *J* 7.6 Hz, ArH), 7.07 (t, 1H, *J* 7.6 Hz, ArH), 7.22 (d, 1H, *J* 8.8 Hz, ArH), 7.24 (d, 1H, *J* 8.8 Hz, ArH), 7.32 (t, 1H, *J* 7.6 Hz, ArH), 7.51 (d, 1H, *J* 7.6 Hz, ArH), 7.57 (s, 1H, ArH), 7.91 (d, 1H, *J* 8.8 Hz, ArH), 7.93 (d, 1H, *J* 8.8 Hz, ArH), 11.2 (s, 1H, NH), 13.32 (s, 1H, NH).
- RMN^{13}C (100 MHz, DMSO-d_6): δ 106.5 (CH, Ar), 111.0 (CH, Ar), 115.4 (CH, Ar), 115.6 (CH, Ar), 119.7 (C-Ar), 119.8 (CH, Ar), 122.4 (CH, Ar), 127.7 (CH, Ar), 127.8 (CH, Ar), 130.4 (CH, Ar), 130.6 (C-Ph), 132.1 (C=N), 141.3 (C-NH, Ar), 150.0 (C-N, Ar), 160.6 (C-F, Ar), 163.2 (C=O), 166.1 (N=C-S).
- Fórmula Molecular: $C_{17}H_{11}FN_4OS$.
- HRMS: 338,06 $[M+H]^{+}$.

PA-1G: (Z)-3-{2-[4-(4-clorofenil)tiazol-2-il]-hidrazona}indolin-2-ona

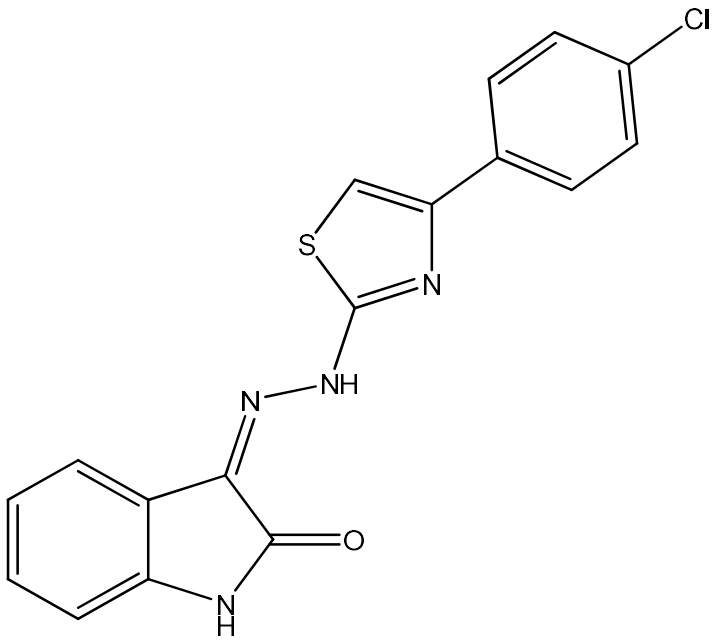

- Ponto de Fusão: 279-280 °C.
- Infravermelho (KBr): 3260 (NH), 1693 (HN-C=O).
- RMN^{1}H (400 MHz, DMSO-d_6): δ 6.95 (d, 1H, *J* 7.2 Hz, ArH), 7.08 (t, 1H, *J* 7.2 Hz, ArH), 7.33 (t, 1H, *J* 7.2 Hz, ArH), 7.46 (d, 2H, *J* 8.8 Hz, ArH), 7.52 (d, 1H, *J* 7.2 Hz, ArH), 7.67 (s, 1H, ArH),7.90 (d, 2H, *J* 8.8 Hz, ArH), 11.23 (s, 1H, NH), 13.33 (s, 1H, NH).
- RMN^{13}C (100 MHz, DMSO-d_6): δ 107.5 (CH, Ar), 111.0 (CH, Ar), 119.7 (C-Ar), 119.8 (CH, Ar), 122.4 (CH, Ar), 127.4 (2CH, Ar), 128.7 (2CH, Ar), 130.5 (CH, Ar), 132.2 (C-Ph), 132.4 (C=N), 132.8 (C-Cl, Ar), 141.3 (C-NH, Ar), 149.8 (C-N, Ar), 163.2 (C=O), 166.2 (N=C-S).
- Fórmula Molecular: $C_{17}H_{11}ClN_4OS$.
- HRMS: 354,03 $[M+H]^+$.

PA-1J: (Z)-3-{2-[4-(2,4-diclorofenil)tiazol-2-il]-hidrazona}indolin-2-ona

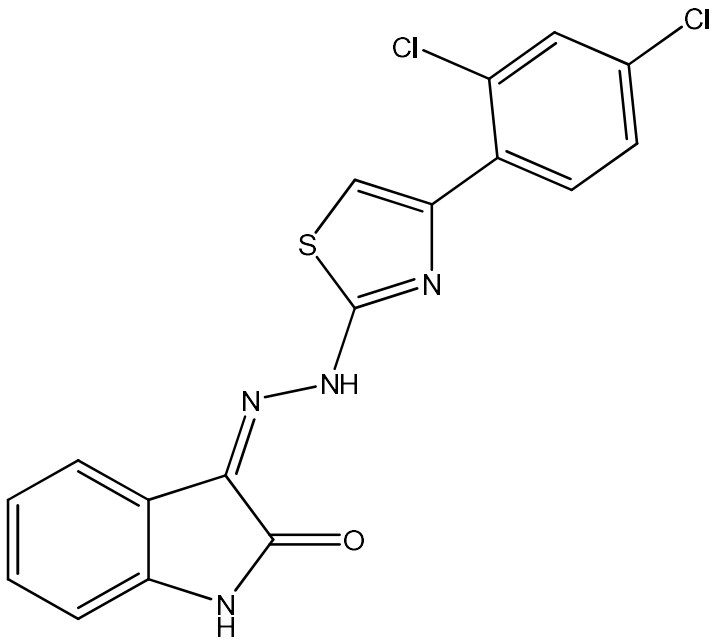

- Ponto de Fusão: 285-286 °C.
- Infravermelho (KBr): 3447 (NH), 1698 e 3264 (HN-C=O).
- RMN^{1}H (400 MHz, DMSO-d_6): δ 6.97 (d, 1H, *J* 7.6 Hz, ArH), 7.1 (t, 1H, *J* 7.6 Hz, ArH), 7.35 (t, 1H, *J* 7.6 Hz, ArH), 7.51 (d, 1H, *J* 8.8 Hz, ArH), 7.55 (d, 1H, *J* 7.6 Hz, ArH), 7.69 (s, 1H, ArH), 7.7 (s, 1H, ArH), 7.94 (d, 1H, *J* 8.8 Hz, ArH), 11.2 (s, 1H, NH), 13.32 (s, 1H, NH).
- RMN^{13}C (100 MHz, DMSO-d_6): δ 110.9 (CH, Ar), 112.2 (CH, Ar), 119.8 (CH, Ar), 119.8 (C-Ar), 122.3 (CH, Ar), 127.4 (2CH, Ar), 129.7 (CH, Ar), 130.5 (CH, Ar), 131.4 (C-Ph), 131.4 (C=N), 132.3 (2CH, Ar), 132.8 (C-Cl, Ar), 141.2 (C-NH, Ar), 163.0 (C=O).
- Fórmula Molecular: $C_{17}H_{10}Cl_2N_4OS$.
- HRMS: 388,00 $[M+H]^+$.

PA-1K: (Z)-3-{2-[4-(clorometil)tiazol-2-il]-hidrazona}indolin-2-ona

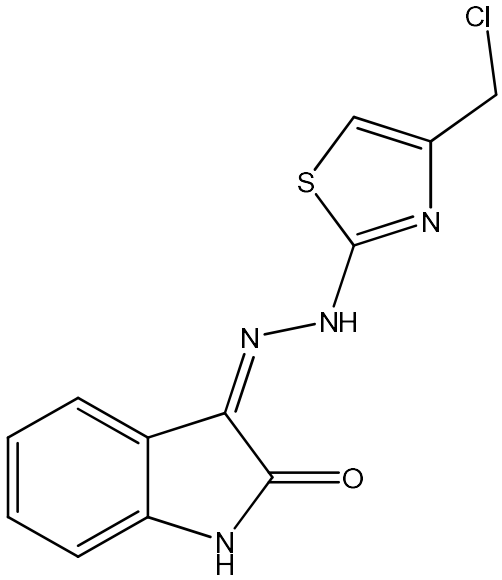

- Infravermelho (KBr): 3180 (NH), 1687 (HN-C=O).
- RMN^{1}H (300 MHz, DMSO-d_6): δ 4.67 (s, 2H, CH_2), 6.95 (d, 1H, *J* 7.8 Hz, ArH), 7.06 (t, 1H, *J* 7.8 Hz, ArH), 7.24 (s, 1H, ArH), 7.32 (t, 1H, *J* 7.8 Hz, ArH), 7.49 (d, 1H, *J* 7.8 Hz, ArH), 11.26 (s, 1H, NH), 13.26 (s, 1H, NH).
- RMN^{13}C (75.5 MHz, DMSO-d_6): δ 111.1 (CH, Ar), 111.7 (CH, Ar), 119.6 (C-Ar), 119.8 (CH, Ar), 122.4 (2CH, Ar), 130.5 (CH, Ar), 132.2 (C=N), 141.4 (C-NH, Ar), 148.5 (C-N, Ar), 163.1 (C=O), 166.5 (N=C-S).
- Fórmula Molecular: $C_{12}H_9ClN_4OS$.
- HRMS: 292,02 $[M+H]^+$.

PA-1L: (Z)-3-{2-[4-(bifenil-4-il)tiazol-2-il]-hidrazona}indolin-2-ona

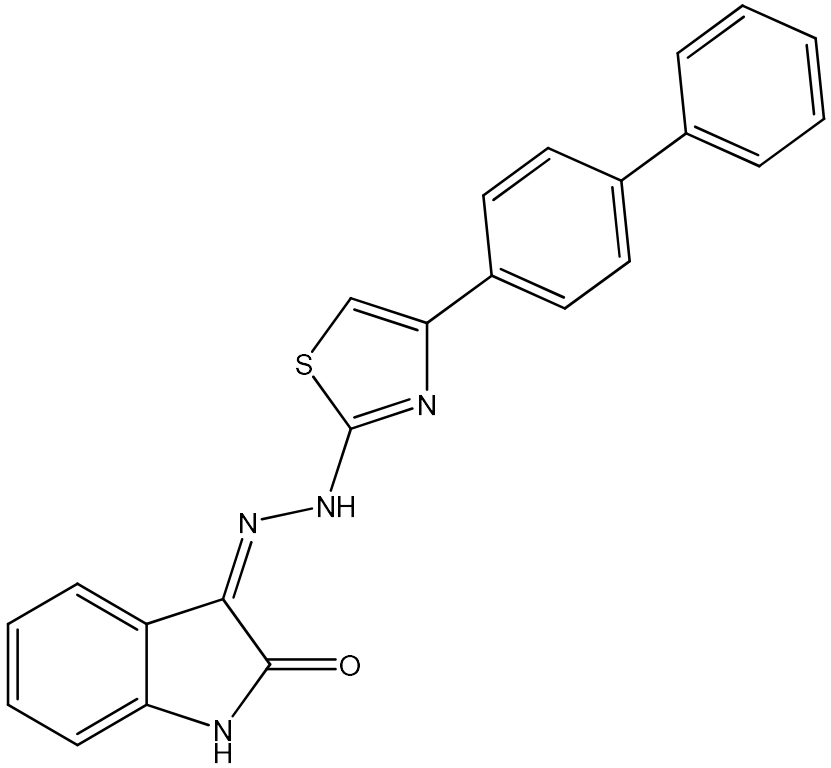

- Fórmula Molecular: $C_{23}H_{16}N_4OS$.
- Peso Molecular: 396,46 g/mol.
- Infravermelho (KBr): 3111 (NH), 1689 (HN-C=O).
- RMN^{1}H (300 MHz, DMSO-d_6): δ 6.98 (d, 2H, *J* 7.2 Hz, ArH), 7.11 (t, 1H, *J* 7.2 Hz, ArH), 7.36 (t, 1H, *J* 7.2 Hz, ArH), 7.38 (t, 1H, *J* 7.2 Hz, ArH), 7.48 (t, 2H, *J* 7.2 Hz, ArH), 7.56 (d, 1H, *J* 7.2 Hz, ArH), 7.68 (s, 1H, ArH), 7.72 (d, 2H, *J* 7.2 Hz, ArH), 7.75 (d, 2H, *J* 7.2 Hz, ArH), 8.0 (d, 2H, *J* 7.2 Hz, ArH), 11.22 (s, 1H, NH), 13.37 (s, 1H, NH).
- RMN^{13}C (75.5 MHz, DMSO-d_6): δ 105.2 (CH, Tiazol), 119.0 (C-Ar), 124.0 (CH-Ar), 125.4 (CH, Ar), 127.0 (2CH, Ar), 127.8 (CH, Ar), 127.9 (2CH, Ar), 128.1 (2CH, Ar), 129.3 (2CH, Ar), 129.5 (CH,Ar), 131.4 (CH, Ar), 132.0 (C, Ar), 133.2 (C=N), 139.5 (C-NH, Ar), 141.0 (2C, Ar), 150.0 (C, Tiazol) 168.6 (C=O), 171,8 (N=C-S).
- Fórmula Molecular: $C_{23}H_{16}N_4OS$.
- HRMS: 396,10 $[M+H]^+$.

PA-3A: (Z)-5-cloro-3-[2-(4-feniltiazol-2-il)-hidrazona]indolin-2-ona

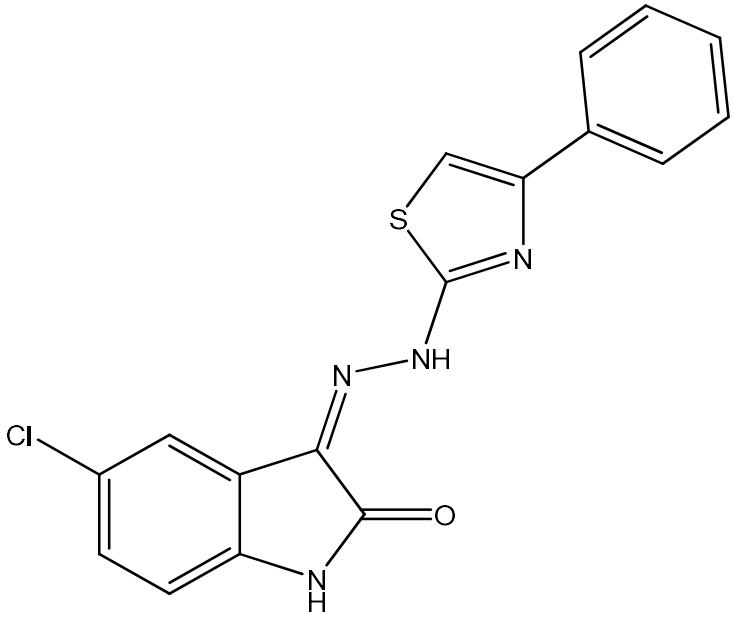

- Peso Molecular: 354,81 g/mol.
- Infravermelho (KBr): 3126.6 (NH), 1709.9 (HN-C=O).
- RMN^{1}H (300 MHz, DMSO-d_6): δ 6.97 (d, 1H, ArH), 7.33-7.9 (m, 8H, ArH), 11.36 (s, 1H, NH), 13.27 (s, 1H, NH).
- RMN^{13}C (75.5 MHz, DMSO-d_6): δ 107.3 (CH, Tiazol), 112.56 (CH, Ar), 119.29 (C-Ar), 119.29 (CH, Ar), 121.46 (CH, Ar), 125.65 (CH, Ar), 125.7 (CH, Ar), 126.56 (CH, Ar), 128.02 (CH, Ar), 128.7 (CH, Ar), 128.89 (CH, Ar), 129.78 (CH, Ar), 130.97 (C-Cl, Ar), 133.84 (C=N), 139.89 (C-NH, Ar), 151.03 (C-N, Ar), 162.96 (C=O), 165.8 (N=C-S).
- Fórmula Molecular: $C_{17}H_{11}ClN_4OS$.
- HRMS: 354,03 $[M+H]^+$.

PA-3B: (Z)-5-cloro-3-[2-(4-*p*-toluiltiazol-2-il)-hidrazona]indolin-2-ona

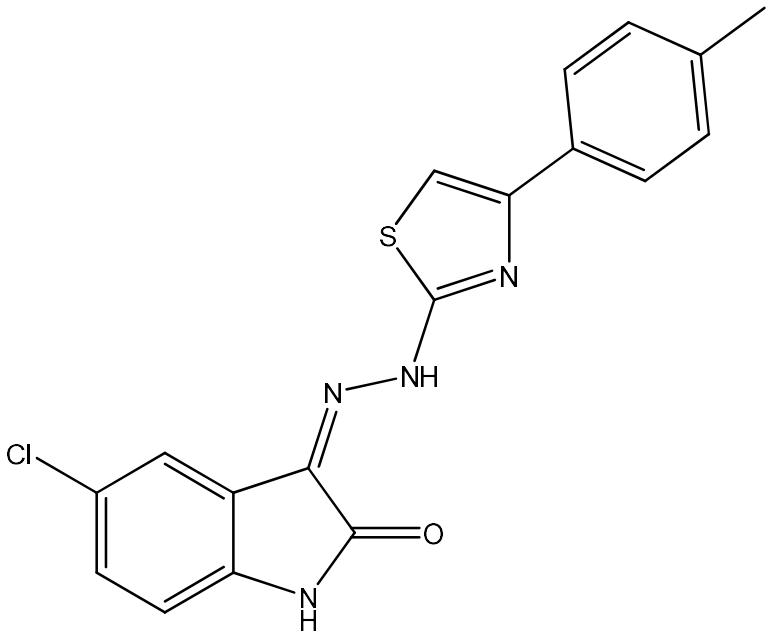

- Peso Molecular: 368,84 g/mol.
- Infravermelho (KBr): 3159.3 (NH), 1686.2 (HN-C=O).
- RMN^{1}H (300 MHz, DMSO-d_6): δ 2.32 (s, 3H, CH_3), 6.97 (d, 1H, ArH), 7.22 (d, 1H, ArH), 7.37 (d, 1H, ArH), 7.5 (s, 1H, ArH), 7.58 (s, 1H, ArH), 7.74 (s, 1H, ArH), 7.78 (s, 1H, ArH), 11.35 (s, 1H, NH), 13.31 (s, 1H, NH).
- RMN^{13}C (75.5 MHz, DMSO-d_6): δ 20.81 (CH_3), 106.36 (CH, Tiazol), 112.49 (CH, Ar), 119.2 (CH, Ar), 120.6 (CH-Ar), 125.52 (CH, Ar), 125.62 (CH, Ar), 129.25 (CH, Ar), 130.4 (C-Cl), 139.84 (C=N), 140.97 (C-NH, Ar), 151.13 (C-N, Ar), 162.36 (C=O), 165.67 (N=C-S).
- Fórmula Molecular: $C_{18}H_{13}ClN_4OS$.
- HRMS: 368,05 $[M+H]^+$.

PA-3C: (Z)-5-cloro-3-{2-[4-(4-metoxifenil)tiazol-2-il]-hidrazona}indolin-2-ona

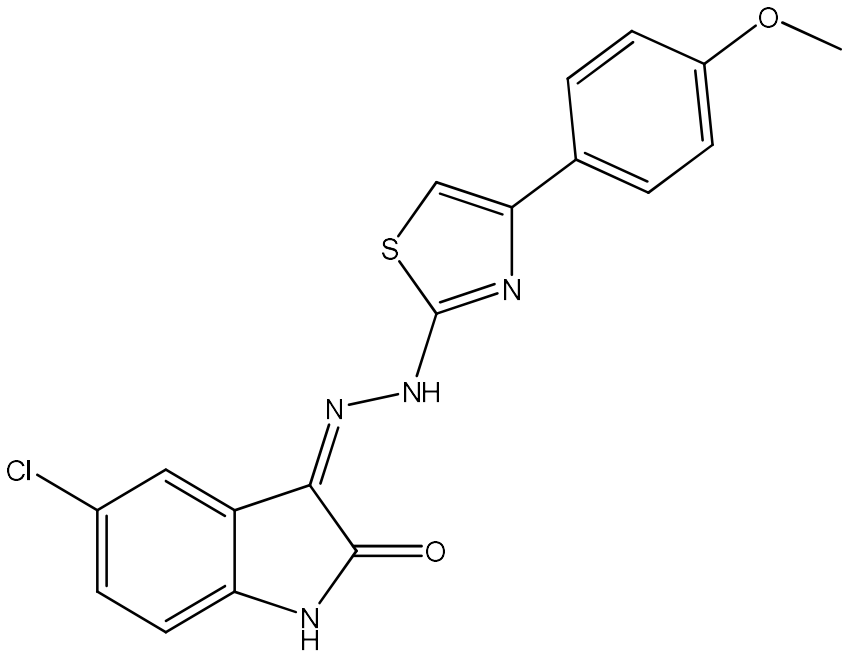

- Peso Molecular: 384,84 g/mol.
- Infravermelho (KBr): 1615.9 (HN-C=O).
- RMN^{1}H (300 MHz, DMSO-d_6): δ 3.78 (s, 3H, CH_3), 6.96-7.82 (m, 8H, ArH), 10.54 (s, 1H, NH), 11.30 (s, 1H, NH).
- RMN^{13}C (75.5 MHz, DMSO-d_6): δ 55.1 (CH_3), 105.0 (CH, Tiazol), 112.4 (CH, Ar), 114.0 (CH, Ar), 119.1 (CH, Ar), 120.6 (CH-Ar), 125.0 (CH, Ar), 126.0 (CH, Ar), 129.0 (CH, Ar), 130.4 (C-Cl, Ar), 139.84 (C=N), 140.97 (C-NH, Ar), 151.0 (C-N, Tiazol), 160.0 (C-O, Ar), 163.0 (C=O), 165.0 (N=C-S, Tiazol).
- Fórmula Molecular: $C_{18}H_{13}ClN_4O_2S$.
- HRMS: 384,04 $[M+H]^+$.

PA-3D: (Z)-5-cloro-3-{2-[4-(3-nitrofenil)tiazol-2-il]-hidrazona}indolin-2-ona

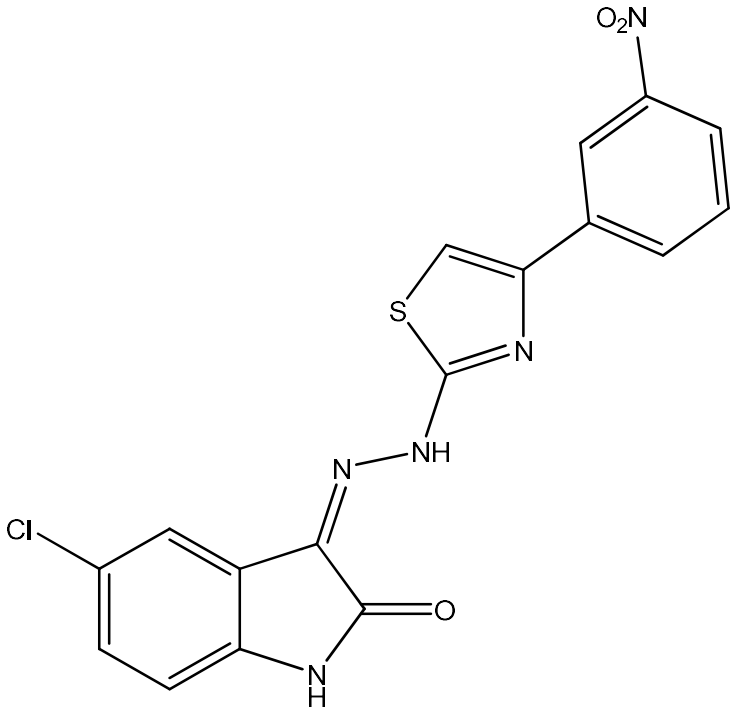

- Peso Molecular: 399,81 g/mol.
- Infravermelho (KBr): 3258.7 (NH), 1692.4 (HN-C=O).
- RMN^{1}H (300 MHz, DMSO-d_6): δ 6.96 (d, 2H, ArH), 7.36 (d, 1H, ArH), 7.51 (d, 1H, ArH), 7.97 (s, 1H, ArH), 8.66 (s, 1H, ArH), 8.78 (s, 1H, ArH), 11.35 (s, 1H, NH), 13.35 (s, 1H, NH).
- RMN^{13}C (75.5 MHz, DMSO-d_6): δ 105.1 (CH, Tiazol), 119.1 (CH, Ar), 120.6 (CH-Ar), 124.0 (CH, Ar), 125.3 (CH, Ar), 126.0 (CH, Ar), 128.9 (CH, Ar), 130.5 (C-Cl, Ar), 133.0 (CH, Ar), 134.0 (C=N), 139.0 (C, Ar), 141.0 (C-NH, Ar), 150.0 (C-N, Tiazol), 148.0 (C-NO_2, Ar), 169.0 (C=O), 170.0 (N=C-S, Tiazol).
- Fórmula Molecular: $C_{17}H_{10}ClN_5O_3S$.
- HRMS: 399,02 $[M+H]^+$.

PA-3E: (Z)-5-cloro-3-{2-[4-(4-nitrofenil)tiazol-2-il]-hidrazona}indolin-2-ona

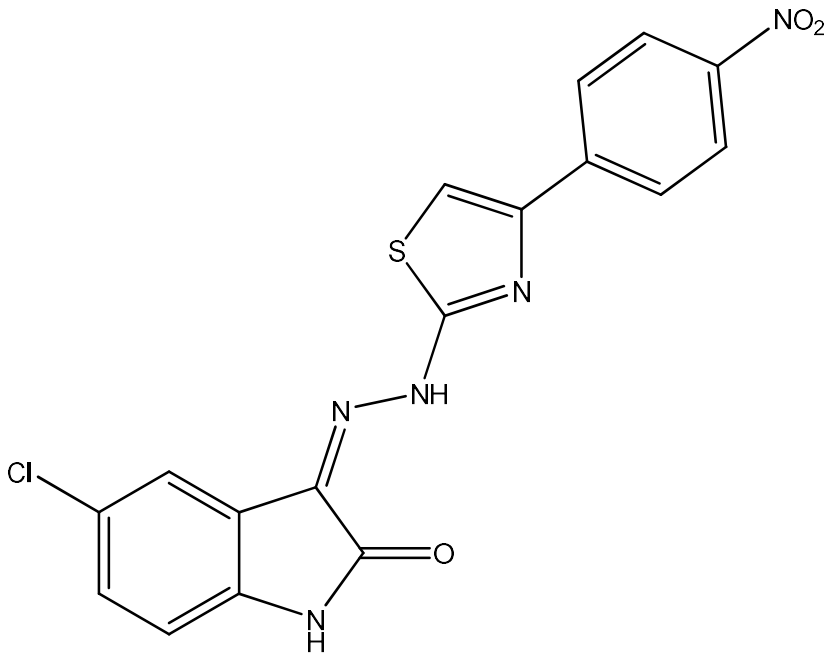

- Peso Molecular: 399,81 g/mol.
- Infravermelho (KBr): 3342.5 (NH), 1683.9 (HN-C=O).
- RMN^{1}H (300 MHz, DMSO-d_6): δ 6.98 (d, 1H, ArH), 7.37 (d, 1H, ArH), 7.52 (s, 1H, ArH), 8.0 (s, 1H, ArH), 8.16 (s, 2H, ArH), 8.27 (d, 2H, ArH), 11.32 (s, 1H, NH), 13.35 (s, 1H, NH).
- RMN^{13}C (75.5 MHz, DMSO-d_6): δ 105.0 (CH, Tiazol), 119.1 (CH, Ar), 120.6 (CH-Ar), 124.0 (CH, Ar), 125.0 (CH, Ar), 126.0 (CH, Ar), 129.0 (CH, Ar), 130.4 (C-Cl, Ar), 134.0 (C=N), 139.0 (C, Ar), 140.0 (C-NH, Ar), 150.0 (C-N, Tiazol), 148.0 (C-NO_2, Ar), 169.0 (C=O), 170.0 (N=C-S, Tiazol).
- Fórmula Molecular: $C_{17}H_{10}ClN_5O_3S$.
- HRMS: 399,02 $[M+H]^+$.

PA-3F: (Z)-5-cloro-3-{2-[4-(4-fluorofenil)tiazol-2-il]-hidrazona}indolin-2-ona

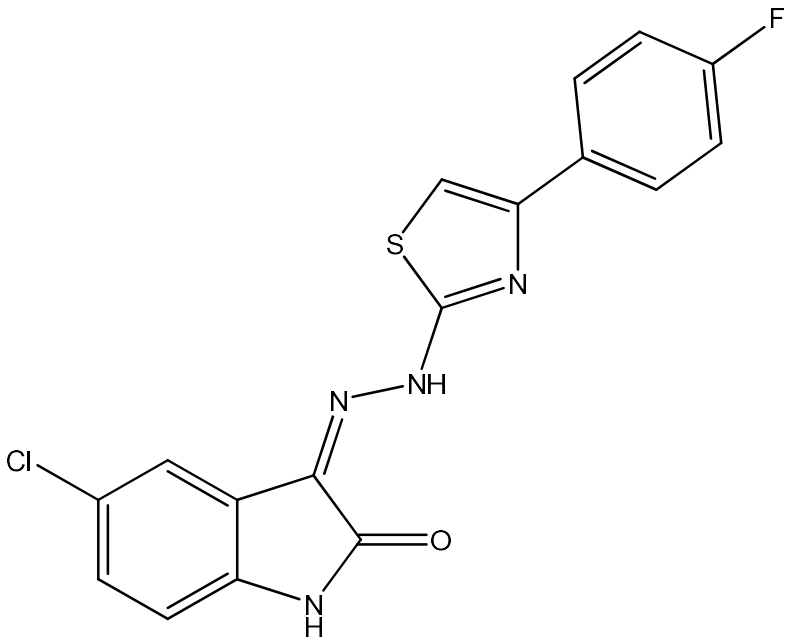

- Peso Molecular: 372,80 g/mol.
- Infravermelho (KBr): 3110.5 (NH), 1691.5 (HN-C=O).
- RMN^{1}H (300 MHz, DMSO-d_6): δ 6.96 (d, 1H, ArH), 7.21-7.36 (m, 3H, ArH), 7.48 (s, 1H, ArH), 7.6 (s, 1H, ArH), 7.92 (d, 2H, ArH), 11.29 (s, 1H, NH), 13.29 (s, 1H, NH).
- RMN^{13}C (75.5 MHz, DMSO-d_6): δ 106.84 (CH, Tiazol), 112.4 (CH, Ar), 115.26 (CH, Ar), 115.48 (C-Ar), 119.14 (CH, Ar), 121.35 (2CH, Ar), 126.46 (CH, Ar), 127.61 (CH, Ar), 127.69 (CH, Ar), 127.84 (CH, Ar), 129.63 (C-Cl), 130.87 (C=N), 139.77 (C-NH, Ar), 150.00 (C-N, Ar), 162.84 (C=O), 165.77 (N=C-S), 178.78 (C-F).
- Fórmula Molecular: $C_{17}H_{10}ClFN_4OS$.
- HRMS: 372,02 $[M+H]^+$.

PA-3G: (Z)-5-cloro-3-{2-[4-(4-clorofenil)tiazol-2-il]-hidrazona}indolin-2-ona

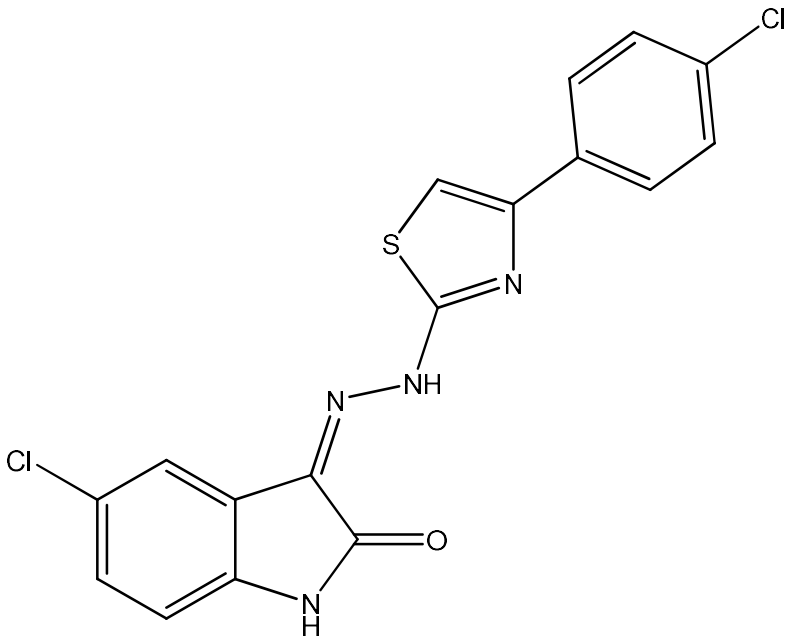

- Peso Molecular: 389,26 g/mol.
- Infravermelho (KBr): 3110.5 (NH), 1688.03 (HN-C=O).
- RMN^{1}H (300 MHz, DMSO-d_6): δ 6.97 (d, 1H, ArH), 7.37 (d, 1H, ArH), 7.48 (d, 2H, ArH), 7.52 (s, 1H, ArH), 7.72 (s, 1H, ArH), 7.92 (d, 2H, ArH), 11.36 (s, 1H, NH), 13.33 (s, 1H, NH).
- RMN^{13}C (75.5 MHz, DMSO-d_6): δ 108.03 (CH, Tiazol), 112.5 (CH, Ar), 119.6 (C-Ar), 121.43 (CH, Ar), 126.56 (CH, Ar), 127.42 (2CH, Ar), 128.7 (2CH, Ar), 129.83 (CH, Ar), 131.11 (CH, Ar), 132.4 (CH, Ar), 132.7 (C=N), 139.9 (C-NH, Ar), 149.83 (C-N, Ar), 162.96 (N=C-S).
- Fórmula Molecular: $C_{17}H_{10}Cl_2N_4OS$.
- HRMS: 388,00 $[M+H]^+$.

PA-3J: (Z)-5-cloro-3-{2-[4-(2,4-diclorofenil)tiazol-2-il]-hidrazona}indolin-2-ona

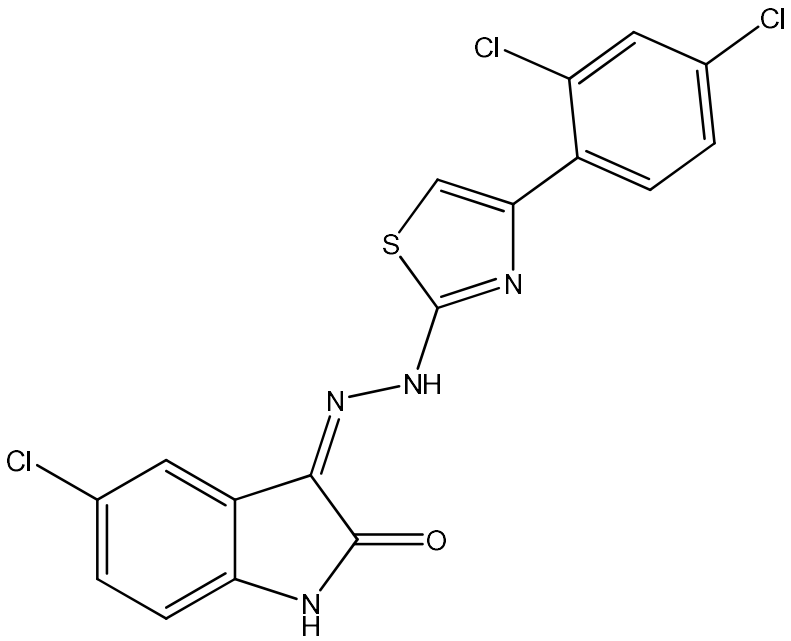

- Fórmula Molecular: $C_{17}H_9Cl_3N_4OS$.
- Infravermelho (KBr): 3110.0 (NH), 1688.0 (HN-C=O).
- RMN^{1}H (300 MHz, DMSO-d_6): δ 7.28 (s, 1H, Tiazol), 7.43 (d, 1H, Ar), 7.48 (s, 1H, Ar), 7.50 (d, 1H, Ar), 7.80 (d, 1H, Ar), 7.89 (d, 1H, Ar), 8.03 (d, 1H, Ar), 11.40 (s, 1H, NH), 13.30 (s, 1H, NH).
- RMN^{13}C (75.5 MHz, DMSO-d_6): δ 105.0 (CH, Tiazol), 119.6 (C-Ar), 125.2 (CH, Ar), 127.4 (CH, Ar), 128.0 (CH, Ar), 129.4 (CH, Ar), 130.0 (C-Cl, Ar), 130.3 (CH, Ar), 130.9 (CH, Ar), 131.3 (CH, Ar), 133.0 (C=N), 133.6 (C-Cl), 139.3 (C-NH, Ar), 147.8 (C-N, Tiazol), 168.5 (C=O), 147.8 (N=C-S, Tiazol).
- HRMS: 421,96 $[M+H]^+$.

PA-3K: (Z)-5-cloro-3-{2-[4-(clorometil)tiazol-2-il]-hidrazona}indolin-2-ona

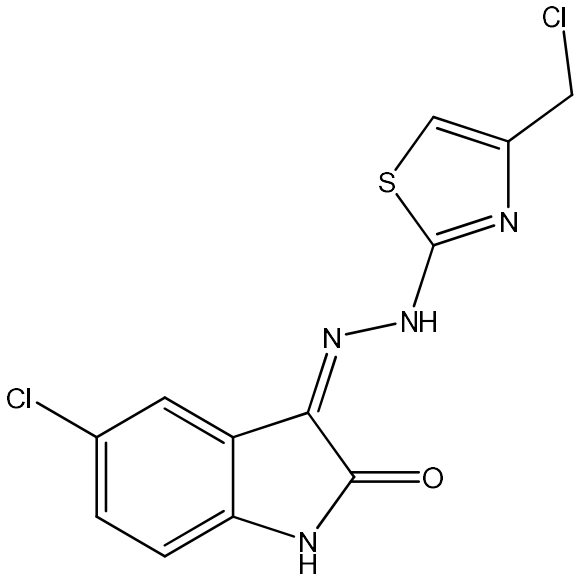

- Fórmula Molecular: $C_{12}H_8Cl_2N_4OS$.
- Infravermelho (KBr): 3112.0 (NH), 1689.0 (HN-C=O).
- RMN^{1}H (300 MHz, DMSO-d_6): δ 4.64 (s, 1H), 6.48 (s, 1H, Tiazol), 7.50 (d, Ar), 7.80 (d, 1H, Ar), 7.89 (s, 1H, Ar), 11.36 (s, 1H, NH), 13.33 (s, 1H, NH).
- RMN^{13}C (75.5 MHz, DMSO-d_6): δ 38.0 (CH_2-Cl), 104.3 (CH, Tiazol), 119.6 (C-Ar), 125.5 (CH, Ar), 129.5 (CH, Ar), 130.0 (CH, Ar), 131.4 (CH, Ar), 133.0 (C=N), 139.3 (C-NH, Ar), 149.83 (C-N, Ar), 168.5 (C=O), 170.4 (N=C-S, Tiazol).
- HRMS: 325,98 $[M+H]^+$.

PA-3L: (Z)-5-cloro-3-{2-[4-(bifenil-4-il)tiazol-2-il]-hidrazona}indolin-2-ona

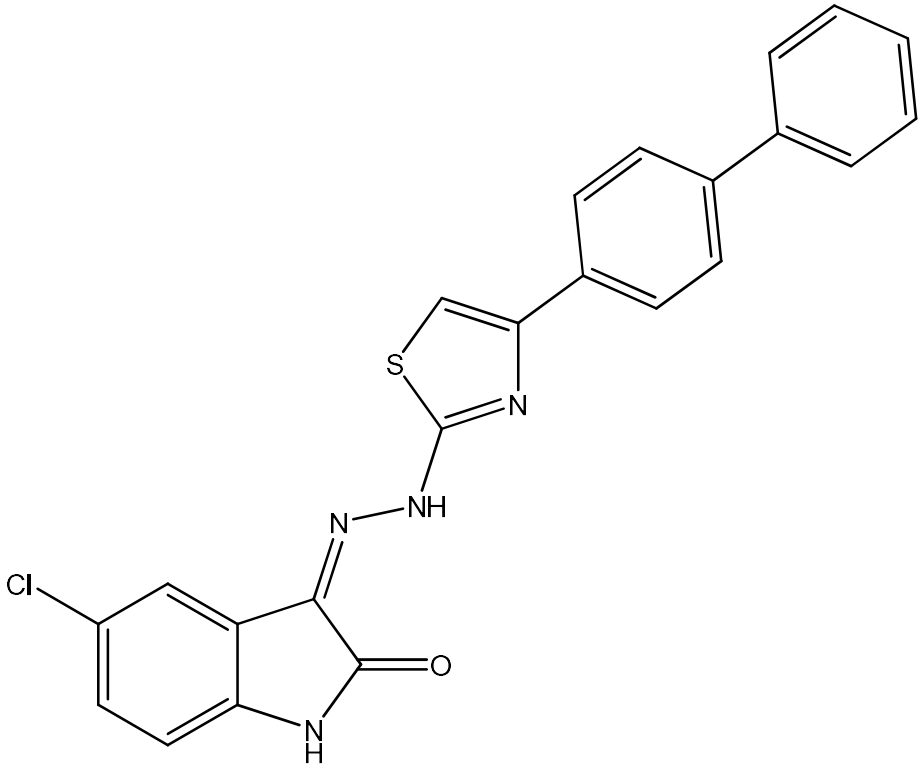

- Peso Molecular: 430,91 g/mol.
- Infravermelho (KBr): 3123.4 (NH), 1684 (HN-C=O).
- RMN^{1}H (300 MHz, DMSO-d_6): δ 6.99 (d, 1H, Ar), 7.37-8.0 (m, 12H, Ar), 11.31 (s, 1H, NH), 13.34 (s, 1H, NH).
- RMN^{13}C (75.5 MHz, DMSO-d_6): δ 105.0 (CH, Tiazol), 119.1 (C-Ar), 125.2 (CH, Ar), 127.2 (2CH, Ar), 127.6 (CH, Ar), 127.9 (2CH, Ar), 128.0 (2CH, Ar), 129.2 (2CH, Ar), 129.4 (CH,Ar), 130.0 (C-Cl), 131.3 (CH, Ar), 131.9 (C, Ar), 133.0 (C=N), 139.3 (C-NH, Ar), 140.8 (2C, Ar), 150.2 (C, Tiazol) 168.5 (C=O), 171,7 (N=C-S).
- Fórmula Molecular: $C_{23}H_{15}ClN_4OS$.
- HRMS: 430,07 $[M+H]^+$.

4.5.2 Parte Biológica

4.5.2.1 Cultura e manutenção das linhagens celulares

As linhagens celulares foram mantidas em garrafas invertidas de poliestireno (TPP®) em estufa úmida a 37ºC e 5% de CO_2 e acompanhadas diariamente com o auxílio de um microscópio invertido. A troca do meio foi realizada sempre que havia necessidade de renovação de nutrientes ou como recomenda o *Data sheet* de cada linhagem.

4.5.2.1.1 Células aderentes

As linhagens aderentes T-47D (Carcinoma ductal de mama) e HeLa (Adenocarcinoma cervical) foram obtidas pelo banco de células do Rio de Janeiro (BCRJ). Tais células foram cultivadas em meio DMEM (Invitrogen®) contendo 10% de soro fetal bovino (SBF) (Gibco®) inativado a 56ºC por 1h; adicionou-se também 3g/litro de Bicarbonato do Sódio (Sigma-Aldrich®) e 200 U/mL de Penicilina/Estreptomicina (Gibco®).

Os repiques foram realizados em fluxo laminar quando as células atingiam a confluência de 80-85%. Para tal o meio foi desprezado e as células foram lavadas com PBS/EDTA (137 mM NaCl, 2,7 mM KCl, 10 mM Na_2HPO_4, 1,8 mM KH_2PO_4, 0,03 mM EDTA, pH 7,4 ajustado com HCl). As células foram deaderidas pela adição de tripsina 0,25% (Invitrogen®) por 5-10 minutos, centrifugadas a 2000 rpm por 3 minutos e distribuídas nas garrafas em uma concentração média de 1.10^4 células/ml.

4.5.2.1.2 Células em suspensão

As linhagens em suspensão HL-60/mx1 (Leucemia aguda resistente a Etoposideo, Teniposideo e Bisantreno) e K-562 (Leucemia mielóide crônica) foram obtidas pelo banco de células do Rio de Janeiro (BCRJ). Tais células foram cultivadas em meio RPMI-1640 (Gibco®) contendo 10 % Soro Fetal Bovino (Gibco®) inativado a 56ºC por 1h, adicionou-se também 3g/litro de Bicarbonato de Sódio (Sigma-Aldrich®) e 1% de Penicilina/Estreptomicina (Gibco®). Para manutenção do meio as células foram centrifugadas por 7 minutos a 1500 rpm e distribuídas em concentração média de 1.10^4 células/ml em garrafas contendo meio novo.

4.5.2.2 Ensaios de toxicidade

As células foram plaqueadas em placas de 96 poços onde cada poço recebeu a quantidade de 1.10^4 de células. Após 24h diferentes concentrações dos compostos foram adicionadas e as placas incubadas em estufa úmida a 37ºC e 5% de CO_2 por 72h. Passado o período de incubação foi adicionado 20 µL da solução de MTT (3-(4,5-dimetilazol-2-il)-2,5-difenil brometo de tetrazolina) na concentração de 5 mg/mL diluída em PBS, as placas foram então protegidas da luz e incubadas mais uma vez em estufa úmida a 37ºC e 5% de CO_2 por um período de 3h. A reação foi então interrompida pela adição de 130 µL de SDS 20% e a densidade óptica medida após 24 horas no comprimento de onda de 560 nm. A leitura foi realizada em um leitor de microplacas (EL808 - Biotek®). A determinação do potencial citotóxico dos compostos testados foi calculada em relação ao controle tratado com o veículo DMSO a 0,01%.

4.5.2.2.1 Ensaio de toxicidade em células saudáveis

Para avaliar a seletividade dos compostos, foram realizados ensaios de redução do MTT com células humanas mononucleares do sangue periférico (PBMCs) de dois indivíduos sadios como descrito acima. Para tal, as PBMCs foram expostas às concentrações de 100 µM de cada composto.

4.5.2.2.2 Avaliação do potencial citotóxico

Com a finalidade de pré-selecionar os compostos com atividade anti-proliferativa significativa, as células de K-562, T-47D, HL-60/mx1 e HeLa foram tratadas com uma concentração única de 10 µM de cada composto. Os compostos que apresentaram viabilidade celular inferior a 59% foram considerados ativos (segundo protocolo do NCI-60).

5 CONCLUSÃO

Foram obtidos inéditos tiazóis derivados dos grupos farmacofóricos ftalimida e isatina. No Capítulo 1 foi apresentado o planejamento estrutural para a obtenção das duas séries de derivados da ftalimida, a metodologia de síntese empregada, a caracterização estrutural e avaliação das propriedades antichagásicas de tais compostos. A estratégia empregada para melhorar a atividade da primeira série de ftalimidas (**2a-n**) mostrou-se eficaz, levando a uma redução da toxicidade e a um aumento na atividade antichagásica. Dos produtos obtidos, podem-se destacar os compostos **2J**, **6A**, **6H**, **6K** e **6J**, sendo este último o mais ativo. O trabalho rendeu uma publicação na *European Journal of Medicinal Chemistry*.

No Capítulo 2 foi apresentado o planejamento estrutural empregado para a obtenção das séries de derivados da istaina, assim como a metodologia de síntese empregada. Os compostos foram caracterizados e estão sendo testados quanto à atividade antitumoral. Nenhum dos compostos apresentou toxicidade em células normais humanas na dose máxima testada. Resultados preliminares indicam a importância da presença de um grupo fenil na posição N3 para a atividade antitumoral, destacando-se o intermediário **PA-Int6**. No entanto, os resultados não são conclusivos, sendo necessários mais testes para a investigação das propriedades antitumorais de tais compostos.

De modo geral, a estratégia de utilização de estruturas privilegiadas como bases estruturais para a obtenção de novos compostos biologicamente ativos mostrou-se promissora. Com a utilização de tal estratégia foi possível identificar potentes agentes antichagásicos, bem como encontrar um prévio direcionamento para síntese de novos protótipos a fármacos antitumorais.

REFERÊNCIAS

ABDEL-AZIZ, A. A. M.; EL-AZAB, A. S.; ATTIA, S. M.; AL-OBAID, A. M.; AL-OMAR, M. A.; EL-SUBBAGH, H. I. Synthesis and biological evaluation of some novel cyclic-imides as hypoglycaemic, anti-hyperlipidemic agents, Eur. J. Med. Chem. 46 (2011) 4324–4329. doi:10.1016/j.ejmech.2011.07.002.

ABOUL-FADL, T.; RADWAN, A. A.; ATTIA, M. I.; AL-DHFYAN, A.; ABDEL-AZIZ, H. A. Schiff bases of indoline-2,3-dione (isatin) with potential antiproliferative activity. **Chemistry Central Journal**, v. 6, p. 49, 2012.

AKGÜN, H.; KARAMELEKOĞLU, İ.; BERK, B.; KURNAZ, I.; SARIBIYIK, G.; ÖKTEM, S. *et al*., Synthesis and antimycobacterial activity of some phthalimide derivatives. **Bioorg. Med. Chem.** v. 20, p. 4149–4154, 2012.

ALANAZI, A.M.; EL-AZAB, A.S.; AL-SUWAIDAN, I.A.; ELTAHIR, K. E. H.; ASIRI, Y. A.; ABDEL-AZIZ, N. I. *et al*., Structure-based design of phthalimide derivatives as potential cyclooxygenase-2 (COX-2) inhibitors: Anti-inflammatory and analgesic activities. **Eur. J. Med. Chem.,** v. 92, p. 115–123, 2015.

ALIABADI, A.; SHAMSA, F.; OSTAD, S. N.; EMAMI, S.; SHAFIEE, A.; DAVOODI, J.; FOROUMADI, A. Synthesis and biological evaluation of 2-phenylthiazole-4-carboxamide derivatives as anticancer agents. **European Journal of Medicinal Chemistry**. v. 45, p. 5384-5389, 2010.

AL-RASHOOD, K. A.; MUSTAFA, A. A.; ALHAIDER, A. A.; GINAWI, O. T.; MADANI, A. A. E.; EL-OBEID, H. A. Antipsychotic properties of new N-(4-substituted-1-piperazinylethyl) and N-(4-substituted-l-piperidinylethyl)-phthalimides. **J. Pharm. Sci.**, v. 77, p. 898-901, 1988.

AMIT, C.; SHEELMANI; SINGH, A.; PAYAL, C.; DHAWAN, R. K. **Chemistry of anticancer thiazole compounds**. Adv J Pharm Life sci Res, 2;1:1-7. 2014.

ANJOS, A. C. Y. dos**. As representações do Cuidar do Idoso em Quimioterapia Oncológica na Vida do Familiar Cuidador**. Tese, Ribeirão Preto, PPGEF/USP, 2010.

ANTUNES, R.; BATISTA, H.; SRIVASTAVA, R.; THOMAS, G.; ARAUJO, C. C.; LONGO, R. L. Synthesis, characterization and interaction mechanism of new oxadiazolo-phthalimides as peripheral analgesics. **J. Mol. Str.**, v. 660, p. 1-13, 2003.

ARORA, S.; AGARWAL, S.; SINGHAL, S. **Anticancer activities of thiosemicarbazides/ thiosemicarbazones: a review.** International Journal of Pharmacy and Pharmaceutical Sciences. Vol 6, Issue 9, 2014.

BABU, A. H.; RAMANA, A. V.; SINHA, R.; YAHAV, J. S.; ARORA, S. K.; Antitubercularagents. Part 1: Synthesis of phthalimido and naphthalimido linked phenazies as a new prototype antitubercular agent. **Bioorg. Med. Chem.**, v. 15, p. 1923-1926, 2005.

BAILLEUX, V.; VALLEE, L.; NUYTS, J. P.; VAMECQ, J. Anticonvulsant activity of some 4-amino-N-phenylphthalimides and N-(3-amino-2-methylphenyl) phthalimides. **Biomed and Pharmacother**, v. 48, p. 95-101, 1994.

BOGO, D. **Avaliação da atividade antitumoral *in vitro* e *in vivo* de compostos de liquens.** Tese. Programa de Pós-Graduação em Saúde e Desenvolvimento na Região Centro-oeste. Universidade Federal de Mato Grosso do Sul. Campo Grande-MS, 2012.

BRAGA M. V, URBINA J.A., SOUZA W., Effects of squalene synthase inhibitors on the growth and ultrastructure of Trypanosoma cruzi., **Int. J. Antimicrob. Agents.** 24 (2004) 72–8.

CAPUTTO, M. E.; CICCARELLI, A.; FRANK, F.; MOGLIONI, A. G.; MOLTRASIO, G. Y.; VEGA, D. *et al*., Synthesis and biological evaluation of some novel 1-indanone thiazolylhydrazone derivatives as anti-*Trypanosoma cruzi* agents. **Eur. J. Med. Chem.,** v.55, p.155–163, 2012.

CARDOSO M., HERNANDES M., MOREIRA D., PONTES F., SIMONE C., LEITE A., *et al.*, Structural Insights Into Bioactive Thiazolidin-4-one: Experimental and Theoretical Data, **Lett. Org. Chem**. 12 (2015) 262–270.

CARDOSO, M. V. O.; SIQUEIRA, L.R.P.; SILVA, E. B.; COSTA, L. B.; HERNANDES, M. Z.; RABELLO, M. M.; *et al*. 2-Pyridyl thiazoles as novel anti- *Trypanosoma cruzi* agents : Structural design , synthesis and pharmacological evaluation. **Eur. J. Med. Chem.**, v. 86, p.48–59, 2014.

CARDOSO, M.V.D.O., , D.R.M., FILHO, G.B.O., CAVALCANTI, S.M.T., COELHO, L.C.D., ESPÍNDOLA, J.W.P., *et al*., Design, synthesis and structure–activity relationship of phthalimides endowed with dual antiproliferative and immunomodulatory activities, Eur**. J. Med. Chem.** 96 (2015) 491–503.

CHEN H., ZHOU X., WANG A., ZHENG Y., GAO Y., ZHOU J., Evolutions in fragment-based drug design: the deconstruction–reconstruction approach, **Drug Discov. Today**. 20 (2015) 105–113.

COÊLHO, L.C.D., CARDOSO, M.V. de O., MOREIRA, D.R.M., GOMES, P.A.T. M., CAVALCANTI, S.M.T., OLIVEIRA, A.R., *et al.*, Novel phthalimide derivatives with TNF-α and IL-1β expression inhibitory and apoptotic inducing properties, **Medchemcomm.** 5 (2014) 758.

COLLIN, X.; ROBERT, J.; WIELGOSZ, G.; LE, B. G.; BOBIN-DUBIGEN, C.; GRIMAUD, N. New anti-inflammatory N-pyridinyl (alkyl) phthalimides acting as tumour necrosis factor-alpha production inhibitors. **Eur. J. Chem**., v. 36, p. 639-649, 2001.

CONGREVE M., CARR R., MURRAY C., JHOTI H. A "Rule of Three" for fragment-based lead discovery?, Drug Discov. Today. 8 (2003) 876–877.

COSTA, P. M. **Avaliação do potencial antitumoral e antiangiogênico de novos análogos ftalimídicos da talidomida**. Fortaleza, CE. Tese. Programa de Pós-Graduação em Farmacologia/UFCE. 2011.

COSTA, P.; PILLI, R.; PINHEIRO, S.; VASCONCELLOS, M.; **Substâncias carboniladas e seus derivados**, 1ª ed., Bookman: Porto Alegre/MG, 2003

COSTA, P.M., COSTA, M.P., CARVALHO, A.A., CAVALCANTI, S.M.T., CARDOSO M.V. OLIVEIRA, OLIVEIRA FILHO G.B., *et al.*, Improvement of in vivo anticancer and antiangiogenic potential of thalidomide derivatives, **Chem. Biol. Interact.** 239 (2015) 174–183.

COSTA-LOTUFO, L. V.; MONTENEGRO, R. C.; ALVES, A. P. N. N., MADEIRA, S. V. F.; PESSOA, C.; MORAES, M. E. A.; MORAES, M. O. A Contribuição dos Produtos Naturais como Fonte de Novos Fármacos Anticâncer: Estudos no Laboratório Nacional de Oncologia Experimental da Universidade Federal do Ceará. **Revista Virtual de Química**. v. 2(1), p. 47-58, 2010.

COSTANTINO, L.; BARLOCCO, D. Privileged Structures as Leads in Medicinal Chemistry. **Current Medicinal Chemistry**, v. 13, p. 65-85, 2006.

CRUZ, M.; ENES, M.; PEREIRA, M.; DOURADO, M.; RIBEIRO, A. B. S. Experimental models in oncology: Contribution of cell culture on understanding the biology of cancer. **Rev. Port. Pneumol.,** v. 15, p. 669, 2009.

DANTAS A.P., SALOMÃO K., BARBOSA H.S., CASTRO S.L.. The effect of Bulgarian propolis against Trypanosoma cruzi and during its interaction with host cells, **Mem. Inst. Oswaldo Cruz.** 101 (2006) 207–211.

DESIMONE, R. W.; CURRIE, K. S.; MITCHELL, S. A.; DARROW, J. W.; PIPPIN, D. A. Privileged structures: applications in drug discovery. **Comb Chem High Throughput Screen.**, v. 7, n. 5, p. 473-494, 2004.

DRANOFF, G. Cytokines in cancer pathogenesis and cancer therapy. **Nature reviews. Cancer**, v. 4, n. 1, p. 11–22, 2004.

E.-N., Collect, Nonius BV. Delft, The Netherlands. 2000 (1997) 585.

ELUMALAI, K., ALI, M.A., ELUMALAI, M., ELURI, K., SRINIVASAN, S., SIVANNAN, S., *et al.*, Synthesis, characterization and biological evaluation of acetazolamide, cycloserine and isoniazid condensed some novel phthalimide derivatives, **Int. J. Chem. Anal. Sci.** 4 (2013) 57–61.

ESPÍNDOLA, J. W. P.; CARDOSO, M. V. O.; OLIVEIRA FILHO, G. B.; SILVA, D. A. O.; MOREIRA, D. R. M.; BASTOS, T. M. *et al*., Synthesis and structure–activity relationship study of a new series of antiparasitic aryloxyl thiosemicarbazones inhibiting *Trypanosoma cruzi* cruzain. **Eur. J. Med. Chem.,** v. 10 p. 818–835, 2015.

FALLAH-TAFTI, A.; FOROUMADI, A.; TIWARI, R.; SHIRAZI, A. N.; HANGAUER, D. G.; BU, Y.; AKBARZADEH, T.; PARANG, K.; SHAFIEE, A. Thiazolyl N-benzyl-substituted acetamide derivatives: Synthesis, Src kinase inhibitory and anticancer activities. **European Journal of Medicinal Chemistry**. v. 46, p. 4853-4858, 2011.

FARRUGIA L.J., ORTEP -3 for Windows - a version of ORTEP -III with a Graphical User Interface (GUI), J. Appl. Crystallogr. 30 (1997) 565–565.

FARRUGIA L.J., WIN G.X. suite for small-molecule single-crystal crystallography, J. Appl. Crystallogr. 32 (1999) 837–838.

FDA. U.S. Food and Drug Administration. **Hematology/Oncology (Cancer) Approvals & Safety Notifications.** Disponível em: <http://www.fda.gov/Drugs/InformationOnDrugs/ApprovedDrugs/ucm279174.htm>. Acesso em 20 fev 2015.

GAJARE, S. P.; MAHAJAN, S. S. QSAR Studies of Phthalimide Derivatives for their Potent Anxiolytic Activity. **Int. J. Cur. Res. and Rev.,** v. 4, 2012.

GARZONI L.R., CALDERA A., MEIRELLES M. N.L., CASTRO S.L. D., DOCAMPO R., MEINTS G.A., *et al.*, Selective in vitro effects of the farnesyl pyrophosphate synthase inhibitor risedronate on Trypanosoma cruzi, **Int. J. Antimicrob. Agents**. 23 (2004) 273–285.

GAWANDE, S. S.; WARANGKAR, S. C. BANDGAR, B. P.; KHOBRAGADE, C. N. Synthesis of new heterocyclic hybrids based on pyrazole and thiazolidinone scaffolds as potent inhibitors of tyrosinase. **Bioorg. Med. Chem.,** v.21, n. 10 p. 2772–2777, 2013.

GERMANO, G.; ALLAVENA, P.; MANTOVANI, A. Cytokines as a key component of cancer-related inflammation. **Cytokine**, v. 43, n. 3, p. 374–9, set. 2008.

GILLAM, E.M.J.; NOTLEY, L.M.; CAI, H.L.; DE VOSS, J.J.; GUENGERICH, F.P. **Oxidation of indole by cytochrome P450 enzymes.** Biochemistry, 39(45), 13817-13824, 2000.

GONZALES-PERDOMO M., CASTRO S.L., MEIRELLES M.N., GOLDENBERG S.. Trypanosoma cruzi proliferation and differentiation are blocked by topoisomerase II inhibitors., **Antimicrob. Agents Chemother**. 34 (1990) 1707–1714.

GONZÁLEZ, M. A.; CLARK, J.; CONNELLY, M.; RIVAS, F. Antimalarial activity of abietane ferruginol analogues possessing a phthalimide group. **Bioorganic & Medicinal Chemistry Letters,** v. 24, p. 5234–5237, 2014.

GRIVENNIKOV, S. I.; GRETEN, F. R.; KARIN, M. Immunity, inflammation, and cancer. **Cell**, v. 140, n. 6, p. 883–99, 19 mar. 2010.
HANAHAN, D.; COUSSENS, L. M. Accessories to the crime: functions of cells recruited to the tumor microenvironment. **Cancer cell**, v. 21, n. 3, p. 309–22, 20 mar. 2012.

HANAHAN, D.; WEINBERG, R. A. Hallmarks of cancer: the next generation. **Cell**, v. 144, n. 5, p. 646–74, mar. 2011.

HASIMA, N.; AGGARWAL, B. B. Cancer-linked targets modulated by curcumin. **Int J Biochem Mol Biol**. v. 3, n. 4, p. 328-351, 2012.

HASSAN, G. S.; EL-MESSERY, S. M.; AL-OMARY, F. A. M.; EL-SUBBAGH, H. I. Substituted thiazoles VII. Synthesis and antitumor activity of certain 2-(substituted amino)-4-phenyl-1,3-thiazole analogs. **Bioorganic & Medicinal Chemistry Letters**. v. 22, p. 6318–6323, 2012.

HASSANZADEH, F.; RABBANI, M.; KHODARAHMI, G. A.; FASIHI, A.; HAKIMELAHI, G. H.; MOHAJERI, M. Synthesis of phthalimide derivative and evaluation of their anxiolytic activity, **Res. Pharm. Sci.**, 2: 35-41. 2007.

HERNANDES, M. Z.; RABELLO, M. M.; LEITE, A. C. L.; CARDOSO, M. V. O.; MOREIRA, D. R. M.; BRONDANI, D. J. *et al*., Studies toward the structural optimization of novel thiazolylhydrazone-based potent antitrypanosomal agents. **Bioorg. Med. Chem.,** v.18, p. 7826–7835, 2010.

INCA. Estimativa 2014: Incidência de Câncer no Brasil / **Instituto Nacional de Câncer José Alencar Gomes da Silva**, Coordenação de Prevenção e Vigilância. Rio de Janeiro. 2014.

JEAN, S. L.; PAULO, Y. R.; CHUNG, C.M.; CELIO, T. H.; FERNANDO, P. R.; CLARICE, L. Q.; Synthesis and *in vitro* anti mycobacterium tuberculosis activity of a series of phthalimide derivatives, **Bioorg. Med. Chem**., v. 17, p. 3795–3799, 2009.

KAMIŃSKI, K.; OBNISKA, J.; WIKLIK, B.; ATAMANYUK, D. Synthesis and anticonvulsant properties of new acetamide derivatives of phthalimide, and its saturated cyclohexane and norbornene analogs. **Eur. J. Med. Chem.** v. 46 p. 4634–4641, 2011.

KARAH, N. Synthesis and primary cytotoxicity evaluation of new 5-nitroindole-2,3-dione derivatives. **Eur. J. Med. Chem.** v. 37, p. 909-918, 2002.

KASHYAP, S. J.; GARG, V. K.; SHARMA, P. K.; KUMAR, N.; DUDHE, R.; GUPTA, J. K. Thiazoles: having diverse biological activities. **Medicinal Chemistry Research.** v. 21, n. 8, p. 2123-2132, 2012.

LEE, S.; MARGOLIN, K. Cytokines in Cancer Immunotherapy. **Cancers**, v. 3, n. 4, p. 3856–3893, 13 out. 2011.

LEFRANC, F.; XU, Z.; BURTH, P.; MATHIEU, V.; REVELANT, G.; FARIA, M. V. de C.; NOYON, C.; GARCIA, D. G.; DUFOUR, D.; BRUYÈRE, C.; GONÇALVES-DE-ALBUQUERQUE, C. F.; ANTWERPEN, P. V.; ROGISTER, B.; HESSE, S.; KIRSCH, G.; KISS, R. 4-Bromo-2-(piperidin-1-yl)thiazol-5-yl-phenyl methanone (12b) inhibits Naþ/Kþ-ATPase and Ras oncogene activity in cancer cells. **European Journal of Medicinal Chemistry**. v. 63, p. 213-223, 2013.

LEITE, A. C. L.; *et al*. Phthaloyl amino acids as anti-inflammatory and immunomodulatory prototypes. **Medicinal Chemistry Research,** v. 23, n. 4, p. 1701-1708, 2014.

LEITE, A. C. L.; LIMA, R. S.; MOREIRA, D. R. M.; CARDOSO, M. V. O.; BRITO, A. C. G.; SANTOS, L. M. F. *et al*. Synthesis, docking, and *in vitro* activity of thiosemicarbazones, aminoacyl-thiosemicarbazides and acyl-thiazolidones against *Trypanosoma cruzi*. **Bioorg. Med. Chem.,** v. 14, p. 3749–57, 2006.

LEITE, A.C.L., BARBOSA, F.F., CARDOSO, M.V.D.O., MOREIRA, D.R.M., COÊLHO, L.C.D., SILVA, E.B., *et al*., Phthaloyl amino acids as anti-inflammatory and immunomodulatory prototypes, **Med. Chem. Res.** (2013).

LEITE, A.C.L.; MOREIRA, D. R. M.; CARDOSO, M. V. O.; HERNANDES, M.Z.; PEREIRA, V. R. A.; SILVA, R. O. *et al*. Synthesis, Cruzain docking, and *in vitro* studies of

aryl-4-oxothiazolylhydrazones against *Trypanosoma cruzi*. **ChemMedChem.,** v. 2 1339–1345, 2007.

MA, X.; WANG, Z. Anticancer drug discovery in the future: an evolutionary perspective. **Drug Discovery Today**. V. 14, Nos. 23/24, p. 1.136- 1.142, 2009.

MANTOVANI, A.; SICA, A. Macrophages, innate immunity and cancer: balance, tolerance, and diversity. **Current opinion in immunology**, v. 22, n. 2, p. 231–7, abr. 2010.

MASOUD, G. N.; YOUSSEF, A. M.; KHALEK, M. M. A.; WAHAB, A. E. A.; LABOUTA, I. M.; HAZZAA, A. A. B. Design, synthesis, and biological evaluation of new 4-thiazolidinone derivatives substituted with benzimidazole ring as potential chemotherapeutic agents. **Med. Chem. Res.**, v. 22, p. 707–725, 2012.

MESHRAM, H. M.; THAKUR, P. B.; BABU, B. M.; BANGALE, V. M. Convenient and simple synthesis of 2-aminothiazoles by the reaction of α-halo ketone carbonyls with ammonium thiocyanate in the present of N-methylimidazole. **Tetrahedron Letters**, v. 53, p. 5265-5269, 2012.

MOREIRA D.R.M., LIMA LEITE A.C., CARDOSO M.V.O., SRIVASTAVA R.M., HERNANDES M.Z., RABELLO M.M., *et al.*, Structural Design, Synthesis and Structure-Activity Relationships of Thiazolidinones with Enhanced Anti-Trypanosoma cruzi Activity., **ChemMedChem**. 9 (2014) 177–88.

MOREIRA, D. R. M.; COSTA, S. P. M.; HERNANDES, M. Z.; RABELLO, M. M.; OLIVEIRA FILHO, G. B.; MELO, C. M. L. *et al*., Structural investigation of anti-*Trypanosoma cruzi* 2-iminothiazolidin-4-ones allows the identification of agents with efficacy in infected mice. **J. Med. Chem.,** v. 55, n. 24, 10918–10936, 2012.

MOTZER, R. J.; MICHAELSON, M. D.; REDMAN, B. G.; HUDES, G. R.; WILDING, G.; FIGLIN, R. A.; GINSBERG, M. S.; KIM, S. T.; BAUM, C. M.; DEPRIMO, S. E.; LI, J. Z.; BELLO, C. L.; THEUER, C. P.; GEORGE, D. J.; RINI, B. I. Activity of SU11248, a multitargeted inhibitor of vascular endothelial growth factor receptor and platelet-derived growth factor receptor, in patients with metastatic renal cell carcinoma. **J. Clin. Oncol.**, v. 24, p. 16–24, 2006.

OLIVEIRA FILHO, G. B.; CARDOSO, M.V. O.; ESPÍNDOLA, J. W. P.; FERREIRA, L. F. G. R.; SIMONE, C. A.; FERREIRA, R. S. *et al*., Structural Design, Synthesis and Pharmacological Evaluation of 4-Thiazolidinones against *Trypanosoma cruzi*. **Bioorg. Med. Chem.**, 2015.

OTWINOWSKI Z., MINOR W. Methods in Enzymology, Macromol. Crystallogr. Part A. 276 (1997) 307–326.

PATEL, H. S.; MISTRY, H. J.; PATEL, N. K.; DESAI, S. N. Synthesis and antimicrobial activity of some new phthalimide derivatives. **Bulgarian Chem. Comm.**, v. 36, p. 167 -172, 2004.

PÉREZ-MOLINA, J. A.; SOJO-DORADO, J.; NORMAN, F.; MONGE-MAILLO, B.; DÍAZ-MENÉNDEZ, M.; ALBAJAR-VIÑAS, P.; LÓPEZ-VÉLEZ, R. Nifurtimox therapy for

Chagas disease does not cause hypersensitivity reactions in patients with such previous adverse reactions during benznidazole treatment. **Acta Trop.,** v. 127, p. 101–104, 2013.

PESSOA, C., FERREIRA, P.M.P., LOTUFO, L.V.C., MORAES, M.O. de, CAVALCANTI, S.M.T., COÊLHO, L.C.D. *et al*., Discovery of phthalimides as immunomodulatory and antitumor drug prototypes., **ChemMedChem**. 5 (2010) 523–8.

PIZZO, C.; SAIZ, C.; TALEVI, A.; GAVERNET, L.; PALESTRO, P.; BELLERA, C.; *et al*., Synthesis of 2-hydrazolyl-4-thiazolidinones based on multicomponent reactions and biological evaluation against *Trypanosoma Cruzi*. **Chem. Biol. Drug Des.**, v. 77, 166–172, 2011.

POULIKAKOS, P. I.; PERSAUD, Y.; JANAKIRAMAN, M.; KONG, X.; NG, C.; MORICEAU, G.; SHI, H.; ATEFI, M.; TITZ, B.; GABAY, M. T.; SALTON, M.; DAHLMAN, K. B.; TADI, M.; WARGO, J. A.; FLAHERTY, K. T.; KELLEY, M. C.; MISTELI, T.; CHAPMAN, P. B.; SOSMAN, J. A.; GRAEBER, T. G.; RIBAS, A.; LO, R. S.; ROSEN, N.; SOLIT, D. B. RAF inhibitor resistance is mediated by dimerization of aberrantly spliced BRAF (V600E). **Nature**, v. 480, p. 387, 2011.

RASSI, A.; RASSI, A. Jr; RASSI, S. G. *et al*. **Doença de Chagas.** In: Lopes AC, ed. Tratado de clinica médica, 2nd edn. Sao Paulo: Editora Roca: 4123–34; 2009.

SABET, R.; MOHAMMADPOUR, M.; SADEGHI, A.; FASSIHI, A. QSAR study of isatin analogues as *in vitro* anti-cancer agents. **European Journal of Medicinal Chemistry.** Volume 45, Issue 3, pp 1113–1118. 2010.

SANTIAGO, E. D. F.; DE OLIVEIRA, S. A.; DE OLIVEIRA FILHO, G. B.; MOREIRA, D. R. M.; GOMES, P. A. T.; DA SILVA, A. L.; DE BARROS, A. F.; DA SILVA, A. C.; DOS SANTOS, T. A. R.; PEREIRA, V. R. A.; GONCALVES, G. G. A.; BRAYNER, F. A.; ALVES, L. C.; WANDERLEY, A. G.; LEITE, A. C. L. Evaluation of the anti-Schistosoma mansoni activity of thiosemicarbazones and thiazoles. Antimicrobial agents and chemotherapy, v. 58, p. 352-363, 2014.

SASAKI, T.; KOIVUNEN, J.; OGINO, A.; YANAGITA, M.; NIKIFOROW, S.; ZHENG, W.; LATHAN, C.; MARCOUX, J. P.; DU, J.; OKUDA, K.; CAPELLETTI, M.; SHIMAMURA, T.; ERCAN, D.; STUMPFOVA, M.; XIAO, Y.; WEREMOWICZ, S.; BUTANEY, M.; HEON, S.; WILNER, K.; CHRISTENSEN, J. G.; ECK, M. J.; WONG, K.-K.; LINDEMAN, N.; GRAY, N. S.; RODIG, S. J.; JÄNNE, P. A. A Novel ALK Secondary Mutation and EGFR Signaling Cause Resistance to ALK Kinase Inhibitors. **Cancer Res.** v. 71, p. 6051, 2011.

SHARMA, U.; KUMAR, P.; KUMAR, N. and SINGH, B. Recent Advances in the Chemistry of Phthalimide Analogues and their Therapeutic Potential. **Mini-Reviews in Medicinal Chemistry,** v. 10, p. 678-704, 2010.

SHARMA, V.; KUMAR, P.; PATHAK, D. Biological importance of the indole nucleus in recent years: A comprehensive review. **Journal of Heterocyclic Chemistry.** v. 47, n. 3, p. 491–502. 2010.

SHELDRICK G.. SHELXL-97 and SHELXS-97, Program for X-ray Crystal Structure Solution and Refinement, Univ. Göttingen. (1997). Program for Crystal Structure Resolution#3.

SHUKLA, S.; SRIVASTAVA, R. S.; SHRIVASTAVA, S. K.; SODHI, A.; KUMAR, P. Synthesis, Molecular docking and Biological evaluation of 4-Cycloalkylidineamino 1, 2-Naphthoquinone Semicarbazones as Anticancer agents. **Asian Pacific Journal of Tropical Biomedicine**. p. S1040-S1046, 2012.

SICA, A.; ALLAVENA, P.; MANTOVANI, A. Cancer related inflammation: the macrophage connection. **Cancer letters**, v. 267, n. 2, p. 204–15, 28 ago. 2008.

SILVA, B. V.; HORTA, B. A. C.; ALENCASTRO, R. B.; PINTO, A. C. **Proteínas quinases: características estruturais e inibidores químicos.** Quím. Nova. 32, 453. 2009.

SILVA, M. M. Síntese, caracterização estrutural e avaliação da atividade anti-*Trypanosoma cruzi* de derivados tiazolidínicos e imidazolidínicos. **Tese. Programa de Pós-Graduação em Ciências Biológicas.** UFPE. Recife, PE. 2009.

SINGH, G.; SAROA, A.; GIRDHAR, S.; RANI, S.; SAHOO, S.; CHOQUESILLO-LAZARTE, D. Synthesis, characterization, electronic absorption and antimicrobial studies of N-(silatranylpropyl)phthalimide derived from phthalic anhydride, **Inorganica Chim. Acta.** v. 427, p. 232–239, 2015.

SOLINAS, G. *et al*. Tumor-associated macrophages (TAM) as major players of the cancer-related inflammation. **Journal of leukocyte biology**, v. 86, n. 5, p. 1065–73, nov. 2009.

SOLOMON, V. R.; HUA, C.; LEE, H. **Hybrid pharmacophore design and synthesis of isatin–benzothiazole analogs for their anti-breast cancer activity.** Bioorganic & Medicinal Chemistry. V. 17, Issue 21, 1. p. 7585–7592. 2009.

SOUZA E.M., LANSIAUX A., BAILLY C., WILSON W.D., HU Q., BOYKIN D.W., *et al.*, Phenyl substitution of furamidine markedly potentiates its anti-parasitic activity against Trypanosoma cruzi and Leishmania amazonensis., **Biochem. Pharmacol.** 68 (2004) 593–600.

SOUZA, M. V. N.; FERREIRA, S. B.; MENDONÇA, J. S.; COSTA, M.; RABELLO, F. R. Métodos de obtenção e aplicação sintética de tiazóis, uma importante classe de compostos heterocíclicos. **Química Nova**, v. 28, n. 1, p. 77-84, 2005.

SWARTZ, M. A. *et al*. Tumor microenvironment complexity: emerging roles in cancer therapy. **Cancer research**, v. 72, n. 10, p. 2473–80, 15 maio 2012.

TENÓRIO R. P.; GÓES A. J. S. Tiossemicarbazonas: métodos de obtenção, aplicações sintéticas e importância biológica. Quim. Nova, Vol. 28, No. 6, 1030-1037, 2005.
TEO, S. K. Properties of Thalidomide and its Analogues: Implications for Anticancer Therapy. **The AAPS Journal**. v. 7, p. 14-19, 2005.

TIMOTHY E. LONG, XIAO LU, MELINA GALIZZI, ROBERTO DOCAMPO, JIRI GUT, PHILIP J. ROSENTHAL. Phosphonium lipocations as antiparasitic agentes. **Bioorganic & Medicinal Chemistry Letters** 22. 2976–2979. 2012.

URBINA, J.; Chemotherapy of Chagas Disease, **Curr. Pharm. Des.** v. 8, p. 287–295, 2002.

VINE, K. L.; LOCKE, J. M.; RANSON, M.; PYNE, S. G.; BREMNER, J. B.; **Bioorg. Med. Chem.** 2007, 15, 931;

VINE, K. L., MATESIC, L., LOCKE, J. M., RANSON, M., SKROPETA, D. Cytotoxic and Anticancer Activities of Isatin and Its Derivatives: A Comprehensive Review from 2000-2008. **Anti-Cancer Agents in Medicinal Chemistry**, 9, 397-414. 2009.

WHO. Cancer (fact sheets). Disponível em: <http://www.who.int/mediacentre/factsheets/fs297 /en/>. Acesso em: 01 jan 2015.

WILLIAMS, R., MANKA, J.T., RODRIGUEZ, A.L., VINSON, P.N., NISWENDER, C.M., WEAVER, C.D., *et al.*, Synthesis and SAR of centrally active mGlu5 positive allosteric modulators based on an aryl acetylenic bicyclic lactam scaffold, **Bioorg. Med. Chem. Lett.** 21 (2011) 1350–1353.

APÊNDICES

APÊNDICE A -

New 1,3-thiazole derivatives and their biological and ultrastructural effects on *Trypanosoma cruzi*

European Journal of Medicinal Chemistry 121 (2016) 387e398

Contents lists available at ScienceDirect

European Journal of Medicinal Chemistry

journalhomepage: http://www.elsevier.com/locate/ejmech

Research paper

New 1,3-thiazole derivatives and their biological and ultrastructural effects on Trypanosoma cruzi

Paulo Andre Teixeira de Moraes Gomes [a], Miria de Oliveira Barbosa [a], Edna Farias Santiago [a], Marcos Veríssimo de Oliveira Cardoso [b], Natali Tereza Capistrano Costa [a], Marcelo Zaldini Hernandes [a], Diogo Rodrigo Magalhaes~ Moreira [c], Aline Caroline da Silva [d], Thiago Andre Ramos dos Santos [d], Valeria Rego^ Alves Pereira [d], Fabio Andre Brayner dos Santosd [d], Glaecia Aparecida do Nascimento Pereira [e, f], Rafaela Salgado Ferreira [f], Ana Cristina Lima Leite [a, *]

[a] Departamento de Ci^encias Farmac^euticas, Centro de Ci^encias da Saúde, Universidade Federal de Pernambuco, 50740-520, Recife, PE, Brazil
[b] Universidade de Pernambuco, 56328-903, Petrolina, PE, Brazil
[c] Centro de Pesquisas Gonçalo Moniz, Fundaçao~ Oswaldo Cruz, CEP 40296-750, Salvador, BA, Brazil
[d] Centro de Pesquisas Aggeu Magalhaes,~ Fundaçao~ Oswaldo Cruz, CEP 50670-420, Recife, PE, Brazil
[e] CAPES Foundation, Ministry of Education of Brazil, Brasília, DF, Brazil
[f] Departamento de Bioquímica e Imunologia, Universidade Federal de Minas Gerais, CEP 31270-901, Belo Horizonte, MG, Brazil

article info

Article history:
Received 24 March 2016
Received in revised form 5 May 2016
Accepted 22 May 2016 Available online 24 May 2016

Keywords:
Antiprotozoal agents
Chagas disease
Thiazole
Hydrazones
Cruzain
Electron microscopy

abstract

In previous studies, the compound 3-(bromopropiophenone) thiosemicarbazone was described as a potent anti-Trypanosoma cruzi and cruzain inhibitor. In view to optimize this activity, 1,3-thiazole core was used as building-block strategy to access new lead generation of anti T. cruzi agents. In this way a series of thiazole derivatives were synthesized and most of these derivatives exhibited antiparasitic activity similar to benznidazole (Bzd). Among them, compounds (1c) and (1g) presented better selective index (SI) than Bzd. In addition, compounds showed inhibitory activity against the cruzain protease. As observed by electron microscopy, compound (1c) treatment caused irreversible and specific morpho-logical changes on ultrastructure organization of T. cruzi, demonstrating that this class of compounds is killing parasites.

1. Introduction

Parasitic diseases continue to take an enormous toll on human health, particularly in tropical regions [1]. Chagas disease, caused by Trypanosoma cruzi, represents a serious and alarming health problem [2]. It is considered to be one of the most concerning in-fectious tropical disease in Latin America [3].

Currently, the only drug in use is nitroheterocyclic benznidazole, which is effective in curing the disease in the acute phase, but is less effective in patients that progressed to the chronic phase [4,5]. Furthermore, benznidazole is less than ideal due to the fact that it causes severe side effects, leading to treatment interruption in a large number of patients [6].

Trypanosomes contain an abundance of cysteine proteases (CPs) which are members of the papain superfamily [7]. The cysteine peptidases present stage-regulated levels, are important virulence factors, modulate mammalian host immune cells and facilitate tissue host invasion, what makes these proteases attractive po-tential targets for chemotherapy [8]. Cruzain is the major Trypa-nosoma cruzi cysteine protease and it has been identified as a crucial enzyme responsible for parasite invasion, differentiation and proliferation in host cells [10]. Among its functions, cruzain induces the production of the proinflammatory peptide Lys bradi-kinin directly by proteolysis of kininogen or by activation of

* Corresponding author.
E-mail address: acllb2003@yahoo.com.br (A.C.L. Leite).

http://dx.doi.org/10.1016/j.ejmech.2016.05.050 0223-5234/

plasmatic pre-kallikrein [9], therefore contributing to the outcome of the infection [11].

Regarding the identification of cruzain inhibitors, most of the efforts have been conducted through the investigation of peptides and peptide-like compounds, such as ureas [9,10], hydrazones [11e14], triazoles [15,16] and thiosemicarbazones [17e19].

Thiosemicarbazones have been largely investigated as anti-T. cruzi agents [17,18,20e24]. Originally, thiosemicarbazones were developed as potential inhibitors of cathepsin-L inhibitors, one of the main proteases involved in cancer development [17]. However, based on the homology and similar biochemical properties be-tween cathepsin-L and cruzain, thiosemicarbazones were investi-gated as a potential class of cruzain inhibitors. Later on, aryl thiosemicarbazones were found to be a class of anti-T. cruzi com-pounds that inhibits cruzain activity [18,19].

Du and co-workers [17] thus identified twelve potent cruzain inhibitors that presented IC_{50} values below 200 nM. Of the active aryl-thiosemicarbazones, the target compound 3-(bromopropio-phenone) thiosemicarbazone (1) was able to inhibit cruzain at a concentration of 100 nM in a time-dependent manner, evidencing the reversible inactivation on the enzyme. Remarkable differences in potency were observed across the congeneric series, probably reflecting the importance of the steric factor in binding to the enzyme. Interestingly, several pyrazoline derivatives seem to be more conformational restricted analogues than aryl-thiosemicarbazones, and have been shown to be as potent as aryl-thiosemicarbazones against cruzain and to act in a similar fashion against the parasite in vitro, being a typical example of a classic bioisosteric relationship between cyclic and non-cyclic scaffolds [25]. This successful example of cruzain inhibitor has led to increased efforts to find new compounds structurally related to 1.

1,3-Thiazole, the cyclic analogue of thiosemicarbazone, is one of the most important scaffolds in heterocyclic chemistry and drug design and discovery. It is widely found in diverse pharmacologi-cally active substances and in some naturally occurring compounds [26]. Thiazole is a versatile building-block for lead generation, and it allows easy access of diverse derivatives for subsequent lead opti-mization [26]. In recent years, many thiazole derivatives have been synthesized and subjected to varied biological activities [26]. Our efforts toward new antiparasitic drug since 2006 have led us to a variety of thiosemicarbazones and thiazolyl hydrazones as trypa-nocidal agents [27e31].

Promising results achieved by compounds bearing a 1,3-thiazole ring motivated us to investigate the trypanocidal activity of novel thiazolyl hydrazones derived from 3-(bromopropiophenone) thio-semicarbazone (1) firstly identified by Du and co-workers [17]. Thus, in this work, the thiosemicarbazone 1 was converted into a set of 4-phenyl-thiazolyl hydrazine, and the effect of antiparasitic activity of different substituents attached at C4 of 1,3-thiazole was investigated. We also studied the influence of a methyl group at the C5 carbon of the thiazole ring, both in the presence or absence of a substituent at the para position of the aromatic ring attached to the 1,3-thiazole and the effect of a methyl or phenyl group at N3 of 1,3-thiazole ring on the antiparasitic activity. (Fig. 1).

2. Results and discussion

2.1. Chemistry

The following thiosemicarbazones 3-(bromopropiophenone)-thiosemicarbazone (1), 2-[1-(3-bromophenyl)propylidene]-N-methylhydrazinecarbothioamide (2) and 2-[1-(3-bromophenyl) propylidene]-N-phenylhydrazinecarbothioamide (3) were pre-pared by reacting commercially available 3^{0}-bromophenyl-1-propanone with corresponding thiosemicarbazide, under reflux in the presence of catalytic HCl. These intermediate compounds then react with different a-halogenated ketones, obtaining the 1a-3c series with yields of 57e72% (Scheme 1). All compounds were identified by infrared (IR) and nuclear magnetic resonance (^{1}H NMR and ^{13}C NMR) spectroscopy, mass spectra (ESI-TOF) and their purity was established by elemental analysis (EA).

NMR data are compatible with the proposed compounds. In theory, two geometrical isomers (E and Z) about the imine (C]N) double bond are possible for the thiosemicarbazones and the respective thiazoles. However, analysis of the ^{1}H NMR spectra of the compounds indicated one predominant isomer; the E isomer by comparison with known analogues [32]. Intramolecular H-bonding involving the proton attached to N4 (in DMSO) with the imine N-atom leads to a distinctive singlet around 10.2 ppm [32] and this is also seen here.

Once thiosemicarbazones were characterized, the respective 1,3-thiazoles were characterized by usual spectroscopy. As exem-plified with the ^{1}H NMR analysis of (E)-4-(biphenyl-4-yl)-2-{2-[1-(3-bromophenyl)propylidene]hydrazinyl}thiazole (1g), the triplet peak at d 1.29 and the quartet peak at d 2.92 correspond to the ethyl group. For the aromatic protons, singlet, doublets or triplets peaks were observed at d 7.19e7.87. For the thiazole ring, a singlet at d 6.76 was found. NH proton appeared as singlet at d 12.89. In ^{13}C NMR spectrum of 1g, peaks d 11.1 and 22.4 ppm correspond to carbons of ethyl group. Peaks of the aromatic carbons were found at d 123.0e140.7 ppm. The presence of peaks at d 101.1 and 170.0 ppm, confirm the thiazole cyclization.

The ^{1}H NMR spectra of 2c and 3c compounds showed that they are composed by diastereomers. Based on previous crystallized compounds by our group, we suggest that the major isomer formed present the E-Z configuration (Fig. 2). Indeed, hydrazine double-bond C2]N2 is commonly assigned as E configuration [3,31,33,34]. Concerning the exocyclic double-bond N3]C3, we suggest that the predominant configuration is Z [17,18,20e24,27,35]. Besides, a representative ^{1}H NMR spectrum of compound 2c is presented in Supplementary Material.

2.2. Cytotoxicity and anti-T. cruzi activity

Comparing host cell cytotoxicity between thiosemicarbazone 1 and 1,3-thiazole 1a, a 2-fold lower cytotoxicity for splenocytes is observed. The insertion of substituents at the para position of the aromatic ring attached at C4 (1,3-thiazole) in series 1a-m reduces the toxicity of eight compounds (1a-g and 1k). Comparing non-substituted compound 1a with 1b (4-methyl substituted) it can be observed that the last is 2-fold less toxic. However, substitution at position 3 (1h, 3-NO_2) and di-substitutions at positions 2,4 (1j, dichloro) or 3,4 (1i, dichloro) do not reduce toxicity when compared with compound 1a (Table 1).

The introduction of a methyl at C5 position of thiazole ring (compounds 1l and 1m) do not reduce the toxicity. Moreover, comparing compound 1 with 2 and 3, it can be seen that the introduction of a methyl (2) at N3 of thiosemicarbazone kept the cytotoxicity, however the substitution with phenyl (3) lead to a 4-fold reduction of cytotoxicity. When the host cell cytotoxicity was compared to Bzd, eight compounds were less toxic (1b-c, 1d-g, 1k and 3), being compounds 1f (4-NO_2), 1g (4-Ph-Ph) and 1k (2-naphthyl) devoid of toxicity in spleen cells (Fig. 3).

Concerning activity against trypomastigotes, the conversion of thiosemicarbazone (1) in 1,3-thiazoles increased the activity, which led us to identify five compounds with similar activity to Bzd (1a, 1c, 1g, 1l and 1m). Specifically, compound 1a showed activity and selectivity index similar to Bzd. In contrast, the substitution of phenyl at C4 (1a) by 2-naphthyl (1k) led to a reduction of activity against trypomastigote form.

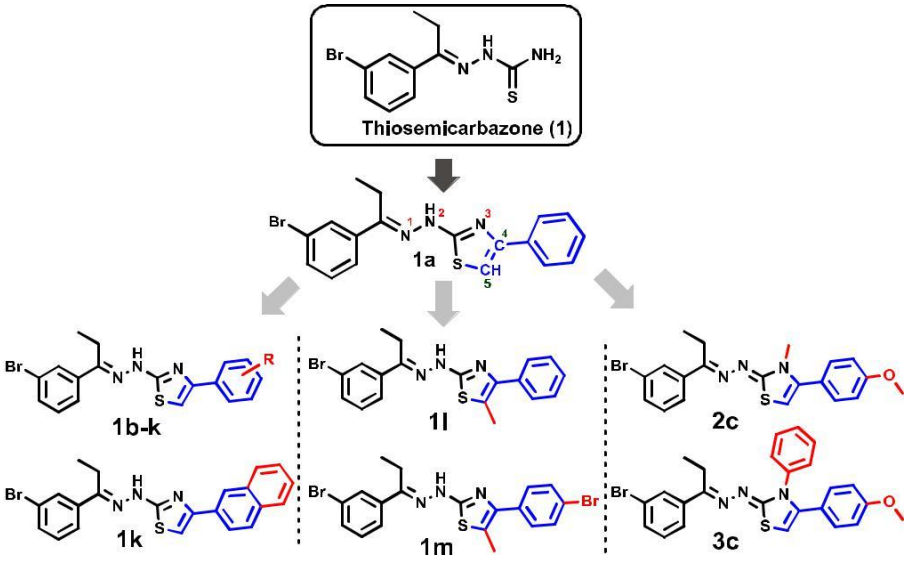

Fig. 1. Structural planning of the proposed series of compounds.

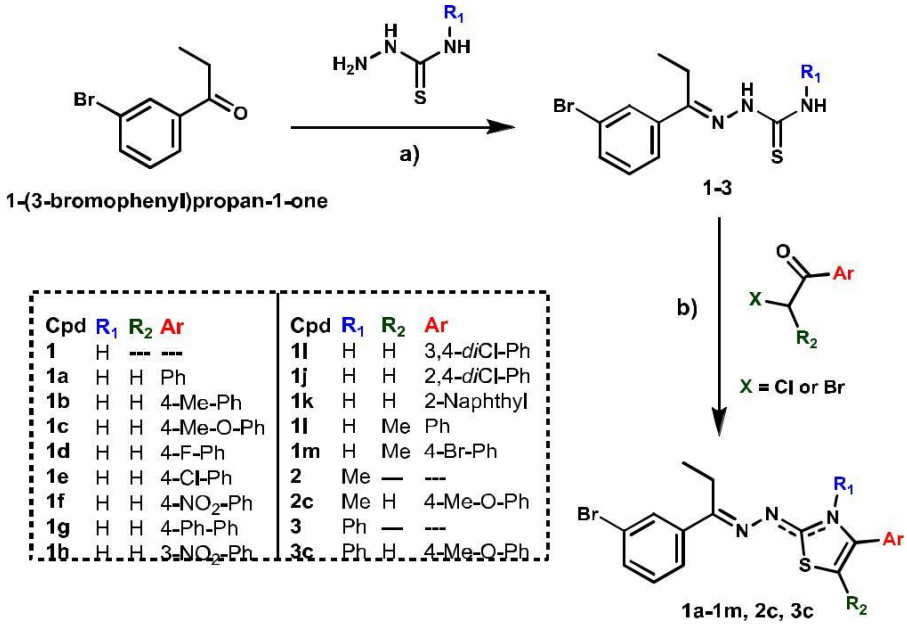

Cpd	R_1	R_2	Ar
1	H	---	---
1a	H	H	Ph
1b	H	H	4-Me-Ph
1c	H	H	4-Me-O-Ph
1d	H	H	4-F-Ph
1e	H	H	4-Cl-Ph
1f	H	H	4-NO_2-Ph
1g	H	H	4-Ph-Ph
1h	H	H	3-NO_2-Ph
1l	H	H	3,4-*di*Cl-Ph
1j	H	H	2,4-*di*Cl-Ph
1k	H	H	2-Naphthyl
1l	H	Me	Ph
1m	H	Me	4-Br-Ph
2	Me	—	---
2c	Me	H	4-Me-O-Ph
3	Ph	—	---
3c	Ph	H	4-Me-O-Ph

Scheme 1. Global synthesis of compounds 1-3c. Reagents and conditions: (a) corresponding thiosemicarbazide, ethanol, HCl, reflux, 2e3 h; (B) corresponding a-haloketone, 2-propanol, rt, 1 h.

Halogens in para position (1d and 1e) of aromatic ring attached to thiazole lead to reduced activity in trypomastigotes. The pres-ence of a methyl (2c) or phenyl (3c) substituent at N3 (thiazole) was also not beneficial to antiparasitic activity. Although the presence of methyl at C5 of thiazole ring was beneficial to cytotoxicity in splenocytes, it improved the antiparasitic activity, as seen with compounds 1l and 1m.

Derivatives 1c (4-OMe) and 1g (4-Ph-Ph) presented better antiparasitic activity, with 1c showing a selectivity index (cyto-toxicity/IC_{50} trypomastigote) about two-times better than Bzd and 1. These results may indicate that the methoxy group present in the molecule 1c is an important substituent for antiparasitic activity.

The compound 1g (4-Ph-Ph) showed a parasite selectivity 4-folds great than Bzd and compound 1. Concerning compound 1k, which contains a bulky 2-naphthyl group, it did not present good trypanocidal activity. The main difference about 1g and 1k is that 1g present more flexibility than 1k, indicating that steric effect and lipophilicity of substituents is not directly related to trypanocidal activity, being mainly flexibility features an important tool to be explored in the future.

Even though thiosemicarbazone (1), synthesized firstly by Du et al. presented the lowest IC_{50} value against trypomastigote form, compounds 1c and 1g showed the highest SI values, (31.3 and 64.5 respectively) being thus promising anti-T. cruzi candidates (Fig. 4).

2.3. Cruzain inhibition

In view to investigate a possible biologic target, compounds were tested against the enzyme cruzain of the T. cruzi. Enzyme inhibition was measured using a fluorimetric assay with the

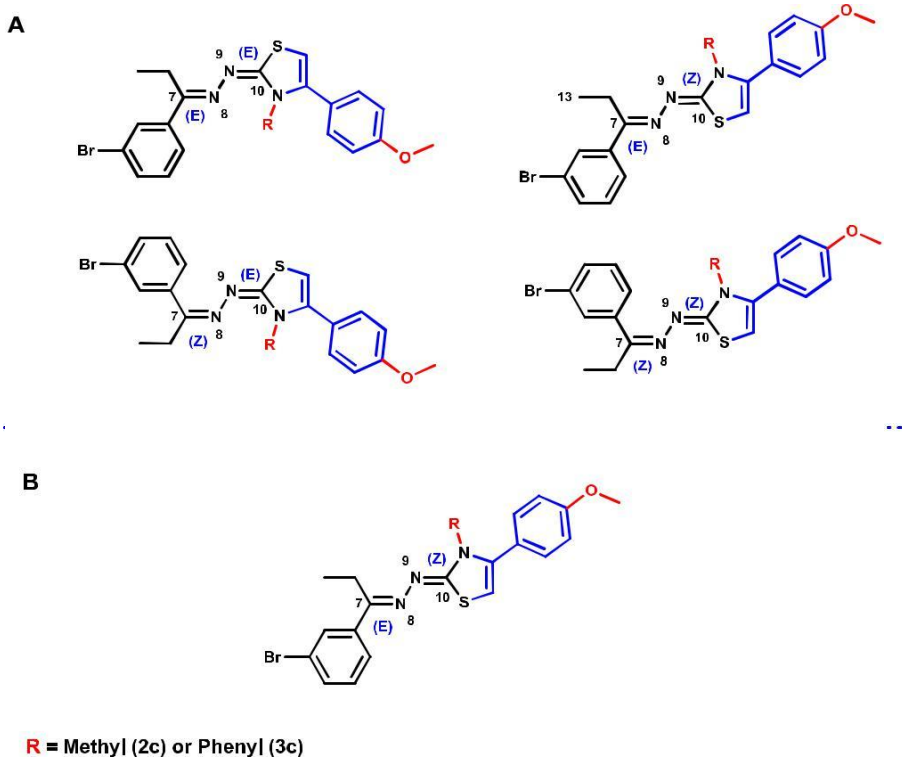

Fig. 2. Isomers representation of compounds 2c and 3c. A- Possible isomers for compounds 2c and 3c. B- Suggested isomer for compounds 2c and 3c.

Table 1

In vitro effect of 3^{0}-(bromopropiophenone)-hydrazinyl-thiazole derivatives on Trypanosoma cruzi (tripomatigotes) and toxicity against mouse splenocytes.

Cpd	R1	R2	Ar	Y strain T. cruzi, IC_{50} (mM) trypomastigote[a]	Toxicity (mM)[b]	SI[c]
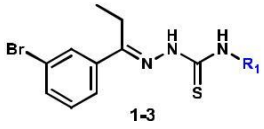 1-3						
1	H	e	e	2.41	34.94	14.5
2	Me	e	e	36.31	33.31	0.9
3	Ph	e	e	13.33	138.01	10.4
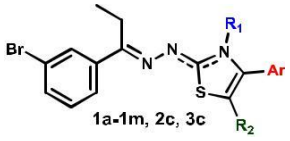 1a-1m, 2c, 3c						
1a	H	H	Ph	5.51	64.71	11.7
1b	H	H	4-Me-Ph	16.64	125.30	7.5
1c	H	H	4-Me-O-Ph	3.84	120.10	31.3
1d	H	H	4-F-Ph	146.05	123.67	0.8
1e	H	H	4-Cl-Ph	140.34	118.83	0.8
1f	H	H	4-NO_2-Ph	60.00	>231.85	>3.9
1g	H	H	4-Ph-Ph	3.35	>216.26	>64.5
1h	H	H	3-NO_2-Ph	15.05	23.18	1.5
1i	H	H	3,4-diCl-Ph	129.72	54.92	0.4
1j	H	H	2,4-diCl-Ph	59.20	54.92	0.9
1k	H	H	2-Naphthyl	50.98	>229.16	>4.5
1l	H	Me	Ph	4.79	12.49	2.6
1m	H	Me	4-Br-Ph	5.80	20.87	3.6
2c	Me	H	4-Me-O-Ph	76.56	58.09	0.7
3c	Ph	H	4-Me-O-Ph	53.10	50.77	0.9
Bzd	e	e	e	6.26	96.1	15.4

[a] Determined 24 h after incubation of trypomastigotes with the compounds. The dose-response curves were determined and the IC_{50} values (mM) were calculated using at least seven concentrations.

[b] Highest non-toxic concentration (>90% incorporation of tritiated thymidine) for mouse splenocytes after 24 h of incubation in the presence of the compounds.

[c] Selective Index (SI) ¼ Cytotoxicity/IC_{50} trypomastigote. Bzd ¼ benznidazole.

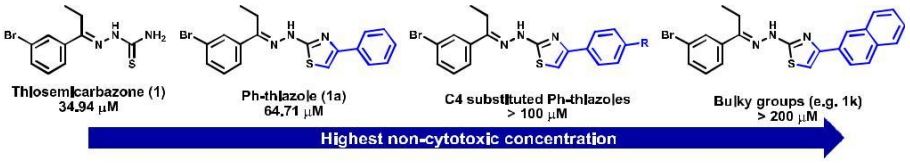

Fig. 3. Highest non-toxic concentration for mouse splenocytes.

substrate Z-Phe-Arg-aminomethylcoumarin (Z-FR-AMC) [36]. All compounds were screened at 300 mM with exception of 2, 2c, 3 (200 mM) and 3c (100 mM), which had to be evaluated at lower concentrations due to their lower solubility. Compounds that inhibited cruzain by at least 80% at the screening concentration were selected for IC_{50} determination (Table 2). Overall, 11 com-pounds had their IC_{50} determined, with values ranging from 0.5 to 45 mM.

Firstly, it was observed that a substitution at N3 for thio-semicarbazones 2 and 3 was deleterious to cruzain inhibition. Comparing compound 1 (IC_{50} ¼ 0.04 ± 0.00 mM) to unsubstituted thiazole 1a (IC_{50} ¼ 44.6 ± 2.2 mM) it is observed that the cyclization was also deleterious for cruzain inhibition, reducing potency 100-fold. In fact, none of the cyclic derivatives 1a-m were more active than thiosemicarbazone 1. Comparing substituted compounds to unsubstituted 1a, it was observed that halogenated substituents (1d-e and 1i,j) at the phenyl ring slightly improved the potency against cruzain (IC_{50}s ranging from 11 to 33 mM). Methoxy de-rivatives did not present cruzain inhibition, even substitution of methyl (1b) and phenyl (1c) at N3 did not only reduced but worsens the activity.

Methyl substituted compounds at C5, 1l and 1m, present a reasonable potency (IC_{50}s ¼ 0.51 ± 0.02 mM and 3.8 ± 0.7 mM, respectively) highlighting compound 1l, which improved the po-tency in comparison to compound 1a, unsubstituted at C5. This improvement can be due a better interaction in the active site of the enzyme. Amongst the cyclic derivatives, the most potent was compound 1l, however, it shows a 12-fold lower potency than 1 (IC_{50} ¼ 0.51 ± 0.02 mM vs IC_{50} ¼ 0.04 ± 0.0 mM).

Curiously, compounds 1c and 1g, which are the most active against T. cruzi trypomastigotes (IC_{50}s ¼ 3.8 and 3.4 mM, respec-tively), did not present high inhibitory activity against cruzain, indicating that their anti-parasite activity occurs through a different target.

As proposed by Du et al. [17], the thioamide moiety has an

Table 2
Inhibitory activity in vitro of inhibitory activity against the cysteine protease cruzain of Trypanosoma cruzi.

Cpd.	R1	R2	Ar	% of inhibition[a]	IC_{50} (mM) ± SEM[b]
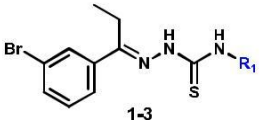 1-3					
1	H	e	e	93.0 ± 0.4	0.04 ± 0.0
2	Me	e	e	11.7 ± 4.9	ND
3	Ph	e	e	49.5 ± 1.3	ND
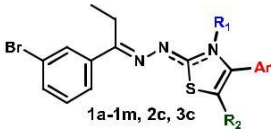 1a-1m, 2c, 3c					
1a	H	H	Ph	80.7 ± 1.7	44.6 ± 2.2
1b	H	H	4-Me-Ph	97.7 ± 0.2	19.2 ± 4.7
1c	H	H	4-Me-O-Ph	72.0 ± 0.2	ND
1d	H	H	4-F-Ph	95.8 ± 0.4	16.5 ± 0.3
1e	H	H	4-Cl-Ph	90.4 ± 0.8	32.7 ± 0.7
1f	H	H	4-NO_2-Ph	68.9 ± 1.1	ND
1g	H	H	4-Ph-Ph	18.1 ± 3.6	ND
1h	H	H	3-NO_2-Ph	85.3 ± 1.2	14.6 ± 4.0
1i	H	H	3,4-diCl-Ph	86.8 ± 1.3	11.3 ± 3.6
1j	H	H	2,4-diCl-Ph	99.7 ± 0.4	15.1 ± 3.6
1k	H	H	2-Naphthyl	88.2 ± 0.1	9.5 ± 3.0
1l	H	Me	Ph	99.5 ± 0.3	0.51 ± 0.02
1m	H	Me	4-Br-Ph	100.0 ± 0.4	3.8 ± 0.7
2c	Me	H	4-Me-O-Ph	33.1 ± 4.1	ND
3c	Ph	H	4-Me-O-Ph	34.3 ± 1.3	ND

[a] Compounds were tested at 100 mM (3c), 200 mM (2, 2c and 3) and 300 mM (1, 1a-m) and the percent inhibition of catalytic activity was determined.

[b] IC50 values (mM) represent the mean ± standard error of the mean (SEM) of three measurements.

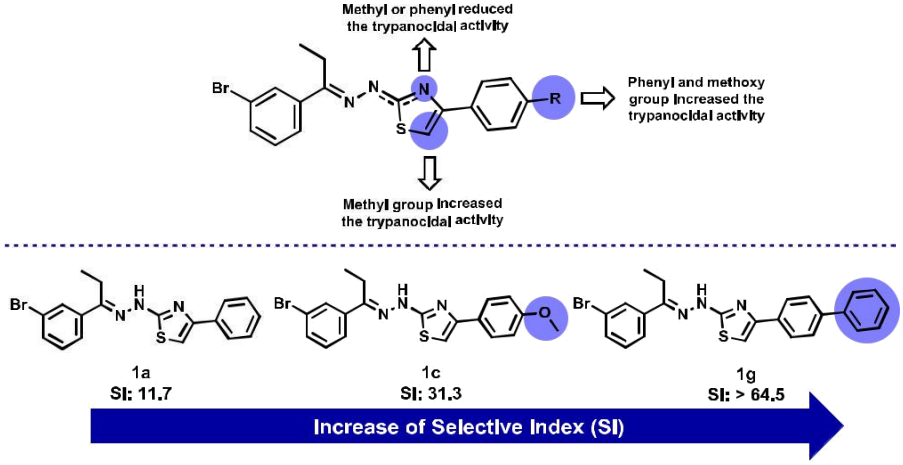

Fig. 4. Summary of SAR of trypanocidal activity and increase of SI of compounds. Selective index (SI) ¼ highest non-toxic concentration in spleen cells of BALB/c mice/IC_{50} trypomastigotes.

important role in the cruzain inhibition mechanism, however it has been demonstrated that cyclic derivatives, as 1,3-thiazoles [31], 2-thiazolidin-4-ones [27] and 2,4-oxadiazoles [13], may also inhibit this enzyme. In this work, most cyclic derivatives present only modest inhibitory activity of cruzain and none of them were most potent than lead thiosemicarbazone 1, however, the most active compounds for tripomastigote form (1c and 1g) did not present inhibitory activity of cruzain, indicating that cyclic derivatives may act by different paths in the parasite.

2.4. Docking studies

To define the structural determinants for cruzain inhibition, and in order to understand the mode of binding in such compounds, their interactions with cruzain (PDB ID: 3IUT) were investigated by docking studies. The binding modes were determined as the highest (most negative) score among the possible solutions for each ligand. Fig. 5 shows the superposition of the best docking solutions for compounds (1a,b, 1d,e and 1h-m), which have IC_{50} values experimentally available for inhibition against the cruzain target. The respective Autodock score values for compounds 1a-1b, 1d-e and 1h-m, are 8.59, 8.76, 6.86, 7.46, 7.99, 7.52, 7.15, 8.29, 8.24 and 8.53 kcal/mol, respectively.

In order to identify the molecular reasons for high affinities towards the cruzain target, it was selected the compound with the highest potency, 1l (IC_{50} ¼ 0.51 ± 0.02 mM), in addition the one which presents one of the lowest inhibitions, 1d (IC_{50} ¼ 16.5 ± 0.3 mM). Additionally, compound 1d presents the lowest inhibition (IC_{50} ¼ 146.05 mM) when tested against the try-pomastigotes forms of T. cruzi Y strains (see Table 1). A detailed analysis of the intermolecular interactions observed in the docking solutions was performed for these molecules. The differences be-tween these two compounds are: (i) the presence of a 4-fluorphenyl linked to the thiazole ring of molecule 1d, instead of a phenyl in molecule 1l; (ii) a methyl group linked to thiazole ring in molecule 1l, rather than a hydrogen atom, for molecule 1d.

The difference between the binding modes of these two mole-cules is show in detail in Fig. 6 and Table 3. It was found a p-p T-shaped interaction for molecule 1l and a p-p interaction for 1d. The hydrogen bond found for 1l, with the residue CYS25, is shorter (2.14 Å) and stronger than the hydrogen bond found for molecule 1d (2.26 Å) with the residue TRP184. It was also found a weak polar interaction (data not shown) for molecule 1l, with the CYS25 residue (2.68 Å) of cruzain. These different intermolecular in-teractions are responsible for the greater stability of the complex formed with 1l than 1d, with docking scores of 8.24 and 6.86 kcal/mol, respectively. These findings corroborate with the in vitro inhibition potency measured for cruzain target.

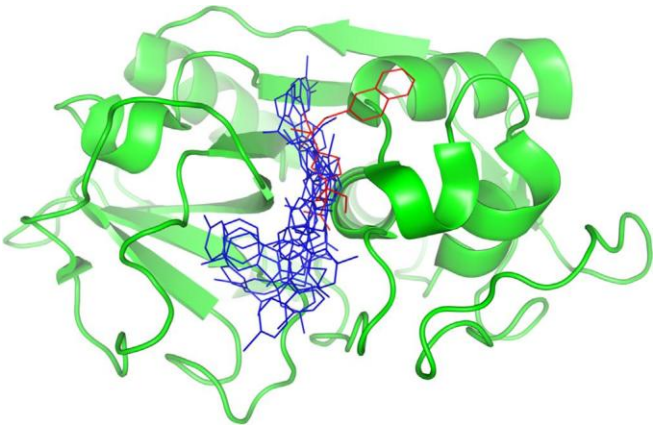

Fig. 5. Superposition of the docking solutions for compounds 1a-1b, 1d-e and 1h-m (blue), bound to T. cruzi cruzain (green), besides the experimental position of the KB2 co-crystallized ligand (red). (For interpretation of the references to color in this figure legend, the reader is referred to the web version of this article.)

2.5. Ultrastructural studies

To investigate the parasite morphological alterations caused by compound 1c, one of the most potent compounds tested (IC_{50} of 3.84 mM), its effects were evaluated at the ultrastructural level. The ultrastructural effects of 1c on trypomastigotes after 24 h were analyzed by Transmission Electron Microscopy (TEM) and Scanning Electron Microscopy (SEM), in concentrations corresponding to once or twice the IC_{50} value (3.4 and 6.8 mM) (Table 1), and revealed several morphological alterations (Fig. 7).

The control group analyzed by SEM showed typical morphology with elongated body (Fig. 7A), whereas the group treated with 1c showed contortion of the parasite body with presence of blebs and alteration in morphology and size of the flagellum which also presented blebs (Fig. 7B).

The control group analyzed by TEM showed normal

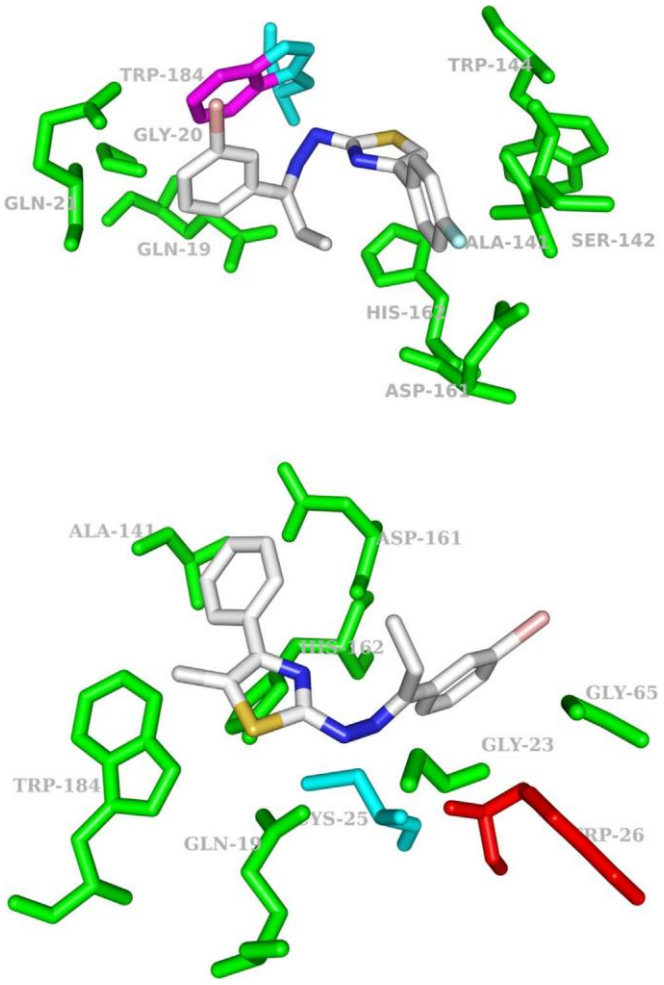

Fig. 6. Detailed view of the docking solutions for compound 1d (above) and 1l (below). The cruzain's residues forming hydrophobic contacts (HC) are colored in green, resi-dues forming hydrogen bonds are colored in blue, residues forming p-p T-shaped are colored in red, and residues forming p- p interactions are colored in margenta. (For interpretation of the references to color in this figure legend, the reader is referred to the web version of this article.)

Table 3
Molecular interactions between the cruzain target and molecules 1d and 1l.

Residues (cruzain)	Molecular interactions	
	1d	1l
GLN19	HC	HC
GLY20	HC	e
GLN21	HC	e
GLY23	e	HC
CYS25	e	2.14
TRP26	e	PIT
GLY65	e	HC
ALA141	HC	HC
SER142	HC	e
TRP144	HC	e
ASP161	HC	HC
HIS162	HC	HC
TRP184	2.26 and PI	HC
Autodock Score	6.86	8.24

HC ¼ hydrophobic contacts. PIT ¼ p-p T-shaped interaction. HB ¼ Hydrogen bond, with distances [Å] between donor and acceptor. PI ¼ p-p interactions. Autodock Score in kcal/mol.

ultrastructural morphology of organelles such as kinetoplast, nu-cleus, nucleolus, flagellum, ribosomes and microtubules membrane (Fig. 7E). The groups treated with 1c analyzed showed intense cytosolic vacuolization, formation of blebs in the membrane, al-terations in the reservosomes, swelling of the mitochondrion and abnormal chromatin condensation (Fig. 7G and H). At the highest compound concentration (6.8 mM) these alterations were empha-sized, and alterations of the parasite morphology were induced. Furthermore, the cytosolic vacuolization was significantly more intense, indicating a dose-dependent action of compound 1c (Fig. 7G and H).

Mitochondrial swelling had already been observed upon treat-ment with various compounds [33,37,38] and published data demonstrate that T. cruzi mitochondrial membranes, in contrast to those of vertebrate cells, are rich in endogenous parasite sterols, which are thought to be required for their energy transducing ac-tivities, being an important action target [34].

The intense cytoplasmic vacuolization observed (Fig. 7G and H), has also been reported in the study of several other compounds described in literature [38e40]. Braga et al. [39] reports that under stress conditions, the cell reacts developing a contractile vacuole. Alterations in the reservosomes could also be important in growth inhibition, since they are involved in endocytosis, storage and breakdown of nutrients and could hamper the proliferation process of the parasite [38]. Observation of alterations in the nucleus can also indicate an effect on parasite proliferation [33].

3. Conclusions

New 3-(bromopropiophenone)hydrazinyl-1,3-thiazoles were prepared from the reaction between 3-(bromopropiophenone)-thiosemicarbazone and a-haloketones. The in vitro bioassay showed that compounds possess substantial antiparasitic activity against the trypomastigote form of T. cruzi. Most compounds were characterized as cruzain inhibitors. However, some of the most potent trypanocidal compounds did not inhibit this enzyme indi-cating that other targets are probably important to kill the parasite. The derivatives 1c and 1g exhibited improved selectivity for para-sites when compared to the reference drug benznidazole. Ultra-structural analysis showed that the compound 1c caused irreversible lesions and changes in parasite morphology in a dose-dependent manner. Our results pointed out the importance of 1,3-thiazoles core as building-blocks for lead generation and showed that adjustment of conformational flexibility could represent a key event to be explored in the future.

4. Experimental section

4.1. Chemistry

Reagents were purchased from Acros Organics, Fluka, Sigma-Aldrich or Vetec and solvents from Vetec or Din^amica. The deuterated solvents (DMSO-d_6, $CDCl_3$, D_2O) were of the CIL brand (Tedia Brazil). The reactions were monitored in thin layer chro-matography (TLC) using silica gel 60 containing fluorescent indi-cator F_{254}. The chromatographic plates were visualized under UV light (at dual wavelength 365 or 254 nm). Melting points were measured using a capillary Thomas Hoover apparatus and the values (C) were not subsequently corrected. For all novel com-pounds, ^1H and ^{13}C NMR analyses were performed, and, when necessary, two-dimensional analysis (DEPT) as well as the addition of D_2O for locating NH signals. All compounds were solubilized in DMSO-d_6. The ^1H and ^{13}C NMR spectra were obtained using Unity Plus model Varian instruments (400 MHz for ^1H, 100 MHz for ^{13}C) or Bruker AMX (300 MHz for ^1H, 75.5 MHz for ^{13}C), using tetra-methylsilane (tms) as internal standard. The number of signals in the ^1H NMR spectra were designated as follows: s/singlet;/ d doublet, t/triplet, dd/double doublet, q/quartet, m/multiplet and the coupling constants, in hertz, as J. Infrared spectroscopy was performed on a Bruker instrument (model IFS 66) using KBr pellets.

4.1.1. General procedure for synthesis of compounds 1, 2 and 3

In a round bottom flask of 100 mL, 1-(3-bromophenyl)propan-1-one (5.5 mmol) and the respective thiosemicarbazide (5.5 mmol) were dissolved in ethanol (20 mL) and HCl (cat.). The mixture was maintained under magnetic stirring and heating reflux for 2e3 h. The reaction was monitored by thin-layer chromatographic plate (TLC). The resulting solid was filtered through a sintered funnel and washed with ethanol to yield pure product.

4.1.1.1. (E)-2-[1-(3-bromophenyl)propylidene]hydrazinecarbothioa-mide (1). 90%yield; mp (C): 144e146; IR (KBr, cm ^{1}) 3415.33 (NH), 1507.11 (C]N); ^1H NMR (DMSO-d_6, 300 MHz) d $_{ppm}$: 0.99 (t, 3H, J ¼ 7.4 Hz, CH_3), 2.86 (q, 2H, J ¼ 7.6 Hz, CH_2), 7.34 (t, 1H, J ¼ 8.0 Hz, Ar), 7.56 (d, 1H, J ¼ 8.0 Hz, Ar), 7.86 (d, 1H, J ¼ 7.6 Hz, Ar), 8.08 and 8.15 (2 s, 2H, NH_2), 8.31 (s, 1H, Ar), 10.35 (s, 1H, NH); ^{13}C NMR (DMSO-d_6, 75.5 MHz) d $_{ppm}$: 10.8 (CH_3), 19.1 (CH_2), 122.1 (Ar), 125.7 (Ar), 129.0 (Ar), 130.4 (Ar), 131.8 (Ar), 138.8 (Ar), 150.2 (C]N), 179.0 (C]S). Anal. Calcd for $C_{10}H_{12}BrN_3S$: C, 41.97; H, 4.23; N, 14.68; S, 11.20. found: C, 41.93; H, 4.26; N, 14.62; S, 11.27. HRMS: 284.9940 [MþH]^þ.

4.1.1.2. (E)-2-[1-(3-bromophenyl)propylidene]-N-methylhy-drazinecarbothioamide (2). 89% yield; mp (C): 148e150; IR (KBr, cm ^{1}): 1552.22 (C]N); ^1H NMR (DMSO-d_6, 300 MHz) d $_{ppm}$: 1.21 (t, J ¼ 7.6 Hz, 3H, CH_3), 2.69 (q, J ¼ 7.6 Hz, 2H, CH_2), 3.29 (d, 3H, CH $_3$), 7.29 (t, J ¼ 7.8 Hz, 1H, Ar), 7.53 (d, J ¼ 7.8 Hz, 1H, Ar), 7.60 (d, J ¼ 7.8 Hz, 1H, Ar), 7.84 (s, 1H, Ar), 8.42 (s, 1H, NH), 8.81 (s, 1H, NH); ^{13}C NMR (DMSO-d_6, 75.5 MHz) d $_{ppm}$: 10.4 (CH_3), 20.1 (CH_2), 31.4 (CH_3), 122.9 (Ar), 124.9 (Ar), 129.2 (Ar), 130.1 (Ar), 132.5 (Ar), 138.4 (Ar), 149.9 (C]N), 178.9 (C]S). Anal. Calcd for $C_{11}H_{14}BrN_3S$: C, 44.01; H, 4.70; N, 14.00; S, 10.68. found: C, 43.93; H, 4.84; N, 14.02; S, 9.83. HRMS: 300.0316 [MþH]^þ.

4.1.1.3. (E)-2-[1-(3-bromophenyl)propylidene]-N-phenyl-hydrazinecarbothioamide (3). 87% yield; mp (C): 169e173; IR (KBr, cm ^{1}): 1588.14 (C]N); ^1H NMR (DMSO-d_6, 300 MHz) d $_{ppm}$: 1.05 (t, J ¼ 7.5 Hz, 3H, CH_3), 2.94 (q, J ¼ 7.5 Hz, 2H, CH_2), 7.22 (t, J ¼ 7.5 Hz, 1H, Ar), 7.35e7.61 (m, 6H, Ar), 7.95 (d, J ¼ 8.1 Hz, 1H, Ar), 8.21 (s, 1H,

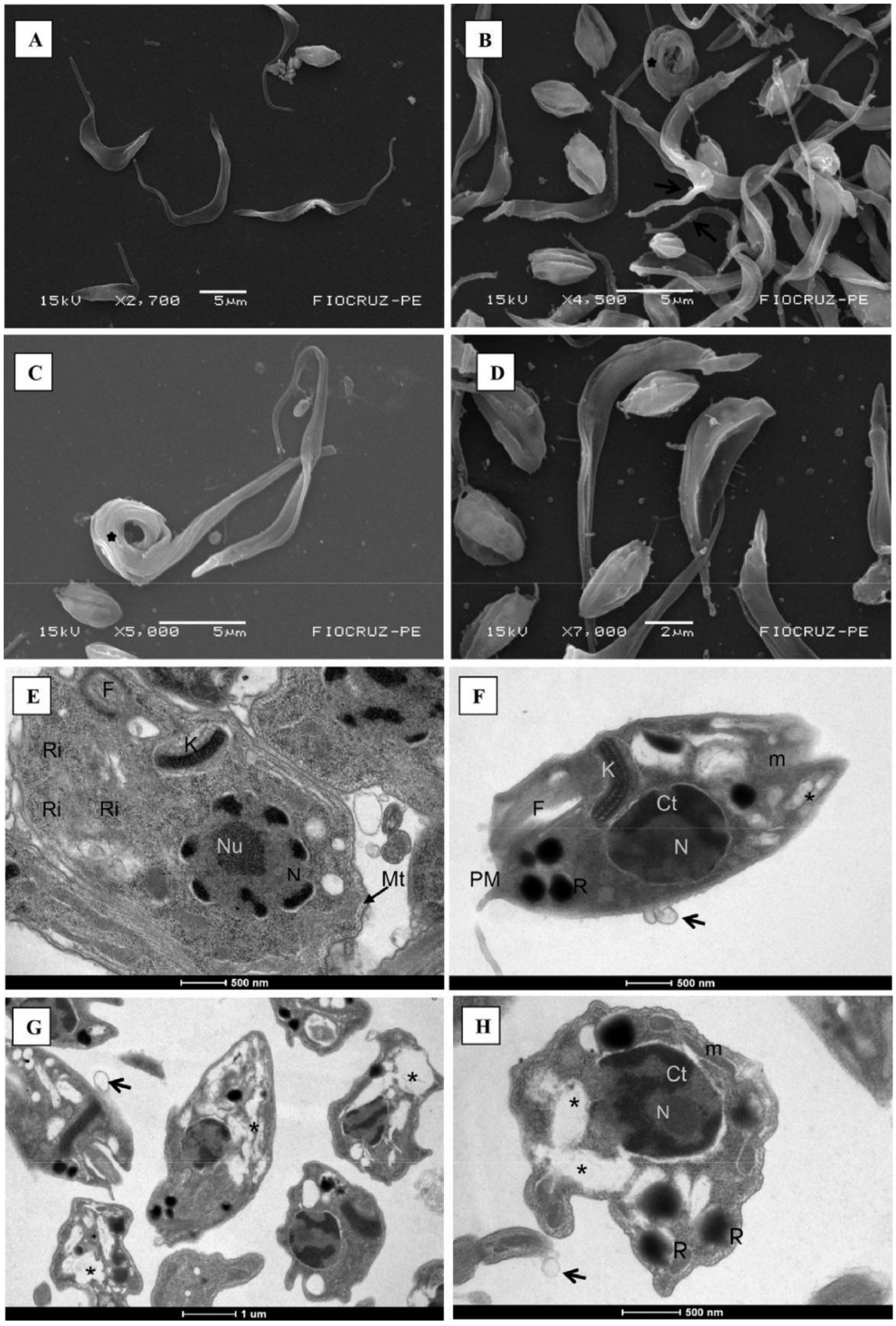

Fig. 7. Effect of 1c on trypomastigotes of T. cruzi morphology observed by SEM and TEM. A- SEM of control untreated trypomastigotes showing the typical elongated body. B- SEM of parasite treated with 3.4 mM of 1c showing contortion (star) of the parasite body and blebs in the flagellum and parasite body. C and D- SEM of parasite treated with 6.8 mM of 1c showing contortion (star) of the parasite body and alteration in morphology and size of the flagellum. E TEM of untreated trypomastigotes showing the normal morphology, with kinetoplast (K), nucleus (N), nucleolus (n), flagellum (F), ribosomes (Ri) and Microtubules membrane (Mt). F- TEM of parasite treated with 3.4 mM of 1c showing alterations in the reservosomes (R), formation of vacuoles (asterisk), bubbles in the membrane (black arrow), abnormal chromatin condensation (Ct), membrane projections (PM) and swelling of the mitochondrion. G and H- TEM of parasite treated with 6.8 mM of 1c showing alterations of the parasite morphology, abnormal chromatin condensation (Ct), intense vacuolization in the cytoplasm (asterisk), swelling of the mitochondrion, bubbles in the membrane (black arrow) and alterations in the reservosomes (R).

Ar), 10.15 (s, 1H, NH), 10.76 (s, 1H, NH); ^{13}C NMR (DMSO-d_6, 75.5 MHz) δ_{ppm}: 10.9 (CH_3), 19.5 (CH_2), 122.1 (Ar), 125.5 (Ar), 126.1 (Ar), 126.3 (Ar), 128.1 (Ar), 129.3 (Ar), 130.4 (Ar), 132.0 (Ar), 138.7 (Ar), 139.2 (Ar), 151.1 (C]N), 177.3 (C]S). Anal. Calcd for $C_{16}H_{16}BrN_3S$: C, 53.04; H, 4.45; N, 11.60; S, 8.85. found: C, 52.93; H, 4.39; N, 11.56; S, 8.79. HRMS: 361.0602 [MþH]$^+$.

4.1.2. General procedure for synthesis of the series (1a-3c)

In round bottom flask, aryl thiosemicarbazone (1, 2 or 3) and the respective 2-bromoacetophenone were dissolved in 2-propanol (20 mL). The reaction mixture was kept at room temperature for 1 h. The reactions were monitored by thin-layer chromatographic plate (TLC). The resulting solid was filtered through sintered funnel with distilled water, yielding the pure product.

4.1.2.1. (E)-2-{2-[1-(3-bromophenyl)propylidene]hydrazinyl}-4-phenylthiazole (1a). 72% yield; mp (C): 196e199; IR (KBr, cm ^{1}): 1516.36 (C]N); ^{1} d H NMR (DMSO- 6, 300 MHz) d ppm: 1.03 (t, J ¼ 6.8 Hz, 3H, CH_3), 2.82 (d, J ¼ 7.2 Hz, 2H, CH_2), 7.28e7.39 (m, 5H, Ar), 7.53 (d, ^{J} ¼ 7.2 Hz, 1H, Ar), 7.73 (d, ^{J} ¼ 7.2 Hz, 1H, $_{13}$Ar), 7.82 (d, J ¼ 7.2 Hz, 2H, Ar), 7.91 (s, 1H, thiazole), 10.64 (s, 1H, NH); C NMR (DMSO-d_6, 75.5 MHz) d ppm: 10.1 (CH_3), 19.6 (CH_2), 104.4 (CH, thiazole), 122.1 (Ar), 124.9 (Ar), 125.6 (Ar), 127.8 (Ar), 127.9 (Ar), 128.2 (Ar), 128.6 (Ar), 130.7 (Ar), 131.4 (Ar), 134.0 (Ar), 138.9 (CeN, thiazole), 149.8 (C]N), 169.6 (SeC]N, thiazole). Anal. Calcd for $C_{18}H_{16}BrN_3S$: C, 55.96; H, 4.17; N, 10.88; S, 8.30. found: C, 56.02; H, 4.14; N, 10.83; S, 8.27. HRMS: 387.1737 [MþH]^{þ}.

4.1.2.2. (E)-2-{2-[1-(3-bromophenyl)propylidene]hydrazinyl}-4-p-tolylthiazole (1b). 69% yield; mp (C): 192e196; IR (KBr, cm ^{1}): 1505.60 (C]N); ^{1} H NMR (DMSO-d_6, 300 MHz) d ppm: 1.06 (s, 3H, CH_3), 2.31 (s, 3H, CH_3), 2.86 (d, ^{J} ¼ 6.8 Hz, 2H, $_{13}$CH), 6.32 (s, 1H, NH), 7.21e7.75 (m, 8H, Ar), 7.94 (s, 1H, thiazole); C NMR (DMSO-d_6, 75.5 MHz) d ppm: 10.6 (CH_3), 19.6 (CH_3), 20.8 (CH_2), 103.4 (CH, thiazole), 122.1 (Ar), 124.8 (Ar), 125.6 (Ar), 127.8 (Ar), 128.2 (Ar), 129.2 (Ar), 130.7 (Ar), 131.3 (Ar), 134.0 (Ar), 137.0 (Ar), 138.9 (CeN, thiazole), 149.0 (C]N), 169.5 (SeC]N, thiazole). Anal. Calcd for $C_{19}H_{18}BrN_3S$: C, 57.00; H, 4.53; N, 10.50; S, 8.01. found: C, 57.07; H, 4.58; N, 10.48; S, 8.05. HRMS: 399.1896 [MþH]^{þ}.

4.1.2.3. (E)-2-{2-[1-(3-bromophenyl)propylidene]hydrazinyl}-4-(4-methoxyphenyl)thiazole (1c). 62% yield; mp (C): 197e200; IR (KBr, cm ^{1}): 3115.41 (NH), 2954.46 and 2831.76 (CH Ar), 1509.43 (C]N); ^{1} H NMR (DMSO-d_6, 300 MHz) d ppm: 1.06 (t, J ¼ 7.3 Hz, 3H, CH_3), 2.78 (q, J ¼ 7.5 Hz, 2H, CH_2), 3.78 (s, 3H, CH_3), 5.71 (s, 1H, NH), 6.98 (d, J ¼ 8.7 Hz, 2H, Ar), 7.16 (s, 1H, Ar), 7.39 (t, J ¼ 7.8 Hz, 1H, Ar), 7.57 (dd, J ¼ 8.1 Hz, 1H, Ar), 7.78 (d, $_{13}$ ¼7.8 Hz, 1H, Ar), 7.79 (d, ¼ 8.4 Hz, 2H, Ar), 7.95 (s, 1H, thiazole); C NMR (DMSO-d_6, 75.5 MHz) d ppm: 10.7 (CH_3), 19.6 (CH_2), 55.2 (CH_3), 102.3 (CH, thiazole), 114.0 (Ar), 122.2 (Ar), 124.9 (Ar), 125.6 (Ar), 127.0 (Ar), 127.9 (Ar), 128.2 (Ar), 130.8 (Ar), 131.4 (Ar), 137.0 (Ar), 139.0 (CeN, thiazole), 158.9 (C]N), 169.5 (SeC]N, thiazole). Anal. Calcd for $C_{19}H_{18}BrN_3OS$: C, 54.81; H, 4.36; N, 10.09; O, 3.84; S, 7.70. found: C, 54.96; H, 4.20; N, 10.02; S, 7.74. HRMS: 414.8419 [M H] .

4.1.2.4. (E)-2-{2-[1-(3-bromophenyl)propylidene]hydrazinyl}-4-(4-fluorophenyl)thiazole (1d). 65% yield; mp (C): 207e210; IR (KBr, cm ^{1}): 1509.35 (C]N); ^{1}H NMR (DMSO-d_6, 300 MHz) d ppm: 1.07 (t, ^{J} ¼ 7.4 Hz, 3H, CH 3), 2.85 (q, $_{13}$ ¼ 7.4 Hz, 2H, CH), 4.28 (s, 1H, NH), 7.22e7.93 (m, 9H, Ar); C NMR (DMSO-d_6, 75.5 MHz) d ppm: 10.6 (CH_3), 19.5 (CH_2), 104.1 (CH, thiazole), 115.3 (Ar), 115.6 (Ar), 122.1 (Ar), 124.8 (Ar), 127.5 (Ar), 127.6 (Ar), 128.1 (Ar), 129.2 (Ar), 130.7 (Ar), 131.3 (Ar), 139.1 (CeN, thiazole), 149.2 (C]N), 169.7 (SeC]N, thiazole). Anal. Calcd for $C_{18}H_{15}BrFN_3S$: C, 53.47; H, 3.74; N, 10.39; S, 7.93. found: C, 54.14; H, 3.69; N, 10.41; S, 7.98. HRMS: 404.0101 [MþH]^{þ}.

4.1.2.5. (E)-2-{2-[1-(3-bromophenyl)propylidene]hydrazinyl}-4-(4-chlorophenyl)thiazole (1e). 62% yield; mp (C): 204e209; IR (KBr, cm ^{1}): 3922.26 (NH); ^{1}H NMR (DMSO-d_6, 300 MHz) d ppm: 1.09 (t, ^{J} ¼ 5.8 Hz, 3H, CH 3), 2.83 (q, $_{13}$ ¼ 5.8 Hz, 2H, CH), 6,01 (s, 1H, NH), 7.36e7.93 (m, 9H, Ar); C NMR (DMSO-d_6, 75.5 MHz) d ppm: 10.6 (CH_3), 19.6 (CH_2), 105.2 (CH, thiazole), 122.1 (Ar), 124.8 (Ar), 127.3 (Ar), 128.7 (Ar), 129.6 (Ar), 130.8 (Ar), 131.3 (Ar), 132.0 (Ar), 132.4 (Ar), 133.5 (Ar), 139.1 (CeN, thiazole), 149.2 (C]N), 169.8 (SeC]N, thiazole). Anal. Calcd for $C_{18}H_{15}BrClN_3S$: C, 51.38; H, 3.59; N, 9.99; S, 7.62. found: C, 52.04; H, 3.60; N, 9.97; S, 7.64. HRMS: 421.1562 [MþH]^{þ}.

4.1.2.6. (E)-2-{2-[1-(3-bromophenyl)propylidene]hydrazinyl}-4-(4-nitrophenyl)thiazole (1f). 63% yield; mp (C): 193e196; IR (KBr, cm ^{1}): 3332.81 (NH), 1508.37 (C]N); ^{1}H NMR (DMSO-d_6, 300 MHz) d ppm: 1.07 (t, ^{J} ¼7.8 Hz, 3H, CH_3), 2.86 (q, J ¼ 7.8 Hz, 2H, $_{13}$ CH_2), 7.39e8.29 (m, 9H, Ar), 11.66 (s, 1H, NH); C NMR (DMSO-d_6, 75.5 MHz) d ppm: 10.5 (CH_3), 19.6 (CH_2), 109.2 (CH, thiazole), 122.1 (Ar), 124.1 (Ar), 124.8 (Ar), 126.3 (Ar), 128.2 (Ar), 130.7 (Ar), 131.3 (Ar), 132.4 (Ar), 133.5 (Ar), 139.0 (Ar), 140.7 (CeN, thiazole), 146.2 (C]N), 170.0 (SeC]N, thiazole). Anal. Calcd for $C_{18}H_{15}BrN_4O_2S$: C, 50.13; H, 3.51; N, 12.99; S, 7.43. found: C, 50.15; H, 3.55; N, 12.97; S, 7.39. HRMS: 430.9228 [MþH]^{þ}.

4.1.2.7. (E)-4-(biphenyl-4-yl)-2-{2-[1-(3-bromophenyl)propylidene] hydrazinyl}thiazole (1g). 64% yield; mp (C): 218e221; IR (KBr, cm ^{1}): 1611.72 (C]N); ^{1}H NMR (DMSO-d_6, 300 MHz) d ppm: 1.29 (t, ^{J} ¼ 7.8 Hz, 3H, CH_3), 2.92 (q, J ¼ 7.8 Hz, 2H, CH_2), 6.76 (s, 1H, Thiazole), 7.19e7.87 (m, 13H, Ar), 12.89 (s, 1H, NH); ^{13} C NMR (DMSO-d_6, 75.5 MHz) d ppm: 11.1 (CH_3), 22.4 (CH_2), 101.1 (CH, thiazole), 123.0 (Ar), 125.4 (Ar), 125.8 (Ar), 126.0 (Ar), 126.9 (Ar), 128.1 (Ar), 128.2 (Ar), 128.9 (Ar), 129.7 (Ar), 130.2 (Ar), 133.5 (Ar), 136.9 (Ar), 139.5 (Ar), 140.7 (Ar), 143.2 (CeN, thiazole), 159.7 (C]N), 170.0 (SeC]N, thiazole). Anal. Calcd for $C_{24}H_{20}BrN_3S$: C, 62.34; H, 4.36; N, 9.09; S, 6.93. found: C, 62.35; H, 4.38; N, 9.07; S, 6.96. HRMS: 461.9808 [MþH]^{þ}.

4.1.2.8. (E)-2-{2-[1-(3-bromophenyl)propylidene]hydrazinyl}-4-(3-nitrophenyl)thiazole (1h). 64% yield; mp (C): 220e223; IR (KBr, cm ^{1}): 1530.66 (C]N); ^{1}H NMR (DMSO-d_6, 300 MHz) d ppm: 1.07 (t, ^{J} ¼ 7.8 Hz, 3H, CH), 2.86 (q, $_{3}$ ¼ 7.8 Hz, 2H, $_{13}$CH), 6.83 (s, 1H, NH), 7.39e8.72 (m, 9H, Ar), 11.6 (s, 1H, NH); C NMR (DMSO-d_6, 75.5 MHz) d ppm: 10.5 (CH_3), 19.5 (CH_2), 107.1 (CH, thiazole), 120.0 (Ar), 122.1 (Ar), 124.8 (Ar), 128.2 (Ar), 130.2 (Ar), 130.7 (Ar), 131.3 (Ar), 131.5 (Ar), 133.5 (Ar), 136.2 (Ar), 139.0 (Ar), 140.7 (Ar), 148.3 (CeN, thiazole), 149.3 (C]N), 169.9 (SeC]N, thiazole). Anal. Calcd for $C_{18}H_{15}BrN_4O_2S$: C, 50.13; H, 3.51; N, 12.99; S, 7.43. found: C, 50.09; H, 3.56; N, 12.97; S, 7.45. HRMS: 431.2205 [MþH]^{þ}.

4.1.2.9. (E)-2-{2-[1-(3-bromophenyl)propylidene]hydrazinyl}-4-(3,4-dichlorophenyl)thiazole (1i). 60% yield; mp (C): 228e231; IR (KBr, cm ^{1}): 3642.77 and 2971.43 (CH Ar), 1475.20 (C]N); ^{1}H NMR (DMSO-d_6, 300 MHz) d ppm: 1.04 (t, ^{J} ¼ 7.5 Hz, 3H, CH_3), $_{13}$ 2.84 (q, J ¼ 7.5 Hz, 2H, CH_2), 5.29 (s, 1H, NH), 7.35e8.10 (m, 8H, Ar); C NMR (DMSO-d_6, 75.5 MHz) d ppm: 10.6 (CH_3), 19.6 (CH_2), 106.6 (CH, thiazole), 122.2 (Ar), 124.8 (Ar), 125.6 (Ar), 127.2 (Ar), 128.2 (Ar), 129.7 (Ar), 130.8 (Ar), 131.5 (Ar), 135.2 (Ar), 139.0 (Ar), 147.9 (Ar), 149.3 (Ar), 150.4 (CeN, thiazole), 149.3 (C]N), 169.8 (SeC]N, thiazole). Anal. Calcd for $C_{18}H_{14}BrCl_2N_3S$: C, 47.49; H, 3.10; N, 9.23; S, 7.04. found: C, 47.47; H, 3.13; N, 9.26; S, 7.06. HRMS: 451.8046 [M H] .

4.1.2.10. (E)-2-{2-[1-(3-bromophenyl)propylidene]hydrazinyl}-4-(2,4-dichlorophenyl)thiazole (1j). 66% yield; mp (C): 174e179; IR (KBr, cm ^{1}): 1518.07 (C]N); ^{1}H NMR (DMSO-d_6, 400 MHz) d ppm: 1.06 (t, J ¼ 7.6 Hz, 3H, CH 3), 2.84 (q, $_{13}$ ¼ 7.6 Hz, 2H, CH), 4.04 (s, 1H, NH), 7.38e7.94 (m, 8H, Ar); C NMR (DMSO-d_6, 75.5 MHz) d ppm: 10.6 (CH_3), 19.6 (CH_2), 109.8 (CH, thiazole), 122.1 (Ar), 124.8 (Ar), 125.6 (Ar), 127.5 (Ar), 128.2 (Ar), 129.7 (Ar), 130.7 (Ar), 131.3 (Ar), 131.6 (Ar), 132.3 (Ar), 132.6 (Ar), 135.2 (Ar), 139.0 (CeN, thiazole),

149.3 (C]N), 168.8 (SeC]N, thiazole). Anal. Calcd for $C_{18}H_{14}BrCl_2N_3S$: C, 47.49; H, 3.10; N, 9.23; S, 7.04. found: C, 47.45; H, 3.13; N, 9.28; S, 7.05. HRMS: 451.9214 [M H] .

4.1.2.11. (E)-2-{2-[1-(3-bromophenyl)propylidene]hydrazinyl}-4-(naphthalen-2-yl)thiazole (1k). 57% yield; mp (C): 198e201; IR (KBr, cm ^{1}): 1614.36 (C]N); ^{1}H NMR (DMSO-d_6, 300 MHz) d $_{ppm}$: 1.36 (t, J ¼ 7.6 Hz, 3H, CH_3), 2.97 (q, J ¼ 7.6 Hz, 2H, CH_2), 6.92 (s, 1H, thiazole), 7.31 (t, J ¼ 7.5 Hz, 1H, Ar), 7.52e7.59 (m, 3H, Ar), 7.68e7.73 (m, 2H, Ar), 7.82 (t, J ¼ 4,6 Hz, 1H, Ar), 7.90e7.98 (m, 3H, Ar), 8.26 (s, 1H, Ar), 13.02 (s, 1H, NH); ^{13}C NMR (DMSO-d_6, 75.5 MHz) d $_{ppm}$: 11.1 (CH_3), 22.4 (CH_2), 101.6 (CH, thiazole), 120.0 (Ar), 122.2 (Ar), 123.0 (Ar), 124.2 (Ar), 125.4 (Ar), 125.6 (Ar), 127.3 (Ar), 127.7 (Ar), 128.9 (Ar), 129.6 (Ar), 129.7 (Ar), 130.3 (Ar), 133.1 (Ar), 133.5 (Ar), 133.8 (Ar), 136.9 (Ar), 140.9 (CeN, thiazole), 159.6 (C]N), 170.1 (SeC]N, thiazole). Anal. Calcd for $C_{22}H_{18}BrN_3S$: C, 60.55; H, 4.16; N, 9.63; S, 7.35. found: C, 60.57; H, 4.14; N, 9.59; S, 7.40. HRMS: 436.1018 [MþH]^{þ}.

4.1.2.12. (E)-2-{2-[1-(3-bromophenyl)propylidene]hydrazinyl}-5-methyl-4-phenylthiazole (1l). 62% yield; mp (C): 202e206; IR (KBr, cm ^{1}): 1614.94 (C]N); ^{1}H NMR (DMSO-d_6, 300 MHz) d $_{ppm}$: 1.32 (t, J ¼ 7.6 Hz, 3H, CH_3), 2.46 (s, 3H, CH_3), 2.96 (q, J ¼ 7.6 Hz, 2H, CH $_2$), 7.30 (t, 1H, Ar), 7.45e7.57 (m, 6H, Ar), 7.68 (d, 1H, Ar), 7.93 (s, 1H, Ar), 12.9 (s, 1H, NH); ^{13}C NMR (DMSO-d_6, 75.5 MHz) d $_{ppm}$: 11.1 (CH_3), 12.3 (CH_3), 22.3 (CH_2), 115.9 (C, thiazole), 120.0 (Ar), 122.9 (Ar), 125.3 (Ar), 127.8 (Ar), 129.5 (Ar), 129.6 (Ar), 129.9 (Ar), 130.2 (Ar), 133.3 (Ar), 135.2 (Ar), 137.1 (CeN, thiazole), 159.1 (C]N), 167.6 (SeC]N, thiazole). Anal. Calcd for $C_{19}H_{18}BrN_3S$: C, 57.00; H, 4.53; N, 10.50; S, 8.01. found: C, 57.07; H, 4.49; N, 10.45; S, 8.09. HRMS: 400.0076 [MþH]^{þ}.

4.1.2.13. (E)-4-(4-bromophenyl)-2-{2-[1-(3-bromophenyl)propylidene]hydrazinyl}-5-methylthiazole (1 m). 61% yield; mp (C): 192e197; IR (KBr, cm ^{1}): 1614.94 (C]N); ^{1}H NMR (DMSO-d_6, 300 MHz) d $_{ppm}$: 1.05 (t, J ¼ 7.2 Hz, 3H, CH_3), 2.40 (s, 3H, CH_3), 2.83 (q, J ¼ 7.2 Hz, 2H, CH_2), 4.64 (s, 1H, NH), 7.38 (t, J ¼ 7.8 Hz, 1H, Ar), 7.58 (m, 5H, Ar), 7.76 (d, J ¼ 7.2 Hz, 1H, Ar), 7.94 (s, 1H, Ar); ^{13}C NMR (DMSO-d_6, 75.5 MHz) d $_{ppm}$: 10.6 (CH_3), 12.1 (CH_3), 19.6 (CH_2), 118.2 (C, thiazole), 120.6 (Ar), 122.1 (Ar), 124.8 (Ar), 125.6 (Ar), 127.8 (Ar), 128.2 (Ar), 129.2 (Ar), 130.1 (Ar), 130.7 (Ar), 131.3 (Ar), 138.9 (CeN, thiazole), 149.2 (C]N), 165.8 (SeC]N, thiazole). Anal. Calcd for $C_{19}H_{17}Br_2N_3S$: C, 47.62; H, 3.58; N, 8.77; S, 6.69. found: C, 47.64; H, 3.59; N, 8.73; S, 6.71. HRMS: 475.5986 [M H] .

4.1.2.14. (E)-2-{(Z)-[1-(3-bromophenyl)propylidene]hydrazono}-4-(4-methoxyphenyl)-3-methyl-2,3-dihydrothiazole (2c). 63% yield; mp (C): 185e190; IR (KBr, cm ^{1}): 1583.39 (C]N); ^{1}H NMR (DMSO-d_6, 300 MHz), d $_{ppm}$: 1.80 (t, J ¼ 7.6 Hz, 3H, CH_3), 3.97 (q, J ¼ 7.4 Hz, 2H, CH_2), 4.42 (s, 3H, CH_3), 4.68 (s, 3H, CH_3), 7.56 (d, J ¼ 8.7 Hz, 2H, Ar), 7.81e7.89 (m, 3H, Ar), 8.12 (d, J ¼ 7.5 Hz, 1H, Ar), 8.22 (d, J ¼ 8.4 Hz, 1H, Ar), 8.46 (s, 1H, Ar), 13.61 (s, 1H, NH); ^{13}C NMR (DMSO-d_6, 75.5 MHz), d $_{ppm}$: 11.4 (CH_3), 24.1 (CH_2), 39.9 (CH_3), 55.5 (CH_3), 106.9 (CH, thiazole), 114.8 (Ar), 119.7 (Ar), 122.8 (Ar), 125.8 (Ar), 130.2 (Ar), 130.8 (Ar), 133.3 (Ar), 136.5 (Ar), 137.6 (Ar), 144.5 (Ar), 161.5 (CeN, thiazole), 163.8 (C]N), 171.7 (SeCeN, thiazole). Anal. Calcd for $C_{20}H_{20}BrN_3OS$: C, 55.82; H, 4.68; N, 9.76; S, 7.45. found: C, 55.86; H, 4.63; N, 9.76; S, 7.42. HRMS: 430.0137 [MþH]^{þ}.

4.1.2.15. (E)-2-{(Z)-[1-(3-bromophenyl)propylidene]hydrazono}-3,4-diphenyl-2,3-dihydrothiazole (3c). 69% yield; mp (C): 246e250; IR (KBr, cm ^{1}): 1585.32 (C]N); ^{1}H NMR (DMSO-d_6, 400 MHz), d $_{ppm}$: 1.80 (t, J ¼ 6.0 Hz, 3H, CH_3), 2.58 (q, J ¼ 6.0 Hz, 2H, CH_2), 3.86 (s, 3H, CH_3), 6.63 (s, 1H, Thiazole), 7.01 (d, J ¼ 6.8 Hz, 2H, Ar), 7.18e7.32 (m, 5H, Ar), 7.58e7.70 (m, 5H, Ar), 7.95 (s, 1H, Ar); ^{13}C NMR (DMSO-d_6, 75.5 MHz), d $_{ppm}$: 55.5 (CH_3), 70.7 (CH_2), 99.0 (CH_3), 115.1 (CH, thiazole), 123.0 (Ar), 125.3 (Ar), 127.3 (Ar), 128.2 (Ar), 128.9 (Ar), 129.0 (Ar), 129.5 (Ar), 129.6 (Ar), 131 0.2 (Ar), 130.2 (Ar), 130.6 (Ar), 133.5 (Ar), 138.1 (Ar), 144.0 (Ar), 161.0 (CeN, thiazole), 164.1 (C]N), 172.0 (SeCeN, thiazole). Anal. Calcd for $C_{24}H_{20}BrN_3S$: C, 62.34; H, 4.36; N, 9.09; S, 6.93. found: C, 62.36; H, 4.33; N, 9.06; S, 6.89. HRMS: 492.1973 [MþH]^{þ}.

4.2. Biological assays

4.2.1. Toxicity to splenocytes

Splenocytes from BALB/c mice were divided into plate with 96 wells at a density of 5 10^6 cells per wells in RPMI-1640 medium containing 10% inactivated Fetal Bovine Serum (FBS). Each chemical inhibitor was dissolved in DMSO at the concentration of 10 mg/mL and then the sample was serially diluted in RPMI-1640 medium supplemented with 10% FBS at the concentrations of 1.0, 5.0, 10, 25, 50 and 100 mg/mL, in triplicate. As a positive control, we used saponin in concentration of 0.1 mg/mL, while as the negative control wells received only an RPMI-1640 medium supplemented with 10% FBS and DMSO. The plate was added 1.0 mCi of ^{3}H- hymidine to each well and the plate was incubated for 24 h at 37 C and 5% CO_2. The plate was then read in the counter beta irradiation (Multilabel Reader, Finland) and tritiated thymidine percent incorporation was determined. For cells that were not treated with drugs (negative control) was calculated as 100% of tritiated thymidine incorpora-tion (100% viable cells). For cells treated with saponin, cell viability was 5%. When the percentage of incorporation was higher than 90%, the concentration of the drug was regarded as nontoxic to splenocytes.

4.2.2. Toxicity to trypomastigotes

Strain Y trypomastigotes were collected from Vero cells super-natant and distributed in a plate with 96 wells for a final density of 4 10^5 cells per well. Each chemical inhibitor was added to the wells in triplicate. Benznidazole were used as positive controls in this assay. The plate was then cultivated for 24 h at 37 C containing 5% CO_2. After this time, aliquots from each well were collected and the number of viable parasites (ie, with apparent motility) was counted in a Neubauer chamber. To the wells that did not receive the chemical inhibitors, it was assumed as 100% the number of viable parasites. The dose-response curves were determined and the IC_{50} values (mM) were calculated using at least seven concen-trations (data-points) using nonlinear regression (Prism, version 4.0).

4.2.3. Ultrastructural studies

The parasites were cultured for 24 h in medium RPMI 1640 medium (SigmaAldrich, St. Louis, MO, USA) buffered to pH 7.5, supplemented with HEPES (20 mM), 10% fetal bovine serum, penicillin (100 U/mL), and streptomycin (100 mg/mL) containing the compound 1c in IC_{50} concentration and twice the value of IC_{50}. The parasites were collected, washed in PBS and fixed with 2.5% glutaraldehyde, 4% formaldehyde, and 0.1 M cacodylate buffer at pH 6.8. They were then postfixed in 2% osmium tetroxide (OsO_4) in a 0.1 M cacodylate buffer at pH 6.8 and processed for routine transmission electron microscopy (TEM) and scanning electron microscopy (SEM). For SEM analysis, the parasites were dehydra-tion in a graded ethanol, dried by the critical point method with CO_2. The samples were mounted on aluminum stubs, coated with gold and examined under a JEOL-5600LV microscope. For TEM analysis, the parasites were dehydration in a graded series of acetone and finally embedded in epon. Sections were stained with uranyl acetate and lead citrate and observed with Tecnai spirit G2 Biotwin microscope.

4.2.4. Cruzain analysis

Recombinant cruzain truncated at the C-terminal was kindly provided by Allison Doak and Brian Shoichet (UCSF, USA). Cruzain activity was monitored as previously reported, based on the fluo-rescence resulting from the cleavage of the substrate Z-Phe-Arg-aminomethylcoumarin (Z-FR-AMC), with 340/440 nm excitation/ emission filters. The assays were carried in a microplate reader Synergy 2 (Biotek®) from the Center of Flow Cytometry and Fluo-rimetry at the Biochemistry and Immunology Department (UFMG). Fluorescence was measured at 25 C, for five minutes at 12 s in-tervals, using BioTek's Gen5™ Reader Control and Data Analysis Software. Reaction rates were calculated from initial velocity rates compared to a DMSO control. Compounds were tested in sodium acetate buffer 0.1 M, pH 5.5, containing 0.01% Triton X-100, 1 mM b-mercaptoethanol, 1 nM cruzain and 2,5 mM substrate. There was no pre-incubation with the enzyme. All assays were performed in at least twice in independent experiments, each performed in tripli-cate. When the inhibition was higher than 80% at highest soluble concentration for the compounds evaluated (300, 200 and 100 mM), IC_{50} curves were determined based on seven different compound concentrations and calculated using GraphPad Prism 6 (GraphPad, San Diego, USA), employing the nonlinear regression "log (inhibi-tor) vs response with variable slope e four parameters" analysis.

4.3. Docking studies

The compounds 1a-b, 1d-e and 1h-m were selected for in silico studies, because their inhibitory potency (IC_{50}) was measured against the cysteine protease of Trypanosoma cruzi (cruzain), as one can see in Table 3. The structures and conformational analysis were obtained through the application of the RM1 semi-empirical approach [41], which is available as part of the SPARTAN 08^0 pro-gram [42], using internal default settings for convergence criteria. The analysis and docking calculation were carried using the T. cruzi cruzain target [15], available at the RCSB Protein Data Bank (PDB ID: 3IUT), which is composed of a co-crystallized complex with an inhibitor (referred as KB2). The space for searching of docking so-lutions was defined to lie within a region of 27.0 Å in direction X, 25.5 Å in direction Y, and 31.5 Å in direction Z, centered on the coordinates based on the reference of the co-crystallized ligand KB2 (X ¼ 2.772; Y ¼ 12.987; Z ¼ 4.357; all in Å). The docking cal-culations were carried out using the AutoDockTools and AutoDock (v.4.2) programs [43], using the default parameters for all the var-iables, except for the number of docking runs (50), the maximum number of energy evaluations on Genetic Algorithm-GA (25,000,000), and the maximum number of generations in GA (10,000). Preliminary calculations indicate that these three specific parameter modifications provide significant improvement in the results obtained using the docking procedure, thereby producing more significant solutions. The ligands were then docked using the Genetic Algorithm followed by a Local Search procedure (GA_LS), also known as a Lamarckian Genetic Algorithm (LGA), and the 50 lowest energy structures were stored for further analysis. The res-idues GLN19, CYS25, SER61, LEU67, MET68, ASN70, ASP161, HIS162 and TRP184 were treated as flexible during the calculations, in or-der to take into account some induced fit effects. The Binana pro-gram [44] was used to analyze the molecular interactions present in the best docking solutions, using default setting, except for hydrogen bond distance, which was changed to a maximum of 3.5 Å. Figures were generated with Pymol software [45].

Acknowledgement

This work received funding by CNPq (grant number 471461/ 2011-3 to A.C.L.L.), CAPES (grant number 23038.003155/2011-37 to V.R.A.P.) PRONEX-FAPESB (grant number 8804-2014 to D.R.M.M.) and PRONEM/FACEPE/CNPq (grant number APQ-054902.11/14 to V.R.A.P.). P.A.T.M.G. is supported by FACEPE (grant number IBPG-0117-4.03/12). A.C.L.L. and M.Z.H. is receiving a CNPq senior fellowship.

Appendix A. Supplementary data

Supplementary data related to this article can be found at http://dx.doi.org/10.1016/j.ejmech.2016.05.050.

References

[1] WHO, Chagas Disease (American Trypanosomiasis), 2015. http://www.who.int/mediacentre/factsheets/fs340/en/index.html.

[2] J.R. Coura, J.C.P. Dias, Epidemiology, control and surveillance of Chagas dis-ease: 100 years after its discovery, Mem. Inst. Oswaldo Cruz. 104 (Suppl) (2009) 31e40, http://dx.doi.org/10.1590/S0074-02762009000900006.

[3] R.L. Tarleton, J.W. Curran, Is chagas disease really the "new HIV/AIDS of the Americas"? PLoS Negl. Trop. Dis. 6 (2012) e1861, http://dx.doi.org/10.1371/journal.pntd.0001861.

[4] F.S. Buckner, J.A. Urbina, Recent developments in sterol 14-demethylase in-hibitors for Chagas disease, Int. J. Parasitol. Drugs Drug Resist. 2 (2012) 236e242, http://dx.doi.org/10.1016/j.ijpddr.2011.12.002.

[5] F.S. Machado, L.A. Jelicks, L.V. Kirchhoff, J. Shirani, F. Nagajyothi, S. Mukherjee, et al., Chagas heart disease, Cardiol. Rev. 20 (2012) 1, http://dx.doi.org/10.1097/CRD.0b013e31823efde2.

[6] M.-J. Pinazo, J. Munoz,~ E. Posada, P. Lopez-Chejade, M. Gallego, E. Ayala, et al., Tolerance of benznidazole in treatment of Chagas' disease in adults, Anti-microb. Agents Chemother. 54 (2010) 4896e4899, http://dx.doi.org/10.1128/ AAC.00537-10.

[7] J.C. Mottram, D.R. Brooks, G.H. Coombs, Roles of cysteine proteinases of try-panosomes and Leishmania in host-parasite interactions, Curr. Opin. Micro-biol. 1 (1998) 455e460.

[8] E.E. Caroselli, D.M. Assis, C.L. Barbieri, W.A.S. Júdice, M.A. Juliano, M.L. Gazarini, et al., Leishmania (L.) amazonensis peptidase activities inside the living cells and in their lysates, Mol. Biochem. Parasitol. 184 (2012) 82e89, http://dx.doi.org/10.1016/j.molbiopara.2012.04.012.

[9] X. Du, E. Hansell, J.C. Engel, C.R. Caffrey, F.E. Cohen, J.H. McKerrow, Aryl ureas represent a new class of anti-trypanosomal agents, Chem. Biol. 7 (2000) 733e742, http://dx.doi.org/10.1016/S1074-5521(00)00018-1.

[10] H.J. Wiggers, J.R. Rocha, W.B. Fernandes, R. Sesti-Costa, Z.A. Carneiro, J. Cheleski, et al., Non-peptidic cruzain inhibitors with trypanocidal activity discovered by virtual screening and in vitro assay, PLoS Negl. Trop. Dis. 7 (2013) e2370, http://dx.doi.org/10.1371/journal.pntd.0002370.

[11] J.M. dos Santos Filho, A.C.L. Leite, B.G. de Oliveira, D.R.M. Moreira, M.S. Lima, M.B.P. Soares, et al., Design, synthesis and cruzain docking of 3-(4-substituted-aryl)-1,2,4-oxadiazole-N-acylhydrazones as anti-Trypanosoma cruzi agents, Bioorg. Med. Chem. 17 (2009) 6682e6691, http://dx.doi.org/ 10.1016/j.bmc.2009.07.068.

[12] N.C. Romeiro, G. Aguirre, P. Hernandez, M. Gonzalez, H. Cerecetto, I. Aldana, et al., Synthesis, trypanocidal activity and docking studies of novel quinoxaline-N-acylhydrazones, designed as cruzain inhibitors candidates, Bioorg. Med. Chem. 17 (2009) 641e652, http://dx.doi.org/10.1016/j.bmc.2008.11.065. [13] J.M. dos Santos Filho, D.R.M. Moreira, C.A. De Simone, R.S. Ferreira, J.H. McKerrow, C.S. Meira, et al., Optimization of anti-Trypanosoma cruzi oxadiazoles leads to identification of compounds with efficacy in infected mice, Bioorg. Med. Chem. 20 (2012) 6423e6433, http://dx.doi.org/10.1016/ j.bmc.2012.08.047.

[14] T. Franklim, L. Freire-de-Lima, J. de Nazareth Sa Diniz, J. Previato, R. Castro, L. Mendonça-Previato, et al., Design, synthesis and trypanocidal evaluation of novel 1,2,4-Triazoles-3-thiones derived from natural piperine, Molecules 18 (2013) 6366e6382, http://dx.doi.org/10.3390/molecules18066366.

[15] K. Brak, I.D. Kerr, K.T. Barrett, N. Fuchi, M. Debnath, K. Ang, et al., Nonpeptidic tetrafluorophenoxymethyl ketone cruzain inhibitors as promising new leads for Chagas disease chemotherapy, J. Med. Chem. 53 (2010) 1763e1773, http://dx.doi.org/10.1021/jm901633v.

[16] K. Brak, P.S. Doyle, J.H. McKerrow, J.A. Ellman, Identification of a new class of nonpeptidic inhibitors of cruzain, J. Am. Chem. Soc. 130 (2008) 6404e6410, http://dx.doi.org/10.1021/ja710254m.

[17] X. Du, C. Guo, E. Hansell, P.S. Doyle, C.R. Caffrey, T.P. Holler, et al., Synthesis and structure activity relationship study of potent trypanocidal thio semi-carbazone inhibitors of the trypanosomal cysteine protease cruzain, J. Med. Chem. 45 (2002) 2695e2707, http://dx.doi.org/10.1021/jm010459j.

[18] D.C. Greenbaum, Z. Mackey, E. Hansell, P. Doyle, J. Gut, C.R. Caffrey, et al., Synthesis and structure-activity relationships of parasiticidal thio-semicarbazone cysteine protease inhibitors against Plasmodium falciparum, Trypanosoma brucei, and Trypanosoma cruzi, J. Med. Chem. 47 (2004) 3212e3219, http://dx.doi.org/10.1021/jm030549j.

[19] R. Siles, S.-E. Chen, M. Zhou, K.G. Pinney, M.L. Trawick, Design, synthesis, and biochemical evaluation of novel cruzain inhibitors with potential application

in the treatment of Chagas' disease, Bioorg. Med. Chem. Lett. 16 (2006) 4405e4409, http://dx.doi.org/10.1016/j.bmcl.2006.05.041.

[20] J.W.P. Espíndola, M.V. de O. Cardoso, G.B. de O. Filho, D.A. Oliveira e Silva, D.R.M. Moreira, T.M. Bastos, et al., Synthesis and structureeactivity relation-ship study of a new series of antiparasitic aryloxyl thiosemicarbazones inhibiting Trypanosoma cruzi cruzain, Eur. J. Med. Chem. 101 (2015) 818e835, http://dx.doi.org/10.1016/j.ejmech.2015.06.048.

[21] N. Fujii, J.P. Mallari, E.J. Hansell, Z. Mackey, P. Doyle, Y.M. Zhou, et al., Dis-covery of potent thiosemicarbazone inhibitors of rhodesain and cruzain, Bioorg. Med. Chem. Lett. 15 (2005) 121e123, http://dx.doi.org/10.1016/ j.bmcl.2004.10.023.

[22] I. Chiyanzu, E. Hansell, J. Gut, P.J. Rosenthal, J.H. McKerrow, K. Chibale, Syn-thesis and evaluation of isatins and thiosemicarbazone derivatives against cruzain, falcipain-2 and rhodesain, Bioorg. Med. Chem. Lett. 13 (2003) 3527e3530, http://dx.doi.org/10.1016/S0960-894X(03)00756-X.

[23] N.C. Fonseca, L.F. da Cruz, F. da Silva Villela, G.A. do Nascimento Pereira, J.L. de Siqueira-Neto, D. Kellar, et al., Synthesis of a sugar-based thiosemicarbazone series and structure-activity relationship versus the parasite cysteine pro-teases rhodesain, cruzain, and schistosoma mansoni cathepsin B1, Antimicrob. Agents Chemother. 59 (2015) 2666e2677, http://dx.doi.org/10.1128/AAC.04601-14.

[24] D.R.M. Moreira, A.C. Lima Leite, M.V.O. Cardoso, R.M. Srivastava, M.Z. Hernandes, M.M. Rabello, et al., Structural design, synthesis and structure-activity relationships of thiazolidinones with enhanced anti-trypanosoma cruzi activity, ChemMedChem 9 (2014) 177e188, http:// dx.doi.org/10.1002/cmdc.201300354.

[25] D.R. Magalhaes Moreira, A. Lima Leite, R.R. Santos, M. Soares, Approaches for the development of new anti-trypanosoma cruzi agents, Curr. Drug Targets 10 (2009) 212e231, http://dx.doi.org/10.2174/138945009787581140.

[26] A. Ayati, S. Emami, A. Asadipour, A. Shafiee, A. Foroumadi, Recent applications of 1,3-thiazole core structure in the identification of new lead compounds and drug discovery, Eur. J. Med. Chem. (2015) 1e20, http://dx.doi.org/10.1016/ j.ejmech.2015.04.015.

[27] D.R.M. Moreira, S.P.M. Costa, M.Z. Hernandes, M.M. Rabello, G.B. de Oliveira Filho, C.M.L. de Melo, et al., Structural investigation of anti-Trypanosoma cruzi 2-iminothiazolidin-4-ones allows the identification of agents with efficacy in infected mice, J. Med. Chem. 55 (2012) 10918e10936, http://dx.doi.org/ 10.1021/jm301518v.

[28] M.Z. Hernandes, M.M. Rabello, A.C.L. Leite, M.V.O. Cardoso, D.R.M. Moreira, D.J. Brondani, et al., Studies toward the structural optimization of novel thiazolylhydrazone-based potent antitrypanosomal agents, Bioorg. Med. Chem. 18 (2010) 7826e7835, http://dx.doi.org/10.1016/j.bmc.2010.09.056.

[29] A.C.L. Leite, R.S. de Lima, D.R.D.M. Moreira, M.V.D.O. Cardoso, A.C. Gouveia de Brito, L.M. Farias Dos Santos, et al., Synthesis, docking, and in vitro activity of thiosemicarbazones, aminoacyl-thiosemicarbazides and acyl-thiazolidones against Trypanosoma cruzi, Bioorg. Med. Chem. 14 (2006) 3749e3757, http://dx.doi.org/10.1016/j.bmc.2006.01.034.

[30] A.C.L. Leite, D.R. de M. Moreira, M.V. de O. Cardoso, M.Z. Hernandes, V.R. Alves Pereira, R.O. Silva, et al., Synthesis, Cruzain docking, and in vitro studies of aryl-4-oxothiazolylhydrazones against Trypanosoma cruzi, ChemMedChem 2 (2007) 1339e1345, http://dx.doi.org/10.1002/cmdc.200700022.

[31] M.V. de O. Cardoso, L.R.P. de Siqueira, E.B. da Silva, L.B. Costa, M.Z. Hernandes, M.M. Rabello, et al., 2-Pyridyl thiazoles as novel anti- Trypanosoma cruzi agents: structural design, synthesis and pharmacological evaluation, Eur. J. Med. Chem. 86 (2014) 48e59, http://dx.doi.org/10.1016/ j.ejmech.2014.08.012.

[32] D.R. Richardson, D.S. Kalinowski, V. Richardson, P.C. Sharpe, D.B. Lovejoy, M. Islam, et al., 2-Acetylpyridine thiosemicarbazones are potent iron chelators and antiproliferative agents: redox activity, iron complexation and charac-terization of their antitumor activity, J. Med. Chem. 52 (2009) 1459e1470, http://dx.doi.org/10.1021/jm801585u.

[33] G.F. Santoro, M. das Graças Cardoso, L.G.L. Guimar~aes, A.P.S.P. Salgado, R.F.S. Menna-Barreto, M.J. Soares, Effect of oregano (Origanum vulgare L.) and thyme (Thymus vulgaris L.) essential oils on Trypanosoma cruzi (Protozoa: Kinetoplastida) growth and ultrastructure, Parasitol. Res. 100 (2007) 783e790, http://dx.doi.org/10.1007/s00436-006-0326-5.

[34] C.O. Rodrigues, R. Catisti, S.A. Uyemura, A.E. Vercesi, R. Lira, C. Rodriguez, et al., The sterol composition of Trypanosoma cruzi changes after growth in different culture media and results in different sensitivity to digitonin-per-meabilization, J. Eukaryot. Microbiol. 48 (2001) 588e594.

[35] P. Zhan, X. Liu, Z. Li, Z. Fang, Z. Li, D. Wang, et al., Novel 1,2,3-thiadiazole derivatives as HIV-1 NNRTIs with improved potency: synthesis and pre-liminary SAR studies, Bioorg. Med. Chem. 17 (2009) 5920e5927, http:// dx.doi.org/10.1016/j.bmc.2009.07.004.

[36] R.S. Ferreira, C. Bryant, K.K.H. Ang, J.H. McKerrow, B.K. Shoichet, A.R. Renslo, Divergent modes of enzyme inhibition in a homologous structure-activity series, J. Med. Chem. 52 (2009) 5005e5008, http://dx.doi.org/10.1021/ jm9009229.

[37] E.M. De Souza, A. Lansiaux, C. Bailly, W.D. Wilson, Q. Hu, D.W. Boykin, et al., Phenyl substitution of furamidine markedly potentiates its anti-parasitic ac-tivity against Trypanosoma cruzi and Leishmania amazonensis, Biochem. Pharmacol. 68 (2004) 593e600, http://dx.doi.org/10.1016/j.bcp.2004.04.019.

[38] L.R. Garzoni, A. Caldera, M. de N.L. Meirelles, S.L. d Castro, R. Docampo, G.A. Meints, et al., Selective in vitro effects of the farnesyl pyrophosphate synthase inhibitor risedronate on Trypanosoma cruzi, Int. J. Antimicrob. Agents 23 (2004) 273e285, http://dx.doi.org/10.1016/ j.ijantimicag.2003.07.020.

[39] M.V. Braga, J.A. Urbina, W. de Souza, Effects of squalene synthase inhibitors on the growth and ultrastructure of Trypanosoma cruzi, Int. J. Antimicrob. Agents 24 (2004) 72e78, http://dx.doi.org/10.1016/j.ijantimicag.2003.12.009.

[40] A.P. Dantas, K. Salomao,~ H.S. Barbosa, S.L. De Castro, The effect of Bulgarian propolis against Trypanosoma cruzi and during its interaction with host cells, Mem. Inst. Oswaldo Cruz. 101 (2006) 207e211, http://dx.doi.org/10.1590/ S0074-02762006000200013.

[41] G.B. Rocha, R.O. Freire, A.M. Simas, J.J.P. Stewart, RM1: a reparameterization of AM1 for H, C, N, O, P, S, F, Cl, Br, and I, J. Comput. Chem. 27 (2006) 1101e1111, http://dx.doi.org/10.1002/jcc.20425.

[42] Spartan "08 Tutorial and User"s Guide: Wavefunction, 2008.

[43] G.M. Morris, R. Huey, W. Lindstrom, M.F. Sanner, R.K. Belew, D.S. Goodsell, et al., AutoDock4 and AutoDockTools4: automated docking with selective re-ceptor flexibility, J. Comput. Chem. 30 (2009) 2785e2791, http://dx.doi.org/ 10.1002/jcc.21256.

[44] J.D. Durrant, J.A. McCammon, BINANA: a novel algorithm for ligand-binding characterization, J. Mol. Graph. Model 29 (2011) 888e893, http://dx.doi.org/10.1016/j.jmgm.2011.01.004.

[45] The PyMOL Molecular Graphics System, Version 1.3 Schrodinger,€ LLC., (n.d.).

APÊNDICE B -

Phthalimido-thiazoles as building blocks and their effects on the growth and morphology of *Trypanosoma cruzi*

European Journal of Medicinal Chemistry 111 (2016) 46e57

Contents lists available at ScienceDirect

European Journal of Medicinal Chemistry

journal homepage: http://www.elsevier.com/locate/ejmech

Research paper

Phthalimido-thiazoles as building blocks and their effects on the growth and morphology of Trypanosoma cruzi

Paulo Andre Teixeira de Moraes Gomes [a], Arsenio^ Rodrigues Oliveira [a], Marcos Veríssimo de Oliveira Cardoso [a], Edna de Farias Santiago [a], Miria de Oliveira Barbosa [a], Lucianna Rabelo Pessoa de Siqueira [a], Diogo Rodrigo Magalhaes~ Moreira [b], Tanira Matutino Bastos [b], Fabio Andre Brayner [c], Milena Botelho Pereira Soares [b, d], Andresa Pereira de Oliveira Mendes [e], Maria Carolina Accioly Brelaz de Castro [e], Valeria Rego Alves Pereira [e], Ana Cristina Lima Leite [a, *]

[a] Departamento de Ci^encias Farmac^euticas, Centro de Ci^encias da Saúde, Universidade Federal de Pernambuco, 50740-520 Recife, PE, Brazil
[b] Fundaçao~ Oswaldo Cruz, Centro de Pesquisas Gonçalo Moniz, CEP 40296-710 Salvador, BA, Brazil
[c] Laboratorio de Imunologia Keizo Asami-LIKA/UFPE, CEP, 50670-901 Recife, PE, Brazil
[d] Centro de Biotecnologia e Terapia Celular, Hospital Sao~ Rafael, Avenida Sao~ Rafael, 2152, Sao~ Marcos, CEP 41253-190, Salvador BA, Brazil
[e] Centro de Pesquisas Aggeu Magalhaes,~ Fundaçao~ Oswaldo Cruz, CEP, 50670-420 Recife, PE, Brazil

article info

Article history:
Received 21 September 2015
Received in revised form
21 December 2015
Accepted 9 January 2016
Available online 11 January 2016

Keywords:
Chagas disease
Trypanosoma cruzi
Thiazole
Hydrazone
Phthalimide

abstract

Chagas disease is a parasitic infection caused by protozoan Trypanosoma cruzi that affects approximately 6e7 million people worldwide. Benznidazole is the only drug approved for treatment during the acute and asymptomatic chronic phases; however, its efficacy during the symptomatic chronic phase is controversial. The present work reports the synthesis and anti-T. cruzi activities of a novel series of phthalimido-thiazoles. Some of these compounds showed potent inhibition of the trypomastigote form of the parasite at low cytotoxicity concentrations in spleen cells, and the resulting structure-activity relationships are discussed. We also showed that phthalimido-thiazoles induced ultrastructural alter-ations on morphology, flagellum shortening, chromatin condensation, mitochondria swelling, reservo-somes alterations and endoplasmic reticulum dilation. Together, these data revealed, for the first time, a novel series of phthalimido-thiazoles-structure-based compounds with potential effects against T. cruzi and lead-like characteristics against Chagas disease.

1. Introduction

Chagas disease, also known as American trypanosomiasis, is a potentially life-threatening illness caused by the protozoan parasite Trypanosoma cruzi (T. cruzi). Approximately 6e7 million people are estimated to be infected worldwide, mostly in Latin America, where Chagas disease is endemic [1].

Despite the efforts of many investigators to research new anti-Chagas drugs, only one drug is currently used in therapy, benzni-dazole (Bdz) [2,3]. Current chemotherapy for Chagas disease is unsatisfactory due to the limited efficacy of Bdz, particularly during the chronic phase, with frequent side effects that can lead to discontinuation of treatment [4].

One pragmatic way to improve the quality of both the candidate drugs and screening collections is by improving the quality of the building blocks (reagents) that are used to synthesize them. Our strategic program focused on substructures and properties that are known to have imparted biological activity and good 'drug-like' properties previously. Among the chemical groups explored for anti-Chagas activity, thiazolyl hydrazones are noteworthy because of their wide biological, especially anti-parasitic, activities [5e8]. Caputo et al. have demonstrated trypanocidal activity for a series of 4-arylthiazolylhydrazones [9], which have broad and potent ac-tivities for all forms of the parasite.

Our efforts toward new antichagasic drugs since 2006 have led

* Corresponding author.
E-mail address: acllb2003@yahoo.com.br (A.C.L. Leite).

http://dx.doi.org/10.1016/j.ejmech.2016.01.010
0223-5234/

us to develop a variety of thiosemicarbazones and 1,3-thiazolyl hydrazones as trypanocidal agents [4,7,10e14]. In continuation of our search for bioactive molecules, we envisaged that the deriva-tization of the thiosemicarbazone group into a thiazole moiety would generate novel templates that are likely to exhibit anti-T. cruzi activity [4].

However, much effort has been invested to identify the key differences between drugs and other organic compounds. High-quality libraries are expected to exhibit drug-likeness to produce compounds with desirable pharmacokinetic and safety profiles. The phthalimide functional group has been used as an important tool in organic synthesis because it protects against unwanted re-actions. Many research teams have used this nucleus as a building block to improve compound quality. In fact, phthalimide de-rivatives have shown a broad spectrum of pharmacological prop-erties, such as analgesic [15], anticonvulsant [16], antitubercular [17,18], hypolipidaemic [18], anxiolytic [15], anti-inflammatory [15], antimicrobial [17,19,20] and antipsychotic [21].

For this reason, our research group has explored the pharma-cological properties of phthalimide derivatives. As a result, bioac-tive prototypes were identified with potent anti-inflammatory [22], anti-proliferative [23], immunomodulatory [22,24,25], antitumor [23], antiangiogenic [26] and schistosomicidal properties [27], Indeed, Santiago et al. identified phthalimido-thiazole derivatives with potent schistosomicidal activities. The phthalimide LpQM-45 caused significant ultrastructural changes, including destruction of the integument in both male and female worms [27], however, their antichagasic properties have not been explored.

Considering the promising results achieved by compounds bearing a thiazole ring and phthalimides nuclei, they were chosen as common pharmacophores that exist in diverse drug classes. In this way, we synthesized a set of molecules with phthalimide and thiazole nucleus. In this synthetic design of a substructure-based compound library, substituents around the phenyl ring attached at C4 in the thiazole ring (compounds 2b-n) were explored. In addition, a spacer group between phthalimide and the thiazole ring was inserted and a phenyl group at N3 of the thiazole ring was also introduced (6b-l). To investigate the influence of the phthalimido moiety at the anti-T. cruzi activity, 26 new compounds were tested in vitro against the T. cruzi parasite epimastigote and trypomasti-gote forms. Ultrastructural studies and flow cytometry analysis were also investigated (Fig. 1).

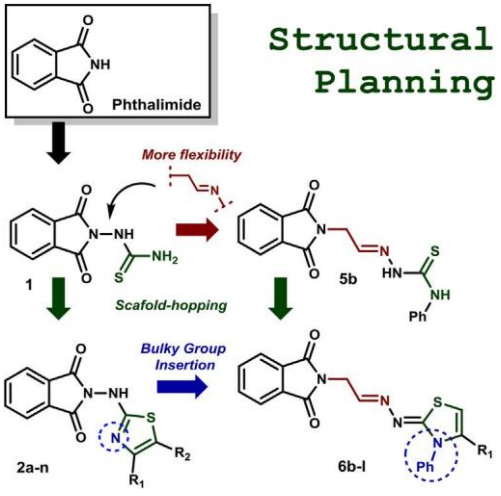

Fig. 1. Structural planning of the proposed compounds.

2. Results and discussion

2.1. Chemistry

Initially, 14 phthalimido-thiazoles (2a-n) were synthesized in a two-step reaction, following the procedures reported by Pessoa et al. [25]. Firstly, a reaction of phthalic anhydride with thio-semicarbazide, in DMF under reflux for 4 h, with a catalytic amount of DMAP, led us to compound 1. The synthesis of the series 2a-n was performed via Hantsch cyclization between compound 1 and the appropriate a-halogenated ketone (1,3-dichloroacetone for com-pound 2a), under ultrasound irradiation, at room temperature (rt) for 1 h. This reaction condition led to average yields from 36 to 65%. To synthesize the series 6a-l, was followed the reaction protocol reported by Cardoso et al. [23]. The desired compounds 6a-l were obtained by the reaction of Intermediate 5b (or 5a, for compound 6a) with the appropriate a-halogenated ketone (1,3-dichloroacetone for compound 6a), via Hantsch cyclization, lead-ing good yields (46e82%) (Scheme 1). All the synthesized com-pounds were well characterized by infrared (IR), nuclear magnetic resonance (^{1}H, ^{13}C NMR), mass spectroscopy (ESI-TOF) and, in case of compounds 2e, 2f and 2g, by single crystal X-ray diffraction analysis (Fig. 2).

The ^{1}H NMR spectra of some compounds showed that phthalimido-thiazoles 6a-l are composed by diastereomers. Next, we aimed to define the configuration of the major isomer by crystallographic analysis. However, we did not succeed in crystal-lizing phthalimido-thiazoles 6a-l suitable for X-ray analysis. Based on previous crystallized compounds by our group, we suggest that the major isomer formed present the E-Z configuration (Fig. 3). Indeed, hydrazine double-bond C2¼N2 is commonly assigned as E configuration [4,23,28]. Concerning the exocyclic double-bond N3¼C3, we suggest that the predominant configuration is in Z-configuration [7,29]. Besides, a representative ^{1}H-NMR spectrum of compound 6i is presented in Supplementary Material.

2.2. Anti-T. cruzi evaluation

Initially, compounds 2a-n were planned to improve the trypa-nocidal activity and cytotoxic tolerance with the cyclization of phthalimido-thiosemicarbazone to the phthalimido-thiazole ring. From the results, it was observed in most of the cases that new phthalimido-thiazoles showed high cytotoxic activity in spleen cells. In opposition, only compounds 2i and 2j showed low cytotoxicity.

Concerning trypanocidal activity for epimastigotes, it is observed that 16 compounds (of 28) present better potency than Benznidazole (Table 1). Among series 2a-n, compound 2i was the most active, among the series and the entire work. The most active compound in series 6 is 6k, a 3-NO_2 derivative, presenting an IC_{50} of 6.0 mM. Observing compounds with withdrawer substituents (2e-h, 2k-n), compound 2,4-dichloro substituted (2m) was the most active. It analogue disubstituted 3,4-dichloro (2l) present lower trypanocidal activity and high toxicity for BALB/c mice spleen cells, denoting that the orientation of the substituents is important for the activity. Observing bulk substituted compounds (phenyl, 2-naphthyl and 4-biphenylyl), in series 2a-n, a relationship of LogP and trypanocidal activity (Fig. 4) is observed, being compound 2i the most active of this sub-series.

The trend of bulky substituents (LogP) observed for series 2a-n is not observed for series 6a-l, being compound 6k (3-NO_2) the most active of the series 6a-l.

When comparing the trypanocidal activity against the trypo-mastigote form of the series 2a-n of phthalimido-thiazole de-rivatives, compound 2j was found to be the most potent of this sub-

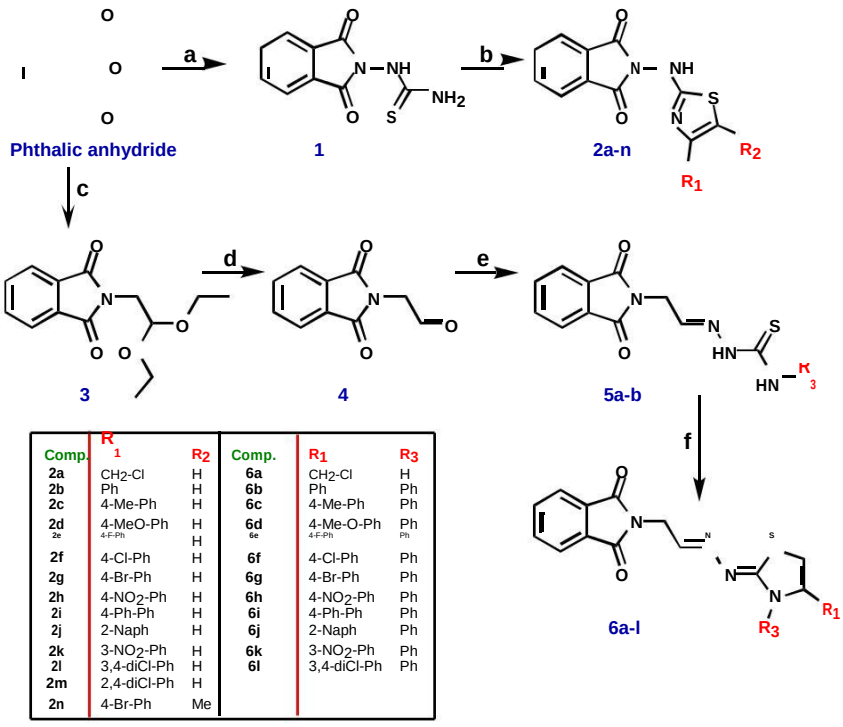

Comp.	R_1	R_2
2a	CH_2-Cl	H
2b	Ph	H
2c	4-Me-Ph	H
2d	4-MeO-Ph	H
2e	4-F-Ph	H
2f	4-Cl-Ph	H
2g	4-Br-Ph	H
2h	4-NO_2-Ph	H
2i	4-Ph-Ph	H
2j	2-Naph	H
2k	3-NO_2-Ph	H
2l	3,4-diCl-Ph	H
2m	2,4-diCl-Ph	H
2n	4-Br-Ph	Me

Comp.	R_1	R_3
6a	CH_2-Cl	H
6b	Ph	Ph
6c	4-Me-Ph	Ph
6d	4-Me-O-Ph	Ph
6e	4-F-Ph	Ph
6f	4-Cl-Ph	Ph
6g	4-Br-Ph	Ph
6h	4-NO_2-Ph	Ph
6i	4-Ph-Ph	Ph
6j	2-Naph	Ph
6k	3-NO_2-Ph	Ph
6l	3,4-diCl-Ph	Ph

Scheme 1. Global synthesis of compounds 2a-n and 6a-l. Reagents and conditions: (a) thiosemicarbazide, DMF, DMAP, reflux, 4h; (b) corresponding a-halogenated ketone (1,3-dichloroacetone for compound 2a), 2-propanol, ultrasound, rt, 1 h; (c) 1-aminoacetaldehyde diethyl acetal, toluene, reflux, DMAP, 2 h; (d) H_2SO_4 (70%), reflux, 2 h; (e) thio-semicarbazide (5a) or 4-phenyl-3-thiosemicarbazide (5b), EtOH, HCl, reflux, 4 h; (f) for 6a, 1,3-dichloroacetone, DMF, rt, 1 h; for 6b-l, corresponding a-halogenated ketone, 2-propanol, rt, 1 h.

series, presenting lower cytotoxic levels (269.2 mM) and equipotent trypanocidal activity compared with Bdz (4.7 vs 6.3 mM) (Table 1).

No clear correlation was observed between the substituents at the thiazole C4 and the biological activity. For example, 2-naphthyl is a bulky substituent present in 2j; however, compound 2i, which was also substituted with a bulky biphenylyl substituent, did not present good activity. The influence of the phenyl linked at C4 in the thiazole ring was also investigated, but no noticeable improvement in activity was observed. Comparing compound 2a with the phenyl-unsubstituted compound 2b, a decrease in trypanocidal activity and higher cytotoxicity were observed, while the phenyl-substituted compounds maintained or increased both activities.

A structural optimization involving addition of a spacer group (eCH2eCH ¼) between the phthalimide and the thiazole core was performed in order to increase the flexibility of the molecules and to investigate its influence on biological activities (Fig. 5). A sub-stitution of H with phenyl at N3 was also performed to explore the influence of bulky substituents based on the results of compounds 2i and 2j, both substituted with 4-biphenylyl and 2-naphthyl at C4, respectively, which displayed lower cytotoxicity.

Compounds that contained a spacer group (6a-l) and phenyl at N3 (6b-l) in general showed low cytotoxicity profiles and improved trypanocidal activity for trypomastigote form, highlighting com-pounds 6a (2.2 mM), 6h (3.2 mM), 6j (0.5 mM) and 6k (0.9 mM). In fact, compound 6j presented a selective index (SI, for trypomasti-gote form) of 409.8, which was approximately 27-fold more se-lective than Bdz (SI: 15.25), the standard drug in clinical use. As observed in the 2a-n series, the compound substituted at C4 with chloromethyl (6a, 2.2 mM) was more active than compounds substituted with phenyl (6b, 8.8 mM); indeed, phenyl-substituted compounds 6j (0.5 mM) and 6k (0.9 mM) were more active than 6a. Comparing compound 6a with 2a, which were both substituted with chloromethyl at C4 with the unique difference of the presence of the spacer group in 6a, a 24-fold improvement in trypanocidal activity (2.2 vs 54.4 mM) and a 4-fold increase in cytotoxicity (73.7 vs 17.0 mM) were observed for 6a. Compounds 6k and 6h, both nitro-substituted compounds at the meta and para positions, respectively, presented high trypanocidal activity with selective indexes of 114.9 and 64.6, respectively (Table 1). Compound 6e (with the electron withdrawing fluorine substituent) and 6i (with 4-biphenylyl substituent) did not present good trypanocidal ac-tivity. Compound 6j, which was substituted with the bulky sub-stituent 2-naphthyl, presented the highest trypanocidal activity.

The SAR studies revealed that a series of phthalimido-thiazoles were interesting anti-T. cruzi compounds, which five new com-pounds showed low cytotoxicity in spleen cells of BALB/c mice and anti-trypanocidal activity against the trypomastigote form of the parasite.

Congreve et al. proposed a rule-of-three (RO3) [30] representing a set of guidelines for constructing a fragment library (molecular weight, <300; cLogP, 3; number of hydrogen bond donors, 3; and the number of hydrogen bond acceptors, 3). Recently, RO3 was accredited by most medicinal chemists and could be useful for efficient fragment selection [31]. As seen in Table 2, the phthalimide and thiazole fragments are in agreement with RO3.

The trypanocidal profile of these phthalimido-thiazoles revealed a group of privileged structure-based compounds that can be used as building blocks to obtain new lead-like compounds. They possess some structural features, such as lower molecular weights, decreased complexity and decreased hydrophobicity, which are consistent with lead-like characteristics. These com-pounds can be used to produce structurally simple leads with modest activity, allowing for further derivatization at a later stage to improve affinity and selectivity while retaining drug-like

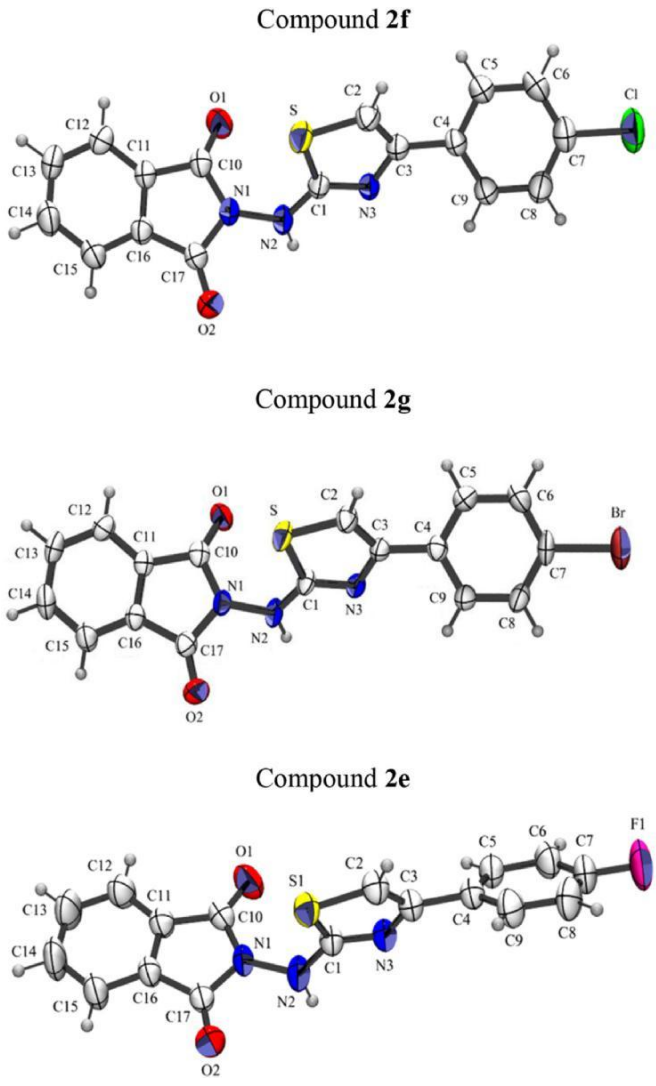

Fig. 2. The molecular structure of the title compounds showing the atom-labelling scheme and displacement ellipsoids at the 50% probability level.

characteristics.

2.3. Ultra structural studies

In view to investigate the effects of phthalimido-thiazoles on parasite morphology, compound 6k, one of the most active com-pound of this work, was selected. The ultrastructural effects of 6k on trypomastigotes after 24 h were analysed by TEM and SEM at the IC_{50} concentration and twice the IC_{50} value (Table 1), and the ul-trastructural analysis showed several morphological alterations (Fig. 6).

SEM analysis revealed that treatment with 0.9 mM (1 IC_{50}) and 1.8 mM (2 IC_{50}) of 6k caused blebs in the flagellum and shortening of the flagellum with a drastic decrease in the number of parasites, respectively (Fig. 6BeC), while the control group retained its typical morphology (Fig. 6A).

TEM analysis revealed that untreated parasites showed normal ultrastructural morphologies of organelles, such as kinetoplast, nucleus, nucleolus, flagellum, ribosomes and microtubule mem-branes (Fig. 6D), whereas parasites treated with 0.9 mM of 6k showed alterations in the reservosomes, and a large number of cells showed intense cytoplasmic vacuolization. In addition, alterations

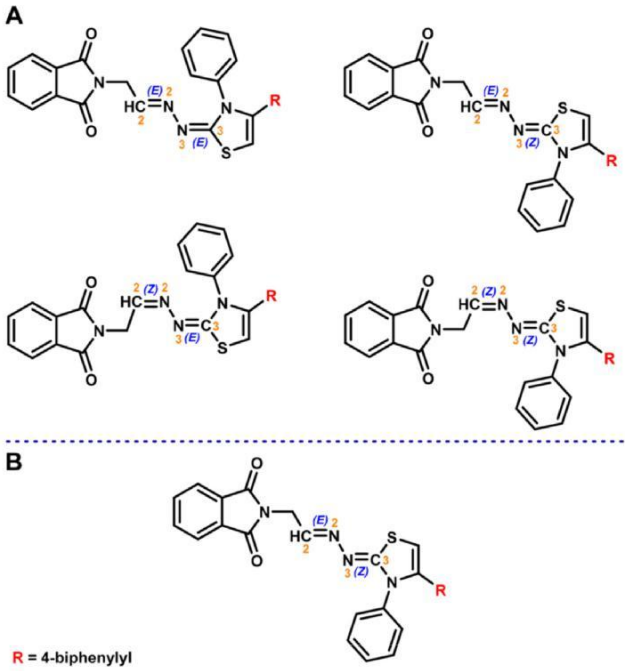

Fig. 3. Isomers representation of compound 6i. A- Possible isomers for compound 6i. B- Suggested isomer for compound 6i.

of the parasite morphology, large nuclear chromatin clumps that resembled the nuclei of apoptotic cells, mitochondria swelling and loss of cytoplasmic material were observed (Fig. 6EeF). The para-sites treated with 1.8 mM of 6k showed alterations of parasite morphology, abnormal chromatin condensation, dilated endo-plasmic reticula, intense vacuolization in the cytoplasm, swelling of the kinetoplast and alterations in the reservosomes (Fig. 6G).

Ultrastructural analysis was applied to explore the damages induced by the drugs in trypomastigotes T. cruzi parasites and clearly showed severe morphological changes, of which intense cytoplasmic vacuolization, chromatin condensation, alterations in the reservosomes and swelling of the mitochondria were most frequent. These ultrastructural alterations are similar to those previously reported [32e36]. The ultrastructural evaluation indi-cated a dose-dependent action because a drastic decrease in the number of parasites was observed with increasing drug doses.

2.4. Flow cytometry analysis

After confirming that 6k was an antiparasitic compound that affected ultrastructural cellular organization, we sought to deter-mine whether 6k caused parasite cell death. To this end, Y strain trypomastigotes were treated with different concentrations of 6k. After 24 h incubation, parasite cells were stained with propidium iodide (PI) and annexin-V and analysed by flow cytometry. The results are shown in Fig. 7.

Compared with untreated cells, benznidazole resulted in PI-staining in a concentration-dependent manner, while no signifi-cant annexin-V staining was observed (data not shown). At 25 mM, benznidazole induced 56 ± 6% PI-staining in parasite cells. At the same concentration, treatment with compound 6k induced PI-staining in 11 ± 3% of parasite cells. No PI or annexin-V staining were observed under treatment with 6k (data not shown). There-fore, these phthalimido-thiazoles do not destroy parasite cells by classical cell death processes. Based on electronic microscopy ob-servations, it is possible that phthalimido-thiazoles decrease

Table 1
Cytotoxicity and trypanocidal activity against epimastigotes and trypomastigotes forms.

CODE	R_1	R_2	R_3	Cytotoxicity mM[a]	IC_{50} epimastigotes (T. cruzi) - mM[b]	IC_{50} trypomastigotes (T. cruzi) - mM[c]
1	e	H	e	4.5	56.8	52.0
				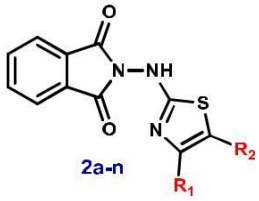		
				2a-n		
2a	CleMe	H	e	17.0	225.7	54.4
2b	Ph	H	e	3.1	70.2	107.5
2c	4-Me-Ph	H	e	14.9	70.4	107.0
2d	4-Me-O-Ph	H	e	14.2	6.4	50.3
2e	4-F-Ph	H	e	2.9	26.5	52.1
2f	4-Cl-Ph	H	e	2.8	30.6	86.2
2g	4-Br-Ph	H	e	2.5	14.8	89.8
2h	4-NO_2-Ph	H	e	2.7	13.3	84.9
2i	4-Ph-Ph	H	e	251.6	4.0	27.5
2j	2-Naph	H	e	269.2	8.0	4.7
2k	3-NO_2-Ph	H	e	2.7	43.2	91.1
2l	3,4-diCl-Ph	H	e	2.6	69.3	88.8
2m	2,4-diCl-Ph	H	e	12.8	10.1	22.7
2n	4-Br-Ph	Me	e	2.4	13.9	38.2
5b	e	e	Ph	50	36.9	ND
				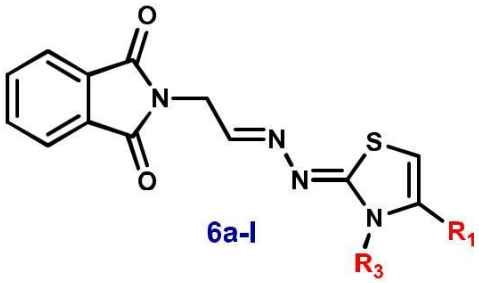		
				6a-l		
6a	CleMe	e	H	73.7	85.7	2.2
6b	Ph	e	Ph	228.1	ND	8.8
6c	4-Me-Ph	e	Ph	221.2	57.8	33.3
6d	4-Me-O-Ph	e	Ph	213.4	ND	10.0
6e	4-F-Ph	e	Ph	219.1	ND	73.8
6f	4-Cl-Ph	e	Ph	211.4	10.6	18.4
6g	4-Br-Ph	e	Ph	96.6	ND	9.7
6h	4-NO_2-Ph	e	Ph	206.8	12.2	3.2
6i	4-Ph-Ph	e	Ph	194.3	44.2	98.0
6j	2-Naph	e	Ph	204.9	11.9	0.5
6k	3-NO_2-Ph	e	Ph	103.4	6.0	0.9
6l	3,4-diCl-Ph	e	Ph	197.1	ND	ND
Bdz	e	e	e	96.1	48.8	6.3

[a] Highest non-toxic concentration (>90% incorporation of tritiated thymidine) in spleen cells of BALB/c mice.

[b] Determined 24 h after incubation of Y strain trypomastigotes with the compounds.

[c] Determined 11 days after incubation of epimastigotes with the compounds.[a,b] Only values with a standard deviation < 10% were included.[a,b] IC_{50} was calculated from at least five concentrations, in triplicate (SD < 10%). Bdz ¼ Benznidazole; ND ¼ Not Determined.

parasite viability by altering cytosol organization, mainly by causing intense cytoplasmic vacuolization.

3. Conclusion

Twenty-six phthalimido-thiazoles were obtained in reasonable yields using a simple methodology. Compounds with important trypanocidal activity, especially compounds 2j, 6a, 6h, 6j and 6k, were identified. Flow cytometry and ultrastructural studies showed that compound 6k did not kill the parasite via necrosis or apoptosis; however, it promoted several morphological changes in the parasite. Compound 6j, the most potent trypanocidal agent identified in this work, presented a selective index of 409, which was approximately 26-fold more selective than Bdz, the standard drug in clinical use. Our results indicated that phthalimido-thiazoles can be used as building blocks to design promising can-didates to treat Chagas disease.

4. Experimental section

4.1. Chemistry

4.1.1. Equipment and reagents

All reagents were used as purchased from commercial sources (SigmaeAldrich, Acros Organics, Vetec or Fluka). Reaction progress was followed by thin-layer chromatography (TLC) analysis (Merck, silica gel 60 F_{254} in aluminium foil). The purities of the target compounds were confirmed by combustion analysis (for C, H, N,

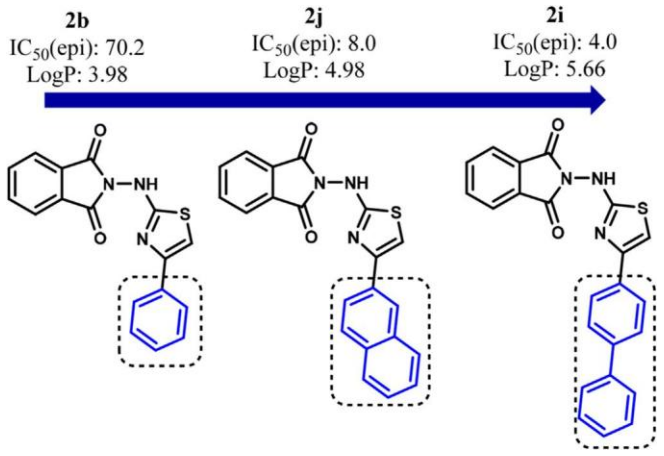

Fig. 4. Trend in trypanocidal activity for epimastigote form.

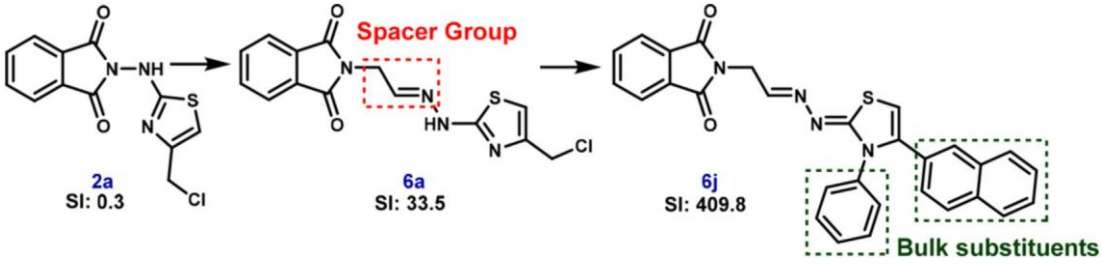

Fig. 5. Structural optimization of proposed compounds. Selective index (SI) ¼ highest non-toxic concentration in spleen cells of BALB/c mice/IC_{50} trypomastigotes.

Table 2
Rule-of-three (RO3) calculations of the fragments phthalimide and thiazole.

Rule	Phthalimide	Thiazole	Criteria met
Molecular weight (<300)	147.13	85.12	Yes
cLogP (<3)	1.148	0.486	Yes
Number of hydrogen bond donors (<3)	1	0	Yes
Number of hydrogen bond acceptors (<3)	2	1	Yes

and S) performed using a Carlo-Erba instrument (model EA 1110). Melting points were determined on a Fisatom 430D electrothermal capillary melting point apparatus and were uncorrected. NMR spectra were measured on either a Varian UnityPlus 400 MHz (400 MHz for ^{1}H and 100 MHz for ^{13}C) or a Bruker AMX-300 MHz (300 MHz for ^{1}H and 75.5 MHz for ^{13}C) instrument. DMSO-d_6 and D_2O were purchased from CIL or SigmaeAldrich. Chemical shifts were reported in ppm, and multiplicities were given as s (singlet), d (doublet), t (triplet), m (multiplet), dd (double doublet), and coupling constants (J) in hertz. Mass spectrometry experiments were performed on a LC-IT-TOF (Shimadzu). Unless otherwise specified, ESI was conducted in positive ion mode. Typical conditions were as follows: capillary voltage of 3 kV, cone voltage of 30 V, and peak scan between 50 and 1000 m/z. IR spectra were recorded with a Bruker model IFS66 FT-IR spectrophotometer using KBr pellets.

4.1.2. General procedure for the syntheses of 2a-n

The compound 1 was prepared by reacting commercially available thiosemicarbazide with the phthalic anhydride (1:1 mol ratio) using DMF under reflux in the presence of a catalytic amount of DMAP, for 4 h. This reaction condition led to satisfactory yield (58%). The phthalimido-thiazoles (2a-n) were prepared via cyclization between 1 and respective a-halogenated ketone (1,3-dichloroacetone for compound 2a), via ultrasound irradiation for 1 h, as previously related [4]. These reactions proceeded well under ultrasound conditions at room temperature using 2-propanol as solvent, resulting in satisfactory yields (36e65%) and shorter re-action times (60 min in most cases).

4.1.2.1. 2-[4-(chloromethyl)thiazol-2-ylamino]isoindoline-1,3-dione (2a). White crystals; Yield: 50%; m.p. (C) 207e208; Rf: 0.53 (hexane/ethyl acetate 1:1). IR (KBr, cm^{-1}): 3119.15 (NH), 1743.24 (C]O). ^{1}H NMR (300 MHz, DMSO-d_6), d $_{ppm}$: 4.54 (s, 2H, CH_2), 7.03 (s, 1H, thiazole), 7.93e7.99 (m, 4H, Ar), 10.54 (s, 1H, NH). ^{13}C NMR (75.5 MHz, DMSO-d_6), d $_{ppm}$: 41.1 (CH_2), 109.8 (CH, thiazole), 123.9 (CH, Ar), 129.4 (C, Ar), 135.4 (CH, Ar), 147.1 (C, thiazole), 165.6 (C] O), 168.3 (SeC]N, thiazole). Anal. Calcd for $C_{12}H_8ClN_3O_2S$: C, 49.07; H, 2.75; N, 14.31; S, 10.92. found: C, 48.50; H, 2.81; N, 14.34; S 10.43. HRMS: 294.0097 [MþH]^{þ}.

4.1.2.2. 2-(4-Phenylthiazol-2-ylamino)isoindoline-1,3-dione (2b). Light yellow crystals; Yield: 65%; m.p. (C) 194e196; Rf: 0.60 (hexane/ethyl acetate 1:1). IR (KBr, cm^{-1}): 3123.66 (NH), 1742.23 (C] O). ^{1}H NMR (400 MHz, DMSO-d_6), d $_{ppm}$: 7.25 (t, J ¼ 7.4 Hz, 1H, Ar), 7.33 (t, J ¼ 7.4 Hz, 2H, Ar), 7.38 (s, 1H, thiazole), 7.70 (d, J ¼ 7.6 Hz, 2H, Ar), 7.95e8.02 (m, 4H, Ar), 10.65 (s, 1H, NH). ^{13}C NMR (100 MHz, DMSO-d_6), d $_{ppm}$: 104.8 (CH, thiazole), 123.8 (CH, Ar), 125.5 (CH, Ar), 127.7 (CH, Ar), 128.6 (CH, Ar) 129.3 (C, Ar), 133.9 (C, Ar), 135.4 (CH, Ar), 149.9 (C, thiazole), 165.5 (C]O), 167.6 (SeC]N, thiazole). Anal. Calcd for $C_{17}H_{11}N_3O_2S$: C, 62.08; H, 3.41; N, 12.98; S, 9.71. found: C, 63.54; H, 3.45; N, 12.53; S, 9.98. HRMS: 322.0619 [MþH]^{þ}.

4.1.2.3. 2-(4-p-Tolylthiazol-2-ylamino)isoindoline-1,3-dione (2c). Light yellow crystals; Yield: 37%; m.p. (C) 214e216; Rf: 0.65 (hexane/ethyl acetate 1:1). IR (KBr, cm^{-1}): 3117.64 (NH), 1738.51 (C]O). ^{1}H NMR (400 MHz, DMSO-d_6), d $_{ppm}$: 2.26 (s, 3H, CH_3), 7.14 (d, J ¼ 6.8 Hz, 2H, Ar), 7.30 (s, 1H, thiazole), 7.59 (d, J ¼ 6.8 Hz, 2H, Ar), 7.99 (m, 4H, Ar), 10.41 (s, 1H, NH). ^{13}C NMR (100 MHz, DMSO-d_6), d $_{ppm}$: 20.8 (CH_3), 103.9 (CH, thiazole), 123.9 (CH, Ar), 125.5 (CH, Ar), 129.17 (CH, Ar), 129.3 (C, Ar), 131.4 (C, Ar), 135.4 (C, Ar), 137.1 (C, Ar), 150.2 (C, thiazole), 165.6 (C]O), 167.5 (SeC]N, thiazole). Anal. Calcd for $C_{18}H_{13}N_3O_2S$: C, 63.17; H, 3.81; N, 18.12; S, 9.17. found: C,

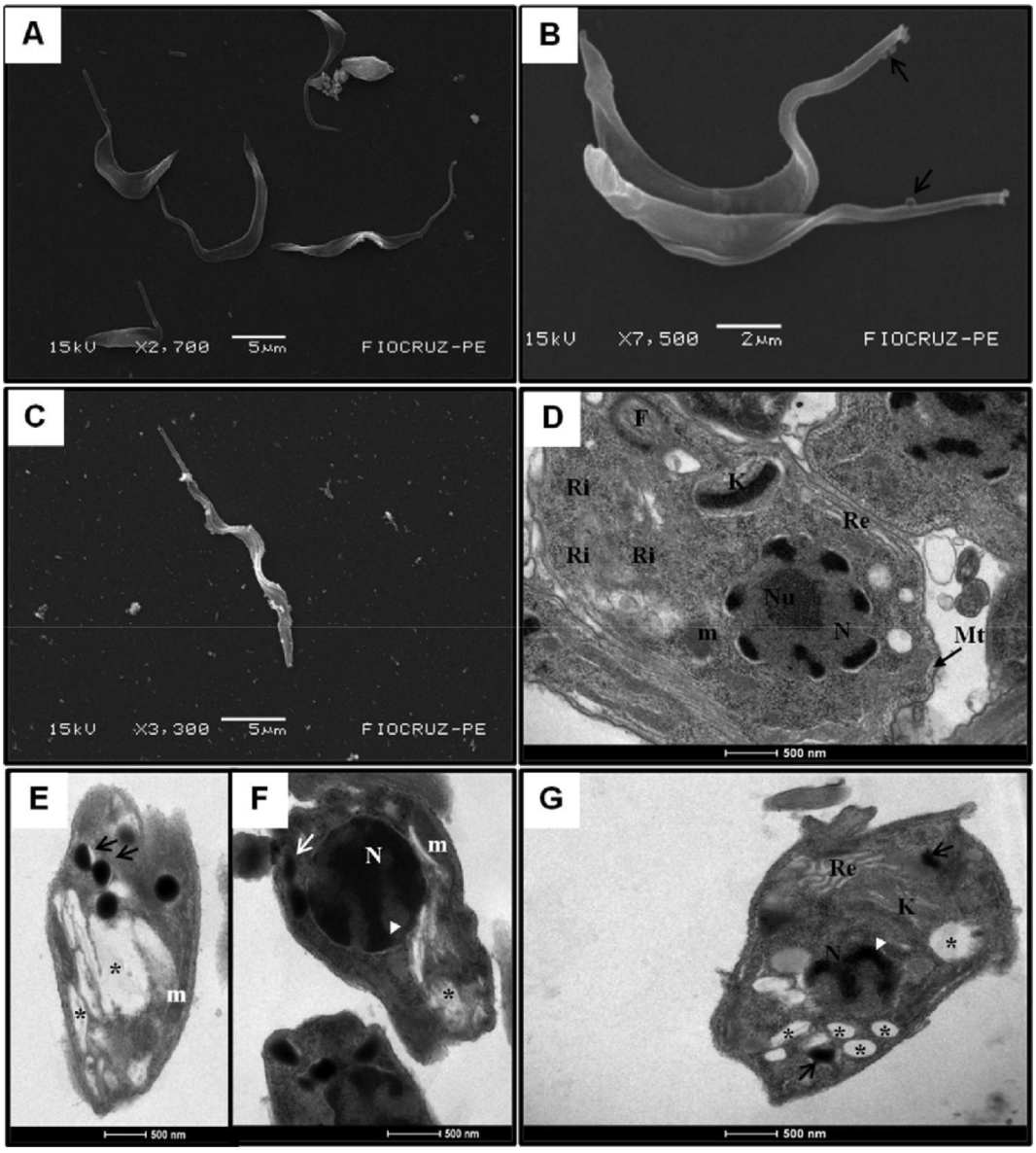

Fig. 6. Ultrastructural alterations in trypomastigotes forms of T. cruzi treated with 6k as observed by SEM and TEM. A- SEM of control untreated trypomastigotes showing the typical elongated body. B- SEM of parasite treated with 0.9 mM of 6k showing blebs in the flagellum. C- SEM of parasite treated with 1.8 mM of 6k showing drastic reduction in the number of parasites and shortening of the flagellum. D- TEM of untreated trypomastigotes showing the normal morphology with kinetoplast (K), nucleus (N), nucleolus (Nu), flagellum (F), ribosomes (Ri), mitochondria (m) and Microtubules Mt). E and F- TEM of parasite treated with 0.9 mM of 6k showing alterations of the parasite morphology, abnormal chromatin condensation (arrowhead) no nucleus (N), swelling of the mitochondrion (m), alterations in the reservosomes (arrows) and loss of cytoplasmic material (asterisks). G-TEM of parasite treated with 1.8 mM of 6k showing alterations of the parasite morphology, abnormal chromatin condensation (arrowhead), endoplasmic reticulum dilated (Re), intense vacuolization in the cytoplasm (asterisk), swelling of the kinetoplast (K) and alterations in the reservosomes (arrows).

64.46; H, 3.91; N, 18.53; S, 9.56. HRMS: 336.0812 [MþH]^{þ}.

4.1.2.4. 2-[4-(4-methoxyphenyl) thiazol-2-ylamino]isoindoline-1,3-dione (2d). Light yellow crystals; Yield: 72%; m.p. (C) 215e218; Rf: 0.53 (hexane/ethyl acetate 3:2). IR (KBr, cm ^{1}): 3232.68 (NH), 1748.64 (C]O). ^{1}H NMR (300 MHz, DMSO-d_6), d $_{ppm}$: 1.025 (s, 3H, CH_3), 6.90 (d, J ¼ 11.6 Hz, 2H, Ar), 7.20 (s, 1H, thiazole), 7.62 (d, J ¼ 11.6 Hz, 2H, Ar), 7.98 (m, 4H, Ar), 10.72 (s, 1H, NH). ^{13}C NMR (75.5 MHz, DMSO-d_6), d $_{ppm}$: 25.5 (CH_3), 102.7 (CH, thiazole), 114.0 (CH, Ar), 123.9 (CH, Ar), 126.7 (C, Ar), 127.0 (CH, Ar), 129.4 (C, Ar), 135.4 (CH, Ar), 149.5 (C, thiazole), 158.6 (CO, Ar), 165.6 (C]O), 167.6 (SeC]N, thiazole). Anal. Calcd for $C_{18}H_{13}N_3O_3S$: C, 58.88; H, 3.87; N, 11.38; S, 8.77. found: C, 61.53; H, 3.73; N, 11.96; S, 9.13. HRMS: 352.0825 [MþH]^{þ}.

4.1.2.5. 2-[4-(4-fluorophenyl)thiazol-2-ylamino]isoindoline-1,3-dione (2e). Yellow crystals; Yield: 51%; m.p. (C) 208e210; Rf: 0.53 (hexane/ethyl acetate 3:2). IR (KBr, cm ^{1}): 3130.14 (NH), 1743.63 (C]O). ^{1}H NMR (400 MHz, DMSO-d_6), d $_{ppm}$: 7.17 (d, J ¼ 17.6 Hz, 2H, Ar), 7.37 (s, 1H, thiazole), 7.73 (d, J ¼ 14.0 Hz, 2H, Ar), 7.99 (m, 4H, Ar), 10.42 (s, 1H, NH). ^{13}C NMR (100 MHz, DMSO-d_6), d $_{ppm}$: 104.6 (CH, thiazole), 115.4 (CH, Ar), 115.6 (CH, Ar), 123.9 (CH, Ar), 127.5 (CH, Ar), 129.3 (C, Ar), 135.4 (CH, Ar), 160.4 (C, thiazole), 162.9 (CF, Ar), 165.5 (C]O), 167.6 (SeC]N, thiazole). Anal. Calcd for $C_{17}H_{10}FN_3O_2S$: C, 60.32; H, 3.02; N, 12.32; S, 9.58. found: C, 60.17; H, 2.97; N, 12.38; S, 9.45. HRMS: 340.0566 [MþH]^{þ}.

4.1.2.6. 2-[4-(4-chlorophenyl)thiazol-2-ylamino]isoindoline-1,3-dione (2f). Light yellow crystals; Yield: 62%; m.p. (C) 217e218; Rf:

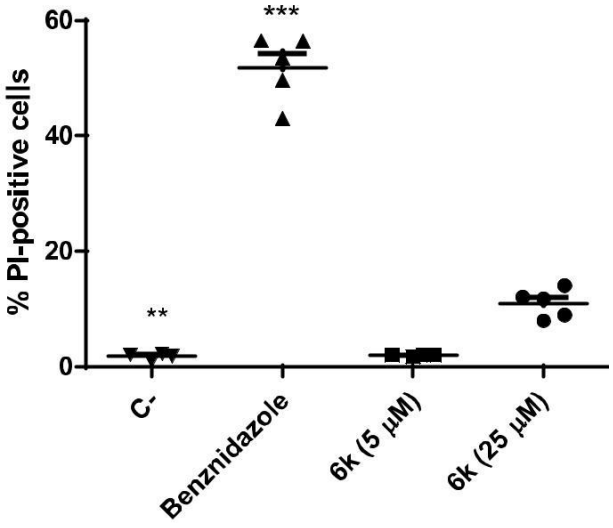

Fig. 7. % of PI-positive cells analysis under 6k treatment. Trypomastigotes were treated with complex for 24 h and examined by flow cytometry with PI staining. (C-) Un-treated; Drug concentration is given in parenthesis. Two independent experiments, each concentration in duplicate. ***p < 0.0001 in comparison to (C-).

0.53 (hexane/ethyl acetate 1:1). IR (KBr, cm ^{1}): 3119.79 (NH), 1739.00 (C]O). ^{1}H NMR (400 MHz, DMSO-d$_6$), d $_{ppm}$: 7.39 (d, J ¼ 8.0 Hz, 2H, Ar), 7.46 (s, 1H, thiazole), 7.72 (d, J ¼ 8 Hz, 2H, Ar). 7.99 (m, 4H, Ar), 10.46 (s, 1H, NH). ^{13}C NMR (100 MHz, DMSO-d$_6$), d $_{ppm}$: 105.7 (CH, thiazole), 123.9 (CH, Ar), 127.3 (CH, Ar), 128.7 (CH, Ar), 129.3 (C, Ar) 132.2 (C, Ar), 132.9 (C, Ar), 135.4 (CCl, Ar), 148.9 (C, thiazole), 165.5 (C]O), 167.7 (SeC]N, thiazole). Anal. Calcd for $C_{17}H_{10}ClN_3O_2S$: C, 57.55; H, 2.96; N, 11.62; S, 9.03. found: C, 57.39; H, 2.83; N, 11.81; S, 9.01. HRMS: 356.0260 [MþH]^{þ}.

4.1.2.7. 2-[4-(4-bromophenyl)thiazol-2-ylamino]isoindoline-1,3-dione (2g). Light yellow crystals; Yield: 55%; m.p. (C) 220e221; Rf: 0.68 (hexane/ethyl acetate 1:1). IR (KBr, cm ^{1}): 3117.68 (NH), 1739.19 (C]O). ^{1}H NMR (400 MHz, DMSO-d$_6$), d $_{ppm}$: 7.47 (s, 1H, thiazole), 7.53 (d, J ¼ 8.4 Hz, 2H, Ar), 7.65 (d, J ¼ 8.0 Hz, 2H, Ar), 7.96 (m, 4H, Ar), 10.46 (s, 1H, NH). ^{13}C NMR (100 MHz, DMSO-d$_6$), d $_{ppm}$: 105.8 (CH, thiazole), 120.8 (CH, Ar), 123.9 (CH, Ar), 127.6 (CH, Ar), 129.3 (C, Ar) 131.6 (C, Ar), 135.4 (CBr, Ar), 148.9 (C, thiazole), 165.5 (C]O), 167.7 (SeC]N, thiazole). Anal. Calcd for $C_{17}H_{10}BrN_3O_2S$: C, 51.15; H, 2.58; N, 11.62; S, 9.03. found: C, 51.01; H, 2.52; N, 11.50; S, 8.91. HRMS: 401.9764 [MþH]^{þ}.

4.1.2.8. 2-[4-(4-nitrophenyl)thiazol-2-ylamino]isoindoline-1,3-dione (2h). Yellow crystals; Yield: 41%; m.p. (C) 239e240; Rf: 0.45 (hexane/ethyl acetate 3:2). IR (KBr, cm ^{1}): 3309.85 (NH), 1724.82 (C]O). ^{1}H NMR (400 MHz, DMSO-d$_6$), d $_{ppm}$: 7.77 (s, 1H, thiazole), 7.97 (m, 4H, Ar), 8.02 (d, J ¼ 8.8 Hz, 2H, Ar), 8.21 (d, J ¼ 8.8 Hz, 2H, Ar), 10.54 (s, 1H, NH). ^{13}C NMR (100 MHz, DMSO-d$_6$), d $_{ppm}$: 109.6 (CH, thiazole), 123.9 (CH, Ar), 124.1 (CH, Ar), 126.4 (CH, Ar), 129.3 (CN Ar), 135.4 (CH, Ar), 139.9 (C, Ar), 146.3 (C, Ar), 147.9 (C, thiazole), 165.382 (C]O), 168,0 (SeC]N, thiazole). Anal. Calcd for $C_{17}H_{10}N_4O_4S$: C, 54.40; H, 2.87; N, 15.23; S, 9.11. found: C, 55.73; H, 2.75; N, 15.29; S, 8.75. HRMS: 367.0517 [MþH]^{þ}.

4.1.2.9. 2-[4-(biphenyl-4-yl)thiazol-2-ylamino]isoindoline-1,3-dione (2i). Light yellow crystals; Yield: 46%; m.p. (C) 240e241; Rf: 0.65 (hexane/ethyl acetate 3:2). IR (KBr, cm ^{1}): 3324.67 (NH), 1660.10 (C]O). ^{1}H NMR (300 MHz, DMSO-d$_6$), d $_{ppm}$: 7.35 (s, 1H, thiazole), 7.48 (t, J ¼ 10.0 Hz, 1H, Ar), 7.63 (m, 4H, Ar), 7.72 (d, J ¼ 11.6 Hz, 2H, Ar), 7.82 (m, 4H, Ar) 7.96 (d, J ¼ 11.6 Hz, 2H, Ar), 10.65 (s, 1H, NH). ^{13}C NMR (75.5 MHz, DMSO-d$_6$), d $_{ppm}$: 103.4 (CH, thiazole), 126.5 (CH, Ar), 126.9 (CH, Ar), 127.5 (CH, Ar), 128.0 (CH, Ar) 129.0 (CH, Ar), 130.1 (CH, Ar), 131.5 (CH, Ar), 133.9 (C, Ar), 136.1 (CH, Ar), 139.0 (C, Ar), 139.7 (C Ar), 150.2 (C, thiazole), 167.6 (C]O), 168.3 (SeC]N, thia-zole). Anal. Calcd for $C_{23}H_{15}N_3O_2S$: C, 66.81; H, 3.98; N, 10.48; S, 7.95. found: C, 66.50; H, 3.80; N, 10.57; S, 8.07. HRMS: 398.0958 [MþH]^{þ}.

4.1.2.10. 2-[4-(naphthalen-2-yl)thiazol-2-ylamino]isoindoline-1,3-dione (2j). Light yellow crystals; Yield: 47%; m.p. (C) 225e227; Rf: 0.50 (hexane/ethyl acetate 3:2). IR (KBr, cm ^{1}): 3169.87 (NH), 1743.89 (C]O). ^{1}H NMR (400 MHz, DMSO-d$_6$), d $_{ppm}$: 7.47 (t, 2H, Ar), 7.53 (s, 1H, thiazole), 7.87 (d, J ¼ 11.6 Hz, 4H, Ar), 8.03 (m, 4H, Ar), 8.23 (s, 1H, Ar), 10.48 (s, 1H, NH). ^{13}C NMR (100 MHz, DMSO-d$_6$) d $_{ppm}$: 105.5 (CH, thiazole), 123.9 (CH, Ar), 124.2 (CH, Ar), 126.1 (CH, Ar), 126.4 (CH, Ar) 127.1 (CH, Ar), 127.6 (CH, Ar), 128.1 (CH, Ar), 128.2 (CH, Ar), 129.3 (C, Ar), 131.5 (C, Ar), 132.4 (C, Ar), 133.0 (C, Ar), 135.4 (CH, Ar), 150.1 (C, thiazole), 165.6 (C]O), 168.0 (SeC]N, thiazole). Anal. Calcd for $C_{21}H_{13}N_3O_2S$: C, 64.89; H, 3.48; N, 11.45; S, 8.26. found: C, 67.91; H, 3.53; N, 11.11; S, 8.63. HRMS: 367.0517 [MþH]^{þ}.

4.1.2.11. 2-[4-(3-nitrophenyl)thiazol-2-ylamino]isoindoline-1,3-dione (2k). Light yellow crystals; Yield: 44%; m.p. (C) 206e207; Rf: 0.55 (hexane/ethyl acetate 3:2). IR (KBr, cm ^{1}): 3287.35 (NH), 1732.47 (C]O). ^{1}H NMR (300 MHz, DMSO-d$_6$) d $_{ppm}$: 7.65 (t, J ¼ 7.2 Hz, 1H, Ar), 7.73 (s, 1H, thiazole), 8.00 (m, 4H, Ar), 8.13 (m, 2H, Ar), 8.48 (s, 1H, Ar) 10.36 (s, 1H, NH). ^{13}C NMR (75.5 MHz, DMSO-d$_6$), d $_{ppm}$: 107.7 (CH, thiazole), 119.9 (CH, Ar), 122.3 (CH, Ar), 123.9 (CH, Ar), 129.3 (CN, Ar) 130.3 (CH, Ar), 131.7 (CH, Ar), 135.5 (CH, Ar), 147.7 (C, Ar), 148.2 (C, thiazole), 165.5 (C]O), 168.2 (SeC]N, thiazole). Anal. Calcd for $C_{17}H_{10}N_4O_4S$: C, 53.04; H, 2.88; N, 15.49; S, 8.90. found: C, 54.73; H, 2.75; N, 15.29; S, 8.75. HRMS: 367.0517 [MþH]^{þ}.

4.1.2.12. 2-[4-(3,4-dichlorophenyl)thiazol-2-ylamino]isoindoline-1,3-dione (2l). Light yellow crystals; Yield: 57%; m.p. (C) 217e218; Rf: 0.53 (hexane/ethyl acetate 3:2). IR (KBr, cm ^{1}): 3337.03 (NH), 1742.53 (C]O). ^{1}H NMR (300 MHz, DMSO-d$_6$), d $_{ppm}$: 7.52 (s, 1H, thiazole), 7.62 (s, 1H, Ar), 7.68 (d, J ¼ 2.1 Hz, 1H, Ar), 7.94 (d, J ¼ 1.8 Hz, 1H, Ar), 8.00 (m, 4H, Ar), 10.51 (s, 1H, NH). ^{13}C NMR (75.5 MHz, DMSO-d$_6$), d $_{ppm}$: 107.1 (CH, thiazole), 123.9 (CH, Ar), 127.1 (CH, Ar), 129.3 (CCl, Ar), 129.5 (CH, Ar), 130.9 (CCl, Ar), 131.4 (C, Ar), 134.5 (CH, Ar), 135.4 (C, Ar), 136.0 (CH, Ar), 147.9 (C, thiazole), 165.4 (C]O), 167.9 (SeC]N, thiazole). Anal. Calcd for $C_{17}H_9Cl_2N_3O_2S$: C, 51.19; H, 2.43; N, 11.04; S, 8.58. found: C, 52.32; H, 2.32; N, 10.77; S, 8.22. HRMS: 356.0260 [MþH]^{þ}.

4.1.2.13. 2-[4-(2,4-dichlorophenyl)thiazol-2-ylamino]isoindoline-1,3-dione (2m). Colourless crystals; Yield: 46%; m.p. (C) 217e218; Rf: 0.55 (hexane/ethyl acetate 3:2). IR (KBr, cm ^{1}): 3130.90 (NH), 1741.75 (C]O). ^{1}H NMR (400 MHz, DMSO-d$_6$), d $_{ppm}$: 7.41 (d, J ¼ 7.2 Hz, 1H, Ar), 7.45 (s, 1H, thiazole), 7.63 (s, 1H, Ar), 7.65 (d, J ¼ 8.4 Hz, 1H, Ar). 7.97 (m, 4H, Ar), 10.46 (s, 1H, NH). ^{13}C NMR (100 MHz, DMSO-d$_6$), d $_{ppm}$: 110.45 (CH, thiazole), 123.8 (CH, Ar), 127.5 (CH, Ar), 129.3 (CCl, Ar), 129.7 (CH, Ar), 131.5 (CCl, Ar), 131.5 (C, Ar), 132.1 (CH, Ar), 132.7 (C, Ar), 135.4 (CH, Ar), 145.4 (C, thiazole), 165.4 (C]O), 166.7 (SeC]N, thiazole). Anal. Calcd for $C_{17}H_9Cl_2N_3O_2S$: C, 52.25; H, 2.26; N, 10.50; S, 7.91. found: C, 52.32; H, 2.32; N, 10.77; S, 8.22. HRMS: 356.0260 [MþH]^{þ}.

4.1.2.14. 2-[4-(4-bromophenyl)-5-methylthiazol-2-ylamino]isoindo-line-1,3-dione (2n). Yellow crystals; Yield: 36%; m.p. (C) 235e236; Rf: 0.60 (hexane/ethyl acetate 3:2). IR (KBr, cm ^{1}): 3188.90 (NH), 1745.97 (C]O). ^{1}H NMR (400 MHz, DMSO-d$_6$), d $_{ppm}$: 2.36 (s, 3H, CH_3), 7.41 (d, J ¼ 8.4 Hz, 2H, Ar), 7.55 (d, J ¼ 8.4 Hz, 2H, Ar), 7.96 (m, 4H, Ar), 10.23 (s, 1H, NH); ^{13}C NMR (100 MHz, DMSO-d$_6$), d $_{ppm}$: 12.1

(CH_3), 119.3 (C, thiazole), 120.4 (C, Ar), 123.8 (CH, Ar), 129.3 (C, Ar), 129.8 (CH, Ar), 131.2 (CH, Ar), 133.7 (CBr, Ar), 135.3 (CH, Ar), 144.0 (C, thiazole), 163.5 (C]O), 165.5 (SeC]N, thiazole). Anal. Calcd for $C_{17}H_{12}BrN_3O_2S$: C, 51.75; H, 3.00; N, 9.93; S, 7.58. found: C, 52.19; H, 2.92; N, 10.10; S, 7.74. HRMS: 401.9764 [MþH]þ.

4.1.3. Procedure for the syntheses of intermediate compounds 5a-b

Compound 3 was prepared by the condensation of commercially available aminoacetaldehyde diethyl acetal with the phthalic an-hydride (1:1 mol ratio), using toluene under reflux, in the presence of a catalytic amount of DMAP (yield 52%) for 2 h. In the next step, 2-(2,2-diethoxyethyl)isoindoline-1,3-dione (3) underwent acid hydrolysis (sulphuric acid at 70%) in reflux for 2 h. After the reaction was completed, it was allowed to reach at room temperature and was then cooled to induce precipitation. The formed precipitate was filtered on a sintered funnel with distilled water, yielding 55% of the pure product. For the synthesis of 5a and 5b, 2-(1,3-dioxoisoindol-2-yl) acetaldehyde (4) reacted with thio-semicarbazide (in the ratio 1:1) (for 5a) or 4-phenyl-3-thiosemicarbazide (for 5b), in ethanol, under reflux with catalytic amount of HCl (4 drops) for 4 h. The reactions were followed by thin layer chromatographic plate analysis. The formed precipitate was filtered on a sintered funnel with ethanol to yield the pure product (yield 76% for 5a and 70% for 5b).

4.1.3.1. (E)-2-[2-(1,3-dioxoisoindolin-2-yl)ethylidene]hydrazine-carbothioamide (5a). White crystals; Yield: 76%; m.p. (C) 223e224; Rf 0.45 (hexane/ethyl acetate 3:2); IR (KBr, cm ^{1}): 3423 and 3308 (NeH), 1769 and 1713 (C]O), 1602 (C]N); ^{1}H NMR (300 MHz, DMSO-d_6), d $_{ppm}$: 4.36 (d, J ¼ 3.6 Hz, 2H, CH_2), 7.36 (s, 1H, NH), 7.42 (t, J ¼ 3.6 Hz, 1H, CH]N), 7.83e7.90 (m, 4H, Ar), 8.03 and 11.27 (s, 1H, NH_2); ^{13}C NMR (75.5 MHz, DMSO-d_6), d $_{ppm}$: 40.1 (CH_2), 123.1 (Ar), 131.7 (Ar), 134.4 (Ar), 140.4 (C]N), 167.5 (C]O), 177.9 (C]S). Anal. Calcd for $C_{11}H_{10}N_4O_2S$: C, 50.37; H, 3.84; N, 21.36; S, 12.22. found: C, 50.03; H, 3.45; N, 20.98; S, 12.30. HRMS: 262.3388 [MþH]þ.

4.1.3.2. (E)-2-[2-(1,3-dioxoisoindolin-2-yl)ethylidene]-N-phenyl-hydrazinecarbothioamide (5b). White crystals; Yield: 70%; m.p. (C) 174e176; Rf 0.52 (hexane/ethyl acetate 3:2); ^{1}H NMR (300 MHz, DMSO-d_6), d $_{ppm}$: 4.46 (d, J ¼ 4.2 Hz, 2H, CH_3), 7.14 (t, J ¼ 7.8 Hz, 1H, Ar), 7.29 (t, J ¼ 7.8 Hz, 2H, Ar), 7.42 (d, J ¼ 7.8 Hz, 2H), 7.52 (t, J ¼ 4.2 Hz, 1H, Ar), 7.85e7.99 (m, 4H, Ar), 9.66 (s, 1H, NH), 11.72 (s, 1H, NH); ^{13}C NMR (75.5 MHz, DMSO-d_6), d $_{ppm}$: 40 (CH_2), 123.2 (Ar), 124.7 (Ar), 125.1 (Ar), 128.1 (Ar), 131.7 (Ar), 134.5 (Ar), 138.7 (Ar), 140.9 (C]N), 167.6 (C]O), 175.8 (C]S). Anal. Calcd for $C_{17}H_{14}N_4O_2S$: C, 60.34; H, 4.17; N, 16.56; S, 9.48. found: C, 60.03; H, 4.45; N, 16.35; S, 11.30. HRMS: 339.0845 [MþH]þ.

4.1.4. Procedure for the synthesis of 6a

In a round bottom flask was added 2-(2-(1,3-dioxoisoindolin-2-yl) ethylidene)hydrazinecarbothioamide (5a), 1,3-dichloroacetone and DMF. The reaction mixture was stirred at room temperature for about 1 h. The reaction was followed by thin layer chromato-graphic plate. After addition of distilled water, the pure product precipitates.

4.1.4.1. (E)-2-(2-{2-[4-(chloromethyl)thiazol-2-yl]hydrazono}ethyl) isoindoline-1,3-dione (6a). White crystals; Yield: 82%; m.p. (C) 191e193; Rf 0.23 (hexane/ethyl acetate 3:2); IR (KBr, cm ^{1}): 3159.36 and 3113.44 (NeH), 1771.01 and 1717.67 (C]O), 1565.77 (C]N). ^{1}H NMR (400 MHz, DMSO-d_6), d $_{ppm}$: 4.41 (d, J ¼ 3.2 Hz, 2H, CH_2), 4.53 (s, 2H, CH $_2$), 6.76 (s, 1H, CH, thiazole), 7.32 (s, 1H, CH), 7.86e7.89 (m, 4H, CH Ar), 11.75 (s, 1H, NH); ^{13}C NMR (75.5 MHz, DMSO-d_6), d $_{ppm}$: 38 (CH_2), 41.7 (CH_2), 107.9 (CH, thiazole), 123.1 (Ar), 131.7 (Ar), 134.5 (Ar), 138.4 (C, thiazole), 147.8 (C]N), 167.5 (C]O), 168.6 (SeC]N, thiazole). Anal. Calcd for $C_{14}H_{11}ClN_4O_2S$: C, 50.23; H, 3.31; N, 16.74; S, 9.58. found: C, 49.91; H, 3.30; N, 16.82; S, 10.03. HRMS: 335.0463 [MþH]þ.

4.1.5. General procedure for the synthesis of 6b-l

In round bottom flask was added 2-(2-(1,3-dioxoisoindolin-2-yl)ethylidene)-N-phenyl-hydrazine-carbothioamide (5b), the respective a-halogenated ketone and 2-propanol. The reaction mixture was kept under magnetic stirring, at room temperature, for 1 h. The reactions were followed by thin layer chromatographic plate. The formed precipitate was filtered on sintered funnel with distilled water, yielding the pure product.

4.1.5.1. 2-((E)-2-{(Z)-[3,4-diphenylthiazol-2(3H)-ylidene]hydrazono} ethyl)isoindoline-1,3-dione (6b). Orange crystals; Yield: 56%; m.p. (C) 196e198; Rf 0.46 (hexane/ethyl acetate 3:2); IR (KBr, cm ^{1}): 1712.40 (C]O). ^{1}H NMR (300 MHz, DMSO-d_6), d $_{ppm}$: 4.42 (d, J ¼ 3 Hz 2H, CH_2), 6.45 (s, 1H, CH, thiazole), 7.09e7.32 (m, 10H, CH Ar), 7.44 (t, J ¼ 3 Hz, 1H, HC]N), 7.91e7.88 (m, 4H, CH Ar, phtha-limide); ^{13}C NMR (75.5 MHz, DMSO-d_6), d $_{ppm}$: 40.3 (CH_2), 104.2 (CH, thiazole), 123.0 (Ar), 125.2 (Ar), 128.0 (Ar), 128.1 (Ar), 128.3 (Ar), 128.6 (Ar), 128.8 (Ar), 130.6 (Ar), 131.8 (Ar), 134.4 (Ar), 137.3 (Ar), 139.3 (C, thiazole), 148.2 (C]N), 167.5 (C]O), 169.9 (SeCeN, thiazole). Anal. Calcd for $C_{25}H_{18}N_4O_2S$: C, 68.48; H, 4.14; N, 12.78; S,

7.31. found: C, 66.88; H, 4.30; N, 12.48; S, 7.12. HRMS: 439.1028 [MþH]þ.

4.1.5.2. 2-((E)-2-{(Z)-[3-phenyl-4-p-tolylthiazol-2(3H)-ylidene] hydrazono}ethyl)isoindoline-1,3-dione (6c). Yellow crystals; Yield: 52%; m.p. (C) 156e158; Rf: 0.7 (hexane/ethyl acetate 3:2). IR (KBr, cm ^{1}): 1712.39 (C]O). ^{1}H NMR (300 MHz, DMSO-d_6), d $_{ppm}$: 2.19 (s, 3H,CH_3), 4.42 (d, J ¼ 3 Hz, 2H, CH_2), 6.41 (s, 1H, CH thiazole), 6.95e6.99 (m, 4H, CH Ar), 7.17e7.45 (m, 6H, CH Ar), 7.88e7.95 (m, 4H, CH Ar phthalimide); ^{13}C NMR (75.5 MHz, DMSO-d_6), d $_{ppm}$: 20.7 (CH_3), 38.9 (CH_2), 100.7 (CH, thiazole), 123.1 (Ar), 127.7 (Ar), 128.1 (Ar), 128.7 (Ar), 128.8 (Ar), 128.9 (Ar), 129.8 (Ar), 131.8 (Ar), 134.5 (Ar), 137.4 (Ar), 137.9 (Ar), 139.456 (C, thiazole), 148.2 (C]N), 167.6 (C]O), 170.1 (SeCeN, thiazole). Anal. Calcd for $C_{26}H_{20}N_4O_2S$: C, 69.01; H, 4.45; N, 12.38; S, 7.09. found: C, 68.66; H, 4.36; N, 12.12; S, 6.96. HRMS: 453.1138 [MþH]þ.

4.1.5.3. 2-((E)-2-{(Z)-[4-(4-methoxyphenyl)-3-phenylthiazol-2(3H)-ylidene]hydrazono}ethyl)isoindoline-1,3-dione (6d). Yellow crystals; Yield: 54%; m.p. (C) 173e175; Rf 0.49 (hexane/ethyl acetate 3:2); IR (KBr, cm ^{1}): 1713.83 (C]O). ^{1}H NMR (300 MHz, DMSO-d_6), d $_{ppm}$: 4.18 (s, 3H, CH_3), 4.44 (d, J ¼ 3 Hz, 2H, CH_2), 6.83e8.10 (m, 14H, Ar); ^{13}C NMR (75.5 MHz, DMSO-d_6), d $_{ppm}$: 40.1 (CH_2), 56.4 (CH_3), 104.3 (CH, thiazole), 123.1 (Ar), 123.3 (Ar), 127.9 (Ar), 128.4 (Ar), 128.8 (Ar), 129.2 (Ar), 131.7 (Ar), 134.5 (Ar), 136.6 (Ar), 136.7 (Ar), 137.6 (Ar), 139.0 (C, thiazole), 146.8 (C]N), 167.5 (C]O), 169.6 (SeCeN, thia-zole). Anal. Calcd for $C_{26}H_{20}N_4O_3S$: C, 66.65; H, 4.30; N, 11.96; S,

6.84. found: C, 65.60; H, 4.08; N, 11.85; S, 6.68. HRMS: 469.1276 [MþH]þ.

4.1.5.4. 2-((E)-2-{(Z)-[4-(4-fluorophenyl)-3-phenylthiazol-2(3H)-ylidene]hydrazono}ethyl)isoindoline-1,3-dione (6e). Yellow crystals; Yield: 50%; m.p. (C)176e179; Rf: 0.63 (hexane/ethyl acetate 3:2); IR (KBr, cm ^{1}): 1714.47 (C]O); ^{1}H NMR (300 MHz, DMSO-d_6), d $_{ppm}$: 4.43 (d, J ¼ 3 Hz, 2H, CH_2), 6.47 (s, 1H, CH thiazole), 7.02e7.36 (m, 9H, CH Ar), 7.45 (t, J ¼ 3 Hz, 1H, CH), 7.86e7.95 (m, 4H, CH Ar phthalimide); ^{13}C NMR (75.5 MHz, DMSO-d_6), d $_{ppm}$: 38.9 (CH_2), 101.3 (CH, thiazole), 115.1 (Ar), 115.3 (Ar), 123.1 (Ar), 127.1 (Ar), 128.0 (Ar), 128.7 (Ar), 128.9 (Ar), 130.6 (Ar), 131.8 (Ar), 134.5 (Ar), 137.2 (Ar),138.3 (C, thiazole), 148.3 (C]N), 160.2 and 163.4 (CeF), 167.6

(C]O), 169.9 (SeCeN, thiazole). Anal. Calcd for $C_{25}H_{17}FN_4O_2S$: C, 65.78; H, 3.75; N, 12.27; S, 7.02. found: C, 63.91; H, 3.79; N, 12.01; S, 6.94. HRMS: 457.1083 [MþH] þ.

4.1.5.5. 2-(2-{(Z)-[4-(4-chlorophenyl)-3-phenylthiazol-2(3H)-ylidene]hydrazono}ethyl)isoindoline-1,3-dione (6f). Yellow crystals; Yield: 58%; m.p. (C) 176e179; Rf: 0.84 (hexane/ethyl acetate 3:2); IR (KBr, cm ^{1}): 1717.30 (C]O). ^{1}H NMR (300 MHz, DMSO-d_6), d $_{ppm}$: 4.41 (d, J ¼ 3 Hz, 2H, CH_2), 6.50 (s, 1H, thiazole), 7.07e7.37 (m, 9H, Ar), 7.44 (t, J ¼ 3 Hz, 1H) 7.85e7.94 (m, 5H, Ar); ^{13}C NMR (75.5 MHz, DMSO-d_6), d $_{ppm}$: 56.0 (CH_2), 101.8 (CH, thiazole), 123.1 (Ar), 127.9 (Ar), 128.1 (Ar), 128.6 (Ar), 128.9 (Ar), 129.5 (Ar), 129.9 (Ar), 131.8 (Ar), 133.1 (Ar), 134.5 (Ar), 137.2 (Ar), 138.7 (C, thiazole), 148.3 (C] N), 167.6 (C]O), 169.9 (SeCeN, thiazole). Anal. Calcd for $C_{25}H_{17}ClN_4O_2S$: C, 63.49; H, 3.62; N, 11.85; S, 6.78. found: C, 61.17; H, 3.43; N, 11.47; S, 6.79. HRMS: 473.0793 [MþH] þ.

4.1.5.6. 2-((E)-2-{(Z)-[4-(4-bromophenyl)-3-phenylthiazol-2(3H)-ylidene]hydrazono}ethyl)isoindoline-1,3-dione (6g). White crystals; Yield: 55%; m.p. (C) 189e193; Rf: 0.73 (hexane/ethyl acetate 3:2); IR (KBr, cm ^{1}): 1717.05 (C]O). ^{1}H NMR (300 MHz, DMSO-d_6), d $_{ppm}$: 4.42 (d, J ¼ 3 Hz, 2H, CH_2), 6.51 (s, 1H, thiazole), 7.01e7.94 (m, 14H, Ar); ^{13}C NMR (75.5 MHz, DMSO-d_6), d $_{ppm}$: 39.3 (CH_2), 101.87 (CH, thiazole), 121.7 (Ar), 123.1 (Ar), 127.9 (Ar), 128.6 (Ar), 128.9 (Ar), 129.8 (Ar), 130.1 (Ar), 131.2 (Ar), 131.8 (Ar), 134.5 (Ar), 137.2 (Ar), 138.1 (C, thiazole), 148.5 (C]N), 167.6 (C]O), 169.9 (SeCeN, thia-zole). Anal. Calcd for $C_{25}H_{17}BrN_4O_2S$: C, 58.03; H, 3.31; N, 10.83; S, 6.20. found: C, 57.27; H, 3.28; N, 10.68; S, 6.06. HRMS: 517.0005 [MþH] þ.

4.1.5.7. 2-((E)-2-{(Z)-[4-(4-nitrophenyl)-3-phenylthiazol-2(3H)-ylidene]hydrazono}ethyl)isoindoline-1,3-dione (6h). Orange crystals; Yield: 46%; m.p. (C) 186e189; Rf: 0.75 (hexane/ethyl acetate 3:2). IR (KBr, cm ^{1}): 1713.38 (C]O). ^{1}H NMR (300 MHz, DMSO-d_6), d $_{ppm}$: 4.45 (d, J ¼ 3 Hz, 2H, CH_2), 6.78e8.10 (m, 15H, Ar); ^{13}C NMR (75.5 MHz, DMSO-d_6), d $_{ppm}$: 40.1 (CH_2), 102.0 (CH, thiazole), 123.2 (Ar), 123.3 (Ar), 124.5 (Ar), 128.0 (Ar), 128.4 (Ar), 129.0 (Ar), 131.7 (Ar), 131.7 (Ar), 134.5 (Ar), 136.7 (Ar), 137.4 (Ar), 138.7 (C, thiazole), 146.7 (C]N), 167.5 (C]O), 169.6 (SeCeN, thiazole). Anal. Calcd for $C_{25}H_{17}N_5O_4S$: C, 62.10; H, 3.54; N, 14.48; S, 6.63. found: C, 59.19; H, 3.65; N, 13.76; S, 6.93. HRMS: 484.0975 [MþH] þ.

4.1.5.8. 2-((E)-2-{(Z)-[4-(biphenyl-4-yl)-3-phenylthiazol-2(3H)-ylidene]hydrazono}ethyl)isoindoline-1,3-dione (6i). Yellow crystals; Yield: 73%; m.p. (C) 157e159; Rf 0.43 (hexane/ethyl acetate 3:2); IR (KBr, cm ^{1}): 1716.38 (C]O). ^{1}H NMR (400 MHz, DMSO-d_6), d $_{ppm}$: 4.48 (d, J ¼ 3.6 Hz, 2H, CH_2), 6.05 (s, 1H, thiazole), 7.00e7.82 (m, 19H, Ar); ^{13}C NMR (75.5 MHz, DMSO-d_6), d $_{ppm}$: 39.2 (CH_2), 101.2 (CH, thiazole), 123.3 (Ar), 126.8 (Ar), 126.9 (Ar), 127.7 (Ar), 128.3 (Ar), 128.4 (Ar), 128.5 (Ar), 128.6 (Ar), 128.7 (Ar), 128.8 (Ar), 129.2 (Ar), 129.6 (Ar), 132.3 (Ar), 133.9 (Ar), 133.9 (Ar), 139.9 (C, thiazole), 141.2 (C]N), 167.8 (C]O), 169.0 (SeCeN, thiazole). Anal. Calcd for $C_{31}H_{22}N_4O_2S$: C, 72.35; H, 4.31; N, 10.89; S, 6.23. found: C, 70.19; H, 4.32; N, 10.35; S, 6.53. HRMS: 515.1416 [MþH] þ.

4.1.5.9. 2-((E)-2-{(Z)-[4-(naphthalen-2-yl)-3-phenylthiazol-2(3H)-ylidene]hydrazono}ethyl)isoindoline-1,3-dione (6j). Yellow crystals; Yield: 68%; m.p. (C) 159e161; Rf 0.43 (hexane/ethyl acetate 3:2); IR (KBr, cm ^{1}): 1713.93 (C]O). ^{1}H NMR (400 MHz, DMSO-d_6), d $_{ppm}$: 4.56 (d, J ¼ 4 Hz, 2H, CH_2), 6.18 (s, 1H, thiazole), 6.99e7.91 (m, 17H, Ar); ^{13}C NMR (75.5 MHz, DMSO-d_6), d $_{ppm}$: 39.2 (CH_2), 101.6 (CH, thiazole), 123.3 (Ar), 125.4 (Ar), 126.5 (Ar), 126.7 (Ar), 127.6 (Ar), 127.7 (Ar) 127.8 (Ar), 128.0 (Ar), 128.1 (Ar), 128.3 (Ar), 128.4 (Ar), 128.7 (Ar), 129.2 (Ar), 132.3 (Ar), 132.8 (Ar), 133.9 (Ar), 137.5 (Ar), 140.3 (C, thiazole), 149.5 (C]N), 167.8 (C]O), 171.0 (SeCeN, thiazole). Anal. Calcd for $C_{29}H_{20}N_4O_2S$: C, 71.29; H, 4.13; N, 11.47; S, 6.56. found: C, 70.09; H, 4.21; N, 11.41; S, 6.70. HRMS: 489.1296 [MþH] þ.

4.1.5.10. 2-((E)-2-{(Z)-[4-(3-nitrophenyl)-3-phenylthiazol-2(3H)-ylidene]hydrazono}ethyl)isoindoline-1,3-dione (6k). Yellow crystals; Yield: 63%; m.p. (C) 154-154; Rf 0.34 (hexane/ethyl acetate 3:2); IR (KBr, cm ^{1}): 1712.80 (C]O). ^{1}H NMR (300 MHz, DMSO-d_6), d $_{ppm}$: 4.43 (d, J ¼ 2.7 Hz, 2H, CH_2), 6.76 (s, 1H, CH thiazole), 7.25e7.38 (m, 5H, CH Ar), 7.48e7.51 (m, 3H, CH Ar), 7.86e7.95 (m, 6H, CH Ar), 8.07 (t, J ¼ 2.4 Hz, 1H, HC]N); ^{13}C NMR (75.5 MHz, DMSO-d_6), d $_{ppm}$: 39.3 (CH_2), 104.3 (CH, thiazole), 123.2 (Ar), 123.4 (Ar), 123.6 (Ar), 128.8 (Ar), 128.9 (Ar), 129.1 (Ar), 129.3 (Ar), 129.5 (Ar), 129.6 (Ar), 130.0 (Ar), 130.3 (Ar), 135.0 (Ar), 135.6 (Ar), 138.8 (C, thiazole), 149.3 (C]N), 167.5 (C]O), 169.6 (SeCeN, thiazole). Anal. Calcd for $C_{25}H_{17}N_5O_4S$: C, 62.10; H, 3.54; N, 14.48; S, 6.63. found: C, 60.45; H, 3.70; N, 14.10; S, 6.48. HRMS: 484.0976 [MþH] þ.

4.1.5.11. 2-((E)-2-{(Z)-[4-(3,4-dichlorophenyl)-3-phenylthiazol-2(3H)-ylidene]hydrazono}ethyl)isoindoline-1,3-dione (6l).
Yellow crystals; Yield: 48%; m.p. (C) 155e157; Rf: 0.89 (hexane/ ethyl acetate 3:2); IR (KBr, cm ^{1}): 1714.45 (C]O). ^{1}H NMR (300 MHz, DMSO-d_6), d $_{ppm}$: 4.45 (d, J ¼ 3 Hz, 2H, CH_2), 6.81e7.92 (m, 14H, Ar); ^{13}C NMR (75.5 MHz, DMSO-d_6), d $_{ppm}$: 40.1 (CH_2), 104.6 (CH, thiazole), 123.1 (Ar), 128.3 (Ar), 128.6 (Ar), 128.9 (Ar), 129.3 (Ar), 130.3 (Ar), 130.5 (Ar), 130.9 (Ar), 131.4 (Ar), 131.7 (Ar), 134.3 (Ar), 134.6 (Ar), 136.1 (Ar), 137.3 (C, thiazole), 149.2 (C]N), 167.5 (C]O), 169.6 (SeCeN, thiazole); Anal. Calcd for $C_{25}H_{16}Cl_2N_4O_2S$: C, 59.18; H, 3.18; N, 11.04; S, 6.32. found: C, 56.85; H, 3.30; N, 10.58; S, 6.02. HRMS: 507.0432 [MþH] þ.

4.2. X-ray analysis

X-ray diffraction data collections were performed on an Enraf-Nonius Kappa-CCD diffractometer (95 mm CCD camera on k-goniostat) using graphite monochromated MoKa radiation (0.71073 Å) at room temperature. Data were collected using the COLLECT software [37] up to 50 (2q). The final unit cell parameters were based on 15666, 9327, and 12333 reflections to 2e, 2f and 2g, respectively. Integration and scaling of the reflections as well as the corrections for Lorentz and polarization effects were performed with the HKL DENZO-SCALEPACK system of programs [38]. The compound structures were solved by direct methods with SHELXS-97 [39]. The model was refined by full-matrix least squares on F2 using SHELXL-97 [39]. The program ORTEP-3 [40] was used for graphic representations, and the program WinGX [41] was used to prepare the material for publication. All H atoms were located by geometric considerations placed (CeH ¼ 0.93 Å; NeH ¼ 0.86 Å) and refined using a riding model with Uiso(H) ¼ 1.5Ueq(C-methyl) or 1.2Ueq(other). An Ortep-3 diagram of the molecules is shown in Fig. 2, and Table S1 shows the main crystallographic data. Crystal-lographic data (excluding structure factors) for the structures re-ported in this paper have been deposited with the Cambridge Crystallographic Data Centre as supplementary material (No. CCDC 1411254, 1411262 and 1411263).

4.3. Biological assays of toxicity to splenocytes

Splenocytes from BALB/c mice were divided into a 96 well plate at a density of 5 10^{6} cells per well in RPMI-1640 medium con-taining 10% inactivated Foetal Bovine Serum (FBS). Each chemical inhibitor was dissolved in DMSO at a concentration of 10 mg/mL, and then the sample was serially diluted in RPMI-1640 medium supplemented with 10% FBS at concentrations of 1.0, 5.0, 10, 25, 50 and 100 mg/mL, in triplicate. As a positive control, saponin was used

at a concentration of 0.1 mg/mL, while RPMI-1640 medium sup-plemented with 10% FBS and DMSO was used as a negative control. A total of 1.0 mCi of 3H-thymidine was added to each well, and the plate was incubated for 24 h at 37 C and 5% CO2.

The plate was then read in the counter beta irradiation reader (Multilabel Reader, Finland), and the percent incorporation of tritiated thymidine was determined. Cells that were not treated with drugs (negative controls) were calculated as 100% of tritiated thymidine incorporation (100% viable cells). For cells treated with saponin, cell viability was 5%. When the percentage of incorpora-tion was higher than 90%, the concentration of the drug was regarded as nontoxic to splenocytes.

4.4. Antiproliferative activity for the epimastigote form

Epimastigotes of Dm28c strain were distributed into a 96 well plate to a final density of 10^6 cells per well. Each chemical inhibitor was dissolved in the respective wells, in triplicate. Benznidazole was used as positive controls in this assay. The plate was then cultivated for 4 days at 27 C. After this time, aliquots from each well were collected, and the number of parasites was calculated in a Neubauer chamber. Epimastigotes not treated with the chemical inhibitors (negative control) were assumed as 100% the number of parasites. The doseeresponse curves were determined, and the IC_{50} values were calculated using at least five concentrations (data points) and a nonlinear equation (Prism, version 4.0).

4.5. Toxicity to trypomastigotes

Strain Y trypomastigotes were collected from Vero cell super-natants and distributed in a 96 well plate to a final density of 4 10^5 cells per well. Each chemical inhibitor was added to the wells, in triplicate. Benznidazole was used as positive controls in this assay. The plate was then cultivated for 24 h at 37 C and 5% CO2. After this time, aliquots from each well were collected, and the number of viable parasites (i.e., with apparent motility) was counted in a Neubauer chamber. The wells that did not receive the chemical inhibitors were assumed as 100% the number of viable parasites. The doseeresponse curves were determined, and the IC_{50} values were calculated by nonlinear regression (Prism, version 4.0) using at least seven concentrations (data points).

4.6. Ultrastructural studies

The parasites were cultured for 24 h in RPMI 1640 medium (SigmaeAldrich, St. Louis, MO, USA) buffered to pH 7.5 and sup-plemented with HEPES (20 mM), 10% foetal bovine serum, peni-cillin (100 U/mL), and streptomycin (100 mg/mL) containing the compound 6k at the IC_{50} concentration and twice the value of IC_{50}. The parasites were collected, washed in PBS and fixed with 2.5% glutaraldehyde, 4% formaldehyde, and 0.1 M cacodylate buffer at pH 6.8. They were then postfixed in 2% osmium tetroxide (OsO_4) in a 0.1 M cacodylate buffer at pH 6.8 and processed for routine transmission electron microscopy (TEM) and scanning electron microscopy (SEM).

For SEM analysis, the parasites were dehydrated in graded ethanol and dried by the critical point method with CO_2. The samples were mounted on aluminium stubs, coated with gold and examined under a JEOL-5600LV microscope.

For TEM analysis, the parasites were dehydrated in a graded series of acetone and finally embedded in epon. Sections were stained with uranyl acetate and lead citrate and observed with Tecnai spirit G2 Biotwin microscope.

4.7. Propidium iodide and annexin V staining

Trypomastigotes (1 10^7) were incubated for 24 h at 37 C in the absence or presence of compound 6k. After incubation, the parasites were labelled with propidium iodide (PI) and annexin V using the annexin V-FITC apoptosis detection kit (SigmaeAldrich), according to the manufacturer's instructions. Acquisition and ana-lyses were performed using a FACS Calibur flow cytometer (Becton Dickinson, CA, USA) with FlowJo software (Tree Star, CA, USA). A total of 30,000 events were acquired in the region previously established as trypomastigote forms of T. cruzi. Two independent experiments were performed.

Acknowledgements

This work was funded by Conselho Nacional de Desenvolvi-mento Científico e Tecnologico (CNPq), Fundaçao~ de Amparo a Ciencia^ e Tecnologia de Pernambuco (FACEPE, APQ-0549-2.11/14, APQ-0289-4.03/13). P.A.T.M.G. holds a FACEPE doctoral scholarship. Authors are thankful to the Departamento de Química Funda-mental (DQF-UFPE) for recording the ^{1}H NMR, ^{13}C NMR, LCMS and IR spectra of compounds. We are also thankful to Julia Campos of Centro de Tecnologias Estrategicas do Nordeste (CETENE) for recording the MS spectra of compounds 6a-l. All authors declare no competing financial interest.

Appendix A. Supplementary data

Supplementary data related to this article can be found at http://dx.doi.org/10.1016/j.ejmech.2016.01.010.

References

[1] WHO, Chagas Disease (American Trypanosomiasis), 2015. http://www.who.int/mediacentre/factsheets/fs340/en/index.html.

[2] J. Urbina, Chemotherapy of chagas disease, Curr. Pharm. Des. 8 (2002) 287e295, http://dx.doi.org/10.2174/1381612023396177.

[3] J.a Perez-Molina, J. Sojo-Dorado, F. Norman, B. Monge-Maillo, M. Díaz-Menendez, P. Albajar-Vinas,~ et al., Nifurtimox therapy for chagas disease does not cause hypersensitivity reactions in patients with such previous adverse reactions during benznidazole treatment, Acta Trop. 127 (2013) 101e104, http://dx.doi.org/10.1016/j.actatropica.2013.04.003.

[4] M.V. de O. Cardoso, L.R.P. de Siqueira, E.B. da Silva, L.B. Costa, M.Z. Hernandes, M.M. Rabello, et al., 2-pyridyl thiazoles as novel anti- Trypanosoma cruzi agents : structural design, synthesis and pharmacological evaluation, Eur. J. Med. Chem. 86 (2014) 48e59, http://dx.doi.org/10.1016/ j.ejmech.2014.08.012.

[5] S.S. Gawande, S.C. Warangkar, B.P. Bandgar, C.N. Khobragade, Synthesis of new heterocyclic hybrids based on pyrazole and thiazolidinone scaffolds as potent inhibitors of tyrosinase, Bioorg. Med. Chem. 21 (2013) 2772e2777, http://dx.doi.org/10.1016/j.bmc.2012.12.053.

[6] G.N. Masoud, A.M. Youssef, M.M. Abdel Khalek, A.E. Abdel Wahab, I.M. Labouta, A.a.B. Hazzaa, Design, synthesis, and biological evaluation of new 4-thiazolidinone derivatives substituted with benzimidazole ring as potential chemotherapeutic agents, Med. Chem. Res. 22 (2012) 707e725, http:// dx.doi.org/10.1007/s00044-012-0057-3.

[7] D.R.M. Moreira, S.P.M. Costa, M.Z. Hernandes, M.M. Rabello, G.B. de Oliveira Filho, C.M.L. de Melo, et al., Structural investigation of anti-Trypanosoma cruzi 2-iminothiazolidin-4-ones allows the identification of agents with efficacy in infected mice, J. Med. Chem. 55 (2012) 10918e10936, http://dx.doi.org/ 10.1021/jm301518v.

[8] C. Pizzo, C. Saiz, A. Talevi, L. Gavernet, P. Palestro, C. Bellera, et al., Synthesis of 2-hydrazolyl-4-thiazolidinones based on multicomponent reactions and bio-logical evaluation against Trypanosoma Cruzi, Chem. Biol. Drug Des. 77 (2011) 166e172, http://dx.doi.org/10.1111/j.1747-0285.2010.01071.x.

[9] M.E. Caputto, A. Ciccarelli, F. Frank, A.G. Moglioni, G.Y. Moltrasio, D. Vega, et al., Synthesis and biological evaluation of some novel 1-indanone thiazo-lylhydrazone derivatives as anti-Trypanosoma cruzi agents, Eur. J. Med. Chem. 55 (2012) 155e163, http://dx.doi.org/10.1016/j.ejmech.2012.07.013.

[10] M.Z. Hernandes, M.M. Rabello, A.C.L. Leite, M.V.O. Cardoso, D.R.M. Moreira, D.J. Brondani, et al., Studies toward the structural optimization of novel thiazolylhydrazone-based potent antitrypanosomal agents, Bioorg. Med. Chem. 18 (2010) 7826e7835, http://dx.doi.org/10.1016/j.bmc.2010.09.056.

[11] A.C.L. Leite, R.S. de Lima, D.R.D.M. Moreira, M.V.D.O. Cardoso, A.C. Gouveia de Brito, L.M. Farias Dos Santos, et al., Synthesis, docking, and in vitro activity of

thiosemicarbazones, aminoacyl-thiosemicarbazides and acyl-thiazolidones against Trypanosoma cruzi, Bioorg. Med. Chem. 14 (2006) 3749e3757, http://dx.doi.org/10.1016/j.bmc.2006.01.034.

[12] A.C.L. Leite, D.R. de M. Moreira, M.V. de O. Cardoso, M.Z. Hernandes, V.R. Alves Pereira, R.O. Silva, et al., Synthesis, Cruzain docking, and in vitro studies of aryl-4-oxothiazolylhydrazones against Trypanosoma cruzi, Chem. Med. Chem. 2 (2007) 1339e1345, http://dx.doi.org/10.1002/cmdc.200700022.

[13] J.W.P. Espíndola, M.V. de O. Cardoso, G.B. de O. Filho, D.A. Oliveira e Silva, D.R.M. Moreira, T.M. Bastos, et al., Synthesis and structureeactivity relation-ship study of a new series of antiparasitic aryloxyl thiosemicarbazones inhibiting Trypanosoma cruzi cruzain, Eur. J. Med. Chem. 101 (2015) 818e835, http://dx.doi.org/10.1016/j.ejmech.2015.06.048.

[14] G.B. de Oliveira Filho, M.V. de Oliveira Cardoso, J.W.P. Espíndola, L.F.G.R. Ferreira, C.A. de Simone, R.S. Ferreira, et al., Structural design, syn-thesis and pharmacological evaluation of 4-thiazolidinones against Trypano-soma cruzi, Bioorg. Med. Chem. 23 (2015) 7478e7486, http://dx.doi.org/ 10.1016/j.bmc.2015.10.048.

[15] A.M. Alanazi, A.S. El-Azab, I.A. Al-Suwaidan, K.E.H. ElTahir, Y.A. Asiri, N.I. Abdel-Aziz, et al., Structure-based design of phthalimide derivatives as potential cyclooxygenase-2 (COX-2) inhibitors: anti-inflammatory and anal-gesic activities, Eur. J. Med. Chem. 92 (2015) 115e123, http://dx.doi.org/ 10.1016/j.ejmech.2014.12.039.

[16] K. Kaminski, J. Obniska, B. Wiklik, D. Atamanyuk, Synthesis and anticonvulsant properties of new acetamide derivatives of phthalimide, and its saturated cyclohexane and norbornene analogs, Eur. J. Med. Chem. 46 (2011) 4634e4641, http://dx.doi.org/10.1016/j.ejmech.2011.07.043.

[17] H. Akgün, I. Karamelekoglu, B. Berk, I. Kurnaz, G. Sar b y k, S. Oktem, et al., Synthesis and antimycobacterial activity of some phthalimide derivatives, Bioorg. Med. Chem. 20 (2012) 4149e4154, http://dx.doi.org/10.1016/ j.bmc.2012.04.060.

[18] A.A.-M. Abdel-Aziz, A.S. El-Azab, S.M. Attia, A.M. Al-Obaid, M.A. Al-Omar, H.I. El-Subbagh, Synthesis and biological evaluation of some novel cyclic-imides as hypoglycaemic, anti-hyperlipidemic agents, Eur. J. Med. Chem. 46 (2011) 4324e4329, http://dx.doi.org/10.1016/j.ejmech.2011.07.002.

[19] G. Singh, A. Saroa, S. Girdhar, S. Rani, S. Sahoo, D. Choquesillo-Lazarte, Syn-thesis, characterization, electronic absorption and antimicrobial studies of N-(silatranylpropyl)phthalimide derived from phthalic anhydride, Inorganica Chim. Acta 427 (2015) 232e239, http://dx.doi.org/10.1016/j.ica.2015.01.011.

[20] K. Elumalai, M.A. Ali, M. Elumalai, K. Eluri, S. Srinivasan, S. Sivannan, et al., Synthesis, characterization and biological evaluation of acetazolamide, cycloserine and isoniazid condensed some novel phthalimide derivatives, Int. J. Chem. Anal. Sci. 4 (2013) 57e61, http://dx.doi.org/10.1016/ j.ijcas.2013.04.004.

[21] R. Williams, J.T. Manka, A.L. Rodriguez, P.N. Vinson, C.M. Niswender, C.D. Weaver, et al., Synthesis and SAR of centrally active mGlu5 positive allosteric modulators based on an aryl acetylenic bicyclic lactam scaffold, Bioorg. Med. Chem. Lett. 21 (2011) 1350e1353, http://dx.doi.org/10.1016/ j.bmcl.2011.01.044.

[22] A.C.L. Leite, F.F. Barbosa, M.V.D.O. Cardoso, D.R.M. Moreira, L.C.D. Coelho,^ E.B. Silva, et al., Phthaloyl amino acids as anti-inflammatory and immuno-modulatory prototypes, Med. Chem. Res. (2013), http://dx.doi.org/10.1007/ s00044-013-0730-1.

[23] M.V.D.O. Cardoso, D.R.M. Moreira, G.B.O. Filho, S.M.T. Cavalcanti, L.C.D. Coelho, J.W.P. Espíndola, et al., Design, synthesis and structureeactivity relationship of phthalimides endowed with dual antiproliferative and immunomodulatory activities, Eur. J. Med. Chem. 96 (2015) 491e503, http://dx.doi.org/10.1016/ j.ejmech.2015.04.041.

[24] L.C.D. Coelho,^ M.V. de O. Cardoso, D.R.M. Moreira, P.A.T. de M. Gomes, S.M.T. Cavalcanti, A.R. Oliveira, et al., Novel phthalimide derivatives with TNF-a and IL-1b expression inhibitory and apoptotic inducing properties, Med-chemcomm 5 (2014) 758, http://dx.doi.org/10.1039/c4md00070f.

[25] C. Pessoa, P.M.P. Ferreira, L.V.C. Lotufo, M.O. de Moraes, S.M.T. Cavalcanti, L.C.D. Coelho,^ et al., Discovery of phthalimides as immunomodulatory and antitumor drug prototypes, Chem. Med. Chem. 5 (2010) 523e528, http://dx.doi.org/10.1002/cmdc.200900525.

[26] P.M. da Costa, M.P. da Costa, A.A. Carvalho, S.M.T. Cavalcanti, M.V. de Oliveira Cardoso, G.B. de Oliveira Filho, et al., Improvement of in vivo anticancer and antiangiogenic potential of thalidomide derivatives, Chem. Biol. Interact. 239 (2015) 174e183, http://dx.doi.org/10.1016/j.cbi.2015.06.037.

[27] E. de F. Santiago, S.A. de Oliveira, G.B. de Oliveira Filho, D.R.M. Moreira, P.A.T. Gomes, A.C.L.A.C.L. da Silva, et al., Evaluation of the anti-schistosoma mansoni activity of Thiosemicarbazones and Thiazoles, Antimicrob. Agents Chemother. 58 (2014) 352e363, http://dx.doi.org/10.1128/AAC.01900-13.

[28] M. Cardosoa, M. Hernandes, D. Moreira, F. Pontes, C. Simone, A. Leite, Struc-tural insights into bioactive Thiazolidin-4-one: experimental and theoretical data, Lett. Org. Chem. 12 (2015) 262e270, http://dx.doi.org/10.2174/1570178612666150203005612.

[29] D.R.M. Moreira, A.C. Lima Leite, M.V.O. Cardoso, R.M. Srivastava, M.Z. Hernandes, M.M. Rabello, et al., Structural design, synthesis and structure-activity relationships of thiazolidinones with enhanced anti-trypanosoma cruzi activity, Chem. Med. Chem. 9 (2014) 177e188, http:// dx.doi.org/10.1002/cmdc.201300354.

[30] M. Congreve, R. Carr, C. Murray, H. Jhoti, A "Rule of Three" for fragment-based lead discovery? Drug Discov. Today 8 (2003) 876e877, http://dx.doi.org/ 10.1016/S1359-6446(03)02831-9.

[31] H. Chen, X. Zhou, A. Wang, Y. Zheng, Y. Gao, J. Zhou, Evolutions in fragment-based drug design: the deconstructionereconstruction approach, Drug Dis-cov. Today 20 (2015) 105e113, http://dx.doi.org/10.1016/ j.drudis.2014.09.015.

[32] M. Gonzales-Perdomo, S.L. de Castro, M.N. Meirelles, S. Goldenberg, Trypa-nosoma cruzi proliferation and differentiation are blocked by topoisomerase II inhibitors, Antimicrob. Agents Chemother. 34 (1990) 1707e1714, http://dx.doi.org/10.1128/AAC.34.9.1707.

[33] E.M. De Souza, A. Lansiaux, C. Bailly, W.D. Wilson, Q. Hu, D.W. Boykin, et al., Phenyl substitution of furamidine markedly potentiates its anti-parasitic ac-tivity against trypanosoma cruzi and Leishmania amazonensis, Biochem. Pharmacol. 68 (2004) 593e600, http://dx.doi.org/10.1016/j.bcp.2004.04.019.

[34] L.R. Garzoni, A. Caldera, M. de N.L. Meirelles, S.L.d. Castro, R. Docampo, G.A. Meints, et al., Selective in vitro effects of the farnesyl pyrophosphate synthase inhibitor risedronate on trypanosoma cruzi, Int. J. Antimicrob. Agents 23 (2004) 273e285, http://dx.doi.org/10.1016/ j.ijantimicag.2003.07.020.

[35] M.V. Braga, J.A. Urbina, W. de Souza, Effects of squalene synthase inhibitors on the growth and ultrastructure of trypanosoma cruzi, Int. J. Antimicrob. Agents 24 (2004) 72e78, http://dx.doi.org/10.1016/j.ijantimicag.2003.12.009.

[36] A.P. Dantas, K. Salomao,~ H.S. Barbosa, S.L. De Castro, The effect of Bulgarian propolis against trypanosoma cruzi and during its interaction with host cells, Mem. Inst. Oswaldo Cruz 101 (2006) 207e211, http://dx.doi.org/10.1590/ S0074-02762006000200013.

[37] E.-N. Collect, Nonius BV, Delft, The Netherlands. 2000 (1997) 585.

[38] Z. Otwinowski, W. Minor, Methods in enzymology, Macromol. Crystallogr. Part A 276 (1997) 307e326, http://dx.doi.org/10.1016/S0076-6879(97)76066-X.

[39] G. Sheldrick, SHELXL-97 and SHELXS-97, Program for X-ray Crystal Structure Solution and Refinement, Univ. Gottingen,€ 1997. http://scholar.google.com.br/scholar?q¼SHELXS-97:Program for Crystal Structure Resolution#3.

[40] L.J. Farrugia, ORTEP -3 for Windows - a version of ORTEP -III with a Graphical User interface (GUI), J. Appl. Crystallogr. 30 (1997) 565, http://dx.doi.org/10.1107/S0021889897003117.

[41] L.J. Farrugia, WinGX suite for small-molecule single-crystal crystallography, J. Appl. Crystallogr. 32 (1999) 837e838, http://dx.doi.org/10.1107/ S0021889899006020.

APÊNDICE C -

Antitumor and immunomodulatory activities of thiosemicarbazones and 1,3-Thiazoles in Jurkat and HT-29 cells

Biomedicine & Pharmacotherapy 82 (2016) 555–560

Available online at
ScienceDirect
www.sciencedirect.com

Elsevier Masson France
EM|consulte
www.em-consulte.com/en

Antitumor and immunomodulatory activities of thiosemicarbazones and 1,3-Thiazoles in Jurkat and HT-29 cells

Thiago André R. dos Santos[a], Aline Caroline da Silva[a], Elany Barbosa Silva[b], Paulo André Teixeira de Moraes Gomes[b], José Wanderlan Pontes Espíndola[b], Marcos Veríssimo de Oliveira Cardoso[b], Diogo Rodrigo Magalhaes Moreira[c], Ana Cristina Lima Leite[b,*], Valéria R.A. Pereira[a,*]

[a] Fundação Oswaldo Cruz, Centro de Pesquisa Aggeu Magalhães, Laboratório de Imunogenética, CEP 50670-420, Recife, PE, Brazil
[b] Universidade Federal de Pernambuco, Departamento de Ciências Farmacêuticas, CEP 50740-520, Recife, PE, Brazil
[c] Fundação Oswaldo Cruz, Centro de Pesquisas Gonçalo Moniz, CEP 40296-710, Salvador, BA, Brazil

ARTICLE INFO

Article history:
Received 7 December 2015
Received in revised form 20 May 2016
Accepted 23 May 2016

Keywords:
Drug development
Cancer
Immune system 1,3-thiazoles
Thiosemicarbazones
Cell death

ABSTRACT

Cancer remains a high incidence and mortality disease, causing around 8.2 million of deaths in the last year. Current chemotherapy needs to be expanded, making research for new drugs a necessary task. Immune system modulation is an emerging concept in cancer cell proliferation control. In fact, there are a number of mechanisms underlying the role immune system plays in tumor cells. In this work, we describe the structural design, synthesis, antitumor and immunomodulatory potential of 31 new 1,3-thiazole and thiosemicarbazone compounds. Cisplatin was used as anticancer drug control. Cytotoxicity against J774A.1 macrophages and antitumor activity against HT-29 and Jurkat cells was determined. These 1,3-thiazole and thiosemicarbazone compounds not only exhibited cytotoxicity in cancer cells, but were able to cause irreversible cancer cell damage by inducing necrosis and apoptosis. In addition, these compounds, especially pyridyl-thiazoles compounds, regulated immune factors such as interleukin 10 and tumor necrosis factor, possible by directing immune system in favor of modulating cancer cell proliferation. By examining their pharmacological activity, we were able to identify new potent and selective anticancer compounds.

1. Introduction

Immune system modulation is an emerging concept in cancer cell proliferation control. In fact, there are a number of mecha-nisms underlying the role immune system plays in tumor cells. The most well-known processes involve minimizing metastasis by attenuating pro-angiogenic cytokines expression, or alternatively by upregulating expression of endothelial factors that are crucial for angiogenic process in metastasis. In addition, enhancing antitumor immunity mediated by interferon-g and interleukins can reduce cancer cell development. In view of this, discovery of anticancer and immunomodulating agents is a line of research that is receiving much attention [1–4].

Among anticancer and immunomodulatory drug candidates that have entered into clinical trials, the majority are synthetic compounds, especially heterocyclic derivatives. Examples are Thalidomide, Imatinib and Sunitinib. Following this direction, phthalimide has commonly been employed in design of potential anti-inflammatory, immunomodulatory, antiangiogenic, and anti-tumor drugs. Given this promising outlook, the strategy of molecular hybridization, using phthalimide as a pharmacophoric fragment has figured prominently in recent research and given rise to many successful outcomes. Our research group has discovered potent and selective anticancer and anti-inflammatory compounds by hybridizing two distinct structural domains: phthalimide and another heterocyclic ring. This has led to the identification of various SARs and the discovery of a new potent hybrid compound containing thiosemicarbazone and 1,3-thiazole moieties, which were observed as having selective toxicity against tumor cells [1,5,6].

Bearing in mind the molecular biophores outlined above and the remarkable pharmacological properties observed in 1,3-

* Corresponding authors.
E-mail addresses: thiago.andre.ufpe@gmail.com (T.A.R. dos Santos), acllb2003@yahoo.com.br (A.C. da Silva), valeria@cpqam.fiocruz.br (V.R.A. Pereira).

http://dx.doi.org/10.1016/j.biopha.2016.05.038 0753-3322/ã 2016

thiazole and thiosemicarbazone compounds, we here describe the design, synthesis and pharmacological evaluation of 31 new potential antitumor and immunomodulatory agents. These 1,3-thiazole and thiosemicarbazones not only exhibited cytotoxicity in cancer cells, but were able to cause irreversible cancer cell damage by inducing necrosis and apoptosis. In addition, especially pyridyl-thiazoles compounds, regulated immune factor such as interleukin 10 and tumor necrosis factor, possible by halting the immune system in favor of modulating cancer cell proliferation.

2. Material and methods

2.1. Compounds

Compounds were obtained from LpQM (Laboratory of planning in Medicinal Chemistry). In general, compounds were developed in two reaction steps: a condensation between ketones and different thiosemicarbazides; and a cyclization of the thiosemicarbazones obtained in the preceding step with different a-halogen-aceto-phenones [7]. The pyridyl-thiosemicarbazones 3a–c, aryl-thiose-micarbazone (6) and phthalyl-thiosemicarbazones (9a, 9b) were prepared from the reaction between thiosemicarbazides (1a–c) and pyridyl-ketone (2), the aryl-ketone (5) and phthalyl ketone (8), respectively (Fig. 1). The thiosemicarbazones obtained were treated with different a-halogen-acetophenones to obtain deriv-atives of 1,3-thiazoles (4a–, (7a–j) and (10a–j). All compounds were chemically characterized and presented purity of >95% [8].

2.2. Cell culture

Colorectal cancer cell line HT-29 and J774A.1 macrophage cell line was cultured in DMEM medium (Cultilab) containing 10% heat-inactivated fetal bovine serum, 100U/mL penicillin G, and 2mMl-glutamine in a humidified atmosphere of 5% CO_2 in air at 37 C. Jurkat cells (human acute T lymphocytic leukemia) cultured in RPMI 1640 medium (Sigma) containing 10% heat-inactivated fetal bovine serum, 100U/mL penicillin G, and 2mMl-glutamine in a humidified atmosphere of 5% CO_2 in air at 37 C. Both cell lines used in this work were obtained from cell bank of Rio de Janeiro (BCRJ). Culture medium was changed 2–3 days and subcultured when cell population density reached to 70–80% confluence.

2.3. Cytotoxicity assessment by MTT assay

MTT-tetrazolium reduction assay was used to evaluate effects of compounds against HT-29, Jurkat and J774A.1 cells [9]. Briefly, 1 10^5 cells/well were added in 96-well plates with appropriated medium and incubated for 24 h (37 C and 5% CO_2). Compounds

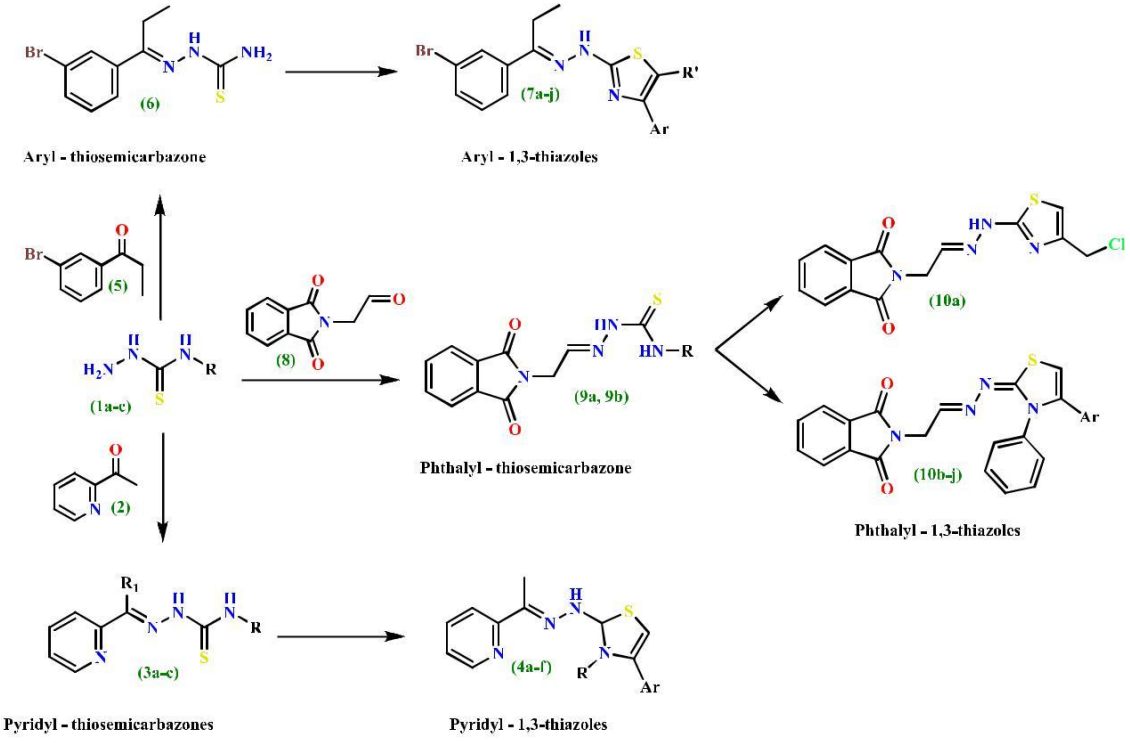

Compounds	R_1	R	Ar
1a	-	H	-
1b	-	CH_3	-
1c	-	Ph	-
3a	CH_3	CH_3	-
3b	CH_3	H	-
3c	Ph	CH_3	-
4a	CH_3	CH_3	Naphthalene
4b	CH_3	CH_3	4-NO_2-Ph
4c	CH_3	CH_3	4-MeO-Ph
4d	CH_3	CH_3	4-Cl-Ph
4e	CH_3	CH_3	4-Br-Ph
4f	CH_3	CH_3	4-F-Ph

Compounds	R'	Ar
7a	-	Ph
7b	-	4-Me-Ph
7c	-	4-MeO-Ph
7d	CH_3	4-Br-Ph
7e	-	3-NO_2-Ph
7f	-	4-NO_2-Ph
7g	-	4-F-Ph
7h	-	4-Cl-Ph
7i	-	3,4-diCl-Ph
7j	-	2,4-diCl-Ph

Compounds	R	Ar
9a	H	-
9b	Ph	-
10b	-	Ph
10c	-	4-Me-Ph
10d	-	4-MeO-Ph
10e	-	3-NO2-Ph
10f	-	4-NO2-Ph
10g	-	4-Cl-Ph
10h	-	4-Br-Ph
10i	-	4-F-Ph
10j	-	3,4-diCl-Ph

Fig. 1. General synthetic procedure.

were then added in different concentrations (1 to 100 μg/mL) and incubated for 72 h. Cisplatin was used as a reference drug. Two hours before the end of the incubation time, 25 μL MTT (3-(4,5-Dimethylthiazol-2-yl)-2,5-diphenyltetrazoliumbromide, 5 mg/mL in PBS) was added to each well. Culture medium was removed and 100 μL of DMSO were added. The amount of formazan was determined by measuring the absorbance at 570 nm [9]. Concen-tration leading to 50% inhibition of viability (CC_{50}) was calculated by regression analysis.

2.4. Flow cytometry assay

HT-29 and Jurkat cells (1 10^6 cells/mL) were treated (72 h, 37 C, 5% CO_2) with compounds in its respective CC_{50}, obtained in previous experiments. Briefly, tumor cells were harvested, washed with PBS, re-suspended in Annexin V biding buffer (eBioscience, San Diego, CA, USA) and stained with propidium iodide (PI) and annexin V-FITC (eBioscience, San Diego, CA, USA) according to manufacturer instructions. The cells were immediately analyzed by flow cytometry (FACSCalibur™, BD BioSciences, San Jose, CA, USA) [10]. Results were analyzed by BD FlowJo 7.6 software.

2.5. Immunomodulatory activity

J774A.1 macrophages were stimulated with compounds for 24, 48 and 72 h in its respective CC_{50} values and culture supernatants were used to measurement of cytokine production [9]. Lipopoly-saccharide (LPS at 50 ng mL-1) was used as positive control, while cells without either LPS or compounds were used as negative control. Concentration of TNF and IL-10 was measured using sandwich enzyme-linked immunosorbent assay (ELISA), according to the manufacturer's suggested protocols (BD OptEIA™, San Jose, CA, USA). Absorbance was read at 415 nm using a spectrophotom-eter (Multiskan™ FC Microplate Photometer, Thermo Scientific, San Jose, CA, USA).

2.6. Statistical analysis

All experiments were done in triplicate. Data were analyzed by one-way analysis of variance (ANOVA) followed by Dunnett's test ($P < 0.05$). GraphPad Prism 5.0 (GraphPad, California, EUA) was used for all analysis.

3. Results

3.1. Antitumor activity on Jurkat and HT-29 cell lines

Using MTT assay we observed that compounds demonstrated antitumor activity in both Jurkat and HT-29 cells. Compounds tested showed a dose-dependent effect (data not shown). All pyridyl-thiosemicarbazones and pyridyl-thiazoles series showed low CC_{50} value in HT-29 and Jurkat cells when compared with cisplatin – 179 and 89,5 μM, respectively (Table 1). The lower CC_{50} value in HT-29 and Jurkat cells was observed with compound 3b (17.18 μM) and compound 7e (2.79 μM) respectively.

3.2. Cell death induction

Once observed that compounds had an antitumor effect, and after determination of CC_{50} value for each compound, we incubated HT-29 and Jurkat cells with these compounds in its respective CC_{50} values for 72 h aiming to evaluate the kind of cell death induced. Cells were stained with annexin V-FITC (AN) and propidium iodide (PI) and analyzed by flow cytometry.

Untreated HT-29 cells presented a lower staining with either AN or PI, demonstrating cell viability. Saponin, used as cell death positive control, caused a high staining (>90%) with PI, indicating cell death by necrosis, as expected. Pyridyl-thiazoles compounds caused higher labeling with AN, under the experimental conditions applied, indicating cell death predominantly by apoptosis. An increase of double staining (AN-PI) was detected after incubation with Phthalyl-thiazoles and Pyridyl-thiazoles, indicating the occurrence of cell death by necrosis or late apoptosis (Fig. 2).

Table 1
Compounds utilized in this study and their cytotoxicity in J774A.1 Macrophages, HT-29 and Jurkat cell lines.

Compound	J774A.1 CC_{50} (μM)	HT-29 CC_{50} (μM)	Jurkat CC_{50} (μM)
3a	21,77	83,09	14,91
3b	182,57	17,18	32,80
3c	21,36	29,46	ND
4a	30,35	57,83	16,23
4b	36,05	65,62	21,30
4c	19,99	108,25	19,59
4d	20,32	78,87	28,18
4e	33,60	51,29	21,54
4f	11,65	25,22	ND
6	51,05	153,67	67,82
7a	75,90	57,49	74,37
7b	113,60	24,13	116,63
7c	114,96	61,97	113,83
7d	21,95	58,34	110,66
7e	40,13	21,02	2.79
7f	67,47	ND	125,69
7g	6,50	79,62	117,88
7h	ND	126,75	406,65
7i	124,76	127,59	271,53
7j	75,37	18,29	25,13
9b	28,66	13,44	88,81
10a	69,33	172,53	17,48
10b	37,01	21,05	83,60
10c	41,03	17,84	23,42
10d	40,51	22,09	114,49
10e	47,38	21,28	21,22
10f	26,47	273,22	21,53
10g	30,07	114,45	11,54
10h	21,20	95,77	ND
10i	26,57	129,71	8,54
10j	ND	0,00	23,99
Cisplatin	58,98	179,07	89,47

Note: ND: Not Determined.

Jurkat untreated cells showed low staining with either AN or PI. The cell treatment with the commercial drug cisplatin caused a double staining (AN-PI) increase. Jurkat cells presented a high double staining with high percentage of PI labeling, for pyridyl-thiazoles. Compound 10c led to an increasing of AN staining, twice higher than untreated control. 10a and 3b compounds induced a high increasing of double staining in Jurkat cells. Results are shown in Fig. 3.

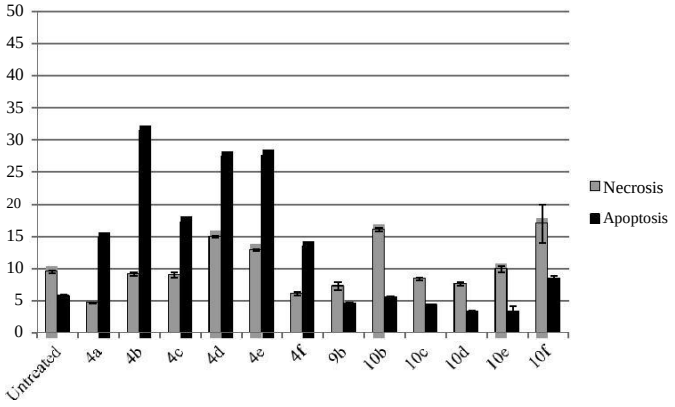

Fig. 2. Percentage of HT-29 cells labeled for necrosis and apoptosis, after 72 h of incubation with the compounds.

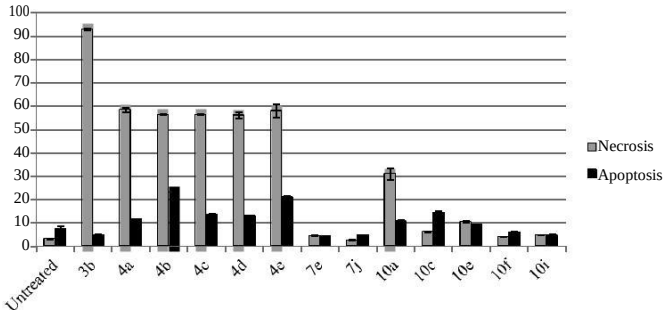

Fig. 3. Percentage of Jurkat cells stained for necrosis and apoptosis, after 72 h of incubation with the compounds.

3.3. Cytotoxicity effect and immunomodulatory activity on macrophages

Cytotoxicity in J774A.1 cells was done by MTT assay and CC_{50} results were used for stimulation of cultures. CC_{50} results varied between 6,5 and 182,57 mM, for 7g and 3b, respectively. Cisplatin showed a CC_{50} of 58.98 mM. All CC_{50} results are shown in Table 1.

Immunomodulatory activity was evaluated by production of cytokines IL-10 and TNF. This quantification was assessed by ELISA assay. For this purpose, J774A.1 macrophages supernatants of culture were collected after incubation with compounds for 24, 48 and 72 h. Results are showed below.

TNF production was observed for all compounds tested after 48 h of incubation, however, significant values were observed only for 6, 7a, 7f, 7h, 7i, 7j, all pyridyl-thiosemicarbazones, pyridyl-thiazoles and phthalyl-thiazoles (except 10f). Similar results were observed after 72 h of incubation. Results are shown in Figs. 4 and 5.

After 24 h of incubation with compounds 4c and 4d was observed a significant ($p < 0.0001$) decrease in IL-10 production, when compared to untreated group. Inhibition of production of this cytokine was sustained with 4c after 48 h of incubation. On the other hand, 7d, 7f, 7g, 10g, 10h, 10j increased this cytokine production after 48 h (Figs. 6 and 7). It was not detected production of IL-10 after 72 h of treatment.

4. Discussion

Despite great efforts made by public and private organizations cancer's characteristics, as severity and often lethality, has persisted over the years [11]. Development of new cancer treatments remains a challenging process, diverse therapy strategies have been developed and tried, and medicinal chemistry is one of this approaches [12]. In this context, several compounds has been noted for its activity in various diseases, including cancer [13].

These compounds include thiosemicarbazones, thiazoles and phthalimides, molecules tested in this study. The choice of these compounds for development of pre-clinical trials are based on the broad spectrum of biological activities related to them, as well as the effects on components of immune system such as cytokines [14,15].

In this work, four classes of compounds were screened for its antitumor activities, and its actions on immune cells. Cisplatin, used as a control, is one of the most remarkable success in the treatment of cancer [16]. It is expected that a potential anticancer drug to stimulate protective immunity against the tumor and in favor of the host [17].

A screening was performed with J774A.1 macrophages, through MTT assay. In this assay, only metabolically viable cells can reduce MTT by mitochondrial dehydrogenases leading to formation of formazan crystals. These experiments aimed to assess cytotoxicity of compounds in this important cell of immune system, present in microenvironment of practically all solid tumors [18]. It is known that macrophages may play both pro and anti-tumor role, due to its polarization capability and high plasticity [19–21]. Faced with this problem, it constitutes an important approach to evaluate whether tested compounds contribute to cytotoxicity of macrophages.

Cytotoxic effect of compounds when treating tumor cells was superior to the observed after treatment with cisplatin. These results showed that these compounds have a potential as a therapeutic tool, despite the cytotoxicity observed in macro-phages. The present data showed that there is a structure-relationship for synthetic compounds tested. The biological activities of compounds are apparently related to the types of modifications on scaffold molecules. Therefore, other experiments were performed, aiming to elucidate this potential in this tumor cell lines.

Antitumor treatment can cause different cell death to neoplastic cells, depending on the lethal stimuli generated [22]. Apoptosis is a strongly regulated process that can be initiated by both intracellular stress signals and extracellular ligands [23]. Apoptosis is morphologically characterized by cell shrink, pyknosis and eventually fragmentation of apoptotic bodies [24]. Inactivation of apoptosis is a central event in cancer development, and its activation, by treatment approaches, can present benefits in patient prognostic [25]. In contrast, necrosis has been considered as an uncontrolled cell death pathway, characterized by cyto-plasmic vacuolization, loss of plasma membrane integrity and cell swelling [23].

After observation that compounds had a considerable cytotoxic effect on tumor cell lines, induction of necrosis and apoptosis was assessed for HT-29 and Jurkat cell lines.

All compounds tested increase significantly the labeling for apoptosis and necrosis. In fact, the triggering of these two types of cell death can have beneficial effects on clinical [23], and these results support the need for further studies in vitro and in vivo in

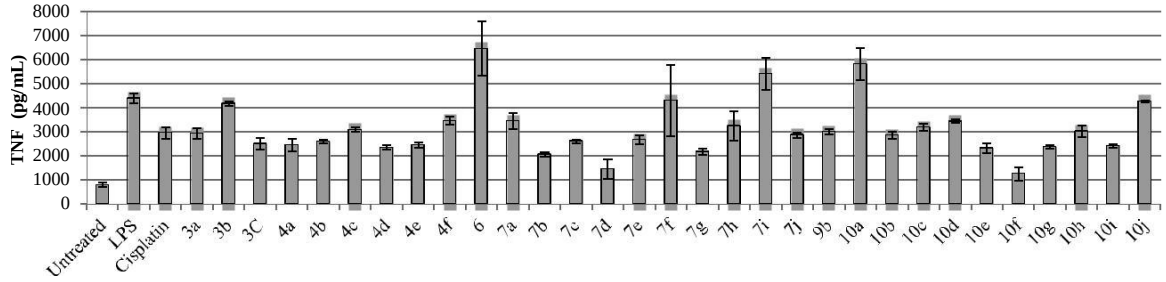

Fig. 4. TNF production in supernatants of macrophage culture in presence of all compounds tested at its respective CC_{50} values, after 48 h of incubation. Horizontal bars represent standard derivation.
Note: Increase was significant for 3a, 3b, 3c, 4a, 4b, 4c, 4d, 4e, 4f, 6, 7a, 7f, 7h, 7i, 7j, 10a, LPS and Cisplatin. $P < 0.0001$.

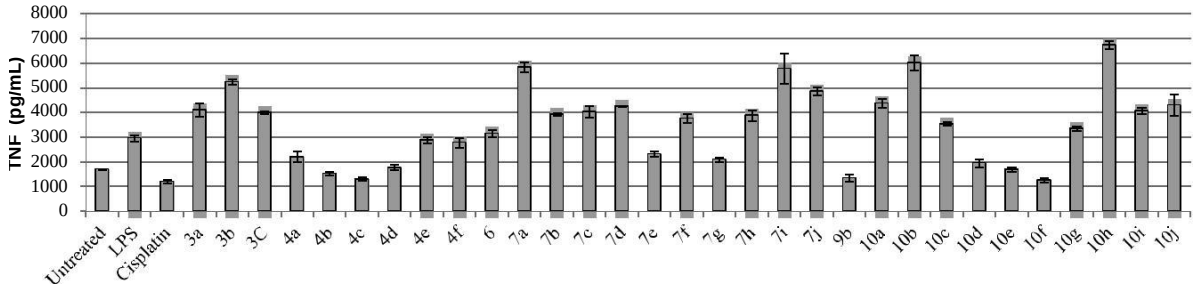

Fig. 5. TNF production in supernatants of macrophage culture after 72 h of incubation. Horizontal bars represent standard derivation.
Note: Increase was significant for 3a, 3b, 3c, 4a, 4e, 4f, 6,7a, 7b, 7c, 7d, 7e, 7f, 7g, 7h, 7i, 7j, 10a, 10b, 10c, 10 g, 10h, 10i, 10j and LPS. $P < 0.0001$.

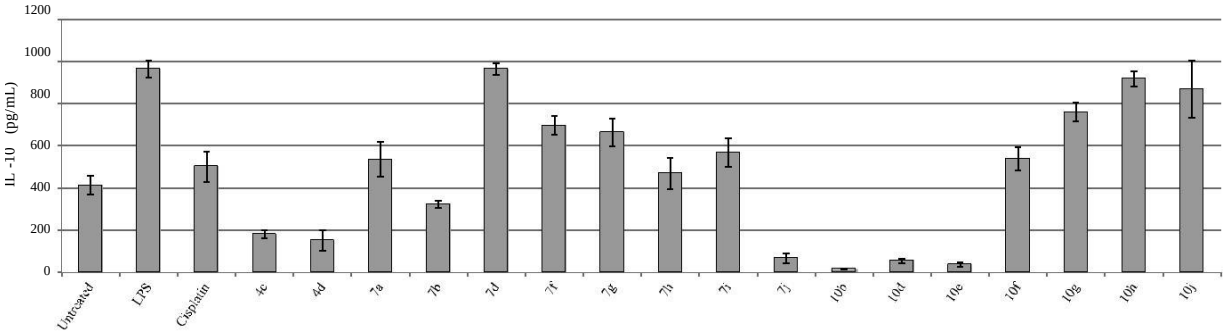

Fig. 6. IL-10 production in supernatants of macrophage culture after 24 h of incubation. Horizontal bars represent standard derivation.
Note: Increase was significant for 7d,7f, 7g, 10g, 10h, 10j, LPS and Cisplatin. $P < 0.0001$. Decrease was significant for 4c, 4d, 7j, 10b, 10d and 10e. $P < 0.0001$.

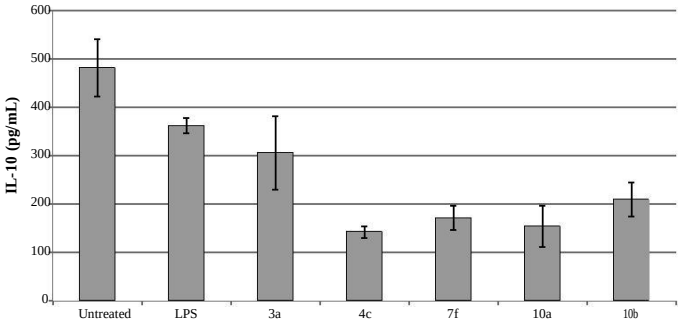

Fig. 7. IL-10 production in supernatants of macrophage culture after 48 h of incubation. Horizontal bars represent standard derivation. Note: Decrease was significant for 3a, 4c, 7f, 10a, 10b. $P < 0.0001$.

order to identify the mechanism of action of this series compounds.

The presence of cytokines are an important component in tumor microenvironment and often more important than the cellular content. The type and amount of cytokines produced in this microenvironment may be critical in tumor development and progression [3].

Cytokine production after incubation with compounds was evaluated with J774A.1 macrophages. IL-10 and TNF production were assessed after 24, 48 and 72 h of incubation.

Among untreated group, production of IL-10 was observed after 24 and 48 h. Its known that under stationary state tissue macrophages presents intrinsic anti-inflammatory functions [26].

IL-10 exerts it function through inhibitory activity on macro-phages and dendritic cells. IL-10 inhibits IL-12 production by activated macrophages in addition to down regulate MHC-II expression by this cells [27]. IL-10 reduction might be considered a desirable phenomenon, mainly if it happens in tumor microenvironment, since that several pro tumor effects have been associated with this cytokine [28,29].

Historically, TNF was the first cytokine used in cancer treatment [30]. Apart of cancer context, TNF was identified as a main regulator of inflammation and a key in cytokine network [31]. In cancer context, this cytokine can present a dichotomous action and can actuate as a pro or antitumor agent, in diverse contexts. For instance, this pro-inflammatory cytokine is an important factor involved in initiation, proliferation, angiogenesis and metastasis of diverse cancer types [32]. Several malign cells constitutively produce small quantities of TNF [31]. Those observations, and TNF roles in cancer development and progression might shade anticancer potential of this cytokine [30]. Defining TNF role in cancer therapy remains a challenging process due to its pleiotropic nature that might stimulate multiple complex and interconnected pathways, often involved in opposite phenomena [30].

Results obtained reveal that some compounds have good activity as immunomodulators on J774A.1 macrophage. Under-standing mechanisms by which a favorable immune context can be

developed and maintained is essential for guiding innovative therapies [33]. New approaches on cancer treatment should consider, and take advantage of mechanisms that interfere in macrophages in several levels, as in attraction, differentiation and activation of this cells [19].

Thus, several series of compounds tested in this work deserve to be further investigated, since it was observed for several of them, low cytotoxic effect on macrophages, cytotoxic action against tumor cells, as well as necrosis/apoptosis induction and stimula-tion of important cytokines production. Results show that these compounds could represent promising prototype for development of new pharmacological agents. As perspectives, further elucida-tion of its mode of action and its effects in vivo models is needed.

5. Conclusions

Anticancer drug development is substantially necessary. By examining pharmacological activity of a set of thiosemicarbazone and 1,3-thiazole, we were able to identify new potent and selective anticancer compounds, such as 4a, 7c, 10e and 3b as most potent anticancer and immunomodulatory agent of each series. These compounds show low cytotoxicity against macrophages and modulated cytokines production. Therefore, these 1,3-thiazole and thiosemicarbazone compounds not only exhibited cytotoxicity in cancer cells, but were able to cause irreversible cancer cell damage by inducing necrosis and apoptosis. It would be worthwhile to conduct further optimization studies with a view to improving the antitumor properties of this 1,3-thiazole and thiosemicarbazone prototypes.

Acknowledgements

We would like to thank the Brazilian National Research Council (CNPq), Research Foundation of Pernambuco State (FACEPE) and FIOCRUZ for the financial support.

Appendix A. Supplementary data

Supplementary data associated with this article can be found, in the online version, at http://dx.doi.org/10.1016/j. biopha.2016.05.038.

References

[1] A.C.L. Leite, F.F. Barbosa, M.V. de, O. Cardoso, D.R.M. Moreira, L.C.D. Coêlho, E.B. da Silva, et al., Phthaloyl amino acids as anti-inflammatory and immunomodulatory prototypes, Med. Chem. Res. 23 (2014) 1701–1708, doi: http://dx.doi.org/10.1007/s00044-013-0730-1.

[2] M.A. Swartz, N. Iida, E.W. Roberts, S. Sangaletti, M.H. Wong, F.E. Yull, et al., Tumor microenvironment complexity: emerging roles in cancer therapy, Cancer Res. 72 (2012) 2473–2480, doi:http://dx.doi.org/10.1158/0008-5472 CAN-12-0122.

[3] S.I. Grivennikov, F.R. Greten, M. Karin, Immunity, inflammation, and cancer, Cell 140 (2010) 883–899, doi:http://dx.doi.org/10.1016/j.cell.2010.01.025.

[4] W.J. Lesterhuis, J.B.A.G. Haanen, C.J.A. Punt, Cancer immunotherapy – revisited, Nat. Rev. Drug Discov. 10 (2011) 591–600, doi:http://dx.doi.org/10.1038/ nrd3500.

[5] L.C.D. Coêlho, M.V. de, O. Cardoso, D.R.M. Moreira, P.A.T. de, M. Gomes, S.M.T. Cavalcanti, A.R. Oliveira, et al., Novel phthalimide derivatives with TNF-a and IL-1b expression inhibitory and apoptotic inducing properties, Medchemcomm 5 (2014) 758, doi:http://dx.doi.org/10.1039/c4md00070f.

[6] C. Pessoa, P.M.P. Ferreira, L.V.C. Lotufo, M.O. de Moraes, S.M.T. Cavalcanti, L.C.D. Coêlho, et al., Discovery of phthalimides as immunomodulatory and antitumor drug prototypes, ChemMedChem 5 (2010) 523–528, doi:http://dx.doi.org/ 10.1002/cmdc.200900525.

[7] M.V. de O. Cardoso, L.R.P. de Siqueira, E.B. da Silva, L.B. Costa, M.Z. Hernandes, M.M. Rabello, et al., 2-Pyridyl thiazoles as novel anti-Trypanosoma cruzi agents: structural design, synthesis and pharmacological evaluation, Eur. J. Med. Chem. 86 (2014) 48–59, doi:http://dx.doi.org/10.1016/j. ejmech.2014.08.012.

[8] P.A.T. de M. Gomes, A.R. Oliveira, M.V. de O. Cardoso, E. de F. Santiago, M. deOBarbosa, L.R.P. deSiqueira, et al., Phthalimido-thiazoles as building blocks and their effects on the growth and morphology of Trypanosoma cruzi, Eur. J. Med. Chem. 111 (2016) 46–57, doi:http://dx.doi.org/10.1016/j. ejmech.2016.01.010.

[9] M.E.S.B. Barros, J.C.R. Freitas, J.M. Oliveira, C.H.B. Da Cruz, P.B.N. Da Silva, L.C.C. De Araújo, et al., Synthesis and evaluation of ( )-Massoialactone and analogues as potential anticancer and anti-inflammatory agents, Eur. J. Med. Chem. 76 (2014) 291–300, doi:http://dx.doi.org/10.1016/j.ejmech.2014.02.013.

[10] E. Augustin, A. Mos-Rompa, D. Nowak-Ziatyk, J. Konopa, Antitumor 1-nitroacridine derivative C-1748, induces apoptosis, necrosis or senescence in human colon carcinoma HCT8 and HT29 cells, Biochem. Pharmacol. 79 (2010) 1231–1241, doi:http://dx.doi.org/10.1016/j.bcp.2009.12.012.

[11] A. Kamb, S. Wee, C. Lengauer, Why is cancer drug discovery so difficult? Rev. Nat. Rev. Drug Discov. 6 (2007) 115–120, doi:http://dx.doi.org/10.1038/ nrd2155.

[12] C.J. Lord, A. Ashworth, Biology-driven cancer drug development: back to the future, BMC Biol. 8 (2010) 38, doi:http://dx.doi.org/10.1186/1741-7007-8-38.

[13] S.J. Sturla, J.J. Irwin, R.N. Loeppky, M.J. Mulvihill, M. Searcey, Chemistry in cancer research: a vital partnership, Cancer Res. 67 (2007) 6539–6543, doi: http://dx.doi.org/10.1158/0008-5472 CAN-07-1619.

[14] S.J. Kashyap, V.K. Garg, P.K. Sharma, N. Kumar, R. Dudhe, J.K. Gupta, Thiazoles: having diverse biological activities, Med. Chem. Res. 21 (2011) 2123–2132, doi: http://dx.doi.org/10.1007/s00044-011-9685-2.

[15] S. Zheng, Q. Zhong, Q. Jiang, M. Mottamal, Q. Zhang, N. Zhu, et al., Discovery of a series of thiazole derivatives as novel inhibitors of metastatic cancer cell migration and invasion, ACS Med. Chem. Lett. 4 (2013) 191–196, doi:http://dx. doi.org/10.1021/ml300322n.

[16] N. Pabla, Z. Dong, Cisplatin nephrotoxicity: mechanisms and renoprotective strategies, Kidney Int. 73 (2008) 994–1007, doi:http://dx.doi.org/10.1038/sj. ki.5002786.

[17] M. Dougan, G. Dranoff, Immune therapy for cancer, Annu. Rev. Immunol. 27 (2009) 83–117, doi:http://dx.doi.org/10.1146/annurev. immunol.021908.132544.

[18] G. Solinas, G. Germano, a Mantovani, P. Allavena, Tumor-associated macrophages (TAM) as major players of the cancer-related inflammation, J. Leukoc. Biol. 86 (2009) 1065–1073, doi:http://dx.doi.org/10.1189/jlb.0609385.

[19] M. Heusinkveld, S.H. van der Burg, Identification and manipulation of tumor associated macrophages in human cancers, J. Transl. Med. 9 (2011) 216, doi: http://dx.doi.org/10.1186/1479-5876-9-216.

[20] A. Mantovani, S. Sozzani, M. Locati, P. Allavena, A. Sica, Macrophage polarization: tumor-associated macrophages as a paradigm for polarized M2 mononuclear phagocytes, Trends Immunol. 23 (2002) 549–555, doi:http://dx. doi.org/10.1016/S1471-4906(02)02302-5.

[21] F.O. Martinez, L. Helming, S. Gordon, Alternative activation of macrophages: an immunologic functional perspective, Annu. Rev. Immunol. (2009), doi:http:// dx.doi.org/10.1146/annurev.immunol.021908.132532.

[22] O. Kepp, A. Tesniere, F. Schlemmer, M. Michaud, L. Senovilla, L. Zitvogel, et al., Immunogenic cell death modalities and their impact on cancer treatment, Apoptosis 14 (2009) 364–375, doi:http://dx.doi.org/10.1007/s10495-008-0303-9.

[23] E.C. de Bruin, J.P. Medema, Apoptosis and non-apoptotic deaths in cancer development and treatment response, Cancer Treat. Rev. 34 (2008) 737–749, doi:http://dx.doi.org/10.1016/j.ctrv.2008.07.001.

[24] R.K. Amaravadi, C.B. Thompson, The roles of therapy-induced autophagy and necrosis in cancer treatment, Clin. Cancer Res. 13 (2007) 7271–7279, doi: http://dx.doi.org/10.1158/1078-0432 CCR-07-1595.

[25] S. Kasibhatla, B. Tseng, Why target apoptosis in cancer treatment? Mol. Cancer Ther. 2 (2003) 573–580. http://www.ncbi.nlm.nih.gov/pubmed/12813137.

[26] P.J. Murray, T.A. Wynn, Protective and pathogenic functions of macrophage subsets, Nat. Rev. Immunol. 11 (2011) 723–737, doi:http://dx.doi.org/10.1038/ nri3073.

[27] S. Lee, K. Margolin, Cytokines in cancer immunotherapy, Cancers (Basel) 3 (2011) 3856–3893, doi:http://dx.doi.org/10.3390/cancers3043856.

[28] E. Itakura, R.-R. Huang, D.-R. Wen, E. Paul, P.H. Wünsch, A.J. Cochran, IL-10 expression by primary tumor cells correlates with melanoma progression from radial to vertical growth phase and development of metastatic competence, Mod. Pathol. 24 (2011) 801–809, doi:http://dx.doi.org/10.1038/ modpathol.2011.5.

[29] L. Zeng, C. O'Connor, J. Zhang, A.M. Kaplan, D.A. Cohen, IL-10 promotes resistance to apoptosis and metastatic potential in lung tumor cell lines, Cytokine. 49 (2010) 294–302, doi:http://dx.doi.org/10.1016/j.cyto.2009.11.015.

[30] L. Bertazza, S. Mocellin, The dual role of tumor necrosis factor (TNF) in cancer biology, Curr. Med. Chem. 17 (2010) 3337–3352. http://www.ncbi.nlm.nih.gov/ pubmed/20712570.

[31] F. Balkwill, Tumour necrosis factor and cancer, Nat. Rev. Cancer 9 (2009) 361– 371, doi:http://dx.doi.org/10.1038/nrc2628.

[32] W. Lin, M. Karin, A cytokine-mediated link between innate immunity, inflammation, and cancer, J.Clin. Invest. 117 (2007) 1175–1183, doi:http://dx. doi.org/10.1172/JCI31537.data.

[33] W.H. Fridman, F. Pagès, C. Sautès-Fridman, J. Galon, The immune contexture in human tumours: impact on clinical outcome, Nat. Rev. Cancer. 12 (2012) 298– 306, doi:http://dx.doi.org/10.1038/nrc3245.

APÊNDICE D -

Compound profiling and 3D-QSAR studies of hydrazone derivatives with activity against intracellular *Trypanosoma cruzi*

Bioorganic & Medicinal Chemistry 24 (2016) 1608–1618

Contents lists available at ScienceDirect

Bioorganic & Medicinal Chemistry

journal homepage: www.elsevier.com/locate/bmc

Compound profiling and 3D-QSAR studies of hydrazone derivatives with activity against intracellular Trypanosoma cruzi

Lívia Bandeira Costa [a,y], Marcos Veríssimo de Oliveira Cardoso [a,y], Gevanio Bezerra de Oliveira Filho [a], Paulo André Teixeira de Moraes Gomes [a], José Wanderlan Pontes Espíndola [a], Thays Gabrielle de Jesus Silva [a], Pedro Henrique Monteiro Torres [b], Floriano Paes Silva Junior [b], Julio Martin [c], Regina Célia Bressan Queiroz de Figueiredo [d], Ana Cristina Lima Leite [a,⇑]

[a] Departamento de Ciências Farmacêuticas, Centro de Ciências da Saúde, Universidade Federal de Pernambuco, 50740-520 Recife, PE, Brazil
[b] Laboratório de Bioquímica Experimental e Computacional de Fármacos, Instituto Oswaldo Cruz, FIOCRUZ, 21040-900 Rio de Janeiro, RJ, Brazil
[c] Molecular Discovery Research, Tres Cantos Medicines Development Campus, GlaxoSmithKline, Tres Cantos, Spain
[d] Departamento de Microbiologia, Centro de Pesquisas Aggeu Magalhães, 50670-420 Recife, PE, Brazil

article info

Article history:
Received 17 December 2015 Revised
15 February 2016 Accepted 21
February 2016 Available online 23
February 2016

Keywords:
Chagas disease
Hydrazones
Thiosemicarbazones
Thiazoles
3D-QSAR
Drug design

abstract

Chagas disease is a tropical disease caused by the parasite Trypanosoma cruzi, which is endemic in Central and South America. Few treatments are available with effectiveness limited to the early (acute) stage of disease, significant toxicity and widespread drug resistance. In this work we report the outcome of a HTS-ready assay chemical library screen to identify novel, nontoxic, small-molecule inhibitors of T. cruzi. We have selected 50 compounds that possess hydrazone as a common group. The compounds were screened using recombinant T. cruzi (Tulahuen strain) expressing beta-galactosidase. A 3D quantitative structure– activity relationship (QSAR) analysis was performed using descriptors calculated from comparative molecular field analysis (CoMFA). Our findings show that of the fifty selected hydrazones, compounds LpQM-19, 28 and 31 displayed the highest activity against T. cruzi, leading to a selectivity index (SI) of 20-fold. The 3D-QSAR analysis indicates that a particular electrostatic arrangement, where electron-defi-cient atoms are aligned along the molecule main axis positively correlates with compound biological activity. These results provide new candidate molecules for the development of treatments against Chagas disease.

1. Introduction

Chagas disease, or American trypanosomiasis, is a devastating neglected disease with no satisfactory treatment.[1] Currently, the World Health Organization estimates that 8–10 million people are infected with Trypanosoma cruzi, the etiological agent of this ill-ness.[2,3] Benznidazole and nifurtimox are the two drugs available for the treatment of Chagas disease. These archaic drugs are asso-ciated with severe side effects that cause discontinuation of treat-ment and limit their long-standing use. Furthermore, their efficacy in the chronic phase of the disease is still controversial, and drug-resistant strains have been observed.[4,5] Hence, the discovery of non-toxic and more effective drugs to combat T. cruzi is urgently needed.[3,5] However, the research for new drugs against many neglected diseases, such as Chagas disease, has faced several draw-backs in drug discovery programs, such as the complex biology of parasites and different life cycle stages.[4]

High-throughput screening (HTS) is an important tool that allows drug discovery through the identification of active com-pounds (hits) from a large number of candidates.[6,7] HTS assays have been restricted to pharmaceutical companies due to the high costs associated with the drug screening experiments. However, with the increasing interest in the development of new platforms for drug prospection, this method has become more accessible and thus has also been used in academic research.[8]

In recent years, there have been significant advances in auto-mated microscopy that enable the testing of compounds against intracellular parasites in high-throughput mode.[9–11] Since the advent of the ‘classical’ screening assay for T. cruzi based on absor-bance readout developed by Fred Buckner and collaborators and used by numerous laboratories on a small scale, advances have been made in terms of the HTS format.[12]

The Chagas disease drug discovery efforts have been facilitated by the development of recombinant T. cruzi parasites used as tools

⇑ Corresponding author. Tel.: +55 81 2126 8511; fax: +55 81 2126 8510. E-mail address: acllb2003@yahoo.com.br (A.C.L. Leite).
y Both authors contributed equally to the work.

http://dx.doi.org/10.1016/j.bmc.2016.02.027 0968-0896/ 2016 Published by Elsevier Ltd.

for drug screening.[13] A T. cruzi strain expressing the b-galactosi-dase reporter gene (b-gal) was the first to allow the use of auto-mated phenotypic assays in vitro for drug screening against T. cruzi.[14,15] The b-gal T. cruzi strain allows detection of parasite growth through the measurement of the b-gal activity, which is correlated with the number of viable parasites.[7]

Regarding the identification of new anti-T. cruzi agents, most of the efforts have been conducted through the investigation of pep-tides and peptide-like compounds containing functional groups such as urea,[5,16] hydrazones,[17–20] triazoles[21,22] and thiosemicar-bazones.[23–26]

Hydrazone moiety is a versatile structural linker highly explored by medicinal chemistry for the development of various classes of bioactive agents. In 2002, Du et al.[23] developed a study about 100 compounds with hydrazone moiety as potent trypanoci-dal compounds, witch motivate us to explore molecules possessing the hydrazone moiety.

Caputto et al. demonstrated the trypanocidal activity for a ser-ies of 4-arylthiazolylhydrazones[27] with broad and potent activity against all forms of the parasite. Our efforts toward new antichaga-sic drugs since 2010 have led us to synthesize a variety of thiosemicarbazones, thiazolyl hydrazones and 2-iminothiazo-lidin-4-ones as trypanocidal agents.[26,28–32] In view to explore the trypanocidal activity of previously hydrazones synthesized by our group, we screened a small chemical library of fifty compounds belonging to the hydrazone chemical class (thiosemicarbazone, thiazolinone and thiazole) through a cell-based assay for HTS-ready assay using a T. cruzi b-gal strain, according to Peña et al.[33] Herein, we report three major compounds that inhibited the devel-opment of intracellular T. cruzi amastigotes in a micromolar range and had low toxicity effects on mammalian cells. In addition, we investigated the structural and chemical features related to the biological activity of these compounds through a 3D QSAR analysis.

2. Results and discussion

2.1. Compound library

Taking into account the bioisosteric relationship between thiosemicarbazones, thiazoles and thiazolidin-4-ones, 50 com-pounds possessing a hydrazone moiety were synthesized. Among these compounds, only compounds (LpQM-01–05 and 22–45) were previously reported in literature,[31,32] therefore the chemical characterization of the new compounds (LpQM-06–21, LpQM-46–50) is reported in Supplementary material. This chemical library comprises four sub-series, which possess some specific structural features (Fig. 1).

Our research group has developed the synthesis of 3,4-dichlorophenyl-4-phenylthiosemicarbazones (LpQM-01–02),[32] 3,4-dichlorophenyl-thiazolidin-4-ones (LpQM-03–05),[32] 3,4-dichlorophenyl-thiazoles (LpQM-06–09), thiophenol-2-ylidene-thiosemicarbazones (LpQM-10–21), pyridyl-arylidene-thiazoles (LpQM-22–45)[31] and m-bromo-phenyl-methylidene-thiazoles (LpQM-46–50) (Fig. 1). All of the compounds were chemically characterized by infrared (IR), nuclear magnetic resonance (^{1}H, ^{13}C NMR), elemental analysis (EA) and mass spectral (MS) studies. Elemental analysis was performed to confirm the degree of purity (>95%). The chemical structures of 50 compounds, as well as the results of testing against T. cruzi are shown in Table 1.

2.2. Structure–activity relationships (SAR) analysis

In this study, we performed a screen of 50 compounds on NIH-3T3 fibroblasts infected with a recombinant Tulahuen strain of T. cruzi expressing the b-galactosidase reporter. This type of assay allows the identification of compounds that inhibit intracellular amastigotes. An important criterion in the search for active com-pounds against intracellular parasites with therapeutic potential is their low toxicity to mammalian host cells.[34]

HepG2 cells are a useful model as a primary toxicity screen due to their human origin, ease of manipulation and because they exhi-bit a variety of cellular responses to different drugs.[14,35] Our cyto-toxicity assay results showed that 43 compounds presented low toxicity (TC_{50} >100 lM) to HepG2 cells.

According to the criteria established for considering a com-pound active on T. cruzi (Section 2.3), our assay identified 26 com-pounds that inhibited the T. cruzi viability into NIH/3T3 cells (Table S1). In parallel, we evaluated the toxicity to mammalian host cells to determine if these compounds were cytotoxic to NIH-3T3 cells and thus false positives. This secondary screen iden-tified 14 compounds that reduced the viability of host NIH-3T3 cells, therefore, these compounds were excluded as viable hits. Twelve compounds, which exhibited selective trypanocidal activ-ity (at least 10-fold activity versus toxicity), were members of two chemical classes (thiosemicarbazone and thiazole) (Table 2).

Analyzing the cytotoxicity data on NIH-3T3 cells we observed that among the compounds tested, the derivatives of 2-pyridine (LpQM 22–45) generally exhibited greater cytotoxicity. Among them, only three compounds (LpQM-26, LpQM-28 and LpQM-32) showed TC_{50} >50.12 lM.

Normally, it is observed a reduction of cytotoxicity in mam-malian cells from the cyclization of the thiosemicarbazone to some of their cyclic derivatives, such as 4-thiazolidinones and thiazoles. Indeed, it was generally observed that characteristic when compar-ing the derivatives of 3,4-dichloro-acetophenone (LpQM 01–09), so that all cyclic derivatives (LpQM 03–09) exhibited low cytotoxicity. On the other hand, it is important to note that the thiophenol-2-ylidene-thiosemicarbazones (LpQM-10–21), which have a spacer group (–S-CH_2–) between the phenyl ring and the thiosemicar-bazone moiety, exhibited low cytotoxicity (which can be associ-ated with the presence of this spacer group), with the exception of compounds LpQM 10 (TC_{50} = 3.55 lM) and LpQM 13 (TC_{50} = 0:52 lM). The latter, was the most cytotoxic compound tested, suggesting that the presence of electron donor group meth-oxy (–OCH_3) in thiophenolic ring contributed to this effect, since its analogs, including unsubstituted (LpQM-10), were less cytotoxic.

Conversely, compounds containing alkyl groups in the various positions of this ring (LpQM-14–17) exhibited significantly lower cytotoxicity. Moreover, the presence of halogens in thiophenolic ring seems to have contributed significantly to increase the selec-tivity of compounds LpQM-11–12, and LpQM-18–21, since it showed low cytotoxic against this NIH-3T3 cells.

Comparing the anti-T. cruzi activity of thiosemicarbazone LpQM-01 (IC_{50} = 0.63 lM) with thiazolidin-4-ones LpQM-03–05 and thiazoles LpQM-06–09, it was found that the cyclization strat-egy was deleterious to the activity against the parasite.

The thiophenol-2-ylidene-thiosemicarbazones (LpQM-10–21), which have a spacer group (–S-CH_2–), exhibited a lower trypanoci-dal profile than the thiosemicarbazone LpQM-01, but showed more promising selectivity indices against the parasite in general, especially compound 1-(2-m-chlorophenylthioethylidene) thiosemicarbazone (LpQM-19), which exhibited an IC_{50} = 1.78 lM for the T. cruzi and TC_{50} >100 lM for HepG2 cells.

Comparing the anti-T. cruzi potency of all classes of compounds evaluated in the HTS-ready assay, the arylidene-pyridyl-thiazoles (LpQM-22–45) were the most promising sub-series. Except for compounds LpQM-31 and LpQM-32, all of the arylidene-pyridyl-thiazoles exhibited IC_{50} 63 lM. Furthermore, compounds LpQM-30, LpQM-43 and LpQM-45 had the most potent trypanocidal activity, with IC_{50} values below 1 lM. Although these compounds

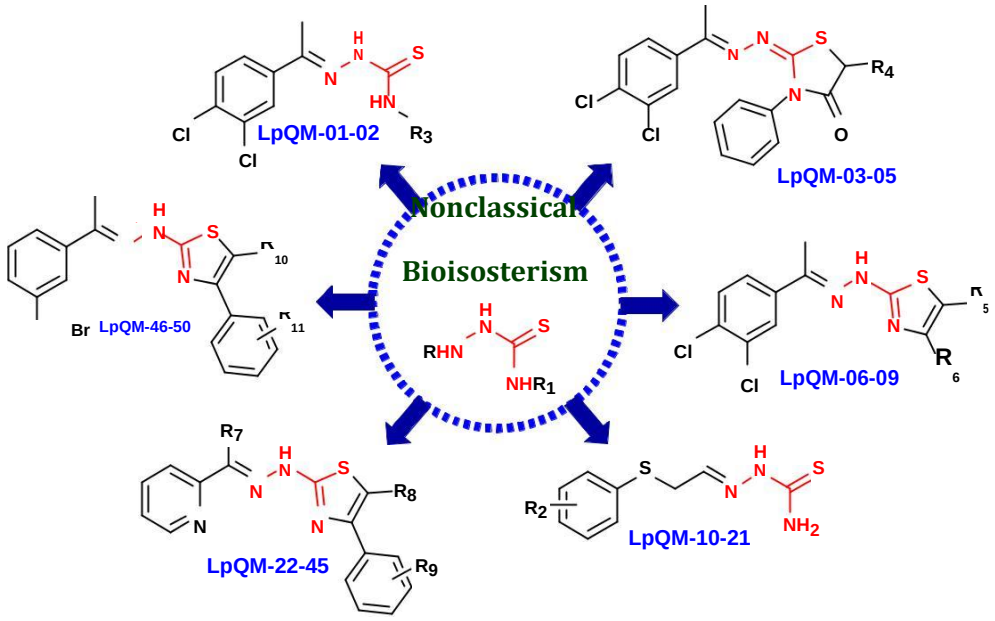

Figure 1. Structural planning of compounds tested.

Table 1
Trypanocidal activity and cytotoxicity of compounds LpQM-01–50

Compound	Structure	T. cruzi IC_{50}[a] (lM)	3T3 TC_{50}[b] (lM)	HepG2 TC_{50}[c] (lM)
LpQM-01	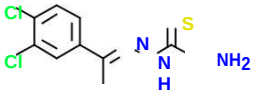	0.63	17.78	43.65
LpQM-02	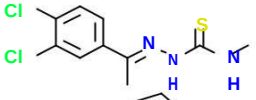	16.98	>50.12	>100
LpQM-03	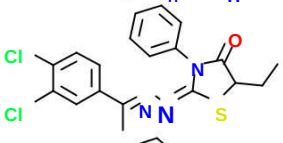	>50.12	>50.12	>100
LpQM-04	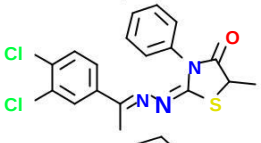	>50.12	>50.12	>100
LpQM-05	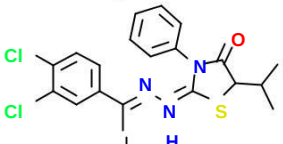	>50.12	>50.12	>100
LpQM-06	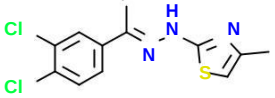	8.32	38.9	>100
LpQM-07	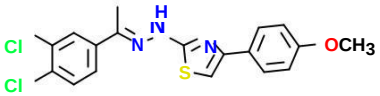	16.98	>50.12	>100
LpQM-08	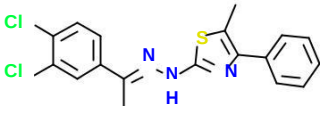	4.9	28.18	>100

Table 1 (continued)

Compound	Structure	T. cruzi IC_{50}[a] (lM)	3T3 TC_{50}[b] (lM)	HepG2 TC_{50}[c] (lM)
LpQM-09	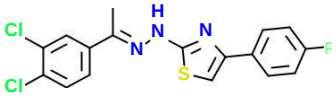	16.22	28.18	>100
LpQM-10	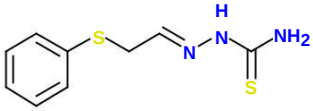	9.33	3.55	>100
LpQM-11	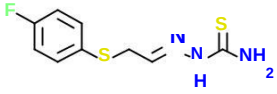	5.89	>50.12	>100
LpQM-12	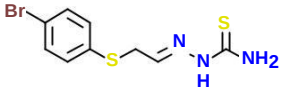	1.62	28.84	53.7
LpQM-13	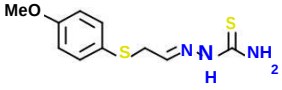	17.38	0.52	>100
LpQM-14	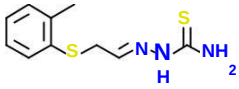	4.9	>50.12	>100
LpQM-15	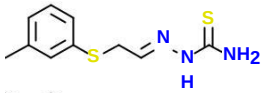	3.24	>50.12	>100
LpQM-16	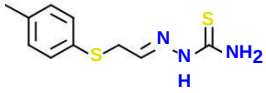	6.46	>50.12	>100
LpQM-17	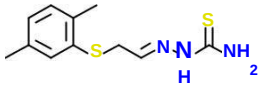	3.24	20.89	>100
LpQM-18	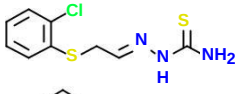	3.09	>50.12	>100
LpQM-19	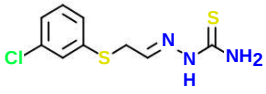	1.78	>50.12	>100
LpQM-20	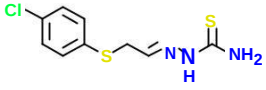	2.09	39.81	75.86
LpQM-21	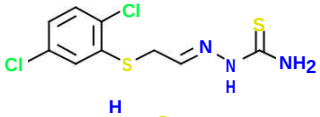	2.57	>50.12	>100
LpQM-22	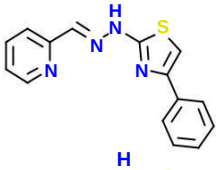	2.19	16.98	>100
LpQM-23	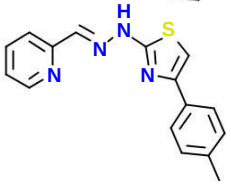	2.63	43.65	>100
LpQM-24	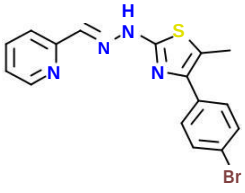	1.38	18.62	>100

(continued on next page)

Table 1 (continued)

Compound	Structure	T. cruzi IC_{50}[a] (lM)	3T3 TC_{50}[b] (lM)	HepG2 TC_{50}[c] (lM)
LpQM-25	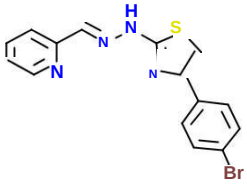	2.24	14.13	>100
LpQM-26	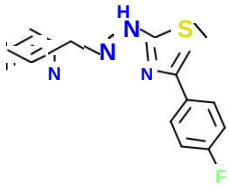	2.29	>50.12	18.2
LpQM-27	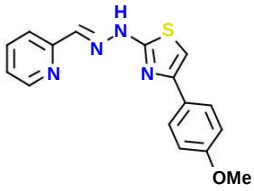	2.69	11.48	>100
LpQM-28	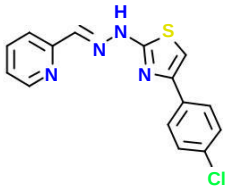	1.86	>50.12	>100
LpQM-29	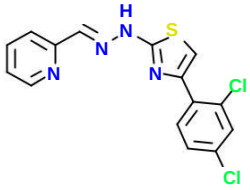	1.05	14.45	>100
LpQM-30	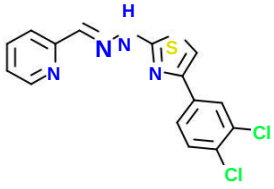	0.79	10.72	>100
LpQM-31	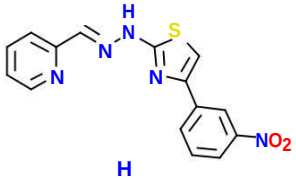	1.62	38.02	>100
LpQM-32	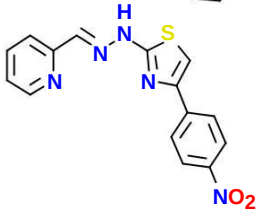	10.96	>50.12	>100
LpQM-33	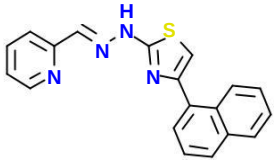	3.39	7.24	>100

Table 1 (continued)

Compound	Structure	T. cruzi IC_{50}[a] (lM)	3T3 TC_{50}[b] (lM)	HepG2 TC_{50}[c] (lM)
LpQM-34	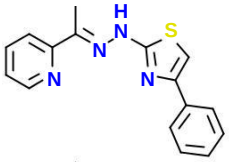	1.12	3.89	91.2
LpQM-35	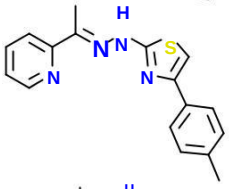	1.7	4.47	>100
LpQM-36	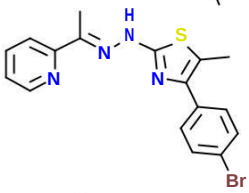	1.35	2	>100
LpQM-37	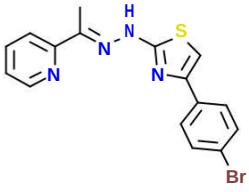	1	3.98	85.11
LpQM-38	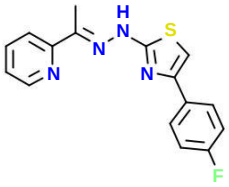	1.32	4.9	91.2
LpQM-39	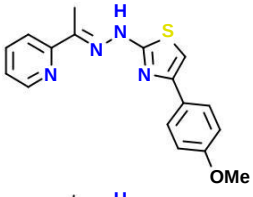	2.24	3.47	>100
LpQM-40	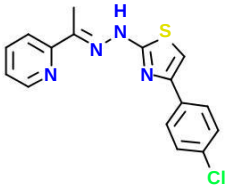	1.05	5.25	>100
LpQM-41	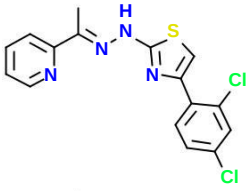	1.55	2	>100
LpQM-42	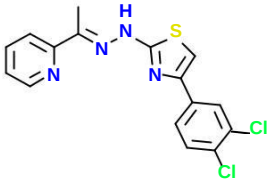	1.26	2.34	>100

(continued on next page)

Table 1 (continued)

Compound	Structure	T. cruzi IC_{50}[a] (lM)	3T3 TC_{50}[b] (lM)	HepG2 TC_{50}[c] (lM)
LpQM-43	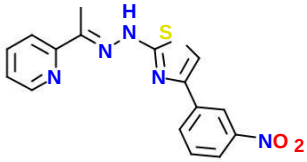	0.89	3.63	>100
LpQM-44	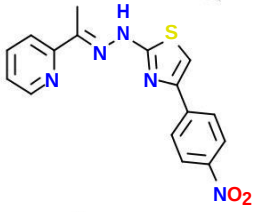	1.26	20.89	>100
LpQM-45	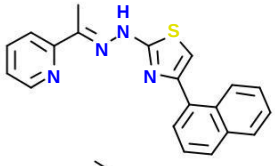	0.93	4.47	>100
LpQM-46	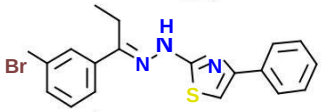	18.2	26.3	>100
LpQM-47	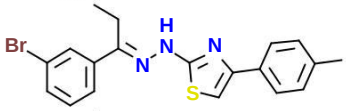	26.3	>50.12	>100
LpQM-48	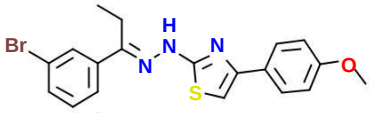	30.2	>50.12	>100
LpQM-49	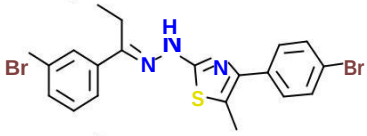	24.55	33.11	>100
LpQM-50	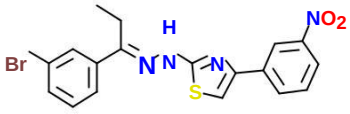	22.91	38.02	>100

[a] IC_{50} determined for a recombinant T. cruzi amastigote strain expressing b-galactosidase after 96 h of incubation with the compounds.
[b] IC_{50} determined for NIH-3T3 after 96 h of incubation in the presence of the compounds.
[c] IC_{50} determined for human Hepg2 after 48 h of incubation in the presence of the compounds.

Table 2
Trypanocidal activity and cytotoxicity of confirmed T. cruzi-positive compounds

Compound	T. cruzi IC_{50}[a] (lM)	3T3 TC_{50}[b] (lM)	HepG2 TC_{50}[c] (lM)
LpQM-14	4.9	>50.12	>100
LpQM-15	3.24	>50.12	>100
LpQM-18	3.09	>50.12	>100
LpQM-19	1.78	>50.12	>100
LpQM-21	2.57	>50.12	>100
LpQM-23	2.63	43.65	>100
LpQM-24	1.38	18.82	>100
LpQM-28	1.86	>50.12	>100
LpQM-29	1.05	14.45	>100
LpQM-30	0.79	10.72	>100
LpQM-31	1.62	38.02	>100
LpQM-44	1.26	20.89	>100

[a] IC_{50} determined for a recombinant T. cruzi amastigote strain expressing b-galactosidase after 96 h of incubation with the compounds.
[b] IC_{50} determined for NIH-3T3 after 96 h of incubation in the presence of the compounds.
[c] IC_{50} determined for human Hepg2 after 48 h of incubation in the presence of the compounds.

exhibited better antiparasitic profiles, they exhibited high toxicity to NIH-3T3, with TC_{50} of 10.72, 3.63 and 4.4 lM, respectively.

In contrast, none of the derivatives of m-bromo-phenyl-methylidene-thiazoles (LpQM-46–50) exhibited significant anti-T. cruzi activity. The main structural difference between the LpQM-22–45 sub-series and LpQM-06–09 and LpQM-46–50 is the pres-ence of the 2-pyridyl group linked at N1. These results indicate that the 2-pyridyl moiety constitutes an important core for antipara-sitic activity.

Taking into account the selectivity of these 2-pyridyl-arylidene-1,3-thiazoles derivatives (LpQM-22–45), compounds 2-(2-(pyri-din-2-ylmethylene)hydrazinyl)-4-(4-chlorophenyl)-1,3-thiazole (LpQM-28) and 2-(2-(pyridin-2-ylmethylene)hydrazinyl)-4-(3-nitrophenyl)-1,3-thiazole (LpQM-31) were the most promising molecules of all series tested. These compounds displayed the highest activity against T. cruzi, with IC_{50} values of 1.86 and 1.62 lM respectively, with a selectivity index (SI) greater than 50. The representative curves of the three best compounds in the

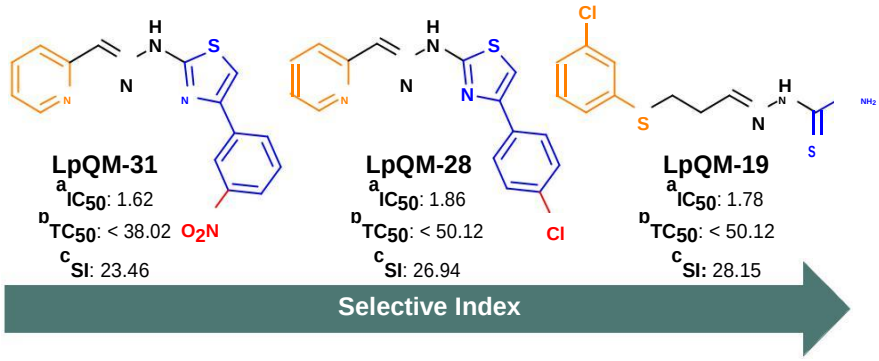

Figure 2. Inhibition of T. cruzi by 3 compounds selected from the HTS-ready assay. [a] IC_{50} (lM) for amastigotes; [b] TC_{50} (lM) for NIH-3T3 mouse fibroblasts; [c] selective index = TC_{50}/IC_{50}.

anti-T. cruzi activity. (LpQM-19, LpQM-28 and LpQM-31) is pre-sented in SI (Fig. S1). The associated anti-T. cruzi activity and toxi-city of these compounds are shown in Figure 2.

2.3. QSAR results

All 50 molecules were initially analyzed with respect to their structural features and were plotted on a structure similarity map (Fig. 3). The structures could be classified into four distinct groups, here identified as A, B, C and D.

The C group was composed of only two molecules (LPQM-01 and LPQM-02) whose structures differed significantly from the others. Besides, these molecules had very different pIC_{50} values despite their structural similarity. The members of the D group, LpQM-03, LpQM-04 and LpQM-05, all displayed very low activity. Therefore, as mentioned in the methods section, both groups were removed from further QSAR analysis. In addition, the aforemen-tioned compound LpQM-32 was also disregarded due to SAR inconsistency, that is, in spite of sharing high structural similarity with the remaining thiazoles, its pIC_{50} was considerably lower. The six compounds that were removed from further analysis are iden-tified with a red ‘ ’ in the structure similarity map. Similarly, the compounds which were assigned to the test group of the QSAR analysis are marked with a black cross.

Regarding the C Log P (Table S2), the calculated values ranged from 1.36 to 8.48, and approximately 66% of the compounds had a C Log P higher than 5.0, including the most active compound (LpQM-30). This indicates that it is possible that many of those

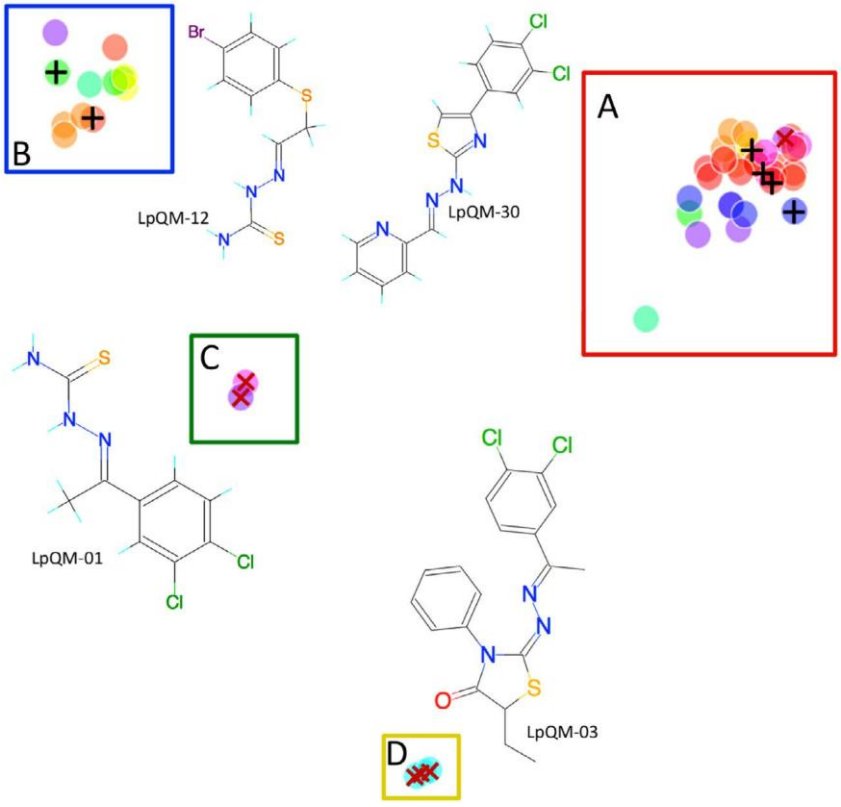

Figure 3. Structure similarity map of the 50 molecules in the initial dataset. The color code indicates the molecule’s pIC_{50}, the red circles show high pIC_{50} and blue circles show low pIC_{50} values. The structures were separated into four distinct groups, referred as A, B C and D. For each group, the molecule with the highest pIC_{50} value was displayed. The compounds which composed the test group are marked with a black cross and the ones that were excluded from the QSAR analysis are marked with a red ‘ ’.

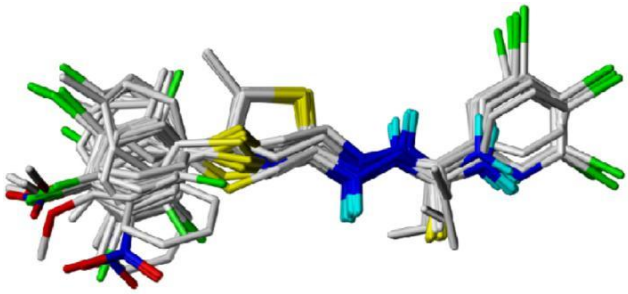

Figure 4. GALAHAD alignment of the 44 molecules selected for the QSAR analysis. The GALAHAD population size and generations were both set to 100.

compounds may require chemical modifications to improve their pharmacokinetic properties. Nevertheless, many promising com-pounds, such as LpQM-19, 31 and 44, had a calculated C Log P lower than 5. 3D-QSAR CoMFA analysis requires prior molecular align-ment. Figure 4 shows the superimposed structures of the 44 mole-cules used in the QSAR analysis after alignment using GALAHAD.[36]

The pharmacophoric model built by the GALAHAD algorithm is also depicted in Figure 5, along with the structure of compound LpQM-30 (the most active compound analyzed). The model is com-posed by eight features: three acceptor atoms (AA), three hydrophobic sites (HY), one positive hydrogen (NP) and one donor atom (DA). The pyridine nitrogen is the center for AA and DA fea-tures while the hydrazine moiety is involved with AA and NP features.

The experimental and predicted pIC_{50} values for both the train-ing (black) and test (red) sets are plotted along with their regres-sion lines in Figure 6 and are listed in Table S2. This CoMFA

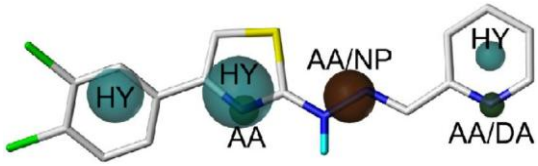

Figure 5. Pharmacophoric model produced by GALAHAD. This model presented an ENERGY value of 12.99, a STERICS value of 139, a MOL_QRY value of 32.62 and a HBOND value of 97. Blue spheres represent hydrophobic centers (HY), green spheres represent acceptor atoms (AA), red spheres represent positive nitrogens (NP) and magenta spheres represent donor atoms (DA). There are two pharma-cophore superpositions AA/NP and AA/DA.

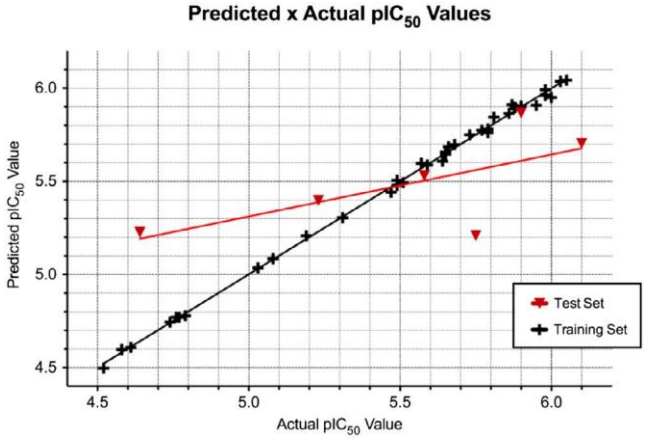

Figure 6. Scatter plots and regression lines of the predicted and actual pIC_{50} values. Red triangles represent the molecules in the test set and black crosses represent the molecules in the training set. The r^2 value was 0.998 for the training set. * Anti-T. cruzi activity.

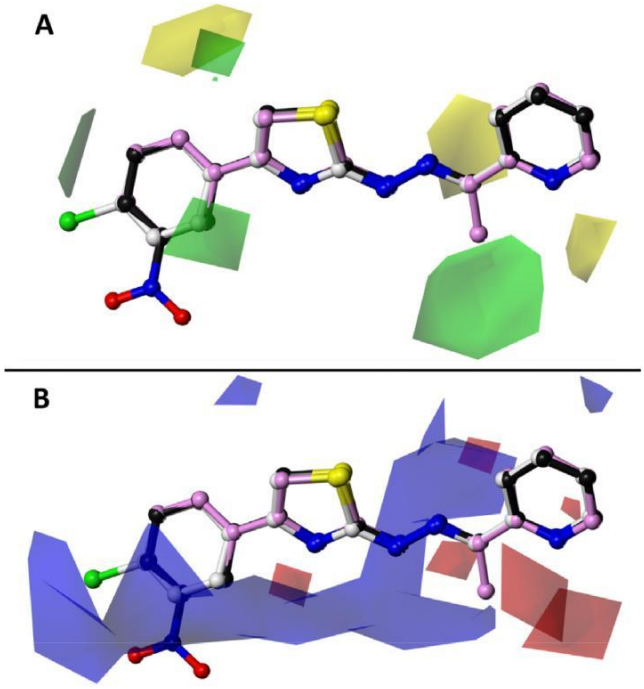

Figure 7. Superimposed ball and stick representation of compounds LpQM-28 (white), LpQM-31 (black) and LpQM-43 (pink) along with CoMFA steric (A) and electrostatic (B) fields. Green areas (80% contribution) indicate regions where bulky groups positively correlates to anti-T. cruzi activity. Yellow areas (20% contribution) indicate regions where bulky groups negatively correlates to anti-T. cruzi activity. Similarly, the electrostatic contributions are also indicated. Blue areas (80% contribution) indicate regions where positive charges positively correlates to anti-T. cruzi activity and red areas (20% contribution) indicate regions where negative charges positively correlates to anti-T. cruzi activity.

model had an r^2 value of 0.998 and a Q^2 of 0.803, indicating good internal predictive power. The pIC_{50} predictions for the structures in the test set were also acceptable, and the differences between the predicted values and the actual values did not exceed one log unit. The latter indicates that we have produced a model that is capable of estimating the biological activity of similar molecules, that is, thiazoles or thioeters, bearing the hydrazine moiety and a cyclic hydrophobic moiety.

Figure 7 shows the CoMFA fields of the QSAR model along with the structure of LpQM-28, LpQM-31 and LpQM-43. LpQM-43 was the most active compound in the training set. The green areas cor-respond to the sites where steric bulk is positively correlated to anti-T. cruzi activity, and the yellow areas correspond to the sites where steric bulk is negatively correlated. Similarly, blue areas cor-respond to sites where positive charges are correlated with the bio-logical activity, and red areas correspond to sites where negative charges are correlated.

Interesting features of the CoMFA model in Figure 7 are the large yellow and green areas around the hydrazone group, indicat-ing both unfavorable and favorable locations for the insertion of bulky substituents, respectively. Distinctly from LpQM-31, LpQM-43 can achieve higher anti-T. cruzi activity by placing a methyl group near this green region, possibly explaining the slight potency difference between the two compounds. Additionally, on the opposite end of the model there are two green areas, suggest-ing that placement of bulky groups in this location is correlated with higher activity. Compounds such as LpQM-19, 28 and 31 sat-isfy this condition by bearing a thiazole and a phenyl ring near those areas. Regarding the electrostatic contribution, the model shows a remarkably large blue area extending from the hydrazone group to the aryl substituent in thiazole containing molecules, indicating that compounds lining electron deficient atoms in these

regions exhibit higher activity. For instance, compounds carrying electron-withdrawing groups in the phenyl ring attached to the thiazole nucleus, such as LpQM-43 (3-NO_2) or LpQM-28 (4-Cl), favourably positions a number of electron deficient atoms. On the opposite end of the model, two red areas indicate regions where higher electron densities are correlated with improved anti-T. cruzi activity. That is the case of thiazoles containing a pyr-idine group, such as LpQM-19, 28 and 31, which favourably locates the electronegative pyridine nitrogen in this region.

3. Conclusions

The HTS-ready assay and QSAR studies were performed on a library of fifty compounds sharing a hydrazone group as a common core. The HTS-ready assay identified compounds LpQM-19, 28 and 31 as high anti-T. cruzi agents and as non-toxic to mammalian cells, leading to a selectivity index of up to 20. Additionally, the QSAR analysis produced a model that was capable of estimating the bio-logical activity for similar molecules. These results provide new candidates for the development of treatments against Chagas disease.

4. Experimental section

4.1. Biological

4.1.1. Parasites and cell lines cultures

LLC-MK2 cells (green monkey kidney epithelial cells) were pur-chased from the European Cell Cultures Collection (ECACC refer-ence 85062804). NIH-3T3 cells (mouse embryonic fibroblast cell line) were provided by the GSK-Biological Reagents and Assay Development Department (BRAD, Stevenage, UK). T. cruzi parasites of Tulahuen strain, expressing b-galactosidase as an intracellular reporter, were kindly provided by Dr. Buckner[37] (University of Washington, Seattle, USA). The parasites were maintained in cul-ture by weekly infection of LLC-MK2 cells. Trypomastigote forms were obtained from the supernatants of LLC-MK2 infected cultures harvested 5 and 9 days post-infection. HepG2 cells (human hep-atoma) were provided by the GSK-Biological Reagents and Assay Development Department (BRAD, Stevenage, UK). All cell lines were cultivated according to Peña et al.[33]

4.1.2. Anti-*Trypanosoma cruzi* activity

The HTS-ready assay and data analysis were performed accord-ing to GSK standard operating procedures.[33] To measure the repro-ducibility and quality of the HTS-ready assay, we used the Z^0 factor.[7,8] Assays with Z factors P0.5 are considered appropriate for HTS-ready assay. Our assay Z factor was 0.75, indicating that it is highly robust. The assay was performed in 1536-well sur-face-treated tissue culture plates at different concentrations rang-ing from 50 to 0.00085 lM in each compound/well, diluted in DMSO. The percentage of DMSO in the experiments never exceeded 0.5%, which is non-toxic for both cells and parasites. To evaluate the growth inhibition of intracellular amastigotes of T. cruzi, a recombinant T. cruzi strain expressing b-galactosidase was used to infect NIH-3T3 cells. A mixed culture of NIH-3T3 and parasites at a final concentration of 1 10^3 cells/well (1:1 par-asites/NIH-3T3 cells) was seeded in a 1536-well culture plate con-taining pre-dispensed tested compounds. The plates were incubated for four days at 37 LC in a 5% CO_2 atmosphere. The sub-strate used for the fluorescence intensity (FLINT) readout was resorufin-b-D-galactopyranoside (Sigma–Aldrich) diluted at 5 lM/ well in PBS supplemented with the soft detergent Igepal (Fluka). The plates were incubated for 4 h at room temperature, and the fluorescent signal was read using an EnVision microtitre plate reader (Perkin–Elmer) at excitation/emission wavelengths of 531/595 nm. Untreated parasites were used as negative controls. The criteria for compound selection in the T. cruzi assay were: (a) pIC_{50} >5 for T. cruzi; (b) pIC_{50} <5 for both mammalian cell lines; and (c) a selectivity index >10. The selectivity index (SI) was deter-mined as the ratio of IC_{50} HepG2/IC_{50} parasite.

4.1.3. Mammalian cell cytotoxicity assay

For the NIH-3T3 cytotoxicity assay, the cell culture (1 10^3 cells/well) was seeded in surface-treated culture plates (1536 well) containing pre-dispensed compounds at a maximum concentra-tion of 100 lM. Cells treated with 0.5% DMSO were used as a neg-ative control (100% viable cells) while cells treated with Amphotericin B at 50 lM were considered a positive control, where the cell toxicity is maximum, that is, 100%. Plates were incu-bated for 4 days at 37 LC and 5% CO_2. The HepG2 cytotoxicity assay was performed according Peña et al.[33] A HepG2 (3000 cells/well) culture was plated into 384-well clear-bottom plates containing pre-dispensed test compounds, as described for the NIH-3T3 assay. Plates were incubated for 48 h at 37 LC in a 5% CO_2 atmosphere. After incubation, to determine the number of viable cells in culture based on quantitation of ATP present, both NIH-3T3 and HepG2 plates were incubated at room temperature with 5 lL CellTiter-Glo Reagent (Promega), following the manufacturer's instruc-tions. Luminiscence was measured using a ViewLux microplate reader. The 50% toxic concentration (TC_{50}) was determined by the Activity-Base XE nonlinear regression function in the full curve analysis bundle, according to Peña et al.[33]

4.2. Computational studies

4.2.1. Molecular structure preparation

The molecules were drawn in 2D and were converted to the SMILES file format. The CONCORD software within the SYBYL-X suite (Tripos Inc., St. Louis) was then used to read the SMILES file and create the tridimensional structures. The structure similarity map was also generated in the SYBYL-X suite based on the UNITY fingerprints with an outlier radius of 30% and an accuracy horizon of 30%.

4.2.2. Molecule alignment and pharmacophore perception with GALAHAD

GALAHAD (Genetic Algorithm with Linear Assignment of Hypermolecular Alignment of Datasets), included in the SYBYL-X suite, was used for the 3D molecular alignment and pharma-cophore perception. GALAHAD[36] generates a 3D pharmacophore, and subsequently aligns a set of ligand molecules that presumably bind at a common target site. For the genetic algorithm settings, we used a population size of 100 and 100 interactions, both values surpassing the recommended values, to enhance the visitation function. All molecules were kept flexible for the procedure.

The GALAHAD software identifies a set of ligand conformations that have an optimal combination of low strain energy (ENERGY), steric overlap (STERICS), and pharmacophoric similarity (MOL_QRY). GALAHAD uses a true multi-objective (MO) function in which each term (ENERGY, STERICS and MOL_QRY) is considered independently. The three MO functions constitute a multi-objec-tive triage (MO Triage) approach, which makes use of the Pareto rank for each individual model. Among models with a Pareto rank-ing of zero, we selected the best model based on two different cri-teria: low energy scores and thorough visual inspection of the best alignment.

4.2.3. 3D-QSAR analysis

A 3D-QSAR model was obtained using the CoMFA (Comparative Molecular Field Analysis) method implemented in the SYBYL-X

suite. The alignment resulting from the pharmacophore model pro-duced by GALAHAD was used as the input for the CoMFA, and sev-eral available charge assignment methods were tested. From the initial dataset containing 50 molecules, 6 molecules were removed, either due to bearing very dissimilar structures (LpQM-01 and LpQM-02), SAR inconsistency (LpQM-32), or very low activity (LpQM-03, 04 and 05).

The remaining 44 molecules were separated in two distinct sets: a training set containing 38 molecules and a test set contain-ing 6 molecules. The limited number of molecules prompted us to keep the training set as large as possible to obtain a robust QSAR model. The selection of the test molecules was designed to span the entire pIC_{50} range; therefore, we selected one test molecule for every 7 training molecules, observing the pIC_{50} scale, from higher to lower values.

Partial least square (PLS) analysis was used to correlate the CoMFA fields to the observed compound potencies in the biological assay and was performed using the SYBYL-X default parameters. The pIC_{50} values, that is, log ($1/IC_{50}$), were used as a measure of the biological activity of the compound. IC_{50} refers to the com-pound concentration required for 50% reduction in the T. cruzi amastigotes load in infected NIH-3T3 mouse fibroblasts. The corre-lation between the predicted and observed values of the created models was calculated, and the Q^2 values were used in the selec-tion of the best model. The pIC_{50} values of the molecules in the test set were then predicted using the generated CoMFA QSAR models. The C Log P, molecular weight, hydrogen bond donors and accep-tors counts were calculated using the software OSISRIS DataWarrior.

Acknowledgments

We would like to thank the Brazilian National Research Council (CNPq) and Coordination for the Improvement of Higher Education Personnel (CAPES) for financial support. From GlaxoSmithKline – Spain, Tres Cantos, Spain, we thank Isro Gloger, Silvia Gonzalez, Imanol Peña, Juan Cantizani, Julio Alonso-Padilla and Vanessa Bar-roso for the technical assistance in the screening. M.V.O.C. Thank FACEPE by granting a researcher fixation scholarship (BFP-0107-4.03/12).

Supplementary data

Supplementary data associated with this article can be found, in the online version, at http://dx.doi.org/10.1016/j.bmc.2016.02.027.

References and notes

1. Diniz, L. de F.; Urbina, J. A.; de Andrade, I. M.; Mazzeti, A. L.; Martins, T. A. F.; Caldas, I. S.; Talvani, A.; Ribeiro, I.; Bahia, M. T. PLoS Negl. Trop. Dis. 2013, 7, e2367.
2. Ayo, C. M.; Dalalio, M. M. de O.; Visentainer, J. E. L.; Reis, P. G.; Sippert, E. Â.; Jarduli, L. R.; Alves, H. V.; Sell, A. M. Biomed. Res. Int. 2013, 2013, 1.
3. Jackson, Y.; Chatelain, E.; Mauris, A.; Holst, M.; Miao, Q.; Chappuis, F.; Ndao, M. BMC Infect. Dis. 2013, 13, 85.
4. Kessler, R. L.; Soares, M. J.; Probst, C. M.; Krieger, M. A. PLoS One 2013, 8, e55497.
5. Wiggers, H. J.; Rocha, J. R.; Fernandes, W. B.; Sesti-Costa, R.; Carneiro, Z. A.; Cheleski, J.; da Silva, A. B. F.; Juliano, L.; Cezari, M. H. S.; Silva, J. S.; McKerrow, J. H.; Montanari, C. A. PLoS Negl. Trop. Dis. 2013, 7, e2370.
6. Siqueira-Neto, J. L.; Song, O.-R.; Oh, H.; Sohn, J.-H.; Yang, G.; Nam, J.; Jang, J.; Cechetto, J.; Lee, C. B.; Moon, S.; Genovesio, A.; Chatelain, E.; Christophe, T.; Freitas-Junior, L. H. PLoS Negl. Trop. Dis. 2010, 4, e675.
7. Bettiol, E.; Samanovic, M.; Murkin, A. S.; Raper, J.; Buckner, F.; Rodriguez, A. PLoS Negl. Trop. Dis. 2009, 3, e384.
8. Alves, H.; Dechering, K.; Van Blitterswijk, C.; De Boer, J. PLoS One 2011, 6, e26678.
9. Moon, S.; Siqueira-Neto, J. L.; Moraes, C. B.; Yang, G.; Kang, M.; Freitas-Junior, L. H.; Hansen, M. A. E. PLoS One 2014, 9, e87188.
10. Aulner, N.; Danckaert, A.; Rouault-Hardoin, E.; Desrivot, J.; Helynck, O.; Commere, P.-H.; Munier-Lehmann, H.; Späth, G. F.; Shorte, S. L.; Milon, G.; Prina, E. PLoS Negl. Trop. Dis. 2013, 7, e2154.
11. Don, R.; Ioset, J.-R. Parasitology 2014, 141, 140.
12. Chatelain, E. J. Biomol. Screen. 2015, 20, 22.
13. Canavaci, A. M. C.; Bustamante, J. M.; Padilla, A. M.; Perez Brandan, C. M.; Simpson, L. J.; Xu, D.; Boehlke, C. L.; Tarleton, R. L. PLoS Negl. Trop. Dis. 2010, 4, e740.
14. Andriani, G.; Chessler, A.-D. C.; Courtemanche, G.; Burleigh, B. A.; Rodriguez, A. PLoS Negl. Trop. Dis. 2011, 5, e1298.
15. Sereno, D.; Cordeiro da Silva, A.; Mathieu-Daude, F.; Ouaissi, A. Parasitol. Int. 2007, 56, 3.
16. Du, X.; Hansell, E.; Engel, J. C.; Caffrey, C. R.; Cohen, F. E.; McKerrow, J. H. Chem. Biol. 2000, 7, 733.
17. dos Santos Filho, J. M.; Leite, A. C. L.; de Oliveira, B. G.; Moreira, D. R. M.; Lima, M. S.; Soares, M. B. P.; Leite, L. F. C. C. Bioorg. Med. Chem. 2009, 17, 6682.
18. Romeiro, N. C.; Aguirre, G.; Hernández, P.; González, M.; Cerecetto, H.; Aldana, I.; Pérez-Silanes, S.; Monge, A.; Barreiro, E. J.; Lima, L. M. Bioorg. Med. Chem. 2009, 17, 641.
19. dos Santos Filho, J. M.; Moreira, D. R. M.; De Simone, C. A.; Ferreira, R. S.; McKerrow, J. H.; Meira, C. S.; Guimarães, E. T.; Soares, M. B. P. Bioorg. Med. Chem. 2012, 20, 6423.
20. Franklim, T.; Freire-de-Lima, L.; de Nazareth Sá Diniz, J.; Previato, J.; Castro, R.; Mendonça-Previato, L.; de Lima, M. Molecules 2013, 18, 6366.
21. Brak, K.; Doyle, P. S.; McKerrow, J. H.; Ellman, J. A. J. Am. Chem. Soc. 2008, 130, 6404.
22. Brak, K.; Kerr, I. D.; Barrett, K. T.; Fuchi, N.; Debnath, M.; Ang, K.; Engel, J. C.; McKerrow, J. H.; Doyle, P. S.; Brinen, L. S.; Ellman, J. A. J. Med. Chem. 2010, 53, 1763.
23. Du, X.; Guo, C.; Hansell, E.; Doyle, P. S.; Caffrey, C. R.; Holler, T. P.; McKerrow, J. H.; Cohen, F. E. J. Med. Chem. 2002, 45, 2695.
24. Greenbaum, D. C.; Mackey, Z.; Hansell, E.; Doyle, P.; Gut, J.; Caffrey, C. R.; Lehrman, J.; Rosenthal, P. J.; McKerrow, J. H.; Chibale, K. J. Med. Chem. 2004, 47, 3212.
25. Siles, R.; Chen, S.-E.; Zhou, M.; Pinney, K. G.; Trawick, M. L. Bioorg. Med. Chem. Lett. 2006, 16, 4405.
26. Espíndola, J. W. P.; Cardoso, M. V. de O.; Filho, G. B. de O.; Oliveira e Silva, D. A.; Moreira, D. R. M.; Bastos, T. M.; de Simone, C. A.; Soares, M. B. P.; Villela, F. S.; Ferreira, R. S.; de Castro, M. C. A. B.; Pereira, V. R. A.; Murta, S. M. F.; Sales Junior, P. A.; Romanha, A. J.; Leite, A. C. L. Eur. J. Med. Chem. 2015, 101, 818.
27. Caputto, M. E.; Ciccarelli, A.; Frank, F.; Moglioni, A. G.; Moltrasio, G. Y.; Vega, D.; Lombardo, E.; Finkielsztein, L. M. Eur. J. Med. Chem. 2012, 55, 155.
28. Moreira, D. R. M.; Costa, S. P. M.; Hernandes, M. Z.; Rabello, M. M.; de Oliveira Filho, G. B.; de Melo, C. M. L.; da Rocha, L. F.; de Simone, C. A.; Ferreira, R. S.; Fradico, J. R. B.; Meira, C. S.; Guimarães, E. T.; Srivastava, R. M.; Pereira, V. R. A.; Soares, M. B. P.; Leite, A. C. L. J. Med. Chem. 2012, 55, 10918.
29. Hernandes, M. Z.; Rabello, M. M.; Leite, A. C. L.; Cardoso, M. V. O.; Moreira, D. R. M.; Brondani, D. J.; Simone, C. A.; Reis, L. C.; Souza, M. A.; Pereira, V. R. A.; Ferreira, R. S.; McKerrow, J. H. Bioorg. Med. Chem. 2010, 18, 7826.
30. Leite, A. C. L.; Moreira, D. R. de M.; Cardoso, M. V. de O.; Hernandes, M. Z.; Alves Pereira, V. R.; Silva, R. O.; Kiperstok, A. C.; Lima, M. da S.; Soares, M. B. P. ChemMedChem 2007, 2, 1339.
31. Cardoso, M. V. de O.; de Siqueira, L. R. P.; da Silva, E. B.; Costa, L. B.; Hernandes, M. Z.; Rabello, M. M.; Ferreira, R. S.; da Cruz, L. F.; Moreira, D. R. M.; Pereira, V. R. A.; de Castro, M. C. A. B.; Bernhardt, P. V.; Leite, A. C. L. Eur. J. Med. Chem. 2014, 86, 48.
32. de Oliveira Filho, G. B.; de Oliveira Cardoso, M. V.; Espíndola, J. W. P.; Ferreira, L. F. G. R.; de Simone, C. A.; Ferreira, R. S.; Coelho, P. L.; Meira, C. S.; Magalhaes Moreira, D. R.; Soares, M. B. P.; Lima Leite, A. C. Bioorg. Med. Chem. 2015, 23, 7478.
33. Peña, I.; Pilar Manzano, M.; Cantizani, J.; Kessler, A.; Alonso-Padilla, J.; Bardera, A. I.; Alvarez, E.; Colmenarejo, G.; Cotillo, I.; Roquero, I.; de Dios-Anton, F.; Barroso, V.; Rodriguez, A.; Gray, D. W.; Navarro, M.; Kumar, V.; Sherstnev, A.; Drewry, D. H.; Brown, J. R.; Fiandor, J. M.; Julio Martin, J. Sci. Rep. 2015, 5, 8771.
34. de B. Moreira, T. L.; Barbosa, A. F. S.; Veiga-Santos, P.; Henriques, C.; Henriques-Pons, A.; Galdino, S. L.; de Lima, M. do C. A.; Pitta, I. da R.; de Souza, W.; de Carvalho, T. M. U. Int. J. Antimicrob. Agents 2013, 41, 183.
35. Sun, R. B.; Xi, Z. G.; Yan, J.; Yang, H. L. Biomed. Environ. Sci. 2012, 25, 495.
36. Richmond, N. J.; Abrams, C. A.; Wolohan, P. R. N.; Abrahamian, E.; Willett, P.; Clark, R. D. J. Comput. Aided Mol. Des. 2006, 20, 567.
37. Buckner, F. S.; Verlinde, C. L.; La Flamme, A. C.; Van Voorhis, W. C. Antimicrob. Agents Chemother. 1996, 40, 2592.

APÊNDICE E -

Evaluation of the *Anti-Schistosoma mansoni* Activity of Thiosemicarbazones and Thiazoles

AAC Journals.ASM.org

Evaluation of the Anti-*Schistosoma mansoni* Activity of Thiosemicarbazones and Thiazoles

Edna de Farias Santiago,[a,b] Sheilla Andrade de Oliveira,[b] Gevânio Bezerra de Oliveira Filho,[a] Diogo Rodrigo Magalhaes Moreira,[e] Paulo André Teixeira Gomes,[a] Anekécia Lauro da Silva,[b] Andréia Ferreira de Barros,[b] Aline Caroline da Silva,[c] Thiago André Ramos dos Santos,[c] Valéria Rêgo Alves Pereira,[c] Gabriel Gazzoni Araújo Gonçalves,[d] Fábio André Brayner,[d] Luiz Carlos Alves,[d] Almir Gonçalves Wanderley,[f] Ana Cristina Lima Leite[a]

Department of Pharmacy, Federal University of Pernambuco, Recife, PE, Brazil[a]; Laboratory of Immunopathology,[b] Laboratory of Immunogenetics,[c] and Laboratory of Immunopathology Keizo Asami/Laboratory of Cell Biology and Molecular,[d] CPqAM/FIOCRUZ, Recife, PE, Brazil; Gonçalo Moniz Research Center/FIOCRUZ, Salvador, BA, Brazil[e]; Department of Physiology and Pharmacology, Federal University of Pernambuco, Recife, Brazil[f]

Schistosomiasis is a chronic and debilitating disease caused by a trematode of the genus *Schistosoma* and affects over 207 million people. Chemotherapy is the only immediate recourse for minimizing the prevalence of this disease and involves predominately the administration of a single drug, praziquantel (PZQ). Although PZQ has proven efficacy, there is a recognized need to develop new drugs as schistosomicides since studies have shown that repeated use of this drug in areas of endemicity may cause a tempo-rary reduction in susceptibility in isolates of *Schistosoma mansoni*. Hydrazones, thiosemicarbazones, phthalimides, and thia-zoles are thus regarded as privileged structures used for a broad spectrum of activities and are potential candidates for sources of new drug prototypes. The present study determined the *in vitro* schistosomicidal activity of 10 molecules containing these struc-tures. During the assays, parameters such motility and mortality, oviposition, morphological changes in the tegument, cytotox-icity, and immunomodulatory activity caused by these compounds were evaluated. The results showed that compounds formed of thiazole and phthalimide led to higher mortality of worms, with a significant decline in motility, inhibition of pairing and ovi-position, and a mortality rate of 100% starting from 144 h of exposure. These compounds also stimulated the production of ni-tric oxide and tumor necrosis factor alpha (TNF-), thereby demonstrating the presence of immunomodulatory activity. The phthalyl thiazole LpQM-45 caused significant ultrastructural alterations, with destruction of the tegument in both male and fe-male worms. According to the present study, phthalyl thiazole compounds possess antischistosomal activities and should form the basis for future experimental and clinical trials.

Schistosomiasis is a chronic and debilitating disease caused by a trematode of the genus *Schistosoma* and is one of the most prevalent and neglected diseases of tropical and subtropical regions. This parasitic disease ranks second after malaria in terms of its public health importance and has a significant economic and social impact. It is estimated that more than 207 million people have been infected worldwide, while 779 million people remain at risk of infection (1–6).

According to the World Health Organization, schistosomiasis is the cause of more than 200,000 deaths per year in sub-Saharan Africa, and this may still be an underestimate (5). *Schistosoma mansoni* is one of the most common etiological agents of human schistosomiasis, and the disease is triggered by the inflammatory granulomatous reaction that occurs during deposition of parasite eggs in the liver and other host tissues (7).

The eggs released during the progression of schistosomiasis produce antigens that induce a stronger Th2 response, leading to the formation of granulomas, whereas the parasite antigen induces a Th1 response, with a predominantly Th1 response being observed in the acute phase that is replaced by a Th2 immune response upon egg antigen production (8–10).

Current schistosomiasis treatment is based on the use of praziquantel (PZQ), a pirazylisoquinoline, which is effective against all *Schistosoma* species infecting humans (11, 12) and has been successfully used over the last 20 years as the drug of choice in most areas where the disease is endemic (3, 13, 14). Even though PZQ the antihelminthic drug of choice and despite its advantages, which include tolerability, safety, efficacy, and low cost, PZQ does not protect individuals from reinfection and is not active against the immature stages of the worm, such as the schistosomula and preadult and juvenile adult stages (13, 15).

Furthermore, the appearance of drug-resistant strains of *Schistosoma* is a constant concern for public health authorities (16–18). Hence, the massive use of PZQ in zones of endemicity with the possibility of the emergence of drug-resistant *Schistosoma*, combined with the lack of any other effective antischistosomal drug, requires new effective schistosomicidal compounds to be developed and further studies to be carried out with a view to developing alternative therapies that could either replace or complement the use of PZQ for treatment of *S. mansoni* infection (4, 13).

It is well known that hydrazones, thiosemicarbazones, and phthalimides as well as thiazoles are considered privileged structures as leads in medicinal chemistry (19–21). These core structures have figured prominently in a vast number of structural subunits used for a broad spectrum of activities, and the mode of action of the nuclei of these pharmacophores is usually attributed to the inhibition of multiple targets. For example, hydrazones and thiosemicarbazones have been shown to possess antimicrobial,

Received 29 August 2013 Accepted 22 October 2013
Published ahead of print 28 October 2013
Address correspondence to Edna de Farias Santiago, ednamity@yahoo.com.br. doi:10.1128/AAC.01900-13

anticonvulsant, analgesic, anti-inflammatory, antiplatelet, antitubercular, and antitumor properties, among others (22).

Likewise, hydrazones, thiazolidinone, and their bioisoster thiazole derivatives are known for their potential pharmaceutical applications and possess antimicrobial (23), antischistosomal (24), antifungal (25), antimalarial (26), herbicidal (27), antiviral (28), antidiabetic (29), and antioxidant (30) properties. Thiazole derivatives have been used to prepare various drugs that are important for antimicrobial (31), antibacterial (32, 33), antifungal (32), anti-inflammatory (34), and antitubercular (35) treatment, and some of the thiazole derivatives are used as antiprotozoals (36).

On the other hand, phthalimide derivatives, such as thalidomide, are known for their immunomodulatory activities, inhibit-ing the cytokine tumor necrosis factor alpha (TNF-), interleu-kins-1 (IL-1), IL-6, and IL-12, and granulocyte-macrophage colony-stimulating factor. They also activate the Th1 response, by increasing gamma interferon (IFN-) and IL-2, have antiangio-genic and antiproliferative properties, activate apoptosis, T cells, and NK cells, and inhibit cell adhesion (37, 38).

With this in mind, we performed a synthesis of a set of molecules whose structures have a hydrazine and/or thiazole nucleus as a common group. With a view to ascertaining whether the new thiosemicarbazone, phthalyl thiosemicarbazone, phthalyl thiazole, and phthalyl thiazolidinone pharmacophores are an essential require-ment for antischistosomal activity, 10 compounds were synthesized, and their antischistosomal potentials were determined.

The efficacy of the compounds was examined in terms of (i) schistosome survival, (ii) egg output (oviposition), (iii) motor activity, (iv) ultrastructural alterations in the tegument of *S. mansoni* as determined by scanning electron microscopy (SEM), and (v) cytotoxicity and immunomodulatory activity induced by these new compounds on splenocytes and macrophages, respectively.

MATERIALS AND METHODS

Compounds. The compounds 2-(1-phenoxypropan-2-ylideno)thiosemicar-bazide (LpQM-01), 2-(1-phenoxypropan-2-ylideno)-4-phenylthiosemicarba-zide (LpQM-02), and 2-(1-phenoxypropan-2-ylideno)-4-methylthiosemicarba-zide (LpQM-03) were prepared as described by Moreira et al. (39). The compounds 2-(2-(1,3-dioxoisoindolin-2-yl)ethylidene)-1-methylthiosemicar-bazide (LpQM-38), (3-methyl-4-oxothiazolidin-2-ylidene)hydrazono)ethyl) isoindoline-1,3-dione (LpQM-40), 2-(2-(2-(4-(4-fluorophenyl)thiazol-2-yl) hydrazono)ethyl)isoindoline-1,3-dione(LpQM-43), 2-(2-(2-(4-(4-methoxy-phenyl)thiazol-2-yl)hydrazono)ethyl)isoindoline-1,3-dione (LpQM-45), and 2-(2-(2-(4-(4-chlorophenyl)thiazol-2-yl)hydrazono)ethyl)isoindoline-1,3-dione (LpQM-47) were prepared as described by Pessoa et al. (40); compounds 2-(2-(1-(3-bromophenyl)propylidene)hydrazinyl)-4-methoxyphenyl)thiazole (LpQM-14) and 2-(2-(1-(3-bromophenyl)propylidene)hydrazinyl)-4-(4-nitro-phenyl)thiazole (LpQM-17) were also used (C. L. Leite and P. A. T. Gomes, un-published data). All compounds were chemically characterized by nuclear mag-netic resonance (NMR), infrared, and mass spectra and by elemental analysis and presented purity of 95%. PZQ (catalog no., 4668; bench, BCBD3257V) was purchased from Sigma-Aldrich (St. Louis, MO, USA).

Parasites and intermediary and definitive hosts. The LE strains (Belo Horizonte, Minas Gerais, Brazil) of *S. mansoni* were used throughout this study. These strains were maintained in *Biomphalaria glabrata* snails and Swiss mice, in the laboratory at the Aggeu Magalhães Research Center (CPqAM) of the Oswaldo Cruz Foundation (FIOCRUZ, PE, Brazil).

Female Swiss mice weighing 20 2 g were used as the definitive host and were infected transcutaneously with about 120 cercariae (LE strain). The animals were kept in a controlled temperature and light environment and had access to food and water *ad libitum*. After 55 days of infection, adult *S. mansoni* specimens were recovered from the mice by perfusion, using the technique developed by Duvall and De Witt (41).The experiments were approved by the Ethics Committee on Animal Use (CEUA), FIOCRUZ (process number 22/2011).

***In vitro* assay.** *S. mansoni* worms harvested from Swiss mice were kept in RPMI 1640 medium (Sigma-Aldrich, St. Louis, MO, USA) buffered to pH 7.5, supplemented with HEPES (20 mM), 10% fetal bovine serum, penicillin (100 U/ml), and streptomycin (100 g · ml ^{1}). Incubation was carried out at 37°C in a humid atmosphere containing 5% CO_2 gas. LpQM-43, LpQM-45, LpQM-47, and LpQM-14 compounds were dis-solved in 1.6% dimethyl sulfoxide (DMSO) and used in concentrations varying from 40 to 100 g · ml ^{1}; compounds were added to the medium containing the worms after a 2-h period of adaptation to the culture me-dium. One pair of adult worms/well was used in this study. The control worms were assayed in RPMI 1640 medium with 1.6% DMSO as a nega-tive-control group. All experiments were carried out in five replicates and were repeated at least three times. The motor activity, egg output (ovipo-sition), tegumental alterations, and survival of the parasites were moni-tored every 24 h for 192 h using an inverted microscope (SMZ 1000; Nikon).

SEM. Male and female worms after *in vitro* exposure to LpQM-45 compound over a period of 24 and 48 h were fixed overnight at room temperature with 2.5% glutaraldehyde, 4% formaldehyde, and 0.1 M cacodylate buffer at pH 6.8. They were then postfixed in 2% osmium tetroxide (OsO_4) in a 0.1 M cacodylate buffer at pH 6.8 for 60 min in the absence of light at room temperature. The next steps included washing and dehydration in a graded ethanol series for 15 min each. The worms were crit-ical-point dried using liquid CO_2, directly sputter coated with colloidal gold for 1 min, and examined under a JEOL-5600LV microscope.

Animals used for cytotoxicity and immunological assays. Male BALB/c mice (6 to 8 weeks old) were raised at the animal facility of the Oswaldo Cruz Foundation (Rio de Janeiro, Brazil) and maintained at the animal facility of the Aggeu Magalhães Research Center, Oswaldo Cruz Foundation, in Recife, Brazil. All mice were euthanized, and their spleens were removed in accordance with the guidelines of the Oswaldo Cruz Foundation Commission for Experiments with Laboratory Animals (Ministry of Health, Brazil, 0266/05).

Spleen cell harvesting. Spleen cells were harvested according to a pre-vious protocol (42). After the BALB/c mice were euthanized with CO_2 gas, the spleen of each mouse was removed aseptically and placed in a Falcon tube containing incomplete RPMI 1640 medium with fetal calf serum (complete medium). In a vertical flow, each spleen was transferred to a petri dish where it was soaked. The cell suspensions obtained were trans-ferred to Falcon tubes containing approximately 10 ml of incomplete medium per spleen and centrifuged at 4°C and 200 *g* for 5 min. After the supernatant was discarded, distilled water was added to the sediment to trigger red blood cell lysis. The supernatant (containing no cell debris) was collected and centrifuged at 4°C and 200 *g* for 5 min. The resulting sediment (containing cells) was resuspended in complete RPMI 1640 me-dium. An aliquot of each cell suspension was separated and diluted in trypan blue for quantification in a Neubauer chamber, and the viability of cells was determined.

***In vitro* cytotoxicity assay.** Spleen cells (6 10^{5} cells/well), obtained as described in the previous paragraph, were cultured in 96-well plates containing RPMI 1640 medium. These cells were incubated with the com-pounds at six concentrations (1, 5, 10, 25, 50, and 100 g · ml ^{1}) in the presence of [^{3}H]thymidine (Amersham Biosciences, USA) (1 Ci · well ^{1}) for 24 h at 37°C and 5% CO_2. Cells treated with saponin (0.05%) were used as a positive control, and cells treated with DMSO (1%) were used as a negative control. Each drug was tested in triplicate.

The contents of the plate were then harvested to determine [^{3}H]thymi-dine incorporation using a beta-radiation counter (Wallac 1209; Rackbeta Pharmacia, Stockholm, Sweden). Compound toxicity was determined by comparing the percentage of [^{3}H]thymidine incorporation (as an indicator of cell viability) in treated cells with that in untreated cells. Noncytotoxic concentrations were defined as those where [^{3}H]thymidine incorporation was

30% lower than the level in untreated controls. Six concentrations were also used for PZQ (1, 5, 10, 25, 50, and 100 g · ml ^{1}).

Measurement of cytokine levels in macrophage supernatants. Cytokines were quantified in supernatants of macrophage cultures treated *in vitro* after 48 h and 72 h with LpQM-43, LpQM-45, LpQM-47, LpQM-14, and PZQ at 56, 58, 55, 50, and 51 g · ml ^{1}, respectively (50% cytotoxic concentration [CC_{50}] in macrophages). As a positive control, cells were stimulated with the mitogens lipopolysaccharide (LPS at 50 g · ml ^{1}) and concanavalin A (ConA at 2.5 g · ml ^{1}), while for the negative con-trols, cells did not receive either mitogen or drugs. The levels of the IL-6, IL-10, IL-12, and TNF- cytokines were measured using sandwich en-zyme-linked immunosorbent assays (ELISAs), according to the manufac-turer's suggested protocols. The monoclonal antibodies used were the OptEIA (BD Biosciences) kit, and these were used after titration. Plates with 96 wells (NalgeNunc International Corp.) were sensitized with spe-cific anticytokine antibodies (according to the manufacturer's instruc-tions) and incubated overnight at 4°C. Cytokine standards were added after serial dilutions from their initial concentrations (16,000 pg · ml ^{1}). After a washing step, 50 l of all samples and standards was added in duplicate, and the plate was incubated for 2 h at room temperature. The specific antibodies were then combined with biotin (according to the manufacturer's instructions) and incubated for 1 h 30 min at room tem-perature. Revealer solution containing 2,2-azino-bis(3-ethylbenzothiazo-line-6-sulfonic acid) diammonium salt (ABTS) was added. The reaction was blocked with 1 M sulfuric acid, and the reading was carried out on a spectrophotometer (3550; Bio-Rad, Hercules, CA) at 415 nm. Sample concentrations were calculated in the linear region of the titration curve of cytokine standards, and final concentrations were expressed in pg · ml ^{1}, using Microplate Manager, version 4.0, software (Bio-Rad Laboratories).

***In vitro* nitrite analysis.** Nitric oxide (NO) production was measured as nitrite (a stable breakdown product of NO) accumulated in the super-natant of the macrophage culture stimulated with LpQM-43, LpQM-45, LpQM-47, LpQM-14, and PZQ at 56, 58, 55, 50, and 51 g · ml ^{1}, respec-tively (the 50% cytotoxic concentration [CC_{50}] in the macrophages) Dul-becco's modified Eagle's medium (DMEM) supplemented with 10% heat-inactivated fetal bovine serum and LPS (50 ng · ml ^{1}) were used as positive and negative controls, respectively.

The Griess indirect method (43) was used, and nitrite levels were quantified using 50 l of each supernatant and an equal volume of Griess reagent [1% sulfanilamide, 0.1% dihydrochloride of *N*-(1-naphthyl)-eth-ylenediamine, 2.5% H_3PO_4], and samples were incubated at room tem-perature for 10 min. Absorbance was measured on a 540-nm reader (Mul-tiskan FC; Thermo Scientific) at 540 nm, and the nitrite levels in each sample after 24 h, 48 h, and 72 h were determined by extrapolation from a previously determined standard curve.

Statistical analysis. The differences between groups were analyzed using Mann-Whitney *U* and Dunnett's nonparametric tests. All results are expressed as mean values of groups standard deviations, and a *P* value of 0.05 was taken to be statistically significant.

RESULTS

Effect of new compounds on adult *S. mansoni* survival. Ten derivatives containing the pharmacophore phthalimide, thiazole, thiazolidinone, and thiosemicarbazone nuclei were tested for schistosomicidal properties (Table 1). Compounds were evalu-ated at a concentration of 40 to 100 g · ml ^{1} every 24 h for a period of 192 h, and mortality, motility, and alterations in the integument of the worms were observed. The mortality after 144 h of exposure at a concentration of 100 g · ml ^{1} was initially used to perform a screening of compounds. Of the tested compounds, those formed of thiazole and phthalimide led to higher mortality among worms (Fig. 1). One exception was LpQM-17, a thiazole derivative that did not kill worms under the conditions cited. We investigated the action of four compounds, LpQM-43, LpQM-45, LpQM-47, and LpQM-14, in greater detail, examining the effect of these compounds on the mortality rate with respect to concentra-tion and incubation time. Other factors evaluated included changes in motility and integument and the 50% inhibitory con-centration (IC_{50}; 50% mortality).

All compounds were tested in concentrations of 5, 10, and 20 g · ml ^{1}, but they did not cause worm mortality in these concentrations (data not shown). Because of this, only concentrations above 40 g · ml ^{1} are described in Table 2. The phthalyl thiazoles LpQM-45 and LpQM-14 caused 100% worm mortality at concen-trations of 100 and 80 g · ml ^{1} within 144 and 168 h, respectively. Similarly, the phthalyl thiazoles LpQM-43 and LpQM-47 caused 67% and 95% worm mortality, respectively, in 192 h at a concen-tration of 100 g · ml ^{1} (Table 2). Interestingly, oviposition by adult worms was not seen with any of the four compounds exam-ined. All of the worms in the control group remained viable until the end of the experiment.

As can be seen in Table 3, there was a significant reduction in motility under the treatment with the LpQM-45 compound at all concentrations. The LpQM-47 compound brought about a reduction in motility at all concentrations, and LpQM-14 reduced motility at 60 to 100 g · ml ^{1}. LpQM-43 caused only a partial reduction in worm motility. Many physiological alterations were observed in adult worms exposed to the new compounds (Table 2). The IC_{50}, the concentration of compound required to cause 50% mortality of worms, was another parameter used to evaluate schistosomicidal activity, and the results are shown in Table 2.

The activity of compounds was evaluated after 120 h of expo-sure in terms of changes in motility and the tegument of the worms and according to the criteria established by Ramirez et al. (44). According to these criteria, LpQM-43 was considered par-tially active at a concentration range of 40 to 100 g · ml ^{1}, while LpQM-45 and LpQM-47 were considered active at a concentra-tion of 40 to 100 g · ml ^{1}, and LpQM-14 was active at a concen-tration of 60 to 100 g · ml ^{1} and partially active at a concentra-tion of 40 g · ml ^{1}.

Scanning electron microscope examination. The compound LpQM-45 caused 100% worm mortality, and it was the most po-tent of the compounds; therefore, we studied its effects on the worm morphology.

The tegument surface of male and female *S. mansoni* worms after *in vitro* exposure to LpQM-45 for periods of 24 and 48 h was examined using scanning electron microscopy (SEM). The worms exposed to DMSO and to medium alone (controls) were also examined using SEM. The control male and female worms that were not exposed to any drugs (negative controls) presented normal surface membrane topography. The male worms exhibited a large number of tubercles with typical spines, sensory papillae, oral and ventral suckers, and no abnormality, and, in the anterior part of the body, the gynecophoral canal showed no abnormality after 24 and 48 h (Fig. 2A to D). In the female worms, parallel fissures, tegument spines, and sensory papillae with no abnormality were observed at 24 and 48 h (Fig. 2E to H).

Exposure of the worms to compound LpQM-45 resulted in ultrastructural alterations, which were already apparent during the first period of exposure (24 h), revealing a variety of changes in the tegument surface. In the male worm, complete destruction of some tubercles was found, with extensive sloughing and exposure of the subtegument layer of muscle tissue (Fig. 3A to D). The

TABLE 1 Structure of new thiosemicarbazone analogs used in this study

Analog	Structure	Compound	Identification of R
Phenoxy-thiosemicarbazones	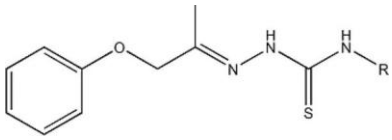	LpQM-01	OH
		LpQM-02	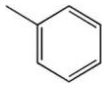
		LpQM-03	OCH_3
Phenyl-thiazoles	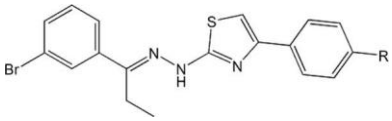	LpQM-14	$OOOCH_3$
		LpQM-17	ONO_2
Phthalyl-thiosemicarbazone	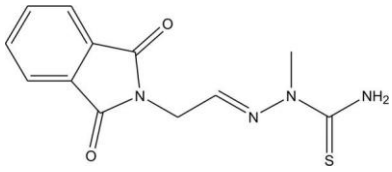	LpQM-38	
Phthalyl-thiazoles	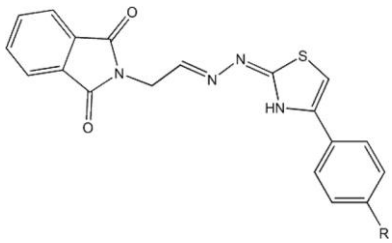	LpQM-47	OCl
		LpQM-43	OF
		LpQM-45	$OOOCH^3$
Phthalyl-thiazolidinone	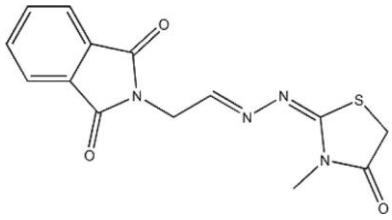	LpQM-40	

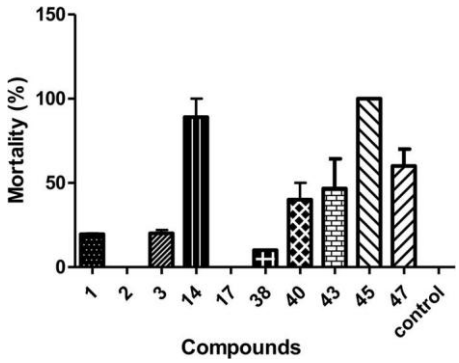

FIG 1 Effects of LpQM compounds on the mortality rate of *S. mansoni* at a concentration of 100 g · ml ^{1} after 144 h. Compounds are indicated by the numerical suffix following LpQM.

severity of tegument damage was higher in the males after 48 h of exposure, with an increasing number of tubercles completely de-structed or eroded, a roughened surface in the same areas, and disintegration of the tegument in this area, as revealed by higher magnification (Fig. 3E to H).

The female worms exposed to LpQM-45 showed serious damage, with extensive sloughing and disintegration of the tegument and exposure and injury of the layer of muscle tissue after 24 and 48 h (Fig. 4).

Cytotoxic activity in splenocytes. After determining the antip-arasitic activity against *S. mansoni* worms, we determined the cyto-toxicity in splenocytes of BALB/c mice for the most potent antipara-sitic compounds. The evaluation of cytotoxic compounds showed that LpQM-43, LpQM-45, and LpQM-47 presented nontoxic effects at concentrations up to 100 g · ml ^{1}, while LpQM-14 presented nontoxic effects at concentrations up to 25 g · ml ^{1} (Table 2). On the other hand, PZQ showed higher toxicity in splenocytes (1 g · ml ^{1}) at all concentrations tested.

TABLE 2 *In vitro* effects of LpQM-43, LpQM-45, LpQM-47, and LpQM-14 against adult worms of *S. mansoni*

Drug	Time (h)	Mortality (%) at the indicated concn (g/ml)				IC_{50} (g/ml)	Cytotoxicity (g/ml)[a]	Worm characteristic(s) observed
		100	80	60	40			
LpQM-43	24	13	0	7	0	82.24	100	Not paired
	48	23	3	10	0	84.13		No sucker adherence
	72	30	7	10	0	83.53		Absence of eggs
	96	37	13	16	0	73.65		Nontransparent blackish tegument
	120	40	20	24	0	64.13		
	144	47	37	29	0	58.01		
	168	60	40	45	0	55.83		
	192	67	53	56	53	32.93		
LpQM-45	24	5	36	9	32	46.20	100	Not paired
	48	40	41	28	41	19.97		No sucker adherence
	72	60	60	57	51	26.36		Absence of eggs
	96	70	80	62	56	31.53		Integument morphology altered (nontransparent blackish tegument, appearance of bubbles)
	120	90	95	76	61	33.78		
	144	100	100	90	70	32.09		
	168	100	100	90	85	25.88		
	192	100	100	90	95	24.69		
LpQM-47	24	5	9	10	5	40.08	100	Not paired
	48	5	9	19	15	51.38		No sucker adherence
	72	15	25	39	21	41.90		Absence of eggs
	96	20	29	53	44	37.48		Integument morphology altered (nontransparent, blackish tegument, appearance of bubbles)
	120	40	46	66	66	23.78		
	144	60	54	74	73	24.92		
	168	80	58	88	83	26.97		
	192	95	58	91	88	30.95		
LpQM-14	24	5	0	5	0	65.70	25	Not paired
	48	25	0	20	0	72.77		No sucker adherence
	72	50	10	25	0	76.17		Absence of eggs
	96	50	40	25	5	60.15		Integument morphology altered (nontransparent, blackish tegument, appearance of bubbles)
	120	78	75	39	22	53.95		
	144	89	95	52	37	48.06		
	168	100	100	57	47	43.41		
	192	100	100	67	61	33.52		

[a] The highest nontoxic concentration on spleen cells of BALB/c mice. Saponin (1.0 g/ml) was used as a positive control.

Immunomodulatory activity in macrophages treated with the compounds. The ability of the compounds to stimulate the secretion of IL-6, IL-10, IL-12, and TNF- was investigated through the measurement of these cytokines in the superna-tants of macrophage cultures. Results are shown in Fig. 5. In comparison to the untreated cells (negative control), a significant (*P* 0.001) production of TNF- was observed after 48 h of treatment with the compound LpQM-47. A similar finding was observed for PZQ-treated cells. After 72 h of treatment, compounds LpQM-43, LpQM-45, and LpQM-47 caused significant TNF- secretion. In contrast, compound LpQM-14 caused significant TNF- secretion only after 72 h of treat-

TABLE 3 Motility score of control and worms treated with PZQ and LpQM-43, LpQM-45, LpQM-47, and LpQM-14 for 120 h

Group	Percentage of worms by motility score after drug treatment at:[a]															
	100 g/ml				80 g/ml				60 g/ml				40 g/ml			
	3	2	1	0	3	2	1	0	3	2	1	0	3	2	1	0
Control	100	0	0	0	100	0	0	0	100	0	0	0	100	0	0	0
PZQ	0	0	0	100	0	0	0	100	0	0	0	100	0	0	0	100
SC-43	17	29	17	38	3	50	27	20	13	46	18	23	4	48	10	38
SC-45	0	0	10	90	0	5	0	95	0	5	19	76	0	20	19	61
SC-47	5	10	45	40	8	13	34	45	0	4	30	66	0	13	21	66
PT-1.4	5	11	6	78	0	20	5	75	0	23	39	39	16	42	20	22

[a] The measurement of mean worm motility is scored on a scale of 0 to 3 as follows: 3, normally active; 2, slowed activity; 1, minimal activity with occasional movement of head and tail and absence of motility apart from gut movements; 0, total absence of mobility.

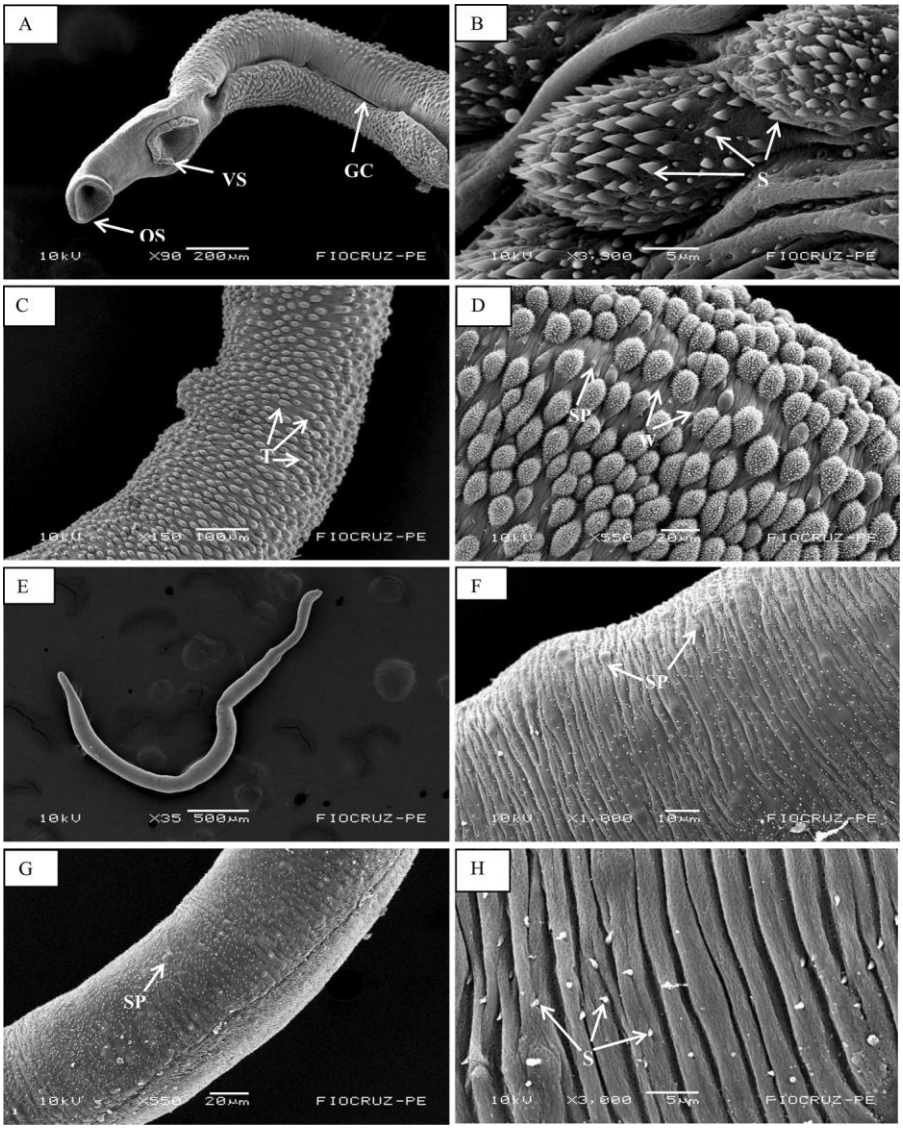

FIG 2 Scanning electron micrographs of adult male and female *S. mansoni* worms from the control group. (A) Male worms kept in medium and DMSO after 24 h, showing the anterior portion of the body with oral (OS) and ventral suckers (VS) and the gynecophoral canal (GC) with no abnormalities. (B) Male worms kept in medium and DMSO after 48 h, showing in detail numerous spines (S) covering the tubercules (T). (C) The dorsal region of male worms kept in medium alone after 48 h, showing numerous tubercles distributed along the body. (D) Male worms kept in medium only after 24 h, showing in detail the dorsal region with sensory papillae (SP) and parallel wrinkles (W) visible. (E) Female worms kept in medium and DMSO after 24 h, showing the whole extent of the body. (F) Female worms kept in medium and DMSO after 48 h, showing the sensory papillae (SP). (G) Female worms kept in medium alone showing the integrity of the tegument. (H) Female worms kept in medium alone, showing spines (S) in detail.

ment. In addition, we observed that the TNF- content under treatment with compound LpQM-14 was quite similar to that observed for LPS-stimulated cells (positive control), indicating that this compound substantially modulates the immune response. After the TNF- content was measured, the secretion of IL-6, IL-10, and IL-12 was evaluated under compound treatment. However, in comparison to the LPS-stimulated cells (positive control), none the compounds induced the secretion of IL-6, IL-10, and IL-12 in macrophages until 72 h after drug incubation (data not shown).

NO content in macrophages. In another set of experiments, the nitrite content was determined in the supernatant of macrophages treated with the drugs LpQM-43, LpQM-45, LpQM-47, and LpQM-14. LPS-treated cells (positive control) and untreated cells (negative control) were included in the experiment (Fig. 6). In comparison to untreated cells, the production of nitrite was significantly higher under compound LpQM-14 treatment, and this was observed during the three data points (24, 48, and 72 h after incubation). In contrast, compound LpQM-45 produced a statistically significant amount of nitrite only at a time point under 48 h after incubation, while PZQ had no effect on the nitrite production.

DISCUSSION

The 10 tested compounds all had a phthalimide nucleus, a hydrazone moiety, and/or a thiazole ring system. In general, compounds that possessed a phthalimide and thiazole ring system showed significant

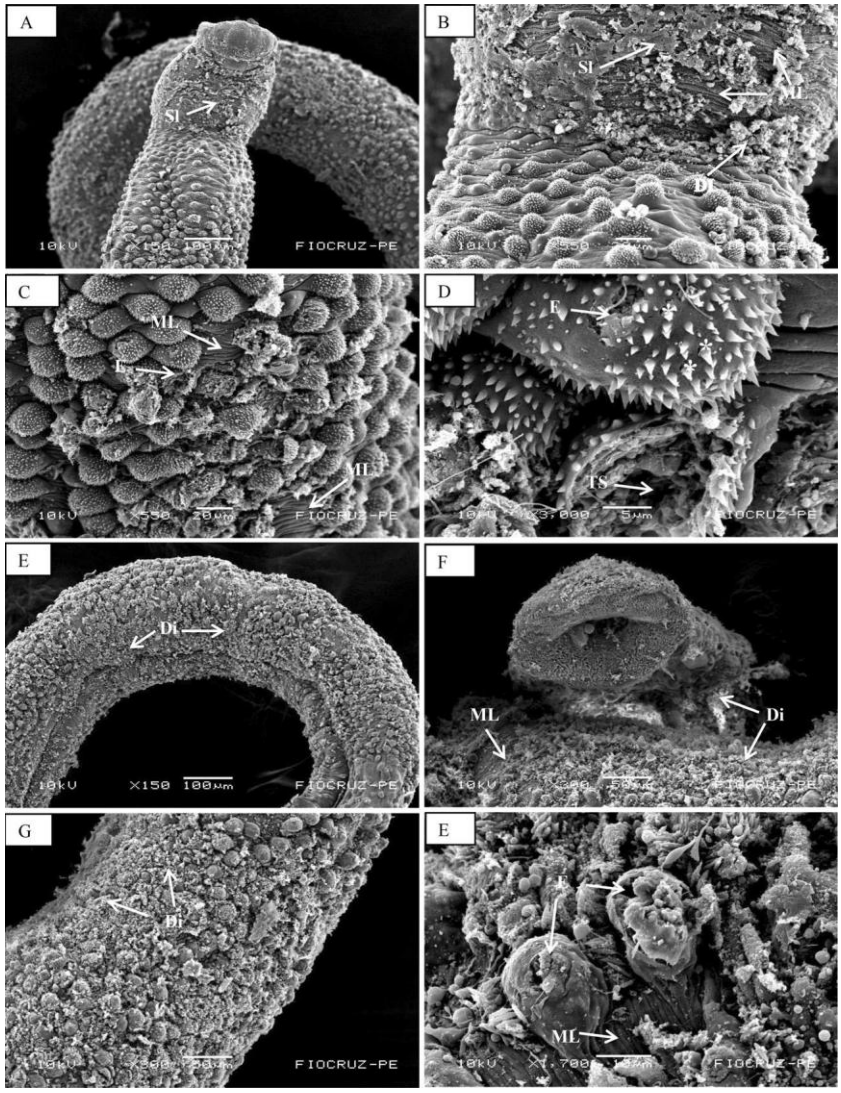

FIG 3 Scanning electron micrographs of adult male *S. mansoni* worms exposed to 80 g · ml ^{1} LpQM-45. (A to D) Worms after 24 h of incubation showing extensive sloughing (Sl), erosion (E), loss of spines (*) and disintegration (Di) of tegument with exposure of subtegumental tissue (TS) and muscle layer (ML). (E to H) Worms after 48 h of incubation showing a greater area of erosion (E) and disintegration (Di) of the tegument and exposure of muscle layer (ML).

antiparasitic activity against *S. mansoni* worms. No antiparasitic activity was observed in the case of LpQM-17, a thiazole derivative that also has a nitro group in the 4-position of the phenyl ring. The cyto-toxicity in mouse cells of PZQ was greater than that of any of the tested compounds that showed anti-*S. mansoni* activity; therefore, the compounds described here were more selective. In terms of the oviposition profile of adult worms (absence), the tested compounds exhibited activity similar to that observed for PZQ.

The thiazole nucleus, which is present in an important class of heterocyclic compounds present in many biologically potent ac-tive molecules (45), is also present in the most active compounds of the whole series. Some thiazoles have, in fact, been shown in the literature as schistosomicidal agents (19, 46). The phthalyl thiazoles LpQM-43, LpQM-45, and LpQM-47 and the thiazole LpQM-14 have been shown to have antischistosomal properties, with the IC_{50}s ranging from 82.24 to 32.93 g · ml ^{1}, 46.20 to 24.69 g · ml ^{1}, 40.08 to 30.95 g · ml ^{1}, and 65.70 to 33.52 g · ml ^{1}, respectively. These results suggest that the efficacy varies according to the substituent in the 4-position of the phenyl group. LpQM-45 exhibited the best schistosomicidal properties in rela-tion to other compounds, with 100% mortality within 144 h at concentrations of 100 and 80 g · ml ^{1}. LpQM-14 also showed significant schistosomicidal activity, with 100% mortality within 168 h at concentrations of 100 and 80 g · ml ^{1}.

The compounds LpQM-14 and LpQM-45 have in common a methoxyl group attached in the 4-position of the phenyl ring.

In comparison to the literature findings, it was also observed that heterocyclic compounds containing a methoxyl group exhib-ited higher schistosomicidal activity than compounds without this group (47). Another interesting structure-activity relationship is observed for the compound LpQM-47, which produced a mortal-ity rate of 95% at 100 g · ml ^{1} and 91% at 60 g · ml ^{1} after 192 h of incubation. This compound has a chloro atom attached to the 4-position of the phenyl ring. In agreement with this, it is de-scribed in the literature that the attachment of a chloro atom im-

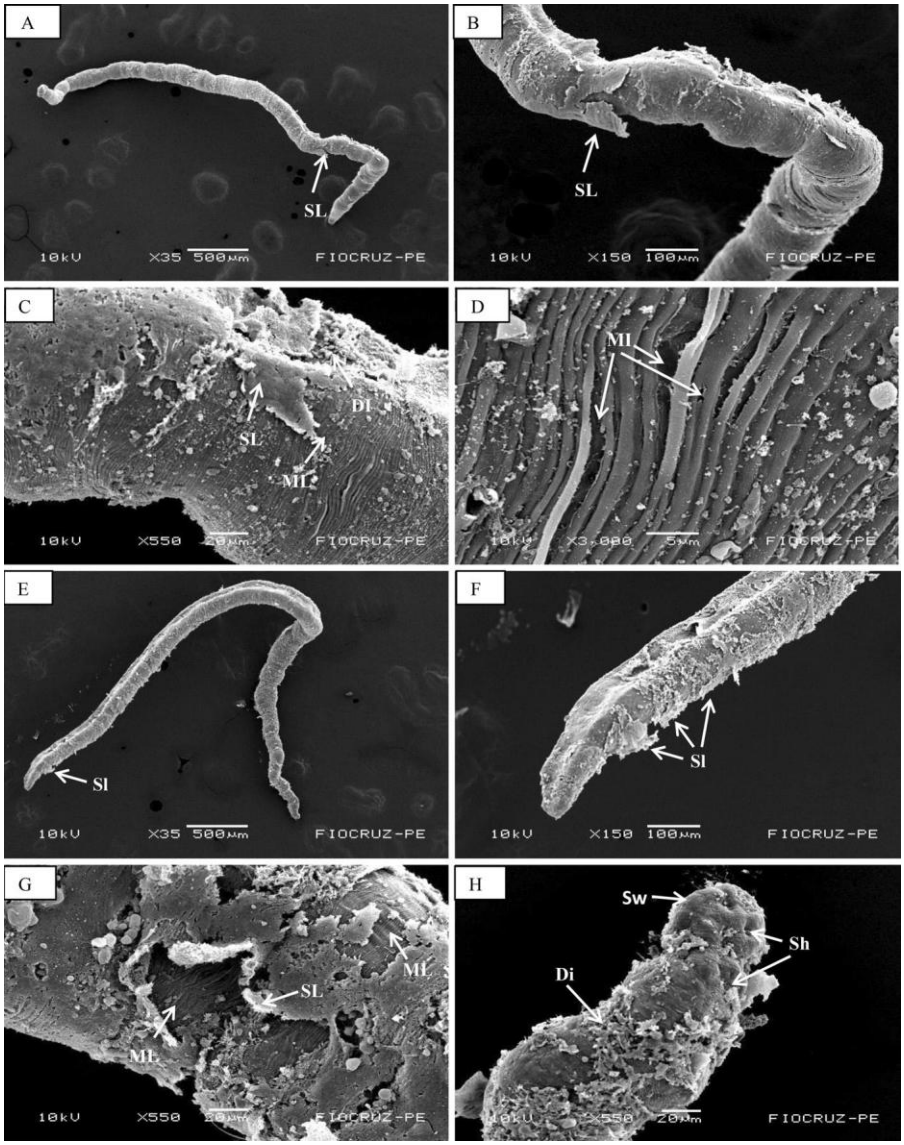

FIG 4 Scanning electron micrograph of adult female *S. mansoni* worms exposed to 80 g · ml ^{1} LpQM-45. (A to D) Worms after 24 h of incubation showing sloughing (Sl), disintegration (Di) of tegument, and exposure of subtegumental muscle layer (ML) with muscle damage (MI). (E to H) Worms after 48 h of incubation showing sloughing (Sl), disintegration (Di) of the tegument with exposure of muscle layer (ML), swelling (Sw), and shrinking (Sh).

proves the schistosomicidal activity for 2-thioxoimidazolidin-4-one compounds (48).

Another common feature of all active compounds described here is the presence of a hydrazone moiety. Some 9-acridanone hydrazones were found to be effective against *S. mansoni* in mice, killing almost all of the skin schistosomules, when administered at a dose of 100 mg/kg (49). In another study, 9-acridanones derived from thiazoles were effective against *S. mansoni* in the skin phase, killing almost all of the parasites in mice at a dose of 100 mg/kg, 24 h after penetration by cercariae. This same study showed that when the compound is administered to monkeys at a dose of 25 mg/kg, worms and eggs are absent from liver tissue and rectal mucosa 7 days after infection, which constitutes cure (20).

Detailed microscopic observation showed that LpQM-43, LpQM-45, LpQM-47, and LpQM-14 molecules caused alterations in the teguments of the worms compared with the untreated control group. These compounds also appear to influence the oviposition of parasites since no eggs were found in the culture medium.

The thick tegument that covers the entire surface of schistosomes is an important target for drugs because the functioning of the surface membrane and the integrity of the tegument are criti-cal for the survival and proliferation of the *Schistosoma* parasite (13). These structures play vital roles in the immune evasion, nu-trient absorption, and cholesterol metabolism of the host (13, 50). Alterations in the surface ultrastructure of schistosome worms have been investigated by a number of authors in order to evaluate antischistosomal drugs (13, 24, 50, 51, 52, 53). The present study thus examined the surface topography of male and female worms to determine the schistosomicidal effect of LpQM-45. We found extensive damage to the tegument in both male and female worms after 24 and 48 h of exposure.

SEM analysis revealed progressive damage to the tegument

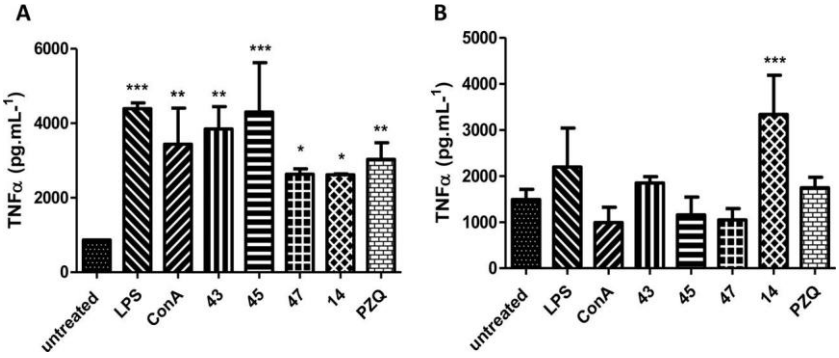

FIG 5 TNF- production in supernatants of the macrophage culture in the presence of LpQM-43,-45,-47, and -14 and PZQ at 56, 58, 55, 50, and 51 g · ml ^{1}, respectively. Assays were performed at 48 h (A) and 72 h (B). The horizontal bars represent median values. *, *P* 0.05; **, *P* 0.01; ***, *P* 0.001.

surface, causing destruction of tubercles in the male, extensive sloughing with disintegration of the tegument in the same areas, and exposure of subtegumental tissue and the layer of muscle tissue in both male and female worms. Similar changes occurred in response to different drugs (13, 50). For instance, Manneck et al. (50) have presented a detailed study of tegument surface alterations caused by 100 g · ml ^{1} of mefloquine in *S. mansoni* worms, finding in females extensive sloughing, with the base membrane exposed along with roughened tegu-ments which have already started to disintegrate. The males showed a roughened surface with disintegration of the tegu-ment, resulting in a fibrous appearance, loss of tubercles, spines, and parallel wrinkles. Bertão et al. (13) also found se-vere damage to the surface of adult male schistosomes caused by exposure to miltefosine, which was characterized by peeling of the tegument, reduction in the size of the spine, erosion, the formation and rupturing of blisters, and the emergence of holes with exposure of layers of muscle tissue.

After 3 h of exposure, PZQ cause severe muscle contraction; the worms became curved, resulting in a decrease in body size (13, 54). In contrast, LpQM-45 caused severe damage to the surface of the worm but no muscle contraction. The lesions were more nu-merous in parasites exposed to LpQM-45 than in those treated with PZQ. Similarly, miltefosine (13) and thioxoimidazolidine (54) have also been shown to be more effective than PZQ in caus-ing tegument damage in *S. mansoni*. In terms of differences be-tween the changes in males and females, it was noted that the tegument of female worms was slightly more affected and that mefloquine (13) and artemether (55) likewise tend to have a greater effect on females.

The outer membrane and lipid bilayers of *S. mansoni* worms proved to be extremely sensitive to LpQM-45. The morphological

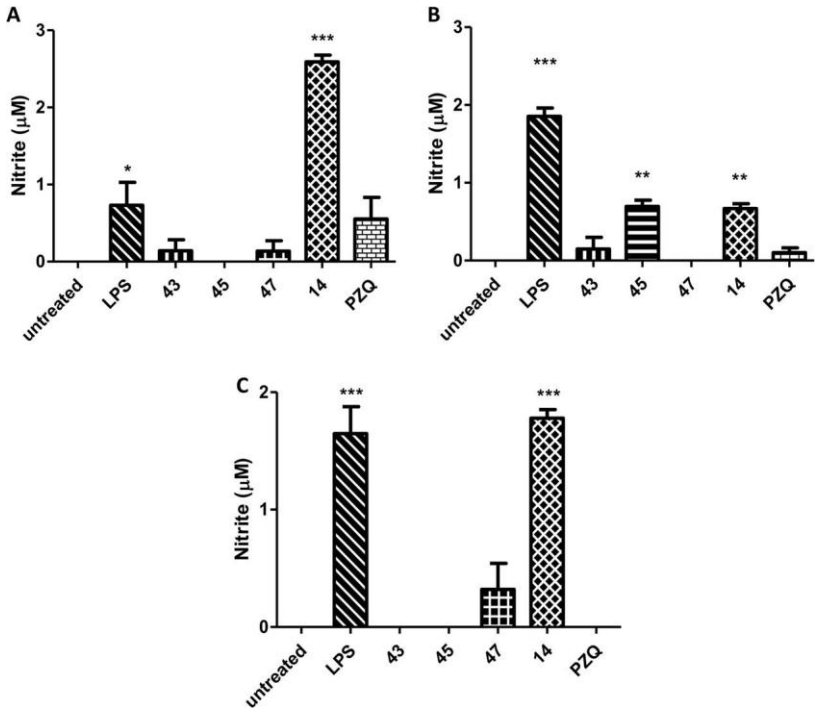

FIG 6 Nitrite production in supernatants of the macrophage culture in the presence of LpQM-43, -45, -47, and -14 and PZQ at 56, 58, 55, 50, and 51 g · ml ^{1}, respectively. Assays were performed at 24 h (A), 48 h (B), and 72 h (C). The horizontal bars represent median values. *, *P* 0.05; **, *P* 0.01; ***, *P* 0.001.

changes brought on by LpQM-45 may therefore have exerted a profound effect upon the metabolic activity of the parasite and may be the mechanism that causes these compounds to kill the worms. The damage to the tegument along the worm's body may impair the functioning of the tegument and destroy the worm's defense system so that it is easy prey to the host's immune system (24).

The morbidity caused by human schistosomiasis is attributed to the granulomatous inflammation caused by an immune response to the egg antigen. Many studies have shown that in schis-tosomotic patients, there is a balance between the Th1 and Th2 responses (12). Furthermore, these same studies strongly suggest that resistance to infection is multifactorial and that it cannot be clearly correlated with a single immune mechanism. The Th1 im-mune response, generated by tumor necrosis factor alpha (TNF-), IL-1, and IL-6, seems to predominate in the acute phase, but it is replaced by a Th2 immune response upon egg antigen produc-tion. The main Th2 cytokine responsible for fibrosis is IL-13 (56). Some mediators such as IL-12, TNF- , NO, and gamma inter-feron (IFN-) prevent production of excess IL-13 during *S. man-soni* infection (9). For immunological assays, the present study investigated IL-6, IL-10, IL-12, and TNF- cytokines and NO pro-duction in the supernatants of macrophage cultures stimulated *in vitro* with LpQM-43, LpQM-45, LpQM-47, and LpQM-14 com-pounds.

In terms of cytokine production, statistically significant levels of TNF- were observed, compared to those of the negative con-trol, for all four compounds analyzed. In the case of LpQM-47, peak production of TNF- was observed after 24 h, decreased production was noted after 48 h, and there was no significant production after 72 h. LpQM-43 and LpQM-45 affected peak pro-duction after 48 h, and LpQM-14 had an effect after 72 h. These results demonstrate that the compounds analyzed stimulate a response with a Th1 cytokine profile. Some compounds that stimulate production of TNF- have shown antiparasitic activ-ity, including meglumine antimoniate, which has been shown to have antileishmania properties involving increased produc-tion of TNF- (57).

NO has been shown to be an important cytotoxic and cyto-static effector for a number of pathogens, including viruses, bac-teria, fungi, and parasites (58). It is implicated as an integral com-ponent of the host armament against invading parasites, and evidence has been put forward for the beneficial role of NO during helminthic infections. In the case of *Schistosoma mansoni*, for ex-ample, NO plays a role in regulation of egg-induced inflamma-tion, acting as an antifibrogenic substance and preventing hepa-tocyte death and widespread tissue damage, in addition to being toxic to the schistosomula (9, 59, 60). It is significant that schisto-somes are known to be more susceptible to oxidative stress than the hosts (61). The production of NO may also contribute to worm mortality by way of *S*-nitrosylation of cysteine proteases, given that schistosomes express cysteine proteases that play a role in digestion, reproduction, and protein turnover and that this appears to be a common and widespread mechanism (58, 62). Studies have also shown that compounds that induce the NO re-lease possess potential immunomodulatory properties (63–65). The present study found that LpQM-14 stimulated NO produc-tion for the three incubation times analyzed, while LpQM-45 stimulated production only after 48 h of exposure. This behavior may indicate the immuno-stimulant properties of these compounds, especially when it is noted that the same compounds caused production of TNF- .

Conclusions. To sum up, our results indicate that the thia-zoles, especially those containing a methoxyl or chloro group, are antiparasitic agents and that they were more potent than their analogs, the thiosemicarbazones. These compounds showed substantial schistosomicidal properties against adult *S. mansoni* worms, with a significant reduction in motility, severe alterations in the integument and mortality of worms, lower toxicity than the reference drug (PZQ), and production of nitric oxide, inhibiting oviposition. The present study revealed LpQM-45 to possess the most effective schistosomicidal properties, suggesting its use as a prototype for the development of new schistosomicidal compounds. The present findings provide a sound basis for further in-depth studies of the antischistosomal properties of phthalyl thiazoles, particularly LpQM-45. It is also important that, in view of the results obtained, further biological studies are needed to shed light on the mechanism(s) of schistosomicidal action.

ACKNOWLEDGMENTS

This study received financial support from the Conselho Nacional de Desenvolvimento Científico e Tecnológico (CPNq) and Fundação Oswaldo Cruz (FIOCRUZ). D.R.M.M. holds a FAPESB postdoctoral schol-arship.

We are also grateful to the Núcleo de Plataformas Tecnológicas of the Aggeu Magalhães Research Center.

REFERENCES

1. **Lescano SZ, Chieffi PP, Canhassi RR, Boulos M, Neto VA.** 2004. Antischistosomal activity of artemether in experimental *Schistosoma mansoni*. Rev. Saúde Pública **38:**71–75. http://dx.doi.org/10.1590/S0034-89102004000100010.
2. **Keiser J, Chollet J, Xiao SH, Mei JY, Jiao PY, Utzinger J, Tanner M.** 2009. Mefloquine—an aminoalcohol with promising antischistosomal properties in mice. PLoS Negl. Trop. Dis. **3:**e350. http://dx.doi.org/10.1371/journal.pntd.0000350.g001.
3. **Moraes J, Nascimento C, Lopes PO, Nakano E, Yamaguchi LF, Kato MJ, Kawano T.** 2011. *Schistosoma mansoni*: *In vitro* schistosomicidal ac-tivity of piplartine. Exp. Parasitol. **127:**357–364. http://dx.doi.org/10.1016 /j.exppara.2010.08.021.
4. **de Oliveira RN, Rehder VL, Santos Oliveira AS, Júnior IM, Carvalho JE, Ruiz AL, Jeraldo VL, Linhares AX, Allegretti SM.** 2012. *Schistosoma mansoni*: *in vitro* schistosomicidal activity of essential oil of Baccharistrimera (less) DC. Exp. Parasitol. **132:**135–143. http://dx.doi.org/10.1016/j.exppara.2012.06.005.
5. **WHO.** 2012. Schistosomiasis: epidemiological situation. World Health Organization, Geneva Switzerland. http://www.who.int/schistosomiasis/epidemiology/en/.
6. **Rollinson D, Knopp S, Levitz S, Stothard JR, Tchuenté LA, Garba A, Mohammed KA, Schur N, Person B, Colley DG, Utzinger J.** 2013. Time to set the agenda for schistosomiasis elimination. Acta Trop. **128:**423– 440. http://dx.doi.org/10.1016/j.actatropica.2012.04.013. http://dx.doi.org/10.1016/j.actatropica.2012.04.013.
7. **Gryseels B, Polman K, Clerinx J, Kestens L.** 2006. Human schistosomiasis. Lancet **368:**1106 –1118. http://dx.doi.org/10.1016/S0140-6736(06)69440-3.
8. **Pearce EJ, MacDonald AS.** 2002. The immunobiology of schistosomiasis. Nat. Rev. Immunol. **2:**499 –511. http://dx.doi.org/10.1038/nri843.
9. **Miranda MA, Kuehn CC, Cardoso JF, Oliveira LG, Magalhães LG, Tiossi RF, Rodrigues V, Zucolloto S, Prado JC, Jr, Bastos JK.** 2013. Immunomodulatory effect of the alkaloidic extract of *Solanumly lycocarpum* fruits in mice infected with *Schistosoma mansoni*. Exp. Parasitol. **133:**396 – 402. http://dx.doi.org/10.1016/j.exppara.2012.12.012.
10. **Stadecker MJ, Asahi H, Finger E, Hernandez HJ, Rutitzky LI, Sun J.** 2004. The immunobiology of Th1 polarization in high-pathology schisto-somiasis. Immunol. Rev. **201:**168 –179. http://dx.doi.org/10.1111/j.0105 -2896.2004.00197.
11. **Gonnert R, Andrews P.** 1977. Praziquantel, a new board-spectrum anti-schistosomal agent. Z. Parasitenkd. **52:**129 –150. http://dx.doi.org/10.1007/BF00389899.

12. **Katz N, Coelho PM.** 2008. Clinical therapy of schistosomiasis mansoni: the Brazilian contribution. Acta Trop. **108:**72–78. http://dx.doi.org/10.1016/j.actatropica.2008.05.006.
13. **Bertão HG, da Silva RA, Padilha RJ, de Azevedo Albuquerque MC, Rádis-Baptista G.** 2012. Ultrastructural analysis of miltefosine-induced surface membrane damage in adult *Schistosoma mansoni* BH strain worms. Parasitol. Res. **110:**2465–2473. http://dx.doi.org/10.1007/s00436 -011-2786-5.
14. **Ridi RE, Aboueldahab M, Tallima H, Salah M, Mahana Fawzi NS, Mohamed SH, Fahmy OM.** 2010. *In Vitro* and *in vivo* activities of arachi-donic acid against *Schistosoma mansoni* and *Schistosoma haematobium*. Antimicrob. Agents Chemother. **54:**3383–3389. http://dx.doi.org/10.1128 /AAC.00173-10.
15. **Holtfreter MC, Loebermanna M, Klammta S, Sombetzkia M, Bodammera P, Riebolda D, Kinzelbachb R, Reisinger EC.** 2011. *Schistosoma mansoni*: schistosomicidal effect of mefloquine and primaquine *in vitro*. Exp. Parasitol. **127:**270 –276. http://dx.doi.org/10.1016/j.exppara.2010.08.008.
16. **Liang YS, Coles GC, Doenhoff MJ, Southgate VR.** 2001. *In vitro* responses of praziquantel-resistant and -susceptible *Schistosoma mansoni* to praziquantel. Int. J. Parasitol. **31:**1227–1235. http://dx.doi.org/10.1016 /S0020-7519(01)00246-6.
17. **Cioli D, Pica-Mattoccia L.** 2003. Praziquantel. Parasitol. Res. **90**(Suppl 1)**:**S3–S9. http://dx.doi.org/10.1007/s00436-002-0751-z.
18. **Pica-Mattoccia L, Doenhoff MJ, Valle C, Basso A, Troiani AR, Liberti P, Festucci A, Guidi A, Cioli D.** 2009. Genetic analysis of decreased praziquantel sensitivity in a laboratory strain of *Schistosoma mansoni*. Acta Trop. **111:**82– 85. http://dx.doi.org/10.1016/j.actatropica.2009.01.012.
19. **Watts SD.** 1986. *Schistosoma mansoni*: Nitrothiazolines and the male tegument. Exp. Parasitol. **62:**157–168. http://dx.doi.org/10.1016/0014 -4894(86)90020-2.
20. **Pereira LH, Coelho PM, Costa JO, Mello RT.** 1995. Activity of 9-acri-danone-hydrazone drugs detected at the pre-postural phase, in the exper-imental *Schistosomiasis mansoni*. Mem. Inst. Oswaldo Cruz. **90:**425– 428. http://dx.doi.org/10.1590/S0074-02761995000300021.
21. **Beraldo H, Gambino D.** 2004. The wide pharmacological versatility of semicarbazones, thiosemicarbazones and their metal complexes. Mini Rev. Med. Chem. **4:**31–39. http://dx.doi.org/10.2174/1389557043487484.
22. **Duarte CD, Barreiro EJ, Fraga CA.** 2007. Privileged structures: a useful concept for the rational design of new lead drug candidates. Mini Rev. Med. Chem. **7:**1108 –1119. http://dx.doi.org/10.2174/138955707782331722.
23. **Kim BY, Ahn JB, Lee HW, Kang SK, Lee JH, Shin JS, Ahn SK, Hong CI, Yoon SS.** 2004. Synthesis and biological activity of novel substituted pyri-dines and purines containing 2,4-thiazolidinedione. Eur. J. Med. Chem. **39:**433– 447. http://dx.doi.org/10.1016/j.ejmech.2004.03.001.
24. **Taha H, Soliman ML.** 2007. Antischistosomal activity of 3-substituted-5-(2-aryl-2-oxoethyl)-2,4-dioxo-1,3-thiazolidine (Ro-354). Int. J. Agric. Biol. **9:**87–93.
25. **Sudo RT, Calasans-Maia JA, Galdino SL, Lima MC, Zapata-Sudo G, Hernandes MZ, Pitta IR.** 2010. Interaction of morphine with a new alpha2-adrenoceptor agonist in mice. J. Pain **11:**71–78. http://dx.doi.org/10.1016/j.jpain.2009.08.001.
26. **Orrling KM, Marzahn MR, Gutierrez-De-Teran H, Aqvist J, Dunn BM, Larhed M.** 2009. -Substituted norstatines as the transition-state mimic in inhibitors of multiple digestive vacuole malaria aspartic proteases. Bioorg. Med. Chem. **17:**5933–5949. http://dx.doi.org/10.1016/j.bmc.2009.06.065.
27. **Sanemitsu Y, Kawamura S, Satoh J, Katayama T, Hashimoto S.** 2006. Synthesis and herbicidal activity of 2-acylimino-3-phenyl-1,3-thiazolines—a new family of bleaching herbicides. J. Pestic. Sci. **31:**305– 310. http://dx.doi.org/10.1584/jpestics.31.305.
28. **Ami E, Nakahara K, Sato A, Nguyen JT, Hidaka K, Hamada Y, Nakatani S, Kimura T, Hayashi Y, Kiso Y.** 2007. Synthesis and antiviral property of allophenylnorstatine-based HIV protease inhibitors incorporating d-cys-teine derivatives as P2/P3moieties. Bioorg. Med. Chem. Lett. **17:**4213– 4217. http://dx.doi.org/10.1016/j.bmcl.2007.05.039.
29. **Murugan R, Anbazhagan S, Narayanan SS.** 2009. Synthesis and *in vivo* antidiabetic activity of novel dispiropyrrolidines through [3 2] cycload-dition reactions with thiazolidinedione and rhodanine derivatives. Eur. J. Med. Chem. **44:**3272–3279. http://dx.doi.org/10.1016/j.ejmech.2009.03.035.
30. **Shih MH, Ke FY.** 2004. Syntheses and evaluation of antioxidant activity of sydnonyl substituted thiazolidinone and thiazoline derivatives. Bioorg. Med. Chem. **12:**4633– 4643. http://dx.doi.org/10.1016/j.bmc.2004.06.033.
31. **Gouda MA, Berghot MA, El-Ghani GE, Abd Khalil AM.** 2010. Synthesis and antimicrobial activities of some new thiazole and pyrazole derivatives based on 4,5,6,7-tetrahydrobenzothiophene moiety. Eur. J. Med. Chem. **45:**1338 –1345. http://dx.doi.org/10.1016/j.ejmech.2009.12.020.
32. **Bharti SK, Nath G, Tilak R, Singh SK.** 2010. Synthesis, anti-bacterial and anti-fungal activities of some novel Schiff bases containing 2,4-disubstituted thiazole ring. Eur. J. Med. Chem. **45:**651– 660. http://dx.doi.org/10.1016/j.ejmech.2009.11.008.
33. **Tomasic´ T, Zidar N, Kovac A, Turk S, Simcic M, Blanot D, Müller-Premru M, Filipic M, Grdadolnik SG, Zega A, Anderluh M, Gobec S, Kikelj D, Peterlin Masic L.** 2010. 5-Benzylidenethiazolidin-4-ones as multitarget inhibitors of bacterial mur ligases. ChemMedChem **5:**286 – 295. http://dx.doi.org/10.1002/cmdc.200900449.
34. **Giri RS, Thaker HM, Giordano T, Williams J, Rogers D, Sudersanam V, Vasu KK.** 2009. Design, synthesis and characterization of novel 2-(2,4-disubstituted-thiazole-5-yl)-3-aryl-3*H*-quinazoline-4-one derivatives as inhibitors of NF- B and AP-1 mediated transcription activation and as potential anti-inflammatory agents. Eur. J. Med. Chem. **44:**2184 –2189. http://dx.doi.org/10.1016/j.ejmech.2008.10.031.
35. **Shiradkar M, Venkata G, Kumar S, Dasai V, Tatikonda S, Chakravarthy AK, Shah R.** 2007. Clubbed triazoles: A novel approach to antitubercular drugs. Eur. J. Med. Chem. **42:**807– 816. http://dx.doi.org/10.1016/j.ejmech.2006.12.001.
36. **Tapia RA, Alegria L, Pessoa CD, Salas C, Cortés MJ, Cortés MJ, Valder-rama JA, Sarciron ME, Pautet F, Walchshofer N, Fillion H.** 2003. Synthesis and antiprotozoal activity of naphthofuranquinones and naphthothiophene-quinones containing a fused thiazole ring. Bioorg. Med. Chem. **11:**2175– 2182. http://dx.doi.org/10.1016/S0968-0896(03)00122-6.
37. **Contino-Pépin C, Parat A, Patinote C, Roscoe WA, Karlik SJ, Pucci B.** 2010. Thalidomide derivatives for the treatment of neuroinflammation. ChemMedChem. **5:**2057–2064. http://dx.doi.org/10.1002/cmdc.201000326.
38. **Hashimoto Y.** 2002. Structural development of biological response modifiers based on thalidomide. Bioorg. Med. Chem. **10:**461– 479. http://dx.doi.org/10.1016/S0968-0896(01)00308-X.
39. **Moreira DR, Costa SP, Hernandes MZ, Rabello MM, de Oliveira Filho GB, de Melo CM, da Rocha LF, de Simone CA, Ferreira RS, Fradico JR, Meira CS, Guimarães ET, Srivastava RM, Pereira VR, Soares MB, Leite AC.** 2012. Structural investigation of anti-*Trypanosoma cruzi* 2-imi-nothiazolidin-4-ones allows the identification of agents with efficacy in infected mice. J. Med. Chem. **55:**10918 – 10936. http://dx.doi.org/10.1021 /jm301518v.
40. **Pessoa C, Ferreira PM, Lotufo LV, de Moraes MO, Cavalcanti SM, Coêlho LC, Hernandes MZ, Leite AC, De Simone CA, Costa VM, Souza VM.** 2010. Discovery of phthalimides as immunomodulatory and antitu-mor drug prototypes. ChemMedChem **5:**523–528. http://dx.doi.org/10.1002/cmdc.200900525.
41. **Duvall RH, De Witt W.** 1967. An improved perfusion technique for recovering adult schistosomes from laboratory animals. Am. J. Trop. Med. Hyg. **16:**483– 486.
42. **Pereira VR, Lorena VM, Da Silva AP, Coutinho EM, Silvas ED, Ferreira AG, Miranda P, Krieger MA, Goldenberg S, Soares MB, Correa-Oliveira R, Gomes YM.** 2004. Immunization with cytoplasmic repetitive antigen and flagellar repetitive antigen of *Trypanosoma cruzi* stimulates a cellular immune response in mice. Parasitology **129:**563–570. http://dx.doi.org/10.1017/S0031182004006043.
43. **Ding AH, Nathan CF, Stuehr D.** 1988. Release of reactive nitrogen intermediates and reactive oxygen intermediates from mouse peritoneal macrophages: comparison of activating cytokines and evidence for independent production. J. Immunol. **141:**2407–2412.
44. **Ramirez B, Bickle Q, Yousif F, Fakorede F, Mouries MA, Nwaka S.** 2007. Schistosomes: challenges in compound screening. Expert Opin. Drug Discov. **2**(Suppl. 1)**:**S53–S61. http://dx.doi.org/10.1517/17460441.2.S1.S53.
45. **Moreira DR, Leite AC, dos Santos RR, Soares MB.** 2009. Approaches for the development of new anti-*Trypanosoma cruzi* agents. Curr. Drug Tar-gets **10:**212–231. http://dx.doi.org/10.2174/138945009787581140.
46. **Pereira HM, Berdini V, Ferri MR, Cleasby A, Garratt RC.** 2010. Crystal structure of *Schistosoma* purine nucleoside phosphorylase complexed with a novel monocyclic inhibitor. Acta Trop. **114:**97–102. http://dx.doi.org/10.1016/j.actatropica.2010.01.010.
47. **Pitta MG, Silva AC, Neves JK, Silva PG, Irmão JI, Malagueño E, Santana JV, Lima MC, Galdino SL, Pitta IR, Albuquerque MC.** 2006. New imidazolidinic bioisosters: potential candidates for antischistosomal

drugs. Mem. Inst. Oswaldo Cruz **101**(Suppl I)**:**313–316. http://dx.doi.org /10.1590/S0074-02762006000900049.

48. **Oliveira SM, Albuquerque MC, Pitta MG, Malagueño E, Santana JV, Lima MC, Pitta IR, Galdino SL.** 2004. A resposta do *Schistosoma mansoni* mantido *in vitro* frente a derivados imidazolidinônicos. Acta Farm. Bo-naerense **23:**343–348.
49. **Sulaiman SM, Ali HM, Homeida MM, Bennett JL.** 1989. Efficacy of a new Hoffmann-La Roche compound (RO-15-5458) against *Schistosoma mansoni* (Gezira strain, Sudan) in vervet monkeys (Cercopithecusa-ethiops). Trop. Med. Parasitol. **40:**335–336.
50. **Manneck T, Haggenmuller Y, Keiser J.** 2010. Morphological effects and tegumental alterations induced by mefloquine on schistosomula and adult flukes of *Schistosoma mansoni*. Parasitology **137:**85–98. http://dx.doi.org /10.1017/S0031182009990965.
51. **Mohamed SH, Fawzi SM.** 1997. Scanning electron microscopy on adults of *Schistosoma mansoni* treated *in vivo* with praziquantel and Ro-15 (5458). Qatar University Sci. J. **17:**439 – 458.
52. **Fawzi SM.** 1999. Ultrastructural studies on the effect of antischistosomal drug Ro15-5458 on the tegument of male *Schistosoma mansoni*. Egypt Zool. **33:**21–31.
53. **Xiao S, Shen B, Utzinger J, Chollet J, Tanner M.** 2002. Ultrastructural alterations in adult *Schistosoma mansoni* caused by artemether. Mem. Inst. Oswaldo Cruz **97:**717–724. http://dx.doi.org/10.1590/S0074-02762002000500023.
54. **Neves JK, de Lima MC, Pereira VR, de Melo CM, Peixoto CA, Pitta Ida R, Albuquerque MC, Galdino SL.** 2011. Antischistosomal action of thioxo-imidazolidine compounds: an ultrastructural and cytotoxicity study. Exp. Parasi-tol. **128:**82–90. http://dx.doi.org/10.1016/j.exppara.2011.01.021.
55. **Xiao SH, Booth M, Tanner M.** 2000. The prophylactic effects of artemether against *Schistosoma japonicum* infections. Parasitol. Today **16:** 122–126. http://dx.doi.org/10.1016/S0169-4758(99)01601-4.
56. **Fallon PG, Richardson EJ, McKenzie GJ, McKenzie ANJ.** 2000. Schis-tosome infection of transgenic mice defines distinct and contrasting pathogenic roles for IL-4 and IL-13: IL-13 is a profibrotic agent. J. Immu-nol. **164:**2585–2591.
57. **Muniz-Junqueira MI, De Paula-Coelho VN.** 2008. Meglumine antimonate directly increases phagocytosis, superoxide anion and TNF-production, but only via TNF- it indirectly increases nitric oxide production by phagocytes of healthy individuals, *in vitro*. Int. Immunopharmacol. **8:**1633–1638. http://dx.doi.org/10.1016/j.intimp.2008.07.011.
58. **Colasanti M, Gradoni L, Mattu M, Persichini T, Salvati L, Venturini G, Ascenzi P.** 2002. Molecular bases for the anti-parasitic effect of NO (re-view). Int. J. Mol. Med. **9:**131–134.
59. **Cioli D, Valle C, Angelucci F, Miele AE.** 2008. Will new antischistosomal drugs finally emerge? Trends Parasitol. **24:**379 –382. http://dx.doi.org/10 .1016/j.pt.2008.05.006.
60. **Brunet LR.** 2001. Nitric oxide in parasitic infections. Int. Immunopharmacol. **1:**1457–1467. http://dx.doi.org/10.1016/S1567-5769(01)00090-X.
61. **Kovacic P, James RA, Douglas LR, Jawdosiuk M, Ryan MD.** 1989. Reduction potentials of anthelmintic drugs: possible relationship to activ-ity. Free Radic. Biol. Med. **6:**131–139. http://dx.doi.org/10.1016/0891 -5849(89)90110-X.
62. **Abdulla MH, Lim KC, Sajid M, Mckerrow JH, Caffrey CR.** 2007. *Schistosomiasis mansoni*: novel chemotherapy using a cysteine protease inhibitor. PLoS Med. **4:**e14. http://dx.doi.org/10.1371/journal.pmed .0040014.
63. **Neves JK, Botelho SP, de Melo CM, Pereira VR, de Lima MC, Pitta Ida R, Albuquerque MC, Galdino SL.** 2010. Biological and immunological activity of new imidazolidines against adult worms of *Schistosoma man-soni*. Parasitol. Res. **107:**531–538. http://dx.doi.org/10.1007/s00436-010 -1886-y.
64. **Curtin JF, Donovan M, Cotter TG.** 2002. Regulation and measurement of oxidative stress in apoptosis. J. Immunol. Methods **265:**49 –72. http: //dx.doi.org/10.1016/S0022-1759(02)00070-4.
65. **Korhonen R, Kosonen O, Hämäläinen M, Moilanen E.** 2008. Nitric oxide-releasing compounds inhibit the production of interleukin-2, -4 and -10 in activated human lymphocytes. Basic Clin. Pharmacol. Toxicol. **103:**322–328. http://dx.doi.org/10.1111/j.1742-7843.2008.00275.x.

APÊNDICE F -

Conformational restriction of aryl thiosemicarbazones produces potent and selective anti-*Trypanosoma cruzi* compounds which induce apoptotic parasite death

European Journal of Medicinal Chemistry 75 (2014) 467e478

Contents lists available at ScienceDirect

European Journal of Medicinal Chemistry

journalhomepage:http://www.elsevier.com/locate/ejmech

Original article

Conformational restriction of aryl thiosemicarbazones produces potent and selective anti-Trypanosoma cruzi compounds which induce apoptotic parasite death

Diogo Rodrigo Magalhaes Moreira [a, *], Ana Daura Travassos de Oliveira [b], Paulo André Teixeira de Moraes Gomes [b], Carlos Alberto de Simone [c], Filipe Silva Villela [d], Rafaela Salgado Ferreira [d], Aline Caroline da Silva [e], Thiago André Ramos dos Santos [e], Maria Carolina Accioly Brelaz de Castro [e], Valéria Rego Alves Pereira [e], Ana Cristina Lima Leite [b, *]

[a] Fundação Oswaldo Cruz, Centro de Pesquisas Gonçalo Moniz, CEP 40296-710 Salvador, BA, Brazil
[b] Universidade Federal de Pernambuco, Departamento de Ciências Farmacêuticas, CEP 50740-520 Recife, PE, Brazil
[c] Universidade de São Paulo, Instituto de Física de São Carlos, CEP 13560-970 São Carlos, SP, Brazil
[d] Universidade Federal de Minas Gerais, Departamento de Bioquímica e Imunologia, CEP 31270-901 Belo Horizonte, MG, Brazil
[e] Fundação Oswaldo Cruz, Centro de Pesquisas Aggeu Magalhães, CEP 50670-420 Recife, PE, Brazil

article info

Article history:
Received 18 November 2013
Received in revised form 30
January 2014
Accepted 2 February 2014 Available
online 3 February 2014

Keywords:
Chagas disease
Trypanosoma cruzi
Thiosemicarbazones
Hydrazones Conformational
restriction Apoptosis

abstract

Chagas disease, caused by Trypanosoma cruzi, is a life-threatening infection leading to approximately 12,000 deaths per year. T. cruzi is susceptible to thiosemicarbazones, making this class of compounds appealing for drug development. Previously, the homologation of aryl thiosemicarbazones resulted in an increase in anti-T. cruzi activity in comparison to aryl thiosemicarbazones without a spacer group. Here, we report the structural planning, synthesis and anti-T. cruzi evaluation of new aryl thiosemicarbazones (9aex), designed as more conformationally restricted compounds. By varying substituents attached to the phenyl ring, substituents were observed to retain, enhance or greatly increase the anti-T. cruzi ac-tivity, in comparison to the nonsubstituted derivative. In most cases, hydrophobic and bulky substituents, such as bromo, biphenyl and phenoxyl groups, greatly increased antiparasitic activity. Specifically, thiosemicarbazones were identified that inhibit the epimastigote proliferation and were toxic for trypomastigotes without affecting mouse splenocytes viability. The most potent anti-T. cruzi thio-semicarbazones were evaluated against cruzain. However, inhibition of this enzyme was not observed, suggesting that the compounds work through another mechanism. In addition, examination of T. cruzi cell death showed that these thiosemicarbazones induce apoptosis. In conclusion, the structural design executed within the series of aryl thiosemicarbazones (9aex) led to the identification of new potent anti-T. cruzi agents, such as compounds (9h) and (9r), which greatly inhibited epimastigote proliferation, and demonstrated a toxicity for trypomastigotes, but not for splenocytes. Mechanistically, these compounds do not inhibit the cruzain, but induce T. cruzi cell death by an apoptotic process.

1. Introduction

Chagas disease, caused by the flagellate protozoan Trypanosoma cruzi, affects approximately 10 million people in Latin America [1]. Currently, the only drug in use is nitroheterocyclic benznidazole (LAFEPE, Brazil), which is effective in curing the disease in the acute phase, but is less effective in patients that progressed to the chronic phase [2,3]. Furthermore, benznidazole is less than ideal due to the fact that it causes severe side effects, leading to treatment inter-ruption in a large number of patients [4]. In fact, Chagas disease is considered to be 'the most concerning' infectious tropical disease in Latin America [5]. Thus, there is a need to identify new pharma-ceuticals for its treatment.

To address this need, a number of molecular targets for anti-T. cruzi drugs have been investigated, increasing the quality of drug identification for Chagas disease treatment. Examples of such

* Corresponding authors.
E-mail addresses: diogollucio@gmail.com, diogollucio@yahoo.com.br (D.R. Magalhaes Moreira), ana.leite@pq.cnpq.br (A.C.L. Leite).

0223-5234/$ e see front matter 2014 Elsevier Masson SAS. All rights reserved.
http://dx.doi.org/10.1016/j.ejmech.2014.02.001

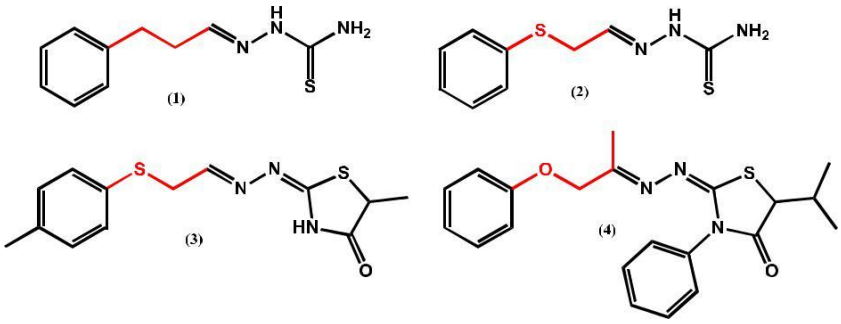

Fig. 1. Structure of thiosemicarbazones (1), (2) and thiazolidinones (3) and (4) previously identified as anti-T. cruzi agents [40e43]. Red lines highlight the spacer groups. (For interpretation of the references to color in this figure legend, the reader is referred to the web version of this article.)

targets are the lanosterol 14 a-demethylase [6], trypanothione reductase [7], cruzain [8], trans-sialidase [9] and phosphatidylino-sitol 3-kinase [10]. By using structure-based drug design, two small-molecules were recently developed and are now considered strong drug candidates: K11777, a vinyl sulfone peptide that in-hibits cruzain [11], and VNI, an oxadiazole derivative inhibitor of 14-a-demethylase activity [12,13]. These compounds are likely to enter into clinical trials; however, the chances of any drug being approved in the clinical stage are very low. Additionally, with the goal of avoiding the development of resistant T. cruzi strains, there is a necessity for combined drug therapy [14,15]. Therefore, the number of potential drug candidates must be enhanced. Given the outcomes observed for K11777 and VNI as anti-T. cruzi agents, the design of compounds to inhibit cruzain and the 14-a-demethylase activity have received special attention [16,17].

Cruzain, the major trypanosomal cysteine protease, is involved during the parasite invasion, differentiation and proliferation in host cells [18]. Specifically, it is responsible for degrading host cell proteins, and therefore contributing to the outcome of the infection [19]. Regarding the identification of cruzain inhibitors, most of the efforts have been conducted through the investigation of peptides and peptide-like compounds, such as ureas [20,21], hydrazones [22e25], triazoles [26,27] and thiosemicarbazones [28e30]. Thio-semicarbazones were originally developed as potential cathepsin-L inhibitors, one of the principal proteases involved in cancer cells [28]. However, based on the homology and similar biochemical properties between cathepsin-L and cruzain, thiosemicarbazones were investigated as a potential class of cruzain inhibitors. Later on, aryl thiosemicarbazones were found to be a class of anti-T. cruzi compounds that inhibits cruzain activity [29,30].

The general binding mode for aryl thiosemicarbazones with cruzain involves covalent binding of a thioamide group to Cys25 amino acid, as well as location of the aryl group within a deep hydrophobic pocket [30,31]. Based on this model, a number of molecular modifications have been investigated, including bis-thi-osemicarbazones, heterocyclic-derived thiosemicarbazones, thio-semicarbazones containing bioreductive groups and metallic complexes [32e37]. This model suggests that aryl thio-semicarbazones contain two different structural determinants and therefore the presence of a spacer group (i.e., the homologation strategy) [38,39] between the aryl group and thiosemicarbazone is a feasible plan to enhance potency of the anti-T. cruzi and cruzain activity.

Our group has observed that the use of homologation strategy produces thiosemicarbazones with enhanced anti-T. cruzi activity in comparison to thiosemicarbazones without a spacer group. Thiosemicarbazones (1) and (2) exhibited higher anti-T. cruzi ac-tivity when compared to their respected analogs lacking a spacer group [40,41]. As limitation, these compounds displayed lower antiparasitic activity as well low selectivity indexes than benzni-dazole. The same strategy was employed in thiosemicarbazone bioisosters, leading to the identification of potent anti-T. cruzi thiazolidinones, exemplified by compounds (3) and (4) (Fig. 1) [42,43].

Recent studies have demonstrated examples of the homologa-tion strategy for drug design by using spacer groups with some degree of conformational restriction (i.e., high rotational energy barrier) [44e48]. The preparation of more conformationally restricted N-acylhydrazones, as well as thiosemicarbazones, has produced compounds with enhanced antiparasitic activity [49,50]. Based on these findings, we hypothesized that applying this strat-egy would increase the anti-T. cruzi activity for the compound (1) chemical class. Therefore, we selected the alkoxyl group displayed in Fig. 2 as the spacer group for aryl thiosemicarbazone homolo-gation, which would increase molecular rigidity, as well as rapidly enable synthesis of multiple derivatives.

Here, we used the alkoxyl spacer group to prepare a new series of aryl thiosemicarbazones (9aex) (Fig. 2). A range of substituents were attached to the phenyl ring to examine their role in terms of electronic and steric contribution to the anti-T. cruzi activity. First, we prepared 4-substituted phenyl derivatives, followed by prepa-ration of derivatives with one substituent at position 3- or 2- in the phenyl ring. Derivatives containing two substituents attached to the phenyl ring were synthesized, as well as the replacement of a phenyl by a naphthyl ring. The substituents were selected based on the Hammett Rho values as well as the hydrophobic parameter Pi, therefore, enabling to examine the substituent effect for the aryl reactivity. Evaluation of the anti-T. cruzi and cruzain activity for the compounds (9aex) led to the identification of a number of struc-tureeactivity relationships, which ultimately resulted to the iden-tification of new compounds equally or more potent than benznidazole.

2. Results

2.1. Synthesis

The synthetic procedures employed in aryl thiosemicarbazones (9aex) preparation is shown in Scheme 1. First, the phenolic compounds (5aex) reacted with 3-chloro-2-butanone (6) in basic conditions at room temperature, similar to previously described protocol [51]. After 12 h of reaction, b-ketoether (7aex) compounds were obtained with yields varying from 66 to 99%. Compounds (7aex) were then reacted with thiosemicarbazide (8) and catalytic HCl in an ultrasound bath at room temperature [52]. After 2 h, thiosemicarbazones (9aex) precipitated in the reaction mixture, which were collected by simple filtration. All thiosemicarbazones (9aex) were recrystallized and obtained at an acceptable purity

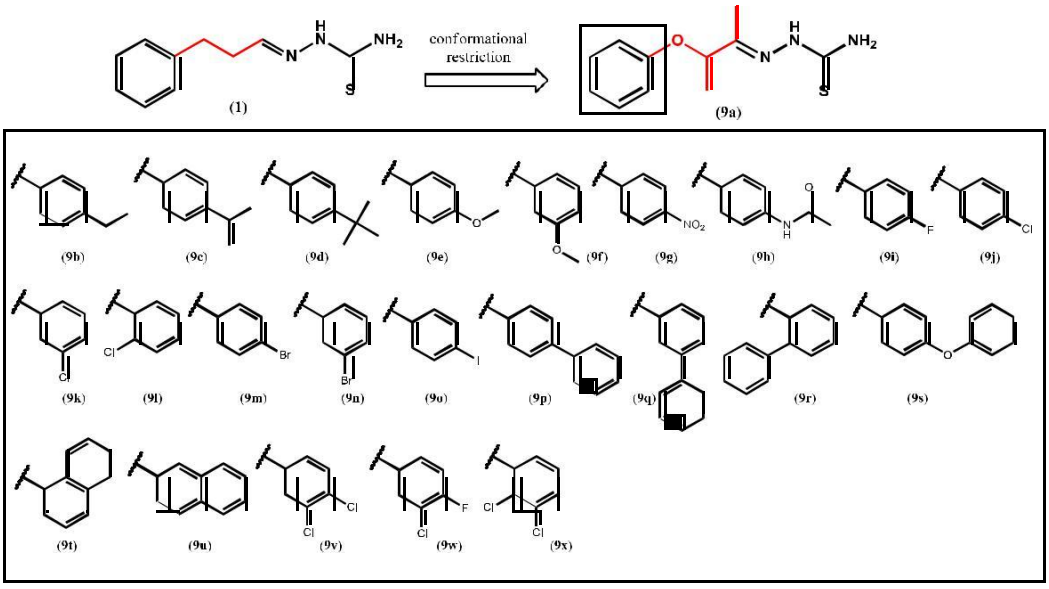

Fig. 2. Conformational restriction of compound (1) leading to the design of (9a). Structure of the aryl groups employed during the aryl thiosemicarbazones (9aex). The red highlights the spacer groups. (For interpretation of the references to color in this figure legend, the reader is referred to the web version of this article.)

(>95%) in yields ranging from 36 to 98%. The structures were determined by ^{1}H and ^{13}C NMR, DEPT, IR and high-resolution mass.

Two diastereoisomers can be produced from these thio-semicarbazones (Fig. 3). However, when the ^{1}H NMR spectra and thin-layer chromatography were analyzed, only the formation of one isomer was observed. These results are consistent with the synthetic procedures, since the last reaction step was performed under room temperature. To determine its configuration, single crystals of the thiosemicarbazone (9a) were analyzed by X-ray crystallography. As we can see from the Ortep-3 diagrams in Fig. 3, the C(2) atom is antiperiplanar to N(2) atom, therefore the thio-semicarbazone (9a) has an E-geometry in the solid state. The same kind of assignment has been described in the literature [53]. In the ^{1}H NMR spectra of all compounds (9aex), the chemical shift of the methine proton C(2) appears at a narrow range, from 4.88 to 5.15 ppm. Based on these findings, it is reasonable to suggest that thiosemicarbazones have an E-geometry. Due to the presence of asymmetric C1 carbon, specific optical rotation was examined and revealed that all analyzed thiosemicarbazones have small optical rotation activity, suggesting that the enantiomeric excess in these compounds is low.

2.2. Pharmacological evaluation

After structural characterization of aryl thiosemicarbazones (9aex), the antiparasitic and host cell cytotoxicity was determined. First, compounds were evaluated by their ability to inhibit the epimastigote proliferation of T. cruzi Dm28 strain, as well as the toxicity against trypomastigotes of Y strain. Results were respec-tively expressed in terms of IC_{50} and CC_{50} values. Following this, cytotoxicity was determined in splenocytes of BALB/c mouse and results were expressed as the highest non-toxic concentration (HNC) and given in mM. Benznidazole and nifurtimox were used as reference anti-T. cruzi drugs (Table 1). Benznidazole exhibited a CC_{50} ¼ 6.2 mM against trypomastigotes. The cutoff between active and inactive compounds was determined using the CC_{50} ¼ 6.2 mM against trypomastigotes, and were considered active anti-T. cruzi agents [54].

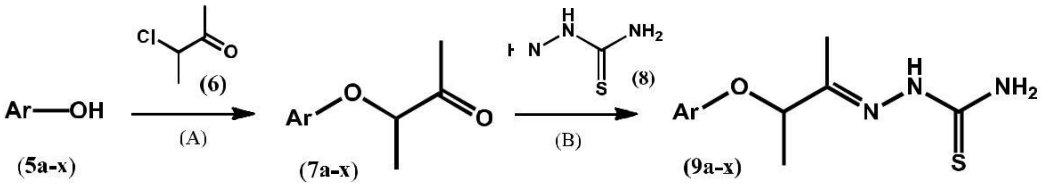

Comp.	Ar	Comp.	Ar	Comp.	Ar
(a)	C_6H_5				
(b)	4-EtC_6H_4	(i)	4-FC_6H_4	(q)	3-(C_6H_5)C_6H_4
(c)	4-*i*PrC_6H_4	(j)	4-ClC_6H_4	(r)	2-(C_6H_5)C_6H_4
(d)	4-*t*BuC_6H_4	(k)	3-ClC_6H_4	(s)	4-(C_6H_5O)C_6H_4
(e)	4-McOC_6H_4	(l)	2-ClC_6H_4	(t)	α-Naphthyl
(f)	3-McOC_6H_4	(m)	4-BrC_6H_4	(u)	β-Naphthyl
(g)	4-$NO_2C_6H_4$	(n)	3-BrC_6H_4	(v)	3,4-*di*ClC_6H_3
(h)	4-(Ac)NHC_6H_4	(o)	4-IC_6H_4	(w)	3-Cl,4-FC_6H_3
		(p)	4-(C_6H_5)C_6H_4	(x)	2,3-*di*ClC_6H_3

Scheme 1. Synthesis of aryl thiosemicarbazones (9aex). Reagents and conditions: (A) K_2CO_3, KI, butanone, r.t., 12 h, yields from 66 to 99%. (B) HCl, EtOH, ultrasound bath for 2 h, yields from 36 to 98%. Ac ¼ acetyl, iPr ¼ isopropyl, tBu ¼ tertbutyl.

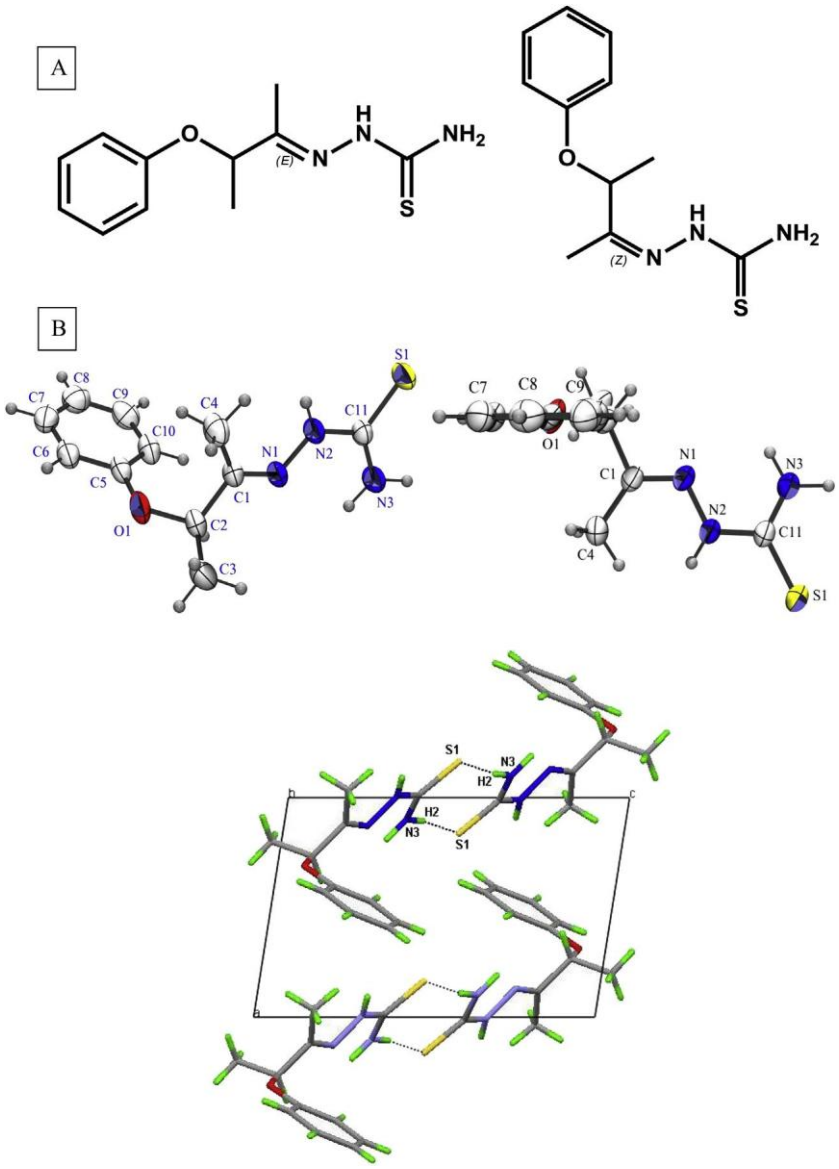

Fig. 3. (A) Representations for the (9a) thiosemicarbazone diastereoisomers. (B) Ortep-3 diagrams with atom-labeling scheme of (9a) and its unit cell showing the formation of centrosymmetric dimmers. Displacement ellipsoids are shown at the 50% probability level.

Regarding the activity against trypomastigotes, nonsubstituted phenyl thiosemicarbazone (9a) was inactive. In comparison to (9a), anti-T. cruzi activity was enhanced when an alkyl group was attached to 4-position of the phenyl ring. The 4-ethylphenyl de-rivative (9b) was 6-times more potent than (9a). When a 4-iso-propyl (9c) or a 4-tertbutyl (9d) substituent is attached to the phenyl ring, the resulting thiosemicarbazones were twice as potent as benznidazole. The 4-methoxyphenyl derivative (9e) was inac-tive, while its isomer (3-methoxyphenyl, 9f) was active. However, the insertion of a 3-methoxyphenyl was not enough to produce a compound more potent than benznidazole. In comparison to a nonsubstituted phenyl thiosemicarbazone (9a), a 4-nitro group (9g) enhanced the anti-T. cruzi activity. More remarkably, attaching an acetamide group (9h) greatly increased the anti-T. cruzi activity. In fact, the potency of (9h) against trypomastigotes was very similar to that observed for nifurtimox and twice as potent as benznidazole.

We evaluated the activity against trypomastigotes for thio-semicarbazones containing halogen atoms attached to the phenyl ring. In these conditions, 4-fluorophenyl (9i) and 4-chlorophenyl (9j) derivatives were inactive. However, when the position of the chloro atom was changed, the potency increased with the following order: (2-Cl, 9l) > (3-Cl, 9k) > (4-Cl, 9j). Bromo atom attachment greatly increases the activity, regardless of its position in the phenyl ring. Likewise, attaching an iodo atom (9o) greatly increases the activity in comparison to nonsubstituted phenyl thio-semicarbazone (9a). Based on the results with bromo and iodo, we evaluated compounds containing biphenyl groups. Placing a biphenyl greatly increased activity against trypomastigotes. When we analyzed the CC_{50} values for compounds (4^0-phenyl, 9p), (3^0-phenyl, 9q) and (2^0-phenyl, 9r), we observed that the position of the biphenyl group did not affect potency. Interestingly, the 4-(phe-noxy)phenyl derivative (9s) was very active against trypomasti-gotes, exhibiting a CC_{50} value in the same range of the thiosemicarbazones containing biphenyl groups.

Next, we tested thiosemicarbazones containing a naphthyl, as opposed to a phenyl ring. While the phenyl thiosemicarbazone (9a) is inactive, the a-naphthyl (9t) and the b-naphthyl (9u)

Table 1
Anti-T. cruzi activity and host cell toxicity for thiosemicarbazones (9aex).

Compd.	Ar	T. cruzi		Cytotoxicity, HNC (mM)[c]
		IC_{50} (mM) epimastigotes[a]	CC_{50} (mM) trypomastigotes[b]	
(9a)	C_6H_5	26.1	27.3	210.6
(9b)	4-EtC_6H_4	11.6	4.6	18.8
(9c)	4-$iPrC_6H_4$	5.9	1.5	17.9
(9d)	4-$tBuC_6H_4$	4.6	1.4	17.0
(9e)	4-$MeOC_6H_4$	27.6	26.8	93.5
(9f)	3-$MeOC_6H_4$	6.8	6.2	37.4
(9g)	4-$NO_2C_6H_4$	176.9	5.9	88.5
(9h)	4-(Ac)NHC_6H_4	71.5	1.4	>339.7 (350)[d]
(9i)	4-FC_6H_4	86.4	23.2	>391.8
(9j)	4-ClC_6H_4	13.5	22.8	92.0
(9k)	3-ClC_6H_4	45.8	5.5	36.8
(9l)	2-ClC_6H_4	10.3	1.5	36.8
(9m)	4-BrC_6H_4	20.1	3.9	31.6
(9n)	3-BrC_6H_4	5.8	4.5	31.6
(9o)	4-IC_6H_4	4.9	1.1	13.7
(9p)	4-(C_6H_5)C_6H_4	4.5	1.3	15.9
(9q)	3-(C_6H_5)C_6H_4	2.2	1.3	31.9
(9r)	2-(C_6H_5)C_6H_4	2.2	1.1	31.9 (50)[d]
(9s)	4-(C_6H_5O)C_6H_4	ND	1.3	30.3
(9t)	a-Naphthyl	4.9	1.5	34.8
(9u)	b-Naphthyl	17.9	5.6	34.8
(9v)	3,4-diClC_6H_3	4.4	4.4	16.3
(9w)	3-Cl-4-FC_6H_3	ND	3.5	34.5
(9x)	2,3-diClC_6H_3	2.2	11.9	32.6
Bdz	e	48.8	6.2	96.0
Nfx	e	5.7	2.7	3.4

HNC ¼ highest non-cytotoxic concentration.

Bdz ¼ benznidazole.

Nfx ¼ nifurtimox.

ND ¼ not determined.

[a] Determined 5 days after incubation with compounds, using Dm28c epimastigotes.

[b] Determined 24 h after incubation with compounds, using Y strain trypomastigotes.

[c] Cell viability of BALB/c mouse splenocytes determined 24 h after treatment.

[d] In parenthesis, CC_{50} values against mouse splenocytes. IC_{50} ¼ inhibitory concentration for 50%. CC_{50} ¼ cytotoxic concentration for 50%. CC_{50} and IC_{50} values were calculated using concentrations in triplicate and experiment was repeated, only values with a standard deviation < 10% mean were considered.

thiosemicarbazones were active. In addition to evaluating com-pounds with a monosubstituted phenyl ring, we tested the thio-semicarbazones containing two substituents attached to the phenyl ring. While the 4-chlorophenyl (9j) was inactive, the 3,4-dichlor-ophenyl derivative (9v) was active. The same was observed for the 3-chloro-4-fluorophenyl derivative (9w). However, attaching chloro atoms at the positions 2- and 3- (9x) slightly decreased the activity against trypomastigotes in comparison to the 3,4-dichlor-ophenyl derivative (9v).

Having ascertained the antiparasitic activity for trypomasti-gotes, we analyzed the antiproliferative activity against epi-mastigotes. Excluding (9g) and (9h), most compounds which were active against trypomastigotes were also able to inhibit epi-mastigote proliferation. Regarding cytotoxicity in splenocytes, some of the thiosemicarbazones that were active against T. cruzi exhibited low cytotoxicity. For instance, compounds (9h), (9r), (9s) and (9t) had CC_{50} < 1.5 mM against trypomastigotes, while they were non-toxic for splenocytes at concentrations up to 30 mM. Compounds (9c), (9d), (9o), (9p) and (9v) were the most cytotoxic thiosemicarbazones for splenocytes, albeit less cytotoxic than nifurtimox. We determined the selectivity index (CC_{50} splenocytes/ CC_{50} trypomastigotes) for compound (9h) and (9r). They displayed indexes 250 and 45, respectively.

We investigated the inhibitory activity for thiosemicarbazones (9aex) against cruzain. To this, we selected thiosemicarbazones with CC_{50} < 5.0 mM against trypomastigotes (i.e., derivatives 9g, 9h, 9k, 9m, 9n, 9o, 9p, 9s, 9t). For comparison reasons only, we included the nonsubstituted phenyl derivative (9a). We measured cruzain mediated enzymatic activity inhibition by using an assay based on competition with the substrate Z-FR-AMC [55].

Compounds (9a), (9h), (9k), (9m), (9n), (9o) and (9s) were screened at 100 mM, while compounds (9g), (9p) and (9t) were tested at 50 mM, the maximum concentration at which they were soluble in the assay buffer. However, cruzain inhibition by these compounds was not observed (data not shown).

To understand the parasite death process caused by thio-semicarbazones, untreated and treated trypomastigotes were treated for 24 h of incubation and then double labeled with annexin V-fluorescein isothiocyanate (FITC) and propidium iodide (PI) [56]. For this assay, compounds (9h, 9r) and (9k) were selected because they contain electron-donor and electron-withdrawing sub-stituents, respectively, and assayed in concentrations equal to the CC_{25} and CC_{100}. The data were acquired and analyzed by flow cytometry and results are shown in Fig. 4. In comparison to un-treated parasites, treatment with thiosemicarbazones (9h, 9k and 9r) decreased parasite cell viability. Until 24 h of treatment with compounds (9h) and (9k), only few parasite cells were stained (data not shown) while in contrast, an increase in the percentage of stained parasites was observed during thiosemicarbazone (9r) treatment and this was concentration-dependent. Parasites treated with compound (9r) at 1.1 mM presented 18.62% positively stained cells, of which 7.8% were early apoptotic (annexin V), 6.2% were late apoptotic (PI þ annexin V), while only 4.62% were necrotic (PI).

3. Discussion

Currently, the only available treatment of Chagas disease is benznidazole, therefore identification of new pharmaceuticals is vital [4]. Aryl thiosemicarbazones were previously demonstrated to act as strong anti-T. cruzi agents, targeting the trypanosomal

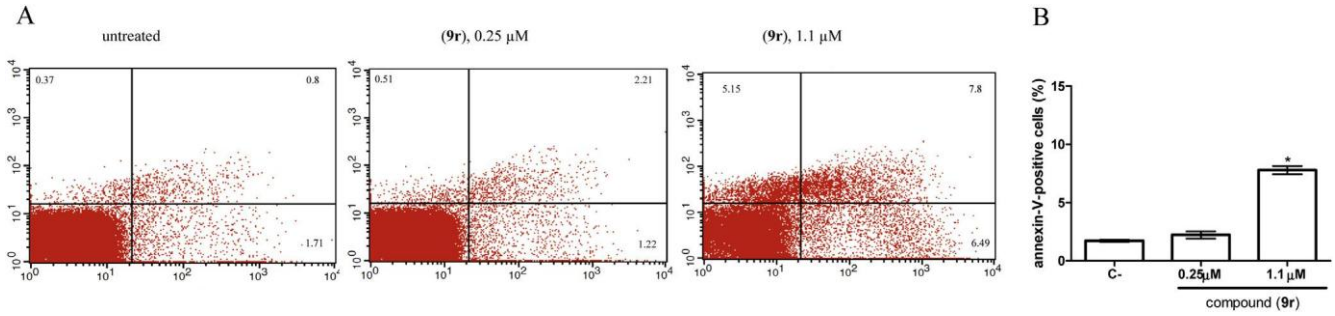

Fig. 4. (A) Thiosemicarbazone (9r)-based treatment causes parasite death through apoptosis induction. Trypomastigotes were treated with compound (9r) for 24 h. Parasites were examined by flow cytometry with annexin V and PI staining. The percentage of cells in each quadrant represent the following: lower left, double negative; upper left, PI single positive; lower right, annexin V single positive; upper right, PI and annexin V double positive. (B) Quantitative analysis of parasites positive only for annexin V. Values were taken from six different readings of two independent experiments. (C) ¼ negative control. *Compared to negative control (ANOVA one-way, $p < 0.05$).

protease cruzain [28e30]. It was recently discovered a sub-class of these inhibitors, which contains a spacer group between aryl ring and thiosemicarbazone, with an enhanced anti-T. cruzi activity in comparison to aryl thiosemicarbazones without the spacer group. Interestingly, the use of a spacer group not only enhanced the thiosemicarbazone activity, but also thiazole and thiazolidinone compound activity [40e43].

In the current study, we sought to use an alkoxyl spacer group to design new aryl thiosemicarbazones. By using the alkoxyl spacer group and varying a number of different substituents attached to the phenyl ring, we were able to observe some structural de-terminants involved in anti-T. cruzi activity. Specifically, sub-stituents were observed to retain, enhance or greatly increase the anti-T. cruzi activity in comparison to the nonsubstituted phenyl thiosemicarbazone. For instance, the attachment of a 4-methoxyl, 4-fluoro or 4-chloro substituents to the phenyl ring led to de-rivatives that retained activity in comparison to the nonsubstituted thiosemicarbazone. However these compounds showed lower po-tency than benznidazole.

Next, we observed that bromo, biphenyl and phenoxyl at 4-position are substituents that greatly increase the anti-T. cruzi ac-tivity in comparison to the nonsubstituted phenyl thio-semicarbazone. In agreement with activity observed for the biphenyl derivatives, the replacement of a phenyl group by a a- or b-naphthyl group also increased the activity. These results demonstrate that hydrophobic substituents may be structural de-terminants. However, we also observed that, while the derivative containing an isopropyl, tertbutyl and iodo substituents greatly increased the anti-T. cruzi activity, an unusual cytotoxicity for host cells was observed.

An interesting structureeactivity relationship was observed by comparing the 4-nitrophenyl and 4-acetamidephenyl derivatives. Nitro is a well-known antiparasitic pharmacophoric group [57], but here its attachment to the phenyl ring was not effective to produce a compound as potent as benznidazole. On the other hand, the insertion of an acetamide greatly increased the activity in com-parison to the nonsubstituted phenyl thiosemicarbazone. In fact, inserting an acetamide group produced one of the most potent anti-T. cruzi thiosemicarbazones observed in this study.

Another set of interesting structureeactivity relationships were observed by comparing the substituent position (i.e, ortho, meta, para). It was evaluated one representative electron-donor substit-uent, which was the biphenyl group, and one electron-withdrawing substituent, the chloro. Variations in the position of the chloro atom when attached to the phenyl group increased the anti-T. cruzi ac-tivity. The position of biphenyl substituents within the phenyl ring did not result in potency variations. This suggests the nature of the substituent is important for the activity, but in same cases, sub-stituent position along the phenyl ring is of less importance.

Next, the effect of electron-donor or electron-withdrawing properties of the substituents was examined here. In regard to moderate electron-donor substituents, the 4-methoxyl derivative was inactive, while the 4-phenoxyl and 4-acetamide were active. Weak electron-donor substituents, such as alkyl and phenyl, also produced active compounds. In regard to electron-withdrawing substituents, strong deactivating substituents, such as the nitro group, produced active compounds. However, bromo and iodo, which are weak electron-withdrawing substituents, produced active compounds and they were more potent than the nitro de-rivative. This shows that the activity cannot be explained by the substituent effect in terms of aryl reactivity. Considering that the thiosemicarbazones containing halogens, biphenyl or phenoxyl substituents exhibited the highest anti-T. cruzi activity, factors such as hydrophobic properties, volume and polarisability (in the pres-ence of halogens) could contribute to the observed activity [58]. An exception to this general rule is the acetamide substituent, which does not fit into these factors, but this substituent produced a highly potent antiparasitic compound.

In general, the thiosemicarbazones were able to reduced epi-mastigote proliferation with IC_{50} values similar to nifurtimox. In addition, these compounds exhibited, in most cases, low cytotox-icity for host cells in comparison to the anti-T. cruzi drugs, benz-nidazole and nifurtimox. Specifically, compound (9h) and (9r) displayed selectivity indexes comparable with some anti-T. cruzi lead-compounds described in the literature [13,59,60]. Another important comparison is that the antiparasitic activity and selec-tivity observed for these molecules are higher than the thio-semicarbazone previously investigated (1, CC_{50} ¼ 3.7 mM for trypomastigotes and HNC < 1.0 mM for splenocytes) [40e43]. Therefore, indicating the structural design employed here for compounds (9aex), which was based on the conformational re-striction, was successful in producing compounds with enhanced anti-trypanosomal activity. Regarding the mechanism of action, most the literature points out that thiosemicarbazones inhibit the major trypanosomal protease, cruzain. Moreover, few reports suggest that this class of compounds also inhibits trypanothione reductase [32]. In this study, the compounds did not exhibit cruzain inhibition, thus, other mechanisms of action must be involved. Regarding the mechanism of action of parasite cell death, we observed thiosemicarbazone (9r) causes parasite death by an apoptotic process, suggesting this compound has more effects on cytoplasm and cell nucleus than affecting cell membrane.

4. Conclusions

Thiosemicarbazones were structurally designed by employing a homologation strategy followed by conformational restriction. This led to the synthesis and chemical characterization of compounds

(9aex), which were evaluated as anti-T. cruzi and cruzain inhibitors. The pharmacological evaluation led to the identification of thio-semicarbazones (9h) and (9r) as potent and selective anti-T. cruzi agents, as similarly observed in benznidazole-treated cells. Anti-T. cruzi activity was observed to be dependent on the nature of the employed substituent, but the substituent position in the phenyl ring had less importance for activity. Mechanistically, these com-pounds did not inhibit cruzain and were observed to induce para-site cell death through an apoptotic process. The data argue that the conformational restriction is a feasible strategy to modify the structure of antiparasitic thiosemicarbazones.

5. Experimental section

5.1. General

Most the chemicals were purchased from SigmaeAldrich (St. Louis, USA), Merck (Berlin, Germany) or Alfa-Aesar (Massachusetts, USA). Reactions in ultrasound bath were performed in a Unique EM-804 TGR instrument, with a frequency of 40 kHz and a nominal power of 180 W, and without external heating. Precoated aluminum sheets (silica gel 60 F254, Merck) were used for thin-layer chromatography (TLC) and spots were visualized under UV light. Elemental analysis was performed with a Carlo Erba instru-ment model E-1110. IR spectra in KBr pellets were acquired at Bruker FT-IR spectrophotometer. ^{1}H and ^{13}C NMR were recorded on a UnityPlus 400 MHz and Bruker AMX-300 MHz spectrometer, using DMSO-d_6 as a solvent and trimethylsilane (TMS) as the in-ternal standard. Splitting patterns were defined as; s, singlet; d, doublet; t, triplet; q, quartet; m, multiplet. Chemical shift values were given in ppm. DEPT was employed to confirm the carbon assignment. High-resolution electrospray ionization mass spectra (HRESIMS) were acquired on a nanoUPLC-Xevo G2 Tof (Waters) in the positive ionization mode. Optical rotations were recorded using a JASCO Dichron model P-2000 polarimeter using tetrahydrofuran as solvent. X-ray diffraction of compound (9a) was performed on an Enraf-Nonius Kappa-CCD diffractometer (95 mm CCD camera on k-goniostat) using graphite monochromated MoKa radiation

(0.71073 A), at room temperature.

5.2. Synthesis of b-ketoethers (7aex). Example for 3-phenoxybutan-2-one (7a)

In a round bottom flask for 100 mL, phenol (5a, 5.0 g, 53 mmol) was dissolved in 30 mL butanone and stirred at room temperature. K_2CO_3 (11 g, 80 mmol) and KI (0.8 g, 5 mmol) were added to the mixture, following by addition of 3-chloro-2-butanone (6, 5.6 g, 53 mmol). The reaction mixture was then maintained under stir-ring for 12 h. After this time, the precipitate was removed under filtration and rinsed with ethyl acetate, and the organic phase was washed with water, and the with saturated KOH solution until the complete removal of unreacted phenol. The combined organic phases were dried over anhydrous Na_2SO_4, concentrated and then dried under vacuum. The resulting product was used in the next step without further purification.

5.3. Synthesis of thiosemicarbazones (9aex). Example for compound (9a)

In a round bottom flask for 50 mL, the b-ketoether (7a, 7.5 g, 46 mmol) was dissolved in 15 mL EtOH, following by the addition of two drops HCl. The flask was placed in an ultrasound bath (40 kHz, 180 W) and under sonication, 4.2 g (46 mmol) of thiosemicarbazide (8) was added in portions to the reaction. After 2 h, the mixture was cooled at 0 C and the precipitate was filtered in a Büchner funnel with a sintered disc filter, washed with cold water, ethanol and then dried over SiO_2. The resulting powder was recrystallized in EtOH to yield 9.7 g (89%) of colorless crystals.

5.3.1. 2-(3-Phenoxybutan-2-ylidene)thiosemicarbazide (9a)

(KBr): 3390 (NH_2), 3228 (NeH), 1598 (C]N) cm ^{1}. ^{1}H NMR (400 MHz, DMSO-d_6): d 1.41 (d, 3H, J 6 Hz, CH_3), 1.82 (s, 3H, CH_3), 4.97 (q, 1H, J 6 Hz, CHeO), 6.89 (d, 2H, J 6 Hz, ArH), 6.97 (d, 2H, J 6 Hz, ArH), 7.25 (t, 1H, J 8.1 Hz, ArH), 7.83 (s, 1H, NH_2), 8.24 (s, 1H, NH_2), 10.18 (s, 1H, NH). ^{13}C NMR (100 MHz, DMSO-d_6): d 11.7 (CH_3), 19.5 (CH_3), 76.7 (CHeO), 116.2 (Ar), 121.6 (CH, Ar), 130.1 (Ar), 152.5 (C]N), 157.9 (CeO), 179.8 (C]S). HRESIMS: 238.0575 [MþH]^{þ}. Anal. Calcd. for $C_{11}H_{15}N_3OS$: C, 55.67; H, 6.37; N, 17.71. Found: C, 56.02; H, 6.60; N, 17.98. Crystallization from ethanol gave (9a) as light white prisms suitable for X-ray analysis. Formula: $C_{11}H_{15}N_3OS$.

5.3.2. 2-(3-(4-Ethylphenoxy)butan-2-ylidene)thiosemicarbazide (9b)

Recrystallization in ethanol afforded yellowish crystals, yield 72%. M.p. (C): 87-89. a 18 2.7 1.3 (c 1.0, THF). IR (KBr):3491 (NH_2), 3192 (NH),1571 (C]N) cm ^{1}. ^{1}H NMR (400 MHz, DMSO-d_6): d 1.13 (t, 3H, J 7.6 Hz, CH_3), 1.40 (d, 3H, J 6.4 Hz, CH_3), 1.82 (s, 3H, CH_3), 2.51 (q, 2H, J 7.6 Hz, CH_2), 4.92 (q, 1H, J 6.4 Hz, CH), 6.88 (d, 2H, J 8.4 Hz, ArH), 7.07 (d, 2H, J 8.4 Hz, ArH), 7.82 (s, 1H, NH_2), 8.23 (s, 1H, NH_2), 10.16 (s, 1H, NH). ^{13}C NMR (75.5 MHz, DMSO-d_6): d 10.9 (CH_3), 15.7 (CH_3), 18.8 (CH_3), 27.2 (CH_2), 76.2 (CH), 115.5 (CH, Ar), 128.6 (CH, Ar), 136.2 (Ar), 152.0 (CeO), 155.2 (C]N), 179.1 (C]S). HRESIMS: 266.1264 [M]^{þ}. Anal. Calcd. for $C_{13}H_{19}N_3OS$: C, 58.84; H, 7.22; N, 15.83. Found: C, 59.11; H, 6.70; N, 16.42.

5.3.3. 2-(3-(4-Isopropylphenoxy)butan-2-ylidene) thiosemicarbazide (9c)

Recrystallization in ethanol afforded colorless crystals, yield ¼ 55%. M.p. (C): 106e108. IR (KBr): 3492 (NH_2), 3193 (NH), 1571 (C]N) cm ^{1}. ^{1}H NMR (300 MHz, DMSO-d_6): d 1.14 (d, 6H, J 6.4 Hz, CH_3), 1.39 (d, 3H, J 6.4 Hz, CH_3), 1.82 (s, 3H, CH_3), 2.74e2.84 (m, 1H, CH), 4.91 (q, 1H, J 6.4 Hz, CHeO), 6.88 (d, 2H, J 8.8 Hz, ArH), 7.10 (d, 2H, J 8.8 Hz, ArH), 7.81 (s, 1H, NH_2), 8.23 (s, 1H, NH_2), 10.16 (s, 1H, NH). ^{13}C NMR (100 MHz, DMSO-d_6): d 10.9 (CH_3), 18.8 (CH_3), 24.0 (CH_3), 24.0 (CH_3), 32.5 (CH), 76.1 (CHeO), 115.3 (CH, Ar), 127.1 (CH, Ar), 140.7 (CH, Ar), 152.1 (CeO), 155.3 (C]N), 179.1 (C]S). HRE-SIMS: 280.1516 [M]^{þ}. Anal. Calcd. for $C_{14}H_{21}N_3OS$: C, 60.18; H, 7.58; N, 15.04. Found: C, 60.88; H, 6.54; N, 15.76.

5.3.4. 2-(3-(4-Tertbutylphenoxy)butan-2-ylidene) thiosemicarbazide (9d)

Recrystallization in methanol afforded colorless crystals, yield ¼ 71%. M.p. (C): 69e71. IR (KBr): 3408 (NH_2), 3254 (NeH), 1603 (C]N) cm ^{1}. ^{1}H NMR (300 MHz, DMSO-d_6): d 1.23 (s, 9H, CH_3), 1.40 (d, 3H, J 6 Hz, CH_3), 1.83 (s, 3H, CH_3), 4.92 (q, 1H, J 6 Hz, CH), 6.89 (d, 2H, J 9 Hz, ArH), 7.25 (d, 2H, J 9 Hz, ArH), 7.83 (s, 1H, NH_2), 8.25 (s, 1H, NH_2), 10.17 (s, 1H, NH). ^{13}C NMR and DEPT (75.5 MHz, DMSO-d_6): d 16.4 (CH_3), 24.3 (CH_3), 36.7 (CH_3), 38.5 (Cq), 81.5 (CHeO), 120.4 (CH, Ar), 131.5 (CH, Ar), 148.5 (C, Ar), 157.3 (CeO), 160.4 (C]N), 183.90 (C]S). HRESIMS: 293.9266 [M]^{þ}. Anal. Calcd. for $C_{15}H_{23}N_3OS$: C, 61.40; H, 7.90; N, 14.32. Found: C, 60.66; H, 6.88; N, 14.44.

5.3.5. 2-(3-(4-Methoxyphenoxy)butan-2-ylidene) thiosemicarbazide (9e)

Recrystallization in ethanol afforded yellowish crystals, yield ¼ 92%. M.p. (C): 120e122. IR (KBr): 3393 (NH_2), 3224 (NeH), 1600 (C]N) cm ^{1}. ^{1}H NMR (300 MHz, DMSO-d_6): d 1.38 (d, 3H, J 6.6 Hz, CH_3), 1.82 (s, 3H, CH_3), 3.68 (s, 3H, OCH_3), 4.85 (q, 1H, J 6.6 Hz, CHeO), 6.80 (d, 2H, J 9 Hz, ArH), 6.90 (d, 2H, J 9 Hz, ArH), 7.79 (s, 1H, NH_2), 8.23 (s, 1H, NH_2), 10.16 (s, 1H, NH). ^{13}C NMR (75.5 MHz, DMSO-d_6): d 10.9 (CH_3), 18.8 (CH_3), 55.2 (OCH_3), 76.7 (CHeO), 114.4 (CH, Ar), 116.7 (CH, Ar), 151.0 (CeO), 152.1 (CeO), 153.5 (C]N), 179.1 (C]S). HRESIMS: 268.0632 [MþH]^{þ}. Anal. Calcd. for $C_{12}H_{17}N_3O_2S$: C, 53.91; H, 6.41; N, 15.72. Found: C, 54.50; H, 6.53; N, 15.95.

5.3.6. 2-(3-(3-Methoxyphenoxy)butan-2-ylidene) thiosemicarbazide (9f)

Recrystallization in ethanol afforded yellowish crystals, yield ¼ 52%. M.p. (C): 110e112. IR (KBr): 3403 (NH_2), 3255 (NeH), 1596 (C]N) cm ^{1}. ^{1}H NMR (400 MHz, DMSO-d_6): d 1.40 (d, 3H, J 6.6 Hz, CH_3), 1.82 (s, 3H, CH_3), 3.69 (s, 3H, OCH_3), 4.94 (q, 1H, J 6.6 Hz, CHeO), 6.48e6.56 (m, 3H, ArH), 7.14 (t, 1H, J 7.8 Hz, ArH), 7.82 (s, 1H, NH_2), 8.20 (s, 1H, NH_2), 10.16 (s, 1H, NH). ^{13}C NMR (100 MHz, DMSO-d_6): d 10.9 (CH_3), 18.7 (CH_3), 54.9 (OCH_3), 76.2 (CHeO), 101.6 (CH, Ar), 106.6 (CH, Ar), 107.7 (CH, Ar), 129.9 (CH, Ar), 151.7 (C]N), 158.4 (CeO), 160.3 (CeO), 179.16 (C]S). HRESIMS: 268.1216 [MþH]^{þ}. Anal. Calcd. for $C_{12}H_{17}N_3O_2S$: C, 53.91; H, 6.41; N, 15.72. Found: C, 54.15; H, 5.96; N, 15.98.

5.3.7. 2-(3-(4-Nitrophenoxy)butan-2-ylidene)thiosemicarbazide (9g)

Recrystallization in ethanol afforded bright yellowish crystals, yield: 87%. M.p. (C): 160e162. IR (KBr): 3453 (NH_2), 3291 (NeH), 1589 (C]N) cm ^{1}. ^{1}H NMR (400 MHz, DMSO-d_6): d 1.47 (d, 3H, J 6.6 Hz, CH_3), 1.85 (s, 3H, CH_3), 5.15 (q, 1H, J 6.6 Hz, CHeO), 7.20 (d, 2H, J 9.3 Hz, ArH), 7.82 (s, 1H, NH_2), 8.16 (d, 2H, J 9.3 Hz, ArH), 8.26 (s, 1H, NH_2), 10.21 (s, 1H, NH). ^{13}C NMR (100 MHz, DMSO-d_6): d 11.1 (CH_3), 18.4 (CH_3), 77.2 (CHeO), 116.0 (CH, Ar), 125.7 (CH, Ar), 141.0 (CeN, Ar), 150.2 (C]N), 162.6 (CeO), 179.3 (C]S). HRESIMS: 283.0980 [MþH]^{þ}. Anal. Calcd. for $C_{11}H_{14}N_4O_3S$: C, 46.80; H, 5.00; N, 19.85. Found: C, 47.63; H, 4.88; N, 19.20.

5.3.8. N-(4-(((3-(thiosemicarbazide)butan-2-ylidene)oxy)phenyl) acetamide (9h)

Recrystallization in ethanol afforded pale yellow crystals, yield ¼89%. M.p. (C): 177e179. $[\alpha]_D^{18}$ 2.4 5.2 (c 1.0, THF). IR (KBr): 3406 (NH_2), 3270 (NeH), 1658 (C]N) cm ^{1}. ^{1}H NMR (300 MHz, DMSO-d_6): d 1.39 (d, 3H, J 6.3 Hz, CH_3), 1.82 (s, 3H, CH_3), 1.99 (s, 3H, CH_3), 4.89 (q, 1H, J 6.3 Hz, CHeO), 6.90 (d, 2H, J 8.7 Hz, ArH), 7.43 (d, 2H, J 8.7 Hz, ArH), 7.78 (s, 1H, NH_2), 8.19 (s, 1H, NH_2), 9.77 (s, 1H, NHCO), 10.11 (s, 1H, NH). ^{13}C NMR (75.5 MHz, DMSO-d_6): d 11.0 (CH_3), 18.4 (CH_3), 77.1 (CHeO), 116.5 (CH, Ar), 117.7 (CH, Ar), 122.9 (Ar), 130.9 (CH, Ar), 131.55 (Ar), 150.5 (C]N), 156.7 (CeO), 179.3 (S]C). HRESIMS: 295.0880 [MþH]^{þ}. Anal. Calcd. for $C_{13}H_{18}N_4O_2S$: C, 53.04; H, 6.16; N, 19.03. Found: C, 53.29; H, 5.60; N, 19.20.

5.3.9. 2-(3-(4-Fluorophenoxy)butan-2-ylidene)thiosemicarbazide (9i)

Recrystallization in ethanol afforded colorless crystals, yield ¼ 83%. M.p. (C): 148e150. IR (KBr): 3427 (NH_2), 3265 (NH), 1605 (C]N) cm ^{1}. ^{1}H NMR (300 MHz, DMSO-d_6): 1.40 (d, 3H, J 6.8 Hz, CH_3), 1.82 (s, 3H, CH_3), 4.91 (q, 1H, J 6.4 Hz, CHeO), 6.97e7.10 (m, 4H, ArH), 7.81 (s, 1H, NH_2), 8.24 (s, 1H, NH_2), 10.17 (s, 1H, NH). ^{13}C NMR (100 MHz, DMSO-d_6): d 10.9 (CH_3), 18.7 (CH_3), 76.8 (CHeO), 115.6 (CH, Ar), 115.9 (CH, Ar), 116.9 (CH, Ar), 117.0 (CH, Ar), 151.5 (CeO), 153.5 (C]N), 155.4 (CeF, Ar), 157.8 (CeF, Ar), 179.1 (C]S). HRESIMS: 256.0987 [MþH]^{þ}. Anal. Calcd. for $C_{11}H_{14}N_3OSF$: C, 51.75; H, 5.53; N, 16.46. Found: C, 52.18; H, 5.09; N, 17.14.

5.3.10. 2-(3-(4-Chlorophenoxy)butan-2-ylidene)thiosemicarbazide (9j)

Recrystallization in ethanol afforded yellowish crystals, yield ¼ 59%. M.p. (C): 119e121. IR (KBr): 3400 and 3353 (NH_2), 3246 (NeH), 1608 (C]N) cm ^{1}. ^{1}H NMR (300 MHz, DMSO-d_6): d 1.42 (d, 3H, J 6.6 Hz, CH_3), 1.82 (s, 3H, CH_3), 4.96 (q, 1H, J 6.6 Hz, CHeO), 7.01 (d, 2H, J 6.6 Hz, ArH), 7.29 (d, 2H, J 6.6 Hz, ArH), 7.85 (s, 1H, NH_2), 8.27 (s, 1H, NH_2), 10.21 (s, 1H, NH). ^{13}C NMR (75.5 MHz, DMSO-d_6): d 11.0 (CH_3), 18.6 (CH_3), 76.5 (CHeO), 117.4 (CH, Ar), 124.6 (Ar), 129.2 (CH, Ar), 151.2 (C]N), 156.0 (CeO), 179.1 (C]S). HRESIMS: 272.0127 [M]^{þ}. Anal. Calcd. for $C_{11}H_{14}N_3OSCl$: C, 48.61; H, 5.19; N, 15.46. Found: C, 49.01; H, 5.12; N, 16.11.

5.3.11. 2-(3-(3-Chlorophenoxy)butan-2-ylidene)thiosemicarbazide (9k)

Recrystallization in ethanol afforded brown crystals, yield ¼ 89%. M.p. (C): 96e98. IR (KBr): 3323 (NH_2), 3256 (NH),1603 (C]N) cm ^{1}. ^{1}H NMR (400 MHz, DMSO-d_6): d 1.41 (d, 3H, J 6.6 Hz, CH_3), 1.83 (s, 3H, CH_3), 5.00 (q, 1H, J 6.6 Hz, CHeO), 6.94e6.99 (m, 2H, Ar), 7.04e7.06 (m, 1H, Ar), 7.27 (t,1H, J 8.1 Hz, Ar), 7.84 (s, 1H, NH_2), 8.23 (s, 1H, NH_2), 10.18 (s, 1H, NH). ^{13}C NMR (100 MHz, DMSO-d_6): d 11.0 (CH_3), 18.5 (CH_3), 76.6 (CHeO),114.5 (CH, Ar),115.7 (CH, Ar),120.9 (CH, Ar),130.8 (CH, Ar), 133.6 (CeCl), 150.9 (C]N), 158.1 (CeO), 179.2 (C]S). HRESIMS: 272.0702 [MþH]^{þ}. Anal. Calcd. for $C_{11}H_{14}N_3OSCl$: C, 48.61; H, 5.19; N, 15.46. Found: C, 49.28; H, 5.13; N, 16.05.

5.3.12. 2-(3-(2-Chlorophenoxy)butan-2-ylidene)thiosemicarbazide (9l)

Recrystallization in ethanol afforded yellowish crystals, yield ¼ 69%. M.p. (C): 139e141. IR (KBr): 3410 (NH_2), 3240 (NH), 1595 (C]N) cm ^{1}. ^{1}H NMR (300 MHz, DMSO-d_6): 1.46 (d, 3H, J 6.0 Hz, CH_3), 1.85 (s, 3H, CH_3), 5.06 (q, 1H, J 6.4 Hz, CHeO), 6.92e6.96 (m, 1H, ArH), 7.21e7.26 (m, 2H, ArH), 7.41 (d, J 7.6 Hz, 1H, ArH), 7.822 (s, 1H, NH_2), 8.256 (s, 1H, NH_2), 10.210 (s, 1H, NH). ^{13}C NMR (75.5 MHz, DMSO-d_6): d 10.9 (CH_3), 18.5 (CH_3), 77.3 (CHeO), 115.8 (CH, Ar), 121.9 (CH, Ar), 122.0 (Ar), 128.1 (CH, Ar), 130.0 (CH, Ar), 150.8 (CeO), 152.5 (C]N), 179.2 (C]S). HRESIMS: 272.0702 [MþH]^{þ}. Anal. Calcd. for $C_{11}H_{14}N_3OSCl$: C, 48.61; H, 5.19; N, 15.46. Found: C, 48.58; H, 5.18; N, 15.78.

5.3.13. 2-(3-(4-Bromophenoxy)butan-2-ylidene)thiosemicarbazide (9m)

Recrystallization in ethanol afforded yellowish crystals, yield ¼ 70%. M.p. (C): 141e143. IR (KBr): 3393 (NH_2), 3224 (NeH), 1600 (C]N) cm ^{1}. ^{1}H NMR (300 MHz, DMSO-d_6): d 1.41 (d, 3H, J 6.6 Hz, CH_3), 1.81 (s, 3H, CH_3), 4.95 (q, 1H, J 6.6 Hz, CH), 6.95 (d, 1H, J 9 Hz, ArH), 7.40 (d, 1H, J 9 Hz, ArH), 7.83 (s, 1H, NH_2), 8.26 (s, 1H, NH_2), 10.20 (s, 1H, NH). ^{13}C NMR (75.5 MHz, DMSO-d_6): d 11.0 (CH_3), 18.6 (CH_3), 76.5 (CHeO), 112.44 (Ar), 117.9 (CH, Ar), 132.1 (CH, Ar), 151.2 (C]N), 156.5 (CeO), 179.1 (C]S). HRESIMS: 315.9171 [MþH]^{þ}. Anal. Calcd. for $C_{11}H_{14}N_3OSBr$: C, 41.78; H, 4.46; N, 13.29. Found: C, 41.63; H, 4.52; N, 13.23.

5.3.14. 2-(3-(3-Bromophenoxy)butan-2-ylidene)thiosemicarbazide (9n)

Recrystallization in ethanol afforded yellowish crystals, yield ¼ 36%. M.p. (C): 121e123. IR (KBr): 3393 (NH_2), 3224 (NeH), 1600 (C]N) cm ^{1}. ^{1}H NMR (300 MHz, DMSO-d_6): d 1.41 (d, 3H, J 6.3 Hz, CH_3), 1.82 (s, 3H, CH_3), 5.00 (q, 1H, J 6.3 Hz, CHeO), 7.00 (d, 1H, J 8.4 Hz, ArH), 7.11 (d, 1H, J 8.4 Hz, ArH), 7.18 (s, 1H, ArH), 7.21 (t, 1H, J 8.1 Hz, ArH), 7.86 (s, 1H, NH_2), 8.27 (s, 1H, NH_2), 10.22 (s, 1H, NH). ^{13}C NMR (75.5 MHz, DMSO-d_6): d 11.0 (CH_3), 18.5 (CH_3), 76.6 (CHeO),

114.9 (CH, Ar), 118.6 (CH, Ar), 121.9 (Ar), 123.9 (CH, Ar), 131.2 (CH, Ar), 150.9 (C]N), 158.2 (CeO), 179.2 (C]S). HRESIMS: 315.962 [MþH]þ. Anal. Calcd. for $C_{11}H_{14}N_3OSBr$: C, 41.78; H, 4.46; N, 13.29. Found: C, 41.85; H, 4.12; N, 13.39.

5.3.15. 2-(3-(4-Iodophenoxy)butan-2-ylidene)thiosemicarbazide (9o)

Recrystallization in ethanol afforded yellowish crystals, yield ¼ 83%. M.p. (C): 154e156. IR (KBr): 3347 (NH_2), 3243 (NH), 1579 (C]N) cm ^{1}. ^{1}H NMR (400 MHz, DMSO-d_6): d 1.41 (d, 3H, J 6.4 Hz, CH_3), 1.81 (s, 3H, CH_3), 4.94 (q, 1H, J 6.4 Hz, CHeO), 6.83 (d, 2H, J 8.4 Hz, CH, ArH), 7.55 (d, 2H, J 8.4 Hz, 2CH, ArH), 7.81 (s, 1H, NH_2), 8.24 (s, 1H, NH_2), 10.18 (s, 1H, NH). ^{13}C NMR (75.5 MHz, DMSO-d_6): d 11.0 (CH_3), 18.6 (CH_3), 76.3 (CHeO), 83.8 (Ar), 118.4 (CH, Ar), 137.9 (CH, Ar), 151.2 (C]N), 157.1 (CeO), 179.1 (C]S). HRESIMS: 364.0118 [M]þ. Anal. Calcd. for $C_{11}H_{14}N_3OSI$: C, 36.37; H, 3.89; N, 11.57. Found: C, 36.45; H, 3.65; N, 11.65.

5.3.16. 2-(3-([1,1^{0}-Biphenyl]-4-yloxy)butan-2-ylidene) thiosemicarbazide (9p)

Recrystallization in ethanol afforded white crystals, yield ¼ 91%. M.p. (C): 164e166. IR (KBr): 3404 (NH_2), 3236 (NeH), 1592 (C]N) cm ^{1}. ^{1}H NMR (400 MHz, DMSO-d_6): d 1.46 (d, 3H, J 6 Hz, CH_3), 1.87 (s, 3H, CH_3), 5.04 (q, 1H, J 6 Hz, CHeO), 7.09 (d, 2H, J 9 Hz, ArH), 7.20e7.47 (m, 1H, ArH), 7.49e7.73 (m, 2H, ArH), 7.78e 7.99 (m, 4H, ArH), 7.89 (s, 1H, NH_2), 8.30 (s, 1H, NH_2), 10.24 (s, 1H, NH). ^{13}C NMR (100 MHz, DMSO-d_6): d 11.7 (CH $_3$), 19.5 (CH_3), 81.7 (CHeO), 116.7 (CH, Ar), 126.9 (CH, Ar), 128.4 (CH, Ar), 129.1 (CH, Ar), 129.5 (CH, Ar), 133.6 (CH, Ar), 140.4 (C, Ar), 152.4 (C]N), 157.6 (Ce O), 179.8 (C]S). HRESIMS: 314.1336 [MþH]þ. Anal. Calcd. for $C_{17}H_{19}N_3OS$: C, 65.15; H, 6.11; N, 13.41. Found: C, 64.93; H, 5.77; N, 13.70.

5.3.17. 2-(3-([1,1^{0}-Biphenyl]-3-yloxy)butan-2-ylidene) thiosemicarbazide (9q)

Recrystallization in ethanol afforded white crystals, yield ¼ 79%. M.p. (C): 138e140. IR (KBr): 3437 (NH_2), 3324 (NeH), 1586 (C]N) cm ^{1}. ^{1}H NMR (400 MHz, DMSO-d_6): d 1.45 (d, 3H, J 8.8 Hz, CH_3), 1.85 (s, 3H, CH_3), 5.09 (q, 1H, J 8.8 Hz, CHeO), 6.96 (d, 1H, ArH), 7.20e7.26 (m, 2H, ArH), 7.31e7.37 (m, 1H, ArH), 7.45 (t, 2H, ArH), 7.62 (d, 2H, ArH), 7.90 (s, 1H, NH_2), 8.26 (s, 1H, NH_2), 10.20 (s, 1H, NH). ^{13}C NMR (100 MHz, DMSO-d_6): d 11.0 (CH_3), 18.8 (CH_3), 76.4 (CHeO), 113.9 (CH, Ar), 114.8 (CH, Ar), 119.4 (CH, Ar), 126.7 (CH, Ar), 127.6 (CH, Ar), 128.9 (CH, Ar), 130.0 (CH, Ar), 139.8 (C, Ar), 141.6 (C, Ar), 151.7 (C]N), 157.8 (CeO), 179.3 (C]S). HRESIMS: 314.1422 [MþH]þ. Anal. Calcd. for $C_{17}H_{19}N_3OS$: C, 65.15; H, 6.11; N, 13.41. Found: C, 65.17; H, 6.11; N, 13.86.

5.3.18. 2-(3-([1,1^{0}-Biphenyl]-2-yloxy)butan-2-ylidene) thiosemicarbazide (9r)

Recrystallization in ethanol afforded white crystals, yield ¼ 83%. M.p. (C): 179e181. IR (KBr): 3416 (NH_2), 3226 (NeH), 1596 (C]N) cm ^{1}. ^{1}H NMR (400 MHz, DMSO-d_6): d 1.32 (d, 3H, J 6.0 Hz, CH_3), 1.76 (s, 3H, CH_3), 4.97 (q, 1H, J 6.4 Hz, CHeO), 7.02 (t, 1H, J 7.6 Hz, ArH), 7.14 (d, 2H, J 8.4 Hz, ArH), 7.25e7.34 (m, 3H, ArH), 7.41 (t, 2H, J 7.2 Hz, ArH), 7.49 (d, 2H, J 7.2 Hz, ArH), 7.73 (s, 1H, NH_2), 8.22 (s, 1H, NH_2), 10.16 (s, 1H, NH). ^{13}C NMR and DEPT (100 MHz, DMSO-d_6): d 11.7 (CH_3), 19.0 (CH_3), 77.2 (CHeO), 114.8 (CH, Ar), 121.8 (CH, Ar), 127.3 (CH, Ar), 128.4 (CH, Ar), 129.2 (CH, Ar), 129.7 (CH, Ar), 130.9 (C, Ar), 131.1 (CH, Ar), 138.6 (C, Ar), 152.2 (CeO), 154.4 (C]N), 179.6 (C]S). HRESIMS: 314.1336 [MþH]þ. Anal. Calcd. for $C_{17}H_{19}N_3OS$: C, 65.15; H, 6.11; N, 13.41. Found: C, 65.70; H, 5.44; N, 13.67.

5.3.19. 2-(3-(4-Phenoxyphenoxy)butan-2-ylidene) thiosemicarbazide (9s)

Recrystallization in ethanol afforded yellow crystals, yield ¼ 71%. M.p. (C): 111e112. IR (KBr): 3423 (NH_2), 3238 (NeH), 1593 (C]N) cm ^{1}. ^{1}H NMR (300 MHz, DMSO-d_6): d 1.42 (d, 3H, J 6 Hz, CH_3), 1.86 (s, 3H, CH_3), 4.93 (q, 1H, J 6 Hz, CHeO), 6.90e6.95 (m, 4H, ArH), 7.00e7.05 (m, 3H, ArH), 7.32e7.38 (m, 2H, ArH), 7.81 (s, 1H, NH_2), 8.26 (s, 1H, NH_2), 10.20 (s, 1H, NH). ^{13}C NMR (75.5 MHz, DMSO-d_6): d 11.8 (CH_3), 19.5 (CH_3), 77.3 (CHeO), 117.6 (CH, Ar), 118.2 (CH, Ar), 121.0 (CH, Ar), 123.4 (CH, Ar), 130.6 (CH, Ar), 133.6 (CH, Ar), 150.5 (CeO, Ar), 152.5 (C]N), 154.2 (CeO, Ar), 158.3 (CeO), 179.8 (C]S). HRESIMS: 330.0697 [MþH]þ. Anal. Calcd. for $C_{17}H_{19}N_3O_2S$: C, 61.98; H, 5.81; N, 12.76. Found: C, 61.83; H, 5.90; N, 12.95.

5.3.20. 2-(3-(Naphthalen-1-yloxy)butan-2-ylidene) thiosemicarbazide (9t)

Recrystallization in ethanol afforded white crystals, yield ¼ 98%. M.p. (C): 158e160. IR (KBr): 3408 (NH_2), 3228 (NeH), 1597 (C]N) cm ^{1}. ^{1}H NMR (300 MHz, DMSO-d_6): d 1.56 (d, 3H, J 6.8 Hz, CH_3), 1.86 (s, 3H, CH_3), 5.18 (q, 1H, J 6.4 Hz, CHeO), 7.05 (d, 1H, J 8 Hz, ArH), 7.36 (t, 1H, J 7.6 Hz, ArH), 7.45e7.53 (m, 3H, ArH), 7.84e 7.86 (m, 1H, ArH), 7.88 (s, 1H, NH_2), 8.19e8.22 (m, 1H, ArH), 8.26 (s, 1H, NH_2), 10.20 (s, 1H, NH). ^{13}C NMR (75.5 MHz, DMSO-d_6): d 10.4 (CH_3), 18.3 (CH_3), 76.0 (CHeO), 106.6 (CH, Ar), 119.8 (CH, Ar), 121.0 (CH, Ar), 124.7 (CH, Ar), 124.9 (CH, Ar), 125.6 (CH, Ar), 125.9 (CH, Ar), 127.0 (CH, Ar), 133.6 (CH, Ar), 151.3 (C]N), 152.0 (CeO, Ar), 179.7 (C]S). HRESIMS: 288.1283 [MþH] þ. Anal. Calcd. for $C_{15}H_{17}N_3OS$: C, 62.69; H, 5.96; N, 14.62. Found: C, 62.63; H, 6.07; N, 14.92.

5.3.21. 2-(3-(Naphthalen-2-yloxy)butan-2-ylidene) thiosemicarbazide (9u)

Recrystallization in ethanol afforded white crystals, yield ¼ 89%. M.p. (C): 150e152. IR (KBr): 3341 (NH_2), 3270 (NeH), 1614 (C]N) cm ^{1}. ^{1}H NMR (400 MHz, DMSO-d_6): d 1.49 (d, 3H, J 6.4 Hz, CH_3), 1.85 (s, 3H, CH_3), 5.13 (q, 1H, J 6.3 Hz, CHeO), 7.19 (d, 1H, J 9.2 Hz, ArH), 7.19 (d, 1H, J 9.2 Hz, ArH), 7.33 (t, 1H, J 7.6 Hz, ArH), 7.41e7.46 (m, 2H, ArH), 7.74 (d, 1H, J 8.4 Hz, ArH), 7.80 (d, 1H, J 8.8 Hz, ArH), 7.98 (s, 1H, NH_2), 8.27 (s, 1H, NH_2), 10.20 (s, 1H, NH). ^{13}C NMR (100 MHz, DMSO-d_6): d 10.9 (CH_3), 18.6 (CH_3), 76.2 (CHeO), 108.9 (CH, Ar), 118.9 (CH, Ar), 123.7 (CH, Ar), 126.3 (CH, Ar), 126.7 (CH, Ar), 127.4 (CH, Ar), 128.5 (CH, Ar), 129.3 (CH, Ar), 134.0 (CH, Ar), 151.6 (C]N), 154.9 (CeO, Ar), 179.2 (C]S). HRESIMS: 288.1283 [MþH]þ. Anal. Calcd. for $C_{15}H_{17}N_3OS$: C, 62.69; H, 5.96; N, 14.62. Found: C, 62.78; H, 6.01; N, 14.97.

5.3.22. 2-(3-(3,4-Dichlorophenoxy)butan-2-ylidene) thiosemicarbazide (9v)

Recrystallization in ethanol afforded white crystals, yield ¼ 74%. M.p. (C): 154e156. IR (KBr): 3420 (NH_2), 3259 (NeH), 1593 (C]N) cm ^{1}. ^{1}H NMR (300 MHz, DMSO-d_6): d 1.42 (d, J 6.6 Hz, 3H, CH_3), 1.82 (s, 3H, CH_3), 5.00 (q, 1H, J 6.6 Hz, CHeO), 7.00 (dd, 1H, J 9.0 Hz, ^{4}J 3.0 Hz, ArH), 7.27 (d, 1H, ^{4}J 3.0 Hz, ArH), 7.47 (d, 1H, J 9.0 Hz, ArH), 7.85 (broad s, 1H, NH_2), 8.24 (broad s, 1H, NH_2), 10.19 (s, 1H, NH). ^{13}C NMR (75.5 MHz, DMSO-d_6): d 11.0 (CH_3), 18.4 (CH_3), 77.1 (CHeO), 116.5 (CH, Ar), 117.7 (CH, Ar), 122.9 (CeCl, Ar), 130.9 (CH, Ar), 131.5 (Ar), 150.5 (C]N), 156.7 (CeO), 179.3 (C]S). HRE-SIMS: 306.0320 [MþH]þ. Anal. Calcd. for $C_{11}H_{13}N_3OSCl_2$: C, 43.15; H, 4.28; N, 13.72. Found: C, 43.39; H, 4.09; N, 13.69.

5.3.23. 2-(3-(3-Chloro-4-fluorophenoxy)butan-2-ylidene) thiosemicarbazide (9w)

Recrystallization in ethanol afforded yellowish crystals, yield ¼ 91%. M.p. (C): 134e136. IR (KBr): 3423 (NH_2), 3236 (NH), 1579 (C]N) cm ^{1}. ^{1}H NMR (300 MHz, DMSO-d_6): d 1.41 (d, 3H, J 6.4 Hz, CH_3), 1.82 (s, 3H, CH_3), 4.96 (q, 1H, J 6.4 Hz, CHeO), 6.97e7.01

(m, 1H, ArH), 7.20e7.22 (m, 1H, ArH), 7.28 (t, 1H, J 9.2 Hz, ArH), 7.88 (s, 1H, NH_2), 8.26 (s, 1H, NH_2), 10.21 (s, 1H, NH). ^{13}C NMR (100 MHz, DMSO-d_6): d 11.0 (CH_3), 18.5 (CH_3), 77.1 (CHeO), 116.0 (CH, Ar), 117.0 (CH, Ar), 117.4 (CH, Ar), 119.7 (Ar), 150.7 (CeF, Ar), 153.1 (CeO), 153.8 (C]N), 179.2 (C]S). HRESIMS: 290.0551 [MþH]þ. Anal. Calcd. for $C_{11}H_{13}N_3OSFCl$: C, 45.60; H, 4.52; N, 14.50. Found: C, 45.35; H, 4.49; N, 14.42.

5.3.24. 2-(3-(2,3-Dichlorophenoxy)butan-2-ylidene) thiosemicarbazide (9x)

Recrystallization in ethanol afforded yellowish crystals, yield ¼ 55%. M.p. (C): 132e134. IR (KBr): 3423 (NH_2), 3236 (NH), 1507 (C]N) cm^{-1}. ^{1}H NMR (300 MHz, DMSO-d_6): d 1.47 (d, 3H, J 6.0 Hz, CH_3), 1.85 (s, 3H, CH_3), 5.09 (q, 1H, J 6.0 Hz, CHeO), 7.18e7.27 (m, 3H, ArH), 7.84 (s, 1H, NH_2), 8.28 (s, 1H, NH_2), 10.23 (s, 1H, NH). ^{13}C NMR (100 MHz, DMSO-d_6): d 10.9 (CH_3), 18.5 (CH_3), 78.0 (CHeO), 114.1 (CH, Ar), 120.6 (CH, Ar), 122.5 (Ar), 128.3 (CH, Ar), 132.3 (Ar), 150.33 (CeO, Ar), 154.0 (C]N), 179.2 (C]S). HRESIMS: 306.0235 [MþH]þ. Anal. Calcd. for $C_{11}H_{13}N_3OSCl_2$: C, 43.15; H, 4.28; N, 13.72. Found: C, 42.61; H, 3.99; N, 13.62.

5.4. Cells

BALB/c mouse, housed in the Centro de Pesquisas Aggeu Mag-alhaes (Recife, Brazil), were used to collect splenocytes accordingly to a previously reported protocol [61]. T. cruzi Dm28c epi-mastigotes, cloned derived from Dm28 strain (TcI) [62], were maintained at 26 C in LIT (Liver Infusion Tryptose) medium sup-plemented with 10% fetal bovine serum (FBS) (Life, Carlsbad, USA), 1% hemin (SigmaeAldrich, St. Louis, USA), 1% R9 medium (Sigmae Aldrich, St. Louis, USA), and 50 mg/mL gentamycin (Novafarma, Anápolis, Brazil). Y strain (TcII) trypomastigotes were obtained from the supernatant of infected LLC-MK2 cells and were main-tained in RPMI-1640 medium (SigmaeAldrich, St. Louis, USA) supplemented with 10% FBS, and 50 mg/mL gentamycin at 37 C and 5% CO_2. Experiments were carried out in accordance with the rec-ommendations of ethical issues guidelines and were approved by the local Animal Ethics Committee (number 0266/05).

5.5. Host cell cytotoxicity

BALB/c mouse splenocytes were seeded at 5 10^6 cells/well in 96-well plate. Compounds were dissolved in DMSO and then diluted in RPMI-1640 medium in a serial dilution (1.23, 3.7, 33.33 and 100 mg/mL) and added to respective wells, in triplicate. The final DMSO concentration was 1%. The plate was incubated for 24 h at 37 C and 5% CO_2 containing 1.0 mCi of ^{3}H-thymidine (Perkine Elmer, Waltham, MA). Cells were harvested and then transferred to a liquid scintillation counter (WALLAC 1209, Rackbeta Pharmacia, Stockholm, Sweden) and the percent of ^{3}H-thymidine incorpora-tion was determined. The highest non-cytotoxic concentration (HNC) was determined for each compound. For determining the CC_{50} values, five different concentrations were used.

5.6. Anti-T. cruzi activity (epimastigotes)

Epimastigotes (Dm28c) in LIT media were counted in a hemo-cytometer and then seeded at 10^6 cells/well into a 96-well plate. Compounds were dissolved in DMSO and then diluted in LIT me-dium in a serial dilution (1.23, 3.70, 11.11, 33.33 and 100 mg/mL) and added to respective wells, in triplicate. The final DMSO concen-tration in the plate was 1%. Plate was incubated for 5 days at 26 C, aliquots of each well were collected, and the number of viable parasites were counted in a Neubauer chamber and compared to untreated parasite culture. Inhibitory concentration for 50% (IC_{50}) was calculated using nonlinear regression on Prism 4.0 GraphPad software. Benznidazole and nifurtimox were used as the reference drugs.

5.7. Anti-T. cruzi activity (trypomastigotes)

Metacyclic trypomastigotes were collected from the superna-tant of infected LLC-MK2 cells and then seeded at 4 10^5 cells/well in RPMI-1640 medium. All compounds were dissolved in DMSO and then diluted in RPMI-1640 medium in a serial dilution (1.23, 3.70, 11.11, 33.33 and 100 mg/mL) and added to respective wells, in triplicate. The final DMSO concentration was 1%. Plate was incu-bated for 24 h at 37 C and 5% of CO_2. Aliquots of each well were collected, and the number of viable parasites was counted in a Neubauer chamber. The percentage of inhibition was calculated in relation to untreated cultures. Cytotoxic concentration for 50% (CC_{50}) calculation was also carried out using nonlinear regression with Prism 4.0 GraphPad software. Benznidazole and nifurtimox were used as the reference drugs.

5.8. Inhibition of catalytic activity of cruzain

Recombinant cruzain was gently provided by Allison Doak and Dr. Brian Shoichet, from the University of California San Francisco. Cruzain activity was measured as previously described, by moni-toring the cleavage of the fluorogenic substrate Z-Phe-Arg-amino-methylcoumarin (Z-FR-AMC) in a Synergy 2 (Biotek), from the Center of Flow Cytometry and Fluorimetry at the Biochemistry and Immunology Department (UFMG), using filters of 340 nm for excitation and 440 nm for emission. Assays were performed in sodium acetate 0.1 M pH 5.5 and in the presence of 1 mM b-mer-captoethanol and 0.01% Triton X-100. The final concentration of cruzain was 0.5 nM, and the substrate concentration was 2.5 mM (K_m ¼ 1.0 mM). Compounds (9a, 9h, 9k, 9m, 9n, 9o and 9s) were screened at 100 mM, while (9g, 9p and 9t) were tested at 50 mM. Screening was performed in two conditions, without pre-incubation with the enzyme and after a 10-min pre-incubation with enzyme. All compounds were assayed in two independent experiments, each performed in triplicates. Assays were followed for 5 min, and activity was calculated based on a DMSO control.

5.9. Flow cytometry analysis

Trypomastigotes (4 10^5 cells/mL) were resuspended in RPMI-1640 medium and treated with compound (9r) (0.25 and 1.1 mM) for 24 h at 37 C with 5% CO_2. Parasites were labeled with propi-dium iodide (PI) and annexin V using the annexin V-FITC apoptosis detection kit (Ebioscience, San Diego, USA) according to the manufacturer instructions. Experiment was performed using a BD Calibur flow cytometer (San Jose, USA) by acquiring 50,000 events at least, and data were analyzed by BD CellQuest software (San Jose, USA). Two independent experiments, in triplicate, were performed.

Acknowledgments

This work was funded by CNPq (grant 471461/2011-3 to A.C.L.L. and 477435/2012-2 to R.S.F.) and FACEPE. A.C.L.L. and C.A.S. and V.R.A.P. are recipients of a CNPq fellowship, A.D.T.O. held a FACEPE scholarship and D.R.M.M. holds a FAPESB post-doctoral scholarship. Authors are thankful to the CPqGM Proteomic facility for deter-mining mass spectral, Instituto de Física de São Carlos for allowing the use of the diffractometer and Centro de Citometria e Fluorimetria da UFMG/FAPEMIG for allowing the use of the fluorimeter. We are very thankful to Allison Doak and Dr. Brian Shoichet (University of California San Francisco) for providing recombinant cruzain.

Crystallographic data for compound (9a) can be obtained free of charge from the Cambridge Crystallographic Data Centre (deposi-tion number 945350, www.ccdc.cam.ac.uk/data_request/cif).

References

[1] A. Rassi Jr., A. Rassi, J.A. Marin-Neto, Chagas disease, Lancet 375 (2010) 1388e 1402, http://dx.doi.org/10.1016/S0140-6736(10)60061-X.

[2] J.A. Urbina, New advances in the management of a long-neglected disease, Clinical Infectious Diseases 49 (2009) 1685e1687, http://dx.doi.org/10.1086/ 648073.

[3] F.S. Machado, L.A. Jelicks, L.V. Kirchhoff, J. Shirani, F. Nagajyothi, S. Mukherjee, R. Nelson, C.M. Coyle, D.C. Spray, A.C. de Carvalho, F. Guan, C.M. Prado, M.P. Lisanti, L.M. Weiss, S.P. Montgomery, H.B. Tanowitz, Chagas heart dis-ease: report on recent developments, Cardiology in Review 20 (2012) 53e65, http://dx.doi.org/10.1097/CRD.0b013e31823efde2.

[4] M.J. Pinazo, J. Muñoz, E. Posada, P. López-Chejade, M. Gállego, E. Ayala, E. del Cacho, D. Soy, J. Gascon, Tolerance of benznidazole in treatment of Chagas' disease in adults, Antimicrobial Agents and Chemotherapy 54 (2010) 4896e 4899, http://dx.doi.org/10.1128/AAC.00537-10.

[5] R.L. Tarleton, J.W. Curran, Is Chagas disease really the "New HIV/AIDS of the Americas"? PLOS Neglected Tropical Diseases 6 (2012) e1861, http:// dx.doi.org/10.1371/journal.pntd.0001861.

[6] F.S. Buckner, J.A. Urbina, Recent developments in sterol 14-demethylase in-hibitors for Chagas disease, International Journal for Parasitology e Drugs and Drug Resistance 2 (2012) 236e242, http://dx.doi.org/10.1016/ j.ijpddr.2011.12.002.

[7] C.B. Lantwin, I. Schlichting, W. Kabsch, E.F. Pai, R.L. Krauth-Siegel, The struc-ture of Trypanosoma cruzi trypanothione reductase in the oxidized and NADPH reduced state, Proteins 18 (1994) 161e173, http://dx.doi.org/10.1002/ prot.340180208.

[8] J.C. Engel, P.S. Doyle, I. Hsieh, J.H. McKerrow, Cysteine protease inhibitors cure an experimental Trypanosoma cruzi infection, Journal of Experimental Medi-cine 188 (1998) 725e734, http://dx.doi.org/10.1084/jem.188.4.725.

[9] S.S. Dc-Rubin, S. Schenkman, Trypanosoma cruzi trans-sialidase as a multi-functional enzyme in Chagas' disease, Cellular Microbiology 14 (2012) 1522e 1530, http://dx.doi.org/10.1111/j.1462-5822.2012.01831.x.

[10] S.E. Wilkowsky, M.A. Barbieri, P. Stahl, E.L. Isola, Trypanosoma cruzi: phos-phatidylinositol 3-kinase and protein kinase B activation is associated with parasite invasion, Experimental Cell Research 264 (2001) 211e218, http:// dx.doi.org/10.1006/excr.2000.5123.

[11] P.S. Doyle, Y.M. Zhou, J.C. Engel, J.H. McKerrow, A cysteine protease inhibitor cures Chagas' disease in an immunodeficient-mouse model of infection, Antimicrobial Agents and Chemotherapy 51 (2007) 3932e3939, http:// dx.doi.org/10.1128/AAC.00436-07.

[12] F. Villalta, M.C. Dobish, P.N. Nde, Y.Y. Kleshchenko, T.Y. Hargrove, C.A. Johnson, M.R. Waterman, J.N. Johnston, G.I. Lepesheva, VNI cures acute and chronic experimental Chagas disease, Journal of Infectious Diseases 208 (2013) 504e 511, http://dx.doi.org/10.1093/infdis/jit042.

[13] M.D. Soeiro, E.M. de Souza, C.F. da Silva, D.G.J. Batista, M.M. Batista, B.P. Pavão, J.S. Araújo, C.A. Aiub, P.B. da Silva, J. Lionel, C. Britto, K. Kim, G. Sulikowski, T.Y. Hargrove, M.R. Waterman, G.I. Lepesheva, In Vitro and in vivo studies of the antiparasitic activity of sterol 14α-demethylase (CYP51) inhibitor VNI against drug-resistant strains of Trypanosoma cruzi, Antimicrobial Agents and Chemotherapy 57 (2013) 4151e4163, http://dx.doi.org/10.1128/AAC.00070-13.

[14] A.F. Francisco, P.M. de Abreu Vieira, J.M. Arantes, M.L. Pedrosa, H.R. Martins, M. Silva, V.M. Veloso, M. de Lana, M.T. Bahia, W.L. Tafuri, C.M. Carneiro, Try-panosoma cruzi: desferrioxamine decreases mortality and parasitemia in infected mice through a trypanostatic effect, Experimental Parasitology 120 (2008) 314e319, http://dx.doi.org/10.1016/j.exppara.2011.05.011.

[15] S. Cencig, N. Coltel, C. Truyens, Y. Carlier, Evaluation of benznidazole treat-ment combined with nifurtimox, posaconazole or AmBisome in mice infected with Trypanosoma cruzi strains, International Journal of Antimicrobial Agents 40 (2012) 527e532, http://dx.doi.org/10.1016/ j.ijantimicag.2012.08.002.

[16] D.R.M. Moreira, A.C.L. Leite, R.R. dos Santos, M.B.P. Soares, Approaches for the development of new anti-Trypanosoma cruzi agents, Current Drug Targets 10 (2009) 212e231, http://dx.doi.org/10.2174/138945009787581140.

[17] A.A. Rascón Jr., J.H. McKerrow, Synthetic and natural protease inhibitors provide insights into parasite development, virulence and pathogenesis, Current Medicinal Chemistry 20 (2013) 3078e3102, http://dx.doi.org/ 10.2174/0929867311320250005.

[18] V.G. Duschak, M. Ciaccio, J.R. Nassert, M.A. Basombrio, Enzymatic activity, protein expression and gene sequence of cruzipain in virulent and attenuated Trypanosoma cruzi strains, Journal of Parasitology 87 (2001) 1016e1022.

[19] P.S. Doyle, Y.M. Zhou, I. Hsieh, D.C. Greenbaum, J.H. McKerrow, J.C. Engel, The Trypanosoma cruzi protease cruzain mediates immune evasion, Plos Patho-gens 7 (2011) e1002139, http://dx.doi.org/10.1371/journal.ppat.1002139.

[20] X. Du, E. Hansell, J.C. Engel, C.R. Caffrey, F.E. Cohen, J.H. McKerrow, Aryl ureas represent a new class of anti-trypanosomal agents, Chemistry & Biology 7 (2000) 733e742, http://dx.doi.org/10.1016/S1074-5521(00)00018-1.

[21] H.J. Wiggers, J.R. Rocha, W.B. Fernandes, R. Sesti-Costa, Z.A. Carneiro, J. Cheleski, A.B. da Silva, L. Juliano, M.H. Cezari, J.S. Silva, J.H. McKerrow, C.A. Montanari, Non-peptidic cruzain inhibitors with trypanocidal activity discovered by virtual screening and in vitro assay, PLOS Neglected Tropical Diseases 7 (2013) e2370, http://dx.doi.org/10.1371/journal.pntd.0002370.

[22] J.M. dos Santos Filho, A.C.L. Leite, B.G. de Oliveira, D.R.M. Moreira, M.S. Lima, M.B.P. Soares, L.F.C. Leite, Design, synthesis and cruzain docking of 3-(4-substituted-aryl)-1,2,4-oxadiazole-N-acylhydrazones as anti-Trypanosoma cruzi agents, Bioorganic & Medicinal Chemistry 17 (2009) 6682e6691, http:// dx.doi.org/10.1016/j.bmc.2009.07.068.

[23] N.C. Romeiro, G. Aguirre, P. Hernández, M. González, H. Cerecetto, I. Aldana, S. Pérez-Silanes, A. Monge, E.J. Barreiro, L.M. Lima, Synthesis, trypanocidal activity and docking studies of novel quinoxaline-N-acylhydrazones, designed as cruzain inhibitors candidates, Bioorganic & Medicinal Chemistry 17 (2009) 641e652, http://dx.doi.org/10.1016/j.bmc.2008.11.065.

[24] J.M. dos Santos-Filho, D.R. Moreira, C.A. de Simone, R.S. Ferreira, J.H. McKerrow, C.S. Meira, E.T. Guimarães, M.B.P. Soares, Optimization of anti-Trypanosoma cruzi oxadiazoles leads to identification of compounds with efficacy in infected mice, Bioorganic & Medicinal Chemistry 20 (2012) 6423e 6433, http://dx.doi.org/10.1016/j.bmc.2012.08.047.

[25] T.N. Franklim, L. Freire-de-Lima, J.N.S. Diniz, J.O. Previato, R.N. Castro, L. Mendonça-Previato, M.E.F. de Lima, Design, synthesis and trypanocidal evaluation of novel 1,2,4-triazoles-3-thiones derived from natural piperine, Molecules 18 (2013) 6366e6382, http://dx.doi.org/10.3390/ molecules18066366.

[26] K. Brak, P.S. Doyle, J.H. McKerrow, J.A. Ellman, Identification of a new class of nonpeptidic inhibitors of cruzain, Journal of the American Chemical Society 130 (2008) 6404e6410, http://dx.doi.org/10.1021/ja710254m.

[27] K. Brak, I.D. Kerr, K.T. Barrett, N. Fuchi, M. Debnath, K. Ang, J.C. Engel, J.H. McKerrow, P.S. Doyle, L.S. Brinen, J.A. Ellman, Nonpeptidic tetra-fluorophenoxymethyl ketone cruzain inhibitors as promising new leads for Chagas disease chemotherapy, Journal of Medicinal Chemistry 53 (2010) 1763e1773, http://dx.doi.org/10.1021/jm901633v.

[28] X. Du, C. Guo, E. Hansell, P.S. Doyle, C.R. Caffrey, T.P. Holler, J.H. McKerrow, F.E. Cohen, Synthesis and structure-activity relationship study of potent try-panocidal thio semicarbazone inhibitors of the trypanosomal cysteine pro-tease cruzain, Journal of Medicinal Chemistry 45 (2002) 2695e2707, http:// dx.doi.org/10.1021/jm010459j.

[29] D.C. Greenbaum, Z. Mackey, E. Hansell, P. Doyle, J. Gut, C.R. Caffrey, J. Lehrman, P.J. Rosenthal, J.H. McKerrow, K. Chibale, Synthesis and structure-activity re-lationships of parasiticidal thiosemicarbazone cysteine protease inhibitors against Plasmodium falciparum, Trypanosoma brucei, and Trypanosoma cruzi, Journal of Medicinal Chemistry 47 (2004) 3212e3219, http://dx.doi.org/ 10.1021/jm030549j.

[30] R. Siles, S.E. Chen, M. Zhou, K.G. Pinney, M.L. Trawick, Design, synthesis, and biochemical evaluation of novel cruzain inhibitors with potential application in the treatment of Chagas' disease, Bioorganic & Medicinal Chemistry Letters 16 (2006) 4405e4409, http://dx.doi.org/10.1016/j.bmcl.2006.05.041.

[31] N.B. Lozano, V.G. Maltarollo, K.C. Weber, K.M. Honorio, R.V. Guido, A.D. Andricopulo, A.B. Da Silva, Molecular features for antitrypanosomal ac-tivity of thiosemicarbazones revealed by OPS-PLS QSAR studies, Medicinal Chemistry 8 (2012) 1045e1056.

[32] W. Porcal, P. Hernández, L. Boiani, M. Boiani, A. Ferreira, A. Chidichimo, J.J. Cazzulo, C. Olea-Azar, M. González, H. Cerecetto, New trypanocidal hybrid compounds from the association of hydrazone moieties and benzofuroxan heterocycle, Bioorganic & Medicinal Chemistry 16 (2008) 6995e7004, http:// dx.doi.org/10.1016/j.bmc.2008.05.038.

[33] M. Vieites, L. Otero, D. Santos, C. Olea-Azar, E. Norambuena, G. Aguirre, H. Cerecetto, M. González, U. Kemmerling, A. Morello, J. Diego Maya, D. Gambino, Risedronate metal complexes potentially active against Chagas disease, Journal of Inorganic Biochemistry 103 (2009) 411e418, http:// dx.doi.org/10.1016/j.jinorgbio.2010.08.004.

[34] G.H. Trossini, A. Malvezzi, A.T. Amaral, C.O. Rangel-Yagui, M.A. Izidoro, M.H. Cezari, L. Juliano, C.M. Chin, C.M. Menezes, E.I. Ferreira, Cruzain inhibi-tion by hydroxymethylnitrofurazone and nitrofurazone: investigation of a new target in Trypanosoma cruzi, Journal of Enzyme Inhibition and Medicinal Chemistry 25 (2010) 62e67, http://dx.doi.org/10.3109/14756360902941058.

[35] M.E. Caputto, L.E. Fabian, D. Benítez, A. Merlino, N. Ríos, H. Cerecetto, G.Y. Moltrasio, A.G. Moglioni, M. González, L.M. Finkielsztein, Thio-semicarbazones derived from 1-indanones as new anti-Trypanosoma cruzi agents, Bioorganic & Medicinal Chemistry 19 (2011) 6818e6826, http:// dx.doi.org/10.1016/j.bmc.2011.09.037.

[36] B. Demoro, C. Sarniguet, R. Sánchez-Delgado, M. Rossi, D. Liebowitz, F. Caruso, C. Olea-Azar, V. Moreno, A. Medeiros, M.A. Comini, L. Otero, D. Gambino, New organoruthenium complexes with bioactive thiosemicarbazones as co-ligands: potential anti-trypanosomal agents, Dalton Transactions 41 (2012) 1534e1543, http://dx.doi.org/10.1039/c1dt11519g.

[37] L. Blau, R.F. Menegon, G.H. Trossini, J.V. Molino, D.G. Vital, R.M. Cicarelli, G.D. Passerini, P.L. Bosquesi, C.M. Chin, Design, synthesis and biological evaluation of new aryl thiosemicarbazone as antichagasic candidates, Euro-pean Journal of Medicinal Chemistry 67 (2013) 142e151, http://dx.doi.org/ 10.1016/j.ejmech.2013.04.022.

[38] I.A. Moussa, S.D. Banister, F.N. Akladios, S.W. Chua, M. Kassiou, Effects of linker elongation in a series of N-(2-benzofuranylmethyl)-N′-(methoxyphenylalkyl)

piperazine S1 receptor ligands, Bioorganic & Medicinal Chemistry Letters 21 (2011) 5707e5710, http://dx.doi.org/10.1016/j.bmcl.2011.08.029.

[39] T.E. Pompeu, F.R. Alves, C.D. Figueiredo, C.B. Antonio, V. Herzfeldt, B.C. Moura, S.M. Rates, E.J. Barreiro, C.A.M. Fraga, F. Noël, Synthesis and pharmacological evaluation of new N-phenylpiperazine derivatives designed as homologues of the antipsychotic lead compound LASSBio-579, European Journal of Medicinal Chemistry 66 (2013) 122e134, http://dx.doi.org/10.1016/ j.ejmech.2013.05.027.

[40] A.C.L. Leite, R.S. de Lima, D.R.M. Moreira, M.V.O. Cardoso, A.C.G. Brito, L.M.F. Santos, M.Z. Hernandes, A.C. Kiperstok, R.S. de Lima, M.B.P. Soares, Synthesis, docking, and in vitro activity of thiosemicarbazones, aminoacyl-thiosemicarbazides and acyl-thiazolidones against Trypanosoma cruzi, Bio-organic & Medicinal Chemistry 14 (2006) 3749e3757, http://dx.doi.org/ 10.1016/j.bmc.2006.01.034.

[41] M.Z. Hernandes, M.M. Rabello, A.C.L. Leite, M.V. Cardoso, D.R.M. Moreira, D.J. Brondani, C.A. Simone, L.C. Reis, M.A. Souza, V.R.A. Pereira, R.S. Ferreira, J.H. McKerrow, Studies toward the structural optimization of novel thiazolylhydrazone-based potent antitrypanosomal agents, Bioorganic & Medicinal Chemistry 18 (2010) 7826e7835, http://dx.doi.org/10.1016/ j.bmc.2010.09.056.

[42] D.R.M. Moreira, S.P. Costa, M.Z. Hernandes, M.M. Rabello, G.B.O. Filho, C.M. de Melo, L.F. da Rocha, C.A. de Simone, R.S. Ferreira, J.R. Fradico, C.S. Meira, E.T. Guimarães, R.M. Srivastava, V.R. Pereira, M.B.P. Soares, A.C.L. Leite, Struc-tural investigation of anti-Trypanosoma cruzi 2-iminothiazolidin-4-ones allows the identification of agents with efficacy in infected mice, Journal of Medicinal Chemistry 55 (2012) 10918e10936, http://dx.doi.org/10.1021/jm301518v.

[43] D.R. Moreira, A.C.L. Leite, M.V.O. Cardoso, R.M. Srivastava, M.Z. Hernandes, M.M. Rabello, L.F. da Cruz, R.S. Ferreira, C.A. de Simone, C.S. Meira, E.T. Guimaraes, A.C. da Silva, T.A. Dos Santos, V.R.A. Pereira, M.B.P. Soares, Structural design, synthesis and structure-activity relationships of thiazoli-dinones with enhanced anti-Trypanosoma cruzi activity, ChemMedChem 9 (2014) 177e188, http://dx.doi.org/10.1002/cmdc.201300354.

[44] J.R. Dimmock, R.N. Puthucode, J.M. Smith, M. Hetherington, J.W. Quail, U. Pugazhenthi, T. Lechler, J.P. Stables, (Aryloxy)aryl semicarbazones and related compounds: a novel class of anticonvulsant agents possessing high activity in the maximal electroshock screen, Journal of Medicinal Chemistry 39 (1996) 3984e3997, http://dx.doi.org/10.1021/jm9603025.

[45] N. Selvakumar, M.A. Raheem, M.K. Khera, T.V. Rajale, M.S. Kumar, S. Kandepu, J. Das, R. Rajagopalan, J. Iqbal, S. Trehan, Influence of ethylene-oxy spacer group on the activity of linezolid: synthesis of potent antibacterials possessing a thiocarbonyl group, Bioorganic & Medicinal Chemistry Letters 13 (2003) 4169e4172, http://dx.doi.org/10.1016/j.bmcl.2003.08.068.

[46] A.J. Bojarski, B. Duszynska, M. Ko1aczkowski, P. Kowalski, T. Kowalska, The impact of spacer structure on 5-HT7 and 5-HT1A receptor affinity in the group of long-chain arylpiperazine ligands, Bioorganic & Medicinal Chemistry Let-ters 14 (2004) 5863e5866, http://dx.doi.org/10.1016/j.bmcl.2004.09.029.

[47] A. Kamal, S. Prabhakar, M. Janaki Ramaiah, P. Venkat Reddy, C. Ratna Reddy, A. Mallareddy, N. Shankaraiah, T.L.N. Reddy, S.N.C.V. Pushpavalli, M. Pal-Bhadra, Synthesis and anticancer activity of chalcone–pyrrolobenzodiazepine conjugates linked via 1,2,3-triazole ring side-armed with alkane spacers, European Journal of Medicinal Chemistry 46 (2011) 3820e3831, http:// dx.doi.org/10.1016/j.ejmech.2011.05.050.

[48] S. Yonezawa, H. Yamakawa, C. Muto, M. Hosono, T. Yamamoto, K. Hattori, M. Sakagami, H. Togame, Y. Tanaka, T. Nakano, H. Takemoto, M. Arisawa, S. Shuto, Conformational restriction approach to BACE1 inhibitors II: SAR study of the isocytosine derivatives fixed with a cis-cyclopropane ring, Bio-organic & Medicinal Chemistry Letters 23 (2013) 2912e2915, http:// dx.doi.org/10.1016/j.bmcl.2013.03.056.

[49] S.A. Carvalho, L.O. Feitosa, M. Soares, T.E. Costa, M.G. Henriques, K. Salomão, S.L. de Castro, M. Kaiser, R. Brun, J.L. Wardell, S.M. Wardell, G.H. Trossini, A.D. Andricopulo, E.F. da Silva, C.A.M. Fraga, Design and synthesis of new (E)-cinnamic N-acylhydrazones as potent antitrypanosomal agents, European Journal of Medicinal Chemistry 54 (2012) 512e721, http://dx.doi.org/10.1016/ j.ejmech.2012.05.041.

[50] J.V.D. Molino, D.G. Vital, R.M.B. Cicarelli, G.D. Passerini, P.L. Bosquesi, C. ManChin, Design, synthesis and biological evaluation of new aryl thio-semicarbazone as antichagasic candidates, European Journal of Medicinal Chemistry 67 (2013) 142e151, http://dx.doi.org/10.1016/ j.ejmech.2013.04.022.

[51] M. Aveniente, E.F. Pinto, L.S. Santos, B. Rossi-Bergmann, L.E. Barata, Structure-activity relationship of antileishmanials neolignan analogues, Bioorganic & Medicinal Chemistry 15 (2007) 7337e7343, http://dx.doi.org/10.1016/ j.bmc.2007.08.016.

[52] D.N. Zhang, J.T. Li, Y.L. Song, H.M. Liu, H.Y. Li, Efficient one-pot three-component synthesis of N-(4-arylthiazol-2-yl) hydrazones in water under ultrasound irradiation, Ultrasonics Sonochemistry 19 (2012) 475e478, http:// dx.doi.org/10.1016/j.ultsonch.2011.10.017.

[53] A.M.M. Bastos, A.F.C. Alcântara, H. Beraldo, Structural analyses of 4-benzoyl-pyridine thiosemicarbazone using NMR techniques and theoretical calcula-tions, Tetrahedron 61 (2005) 7045e7053, http://dx.doi.org/10.1016/ j.tet.2005.04.042.

[54] A.J. Romanha, S.L. Castro, M.N. Soeiro, J. Lannes-Vieira, I. Ribeiro, A. Talvani, B. Bourdin, B. Blum, B. Olivieri, C.L. Zani, C. Spadafora, E. Chiari, E. Chatelain, G. Chaves, J.E. Calzada, J.M. Bustamante, L.H. Freitas-Junior, L.I. Romero, M.T. Bahia, M. Lotrowska, M.B. Soares, S.G. Andrade, T. Armstrong, W. Degrave, Z.A. Andrade, In vitro and in vivo experimental models for drug screening and development for Chagas disease, Memorias do Instituto Oswaldo Cruz 105 (2010) 233e238, http://dx.doi.org/10.1590/S0074-02762010000200022.

[55] R.S. Ferreira, C. Bryant, K.K. Ang, J.H. McKerrow, B.K. Shoichet, A.R. Renslo, Divergent modes of enzyme inhibition in a homologous structure-activity series, Journal of Medicinal Chemistry 52 (2009) 5005e5008, http:// dx.doi.org/10.1021/jm9009229.

[56] A.L. Matsuo, L.S. Silva, A.C. Torrecilhas, B.S. Pascoalino, T.C. Ramos, E.G. Rodrigues, S. Schenkman, A.C. Caires, L.R. Travassos, In vitro and in vivo trypanocidal effects of the cyclopalladated compound 7a, a drug candidate for treatment of Chagas' disease, Antimicrobial Agents and Chemotherapy 54 (2010) 3318e3325, http://dx.doi.org/10.1128/AAC.00323-10.

[57] J.D. Maya, S. Bollo, L.J. Nuñez-Vergara, J.A. Squella, Y. Repetto, A. Morello, J. Périé, G. Chauvière, Trypanosoma cruzi: effect and mode of action of nitro-imidazole and nitrofuran derivatives, Biochemical Pharmacology 65 (2003) 999e1006, http://dx.doi.org/10.1016/S0006-2952(02)01663-5.

[58] M.Z. Hernandes, S.M. Cavalcanti, D.R.M. Moreira, W.F. de Azevedo-Junior, A.C.L. Leite, Halogen atoms in the modern medicinal chemistry: hints for the drug design, Current Drug Targets 11 (2010) 303e314, http://dx.doi.org/ 10.2174/138945010790711996.

[59] J.M. Kraus, H.B. Tatipaka, A.S. McGuffin, N.K. Chennamaneni, M. Karimi, J. Arif, C.L. Verlinde, F.S. Buckner, M.H. Gelb, Second generation analogues of the cancer drug clinical candidate tipifarnib for anti-Chagas disease drug dis-covery, Journal of Medicinal Chemistry 53 (2010) 3887e3898, http:// dx.doi.org/10.1021/jm9013136.

[60] M.T. Bahia, I.M. de Andrade, T.A. Martins, A.F. do Nascimento, L.F. Diniz, I.S. Caldas, A. Talvani, B.B. Trunz, E. Torreele, I. Ribeiro, Fexinidazole: a po-tential new drug candidate for Chagas disease, PLOS Neglected Tropical Dis-eases 6 (2012) e1870, http://dx.doi.org/10.1371/journal.pntd.0001870.

[61] E.F. Santiago, S.A. de Oliveira, G.B. de Oliveira Filho, D.R.M. Moreira, P.A. Gomes, A.L. da Silva, A.F. de Barros, A.C. da Silva, T.A. Dos Santos, V.R.A. Pereira, G.C. Gonçalves, F.A. Brayner, L.C. Alves, A.G. Wanderley, A.C. Leite, Evaluation of the anti-Schistosoma mansoni activity of thio-semicarbazones and thiazoles, Antimicrobial Agents and Chemotherapy 58 (2014) 352e363, http://dx.doi.org/10.1128/AAC.01900-13. Epub 2013 Oct 28.

[62] B. Zingales, S.G. Andrade, M.R. Briones, D.A. Campbell, E. Chiari, O. Fernandes, F. Guhl, E. Lages-Silva, A.M. Macedo, C.R. Machado, M.A. Miles, A.J. Romanha, N.R. Sturm, M. Tibayrenc, A.G. Schijman, A new consensus for Trypanosoma cruzi intraspecific nomenclature: second revision meeting recommends TcI to TcVI, Memorias do Instituto Oswaldo Cruz 104 (2009) 1051e1054, http:// dx.doi.org/10.1590/S0074-02762009000700021.

APÊNDICE G -

Novel phthalimide derivatives with TNF-a and IL-1b expression inhibitory and apoptotic inducing properties

MedChemComm

CONCISE ARTICLE

View Article Online
View Journal | View Issue

Cite this: Med. Chem. Commun., 2014, 5, 758

Novel phthalimide derivatives with TNF-a and IL-1b expression inhibitory and apoptotic inducing properties

Lucas Cunha Duarte Coelho,[a] Marcos Ver´ıssimo de Oliveira Cardoso,[a] Diogo Rodrigo Magalhaes Moreira,[a] Paulo Andre Teixeira de Moraes Gomes,[a] Suellen Melo Tiburcio Cavalcanti,[a] Arsenio Rodrigues Oliveira,[a] Gevanio Bezerra de Oliveira Filho,[a] Lucianna Rabelo Pessoa de Siqueira,[a] Miria de Oliveira Barbosa,[a] Elizabeth Fernanda de Oliveira Borba,[b] Teresinha Gonçalves da Silva,[b] Belinda Kaskow,[c] Mahdad Karimi,[c] Lawrence J. Abraham[d] and Ana Cristina Lima Leite*[a]

Received 19th February 2014
Accepted 28th March 2014

DOI: 10.1039/c4md00070f

www.rsc.org/medchemcomm

Modulation of the immune system is an emerging concept in the control of tumor growth. Bearing in mind the pharmacological properties of thalidomide and its phthalimide derivatives, we describe here the structural design, synthesis and pharmacological evaluation of N-acylhydrazones derived from phthalimide. The ability of these N-acylhydrazones in inhibiting the secretion of TNF-a in stimulated cells as well as in inhibiting the transcription of the TNF-a gene was evaluated. We identified N-acylhydrazones 6b and 9c, which substantially impaired TNF-a secretion, expression and reduced IL-1b production similar to thalidomide or Revlimid. N-Acylhydrazone 9c was also able to induce apoptosis in Jurkat cells, however it does not have either antiproliferative properties or cytotoxicity for mouse splenocytes. Beyond that, we have assayed the ability of these compounds to induce cell death and a number of them are able to induce apoptosis.

Introduction

The immune system's role in cancer involves many different mechanisms, such as minimizing metastasis by attenuating the expression of pro-angiogenic factors. Another aspect is the enhancement of antitumor immunity facilitated by interferons and interleukins. Overall, reducing in ammation by modu-lating the immune response is important over the course of cancer. In light of these possibilities, the identi cation of immunomodulating agents is a task that is receiving a great deal of attention. In this way, a variety of cytokines, including IL-1 and tumor necrosis factor (TNF), play different roles as regulators of immune, in ammatory, and growth responses.[1] IL-1 ligands (IL-1a and IL-1b, collectively referred to as IL-1) are pluripotent, proin ammatory cytokines that orchestrate in ammatory and host defense responses in the body.[2] IL-1 increases T-cell responses to mitogens (and indirectly activates B cells), increases expression of vascular adhesion molecules, and induces a number of other proin ammatory cytokines, chemokines, and in ammation-associated molecules that form an amplifying cascade to stimulate an immune response.[2] Tumor necrosis factor (TNF) can kill cells by apoptosis, and this ability to induce apoptosis is presently the most intensely studied area of TNF research.[3]

A series of recent papers has provided new hope that TNF could yet be useful as an anti-tumor cytokine.[4–8] The manipu-lation of signaling pathways downstream of TNF receptor (TNF-R) activation showed that TNF negatively regulates its own ability to induce apoptosis. However, despite considerable incentives, viable leads for analogous small-molecule inhibitors of TNF have not been reported.[8]

Phthalimide derivatives have been attracting considerable attention since 1979 when Chapman Jr et al. showed that N-substituted phthalimides possess hypolipidemic activity.[9] Two years later, Hall et al. examined 12 imide analogs and proposed that phthalimides are able to inhibit acetyl CoA carboxylase activity.[10] The same group investigated 10 N-aryl-phthalimides and found that o-(N-phthalimido)acetophenone lowered both serum cholesterol and triglyceride levels by 57% and 44% a er 16 and 14 days of treatment in Swiss white mice.[11] This class of compounds is also endowed with anti-

[a]Departamento de Ci^encias Farmac^euticas, Centro de Ci^encias da Saude,´ Universidade Federal de Pernambuco, 50740-520, Recife, PE, Brazil. E-mail: acllb2003@yahoo.com. br

[b]Departamento de Antibi´oticos, Centro de Ci^encias Biol´ogicas, Universidade Federal de Pernambuco, 50740-520, Recife, PE, Brazil

[c]The School of Chemistry & Biochemistry, The University of Western Australia, Crawley, WA 6009, Australia

[d]School of Pathology & Laboratory Medicine, The University of Western Australia, Crawley, WA 6009, Australia

in ammatory and immunomodulatory properties, with thalid-omide as the best representative of bioactive phthalimides.

Furthermore, a biochemical strategy for derivatization of carboxylic acid-containing non-steroidal anti-in ammatory drugs (NSAIDs) to esters or amides was able to produce mole-cules capable of binding tightly to COX-2, but not COX-1. This single chemical derivatization (amidation or esteri cation) of the carboxylic acid moiety-containing NSAIDs generates an impressive array of potent and highly selective COX-2 inhibi-tors. Several of them exhibited anti-in ammatory and anti-angiogenic activities.[12]

Similarly, a number of hydrazones have been evaluated for new drug development, and some of them have been shown to exhibit anti-cancer properties.[13] Some have demonstrated qual-ities of an apoptotic inducer with anti-proliferative chemo-preventive activity in tongue cancer cells, such as the compound [bromomethyl(phenyl)methyl]-2-(2,4-dinitrophenyl)hydrazine.[14] In fact, because of their functional properties, the attachment of N-acylhydrazones has been employed in the design of new anti-in ammatory and immunomodulatory agents.

In view of this, we describe the synthesis of N-phthaloyl amino acids 2a–c and their chemical derivatization to their respective esters 3a–c, amides 4a–c, hydrazides 5a–c and N-acylhydrazone derivatives 6a–c, 7a–c, 8a–c and 9a–c. All these compounds are phthalimide derivatives designed to compare the bioisosteric relationship between a carboxylic acid and an amide; moreover, we aimed to compare the bioisosteric inter-play between an amide and N-acylhydrazone. This examination also reports the pharmacological evaluation of their properties for inhibiting the secretion and expression of TNF and IL-1b in cells. Beyond that, we have assayed the ability of these compounds in inducing cell death and some of them are indeed apoptosis inducers.

Results and discussion

Chemistry

A single strategy for the production of new chemical entities is the chemical derivatization of acid or amine compounds to esters, amides or hydrazines. Indeed, N-phthaloyl amino acids 2a–c were synthesized following a known procedure[15] that condenses phthalic anhydride 1 with the respective amino acids. Then N-phthaloyl amino acids 2a–c were converted into ethyl esters 3a–c and amides 4a–c (Scheme 1). The reactions of amidi cation to prepare amides 4a–c proceed well by using urea upon re uxing with ethanol (24 h), but we adapted them under ultrasound conditions using NH_4OH and K_2CO_3 as bases which produced excellent yields in general (50–85%) and in shorter time periods (30 min in most of the cases). The hydrazides 5a–c were prepared by reacting commercially available hydrazine hydrate with the appropriate ethyl esters 3a–c under magnetic stirring in EtOH with mild heating. Once hydrazides 5a–c were isolated, we reacted them with aromatic aldehydes. These reactions were carried out in anhydrous EtOH in re ux under the presence of catalytic amounts of H_2SO_4, affording N-acyl-hydrazones 6a–c, 7a–c, 8a–c and 9a–c in low to moderate yields (38–84%). It is worth mentioning that only the desired

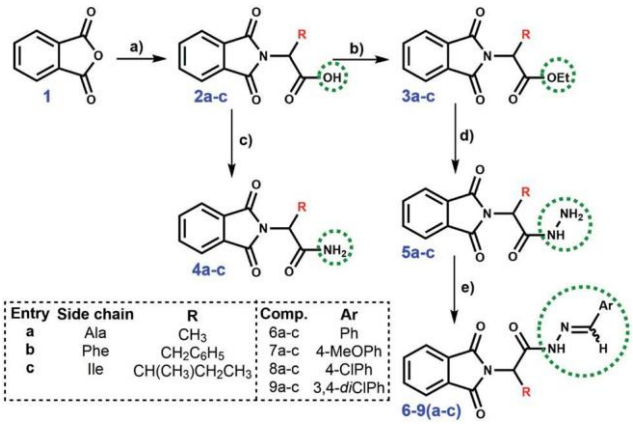

Entry	Side chain	R
a	Ala	CH_3
b	Phe	$CH_2C_6H_5$
c	Ile	$CH(CH_3)CH_2CH_3$

Comp.	Ar
6a-c	Ph
7a-c	4-MeOPh
8a-c	4-ClPh
9a-c	3,4-*di*ClPh

Scheme 1 Synthesis of the compounds. Reagents and conditions: (a) Ala, Phe or Ile, 135 C, 30 min;[15] (b) ethanol, H_2SO_4 (4 drops), magnetic stirring, 60 C, 4 h; (c) THF, imidazole, magnetic stirring, 60 C, 4 h; (d) ethanol, hydrazine hydrate (4 drops), magnetic stirring, 60 C, 4 h; and (e) ethanol, aromatic aldehyde substituted, reflux, 4 h.

S-enantiomers were obtained in all cases as veri ed by the addition of the chiral shi reagent $Eu(hfc)_3$ in ^1H NMR spectra.

Biological activities

To evaluate the levels of TNF and IL-1b, mouse macrophages were incubated with phthalimide derivatives over a 24 h time course. These cells were then stimulated with lipopolysaccha-ride (LPS). The purpose of this test was to evaluate the biological capacity of the molecules that were found to inhibit the synthesis of these extremely important cytokines in in amma-tory processes and cancers. Data presented in Fig. 1 show that twelve compounds were able to inhibit TNF production at 50 mM, better than Thl. Among all series of compounds, the hydrazide and hydrazone series were the most promising. The hydrazide derivative 5b, the phenyl-hydrazone derivative 6c and the 4-methoxy-phenyl-hydrazone derivative 7c all inhibit secre-tion of TNF by macrophages at 50 mM. Concerning IL-1b, in general, each series of compounds was able to inhibit IL-1b at the same concentration (50 mM). The ester derivative 3b was the least potent. Compounds 5b, 6c, 7b and 8c were the most active of the series. These preliminary results indicate that, in general, the chemical derivatization to acylhydrazides and hydrazones and apolar aminoacyl moieties produces new derivatives that are most effective in modulating TNF and IL-1b expression.

To effectively measure the inhibition of the expression of TNF, the compounds were tested and evaluated for inhibition of TNF transcriptional activity via the NFkB signaling pathway. For this purpose, a T cell line containing a transcriptional reporter was used (FRT-Jurkat TNF) as previously described.[16,17] The green uorescent protein (GFP) reporter gene is under the control of the TNF promoter sequence which contains an NFkB binding site. As a measure of TNF expression, the activity of GFP was quanti ed by ow cytometry as previously described.[18] First, it was determined whether the compounds inhibited the expression of TNF at 10 mM and 100 mM doses (Fig. 2). Thalid-omide was used as a standard for comparing the levels of

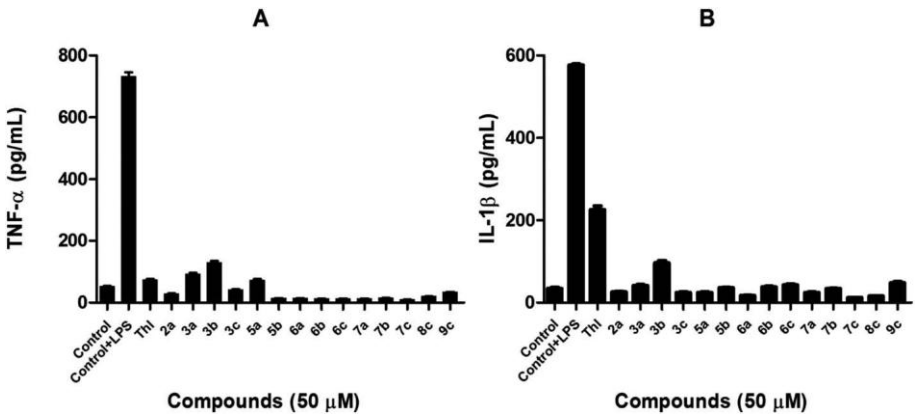

Fig. 1 (a) Effect of phthalimides and Thl on the production of TNF-a in mouse macrophages (2 10^6) stimulated with LPS (2 mg mL^{-1}). TNF-a was measured after 24 h of incubation with compounds (50 mM) by sandwich ELISA (eBioscience kit). Data are mean S.D. obtained in triplicate.
(b) Effect of phthalimides and Thl on the production of interleukin-1b (IL-1b) in mouse macrophages (2 10^6) stimulated with LPS (2 mg mL^{-1}). IL-1b was measured after 24 h of incubation with compounds (50 mM) by sandwich ELISA (eBioscience kit). Data are mean S.D. (error bars) obtained in triplicate. Thl, thalidomide; S.D., standard deviation.

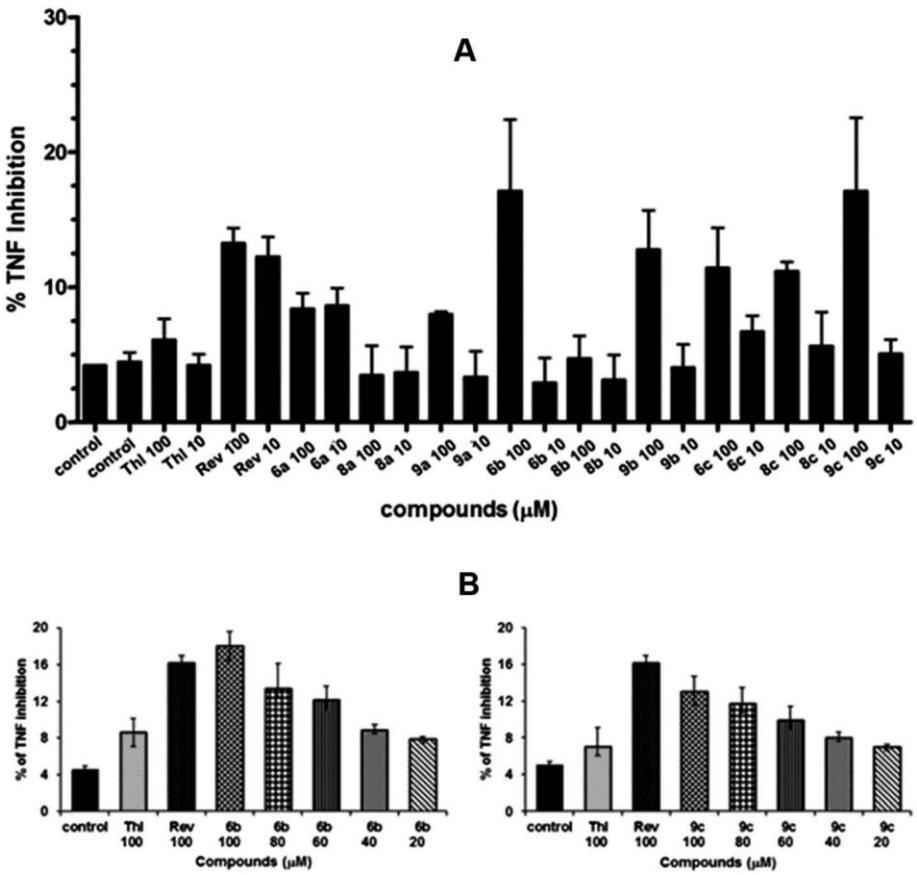

Fig. 2 (a) Effect of phthalimides and Thl on the expression of TNF in the human T cell line. Jurkat cells containing GFP-gene report under control of the TNF gene promoter (FRT-Jurkat TNF) were incubated for 24 h with the compounds (100 or 10 mM). Inhibition of TNF expression was measured as the GFP expression. Data are mean S.D. obtained in duplicate; one single experiment. (b) Dose–response curve of selected phthalimides in the expression of TNF in the human T cell line (Jurkat); two independent experiments. Controls have only buffer and DMSO (0.5%). Thl, thalidomide; Rev, Revlimid; S.D., standard deviation expressed in error bars.

inhibition. Revlimid (pomalidomide), a thalidomide derivative, which has been clinically shown to be 1000 times more powerful in relation to inhibition of TNF, was also used as a standard compound. In this model, Revlimid shows only twice the potency of thalidomide, therefore it suggests that if a compound shows a level of inhibition in this model similar to

Revlimid, in a clinical context, it will be a signi cant improve-ment over thalidomide.

The N-acyl-hydrazone 6a derivative showed a percentage inhibition of TNF-a of 9.8% at both concentrations 100 mM and 10 mM, which is about 3% more than thalidomide (around 5– 6% at 100 mM and 10 mM). The 6b (phenyl-hydrazone derivative) and 9c (3,4-dichloro-phenyl-hydrazone derivative) compounds were the most effective with inhibition around 17% at 100 mM, which is three times more effective than thalidomide and equipotent to Revlimid (Fig. 2A). No signi cant inhibitory activity was veri ed at 10 mM. As we can see in Fig. 2B, compounds 6b and 9c inhibit TNF-a in a dose-dependent manner. The TNF expression inhibition was more effective for the 6, 8 and 9 series. These series have in common an N-phenyl-acyl-hydrazone moiety. In previous studies, it was observed that improvements in thalidomide derivatives bearing hydrophobic groups (phenyl or alkyl) have been found to provide highly potent inhibitors of TNF expression.[19]

As shown in Fig. 3, we analyzed the induction of total cell death by ow cytometry. Observing the DMSO control it is clear that the solvent does not interfere with the test and does not lead to cell death. Therefore, any toxicity observed would be due solely to the presence of the compounds. By adding thalidomide (10 mM) it is possible to observe a rate of 2–3% of cell death, however Revlimid is the less toxic option. In other words, Revlimid is the most effective in inhibiting TNF without killing

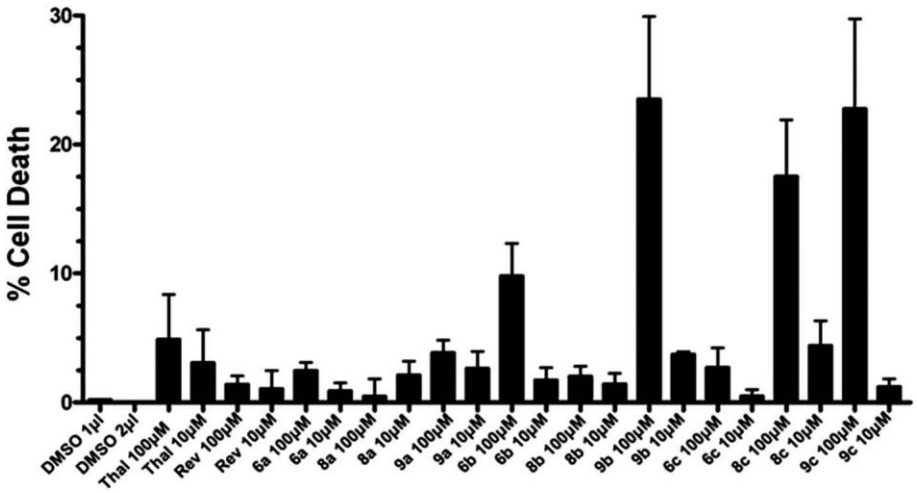

Fig. 3 Induction of total cell death. The effect of each compound on cellular viability was assessed using the FRT-Jurkat TNF reporter cell line using a FACSCalibur 4 colour flow cytometer. Viable and non-viable cells present following either solvent (DMSO) alone or compound treatment for 24 h were assayed. Cells were counted by gating on each cell population using a forward scatter (FSC) versus side scatter (SSC) plot. The percentage of viable cells was determined as the percentage of cells inside the FSC/SSC gate that encompassed the major population in solvent-only treated control cells. Viability was confirmed following propidium iodide staining and detection of fluorescence at 570 nm. Data are mean S.E. (standard error of the mean) obtained in triplicate. Thal, thalidomide, Rev, Revlimid.

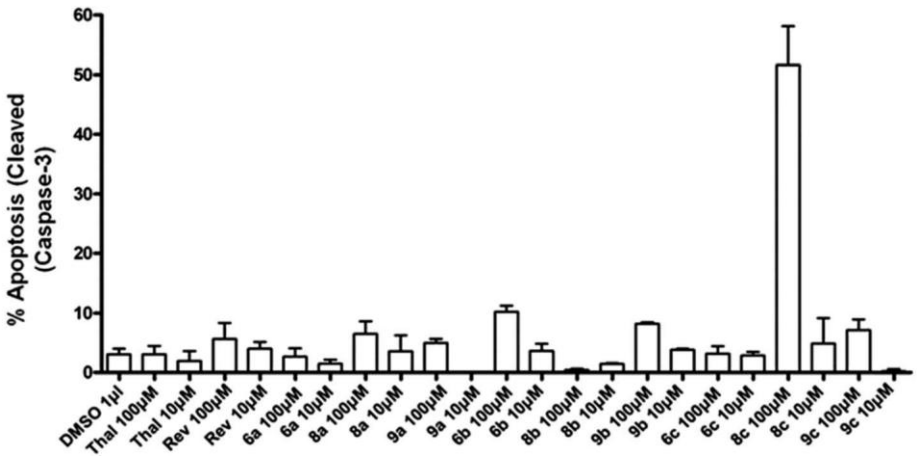

Fig. 4 Induction of apoptosis. Treatments were carried out as in Fig. 3 using the parental Jurkat line. Apoptosis was measured following treatment with a FITC-labelled caspase 3 substrate. The degree of apoptosis was assessed as the percentage of the cleaved caspase 3 substrate measured as an increase in fluorescence at 515 nm due to FITC release. Data are mean S.E. (standard error of the mean) obtained in triplicate. Thal, thalidomide, Rev, Revlimid.

cells. In general, all compounds showed acceptable levels of cell death comparable to thalidomide and even less than the Revlimid like acyl-hydrazones 6a, 6c and 9c (all at 10 mM). The compounds 6b, 9b, 8c and 9c have shown a high rate of cell death at 100 mM (Fig. 3). However, it was not previously possible to say whether this was through programmed cell death.

It is interesting to note that the compound 6a (alanyl-hydrazone derivative), at 10 mM, induced cell death at a lower percentage than Revlimid, also at 10 mM, and showed a percentage of inhibition of TNF similar to Revlimid (9% and 14% respectively, both at 10 mM). To determine whether cell death was via apoptosis (programmed cell death), we used the same T cell line, Jurkat, however without the GFP reporter (Fig. 4). Cells were treated with compounds and a er 24 hours, the degree of caspase 3 cleavage was assessed as a measure of apoptosis. Cleavage could be measured as the release of the added uorescein isothiocyanate (FITC)-labeled substrate against cleaved caspase 3.

In Fig. 4 it can be noted that the compound 6a in this trial had a greater activity than the leading parent compound Revlimid. At both 100 mM and 10 mM concentrations, our synthesized compound 6a showed a lower apoptotic action against the test cells. It is also observed that the compound 8c (4-Cl-phenyl-hydrazone derivative) has a high rate of apoptosis. From the rst test (Fig. 2) it appears that this compound inhibits TNF-a around 13% while Revlimid inhibits 14% at 100 mM. Although the compound 8c does not show more effi-cient inhibition against TNF, it is equivalent to a drug for clinical use. However, this compound is far more effective in promoting programmed cell death.

Conclusion

In conclusion, new analogues of thalidomide and immuno-modulatory activity were obtained. Compounds inhibited the production of TNF-a and IL-1 also in vitro. The pro les of compounds 6a, 6b and 9c showed good inhibition of TNF-a as compared to the standards used (thalidomide and Revlimid). The compounds 6b, 8c, 9b and 9c showed high levels of cyto-toxicity. In addition, compound 8c showed a high rate of induction of apoptosis. These results indicate that, in general the chemical derivatization to acylhydrazones and hydrazones, instead of esters or amides is most effective in modulating TNF and IL-1 expression and also is effective in promoting pro-grammed cell death. These select compounds are important lead candidates to act as immunomodulatory agents.

Experimental

General

Melting points which were measured with a Fisatom (Mod. 430D, 60 Hz) melting point apparatus are uncorrected. ^{1}H NMR spectra were recorded on a 300 MHz spectrometer in appropriate solvents using TMS as an internal standard or the solvent signals as secondary standards, and the chemical shi s are shown in the d (ppm) scale. Multiplicities of NMR signals are designated as s (singlet), d (doublet), br (broad) and m (multiplet, for unresolved lines). ^{13}C NMR spectra were recorded on a 75.5 MHz spec-trometer. All the experiments were monitored by analytical thin layer chromatography (TLC) performed on silica gel GF254 pre-coated plates. A er elution, the plate was visualized under UV illumination at 254 nm for UV active materials.

Chemistry

General procedure for the synthesis of 3a–c. The respective acid 2a–c (4.56 mmol), 15 mL of ethanol and H_2SO_4 (4 drops) were added to a 50 mL round bottom ask under magnetic stirring and warmed to 60 C for 4 h. A er cooling back to rt, the precipitate was ltered off and the solvent was evaporated. A white solid was obtained, ltered in a Buchner funnel with a sintered disc lter, washed with cold water, and then dried over SiO_2.

Ethyl 2-(1,3-dioxoisoindolin-2-yl)propanoate (3a). Chemical formula: $C_{13}H_{13}NO_4$. MW: 247.25 g. Yield: 70.09%. R_f: 0.6 (Hex/ AcEt: 8/2). M.p.: liquid product. IR (KBr, cm ^{1}): 3008 (C–H), 1711 (C]O) cm ^{1}. ^{1}H NMR (300 MHz, DMSO-d_6), d (ppm): 0.98 (M, 3H, CH_3), 1.12 (d, 3H, CH_3), 2.49 (m, 3H, CH and CH_2), 7.85– 8.05 (m, 4H, Ar). ^{13}C NMR (75.5 MHz, DMSO-d_6), d (ppm): 10.8 (CH_3), 15.4 (CH_3), 20.8 (CH), 125.5 (Ar), 127.6 (Ar), 132.9 (Ar), 152.2 (C]O), 170.1 (C]O). Elemental analysis: liquid product.

Ethyl 2-(1,3-dioxoisoindolin-2-yl)-3-phenylpropanoate (3b). Chemical formula: $C_{19}H_{17}NO_4$. MW: 323.34 g. Yield: 74.89%. R_f: 0.5 (Hex/AcEt: 8/2). M.p.: liquid product. IR (KBr, cm ^{1}): 3447 (NH_2), 3018 (N–H), 1679 (C]O) cm ^{1}, 2918 (C–H), 1679 (C]O) cm ^{1}. ^{1}H NMR (300 MHz, DMSO-d_6), d (ppm): 1.09 (m, 3H, CH_3), 3.50 (m, 4H, 2 CH_2), 4.91 (m, 1H, CH), 7.08–7.14 (m, 5H, Ar), 7.12 (br, 2H, NH_2), 7.78–7.91 (m, 4H, Ar). ^{13}C NMR (75.5 MHz, DMSO-d_6), d (ppm): 10.0 (CH_3), 37.34 (CH_2), 55.8 (CH), 123.6 (Ar), 126.8 (Ar), 128.6 (Ar), 129.1 (Ar), 134.9 (Ar), 168.1 (C] O). Elemental analysis: liquid product.

Ethyl 2-(1,3-dioxoisoindolin-2-yl)-3-methylpentanoate (3c). Chemical formula: $C_{16}H_{19}NO_4$. MW: 289.33 g. Yield: 72.46%. R_f: 0.6 (Hex/AcEt: 8/2). M.p.: liquid product. IR (KBr, cm ^{1}): 3062 (C–H), 1776 (C]O) cm ^{1}. ^{1}H NMR (300 MHz, DMSO-d_6), d (ppm): 0.77 (m, 6H, 2 CH_3), 0.91 (m, 2H, CH_2), 0.98 (m, 3H, CH_3), 2.51 (m, 1H, CH), 4.34 (m, 1H, CH), 7.87–7.86 (m, 4H, Ar). ^{13}C NMR (75.5 MHz, DMSO-d_6), d (ppm): 10.5, 11.2 (CH_3), 17.1 (CH_3), 25.8 (CH_2), 33.3 (CH), 58.5 (CH), 123.6 (Ar), 135.0 (Ar), 168.1 (C]O), 170.1 (C]O). Elemental analysis: liquid product.

General procedure for the synthesis of 4a–c. The respective acid (2a–c, 4.56 mmol), 15 mL of THF and imidazole (0.31 g, 4.56 mmol) were added to a 50 mL round bottom ask under magnetic stirring and warmed to 60 C for 4 h. A er cooling back to rt, the precipitate was ltered off and the solvent was evaporated. A white solid was obtained, ltered in a Buchner funnel with a sintered disc lter, washed with cold water, and then dried over SiO_2.

2-(1,3-Dioxoisoindolin-2-yl)propanamide (4a). Chemical formula: $C_{11}H_{10}N_2O_3$. MW: 218.21 g. Yield: 58.31%. R_f: 0.2 (Hex/ AcEt: 3/7). M.p.: 187–189 C. IR (KBr, cm ^{1}): 3439 (NH); 1683 (C]O); 1467 (C–N–C); 1387 (C–N–C). ^{1}H NMR (300 MHz, DMSO-d_6), d (ppm): 1.12 (d, 3H, CH_3), 2.49 (m, 1H, CH), 6.91 (br, 2H, NH_2), 7.85–7.91 (m, 2H, Ar), 8.05 (m, 2H, Ar). ^{13}C NMR (75.5 MHz, DMSO-d_6), d (ppm): 15.4 (CH_3), 20.9 (CH), 125.5 (Ar), 127.6

(Ar), 132.9 (Ar), 152.2 (C]O), 170.1 (C]O). Elemental analysis – EA_{theor}: N 12.84%; C 60.55%; H 4.62%; EA_{exp}: N 12.74%; C 60.79%; H 4.71%.

2-(1,3-Dioxoisoindolin-2-yl)-3-phenylpropanamide (4b). Chemical formula: $C_{17}H_{14}N_2O_3$. MW: 294.30 g. Yield: 59.05%. R_f: 0.5 (Hex/AcEt: 3/7). M.p.: 233–234 C. IR (KBr, cm ^{1}): 3387 (NH); 1687 (C]O); 1468 (C–N–C); 1384 (C–N–C). ^{1}H NMR (300 MHz, DMSO-d_6), d (ppm): 3.50 (m, 2H, CH_2), 4.91 (m, 1H, CH), 7.08–7.14 (m, 5H, Ar), 7.12 (br, 2H, NH_2), 7.78–7.91 (m, 4H, Ar). ^{13}C NMR (75.5 MHz, DMSO-d_6), d (ppm): 37.3 (CH_2), 54.7 (CH), 123.6 (Ar), 126.8, 128.6, 129.1 (Ar), 134.9 (Ar), 168.1 (C]O), 170.1 (C]O). Elemental analysis – EA_{theor}: N 9.52%; C 69.38%; H 4.79%; EA_{exp}: N 9.36%; C 69.49%; H 4.87%.

2-(1,3-Dioxoisoindolin-2-yl)-3-methylpentanamide (4c). Chemical formula: $C_{14}H_{16}N_2O_3$. MW: 260.29 g. Yield: 56.39%. R_f: 0.6 (Hex/AcEt: 3/7). M.p.: 218–219 C. IR (KBr, cm ^{1}): 3402 (NH); 1650 (C]O); 1458 (C–N–C); 1389 (C–N–C). ^{1}H NMR (300 MHz, DMSO-d_6), d (ppm): 0.77 (m, 3H, CH_3), 0.91 (m, 2H, CH_2), 0.98 (m, 2H, CH_3), 2.51 (m, 1H, CH), 4.34 (m, 1H, CH), 7.12 and 7.49 (2 br, 2H, NH_2), 7.87–7.86 (m, 4H, Ar). ^{13}C NMR (75.5 MHz, DMSO-d_6), d (ppm): 11.2 (CH_3), 17.1 (CH_3), 25.8 (CH_2), 33.3 (CH), 58.5 (CH), 123.6 (Ar), 135.0 (Ar), 168.1 (C]O), 170.1 (C] O). Elemental analysis – EA_{theor}: N 10.76%; C 64.60%; H 6.20%; EA_{exp}: N 10.57%; C: 64.74%; H: 6.36%.

General procedure for the synthesis of 5a–c. The respective ester (3a–c, 4.04 mmol), 15 mL of ethanol and hydrazine hydrate (4 drops) were added to a 50 mL round bottom ask under magnetic stirring and warmed to 60 C for 4 h. A er cooling back to rt, the precipitate was ltered off and the solvent was evaporated. A white solid was obtained, ltered in a Buchner funnel with a sintered disc lter, washed with cold water, and then dried over SiO_2.

2-(1,3-Dioxoisoindolin-2-yl)propanehydrazide (5a). Chemical formula: $C_{11}H_{11}N_3O_3$. MW: 233.22 g. Yield: 61.45%. IR (KBr, cm ^{1}): 3018 (NH); 1661 (C]O); 1458 (C–N–C); 1377 (C–N–C). ^{1}H NMR (300 MHz, DMSO-d_6), d (ppm): 1.12 (d, 3H, CH_3), 2.49 (m, 1H, CH), 4.11 (br, 2H, NH_2), 7.85–8.05 (m, 4H, Ar). The signal in 4.11 disappears a er the addition of 3 drops of D_2O. ^{13}C NMR (75.5 MHz, DMSO-d_6), d (ppm): 15.4 (CH_3), 20.8 (CH), 125.5 (Ar), 127.6 (Ar), 132.9 (Ar), 152.2 (C]O), 170.1 (C]O). EA_{theor}: N 18.02%; C 56.65%; H 4.75%. Elemental analysis – EA_{exp}: N 17.99%; C 56.68%; H 4.68%.

2-(1,3-Dioxoisoindolin-2-yl)-3-phenylpropanehydrazide (5b). Chemical formula: $C_{17}H_{15}N_3O_3$. MW: 309.32 g. Yield: 69.96%. IR (KBr, cm ^{1}): 3026 (NH); 1662 (C]O); 1493 (C–N–C); 1378 (C– N–C). ^{1}H NMR (300 MHz, DMSO-d_6), d (ppm): 3.50 (m, 2H, CH_2), 4.91 (m, 1H, CH), 7.08–7.14 (m, 5H, Ar), 7.12 (br, 2H, NH), 7.46 (NH_2), 7.78–7.91 (m, 4H, Ar). ^{13}C NMR (75.5 MHz, DMSO-d_6), d (ppm): 37.3 (CH_2), 54.7 (CH), 126.8 (Ar), 128.6 (Ar), 129.1 (Ar), 123.6 (Ar), 134.9 (Ar), 168.1 (C]O), 170.1 (C]O). EA_{theor}: N 13.58%; C 66.01%; H 4.89%; elemental analysis – EA_{exp}: N 13.43%; C 66.17%; H 5.06%.

2-(1,3-Dioxoisoindolin-2-yl)-3-methylpentanehydrazide (5c). Chemical formula: $C_{14}H_{17}N_3O_3$. MW: 275.30 g. Yield: 75.17%. IR (KBr, cm ^{1}): 3018 (NH); 1662 (C]O); 1494 (C–N–C); 1378 (C– N–C). ^{1}H NMR (300 MHz, DMSO-d_6), d (ppm): 0.77 (m, 3H, CH_3), 0.91 (m, 2H, CH_2), 0.98 (m, 2H, CH_3), 2.51 (m, 1H, CH), 4.34 (m, 1H, CH), 7.12–7.49 (2 br, 2H, NH_2), 7.87–7.86 (m, 4H, Ar), 7.99 (s, 1H, NH). ^{13}C NMR (75.5 MHz, DMSO-d_6), d (ppm): 11.2 (CH_3), 17.1 (CH_3), 25.8 (CH_2), 33.3 (CH), 58.5 (CH), 123.6 (Ar), 135.0 (Ar), 168.1 (C]O), 170.1 (C]O). Elemental analysis – EA_{theor}: N 15.26%; C 61.08%; H 6.22%; EA_{exp}: N 15.13%; C 61.21%; H 6.31%.

General procedure for the synthesis of 6a–9c. The respective hydrazide (5a–c, 4.22 mmol), 15 mL of ethanol and aromatic aldehyde p-substituted (4.22 mmol) were added to a 50 mL round bottom ask, under magnetic stirring and re ux for 4 h. A er cooling back to rt, the precipitate was ltered off and the solvent was evaporated. A white solid was obtained, ltered in a Buchner funnel with a sintered disc lter, washed with cold water, and then dried over SiO_2.

(Z)-N^{0}-Benzylidene-2-(1,3-dioxoisoindolin-2-yl)propanehydrazide (6a). Chemical formula: $C_{18}H_{15}N_3O_3$. MW: 321.33 g. Yield: 44.77%. R_f: 0.6 (Hex/AcEt: 9/1). M.p.: 86–88 C. IR (KBr, cm ^{1}): 3018 (NH_2), 2897 (C–H), 1661 (C]O) cm ^{1}. ^{1}H NMR (300 MHz, DMSO-d_6), d: 1.11 (d, 3H, CH_3), 2.49 (m, 1H, CH), 4.15 (s, 3H, CH_3), 7.51–7.72 (m, 4H, Ar), 7.85–8.05 (m, 4H, Ar), 8.09 (s, 1H, CH]N). ^{13}C NMR (75.5 MHz, DMSO-d_6), d (ppm): 15.4 (CH_3), 20.8 (CH), 123.6 (Ar), 125.5 (Ar), 128.6 (Ar), 129.1 (Ar), 132.9 (Ar), 134.9 (Ar), 152.2 (C]O), 159.5 (CH]N), 170.1 (C]O). Elemental analysis – EA_{theor}: N 13.08%; C 67.28%; H 4.71%; EA_{exp}: N 12.98%; C 67.17%; H 4.76%.

(Z)-N^{0}-Benzylidene-2-(1,3-dioxoisoindolin-2-yl)-3-phenylpropanehydrazide (6b). Chemical formula: $C_{24}H_{19}N_3O_3$. MW: 397.43 g. Yield: 42.22%. R_f: 0.6 (Hex/AcEt: 9/1). M.p.: 90–92 C. IR (KBr, cm ^{1}): 1664 (C]N); 1624 (C]O). ^{1}H NMR (300 MHz, DMSO-d_6), d (ppm): 0.77 (m, 3H, CH_3), 0.91 (m, 2H, CH_2), 0.98 (m, 2H, CH_3), 2.51 (m, 1H, CH), 4.34 (m, 1H, CH), 7.10–7.52 (m, 8H, Ar), 7.87–7.86 (m, 4H, Ar), 7.99 (s, 1H, NH), 8.01 (s, 1H, CH]N). ^{13}C NMR (75.5 MHz, DMSO-d_6), d (ppm): 25.8 (CH_2), 33.3 (CH), 58.5 (CH), 123.6 (Ar), 125.0 (Ar), 126.5 (Ar), 131.0 (Ar), 135.0 (Ar), 168.1 (C]O), 170.1 (C]O). Elemental analysis – EA_{theor}: N 10.57%; C 72.53%; H 4.82%; EA_{exp}: N 10.52%; C 72.38%; H 4.77%.

(Z)-N^{0}-Benzylidene-2-(1,3-dioxoisoindolin-2-yl)-3-methylpentanehydrazide (6c). Chemical formula: $C_{21}H_{21}N_3O_3$. MW: 363.41 g. Yield: 42.84%. R_f: 0.6 (Hex/AcEt: 9/1). M.p.: 93–95 C. IR (KBr, cm ^{1}): 1664 (C]N); 1623 (C]O). ^{1}H NMR (300 MHz, DMSO-d_6), d (ppm): 0.77 (m, 3H, CH_3), 0.91 (m, 2H, CH_2), 0.98 (m, 2H, CH_3), 2.51 (m, 1H, CH), 4.34 (m, 1H, CH), 7.19–7.32 (m, 5H, Ar), 7.87–7.86 (m, 4H, Ar), 7.99 (s, 1H, NH), 8.01 (s, 1H, CH]N). ^{13}C NMR (75.5 MHz, DMSO-d_6), d (ppm): 11.2 (CH_3), 17.1 (CH_3), 25.8 (CH_2), 33.3 (CH), 58.5 (CH), 123.6 (Ar), 135.0 (Ar), 168.1 (C]O), 170.1 (C]O). Elemental analysis – EA_{theor}: N 11.56%; C 69.41%; H 5.82%; EA_{exp}: N 11.49%; C 69.58%; H 5.73%.

(Z)-2-(1,3-Dioxoisoindolin-2-yl)-N^{0}-(4-methoxybenzylidene-propanehydrazide) (7a). Chemical formula: $C_{19}H_{17}N_3O_4$. MW: 351.36 g. Yield: 47.95%. R_f: 0 : 3 (Hex/AcEt: 9/1). M.p.: 169–170 C. IR (KBr, cm ^{1}): 3018 (NH_2), 2897 (C–H), 1661 (C]O) cm ^{1}. ^{1}H NMR (300 MHz, DMSO-d_6), d (ppm): 1.12 (d, 3H, CH_3), 2.49 (m, 1H, CH), 4.11 (s, 3H, CH_3), 7.21–7.31 (m, 4H, Ar), 7.85–8.05 (m, 4H, Ar), 8.09 (s, 1H, CH]N). ^{13}C NMR (75.5 MHz, DMSO-d_6), d (ppm): 15.4 (CH_3), 20.8 (CH), 123.6 (Ar), 125.5 (Ar), 128.6

(Ar), 129.1 (Ar), 132.9 (Ar), 134.9 (Ar), 152.2 (C]O), 159.5 (CH] N), 170.1 (C]O). Elemental analysis – EA_{theor}: N 11.96%; C 64.95%; H 4.88%; EA_{exp}: N 11.83%; C 64.90%; H 5.04%.

(Z)-2-(1,3-Dioxoisoindolin-2-yl)-N^0-(4-methoxybenzylidene)-3-phenylpropanehydrazide (7b). Chemical formula: $C_{25}H_{21}N_3O_4$. MW: 427.45 g. Yield: 49.12%. R_f: 0.3 (Hex/AcEt: 9/1). M.p.: 169–170 C. IR (KBr, cm ^{1}): 1620 (C]N); 1602 (C]O). ^{1}H NMR (300 MHz, DMSO-d_6), d (ppm): 2.61 (m, 1H, CH), 4.11 (s, 3H, OCH_3), 4.34 (m, 1H, CH), 7.12 and 7.49 (2 br, 2H, NH_2), 7.10–7.52 (m, 8H, Ar), 7.86–7.87 (m, 4H, Ar), 7.99 (s, 1H, NH), 8.01 (s, 1H, CH]N). ^{13}C NMR (75.5 MHz, DMSO-d_6), d (ppm): 25.8 (CH_2), 33.3 (CH), 45.9 (CH_3O), 58.5 (CH), 123.6 (Ar), 125.0 (Ar), 126.5 (Ar), 131.0 (Ar), 135.0 (Ar), 168.1 (C]O), 170.1 (C]O). 7b – elemental analysis – EA_{theor}: N 9.83%; C 70.25%; H 4.95%; EA_{exp}: N 10.02%; C 70.13%; H 4.98%.

(Z)-2-(1,3-Dioxoisoindolin-2-yl)-N^0-(4-methoxybenzylidene)-3-methylpentanehydrazide (7c). Chemical formula: $C_{22}H_{23}N_3O_4$. MW: 393.44 g. Yield: 48.75%. R_f: 0.2 (Hex/AcEt: 9/1). M.p.: 169–171 C. IR (KBr, cm ^{1}): 1661 (C]N); 1623 (C]O). ^{1}H NMR (300 MHz, DMSO-d_6), d (ppm): 0.77 (m, 3H, CH_3), 0.91 (m, 2H, CH_2), 0.98 (m, 2H, CH_3), 2.51 (m, 1H, CH), 4.11 (s, 3H, OCH_3), 4.34 (m, 1H, CH), 7.12 and 7.49 (2 br, 2H, NH_2), 7.19–7.32 (m, 4H, Ar), 7.87–7.86 (m, 4H, Ar), 7.99 (s, 1H, NH), 8.01 (s, 1H, CH]N). ^{13}C NMR (75.5 MHz, DMSO-d_6), d (ppm): 11.2 (CH_3), 17.1 (CH_3), 25.8 (CH_2), 33.3 (CH), 45.9 (CH_3O), 58.5 (CH), 123.6 (Ar), 135.0 (Ar), 168.1 (C]O), 170.1 (C]O). Elemental analysis – EA_{theor}: N 10.68%; C 67.16%; H 5.89%. EA_{exp}: N 10.85%; C 67.30%; H 5.69%.

(Z)-N^0-(4-Chlorobenzylidene)-2-(1,3-dioxoisoindolin-2-yl)propanehydrazide (8a). Chemical formula: $C_{18}H_{14}ClN_3O_3$. MW: 355.78 g. Yield: 60.04%. R_f: 0.7 (Hex/AcEt: 9/1). M.p.: 209– 210 C. IR (KBr, cm ^{1}): 1660 (C]N); 1624 (C]O). ^{1}H NMR (300 MHz, DMSO-d_6), d (ppm): 1.11 (d, 3H, CH_3), 2.49 (m, 1H, CH), 4.11 (s, 3H, CH_3), 7.51–7.72 (m, 4H, Ar), 7.85–8.05 (m, 4H, Ar), 8.09 (s, 1H, CH]N). ^{13}C NMR (75.5 MHz, DMSO-d_6), d (ppm): 15.4 (CH_3), 20.8 (CH), 123.6 (Ar), 125.5 (Ar), 128.6, 129.1 (Ar), 132.9 (Ar), 134.9 (Ar), 147.9 (Ar, C–Cl), 152.2 (C]O), 159.5 (CH] N), 170.1 (C]O). Elemental analysis – EA_{theor}: N 11.81%; C 60.77%; H 3.97%; EA_{exp}: N 11.72%; C 60.68%; H 3.89%.

(Z)-N^0-(4-Chlorobenzylidene)-2-(1,3-dioxoisoindolin-2-yl)-3-phenylpropanehydrazide (8b). Chemical formula: $C_{24}H_{18}ClN_3O_3$. MW: 431.87 g. Yield: 50.25%. R_f: 0.7 (Hex/AcEt: 9/1). M.p.: 210–211 C. IR (KBr, cm ^{1}): 1658 (C]N); 1624 (C]O). ^{1}H NMR (300 MHz, DMSO-d_6), d (ppm): 2.51 (m, 2H, CH_2), 4.34 (m, 1H, CH), 7.10–7.52 (m, 8H, Ar), 7.87–7.86 (m, 4H, Ar), 7.99 (s, 1H, NH), 8.01 (s, 1H, CH]N). ^{13}C NMR (75.5 MHz, DMSO-d_6), d (ppm): 25.8 (CH_2), 33.3 (CH), 45.9 (CH_3O), 58.5 (CH), 123.6 (Ar), 125.0 (Ar), 126.5 (Ar), 131.0 (Ar), 135.0 (Ar), 168.1 (C]O), 170.1 (C]O). Elemental analysis – AE_{teor}: N 9.73%; C 66.75%; H 4.20%; AE_{exp}: N 9.92%; C 66.83%; H 4.47%.

(Z)-N^0-(4-Chlorobenzylidene)-2-(1,3-dioxoisoindolin-2-yl)-3-methylpentanehydrazide (8c). Chemical formula: $C_{21}H_{20}ClN_3O_3$. MW: 397.86 g. Yield: 55.54%. R_f: 0.7 (Hex/AcEt: 9/1). M.p.: 210– 211 C. IR (KBr, cm ^{1}): 1660 (C]N); 1624 (C]O). ^{1}H NMR (300 MHz, DMSO-d_6), d (ppm): 0.77 (m, 3H, CH_3), 0.91 (m, 2H, CH_2), 0.98 (m, 2H, CH_3), 2.51 (m, 1H, CH), 4.11 (s, 3H, OCH_3), 4.34 (m, 1H, CH), 7.19–7.32 (m, 4H, Ar), 7.87–7.86 (m, 4H, Ar), 7.99 (s, 1H, NH), 8.01 (s, 1H, CH]N). ^{13}C NMR (75.5 MHz, DMSO-d_6), d (ppm): 11.2 (CH_3), 17.1 (CH_3), 25.8 (CH_2), 33.3 (CH), 45.9 (CH_3O), 58.5 (CH), 135.0 (Ar), 123.6 (Ar), 168.1 (C]O), 170.1 (C]O). Elemental analysis – EA_{theor}: N 10.56%; C 63.40%; H 5.07%; EA_{exp}: N 10.72%; C 63.51%; H 5.11%.

(Z)-N^0-(3,4-Dichlorobenzylidene)-2-(1,3-dioxoisoindolin-2-yl)-propanehydrazide (9a). Chemical formula: $C_{18}H_{13}Cl_2N_3O_3$. MW: 390.22 g. Yield: 45.76%. R_f: 0.7 (Hex/AcEt: 9/1). M.p.: 170–172 C. IR (KBr, cm ^{1}): 3442 (NH_2), 2997 (C–H), 1710 (C]O), 1627 (C]N) cm ^{1}. ^{1}H NMR (300 MHz, DMSO-d_6), d (ppm): 1.11 (d, 3H, CH_3), 2.49 (m, 1H, CH), 4.11 (s, 3H, CH_3), 7.51–7.63 (4H, Ar), 7.85–8.05 (m, 4H, Ar), 8.19 (s, 1H, CH]N). ^{13}C NMR (75.5 MHz, DMSO-d_6), d (ppm): 15.4 (CH_3), 20.8 (CH), 125.5 (Ar), 128.6 (Ar), 129.1 (Ar), 132.9 (Ar), 134.9 (Ar), 147.9 (Ar, C–Cl), 152.2 (C]O), 159.5 (CH] N), 170.1 (C]O). Elemental analysis – EA_{theor}: N 10.77%; C 55.40%; H 3.36%; EA_{exp}: N 10.67%; C 55.46%; H 3.25%.

(Z)-N^0-(3,4-Dichlorobenzylidene)-2-(1,3-dioxoisoindolin-2-yl)-3-phenylpropanehydrazide (9b). Chemical formula: $C_{24}H_{17}Cl_2N_3O_3$. MW: 466.32 g. Yield: 46.82%. R_f: 0.7 (Hex/AcEt: 9/1). M.p.: 171–173 C. IR (KBr, cm ^{1}): 3442 (NH_2), 2997 (C–H), 1700 (C]O), 1687 (C]N) cm ^{1}. ^{1}H NMR (300 MHz, DMSO-d_6), d (ppm): 2.49 (m, 1H, CH), 4.11 (s, 3H, CH_3), 7.10–7.52 (m, 8H, Ar), 7.85–8.05 (m, 4H, Ar), 8.19 (s, 1H, CH]N). ^{13}C NMR (75.5 MHz, DMSO-d_6), d (ppm): 25.8 (CH_2), 33.3 (CH), 58.5 (CH), 125.0 (Ar), 126.5 (Ar), 131.0 (Ar), 135.0 (Ar), 143.6 (Ar), 168.1 (C]O), 170.1 (C]O). Elemental analysis – EA_{theor}: N 9.01%; C 61.82%; H 3.67%; EA_{exp}: N 9.24%; C 61.74%; H 3.46%.

(Z)-N^0-(3,4-Dichlorobenzylidene)-2-(1,3-dioxoisoindolin-2-yl)-propanehydrazide (9c). Chemical formula: $C_{21}H_{19}Cl_2N_3O_3$. MW: 432.30 g. Yield: 50.02%. R_f: 0.7 (Hex/AcEt: 9/1). M.p.: 178– 180 C. IR (KBr, cm ^{1}): 3442 (NH_2), 2997 (C–H), 1700 (C]O), 1687 (C]N) cm ^{1}. ^{1}H NMR (300 MHz, DMSO-d_6), d (ppm): 1.11 (d, 3H, CH_3), 2.49 (m, 1H, CH), 4.11 (s, 3H, CH_3), 7.51–7.63 (m, 2H, Ar), 7.85–8.05 (m, 4H, Ar), 8.19 (s, 1H, CH]N). ^{13}C NMR (75.5 MHz, DMSO-d_6), d (ppm): 15.4 (CH_3), 20.8 (CH), 125.5 (Ar), 128.6 (Ar), 129.1 (Ar), 132.9 (Ar), 134.9 (Ar), 147.9 (Ar, C–Cl), 152.2 (C]O), 159.5 (CH]N), 170.1 (C]O). Elemental analysis – EA_{theor}: N 9.72%; C 58.35%; H 4.43%; EA_{exp}: N 9.60%; C 58.27%; H 4.67%.

Biological in vitro evaluation

TNF-a and IL-1 levels. Mice peritoneal macrophages were placed into 96 well plates at a cell density of 2 10^6 cells per mL and incubated for 2 h at 37 C and 5% CO_2. Cells at 2 10^6 concentration were suspended in RPMI 1640 with 5% FBS, 100 UI mL ^{1} of penicillin, 100 mg mL ^{1} of streptomycin and 50 mM 2-mercaptoethanol. 100 mL of suspension and 100 mL of samples were incubated with LPS 2 mg mL ^{1} (positive control) or with the test compounds in different concentrations. A er 24 h, the supernatants were removed and kept at 80 C until the eval-uation of cytokine levels (TNF and IL-1). The doses of cytokines in the exudates were assayed by sandwich ELISA, using mono-clonal antibodies speci c to the detection of cytokines.

TNF-a, cell death and apoptosis inhibition. The effect of each compound on inhibiting TNF expression and decreasing cell viability was determined using the cell line FRT-Jurkat TNF.

The analysis was carried out using a ow cytometer FACSCali-bur 4-Colour (Becton, Dickinson and Company, New Jersey, USA). The data analysis was obtained with FlowJo so ware (Tree-Star, Ashland, OR, USA). The study of cell viability with DMSO and with the compounds, for 24 h, was carried out by ow cytometry. The compounds were suspended and diluted to 100 mM and 10 mM in dimethyl sulfoxide. TNF inhibition was determined as a decrease in GFP uorescence, which was detected at a wavelength of 515 nm, in channel FL3. Viable and non-viable cells, present following either the solvent alone or compound treatment, were counted by gating on each cell population using a forward scatter (FSC) versus side scatter (SSC) plot. Viability was also assessed following propidium iodide staining and detection of uorescence at 570 nm in the FL2 channel. For detection of apoptosis following treatment with each compound, parental Jurkat cells were treated with the substrate, labelled with uorescein isothiocyanate (FITC), against cleaved caspase 3 by the Nucview-488 caspase 3 assay (Biotium Inc., Hayward, USA). The resulting uorescence was quantitated in channel FL3.

Acknowledgements

We would like to thank the Brazilian National Research Council (CNPq), the Research Foundation of Pernambuco State (FACEPE) and the Cancer Council, Western Australia for nancial support. M.V.O.C. is a recipient of the FACEPE scholarship. Our thanks are also due to the Department of Chemistry at the Federal University of Pernambuco (UFPE), for recording the ^{1}H NMR and IR spectra of all compounds.

References

1 A. L. Akeson, C. W. Woods, L. B. Mosher, C. E. Thomas and R. L. Jackson, Atherosclerosis, 1991, 86, 261–270.
2 K. D. Nam, M. Han, J. Yoon, E.-A. Kim, S.-W. Cho and H.-G. Hahn, Bull. Korean Chem. Soc., 2013, 34, 271–274.
3 J. Drewe, S. Kasibhatla, B. Tseng, E. Shelton, D. Sperandio, R. M. Yee, J. Litvak, M. Sendzik, J. R. Spencer and S. X. Cai, Bioorg. Med. Chem. Lett., 2007, 17, 4987–4990.
4 A. A. Beg and D. Baltimore, Science, 1996, 274, 782–784.
5 Z. G. Liu, H. Hsu, D. V. Goeddel and M. Karin, Cell, 1996, 87, 565–576.
6 D. J. Van Antwerp, S. J. Martin, T. Kafri, D. R. Green and I. M. Verma, Science, 1996, 274, 787–789.
7 C. Y. Wang, M. W. Mayo and A. S. Baldwin, Science, 1996, 274, 784–787.
8 M. A. Palladino, F. R. Bahjat, E. A. Theodorakis and L. L. Moldawer, Nat. Rev. Drug Discovery, 2003, 2, 736–746.
9 J. M. Chapman, G. H. Cocolas and I. H. Hall, J. Med. Chem., 1979, 22, 1399–1402.
10 I. H. Hall, J. M. Chapman and G. H. Cocolas, J. Pharm. Sci., 1981, 70, 326–328.
11 J. M. Chapman, P. J. Voorstad, G. H. Cocolas and I. H. Hall, J. Med. Chem., 1983, 26, 237–243.
12 T. O. Daniel, H. Liu, J. D. Morrow, B. C. Crews and L. J. Marnett, Cancer Res., 1999, 59, 4574–4577.
13 S. Rollas and S. G. Kuç¨ukg¨uzel,¨ Molecules, 2007, 12, 1910–1939.
14 N. A. Zulkepli, K. V. K. Rou, W. N. H. W. Sulaiman, A. Salhin, B. Saad and A. Seeni, Asian Pac. J. Cancer Prev., 2011, 12, 259–263.
15 Q. Zeng, Z. Liu, B. Li and F. Wang, Amino Acids, 2004, 27, 183–186.
16 M. Karimi, L. C. Goldie, D. Ulgiati and L. J. Abraham, BioTechniques, 2007, 42, 217–224.
17 K. M. Kroeger, K. S. Carville and L. J. Abraham, Mol. Immunol., 1997, 34, 391–399.
18 S. G. Stewart, C. J. Braun, S.-L. Ng, M. E. Polomska, M. Karimi and L. J. Abraham, Bioorg. Med. Chem., 2010, 18, 650–662.
19 S. Y. Yeung, S. Kampmann, K. A. Stubbs, B. W. Skelton, B. J. Kaskow, L. J. Abraham and S. G. Stewart, MedChemComm, 2011, 2, 1073.